Evaluation of Prenatal Adenoviral Vascular Endothelial Growth Factor Gene Therapy in the Growth-Restricted Sheep Fetus and Neonate

David John Carr

University College London

2013

A thesis submitted for the degree of Doctor of Philosophy

Declaration

I, David Carr, confirm that the work presented in this thesis is my own. Where information has been derived from other sources, I confirm that this has been indicated in the thesis.

Abstract

Background

Fetal growth restriction (FGR) is associated with reduced uterine blood flow (UBF). In normal sheep pregnancies, adenovirus (Ad) mediated over-expression of vascular endothelial growth factor (VEGF) in the uterine arteries (UtA) increases UBF. It was hypothesised that enhancing UBF would improve fetal substrate delivery in an ovine paradigm of FGR characterised by reduced UBF from mid-gestation.

Methods

Singleton pregnancies were established using embryo transfer in adolescent ewes subsequently overnourished to generate FGR (n=81). Ewes were randomised mid-gestation to receive bilateral UtA injections of $5x10^{11}$ particles Ad.VEGF-A_{165} or inactive treatment (saline or $5x10^{11}$ particles Ad.LacZ, a control vector). Fetal growth/wellbeing were evaluated using serial ultrasound. *Late-gestation study*: UBF was monitored using indwelling flowprobes until necropsy at 0.9 gestation. Vasorelaxation, neovascularisation in perivascular adventitia and placental mRNA expression of angiogenic factors/receptors were examined. A group of control-fed ewes with normally-developing fetuses was included (n=12). *Postnatal study*: Pregnancies continued until spontaneous delivery near to term. Lambs were weighed and measured weekly and underwent metabolic challenge at 7 weeks, dual-energy X-ray absorptiometry at 11 weeks, and necropsy at 12 weeks postnatal age. DNA methylation of somatotropic genes was examined in hepatic tissues.

Results

Ultrasonographic fetal growth velocity was greater in Ad.VEGF-A_{165}-treated versus control-treated FGR fetuses at 3-4 weeks post-injection. In late gestation fewer fetuses were markedly growth-restricted following Ad.VEGF-A_{165} therapy. There was evidence of mitigated brain sparing. No effect was seen on UBF/neovascularisation although Ad.VEGF-A_{165}-transduced vessels showed enhanced vasorelaxation. Flt1/KDR expression was increased in the maternal placental compartment. At birth Ad.VEGF-A_{165}-treated lambs tended to be heavier with increased placental efficiency. Postnatal growth, lean tissue accretion and insulin secretion were also increased, however no epigenetic changes were observed.

Conclusions

Ad.VEGF-A_{165} safely increases fetal growth in this ovine model of FGR. This work has supported a successful application to translate this therapy into the clinic.

Table of Contents

List of Figures

List of Tables

Publications

- Carr DJ, Wallace JM, Aitken RP, Milne JS, Mehta V, Martin JF, Zachary IC, Peebles DM, David AL. Uteroplacental adenoviral VEGF gene therapy increases fetal growth velocity in growth-restricted sheep pregnancies [submitted]

- Carr DJ, Aitken RP, Milne JS, David AL, Wallace JM. A case of successful pregnancy in a ewe with uterus didelphys. *Reprod Domest Anim* 2013 [in press]

- Carr DJ, Aitken RP, Milne JS, David AL, Wallace JM. Fetoplacental biometry and umbilical artery Doppler velocimetry in the overnourished adolescent model of fetal growth restriction. *Am J Obstet Gynecol* 2012; 207(2): 141.e6-141.e15

- Mehta V, Abi-Nader KN, Carr D, Wallace J, Coutelle C, Waddington S, Peebles D, David AL. Monitoring for potential adverse effects of prenatal gene therapy: use of large animal models with relevance to human application. *Methods Molecul Biol* 2012; 891: 291-328

- Carr DJ, Aitken RP, Milne JS, David AL, Wallace JM. Ultrasonographic assessment of growth and estimation of birthweight in late gestation sheep fetuses. *Ultrasound Med Biol* 2011; 37(10):1588-1595

Acknowledgements

Above all else, I would like to thank my two incredible supervisors - Anna David and Jacqueline Wallace - for their unrelenting support and encouragement over the past three to four years.

I am very grateful to Anna David for being a great clinical academic role model and for helping me acquire a wide range of new skills that will be invaluable for my career. I greatly appreciate her having given me the freedom to expand my teaching portfolio, develop my own ideas and collaborations for future research, and to maintain my clinical skills over the course of my PhD, which has helped me develop many of the attributes necessary to succeed in clinical academia. Her approachable and down-to-earth nature, plus her talent, make her an exceptional mentor.

Huge respect is also due to Jacqueline Wallace for having succeeded in making a scientist out of me, despite my anxieties about having never before set foot in a laboratory and an inherent fear of sheep that had been repressed since childhood (following an attack by a ram). From the very beginning, Jacqueline encouraged me to find my own answers and develop skills in critical analysis, which have helped shape my way of thinking. Her work ethic, attention to detail and time management skills are inspirational, and I strive to emulate them in my daily working life.

I am also grateful to all the staff at the Rowett Institute for having made me feel so welcome from day one, and for having given me such a comprehensive induction into the basic sciences. I am forever indebted to John Milne for his expert supervision of my early days in the lab, and to Raymond Aitken for everything he taught me working in the sheephouse. I would also like to thank Graham Horgan, Clare Adam, Joel Caton, James Forbes Birnie and Hannah Battensby.

I am extremely grateful to Vedanta Mehta for performing the organ bath analyses detailed in Chapter 4, and for his helpful tips and constant support in countless other matters. Gratitude is also due to Ian Zachary and his group, who welcomed me into their lab in the Rayne Institute and provided me with the bench space for my ongoing lab work back at UCL. Additional thanks go to Donald Peebles and John Martin for academic input. I must also acknowledge the staff of the Genome Centre, Queen Mary University London, particularly Chaz Mein and Eva Wozniak, who were involved in design and optimisation of the epigenetic analyses detailed in Chapter 6.

Last, but certainly not least, I would like to thank my husband, Michael, who unquestioningly gave up his job and agreed to move 500 miles away from our family and friends so I could take up this amazing research opportunity. And, finally, I would just like to acknowledge and keep in mind all the ewes, fetuses and lambs that contributed to the success of this research project.

6FAM	6-carboxyfluorescein
AA	adventitial area
ABC	avidin-biotin complex
ABTS	2,2’-azino-bis(3-ethylbenzothiazoline-6-sulphonic acid)
AC	abdominal circumference
ACTH	adrenocorticotrophic hormone
Ad	adenovirus
AEDF	absent end-diastolic flow
AFW	adjusted fetal weight
AGA	appropriate for gestational age
ALP	alkaline phosphatase
ALT	alanine transaminase
AMP	adenosine monophosphate
ANGPT	angiopoietin
ANOVA	analysis of variance
APRD	anteroposterior renal diameter
APS	adenosine 5' phosphosulphate
AST	aspartate aminotransferase
ATP	adenosine triphosphate
AUC	area under the curve
BCS	body condition score
BK	bradykinin
BMC	bone mineral content
BMD	bone mineral density
BMI	body mass index
BP	blood pressure
BPD	biparietal diameter
BPP	biophysical profile
BrdU	5-bromo-2'-deoxyuridine
BSA	bovine serum albumin
C	control-intake
C/EBP	CCAAT/enhancer binding protein
CABG	coronary artery bypass graft
cAMP	cyclic adenosine monophosphate
CAR	Coxsackievirus and adenovirus receptor
cGMP	cyclic guanosine monophosphate
CHD	coronary heart disease
COBRA	combined bisulphite restriction analysis
CpG	cytosine base adjacent to guanine base
CRH	corticotrophin releasing hormone
CSA	cross-sectional area
CTG	cardiotocography
D	day
DAB	3,3’-diaminobenzidine tetrahydrochloride
dATP	deoxyadenosine triphosphate

dCTP	deoxycytidine triphosphate
DEXA	dual energy X-ray absorptiometry
dGTP	deoxyguanosine triphosphate
DMR	differentially methylated region
DNA	deoxyribonucleic acid
dNTP	deoxyribonucleotide triphosphate
DPX	di-n-butylphthalate in xylene
dTTP	deoxyribothymidine triphosphate
DV	ductus venosus
DVP	deepest vertical pool
EDF	end-diastolic flow
EDHF	endothelium-derived hyperpolarizing factor
EDTA	ethylenediaminetetraacetic acid
EFW	estimated fetal weight
ELISA	enzyme-linked immunosorbent array
eNOS	endothelial nitric oxide synthase
EPROM	erasable programmable read only memory
ET	endotracheal
F	female
FGF2	fibroblast growth factor 2
FGR	fetal growth restriction
FL	femur length
Flt-1	fms-like tyrosine kinase 1
FLT1	fms-like tyrosine kinase 1 (gene)
GA	gestational age
GFP	green fluorescent protein
GGT	gamma-glutamyl transferase
GH	growth hormone
GHR	growth hormone receptor
GLDH	glutamate dehydrogenase
GLM	General Linear Model
GLUT	glucose transporter
GOI	gene of interest
GRIT	Growth Restriction Intervention Trial
GUCY1B3	soluble guanylate cyclase
GWA	genome wide amplification
H	high-intake
H&E	haematoxylin and eosin
HC	head circumference
HELLP	Haemolysis, Elevated Liver enzymes, Low Platelets
HIV	human immunodeficiency virus
HOMA	homeostatic model assessment
HPA	hypothalamic-pituitary adrenal
HR	heart rate
IGF	insulin-like growth factor
IGFBP	insulin-like growth factor binding protein
IGFR	insulin-like growth factor receptor
IgG	immunoglobulin G

i.m.	intramuscular
IMA	intima + media area
IMLA	intima + media + lumen area
IMR	intima to media ratio
IMT	intima-media thickness
iNOS	inducible nitric oxide synthase
i.v.	intravenous
IVC	inferior vena cava
KDR	kinase insert domain receptor
LA	lumen area
LacZ	β-galactosidase (gene)
LBW	low birth weight
LPL	lipoprotein lipase
M	male
MBD	methyl-CpG-binding domain
MCA	middle cerebral artery
miRNA	microRNA
MoM	multiples of the median
mRNA	messenger ribonucleic acid
M.*Sss*I	CpG methyltransferase
NBF	neutral buffered formalin
NBW	necropsy / birth weight
NCBI	National Center for Biotechnology Information
NEC	necrotising enterocolitis
NEFA	non-esterified fatty acid
NICE	National Institute for Health and Clinical Excellence
NO	nitric oxide
NOS	nitric oxide synthase
NOS3	nitric oxide synthase (gene)
NRC31	nuclear receptor subfamily 3, group C, member 1 (glucocorticoid receptor)
OCM	ovum culture medium
oFSH	ovine follicle-stimulating hormone
ORMOSIL	organically modified silica
OSL	occipito-snout length
PAPP-A	pregnancy-associated plasma protein A
PBS	phosphate buffered saline
PCR	polymerase chain reaction
PDS	polydioxanone
PE	phenylephrine
PEG	polyethylene glycol
PGI_2	prostacyclin
PI	pulsatility index
PlGF	placental growth factor
PMSG	pregnant mare serum gonadotrophin
pO_2	partial pressure of oxygen
PPAR	peroxisome proliferator-activated receptor
PPi	pyrophosphate

PV	per vaginum
QC	quality control
RCOG	Royal College of Obstetricians and Gynaecologists
REDF	reversed end-diastolic flow
RI	resistance index
RIA	radioimmunoassay
RL	renal length
RNA	ribonucleic acid
RT	reverse transcription
RV	renal volume
SAA	serum amyloid A
SAM	s-adenosylmethionine
s.c.	subcutaneous
SD	standard deviation
SDR	systolic to diastolic ratio
SE	standard error of the estimate
SEM	standard error of the mean
SFD	symphysio-fundal height
sFlt-1	soluble fms-like tyrosine kinase 1
SGA	small for gestational age
SPSS	Statistical Package for the Social Sciences
SUAL	single umbilical arterial ligation
T3	tri-iodothyronine
T4	thyroxine
TAMAX	time-averaged maximum velocity
TAMRA	tetramethylrhodamine
TAT-1	T-type amino acid transporter
TD	trunk (transverse abdominal) diameter
TEK	endothelial tyrosine kinase
TENS	transcutaneous electrical nerve stimulation
TGF	transforming growth factor
TL	tibia length
TORCH	TOxoplasma gondii, Rubella, Cytomegalovirus, Herpes simplex
TRD	transverse renal diameter
TSH	thyroid stimulating hormone
TVA	total vessel area
UA	umbilical artery
UBF	uterine blood flow
UCD	umbilical cord diameter
UtA	uterine artery
UV	umbilical vein
VEGF	vascular endothelial growth factor
Vmax	maximum (peak systolic) velocity
Vmin	minimum (end-diastolic) velocity
vWF	von Willebrand factor

1.1 Fetal growth restriction

Fetal growth restriction (FGR) is defined as the failure of a fetus to achieve its own genetically pre-determined growth potential. FGR complicates around 8% of pregnancies in the general population of developed countries (Mandruzzato et al. 2008) and is a major cause of perinatal mortality and morbidity (Bernstein et al. 2000; Halliday 2009). The biomedical, psychological, social and economic impact of this complication of pregnancy is huge (Nardozza et al. 2012).

1.1.1 Terminology

In clinical practice, diagnosis of FGR can be difficult as the intrinsic growth potential of a given fetus is generally not known and depends on a number of different factors including ethnicity, parity, fetal gender, maternal height and weight in early pregnancy and the mother's own birth weight (Gardosi et al. 1992; Gardosi et al. 1995; McCowan & Horgan 2009). Paternal weight also makes a modest contribution (Wilcox et al. 1995). The majority of significantly growth-restricted fetuses are also “small for gestational age” (SGA) at birth. This related but not synonymous term is applied when the birth weight falls below a certain threshold, for example the 10th, 5th or 3rd percentile for a given gestational age. However it is important to recognise that not all SGA babies are in fact growth-restricted. For example, by definition 10% of normal babies will weigh less than the 10th percentile at birth. Consequently SGA fetuses represent a heterogeneous group in which those with true FGR are diluted with fetuses that are normally grown yet "constitutionally small". Only 30-50% of those babies whose birth weight falls below the 10th percentile for gestational age are growth-restricted (Ott 1988) and vice versa not all fetuses with FGR are necessarily SGA (Chard et al. 1992). Another term often used is "low birth weight" (LBW), defined as a birth weight less than 2500g. This classification is even less useful in clinical practice than SGA as it does not account at all for the gestational age. Consequently a LBW baby may be small as the result of FGR, constitutional smallness or simply prematurity.

1.1.2 Causes of FGR

FGR is a description of fetal condition rather than a diagnosis, and there are a wide range of underlying causes, associations and contributory factors. Broadly speaking these fall into one of three main categories, which are fetal, maternal and uteroplacental. It should be noted however that there is often some degree of overlap and that many causes will lead to a common end-point of reduced uteroplacental perfusion and hence attenuated fetal nutrient

delivery. For example, numerous maternal medical co-morbidities can adversely affect placentation and/or uterine blood flow (UBF). In clinical practice it is more useful to make the basic distinction between placentally mediated and non placentally mediated FGR with respect to management (see Section 1.1.4).

1.1.2.1 Fetal factors

There are many intrinsic fetal causes of FGR, which broadly fall into one of four categories: chromosomal aberrations, genetic syndromes, structural anomalies and congenital infections.

Chromosomal abnormalities including trisomy 21 (Down's syndrome), trisomy 18 (Edward's syndrome), trisomy 13 (Patau's syndrome) and monosomy X (Turner's syndrome) are present in 7% and 19% cases of fetuses with AC measurements below the 10th and 5th percentiles, respectively (Snijders et al. 1993a; Heydanus et al. 1994). In the latter three examples, slowing of fetal growth is usually apparent by the second trimester (Dicke & Crane 1991; FitzSimmons et al. 1994). This is also true of triploidy (Jauniaux et al. 1996), particularly when the extra set of chromosomes is paternally derived (McFadden & Kalousek 1991). Additional chromosome problems associated with FGR include confined placental mosaicism (particularly trisomy 15, 16 and trisomy 9q), uniparental disomy (particularly of chromosomes 6, 14 and 16) and partial chromosomal deletions such as 4q (Wolf-Hirschhorn syndrome) or 5q (Cri du Chat syndrome) (Fujimoto & Wilson 1990; Sanlaville et al. 2000; Maulik 2006; Wilkins-Haug et al. 2006).

FGR may complicate a large number of different genetic syndromes, many of which are single gene disorders demonstrating Mendelian (mostly autosomal dominant or autosomal recessive) inheritance. Specific examples include Cornelia de Lange, Brachmann de Lange, Russell-Silver, Mulibrey Nanism, Rubenstein-Taybi, Dubowitz, Seckel, De Sanctis-Cachione, Johanson-Blizzard, Roberts and Fanconi pancytopaenia syndrome (Gross 1997). Most of these genetic syndromes are characterised by multiple physical abnormalities, some of which are detectable by fetal ultrasound. The availability of various online dysmorphology databases, such as the London Dysmorphology Database (LDDD) and the recently developed Phenotip (www.phenotip.com) can aid pattern recognition and diagnosis of the rarer genetic syndromes (Guest et al. 1999).

Structural fetal anomalies may be associated with one of the chromosomal problems or single gene disorders described above, but even in karyotypically normal and non-syndromic fetuses, congenital malformations account for a further 1–2% of FGR cases (Hendrix & Berghella 2008). Commonly associated abnormalities include cardiac defects (Fallot's tetralogy, hypoplastic left heart syndrome, pulmonary stenosis, ventricular septal defects), anencephaly, abdominal wall defects (gastroschisis and exomphalos) and congenital diaphragmatic hernia. In addition, some

soft markers are associated with FGR. Soft markers, also known as normal variants, constitute ultrasonographic features that are present in both normal and affected fetuses, but are more prevalent in the latter group and thereby increase the likelihood of a particular condition, e.g. FGR or aneuploidy. For example, the finding of hyperechogenic bowel and a single umbilical artery at the second trimester anomaly scan are each associated with a greater than two-fold increase in the risk of FGR (Hua et al. 2010; Goetzinger et al. 2011).

Finally, intrauterine infection is responsible for approximately 5–10% of cases (Knox 1978). The infective agents that are most frequently encountered in obstetric practice in association with FGR are collectively referred to as the TORCH complex, which consists of TOxoplasma gondii, Rubella, Cytomegalovirus (CMV) and Herpes simplex virus (Kinney & Kumar 1988). Although congenital rubella infection is becoming less common in the UK due to widespread vaccination, there remains a strong association with FGR if susceptible women become exposed during pregnancy. The most common infective cause of FGR in developed countries is CMV (Cox & Marton 2009), however endemic malarial infection (mainly due to *Plasmodium falciparum*) is currently responsible for a larger proportion of infective FGR worldwide (Berghella 2007).

1.1.2.2 Maternal factors

A large number of maternal risk factors have been identified for the development of FGR, and are listed in Table 1.1. These include discrete pathologies such as chronic medical conditions, environmental factors such as living at high altitude or exposure to various toxins, and other socioeconomic markers of maternal deprivation which put the pregnancy at higher risk of adverse perinatal outcomes, for example being unmarried or unemployed. In addition to these maternal factors, it is recognised that paternal factors also have an impact. For example, parous women embarking on a further pregnancy with a new partner are 20-30% more likely to have FGR even if the first pregnancy was unaffected (Krulewitch et al. 1997) and the risk of SGA is elevated if the father himself was born SGA (Shah 2010a).

A further important consideration here is maternal constraint, which is a physiological rather than pathological process, but one which may significantly impact the growth potential of a given fetus. Maternal constraint (see Gluckman and Hanson (2004) for a review) essentially refers to the non-genetic and non-pathological maternal factors that restrict fetal growth in all pregnancies, whether or not they are complicated by FGR or SGA. Maternal constraint may reflect increased demand (for example multiple gestation) and/or reduced supply of nutrients (variations in maternal diet within the normal nutritional range). Classically however uterine size is though to play a particularly important role. This is best illustrated by the seminal work

Table 1.1 – Maternal risk factors for fetal growth restriction and smallness for gestational age

Risk Factor	**Reference**
Diabetes mellitus with associated vascular disease	Howarth et al. 2007
Impaired renal function	Fink et al. 1998
Antiphospholipid syndrome	Yasuda et al. 1995
Chronic (essential) hypertension	Allen et al. 2004
Systemic lupus erythematosus	Yasmeen et al. 2001
Congenital heart disease	Drenthen et al. 2007
Advanced maternal age (>35 years old)	Odibo et al. 2006
Nulliparity	Shah 2010b
Underweight, overweight or obese (BMI <20, >25 or >30)	Gardosi & Francis 2009
Smoking	Kramer et al. 1999
IVF conception	Jackson et al. 2004
Excessive exercise or low pre-pregnancy fruit intake	McCowan et al. 2010
Previous history of SGA, stillbirth or pre-eclampsia	Ananth et al. 2007
Inter-pregnancy interval <6 months or >5 years	Conde-Agudelo et al. 2006
Mother born SGA	Shah et al. 2009
African ethnicity	Kramer 1987
Asian ethnicity	Alexander et al. 2007
Social deprivation	Blumenshine et al. 2010
Being unmarried	Shah et al. 2011
Pregnancy-induced hypertension	Allen et al. 2004
Pre-eclampsia	Ananth et al. 2007
Heavy first trimester PV bleeding (threatened miscarriage)	Weiss et al. 2004
Placental abruption	Tikkanen 2011
Caffeine intake >300mg per day	CARE Study Group 2008
Low maternal weight gain	Lang et al. 1996
Cocaine use	Gouin et al. 2011
Moderate or excessive alcohol intake	Jaddoe et al. 2007
Domestic violence	Shah & Shah 2010
Environmental pollutants	Liu et al. 2003
Maternal stress	Lederman et al. 2004
Living at high altitude	Moore 2003
Human immundeficiency virus (HIV) infection	Brocklehurst & French 1998

of Walton and Hammond (1938) who established reciprocal crosses between Shire horses and Shetland ponies. In these experiments, Shetland pony fetuses developing in Shire horse uteri grew larger than expected. Conversely, Shire horse fetuses developing in Shetland pony uteri did not reach their genetic full potential.

1.1.2.3 Uteroplacental factors

Aside from the fetomaternal causes detailed above, most cases of FGR (>60%) occur secondary to uteroplacental insufficiency (Ghidini 1996). This term is widely used to describe the scenario in which there is reduced uterine blood flow (UBF) and/or failure of normal placental growth and development. As a result transplacental exchange of oxygen and nutrients is insufficient to meet the demands of the growing fetus. This particular form of FGR varies greatly in its timing and severity but, with the exception of very early onset cases, it is usually asymmetrical in its pattern (Cox & Marton 2009). During normal pregnancy, adequate uterine perfusion depends critically on physiological adaptation of the maternal cardiovascular system and establishment of functional uteroplacental and fetoplacental circulations. Key to this process in the human is invasion of the maternal spiral arteries and replacement of the vascular smooth muscle layer (tunica media) by the extravillous trophoblast (Figure 1.1). The end result is a high capacitance, passively dilated vascular bed, which is capable of accommodating the major increases in UBF that are required as pregnancy advances, from 50ml/min at 10 weeks to 500ml/min in mid-gestation to 1300ml/min at term (Lang et al. 2003). At the same time maternal cardiac output increases by 30–40% (Ueland et al. 1969) and plasma volume is expanded by ~50% (Nelson-Piercy 2010). Failure of these adaptive processes results in abnormally high resistance to flow in the uterine arteries (UtA), which in clinical practice can be recognised using UtA Doppler ultrasound. High impedance leads to reduced blood flow, particularly in end-diastole, which results in a raised pulsatility index (PI), resistance index (RI) and systolic to diastolic ratio (SDR). These indices can be calculated using the formulae presented in Section 2.1.3.2. An early diastolic notch (see Figure 1.2) in the waveform is also associated with impaired trophoblast invasion (Harrington et al. 1997), particularly when it persists beyond 24 weeks of gestation (Pijnenborg et al. 1983). In addition, it is increasingly recognised that additional factors are important for UtA adaptation during pregnancy, including changes in maternal arterial stiffness, endothelial function, endogenous hormone levels (mainly oestrogen), nitric oxide availability and sympathetic tone (Owman 1981; Everett & Lees 2012). This may be particularly true of species such as the sheep, in which trophoblast invasion does not occur and yet similar increases in UBF to the human are observed, and in which UBF correlates positively with fetal growth (Lang et al. 2003). Human FGR is characterised by reduced UBF from as early as mid-

gestation, as illustrated in Figure 1.3 (Konje et al. 2003), and deliberate restriction of UBF by gel-foam embolisation or ligation of the UtA in mid to late gestation results in FGR in sheep, rat, mouse and guinea pig pregnancies (Ochi et al. 1998; Carter 2007), which illustrates the importance of adequate UBF in sustaining normal fetal growth. In sheep, an early diastolic notch is also observed in the UtA waveform of embolised pregnancies (Ochi et al. 1998).

Figure 1.1 – Uterine artery invasion by extravillous trophoblast in normal pregnancy and FGR

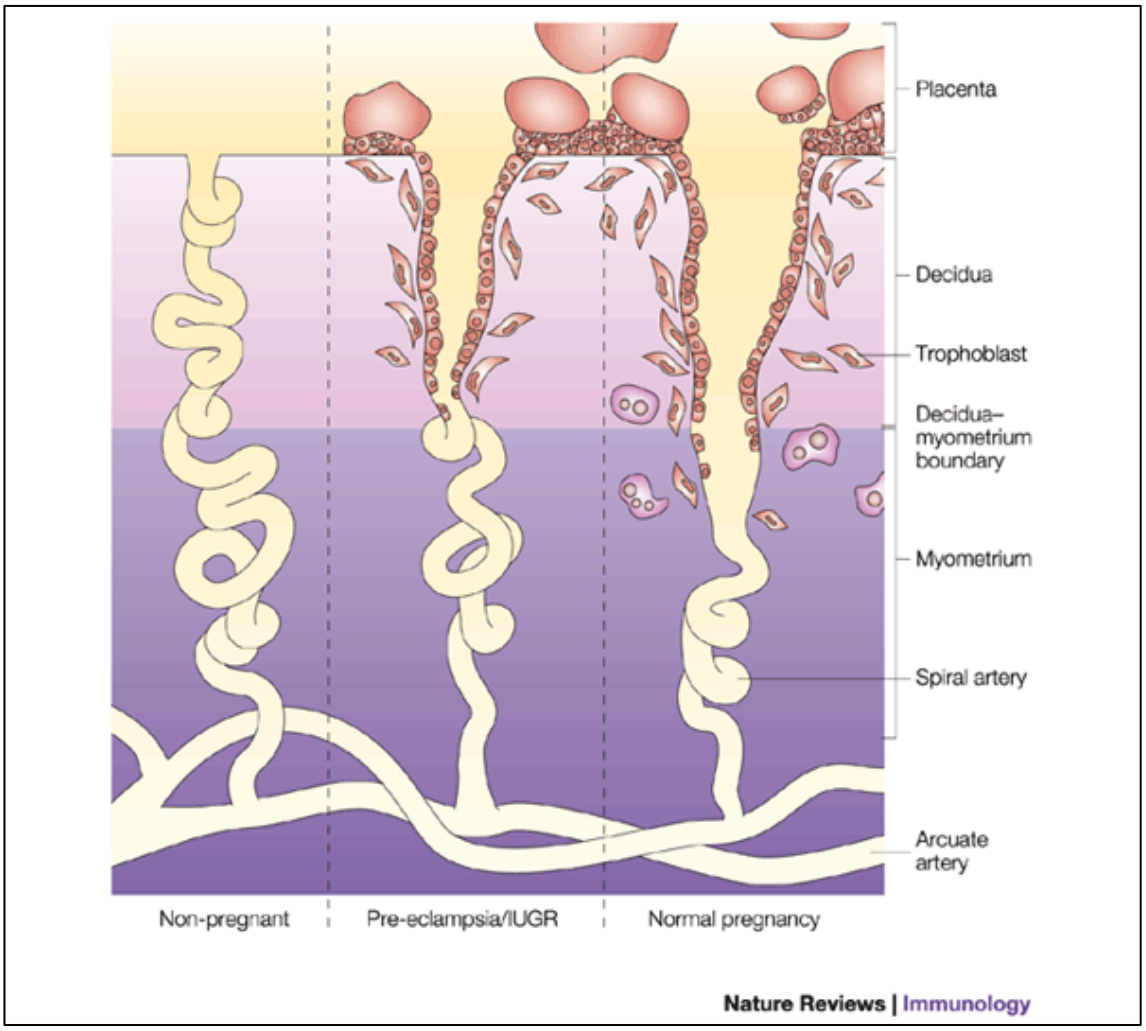

Comparison between uterine arteries in the non-pregnant (uninvaded) state, normal pregnancy and pathological pregnancy - pre-eclampsia and intrauterine growth restriction (IUGR). Both the extent and depth of trophoblast invasion is suboptimal in the latter, resulting in inadequate spiral artery transformation, increased vascular resistance and reduced uterine blood flow. As well as restricting nutrient delivery to the fetus, ischaemia in the placenta can lead to systemic endothelial dysfunction in the mother that results in the maternal syndrome of pre-eclampsia. Figure reproduced with permission from Moffett-King (2002).

Figure 1.2 – Abnormal uterine artery Doppler waveform

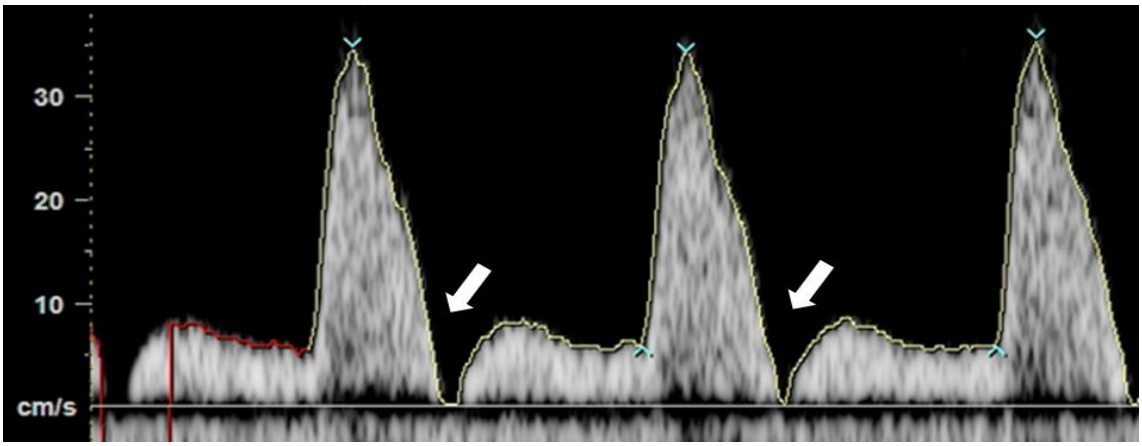

Maternal uterine artery Doppler waveform demonstrating reduced end-diastolic flow and an early diastolic notch (illutstrated by the white arrows), suggestive of impaired trophoblast invasion, increase uteroplacental vascular resistance and reduced uterine blood flow.

Figure 1.3 – Uterine blood flow in growth-restricted versus normally developing pregnancies

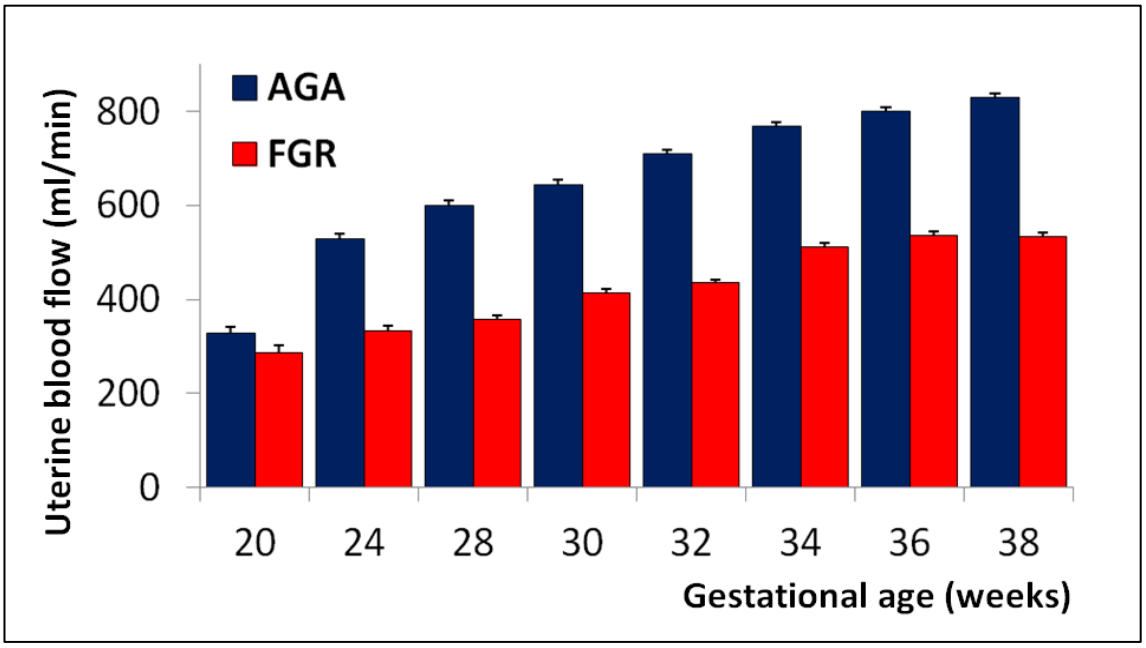

Serial measurements of volume blood flow in the uterine artery measured by transabdominal ultrasound between 20 and 38 weeks gestation in human pregnancies complicated by fetal growth restriction (FGR) compared with appropriate-for-gestational-age (AGA) controls. The criteria for FGR were an estimated fetal weight (and eventual birth weight) between the 3rd and 10th centile for gestational age and evidence of centile crossing (reduced growth velocity). Graph produced using data tables from Konje et al. (2003).

In addition to the uteroplacental blood flow, an adequately matched fetoplacental blood flow is needed to ensure fetal substrate supply, as mismatch between the two placental circulations effectively decreases the available area for gaseous and nutrient exchange. The establishment of a fetoplacental circulation depends on the development and patency of a complex network of secondary and tertiary villi (Kingdom et al. 1997). FGR is associated with a poorly developed villous tree, leading to a reduction in umbilical venous blood flow (Rigano et al. 2001) followed by progressive obliteration of small muscular arteries within the tertiary stem villi. This process is accompanied by increased resistance to blood flow within the umbilical artery (UA), which is reflected by a progressive reduction in end-diastolic flow (EDF) and increasing values of PI, RI and/or SDR (Trudinger et al. 1985; Giles et al. 1985). UA Doppler indices only start to become elevated when >30% of the fetal villous architecture is abnormal (Morrow et al. 1989). UA EDF is usually maintained until ~60-70% of the villous tree has been obliterated, at which point it becomes absent, then reversed (Wilcox et al. 1989) - see Figure 1.4 and Section 1.1.4.6 below.

Figure 1.4 – Normal and abnormal umbilical artery Doppler waveforms

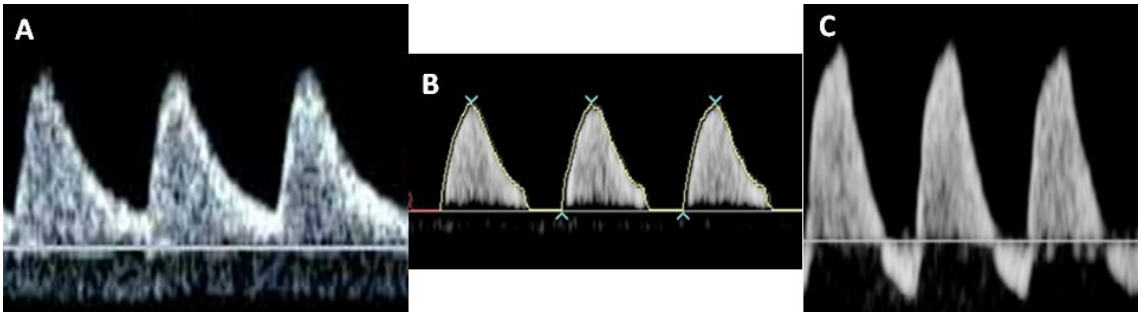

Doppler waveforms of the umbilical artery (UA) taken from human pregnancies complicated by fetal growth restriction. A = normal UA waveform showing positive end-diastolic flow (EDF). B = abnormal UA waveform demonstrating absent EDF. C = abnormal UA waveform featuring reversed EDF.

The placenta in FGR may demonstrate any number of different morphological abnormalities. FGR characterised by UA Doppler abnormalities is associated with reduced placental size with fewer small arteries on histological examination (McCowan et al. 1987; Bracero et al. 1989). Intermediate and terminal villi exhibit a reduced volume and surface area (Jackson et al. 1995) and the exchange barrier may be increased secondary to thickening of the basal lamina, villous

cytotrophoblast hyperplasia and focal degeneration in the vessel wall (van der Veen & Fox 1983; Fok et al. 1990; Macara et al. 1996). Microscopic examination of the placenta in FGR may reveal other contributory microvascular disease processes such as fibrinoid necrosis, atherosis, chronic vasculitis and thrombosis (Salafia 1997).

1.1.3 Consequences of FGR

Faced with a reduced substrate supply, the fetus mounts a number of adaptive responses in order to maximise the limited resources. Unfortunately this initial phase of compensation is frequently followed by relative decompensation leading to tissue damage *in utero*. Moreover some of these adaptive processes, whilst they might improve the chance of fetal survival, are responsible for some of the increased morbidity that is seen in neonatal and later life. A major factor in such adaptation is the degree of hypoxia in the fetus, which is believe to be the main trigger for the cardiovascular redistribution that results in fetal brain sparing and intrauterine programming of cardiovascular dysfunction (Giussani et al. 2012), discussed further in Sections 1.1.3.4 and 1.1.3.8 below. Severely growth-restricted fetuses with evidence of compromise such as abnormal UA Dopplers are frequently hypoxaemic, and this has been demonstrated by umbilical venous blood gas analysis following cordocentesis (Pardi et al. 1993) - see Figure 1.5.

1.1.3.1 Metabolic impact

Attenuated uteroplacental blood flow directly limits the transplacental supply of nutrients to the fetus, resulting in reduced availability of key macronutrients, principally glucose, amino acids and free fatty acids. Fetal nutrient levels are significantly reduced relative to maternal levels, reflecting the elevated maternal-fetal concentration gradients secondary to impaired placental transfer (Hay 2006; Avagliano et al. 2012). Fetal hypoglycaemia has been shown to be directly proportion to the partial pressure of oxygen (pO_2) in mid to late gestation, which reflects the degree of hypoxia (Nicolini et al. 1989). Aiming to reinstate normoglycaemia, fetal pancreatic secretion of glucagon and insulin are increased and decreased, respectively, during the late second and early third trimester (Hubinont et al. 1991). Importantly, the degrees of hypoglycaemia and hypoinsulinaemia during fetal life are often disproportionate, suggesting an element of pancreatic dysfunction (Economides et al. 1991). The proportions of pancreatic insulin-secreting beta-cells have been shown to be decreased in the growth-restricted fetus (van Assche & Aerts 1979), which may contribute to the increased risk of diabetes in later life following FGR (see Section 1.1.3.8). Interestingly in the early stages of fetal hypoxia, relative hyperglycaemia is observed secondary to reduced fetal glucose consumption (Jones et al. 1983) and presumably by increased glucose production via breakdown of glycogen stores and

Figure 1.5 – Evidence of hypoxaemia in severely growth-restricted fetuses

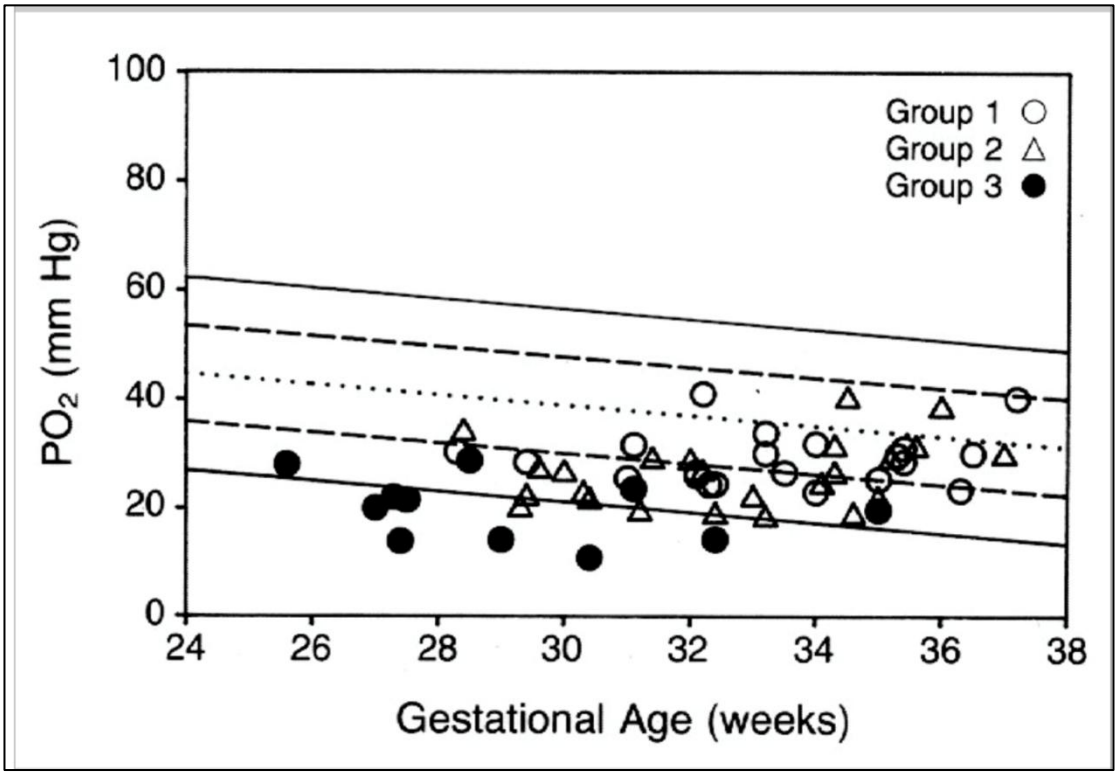

Measurements of venous partial pressure of oxygen (pO_2) in umbilical cord blood obtained via cordocentesis in growth-restricted fetuses with biometric markers (abdominal circumference and head circumference) below the 5th percentile for gestational age. The fetuses were divided into three subgroups: Group 1 fetuses had a normal fetal heart rate (FHR) and umbilical artery (UA) pulsatility indices (PI). Group 2 had a normal FHR but UA PI values more than 2 standard deviations (2SD) above normal. Group 3 had an abnormal FHR and UA PI >2SD above normal. Figure reproduced with permission from Pardi et al. (1993).

---

hepatic gluconeogenesis. However this does not appear to be maintained in the longer term. Fortunately the fetal brain is able to utilise alternative fuels such as ketones and lactate, which confers some degree of protection against the deleterious effects of hypoglycaemia (Vannucci & Vannucci 2000). FGR appears to be associated with impaired glucose tolerance as insulin levels do not change following glucose challenge in severe human FGR (Nicolini et al. 1990).

Amino acid concentrations are similarly reduced in the fetal circulation. Whilst the fetus is able to generate some amino acids through protein breakdown, reduced concentrations of most of the amino acids are apparent in umbilical cord blood (Cetin et al. 1992), particularly those that

are essential (Cetin et al. 1990). Transplacental flux of two essential amino acids, leucine and phenylalanine, has been measured and is attenuated in FGR (Paolini et al. 2001). Whilst placental transfer of essential fatty acids is also reduced, leading to lower circulating levels of linoleic acid and arachidonic acid, there is evidence that growth-restricted fetuses have increased levels of free (non-esterified) fatty acids and triglycerides relative to normally growing fetuses (Economides et al. 1991; Alvino et al. 2008). This is likely to reflect a relatively catabolic state in which fat stores are broken down to provide substrates for fetal metabolism, as an alternative to glucose, and for gluconeogenesis. Free fatty acid levels within the amniotic fluid are also three times higher in FGR pregnancies (Urban & Iwaszkiewicz-Pawlowska 1986). Furthermore umbilical cord blood concentrations of albumin, cholesterol and magnesium are significantly lower at birth following FGR, which is indicative of impaired micronutrient transfer (Nieto-Diaz et al. 1996).

1.1.3.2 Endocrine effects

In addition to the changes in plasma insulin and glucagon levels discussed above in relation to fetal metabolism, FGR has a wide impact upon the maturation and activity of various fetal endocrine pathways. Those alterations in hormone levels that have been demonstrated in human pregnancies complicated by FGR are summarised in Table 1.2. Insulin-like growth factor (IGF-1) and IGF-2 are both down-regulated, whilst the IGF binding proteins (BP) are variably affected: FGR increases IGFBP-1 and 2 and decreases IGFBP-3 (Cianfarani et al. 1998; Street et al. 2006). With respect to thyroid function, growth-restricted fetuses are hypothyroid with low thyroxine (T4) levels in spite of raised thyroid stimulating hormone (TSH) levels. Tri-iodothyronine (T3) levels, however, are unaffected (Thorpe-Beeston et al. 1991). Although plasma renin levels are increased, aldosterone concentrations are not different between FGR and control pregnancies (Ville et al. 1994). FGR activates the hypothalamic-pituitary-adrenal (HPA) axis, thus increasing circulating concentrations of corticotrophin releasing hormone (CRH), adrenocorticotrophic hormone (ACTH) and cortisol. Finally, the observed changes in osteocalcin and 1,25-dihydroxyvitamin D concentrations in FGR are associated with reduced bone mineral density in neonatal life (Namgung et al. 1993). Other fetal parameters which are affected by FGR include the catecholamines, ghrelin, leptin and transforming growth factor-1β (detailed in Table 1.2).

1.1.3.3 Haematological changes

FGR has widespread effects on the circulatory system including redistribution of the cardiac output (see Section 1.1.3.4 below) as well as alterations in the composition of the fetal blood.

Table 1.2 – Effect of FGR on fetal concentrations of various hormones from human studies

Hormone	**Effect of FGR**	**Reference**
Insulin*	↓	Economides et al. 1991
Insulin-like growth factor (IGF)-1	↓	Ostlund et al. 2002
Transforming growth factor (TGF)-1β	↓	
Corticotrophin-releasing hormone (CRH)	↑	Goland et al. 1993
Adrenocorticotrophic hormone (ACTH)	↑	
Cortisol	↑	
Osteocalcin	↓	Verhaeghe et al. 1995
1,24 dihydroxyvitamin D	↓	Namgung et al. 1993
Thyroid stimulating hormone (TSH)*	↑	Thorpe-Beeston & Nicolaides 1993
Total thyroxine (T4)*	↓	
Free thyroxine (T4)*	↓	
Growth hormone	↑	Nieto-Diaz et al. 1996
Renin*	↑	Weiner & Robillard 1988
Adrenaline*	↑	
Noradrenaline*	↑	Greenough et al. 1990
Leptin	↓	Martos-Moreno et al. 2009
Ghrelin	↑	
Insulin-like growth factor (IGF)-2	↓	Smerieri et al. 2011

** Indicates those parameters that were measured during fetal life by means of cordocentesis. All remaining parameters were measured in umbilical cord blood sampled at birth.*

These changes largely occur secondary to a reduction in pH, pO_2 and % oxygen saturation and an increase in the partial pressure of carbon dioxide (pCO_2), bicarbonate and lactate (Weiner & Williamson 1989; Economides et al. 1991). In order to maximise oxygen carriage, erythopoietin secretion and red blood cell production (from both medullary and extramedullary sources) is stimulated, leading to polycythaemia (Snijders et al. 1993b; Maier et al. 1994). Erythroblast and nucleated red blood cell (NRBC) counts are increased and these correlate with the degree of intrauterine hypoxia (Thilaganathan & Nicolaides 1992; Thilaganathan et al. 1994; Bernstein

et al. 1997). In advanced cases, erythopoiesis can become dysfunctional (Stallmach et al. 1998) resulting in anaemia, which is also associated with higher cobalamin and reduced ferritin levels (Abbas et al. 1994). FGR is frequently complicated by thrombocytopaenia (van den Hof & Nicolaides 1990; Baschat et al. 1999), platelet activation and aggregation (Ohshige et al. 1999), increased thrombin concentrations (Trudinger et al. 2003) and increased whole blood viscosity, all of which can predispose to occlusion of small vessels within the placenta and thereby further exacerbate uteroplacental insufficiency.

1.1.3.4 Cardiovascular redistribution

In response to reduced oxygen and metabolic nutrient supply, the fetus adapts by altering the partitioning of blood flow, and thereby substrate delivery, in a way that preferentially supplies the essential organs. Arguably the most important organ of all is the fetal brain. Accordingly, in response to hypoxaemia, the fetal cerebral circulation dilates, reducing the resistance to blood flow and decreasing left ventricular afterload. This becomes apparent on Doppler ultrasound as a reduced PI and increased peak systolic velocity in the middle cerebral artery (Mari & Deter 1992; Mari 2009). At the same time, an opposite effect is occurring in the periphery. The trunk vessels constrict, increasing the peripheral vascular impedance and right ventricular afterload (al-Ghazali et al. 1989). The relative changes in the left and right ventricular outflows results in a greater proportion of the cardiac output being distributed to the fetal head and brain, whilst blood from the descending aorta is preferentially streamed to the placenta for re-oxygenation rather than to the periphery for musculoskeletal growth. The consequence of these alterations in blood flow and nutrient partitioning is a prioritisation of fetal brain growth at the expense of body growth, the so-called "brain sparing effect", which produces an asymmetrical pattern of FGR. Brain sparing can be identified at post-mortem examination by an increased brain to liver weight ratio (Cox & Marton 2009) and on ultrasound by increased biparietal diameter (BPD) to abdominal circumference (AC) ratios. The degree of fetal brain sparing is closely related to the degree of placental vascular resistance (Cheema et al. 2006). In addition to fetal brain sparing, blood flow is also preferentially diverted to the heart and adrenal glands (Baschat et al. 1997; Tekay & Jouppila 2000). This may result in ventricular wall hypertrophy and activation of the hypothalamic-pituitary-adrenal axis, respectively, and is associated with an increase in adrenal secretion of catecholamines (Weiner & Robillard 1988). By contrast, blood flow in the vessels supplying the less essential organs is reduced, for example the pulmonary, mesenteric and renal arteries (Veille & Kanaan 1989; Mari et al. 1995; Rizzo et al. 1996). The latter is associated with oligohydramnios and, whilst the former functions are not required during fetal life, pulmonary and gastrointestinal hypoperfusion can result in respiratory compromise and

susceptibility to necrotising enterocolitis in the neonatal period, respectively. In addition blood flow to the limbs in reduced, classically resulting in a short femur (Papageorghiou et al. 2008).

1.1.3.5 Perinatal mortality

The risk of stillbirth and neonatal death is largely dependent on the cause of FGR and its onset and severity. Published studies imply an overall five- to ten-fold increase in perinatal mortality (McIntire et al. 1999; Lackman et al. 2001). However this thesis is primarily concerned with the particular problem of early-onset severe FGR secondary to uteroplacental insufficiency, which is especially challenging to manage clinically (see Section 1.1.4) and is associated with very poor perinatal outcomes indeed. A recent retrospective analysis of cases characterised by an AC or EFW below the 5th centile and either abnormal UA Dopplers or reduced growth velocity which were referred to the Fetal Medicine Unit at University College London Hospital over a 12 year period (2000 to 2012) found that, of a total of 78 pregnancies that were chromosomally and structurally normal, 31 (40%) resulted in miscarriage, intrauterine fetal death or stillbirth, and the remaining 47 (60%) required delivery for fetal indications prior to 32 weeks gestation (DJ Carr, unpublished data). It has been shown that the chance of fetal survival is dependent upon the gestational age and the estimated fetal weight (EFW) on ultrasound (Baschat 2004). Viability is considered to have been achieved when the pregnancy reaches 24 completed weeks gestation and EFW is >500g. However it is the gestational age that it the most important independent predictor of neonatal survival and, perhaps more importantly, intact survival without disability (Baschat et al. 2007). For example, an increase in gestational age at delivery from 25 to 26 weeks is associated with a doubling (approximately) of intact survival (see Figure 1.6). It is also important to note, that in addition to the mortality from antenatally diagnosed FGR, many cases go undetected and can later result in an otherwise "unexplained" stillbirth (Cousens et al. 2011). Prenatally detected cases may therefore represent the tip of the iceberg.

1.1.3.6 Neonatal morbidity

Survivors of severe FGR are at increased risk of a wide range of medical complications during the neonatal period, which often relates to one or more of the following: (a) the effects of the intrauterine starvation *per se*; (b) the potentially adverse side-effects of adaptive mechanisms designed to promote growth of important organs such as the brain at the expense of others such as the lung and bowel; and (c) iatrogenic prematurity, if early delivery has been indicated because of concerns that continuing the pregnancy is likely to result in fetal demise. Growth-restricted and/or premature babies are at a particularly high risk of hypothermia as they tend to be long and skinny with a low ponderal index (Doctor et al. 2001). Consequently they have a

Figure 1.6 – Survival of placentally growth-restricted neonates born before 32 weeks gestation

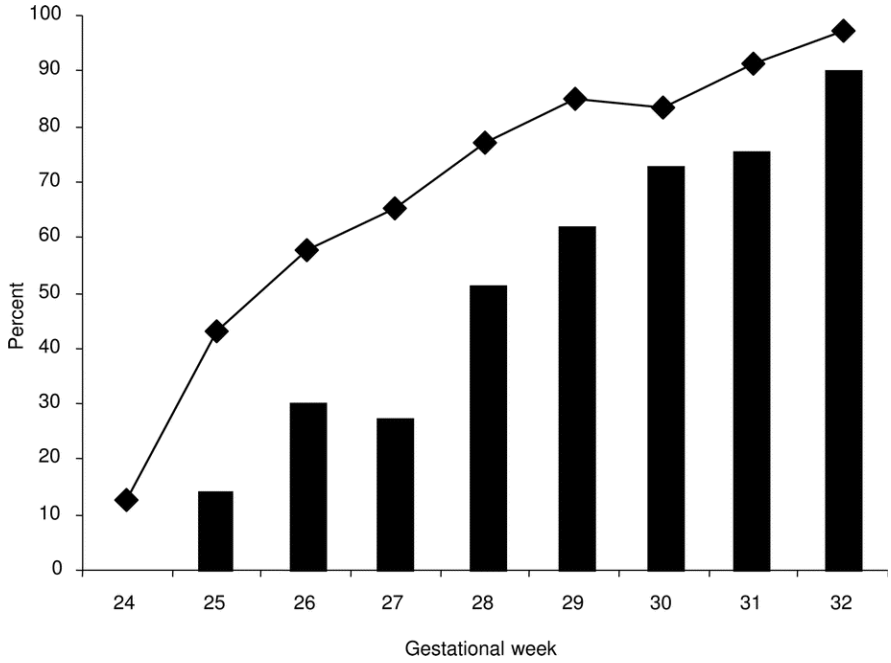

Total survival (black diamonds) and intact survival rates (black bars) until discharge in growth restricted neonates by gestational age. Reproduced with permission from Baschat et al. (2007).

---

large body surface area relative to their size through which they rapidly lose heat. They also usually have greatly reduced body fat stores secondary to *in utero* malnutrition, such that their ability to generate heat via non-shivering thermogenesis is reduced. It is particularly important to avoid hypothermia as it exacerbates other complications such as hypoglycaemia. Growth-restricted neonates tend to remain hypoglycaemic following delivery, which *vice versa* can exacerbate hypothermia, resulting in a vicious cycle. Prematurity is associated with feeding difficulties (due to an absent or weak suck reflex) and these neonates often require tube feeding or parenteral nutrition. However care must be taken when feeding not to overload the gut in view of the risk of necrotising enterocolitis, a potentially life-threatening complication associated with impaired intestinal vascular development (Aucott et al. 2004). Polycythaemia, although of benefit to the fetus by maximising oxygen delivery to the tissues, greatly increases the risk of neonatal jaundice as the excess red cell mass is broken down. If not managed vigilantly with phototherapy it can lead to bilirubin-induced brain damage (kernicterus). Growth-restricted neonates are also at risk of intraventricular haemorrhage (Simchen et al. 2000), which is a further mechanism through which an adverse neurological outcome may result. FGR is associated wtih bronchopulmonary dysplasia and respiratory distress syndrome

(Tyson et al. 1995) and increases susceptibility to infection partly through impaired immunity, which is in turn reflected by reduced immunoglobulin G concentrations, phagocytic indices and neutrophil counts (Chandra & Matsumura 1979).

1.1.3.7 Impact on child health

Prenatally growth-restricted individuals who survive through the neonatal period also have an increased risk of ill health during childhood and beyond. The problems seen with respiratory adaptation to extra-uterine life following FGR, which may require prolonged oxygen therapy ± ventilatory support, confer an increased risk of chronic lung disease (Regev et al. 2003). Lung function is worse in preterm growth-restricted babies compared with preterm AGA babies when measured around 8 years of age (Morsing et al. 2012) and FGR is also associated with an increased risk of asthma (Henderson & Warner 2012). Adverse effects on cardiovascular health are also apparent relatively early following FGR, reflected by smaller aortic dimensions and increased resting heart rate in adolescents (Brodszki et al. 2005). These changes probably contribute to the adverse cardiovascular risk profile observed in adult life (see Section 1.1.3.8). Of particular concern is the risk of poor neurodevelopmental outcome following FGR. At 5 to 8 years of age, cognitive function is reduced following FGR and is notably poorer amongst boys (Morsing et al. 2011). Within the brain, it has been shown that FGR reduces grey matter, white matter and hippocampal volumes (Lodygensky et al. 2008) and adversely affects complexity of the cortex (Tolsa et al. 2004). The latter is associated with immature behavioural scores and an attention deficit. Poorer neurological outcomes appear to be particularly prevalent following severe early-onset FGR, where rates of up to 53% have been reported (Baschat et al. 2007). The risk of cerebral palsy with a birth weight below the 10th percentile is increased six-fold (Jarvis et al. 2003) and prevalence following FGR is reported to be ~22% (Spinillo et al. 2006). Prenatally growth-restricted children also show an increased rate of visual problems at 4 years of age (Matilainen et al. 1987) and FGR is associated with hearing deficits (Baschat et al. 2009) and increased rates of childhood obesity by the age of nine (Chakraborty et al. 2007).

1.1.3.8 Impact on adult health

In the longer term, survivors of FGR are at an increased risk of adult-onset cardiovascular and metabolic disease - coronary artery disease, stroke, hypertension and type 2 diabetes mellitus (Barker et al. 1993; Barker 2006; Ross & Beall 2008). The process by which prenatal exposures can impact on health and disease in later life is known as "intrauterine programming" and has given rise to a rapidly expanding research field - Developmental Origins of Health and Disease (DoHaD). The developmental origins hypothesis proposes that early life nutrition (during the

fetal and neonatal period and infancy) leads to alterations in gene expression that set baseline metabolic function and influence vulnerability to later life exposures.

A number of different epidemiological studies have illustrated the link between birth weight and adult disease. A cohort study of 10,636 men born in Hertfordshire between 1911 and 1930 revealed that the prevalence of adult-onset diabetes and impaired glucose tolerance showed a bimodal peak, being highest in those who were LBW or macrosomic at birth (Hales et al. 1991). The risk of coronary heart disease fell in a stepwise pattern with increased birth weight. There was also a strong relationship between infant weight at one year of age and impaired glucose tolerance. A similar trend was seen in women between glucose tolerance and birth weight but not infant weight, suggesting that men are at greater risk from prenatal nutritional insults. These findings have since been reproduced in several hundred studies worldwide in various different populations and ethnicities - see Barker (2006) for a summary. Some of these studies have specifically assessed confounding by collecting data on lifestyle. For example, the US Nurses' Health Study found that controlling factors such as smoking, alcohol intake, exercise and employment status did not significantly distort the relationship between birth weight and adult-onset diseases (Rich-Edwards et al. 1997). Nevertheless, it is clear that adult lifestyle factors are additive and further increase LBW-related cardiovascular risk. For example, impaired glucose tolerance is greatest amongst individuals born SGA who become obese in later life (McCance et al. 1994). It is also possible that survivors of FGR are more susceptible to the negative impact of various environmental exposures. For example, men who had a high ponderal index at birth suggestive of FGR demonstrate an association between low income and coronary heart disease that is not apparent in men who had an appropriate-for-gestational-age birth weight (Barker et al. 2001). Adults born SGA also demonstrate elevated serum cortisol concentrations in response to stress (Phillips et al. 2000).

Another good illustration of the importance of fetal nutrient supply on adult health was the natural experiment of the Dutch Hunger Winter, which was a period of famine in a German-occupied region of the Netherlands in 1944, shortly before the end of World War II. During the period food rationing was in place, average energy intake was reduced to as little as 400-800 calories per day (Schulz 2010). Late gestational exposure reduced mean birth weight by only approximately ~240g compared to non-exposed controls, a modest perturbation, however the impact of prenatal famine exposure on adult health was considerable - see Painter et al. (2005) for an overview. The specific risks varied with the timing of exposure. Individuals prenatally exposed to famine in early gestation had a greater incidence of coronary heart disease, hyperlipidaemia, clotting disorders, and obesity. Exposure in mid-gestation conferred an

increased risk of obstructive lung disease and microalbuminuria and those exposed in late gestation had reduced glucose tolerance. This suggests that there exist "windows" during which the development of specific fetal organs is vulnerable to nutritional insults. More recent data from this cohort has also shown accelerated cognitive ageing in those exposed to famine in early gestation (de Rooij et al. 2010).

A number of different mechanisms have been proposed to explain these programming effects including epigenetic changes (DNA methylation, histone modifications and microRNAs), which are discussed in detail in Chapter 6. Epigenetic modifications can lead to potentially permanent alterations in gene function in the absence of changes in the genomic DNA sequence through differential effects on gene transcription. In the Dutch Hunger Winter cohort, those exposed to famine in early gestation demonstrated permanent alterations in the methylation status of the IGF-2 gene (Heijmans et al. 2008). Other possible contributors include structural alterations in various organs and tissues as a consequence of compromised fetal growth *in utero*. For example it is known that FGR reduces the number of glomeruli in the kidney at birth and that this may at least partially explain the increased risk of hypertension (Brenner & Chertow 1993). As already mentioned, there is also a reduction in pancreatic beta-cell mass which contributes to an insulin-resistant phenotype. It may well be beneficial during intrauterine life for a fetus to develop relative insulin resistance in an attempt to maintain circulating glucose levels. However in postnatal life, when nutrient supply is often restored, this may lead to a diabetic phenotype (Phillips 1996). It is apparent that a relative mismatch between the prenatal and postnatal environments is a particular risk factor for the development of an adverse metabolic profile in later life (Hanson & Gluckman 2011). Children born small who show catch up growth in the early years (particularly between 4 and 8 years of age) with upward centile crossing are at greatest risk of insulin resistance and cardiovascular disease (Bavdekar et al. 1999) and lack of catch up growth is associated with a reduced risk of disease (Hofman et al. 1997). In the developing world greater risks are associated with moves towards greater nutrient availability in postnatal life e.g. rural to urban migration, adoption and elevated social status (Yajnik 2004).

1.1.3.9 Financial implications

In addition to the biomedical, psychological and social impact of FGR, the economic burden is huge. As well as the longer term child and adult health implications discussed above, the cost of prolonged neonatal intensive care provision when early delivery is indicated is considerable. One recent estimation of the overall cost to society of preterm birth in the England and Wales in 2006 was almost £3 billion, with individual costs per survivor as high as £225,000 for those born at 24 weeks gestation (Mangham et al. 2009). FGR contributes a significant proportion of

preterm birth, particularly of the iatrogenic type. The cost of neonatal care is inversely related to birth weight, which reflects fetal growth as well as the gestational age at delivery. Table 1.3 illustrates the average cost of the hospital stay per neonate, stratified by birth weight category and presented separately for term versus preterm birth, recorded annually across a five-year period at a single tertiary level hospital in the UK. It can be seen that the cost for a baby born weighing less than 1000g is more than double that of a baby born weighing 1000-1499g. This suggests that relatively modest increases in fetal growth might have a major financial impact. In the longer term when FGR is associated with neurosensory disability, individual healthcare costs may exceed £50,000 per annum (Petrou et al. 2006). When the increased health burden of adult-onset diseases is also considered, the financial impact over a lifetime is immeasurable.

1.1.4 Management of FGR

1.1.4.1 Prevention

Preventive strategies are mainly aimed at women with a previous history of FGR or its known risk factors. The overall recurrence rate of FGR is approximately 20% (Patterson et al. 1986), although this can vary dramatically depending on the underlying cause. Short inter-pregnancy intervals are associated with 30% incidence of SGA and 40% incidence of LBW, and the optimal time period between the previous pregnancy and subsequent conception appears to be 18 to 24 months (Zhu et al. 1999). A Cochrane review including 56 randomised controlled trials and nine cluster randomised trials of various interventions to promote smoking cessation during pregnancy found that stopping smoking reduced the incidence of low birth weight by 17% and increased mean birthweight by 54g (Lumley et al. 2009). Furthermore a diet rich in leafy green vegetables prior to pregnancy has been shown to reduce the risk of SGA by 56% (McCowan et al. 2010). Treatment of mild or moderate hypertension with pharmacological agents does not reduce the incidence of SGA (Abalos et al. 2007) and may precipitate a fall in placental perfusion. This is an important consideration in the management of both pre-existing and gestational hypertension, in which the target blood pressure should be around 140/90 to avoid acute fetal compromise. However it is important to avoid sustained elevations in systolic and diastolic blood pressure (>160 and >110 mmHg, respectively) to avoid maternal haemorrhagic stroke (Cantwell et al. 2011). Anti-platelet agents such as aspirin also have a role in the prevention of recurrence of FGR. The latest Cochrane review of 59 randomised controlled trials (n=37,560 women) and an individual patient data-analysis found a reduction in SGA of 10–11% (Askie et al. 2007; Duley et al. 2007). Aspirin is also used in clinical practice for the prevention of pre-eclampsia, a related placental disorder that is characterised by gestational hypertension and proteinuria and shares the same underlying pathogenesis as uteroplacental FGR. It

Table 1.3 – Costs of neonatal care provision associated with low birth weight (<2500g) according to birth weight category and gestational age at delivery

AVERAGE COST UNTIL DISCHARGE FROM HOSPITAL (£)											
Year	**All ≤2500g**	**Term ≤2500g**	**Term 2000- 2499g**	**Term 1500- 1999g**	**Term 1000-1499g**	**All Preterm ≤2500g**	**Preterm 2000- 2500g**	**Preterm 1500-1999g**	**Preterm 1000-1499g**	**Preterm 500-999g**	**Preterm <500g**
2008	13074	2620	2674	1574	5622	14634	3828	8215	15596	34754	52452
2007	12861	2022	2087	1660		13948	4396	7337	14142	33529	
2006	13991	3158	3001	3863		15068	4750	8248	22217	35909	
2005	15236	2420	2446	2378		16731	4605	9409	21036	49524	24055
2004	16896	3329	3081	4199		18094	4162	8346	213599	43688	36418
5-Yr Ave	**14411**	**2709**	**2659**	**2735**	**5622**	**15734**	**4348**	**8310**	**18871**	**39494**	**37640**

Immediate costs of neonatal care until hospital discharge for preterm babies according to birth weight, based on data from a single large NHS university hospital in central England. Over the five year period shown (2004-2008), the average length of stay at each level of neonatal care (intensive care, high dependency care, transitional care or postnatal ward) was calculated for each baby and then stratified according to year, birthweight and gestational age at delivery: term = >37 weeks of gestation; preterm = <37 weeks gestation. Table reproduced with permission from Morris et al. (2010).

been shown that aspirin must be started before 16 weeks to be effective for this indication (Bujold et al. 2010) and the same is probably true for FGR. Unfortunately the latter is usually diagnosed in the mid second trimester (early onset) or during the third trimester (late onset), which is simply too late for aspirin to be effective.

1.1.4.2 Prediction

When pregnant women attend for their booking visit, which should ideally be before 10 weeks gestation (NICE 2008), a full obstetric and medical history is taken along with measurements of height and weight, used to calculate the body mass index (BMI), and blood pressure. At this point a number of risk factors or pre-existing maternal conditions may be identified that confer an increased risk of FGR (detailed above in Table 1.1). Previous obstetric history is particularly relevant. Having previously had an SGA infant increases the risk four-fold (Wolfe et al. 1987), and this risk is further elevated after two or more previous SGA babies (Kleijer et al. 2005). A baseline risk assessment is important given that routine antenatal care in the UK for "low risk" women includes only two ultrasound scans, for pregnancy dating and fetal anomaly screening at 10–14 and 18–22 weeks, respectively. This model of antenatal care is justifiable as routine ultrasound during the third trimester does not improve maternal or perinatal outcome in an unselected or low-risk population (Bricker et al. 2008).

It is currently recommended that women with one or more of the following *major* risk factors for SGA/FGR (odds ratio for SGA >2.0 from published studies) at booking should undergo serial ultrasound assessment of fetal growth in the third trimester (RCOG 2013):

- Maternal age >40 years
- Smoker >10 cigarettes per day
- Cocaine use
- Daily vigorous exercise
- Previous SGA
- Previous stillbirth
- Maternal or paternal SGA
- Chronic hypertension
- Diabetes and vascular disease
- Renal impairment
- Antiphospholipid syndrome

Women who have three or more *minor* risk factors (remainder of those detailed in Table 1.1)

should undergo further screening with UtA Doppler ultrasound at 20 to 24 weeks gestation. As discussed in Section 1.1.2.3, UtA Doppler waveforms are a reflection of downstream resistance to blood flow in the maternal placental circulation. Persistence of an early diastolic notch or low end-diastolic velocity (which are characteristic features of the non-pregnant and first trimester waveforms) after 24 weeks of gestation indicate impaired adaptation, which is associated with inadequate trophoblast invasion of the spiral arteries (Kirkegaard et al. 2011). UtA Doppler can be performed earlier, as abnormalities between 10 and 14 weeks gestation are also associated with impaired trophoblast invasion (Lin et al. 1995) and a large prospective observational study (FASTER) performed in this gestational age range demonstrated that a UtA RI value above the 75th percentile was associated with a 5.5-fold increase in the risk of FGR (Dugoff et al. 2005). However despite a relatively high specificity (91–96%) and negative predictive value (91–99%), the sensitivity of UtA Doppler at this stage of gestation is very poor (12–25%), limiting its use as a screening test (Prefumo et al. 2004). Routine UtA Doppler in the second trimester shows no maternal or fetal benefit and is therefore not warranted (Ghi et al. 2010). However for women at increased risk of SGA/FGR, UtA Doppler screening has a greater predictive value when performed in the early second trimester (Chan et al. 1995). Women who have a high UtA PI (± notching) at this stage have a ~14-fold increased risk of FGR (Cnossen et al. 2008) and should therefore be offered growth scans from 26–28 weeks gestation, as per those with a major risk factor (RCOG 2013).

In recent years, much effort has been directed at developing serum screening tests for FGR. A variety of different biomarkers have been evaluated including markers of angiogenesis (such as placental growth factor (PlGF), soluble fms-like tyrosine kinase 1 (sFlt-1), soluble endoglin, vascular endothelial growth factor (VEGF) and angiopoietin) and markers of endothelial dysfunction and oxidative stress (such as soluble vascular cell adhesion molecule-1, soluble intercellular adhesion molecule-1, pentraxin 3 and homocysteine). A recent systematic review and meta-analysis of 53 studies of 37 different biomarkers in a total of 39,974 women concluded that no marker is sufficiently accurate for clinical use (Conde-Agudelo et al. 2013). Nevertheless it is recognised that low maternal serum levels of pregnancy-associated plasma protein A (PAPP-A), defined as less than 0.415 multiples of the median (MoM) for gestational age, during the first trimester confers a two- to three-fold increase in the risk of uteroplacental FGR (Gagnon et al. 2008). Consequently women with low PAPP-A levels picked up through the Down's syndrome screening programme, in which PAPP-A is used as a serum marker, should have regular fetal growth scans during the third trimester. However, despite this association, PAPP-A is not suitable as a routine screening test for FGR. Currently all pregnant women routinely have regular abdominal measurements of the symphysio-fundal height (SFD) at each

antenatal visit from 24 weeks gestation onwards. This also represents a form of screening for fetal growth disorders, although the sensitivity of SFD to detect an SGA pregnancy has been reported to be as low as 27% (Persson et al. 1986).

1.1.4.3 Diagnosis

The initial suspicion of FGR is usually raised when an SGA fetus is diagnosed antenatally on ultrasound examination. In the UK, SGA has been defined by the Royal College of Obstetricians and Gynaecologists (RCOG) as a fetal abdominal circumference (AC) or estimated fetal weight (EFW) value below the 10th percentile for gestational age. SGA is "severe" if the AC/EFW plot below the 3rd centile (RCOG 2013). Fetal weight can be estimated ultrasonographically using one of many published regression equations (Hoopmann et al. 2010), although this approach is subject to various methodological and analytical flaws. It is well recognised that there is a significant margin of error with respect to ultrasound derived EFW, particularly at the extremes of fetal weight, i.e. in FGR and fetal macrosomia, which is variably defined as a birth weight greater than the 90th percentile for gestational age, or >4.5kg or >4kg irrespective of gestational age (Platz & Newman 2008). Customised fetal growth charts are available which incorporate various maternal factors (e.g, maternal height and weight in early pregnancy, parity and ethnicity) to take the estimated intrinsic fetal growth potential into account, and these may improve the sensitivity to detect a genuinely SGA fetus (Gardosi et al. 1992) and/or growth-restricted fetus (de Jong et al. 1998). Fetuses that are found to be SGA are considered more likely to be truly growth-restricted if they additionally show evidence of fetal compromise, which usually comprises one or more of the following findings: (a) reduced longitudinal growth velocity; (b) abnormal UA Dopplers; or (c) abnormal amniotic fluid volume. Longitudinal fetal growth velocity can be measured by repeating measurements of AC and/or EFW at 2–3 week intervals. In addition the pattern of growth (symmetrical versus asymmetrical) can be determined by additionally comparing head and long bone growth by measurement of biparietal diameter (BPD), head circumference (HC) and femur length (FL). Normative growth charts are available for all these parameters (Chitty et al. 1994a; Chitty et al. 1994b; Chitty et al. 1994c) and measurements that are found to be crossing centiles are indicative of restricted growth (see Figure 1.7). By contrast, a fetus that is SGA but growing parallel to the centile lines with normal UA Dopplers and amniotic fluid indices is much more likely to be constitutionally small (see Section 1.1.1).

1.1.4.4 Investigation

Once a fetus is suspected to be growth-restricted, a number of investigations are normally

Figure 1.7 – Ultrasound growth chart demonstrating EFW trajectory in severe early-onset FGR

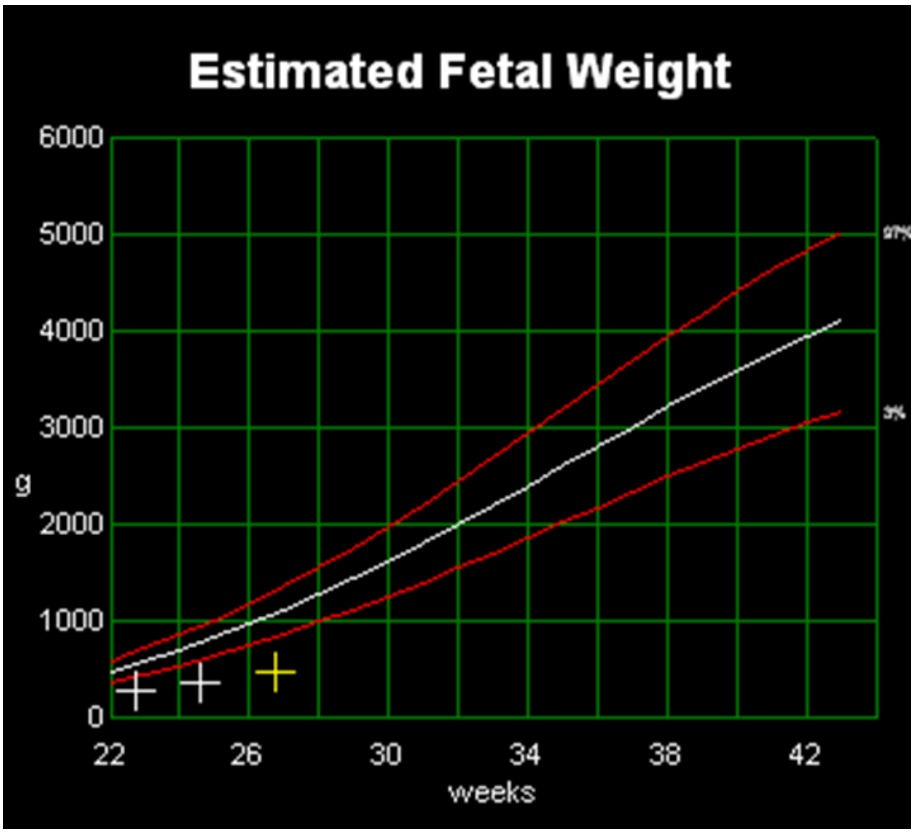

Example of centile chart used for the longitudinal assessment of fetal growth. Ultrasonographic estimated fetal weight (EFW) is shown on the y axis and gestational age in weeks on the x axis. The white line represents the 50th percentile and the upper and lower red lines represent the 97th and 3rd percentiles, respectively. The symbols indicate the growth trajectory of an individual severely growth-restricted fetus, whose EFW is consistently below the 3rd percentile and tailing off (reduced growth velocity) before a viable weight (>500g) has been achieved.

---

considered in view of the many potential fetal and maternal causes that need to be ruled out (see Sections 1.1.2.1 and 1.1.2.2). Maternal factors are identified through history taking and clinical examination. In order to identify anomalous fetuses, a detailed ultrasound examination is performed to look for structural abnormalities and markers of aneuploidy. Uteroplacental blood flow and Doppler waveforms are interrogated to determine if there is any evidence of uteroplacental insufficiency (see Section 1.1.2.3). If there is any ultrasonographic evidence of a chromosomal abnormality then a fetal karyotype will be offered (amniocentesis or chorionic villus sampling). Karyotyping may be offered routinely in severe early-onset cases of SGA/FGR, in which the prevalence of chromosomal abnormality is up to 20% (Anandakumar et al. 1996;

Niknafs & Sibbald 2001). Hyperechogenic bowel should specifically be examined for, as it is more prevalent in FGR and its presence confers an almost ten-fold increased risk of perinatal mortality (Goetzinger et al. 2011). If there is a pattern suggestive of any particular genetic syndrome then an opinion from a clinical geneticist might be sought and targeted genetic testing (if available) may be indicated. A TORCH screen (see Section 1.1.2.1 above) should also be performed to exclude maternal viral infections.

1.1.4.5 Treatment

If a specific maternal medical condition is found then optimisation of treatment is appropriate, although this may or may not benefit fetal growth. For example, treating simple iron deficiency anaemia with ferrous sulphate supplements may improve maternal haemoglobin levels and therefore increase the oxygen carrying capacity of the blood reaching the placenta, however maternal vascular disorders that are known to adversely impact placentation are likely to have already caused irreversible damage to the placental circulation by mid-gestation (Ackerman et al. 1999). If a specific fetal diagnosis is made then the prognosis and management will be dictated by the underlying pathology. Depending on the likelihood of handicap, termination of pregnancy may be offered.

The remainder of this section deals specifically with FGR due to uteroplacental insufficiency, as this is the focus of this PhD thesis. Unfortunately there is currently no effective treatment for this type of FGR (Sibai et al. 2005). A large number of different therapeutic approaches have been evaluated in clinical trials and are detailed in Table 1.4. However none of these therapies have been sufficiently effective to be used in clinical practice. In uteroplacental insufficiency, attenuated UBF ultimately limits the supply of oxygen and nutrients to the developing fetus. In simple terms, fetal nutrient supply is equal to the product of UBF and substrate availability. Consequently there are two basic approaches that can be used to achieve an increase in fetal nutrient supply. Attempts to increase substrate availability by maternal supplementation using various macro- and micro-nutrients have been disappointing and this probably reflects the fact that, with the specific exception of maternal undernutrition, the issue is not generally a lack of availability of these nutrients within the maternal circulation but rather an impairment of placental transfer to the fetal circulation. In support of this hypothesis, it has been shown that balanced nutrient supplementation in women with proven nutritional deficiency reduces SGA, stillbirth and neonatal death rates by 32%, 45% and 38%, respectively, but does not benefit the majority of women (Ota et al. 2012) when applied as a preventive strategy during pregnancy. High protein supplementation of the mother during pregnancy is worryingly associated with increased rates of SGA, prematurity and neonatal death (Rush et al. 1980).

Table 1.4 – Treatments that are ineffective in placentally-mediated fetal growth restriction

Treatment	**Reference**
Bed rest	Crowther et al. 1990
Maternal hyperoxygenation	Nicolaides et al. 1987
Low-dose aspirin*	Leitich et al. 1997
β-adrenergic receptor agonists	Gulmezoglu & Hofmeyr 2001
L-arginine	Winer et al. 2009
Calcium channel blockers	Gulmezoglu & Hofmeyr 2000a
Melatonin and vitamin C	Thakor et al. 2010
Plasma volume expansion	Karsdorp et al. 1992
Transcutaneous electrical nerve stimulation (TENS)	Gulmezoglu & Hofmeyr 2000b
Hormone administration	Say et al. 2003a
Maternal infusion of amino acids	Ronzoni et al. 2002
Salt restriction	Steegers et al. 1991
Iron supplementation	Pena-Rosas et al. 2012
Folate supplementation	Mahomed 2000
Calcium supplementation	Hofmeyr et al. 2010
Vitamin D supplementation	Mahomed & Gulmezoglu 2000
Magnesium supplementation	Makrides et al. 2006
Zinc supplementation	Mori et al. 2012
Fish oil supplementation	Berghella 2007
Diet rich in fish, low-fat meat, grains, fruit and vegetables	Khoury et al. 2005
Maternal glucose supplementation	Viehweg et al. 1987
Maternal carnitine supplementation	Genger et al. 1988
Maternal solcoseryl supplementation	Herre et al. 1976
Balanced energy/protein supplementation	Say et al. 2003b
High protein supplementation	Rush et al. 1980
Isocaloric protein supplementation	Viegas et al. 1982
Multiple micronutrient supplementation	Roberfroid et al. 2008
Maternal nutritional advice	Kafatos et al. 1989
Abdominal decompression	Hofmeyr 2012

** Most likely ineffective if commenced after 16 weeks gestation, i.e. once FGR is diagnosed*

The alternative of direct fetal nutrient supplementation would bypass the problem of placental transfer but is invasive and therefore unlikely to be feasible clinically. This approach has been investigated in various animal models of FGR. Continuous intra-amniotic infusion of dextrose and amino acids in FGR rabbits does not impact fetal growth and lipid administration leads to chronic lipid aspiration and further exacerbates FGR (Flake et al. 1986). Direct intragastric supplementation of amino acids and glucose has also been performed in fetal sheep, which did marginally increase fetal weight but is highly impractical clinically (Charlton & Johengen 1985).

A related treatment that has shown some promise but is unlikely to be translated into clinical practice is intra-amniotic infusion of growth factors. Eremia et al. (2007) showed an increase in fetal weight after IGF-1 was infused directly into the amniotic cavity three times a week (using indwelling catheters) from 100 to 128 days gestation of sheep pregnancy following placental embolisation. The same group more recently evaluated the efficacy of a once weekly injection of IGF-1 in the same model and demonstrated increased fetal growth rates (Wali et al. 2012). A similar approach in the FGR rabbit, by infusion of recombinant human IGF-1, increased serum IGF-1 and placental weight but did not significantly impact fetal weight (Skarsgard et al. 2001). However, an intra-amniotic infusion of epidermal growth factor in FGR rabbits did normalise fetal growth and small intestinal proliferation compared to controls (Cellini et al. 2004). The main drawback of this approach is that, in human pregnancy, invasive procedures are highly likely to result in uterine infection and/or preterm birth if repeated at regular intervals. Consequently the translational potential of these intra-amniotic therapies remains limited. Incidentally, systemic treatment of FGR with growth factors does not look promising. Twice daily injections of growth hormone during late gestation growth-restricted sheep pregnancies modestly increased fetal growth but resulted in profound increases in adiposity (Wallace et al. 2006c) and fetal brain injury (De Boo et al. 2008).

Meanwhile other researchers have investigated the alternative approach of increasing UBF, for example using vasodilator agents such the nitric oxide donor L-arginine (Sieroszewski et al. 2004) or the phosphodiesterase type 5 inhibitor sildenafil citrate (Viagra®). The latter agent is currently being evaluated within a New Zealand based randomised clinical trial called STRIDER (Sildenafil TheRapy In Dismal prognosis Early-onset intrauterine growth Restriction). Results of sildenafil treatment have so far been mixed and have raised a number of doubts and concerns. Sildenafil enhances vasodilatation and reduce vasoconstriction in human myometrial arteries harvested at caesarean section from growth-restricted pregnancies (Wareing et al. 2005) and increases UBF in non-pregnant sheep (Zoma et al. 2004). However, in non-pregnant women, it enhanced UBF when baseline values were normal but not if they were low (Hale et al. 2010),

as would be anticipated in uteroplacental insufficiency. No benefit of sildenafil has been shown in early-onset pre-eclampsia (Samangaya et al. 2009), however a study of 10 pregnancies complicated by severe early-onset FGR showed a significant increase in the fetal AC after oral sildenafil treatment in mid-gestation compared to contemporaneous control pregnancies that were not offered treatment, with a mean interval between eligibity and delivery of 31.5 days (von Dadelszen et al. 2011). There was no effect on any other pregnancy outcomes, although this very small study was clearly underpowered to detect any differences in perinatal mortality or neonatal morbidity. Some concerns were raised by the fact that the most compromised fetus in the study, which (unlike all the others) already showed reversed EDF in the UA at enrolment, died within 48 hours of commencing treatment. Sildenafil citrate crosses the placenta in relatively large amounts and therefore might affect fetal physiological compensation to FGR. In normal and hypoxic rat pregnancies, sildenafil increased fetal weight in the presence of hypoxia, but worryingly reduced fetal weight in non-hypoxic conditions (Refuerzo et al. 2006). The route of delivery appears to be an important consideration. For example, intravenous administration of sildenafil in a sheep model of FGR at 110 to 115 days gestation acutely reduced UBF and impaired fetal oxygenation in both growth-restricted and control fetuses (Miller et al. 2009). Furthermore, in a rat model of Nω-nitro-l-arginine methyl ester induced FGR, sildenafil treatment further reduced fetal growth (Nassar et al. 2012). This illustrates the potential hazard of systemically delivered vasodilators that result in widespread maternal vasodilatation, which can drop maternal blood pressure and further compromise uteroplacental perfusion in an effect called the placental “steal” phenomenon. Satterfield et al. (2010) administered sildenafil subcutaneously three times a day over a longer time period, from 28 to 115 days gestation, to undernourished sheep dams. Although they did not measure UBF in their study, there was an improvement in amino acid availability and fetal weight. Women in the STRIDER trial who are allocated to receive sildenafil treatment will take 50mg orally three times per day from entry until 32 weeks gestation or delivery, whichever is sooner.

1.1.4.6 Surveillance

As there is currently no effective treatment for FGR secondary to uteroplacental insufficiency (see Section 1.1.4.5), contemporary management is comprised of fetal surveillance and timely delivery. With regards to timing, the risks of iatrogenic prematurity must be balanced against the risks of irreversible tissue damage secondary to severe hypoxia or even intrauterine fetal death. Unfortunately it appears that delivering the fetus *per se* does not affect the overall outcomes. The GRIT (Growth Restriction Intervention Trial) study was a clinical trial in which patients were randomised to early versus delayed delivery in cases of FGR in which clinicians

felt uncertainty about the appropriate timing of delivery (GRIT Study Group 2003). There were 196 fetuses enrolled between 24 and 30 weeks, and 352 fetuses between 30 and 36 weeks gestation. The early delivery group were delivered within 48 hours of receiving steroids after a mean interval of 0.9 (range 0.4 to 1.3) days post randomisation. The delayed delivery group were delivered at 4.9 (range 2.0 to 10.8) days post randomisation. There were a greater number of stillbirths in the delayed delivery group and a greater number of neonatal deaths in the early delivery group. Consequently overall perinatal mortality rates were equivalent. Furthermore, at two years of age, death rates, severe disability and neurological outcomes were not different between groups (Thornton et al. 2004). The DIGITAT trial had a similar design to GRIT, but enrolled FGR pregnancies near to term. There were similarly no differences in perinatal mortality rates (Boers et al. 2010), neonatal morbidity (Boers et al. 2012) or neurodevelopmental outcomes at two years of age (van Wyk et al. 2012).

Currently the mainstay of fetal surveillance in FGR is Doppler examination of the umbilical and fetal vessels (Baschat 2010). Although occasional exceptions to the rule occur, there is a relatively predictable sequence of Doppler abnormalities that occur during fetal deterioration in early-onset severe FGR, which may act as a trigger for delivery depending on the gestational age at the time when these emerge (Baschat et al. 2001; Hecher et al. 2001; Ferrazzi et al. 2002). It is currently recommended that UA Doppler waveform analysis should be used as the primary surveillance tool in fetuses with confirmed or suspected FGR as, in the presence of maintained end-diastolic flow (EDF) and the absence of other complications, delivery can generally be delayed until >37 weeks gestation (RCOG 2013). By contrast, absence or reversal of EDF indicates that >70% of the fetal placental circulation is obliterated (Morrow et al. 1989; Wilcox et al. 1989; Kingdom et al. 1997) and pooled data from clinical trials indicate that absent or reversed EDF is associated with a 60-fold increase in perinatal mortality rates (Thornton & Lilford 1993). Meta-analyses of randomised controlled studies of UA Doppler in high risk populations have shown that its use significantly reduces the incidence of intrauterine fetal death (Giles & Bisits 1993; Divon 1995). For example, Alfirevic and Neilson (1995) showed a 38% reduction in perinatal mortality when UA Doppler was utilised for fetal surveillance. When EDF is absent or reversed then additional monitoring and administration of steroids for fetal lung maturation is normally considered. The fetus will generally be delivered if the pregnancy is more than 30–32 weeks gestation (RCOG 2013). Prior to 30 weeks, fetal venous Dopplers are ideally used to decide on timing of delivery (see below).

The middle cerebral artery (MCA) Doppler is a useful adjunct to the UA, and may reveal fetal brain sparing (see Section 1.1.3.4). Under normal circumstances the MCA is characterised by

high impedance to flow with minimal EDF velocities. An increase in EDF velocity is an early sign of fetal hypoxemia (Gudmundsson et al. 1996) and is a sign of redistribution of fetal blood flow in chronic hypoxemia (Wladimiroff et al. 1986; Mari & Deter 1992). The PI of the MCA can also be expressed relative to the UA PI as a cerebro-umbilical Doppler ratio, which increases its ability to predict adverse perinatal outcomes (Gramellini et al. 1992). Notably when EDF is increased in isolation in the MCA, it is not associated with metabolic acidosis (Wladimiroff et al. 1986) or with adverse neurological outcomes (Chan et al. 1996), therefore the MCA is rarely used alone to decide on timing of delivery.

In the presence of UA Doppler abnormalities an additional assessment should be made of the fetal venous system, including the ductus venosus (DV), inferior vena cava (IVC) and umbilical vein (UV). In the advanced stages of fetal decompensation, venous back flow during atrial contraction is seen in the DV (Hecher et al. 1995) and IVC (Rizzo et al. 1995). DV waveform abnormalities in particular are strongly correlated with fetal acidaemia (Baschat et al. 2007; Mari et al. 2007). A pulsatile UV waveform is a particularly ominous sign and may represent fetal congestive heart failure (Gudmundsson et al. 1991; Tulzer et al. 1994). Although there are no specific published guidelines, many obstetricians would recommend delivering fetuses with abnormal DV Dopplers from 26–28 weeks gestation (DM Peebles, personal communication). Currently a multi-centre randomised controlled trial called TRUFFLE (Trial of Umbilical and Fetal Flow in Europe) is underway, which aims to evaluate the use of venous Dopplers to time delivery. Perinatal outcomes are being compared between fetuses delivered on the basis of early versus late venous Doppler changes.

In addition to Doppler evaluation, FGR pregnancies should also ideally undergo assessment of fetal growth velocity (using the AC or EFW) and quantification of amniotic fluid volume, which can be done by measuring either the amniotic fluid index (AFI) or deepest vertical pool (DVP) of amniotic fluid. Reduced amniotic fluid volume reflects reduced perfusion of the fetal kidney as a response to circulatory redistribution (see Section 1.1.3.4). A reduced DVP is associated with increased perinatal mortality (Bastide et al. 1986) and fetal distress (Chauhan et al. 1999). A further means of assessing fetal wellbeing is the use of cardiotocography (CTG). In the UK, it is recommended that computerised analysis of the CTG, which pays particular attention to the short term fetal heart variability, should be used in place of conventional interpretation (RCOG 2013). Computerised CTG has been shown in a Cochrane review to reduce perinatal mortality by 4.2% compared with 1.9% for the traditional CTG (Grivell et al. 2012). In the United States, CTG is often combined with ultrasound assessment of fetal breathing movements, gross body movements, fetal tone and amniotic fluid volume as a "biophysical profile". Evidence suggests

that this test is a poorer predictor of fetal acidaemia with relatively high false negative rates in small fetuses (Kaur et al. 2008) therefore it is not currently recommended. A limitation of all these CTG based tests is that fetal heart rate (FHR) abnormalities do not develop until the later phases of fetal compromise. For example, >60% of fetuses with an abnormal FHR pattern will already be hypoxic and acidotic (Pardi et al. 1993) by this stage. Hence whilst the CTG remains an important tool to pick up fetuses that are already in a critical state, they should not be used in isolation for surveillance.

When delivery is indicated, mode of delivery depends on the gestational age and the likelihood of an individual fetus being able to tolerate labour. If a trial of labour is considered appropriate then continuous electronic fetal monitoring throughout is recommended in view of the high risk of a pathological CTG and possible fetal hypoxia. A skilled neonatal team needs to be present at delivery due to a high risk of neonatal mortality and morbidity (see Section 1.1.3.6).

1.1.5 Animal models of FGR

Given the current lack of effective treatments for FGR, there is an on-going need to use animal models of the condition in preclinical studies aimed at developing new therapeutic approaches for future clinical trials. There are a wide variety of different animal models of FGR available for translational research, however unfortunately none of them is able to completely replicate the pathology that is observed in the human.

The closest model to human pregnancy is the non-human primate. The main advantage is that, unlike many other animals, their pregnancies are characterised by trophoblastic invasion of the spiral arteries as per the human (Blankenship & Enders 2003), and there have been reports of a naturally occurring pre-eclampsia type syndrome (Palmer et al. 1992). Disadvantages include the prohibitively high cost, the high complication rate associated with pregnancy interventions, the lack of facilities in the UK and specific ethical concerns due to their similarity to the human. In the USA, some centres have conducted research into FGR using non-human primate models such as the nutrient-restricted baboon (Li et al. 2013). Alternative large animal models include the sheep (discussed in detail below) and the goat (He et al. 2013).

Small animal models of FGR are used much more frequently. Up until 2001, ~75% of preclinical studies in FGR animal models had been performed in the rat or mouse (Schroeder 2003). In addition to nutritional and surgical models, there are a number of different transgenic models of FGR in the mouse, including placental-specific IGF-2 and eNOS knockout (Hefler et al. 2001; Constancia et al. 2002). The main limitations of rodents are a relatively short gestation period (21 days) and the relative immaturity of the pups at birth, equivalent to the third trimester of

human pregnancy. They are a particularly poor species for studying the neurological impact of prenatal insults and/or therapy, as the majority of brain development occurs in postnatal life. Trophoblast invasion is shallow in rodents and UtA transformation depends more on maternal factors like natural killer cells, than trophoblast invasion (Carter 2007; Greenwood et al. 2000).

1.1.5.1 Sheep models of fetal growth restriction

The sheep has frequently been utilised as a model for human pregnancy and has a wide range of benefits over small animals including the ability to study singleton pregnancies, comparable maternal size, adiposity, maternal to fetal weight ratio and birth weight, similar organogenesis for all major body systems and equivalent rates of fetal protein accretion. Unlike most small animals, the sheep fetus accumulates fat prenatally and is relatively mature at birth. Sheep have a relatively long gestation period (145 to 147 days, depending on the particular genotype) and fetuses can be chronically catheterised for serial assessment of physiological parameters. The relative increase in uteroplacental perfusion that is seen during normal sheep pregnancy is similar to the human, approximately two- to three-fold (Konje et al. 2003; Meschia 1983) and the rates of oxygen and glucose uptake are also similar (Barry & Anthony 2008). Although the human and sheep placenta are similar functionally and much of our understanding of human placental physiology is derived from sheep experiments, there are some important differences in structure and the layers separating maternal and fetal blood (discussed in Section 7.1.1.4). There are a number of different ways of generating FGR in sheep, as summarised in Table 1.5. These sheep models produce variable degrees of fetal growth constraint - 17 to 42% compared to normally grown controls. With the notable exception of maternal undernutrition, the effect on fetal growth appears to be placentally mediated in most of these experimental paradigms, however the associated impact on uterine blood flow is variable. For the work detailed in this thesis, the model of choice was considered to be the one that is characterised by the largest reduction in uterine perfusion, excluding those which involve permanent surgical interference.

1.1.5.2 The overnourished adolescent sheep paradigm

Paradoxically, overnourishing the pregnant adolescent sheep has consistently been shown to result in significant placental and therefore fetal growth restriction, relative to the normally growing fetuses of control ewes fed a moderate intake (Wallace et al. 2006a). High intakes in these overnourished adolescent dams (which are ultimately still growing during pregnancy) result in enhanced maternal growth and nutrient partitioning away from the gravid uterus at the expense of the pregnancy. Elevated peripheral concentrations of glucose, insulin, IGF-1 and thyroid hormones maintain the drive towards maternal tissue deposition (principally

Table 1.5 – Sheep models of fetal growth restriction

Model / Insult	**Effect on fetal weight (days gestation)**	**Effect on placental weight (days gestation)**	**Effect on uterine blood flow (days gestation)**	**Reference(s)**
Overnourished adolescent ewe	↓ 34% (134)	↓ 45% (134)	↓ 42% (88)	Wallace et al. 2002 / 2008b
Undernourished adolescent ewe	↓ 17% (130)	=	=	Luther et al. 2007
Undernourished adult ewe	↓ 16% (140)	=	=	Leury et al. 1990
Multiple pregnancy*	↓ 11% (130)	↓ 63% (130)	↓ 23% (130)	Christenson & Prior 1978
Maternal hyperthermia (from 40 to 120 days gestation)	↓ 42% (134)	↓ 51% (134)	↓ 26% (134)	Regnault et al. 2003
Single umbilical artery ligation (SUAL) (performed at 105-119 days gestation)	↓ 34% (140)	↓ 23–34% (140)	↓ 15% (114)	Oyama et al. 1992 Miller et al. 2009
Uteroplacental embolisation (performed at 104-119 days gestation)	↓ 28% (110)	-	↓ 38–74% (119)	Ochi et al. 1995 Murotsuki et al. 1997
Pre-mating carunclectomy	↓ 32% (114)	↓ 71% (140)	↓ 39–71% (121)	Owens et al. 1986 Phillips et al. 2001
Maternal anaemia	↓ 40% (138)	-	↓ 22–41% (114)	Mostello et al. 1991
Progressive uterine artery occlusion	↓ 39–71% (138)	↓ 27–34% (138)	↓ 30–45% (138)	Lang et al. 2000

* Mean fetal / placental weight and uterine blood flow (UBF) reduced (total fetal / placental weight and uterine blood flow increased - triplets > twins > singletons

adipose tissue) resulting in maternal obesity (Wallace et al. 2000). Despite the abundance of nutrients in the maternal circulation, by late gestation fetal concentrations of glucose, insulin and IGF-1 are significantly reduced and fetuses are hypoxaemic. *In vivo* assessments of glucose and oxygen uptakes have demonstrated that these are reduced in proportion to placental weight (Wallace et al. 2002), which suggests that it is the small size of the placenta *per se* which becomes the major constraint to fetal growth during the final third of gestation.

Whilst these adverse effects of overnutrition are unique to the adolescent, this is nevertheless an excellent model for the study of FGR irrespective of maternal age as it replicates many of the key features of human FGR due to uteroplacental insufficiency. Although the fetal growth trajectory itself is not compromised until relatively late in pregnancy, stigmata of placental dysfunction are evident from as early as day 50 of gestation, at which point various indices of placental vascular development are significantly reduced in overnourished relative to control intake pregnancies (Redmer et al. 2009) At 81 days gestation, placental mRNA expression of several important angiogenic factors (VEGF, angiopoietin 1 and 2, nitric oxidase synthase (NOS)-3) and the VEGF receptor FLT1 is reduced (Redmer et al. 2005) and there is evidence of reduced placental proliferation and possibly increased placental apoptosis (Lea et al. 2005). As illustrated in Figure 1.8, from mid-gestation onwards there is a major (~42%) reduction in UBF (Wallace et al. 2008b) indicating uteroplacental insufficiency, which is similar to that observed in human FGR pregnancies (Section 1.1.2.3). Circulating levels of oestradiol-17β, progesterone and ovine placental lactogen are also reduced, indicating impaired secretory function (Lea et al. 2007; Wallace et al. 2008a). Collectively these observations imply an early insult on uteroplacental development, which precedes the subsequent reduction in placental mass (30–40% lower than controls in late gestation). Maternal switchover studies suggest that it is the second third of gestation in which high nutritional intakes exert their strongest effects on pregnancy outcome in this paradigm. After switching from a high to a control intake from 50 days gestation there is relatively normal fetal and placental growth. By contrast, switching from a control intake to a high intake at the same stage produces a degree of FGR similar to that of continuously overnourished ewes (Wallace et al. 1999). Furthermore, switching from a high to a low intake from 90 days gestation onwards also results in a similar degree of FGR as continuously overnourished ewes, indicating that fetal growth cannot be “rescued” once placental growth has been perturbed (Redmer et al. 2012).

This model utilises embryo transfer techniques to establish singleton pregnancies and thereby avoids multiple gestations. Embryos are sourced from multiparous donor ewes, as these have an inherently higher viability than those derived from adolescents (Quirke & Hanrahan 1977;

Figure 1.8 – Uterine blood flow in overnourished versus control-fed pregnant adolescent ewes from 88 to 135 days gestation

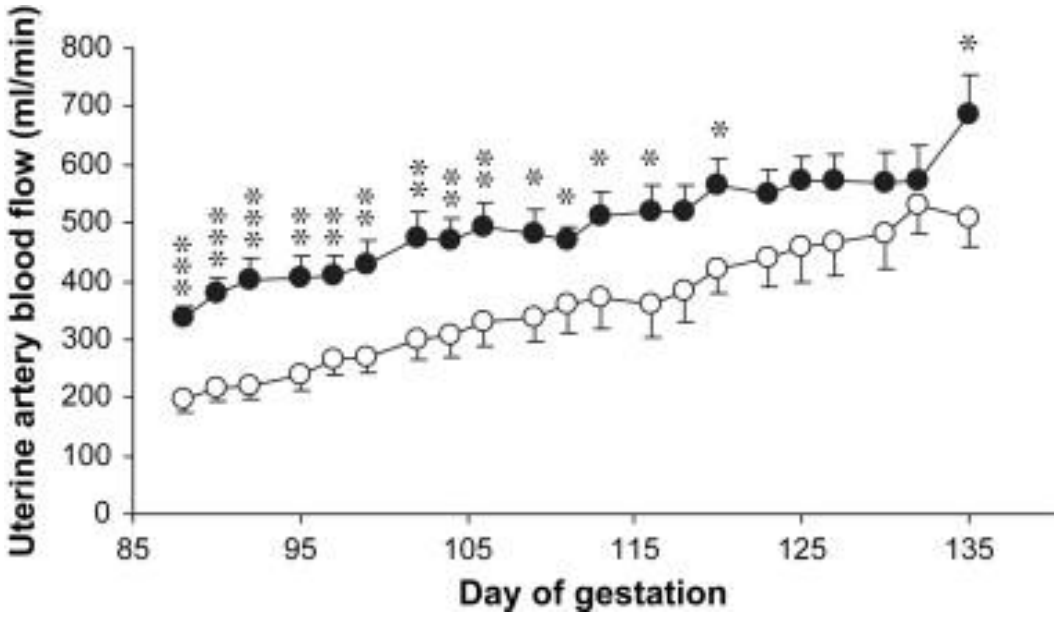

*Average uterine blood flow recorded for 2 hours 3 times per week, measured using indwelling ultrasonic flow probes from 88 to 135 days gestation in singleton-bearing adolescent ewes fed a control-intake (n=9, closed circles) to promote normal placental and thereby fetal growth, or overnourished (n=10, open circles) to induce fetal growth restriction. All data are mean ± SEM. *** p<0.001, ** p<0.01, * p<0.05. Reproduced with permission from Wallace et al. (2008b).*

McMillan & McDonald 1985). The superovulated donor ewes undergo laparoscopic intrauterine insemination because this ensures 100% fertilisation, unlike cervical insemination where only 36% of recovered oocytes are fertilised (Robinson et al. 1969). Thus intrauterine insemination maximises the number of high grade embryos recovered per ewe and these embryos are then transferred in singleton into oestrus synchronised adolescent recipients. Donor superovulation and the use of a single sire maximises the genetic homogeneity of the resultant pregnancies. Precise gestational age is known, which avoids the need to rely on estimated dates of conception and ultrasound pregnancy dating following mating. Following embryo transfer, recipients of equivalent age are evenly allocated to high or control intakes on the basis of baseline body weight, adiposity and ovulation rate, thus controlling for many of the periconceptual factors known to influence fetal and placental growth. A further advantage of this model is that it does not require any surgical interference in order to reduce UBF. The uterine and umbilical circulations remain intact, thus there remains the potential to target UBF

therapeutically. Moreover, fetuses exhibit normal fetal weight-specific metabolic responses to short-term experimental increases in glucose, implying that they can respond favourably to enhanced nutrient supply (Wallace et al. 2007).

1.2 Prenatal Ad.VEGF gene therapy

Over the course of the last eight years, the research group at UCL have been developing a novel maternal gene therapy approach to locally transfect the uteroplacental circulation, with the aim of enhancing UBF and thereby fetal nutrient supply. The potential to locally target UBF and therefore avoid systemic vasodilatation and placental steal (as discussed above) is a significant benefit of this therapy. Clinical grade adenoviruses encoding the human gene for vascular endothelial growth factor (VEGF) are available and have already been used in a number of clinical trials in the field of cardiovascular biology and medicine, which are outlined in Table 1.6. In adult patients, this therapy appears safe. Unfortunately successful therapeutic angiogenesis in ageing, diseased vessels has been limited to date (Zachary & Morgan 2011) but the uterine artery of young, otherwise healthy women may represent a more promising target.

Table 1.6 – Adult clinical trials of adenoviral vascular endothelial growth factor gene therapy

VEGF Isoform	**Indication**	**Route of Administration**	**Reference(s)**
VEGF-A_{165}	Peripheral arterial disease (following percutaneous transluminal angioplasty)	Intra-arterial	Makinen et al. 2002
VEGF-A_{165}	Coronary artery disease (following percutaneous coronary intervention)	Intra-arterial	Hedman et al. 2003
VEGF-A_{121}	Peripheral arterial disease	Intramuscular	Rajagopalan et al. 2003
VEGF-A_{121}	Coronary artery disease (± coronary artery bypass graft, CABG)	Intramyocardial (after CABG or via mini-thoracotomy	Rosengart et al. 1999 Stewart et al. 2006
VEGF-A_{121}	Coronary artery disease	Transendocardial (via catheterisation)	Kastrup et al. 2011

Abbreviations: VEGF = vascular endothelial growth factor; CABG = coronary artery bypass graft

1.2.1 Adenoviral vectors

Gene therapy involves the use of delivery systems called vectors to administer genetic material into cells for potential therapeutic benefit. There are a number of different delivery systems available, which are broadly categorised as viral or non-viral in nature. Different viral species can be adapted including retroviruses, lentiviruses, adenoviruses and adenovirus-associated viruses. For most gene therapy applications, an integrating vector is desirable as the typical aim is to permanently correct or to replace the function of genes that are mutated or missing, respectively. Examples include cystic fibrosis and glycogen storage disorders (David & Waddington 2012). One of the main barriers to long term gene therapy using viruses is the host immune response, which may be pre-existing or develop *de novo*. One of the potential benefits of fetal gene therapy is that treatment can be given at a time when the immune system is relatively immature. Non-viral vectors are much less widely used and are specifically engineered for their purpose. An example might be ORMOSIL (organically modified silica) nanoparticles, which have been successfully used for gene transfer of GFP (green fluorescent protein) to the mouse brain (Bharali et al. 2005).

In the experiments described in this thesis, clinical grade adenovirus vectors were used. The adenovirus is a non-enveloped icosahedral particle that measures approximately 70-90nm in diameter, with an outer protein shell and an inner nucleoprotein core. Adenoviruses are not ideal for most gene therapy applications due to their transient expression (up to a few weeks), however for this particular programme of work the adenovirus was considered to be ideal for this very reason (see Section 1.2.3 below). Adenoviruses provide highly efficient gene transfer without being permanently integrated into the host's genome, hence insertional mutagenesis is avoided. Adenovirus infection *per se* appears to be safe in pregnancy. The virus causes the common cold in humans, which is not generally regarded as problematic during pregnancy. Even when adenovirus has been detected in amniotic fluid samples, suggesting transplacental fetal infection, there is no associated increase in pregnancy loss rates (Wenstrom et al. 1998). In any case the adenoviral vectors used in the studies detailed herein had been rendered first generation replication deficient by complete and partial deletions of the E1 and E3 regions, respectively. The E1 region was replaced by the transgene, VEGF.

1.2.2 Vascular endothelial growth factor

VEGF is a naturally occurring homodimeric glycoprotein that is important for the formation of new blood vessels during embryonic development (vasculogenesis) and the sprouting of new vessels from existing vessels (angiogenesis). The latter serves to increase vascular density and

is important in the development of collateral circulations and revascularisation following injury or ischaemia. There are currently six different members of the VEGF family, designated A to F, with the original VEGF protein now known as VEGF-A. VEGF-A is particularly important for the process of placental angiogenesis (Arroyo & Winn 2008) and is to date the most investigated form of VEGF. VEGF-B has a particular role in embryonic angiogenesis, particularly in the heart, whilst VEGF-C and VEGF-D contribute significantly to lymphangiogenesis. VEGF-E and VEGF-F are of viral and snake venom origin, respectively (Giacca & Zacchigna 2012). Moreover, alternative splicing of VEGF-A produces a number of different isoforms, which are represented by the number of amino acids they contain. Isoforms comprised of 206, 189, 183, 165, 148, 145 and 121 amino acids have been described. VEGF-A_{165} is the dominant and most potent isoform in the human.

The three principal actions of VEGF are vasodilatation, new vessel formation and protection of existing vasculature from insults, such as shear stress secondary to erratic blood flow (Zachary 2003). As implied by its name, the main target of VEGF protein is the vascular endothelial cell and its actions are mediated via the two VEGF receptors, Flt-1 (1) and KDR (2), as well as the neuropilin receptor 1. Actions through the latter receptor may explain its pleiotrophic effects. Vasodilatation may be achieved through one of three different pathways involving nitric oxide (NO), bradykinin and endothelium-derived hyperpolarizing factor (EDHF), respectively. Most of the biologically important actions of VEGF are mediated through the KDR receptor (Holmes et al. 2007). VEGF phosphorylates KDR, which results in activation of phospholipase Cγ, formation of inositol 1,4,5-triphosphate, elevation of intracellular calcium and activation of endothelial nitric oxide synthase (eNOS) (He et al. 1999). VEGF can also generate NO through a calcium independent pathway (Fulton et al. 1999). NO relaxes vascular smooth muscle via activation of soluble guanylate cyclase and increased intracellular levels of cyclic guanosine monophosphate (cGMP) (Ignarro 1989). By contrast, prostayclin induces vasorelaxation via activation of soluble adenylate cylase and increased intracellular levels of cyclic adenosine monophosphate (cAMP) (Moncada & Vane 1978). EDHF-mediated vascular relaxation is less well understood from a mechanistic point of view, but is represented by the residual vasodilatory effect that is seen after both NO and prostacyclin have been pharmacologically blocked. The precise role of VEGF receptor 1 (Flt-1) is less well understood, but is believed to include modulation of the actions of KDR. There is a soluble version of Flt-1 (sFlt-1) that serves as a decoy receptor, binding free VEGF in the bloodstream and reducing its circulating levels, thereby antagonising VEGF action.

VEGF is also important for the physiological changes during normal pregnancy. The extravillous trophoblast secretes a number of different angiogenic factors and local vasodilators including

VEGF, which contributes to the fall in vascular resistance, together with transformation of the spiral arteries (see Section 1.1.2.3). Placental secretion of VEGF occurs preferentially into the maternal circulation, leading to a maternal serum concentration that is ten times higher than that in the fetal circulation. The placenta also secretes sFlt-1 at concentrations which are >20 times higher on the maternal versus fetal sides, resulting in a low level of free VEGF in the maternal circulation (Maynard et al. 2003; Brownbill et al. 2008). Maternal serum sFlt-1 levels are higher in pre-eclampsia and FGR (Sibai et al. 2005), which has the effect of further reducing the bioavailability of VEGF. Accordingly, maternal serum levels of VEGF are significantly lower than in normal pregnancy (Bersinger & Odegard 2005; Savvidou et al. 2006). Interestingly, this increase in sFlt-1 precedes the onset of pre-eclampsia but is only seen in FGR once established.

1.2.3 Work that has led up to the project

Previous work evaluating the effects of bilateral uterine artery injections of Ad.VEGF in normal sheep pregnancy demonstrated a significant short-term increase in uterine blood flow (UBF) when assessed by Doppler ultrasound. Uterine arteries (UtA) harvested at 4–7 days following treatment with Ad.VEGF exhibited a reduced contractile response to phenylephrine as well as enhanced bradykinin induced relaxation (David et al. 2008). More recently the longer term impact of Ad.VEGF on UBF has been evaluated using indwelling ultrasonic flow probes, which are the gold standard for the assessment of blood flow in vivo (Sokol et al. 1996) and which have several advantages over volume flow assessment using Doppler ultrasound, a technqiue which is associated with a high degree of variability (Abi-Nader et al. 2010). Figure 1.9 depicts the sustained increase in UBF (relative to baseline values) that was observed after a unilateral UtA injection of Ad.VEGF in mid-gestation compared with a contralateral injection of a non-vasoactive control vector, Ad.LacZ (= adenovirus encoding the β-galactosidase gene). Ad.VEGF therapy approximately doubled the normal gestational increase in UBF over a >4-week period (Mehta et al. 2011). Examination of the long-term UtA similarly revealed less vasoconstriction, and there was evidence of increased perivascular adventitial neovascularisation and reduced intima-to-media ratios. There was also an upregulation of both VEGF receptors (Flt-1 and KDR) and endothelial nitric oxide synthase (eNOS) when measured using immunohistochemistry and Western blotting, respectively, at the short-term but not long-term time points. There were no adverse effects on maternal or fetal heart rate or blood pressure, and no other concerns about safety were raised. This initial work provided proof of principle that Ad.VEGF can enhance UBF, however it remained unknown whether the same effects could be achieved when UBF is low (i.e. in the state of uteroplacental insufficiency). It was also not known whether or not this would impact fetal growth or wellbeing in pregnancies complicated by fetal growth restriction.

Figure 1.9 - Effect of Ad.VEGF gene therapy on uterine blood flow in normal sheep pregnancy

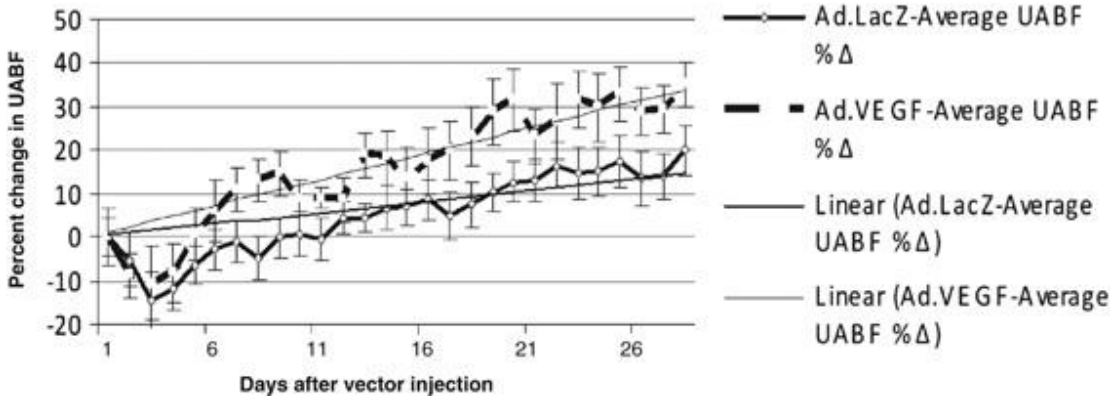

Serial changes in uterine artery blood flow (UABF) following injection with Ad.VEGF or inactive control vector (Ad.LacZ). The percentage increase in UABF relative to a mid-gestation baseline (adjusted to 0) is shown, as well as gradients of the gestational increase over a 4-week period post-injection. Error bars indicate SEM. Reproduced with permission from Mehta et al. (2011).

1.3 Aims of thesis

The aims of the research detailed in this PhD thesis were to evaluate the efficacy, safety and mechanisms of action of prenatal Ad.VEGF gene therapy in an established sheep model of FGR and to consider the ethical issues and translational aspects of this therapy. The overnourished adolescent sheep paradigm was chosen as it replicates many of the key features of human FGF secondary to uteroplacental insufficiency, including a major reduction in UBF by mid-gestation, without the need for any permanent surgical interference at a vascular or placental level.

More specifically, the aims were to evaluate the effects of Ad.VEGF gene therapy for FGR on:

- *In vivo* measurements of uterine blood flow
- Uterine artery vascular reactivity, intima: media ratios and adventitial neovascularisation
- Fetal growth velocity (measured by serial ultrasound)
- Fetal weight, body composition, organ weights and gross morphology in late gestation
- Gestation length and lamb birth weight following spontaneous delivery approaching term
- Neonatal mortality and morbidity, and level of neonatal care required to ensure survival
- Postnatal growth rates to weaning, body composition and metabolic function in early life

2.1 Animal Procedures

All regulated procedures were licensed under the UK Animals (Scientific Procedures) Act 1986 and approved by the Rowett Institute's local ethical review committee. Sheep were housed in individual pens under natural lighting conditions at the Rowett Institute of Nutrition and Health, University of Aberdeen, Scotland (57^{o}N 2^{o}W).

2.1.1 Establishment of singleton pregnancies

Adult Scottish Greyface ewes (Border Leicester x Scottish Blackface) were used as donors of embryos for transfer into adolescent recipient ewe lambs (Dorset Horn x Scotch Mule (Bluefaced Leicester x Scottish Blackface)) of known age, birthweight and growth status. Embryo transfers were carried out on 10 separate days during the mid-breeding season.

2.1.1.1 Oestrus synchronisation and ovulation induction

Oestrus cycles of the adolescent recipients (n=177) and adult donors (n=40) were synchronised by withdrawal of progestogen sponges. Synchronisation was carried out in 10 batches (each consisting of 3 to 4 donors and 16 to 21 recipients) across a 2 week period preceding each embryo transfer day.

Prior to sponge insertion recipient ewe lambs were sheared and weighed. Adiposity was assessed and a body condition score (BCS) assigned following palpation of the lumbar vertebral spinous processes between the lowermost rib and the level of the kidneys, according to the criteria of Russel et al. (1969). Body condition scoring was carried out by a single experienced assessor (Raymond Aitken). Synchronisation of recipients was commenced on Day –15 relative to the onset of oestrus (Day 0) by insertion of vaginal sponges containing 60mg medroxyprogesterone acetate (Veramix®, Intervet UK Ltd, Welwyn Garden City, Herts, UK). Sponges were dusted with terramycin antibiotic powder and well lubricated prior to insertion. Ewe lambs were examined daily to ensure that the sponges remained in situ in view of the risk of displacement secondary to adolescent anatomical variation. Thirteen days later (on Day –2) at 14:00, sponges were removed and 600IU pregnant mare serum gonadotrophin (PMSG, Intervet UK Ltd) was administered by intramuscular (i.m.) injection to stimulate ovulation.

Donor ewes (2 to 3 years old and of known breeding history) were also weighed and body condition scored prior to the start of synchronisation on Day –14, when vaginal sponges

containing 40mg fluorogestone acetate (Chronogest®, Intervet UK Ltd) were inserted using a sponge applicator. Seven days later (Day –7) these sponges were removed and immediately replaced with fresh ones of the same type. A superovulation regime was commenced at 08:00 on Day –4 with the i.m. administration of 1.125mg ovine follicle-stimulating hormone (oFSH) (Ovagen®, Immuno-Chemical Products Ltd, Auckland, New Zealand) immediately followed by 125µg i.m. cloprostenol (Estrumate®, Schering-Plough Ltd, Welwyn Garden City, Herts, UK), a synthetic prostaglandin-F2α. At 18:00 a second dose of oFSH was given together with 400IU i.m. PMSG. Further twice daily doses of oFSH were administered at 08:00 and 18:00 on the following 3 days (Day –3 to –1) and sponges were removed on Day –2 at 18:00. Beginning on Day –1, each donor and recipient ewe was individually exposed to a vasectomised ram three times daily until onset of oestrus had been detected.

2.1.1.2 Laparoscopic intrauterine insemination

On Day 0 at 16:00 (46 hours following sponge removal) donor ewes underwent insemination directly into the uterine cavity under direct laparoscopic visualisation, as previously described by McKelvey et al. (1985).

Fresh semen was harvested from a single sire (Dorset Horn) of proven fertility using an artificial vagina warmed to 37^{o}C. Semen production had been checked during the previous week and viability assessed by staining and scoring on the day before use. After collection semen was diluted 1:3 by volume with phosphate buffered saline and stored in a double-walled glass vessel at 35^{o}C. Sperm motility was evaluated and rechecked immediately prior to insemination into each of the 3 to 4 donor ewes per batch. Food and water were withheld overnight prior to laparoscopy. Ewes initially underwent sedation with 6mg i.m. acepromazine (ACP Injection®, Novartis Animal Health UK Ltd, Frimley, Surrey, UK), which was administered 30 to 45 minutes before the procedure. They were restrained in a custom-made laparoscopy cradle, designed to provide a large degree of “head-down”, allowing the bowel to fall away from the pelvis under gravity and thereby negate the risk of injury (Figure 2.1). The ventral abdomen was shaved and prepared with 4% chlorhexidine gluconate (HiBiSCRUB®, Regent Medical, Manchester, UK). Trochars were inserted at two sites following local subcutaneous (s.c.) infiltration of 10ml 2.0% lidocaine hydrochloride mixed with 0.001% adrenaline (Lignol®, Arnolds Veterinary Products, Shrewsbury, Shropshire, UK). The abdominal cavity was insufflated with carbon dioxide and a 5mm laparoscope (Panoview Lumina SL 8933.441, Richard Wolf UK Ltd, Wimbledon, UK) was introduced via the primary port to visualise the uterus. Under direct vision 0.3ml of diluted semen was deposited into the lumen of each uterine horn using a long finely drawn sterile glass pipette introduced via the secondary port.

Figure 2.1 – Preparation for laparoscopic procedures

Photograph of an anaesthetised adult donor ewe positioned "head-down" for laparoscopic intrauterine insemination in a custom-made cradle.

Once insemination was complete the peritoneal cavity was deflated, the trochars removed and Michel clips applied over the port site incisions. Antibiotics were administered in the form of 4ml i.m. Duphapen®+Strep (Fort Dodge Animal Health UK Ltd, Southampton, UK), containing 200mg procaine benzylpenicillin and 250mg dihydrostreptomycin per ml.

2.1.1.3 Embryo recovery

Four days following insemination, multiple embryos were recovered from donor ewes at laparotomy using a standard surgical technique of retrograde flushing of each oviduct, as described (Hunter et al. 1955). As many donors as necessary were flushed in order to provide enough embryos of sufficient quality for transfer into 12 to 16 adolescent recipients per batch. This varied between 1 and 4 donors per day.

Food and water were withheld overnight. Surgery was performed under general anaesthesia, which was induced and maintained via inhalation of isoflurane (IsoFlo®, Abbott Laboratories

Ltd, Queenborough, Kent, UK) in a mixture of oxygen and nitrous oxide. After mask induction all ewes were intubated using a size 8.0 endotracheal (ET) tube (Phoenix Medical Ltd, Preston, UK) but artificial ventilation (using a Manley Pulmovent MPP 200) was only provided if necessary. Once adequately anaesthetised, ewes were positioned in dorsal recumbency, closely shaved and prepared with povidone-iodine (Vetasept®, Animalcare Ltd, York, UK). Once draped a 10cm midline incision was made on the anterior abdominal wall immediately above the mammary gland and a combination of sharp and blunt dissection was used to safely enter the peritoneal cavity. The uterus and ovaries were located and exteriorised and the ovulation rate was determined by counting the number of corpora lutea on the surface of each ovary (Figure 2.2A). Each oviduct in turn was cannulated using a fine glass catheter, which was carefully threaded into the fimbria and advanced approximately 3cm into the oviduct (Figure 2.2B). 15–20ml ovum culture media (OCM) (ICN Biomedicals, Ohio, USA) warmed to 37^{o}C was injected into the lumen of the ipsilateral uterine horn approximately 5cm from the utero-tubal junction. Media was then milked out through the cannula into a sterile glass embryo dish. Embryo yield was immediately determined by assessment of developmental stage using a stereomicroscope (magnification x40). Once bilateral recovery was complete the rectus sheath was closed with interrupted horizontal mattress sutures using monofilament absorbable polydioxanone (0 PDS®II, W9381H, Ethicon, Norderstedt, Germany). 1ml Duphapen®+Strep was administered directly into the wound during closure of the skin with continuous braided absorbable polyglactin (2 Vicryl®, W9297, Ethicon). A moisture vapour permeable spray dressing (Opsite®, Smith and Nephew Medical Ltd, Hull, UK) was applied over the wound. Perioperatively ewes received systemic antibiotics and analgesia in the form of 4ml i.m. Duphapen®+Strep and 40mg s.c. meloxicam (Metacam®, Boehringer Ingelheim, Ingelheim, Germany), respectively. Embryos were held at 33^{o}C in fresh OCM until transferred to recipients within 6 hours of recovery (Section 2.1.1.4). Induction of anaesthesia and embryo recovery took approximately 45 minutes per animal and ewes were standing within 5 minutes of extubation. Ewes routinely received a further two doses of Duphapen®+Strep (4ml) on post-operative days 1 and 2 and were gradually re-alimented to feed over a 4 day period to prevent the development of ketoacidosis. Further analgesia was provided in the event of inappetance or signs of pain. Ewes received 125µg i.m. cloprostenol between post-operative days 10 and 12 following insemination to induce luteolysis.

2.1.1.4 Embryo transfer

Recovered embryos of appropriate quality and stage were synchronously transferred into the uteri of adolescent recipients using the laparoscopically assisted technique of Tervit (1989).

Figure 2.2 – Embryo recovery at laparotomy

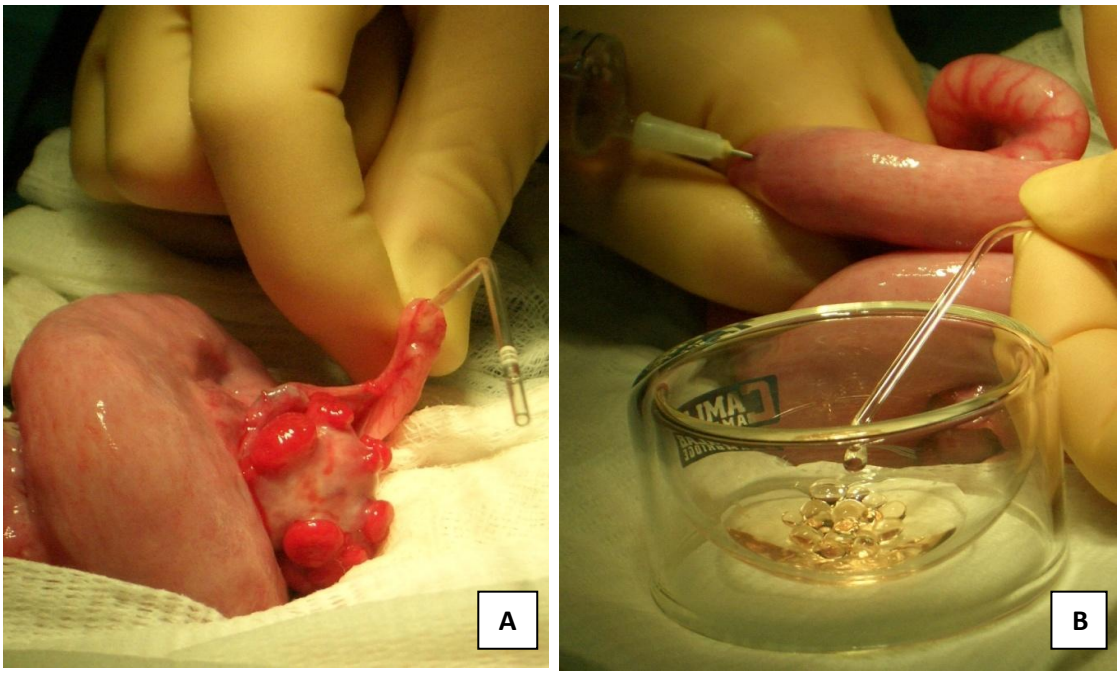

Photographs of open embryo recovery procedure: [A] View of the exteriorised uterus, adjacent superovulated ovary and fallopian tube, cannulated using a fine glass catheter; [B] Injection of ovum culture medium into the uterine cavity and retrograde flushing of embryos into a dish.

Food and water were withheld overnight. General anaesthesia was induced and maintained as described for the embryo recovery procedures (Section 2.1.1.3) and ewe lambs were positioned and prepared for laparoscopy as described for the intrauterine insemination procedures (Section 2.1.1.2). At laparoscopy the ovaries were visualised and ovulation rate was determined (Figure 2.3A). In the event of regressed corpora lutea or complete failure of ovulation, embryo transfer was not carried out. Otherwise the uterine horn ipsilateral to the ovary with the greatest number of corpora lutea was selected for transfer. The ewe was draped and a 1–2cm mini-laparotomy incision was made on the anterior abdominal wall approximately 10cm anterior to the udder and slightly to the right of the midline. The tip of the selected uterine horn was carefully exteriorised through this incision using a pair of endoscopic grasping forceps (Richard Wolf UK Ltd) and gently held in a warm saline-soaked swab. An appropriate embryo (high quality early morula) was selected and loaded into a fine glass pipette attached to a syringe, held in 0.2ml OCM. The pipette was inserted through the wall of the chosen horn approximately 1.5cm anterior to the utero-tubal junction (Figure 2.3B) and discharged into the uterine lumen. The horn was then carefully returned to the abdominal cavity and the rectus sheath and skin closed using interrupted 0 PDS®II.

Figure 2.3 – Laparoscopically assisted embryo transfer

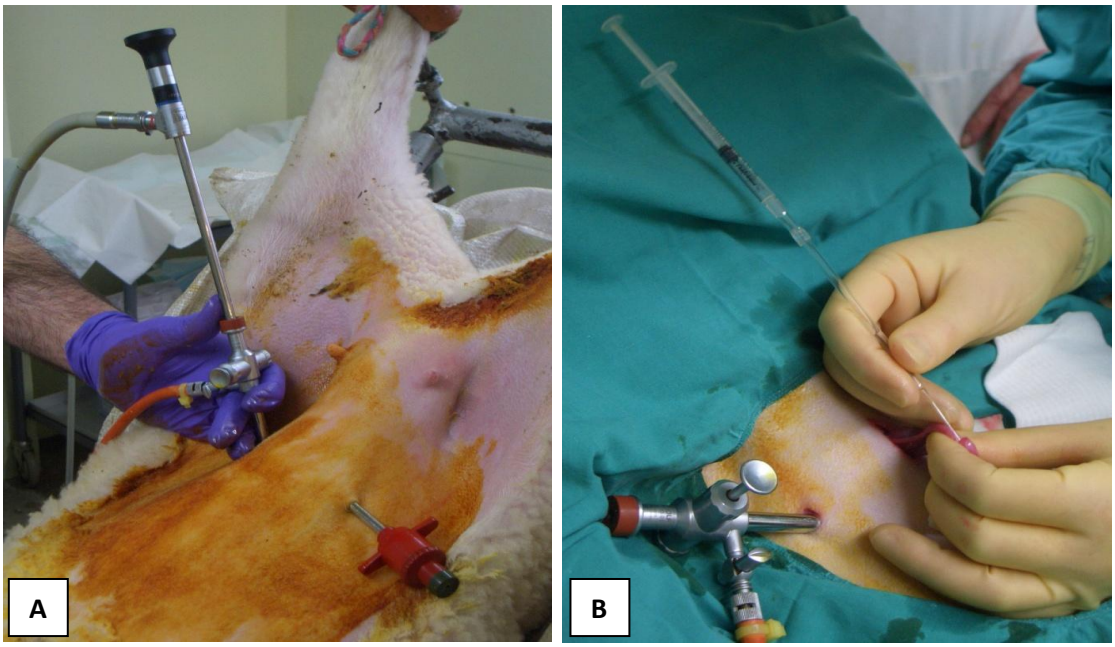

Photographs of embryo transfer procedure on an adolescent recipient ewe: [A] Laparoscopy to determine recipient ovulation rate and to select the uterine horn for embryo transfer; [B] Exteriorisation of chosen uterine horn through a mini-laparotomy incision and transfer of embryo into the uterine cavity using a fine glass pipette.

Perioperatively ewes received 3ml i.m. Duphapen®+Strep and 20mg s.c. meloxicam. Induction of anaesthesia and embryo transfer took approximately 20 minutes per animal and ewes were standing within 5 minutes of extubation. Ewes received two further doses of i.m. Duphapen®+Strep (3ml) on postoperative day 1 and 2.

2.1.1.5 Pregnancy diagnosis

Pregnancy rate following embryo transfer was determined on day 45 of gestation by transabdominal ultrasound using a B-mode linear array scanner (Aloka SSD-210 DXII, BCF Technology Ltd, West Lothian, UK) with a 5.0MHz transducer and ultrasound coupling gel (Ultra/Phonic™, Pharmaceutical Innovations Inc, Newark, NJ, USA). Viability was confirmed by the presence of fetal heart activity.

2.1.2 Nutritional management

Immediately following embryo transfer, ewes were allocated to one of two nutritional regimes: a high intake diet designed to overnourish the mother at the expense of the

pregnancy; or a control intake diet designed to meet but not exceed the requirements of pregnancy and thereby optimise fetal and placental growth. Control-intake and overnourished ewes received different quantities of the same complete diet, the composition of which is detailed in Table 2.1. All ingredients other than home produced barley were bought in and freshly mixed in feed mill at the Rowett Institute. The complete diet supplied a total of 12MJ metabolisable energy and 140g crude protein per kg and had an average dry matter of 86%. The feed was sub-sampled five times per week and the complete sample was submitted weekly to the Rowett Institute's Analytical Department for the determination of crude protein content (nitrogen x 6.25) using the Kjeldahl procedure (Davidson et al. 1970). The amount of soya protein used varied depending on the quality of the hay and barley and was usually adjusted within the range 165–175kg on the basis of nitrogen content. Vitamins and minerals were supplemented by adding Norvite 317 (Insch, Aberdeenshire, UK). The diet was offered in two equal feeds at 08:00 and 16:00 daily. Before the morning ration was provided, any feed left in the trough overnight was weighed and recorded as a daily feed refusal. Ewes were weighed once a week and maternal BCS was recorded fortnightly - described in Section 2.1.1.1.

The level of feed for control-intake ewes was calculated to promote normal maternal weight gain and to maintain baseline maternal adiposity throughout gestation. Control-intake ewes received their entire ration immediately following embryo transfer. Thereafter the amount of feed was adjusted to promote a low to moderate maternal weight gain (approximately 50–65g per day) during the first two-thirds of gestation. From 100 days gestation onwards, step-wise increases in maternal intake were allowed in order to meet the increasing demands of the developing fetus.

Table 2.1 – Composition of the sheep diet (per kg)

Rolled barley	422.5g
Coarsely chopped hay	300.0g
Soybean meal	167.5g
Molasses	100.0g
Salt	3.5g
Limestone	2.5g
Dicalcium phosphate	2.5g
Vitamins and minerals	1.5g

The level of feed for overnourished ewes was calculated to promote rapid maternal growth, and provided (on average) 2.25 times the amount of metabolisable energy as the control diet. Following embryo transfer, these ewes had their level of feed gradually increased over a two week period until the daily level of feed refused was approximately 15% of the total offered, equivalent to *ad libitum* intakes. Thereafter the amount of feed was individually reviewed three times per week and adjusted where appropriate on the basis of weekly increases in live weight and the level of daily feed refusals.

2.1.3 Ultrasound examination

Serial ultrasound examinations were systematically performed to assess fetal growth and wellbeing throughout the second half of pregnancy, beginning with a baseline assessment in mid-gestation. All scans were performed by a single operator (David Carr) using a GE Logiq™ 400 CL machine (GE Medical Systems Ltd, Milwaukee, WI, USA) with cine-loop facility, pulsed wave and colour flow Doppler functionality, and a 3.0–5.0MHz curvilinear abdominal probe.

Ewes were examined whilst standing upright in a modified milking crate and loosely restrained by head collar (Figure 2.4). One-to-one attention and hay was provided by an additional member of the research team in order to reduce anxiety. Prior to applying ultrasound coupling gel, the abdominal wool was clipped anterior to the udder after application of a cleaning solution containing (per litre) 750ml 100% ethanol, 150ml deionised water and 100ml 5% chorhexidine gluconate (HiBiTANE™, Regent Medical). Each ultrasound examination lasted a maximum of 30 minutes, during which time all fetal measurements were repeated until a minimum of three values in reasonable agreement with each other (coefficient of variation <5%) were obtained.

2.1.3.1 Fetal biometry

After confirming the presence of fetal heart activity, a transverse view of the fetal abdomen was obtained at the level of the lowermost rib, just above the umbilical cord insertion. Care was taken to ensure the presence of a complete rib, the stomach bubble and the intrahepatic portion of the umbilical vein in the section. The abdominal circumference (AC) was measured in this plane using an ellipse (Figure 2.5A) and the trunk (transverse abdominal) diameter (TD) was determined at the same level (Figure 2.5B).

Remaining in the axial plane, the transducer was then moved caudally to the level of the fetal kidneys and panned up and down to identify the widest mid-section in this plane (Figure 2.6A). The right kidney was selected for all renal measurements unless satisfactory views were

F*igure 2.4 – Ultrasound examination*

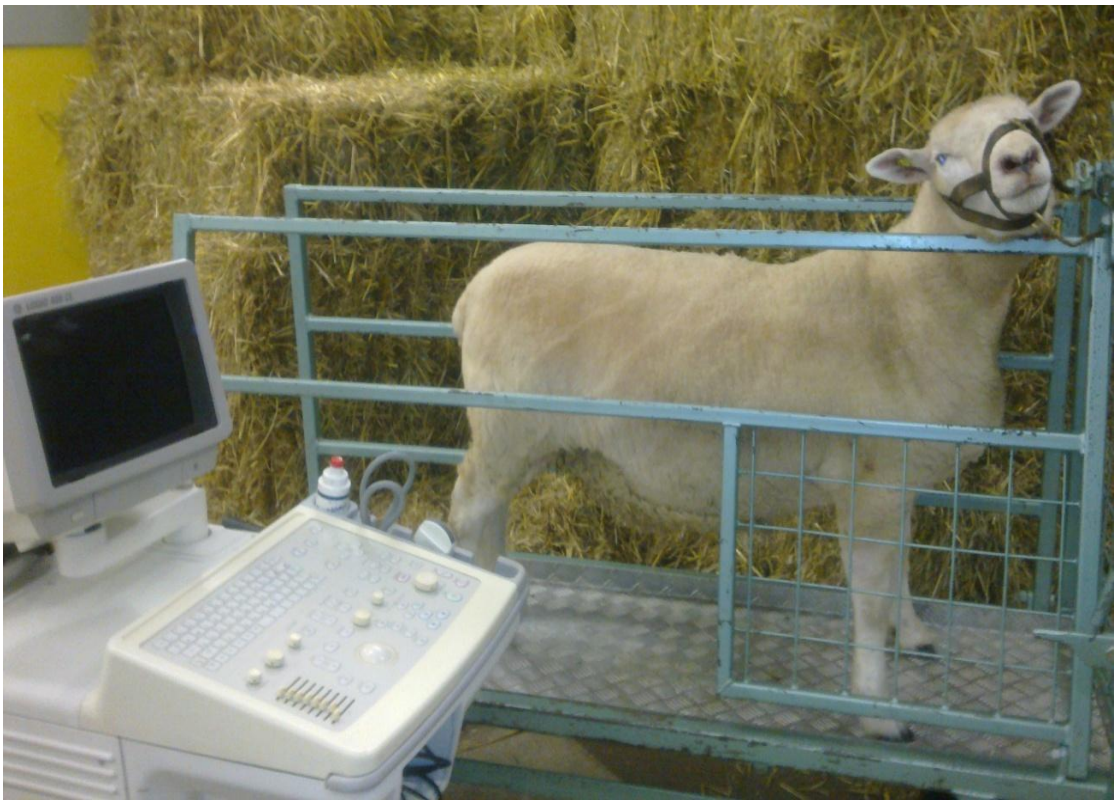

Photograph of the set up for scanning, showing a ewe standing upright in a modified milking crate ready for transabdominal ultrasound examination

---

unobtainable, in which case the left was substituted. At the widest point of the kidney, the transverse and anteroposterior renal diameters (TRD and APRD) were measured at right angles to one another by placing the callipers on the borders of the renal tissue. The probe was then rotated through 90^{o} to obtain a longitudinal view of the same kidney in parasagittal section, taking care to visualise the full length of the organ. In this plane the renal length (RL) was measured between the superior and inferior poles of the kidney (Figure 2.6B). From these three measurements the renal volume (RV) was then calculated, using the ellipsoid equation [RV = RL x TRD x APRD x π/6], as previously described (Jeanty et al. 1982).

After rotating back into a transverse section, the transducer was moved from the level of the kidneys down to the fetal pelvis, where the iliac crests and head of the femur were identified. Fixing on the proximal end of the femoral bone, the probe was then rotated and angled to visualise the full length of the calcified shaft, keeping the long axis of the bone close to 90^{o}

Figure 2.5 – Abdominal measurements

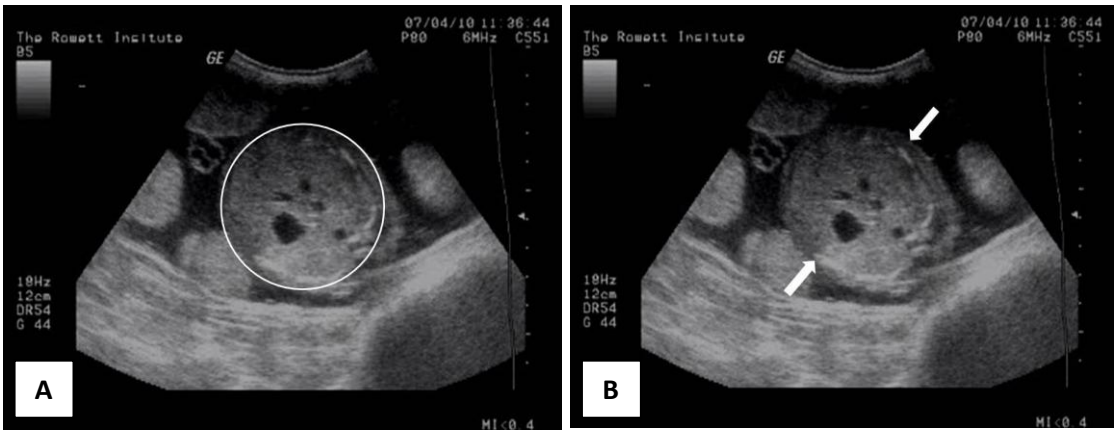

Ultrasound images: [A] Transverse section of the fetal abdomen at the level of the lowermost rib for the measurement of abdominal circumference; [B] Measurement of the trunk diameter.

Figure 2.6 – Renal measurements

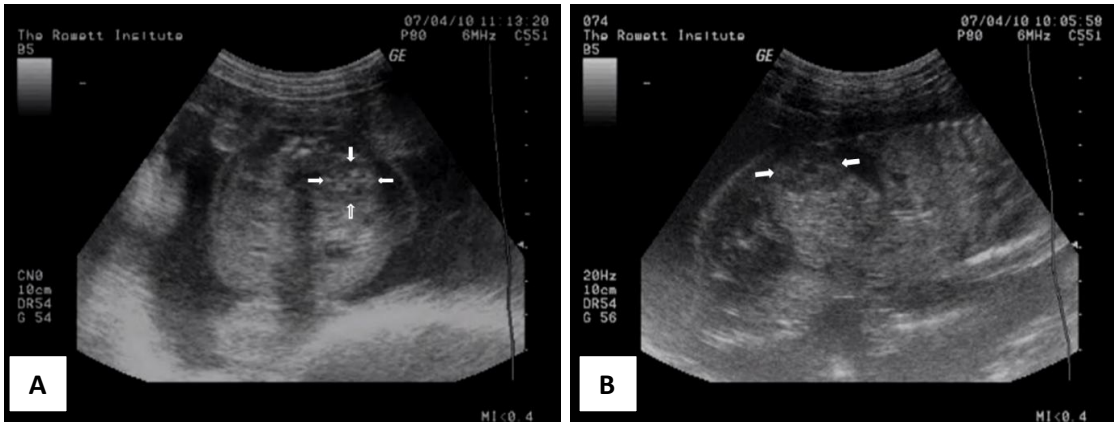

Ultrasound images: [A] Transverse view of the fetal abdomen demonstrating the widest midpoint of the right kidney for measurement of the transverse and anteroposterior renal diameters; [B] Parasagittal section through the right kidney for measurement of renal length.

---

relative to the ultrasound beam (i.e. parallel to the top of the screen) in order to minimise artefact. The femur length (FL) was then measured (Figure 2.7A) between the two metaphyses. Rotating 90^{o} into an axial view of the femur, the bony shaft was followed down to its distal end in order to identify the adjacent tibial bone. After fixing on the proximal end of the tibia, the above steps were repeated in order to visualise the full tibial shaft and to measure the tibia length (TL) (Figure 2.7B).

Figure 2.7 – Long bone measurements

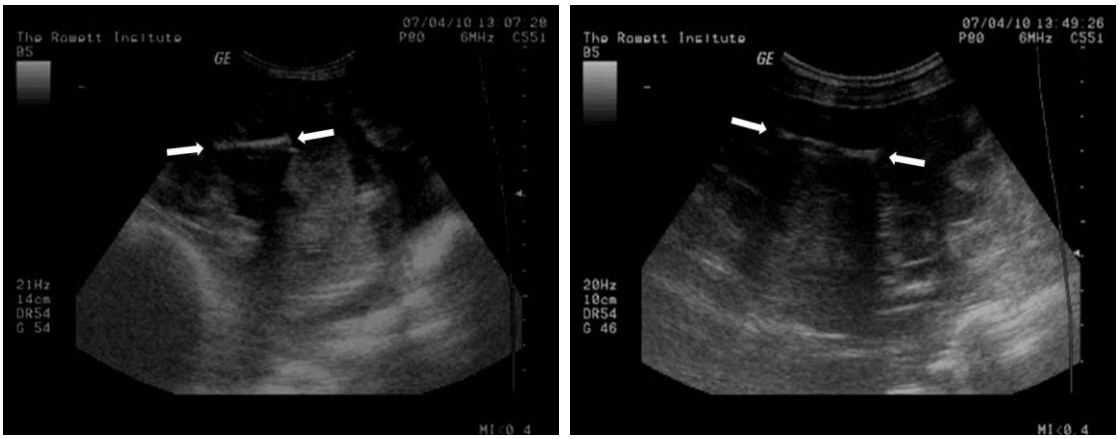

Ultrasound images: [A] View of the full length of the calcified shaft of the femur for the measurement of femur length; [B] Equivalent view for the measurement of the tibia length.

Thereafter the fetal head was located by following the cervical vertebrae from the fetal chest up to the base of the skull. The probe was orientated so that the long axis of the fetal head was at right angles to the ultrasound beam. Care was taken to visualise the full length of the fetal head and to ensure the correct section through the cranium, in which the midline structures of the brain were equidistant from the two parietal bones. In this view the biparietal diameter (BPD) was measured as the widest distance between the proximal and distal parietal bones (outer to outer surface, as shown in Figure 2.8A). The occipito-snout length (OSL) was also measured in this plane, from the occipital bone at the posterior aspect of the skull (outer surface) to the anterior border of the soft tissue at the tip of the snout (Figure 2.8B).

2.1.3.2 Umbilical artery Dopplers

The umbilical cord diameter was first measured within 1cm of its insertion into the fetal abdomen. The cord was then followed distally to identify the nearest appropriate straight section for Doppler waveform analysis. The colour flow mode was enabled and the orientation was adjusted so that the umbilical vessels were directed towards the transducer with the angle of insonation (θ) as close to zero as possible (direction of blood flow parallel with ultrasound beam) and always below 30^{o}. The pulsed wave Doppler mode was then enabled and the gate was positioned over the umbilical artery, distinguishable from the umbilical vein by its characteristic pulsatile waveform. The velocity scale was adjusted to ensure that the waveform was maximised whilst still visible in its entirety, and the gain was altered until a "clean" waveform with minimum background noise was observed. A series of waveforms of uniform

Figure 2.8 – Head measurements

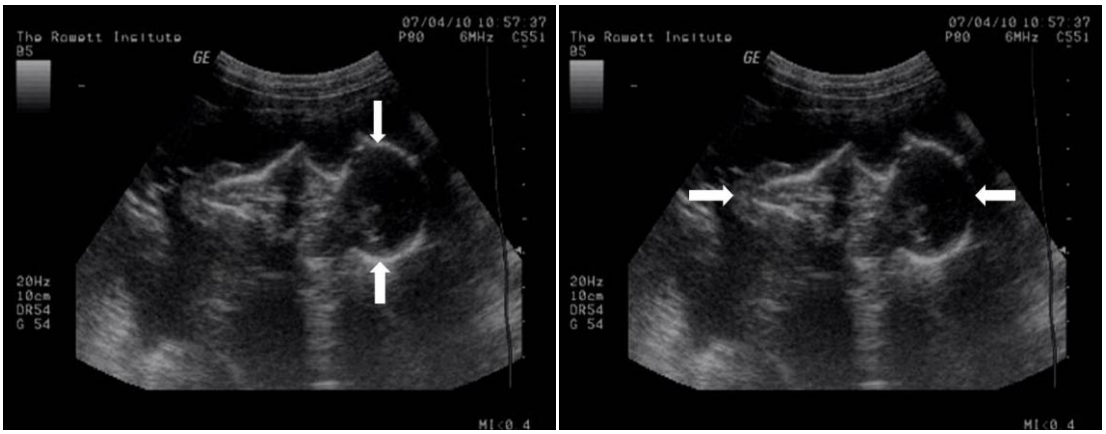

Ultrasound images: [A] Section through the fetal head for the measurement of the biparietal diameter; [B] Measurement of the occipito-snout length.

---

appearance were then recorded in the absence of fetal or maternal movements. The maximum velocity envelope (outline) of three consecutive waveforms was traced manually in order to determine the maximum (peak systolic) velocity (Vmax), minimum (end-diastolic) velocity (Vmin) and time-averaged maximum velocity (TAMAX) (Figure 2.9). The vessel was subsequently re-examined and the above steps repeated at least two more times. Measurements were then averaged for accuracy.

Figure 2.9 – Umbilical artery Dopplers

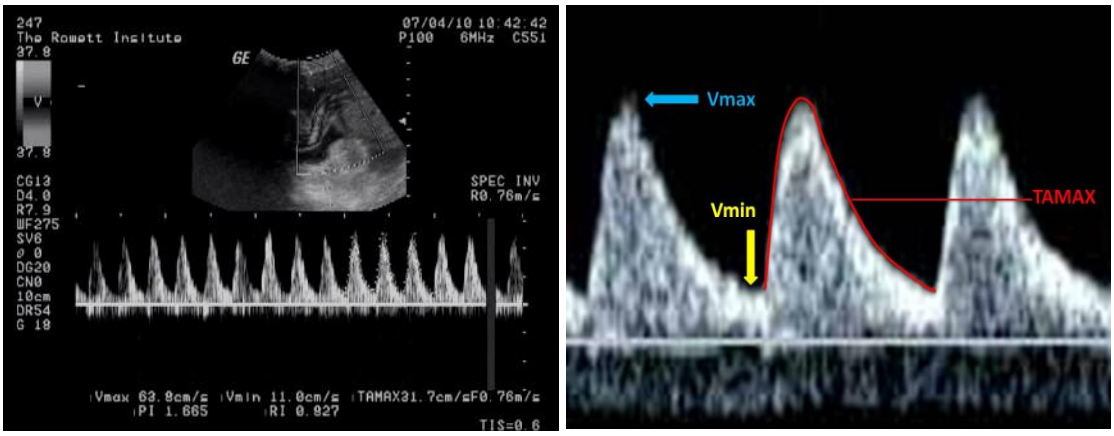

Measurement of umbilical artery Doppler indices: [A] Ultrasound image of waveform captured during Doppler examination of a free loop of umbilical cord, with angle of insonation less than 30 degrees; [B] Close-up of three consecutive waveforms illustrating measurement of maximum velocity (Vmax), minimum velocity (Vmin) and the time-averaged maximum velocity (TAMAX).

From these velocities the following flow-independent indices were calculated:

- Pulsatility index (PI) = (Vmax – Vmin) / TAMAX
- Resistance index (RI) = (Vmax – Vmin) / Vmax
- Systolic : diastolic ratio (SDR) = Vmax / Vmin

2.1.3.3 Placentation and amniotic fluid volume

An initial sweep was made through the gravid horn to survey the approximate number, size and general distribution of the placentomes. Based on the overall appearances, placental quality was subjectively categorised as excellent, good, moderate or poor. In order to more objectively assess placental morphometry, 10 representative placentomes of average size were randomly selected for measurement. A longitudinal mid-section (side-on) view of each chosen placentome was obtained, with its characteristic oval appearance (Figure 2.10A). In this plane the placentome length and width were measured at right angles. The cross-sectional area (CSA) of each placentome was then calculated using the formula: CSA = [π x (placentome length x 0.5) x (placentome width x 0.5)] / 100. Finally, the CSAs of all 10 placentomes were added together to give a "placentome index".

Amniotic fluid was first assessed subjectively by sweeping through the entire uterus and categorising fluid levels as normal, increased or reduced. With the ewe standing straight and upright, a search was made for deep pockets of accumulated fluid, and the deepest vertical pool (DVP) was identified and quantified by averaging 3 vertical measurements (Figure 2.10B).

Figure 2.10 – Assessment of placentation and amniotic fluid

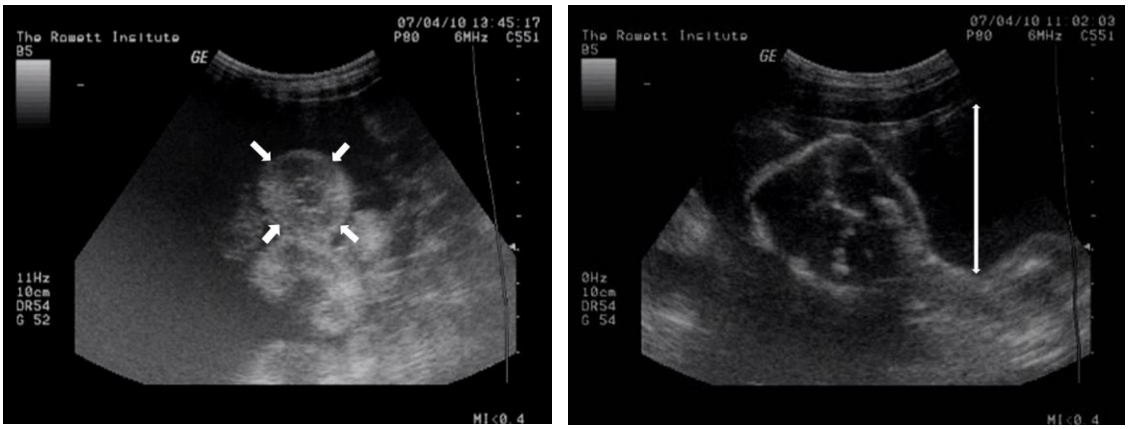

Ultrasound images: [A] Measurement of the width and length of an individual placentome; [B] Measurement of the deepest vertical pool of amniotic fluid.

2.1.4 Gene therapy administration

2.1.4.1 Vectors

Adenoviral constructs containing the gene for the human vascular endothelial growth factor (VEGF) A-165 (Ad.VEGF-A_{165}) or a marker gene encoding the beta-galactosidase enzyme LacZ (Ad.LacZ) were produced in individual lots by the A.I. Virtanen Institute for Molecular Sciences (AIVI), University of Kuopio, Finland. The functionality of each lot was tested by Ark Therapeutics Ltd (Kuopio, Finland) using *in vitro* assays prior to shipping to the Rowett Institute of Nutrition and Health, Aberdeen. HeLa cells were first transduced *in vitro* using each vector lot. Thereafter the cells and conditioned growth media were separately collected for laboratory analysis. VEGF-A_{165} protein concentrations were quantified in the media supernatant using enzyme-linked immunosorbent assay (ELISA). VEGF expression was also assessed semi-quantitatively by visual inspection of band size following Western blotting. Beta-galactosidase expression was assessed in the transduced HeLa cells after straining with X-gal solution (5-bromo-4-chloro-3-indolyl-β-D-galactopyranoside).

Following delivery, vectors were stored at –80^{o}C prior to use. The viral titre of each lot was known and allowed for the calculation of the precise volume required to provide 1 x 10^{12} particles for injection into each uterine artery. Aliquots of vector were thawed out and the required volume (μL) was added to 10ml sterile normal saline by John Milne immediately prior to administration at laparotomy (see Section 2.1.4.2). Syringes and needles used to draw up and/or administer adenoviral vectors were subsequently placed into a designated sharps bin and disinfected overnight in 2% Virkon® (Antec International Ltd, Sudbury, Suffolk, UK) before disposal as clinical waste.

2.1.4.2 Surgery

On the day before surgery the afternoon feed was omitted and water withdrawn from 17:00. Ewes were weighed to ensure accurate dosing of analgesia, antibiotics and anaesthetic agents. On the morning of surgery fetal viability was confirmed by transabdominal ultrasound prior to transfer to the surgical preparation room, where a 14-gauge jugular venous catheter was inserted. Induction of anaesthesia was achieved using 4–5mg/kg intravenous (i.v.) propofol (PropoFlo®, Abbott Laboratories Ltd). A 7.5mm ET tube was inserted, through which anaesthesia was maintained using isoflurane in a mixture of oxygen and nitrous oxide. Ewes were ventilated with an Aestiva 5 unit (Datex-Ohmeda, Madison, WI, USA). Antibiotics were administered in the form of 10mg/kg i.m. benzylpenicillin (Crystapen®, Genus Pharmaceuticals, Berkshire, UK) and 0.4ml/kg i.m. Duphapen®+Strep. Analgesia was provided in the form of

0.006mg/kg i.m. buprenorphine (Vetergesic®, Schering-Plough Ltd) and 0.5mg/kg s.c. meloxicam. The ventral abdomen and an additional area for the application of a diathermy electrode were closely shaved.

Ewes were positioned on the operating table in dorsal recumbency, legs loosely restrained by ankle ties, and completely draped. The abdomen was prepared with povidone-iodine. Maternal heart rate, respiratory rate, oxygen saturations and the concentration of isoflurane in the inspired and expired air were monitored throughout surgery. Once the ewe was anaesthetically stable and taking care to avoid the mammary vein, a 12–15cm midline incision was made on the lower abdominal skin and continued through the subcutaneous fat layer to the rectus sheath beneath. Any bleeding vessels were ligated with artery forceps and cauterised as necessary. The rectus sheath and parietal peritoneum were carefully incised in the midline using a scalpel and the incision was extended with scissors to open the peritoneal cavity. Uterine position was assessed and the gravid horn identified by bilateral inspection, taking care to avoid excessive handling of the uterus. Large gauze swabs soaked in saline were used to gently retract the omentum, bowel and non-gravid uterine horn in order to visualise the lower lateral aspect of the gravid horn. The main trunk of the uterine artery was identified in its course along the posterior aspect of the uterus and passage over the anterior wall within the mesometrium, and the visceral peritoneum overlying the vessel was carefully opened as proximally as possible. The artery beneath was then mobilised by carefully separating it from the underlying tissue using Metzenbaum scissors, an aneurysm needle, right-angled artery forceps and fine cotton buds as required. A vessel loop (Ethicon) was fed beneath the artery and used to gently elevate and stabilise the artery, which was then occluded digitally. A 23-gauge butterfly needle attached to the prepared syringe (containing 10ml normal saline ± adenoviral particles; see above) was carefully inserted through the vessel wall just distal to the occlusion and proximal to the first arterial bifurcation, as shown in Figure 2.11.

After drawing back to ensure the needle tip was in the vessel lumen, the solution was steadily injected over a period of 1 minute, after which the needle was carefully removed and a second digital occlusion applied directly over the injection site. Bimanual occlusion was maintained for a further 4 minutes to maximise transfection of the downstream endothelium and to prevent excessive systemic spread (for ewes receiving adenoviral particles). After 4 minutes the occlusion over the injection site was released and the area inspected for any signs of bleeding. Haemorrhage from the artery was managed by a further digital occlusion for 1 minute, or longer if necessary. Haemorrhage from the dissected peritoneal edges was managed using pressure with a small gauze swab and/or figure-of-eight sutures using nonabsorbable braided

Figure 2.11 – *Gene therapy administration*

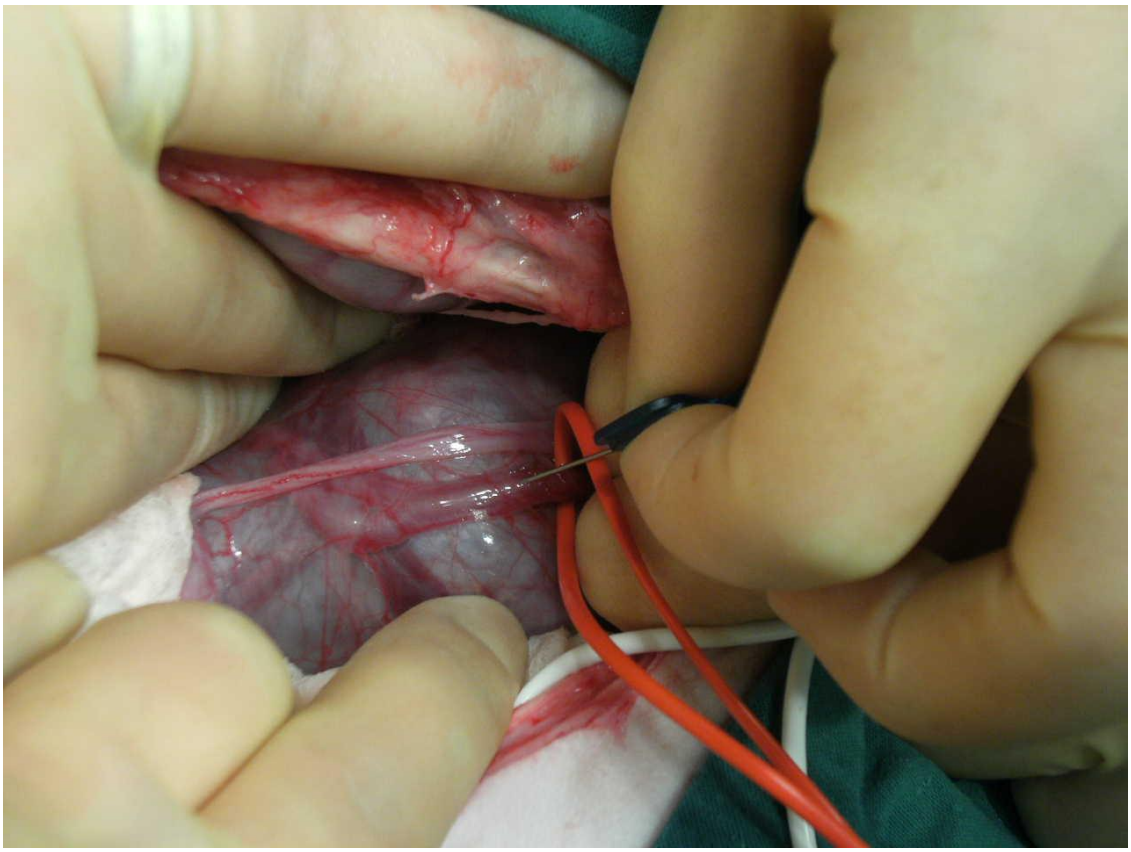

Photograph showing the main trunk of a uterine artery being injected using a butterfly needle at laparotomy. The artery has been dissected out, elevated using a vessel loop and is being digitally occluded just proximal to the site of injection.

---

silk (3.0 Mersilk®, W192, Ethicon). Once haemostasis had been achieved the non-gravid uterine artery was identified and injected in the same manner. Thereafter the uterus was restored to its original position and hydrated with sterile normal saline warmed to 37°C. The rectus sheath and parietal peritoneum were closed using interrupted 2 Mersilk® (W595, Ethicon) and the subcutaneous fat layer was closed with interrupted 2.0 Vicryl® (W9463, Ethicon) to obliterate the dead space and thereby reduce the risk of infection. The skin was closed with continuous 2.0 Vicryl® and the wound sprayed with Opsite®. An abdominal bandage comprising a double fold of Tubigrip® L (Molnlycke Health Care, Dunstables, Beds, UK) was applied around the trunk in order to provide support and to limit direct contact of the surgical wound with dirt in the pen and thereby reduce the risk of infection.

In the recovery area, ewes were extubated and kept under observation in a heated pen. An upright position was encouraged to prevent bloating. Two doses of 3ml Duphapen®+Strep

were administered on day 1 and day 2 post-op. Additional antibiotics in the form of procaine-penicillin (Duphapen Fort®, Fort Dodge Animal Health) were administered if there was perceived to be a higher risk of infection. Further analgesia (meloxicam and/or buprenorphine) was provided if there were signs of pain or inappetance. Overnourished ewes were gradually re-alimented to pre-surgery intakes. Normal step-up was commenced for control-intake ewes.

2.2 Laboratory Techniques

2.2.1 Processing of blood samples

Samples of maternal and lamb venous blood were obtained by jugular venepuncture at various stages throughout pregnancy and the postnatal period, whilst fetal blood samples were obtained at necropsy from the umbilical cord or by cardiac puncture (Section 4.2.5.1). Samples taken into 10ml BD Vacutainer® tubes containing either 18.0mg K2-EDTA or 170 IU lithium-heparin (Becton Dickinson, Plymouth, Devon, UK), 5ml assay tubes (Sarstedt, Nümbrecht, Germany) containing 50µl heparin or 2.5ml syringes containing 25µl heparin (both at 10 IU/ml concentration, Leo Laboratories Ltd, Princes Risborough, Bucks, UK) were placed on ice before being spun down at 3000rpm (2000g) for 20 minutes at 4^{o}C in a refrigerated centrifuge (ALC 4237R or Jouan KR422). The resultant plasma was pipetted off and stored at –20^{o}C. Samples taken in 10ml plain tubes (BD Vacutainer®) were left at room temperature for 8 hours then, after ringing, stored overnight at 4^{o}C. The following morning they were centrifuged at 3000 rpm (2000g) for 90 minutes at 4^{o}C. The resultant serum was pipetted off and stored at -20^{o}C.

2.2.2 Preparation of fixative solutions

Carnoy's solution was made up as follows:

- Absolute ethanol 6 parts
- Chloroform 3 parts
- 10% glacial acetic acid 1 part

4% neutral buffered formalin (NBF) solution was made up as follows:

- Na_2HPO_4 6.5g
- NaH_2POH_2O 4.0g
- Formaldehyde 100ml
- Deionised water (d.H_2O) 900ml

Both of these fixative solutions were stored at 4^{o}C and used within 7 days.

2.2.3 Processing of fixed tissue samples

Tissues immersion-fixed in Carnoy's solution were transferred into 70% ethanol at 6 hours following collection, then rinsed and placed into fresh 70% ethanol at 24 hours. Tissues which had been immersion-fixed in NBF solution were transferred into $d.H_2O$ at 48 hours following collection. At approximately 72 hours they were rinsed and placed into fresh $d.H_2O$ for a further 24 hours before being rinsed again and transferred into 70% ethanol at 96 hours. Within 2 weeks of collection, tissues were trimmed if required prior to being enclosed in histological processing cassettes (Histosette® I (M490-6) or Macrosette® (M512), Simport, Beloell, QC, Canada). Small tissues such as fetal ovaries and narrow uterine artery sections were first wrapped in velin tissue. Up to 60 cassettes per day were subsequently processed through sequential baths of the following solutions during a 19-hour automated cycle (Citadel 1000, Shandon, Pittsburgh, PA, USA):

• 70% ethanol		60 min	
• 80% ethanol		90 min	
• 95% ethanol		90 min	
• 100% ethanol	x 4	60 / 60 / 90 / 90 min	
• Histo-Clear™ II*	x 3	60 / 90 / 90 min	
• Paraffin wax	x 2	180 / 180 min	(*National Diagnostics, Hull, UK)

Tissues were subsequently embedded in paraffin wax blocks using a HistoEmbedder (Leica Microsystems, Wetzlar, Germany).

2.2.4 Measurement of nutrients and metabolic hormones

2.2.4.1 Glucose

Glucose and lactate concentrations were measured directly in amniotic fluid and maternal, fetal and lamb plasma samples using a dual biochemistry analyser (Model 2700, Yellow Springs Instruments, Yellow Springs, OH, USA). Determinations were made in duplicate and repeated if the coefficient of variation exceeded 5%.

2.2.4.2 Insulin

Insulin concentrations were determined in duplicate in maternal, fetal and lamb plasma samples using a double antibody radioimmunoassay technique, as previously described by MacRae et al. (1991).

Insulin assay buffer was first prepared by adding 0.5% bovine serum albumin to 0.05M phosphate buffer, adjusting the pH to 7.4 and storing at 4^{o}C. Eight standard solutions (ranging from 0.205 to 26.3 µU/ml) were prepared from a stock solution of porcine insulin (Ref. I-3505, Sigma Aldrich Co. Ltd., Poole, Dorset, UK). To start, 500µl of first antibody), raised in guinea pig to porcine insulin (Ref. 65-104, ICN Biomedicals Ltd, Thame, Oxfordshire, UK), at 1:75000 initial dilution, was added to 100µl of each standard solution, 100µl of each plasma sample and to two tubes containing 100µl assay buffer only (for total binding). Tubes were vortexed before being incubated at room temperature overnight (a minimum of 16 hours). The following morning, 100µl of ^{125}I-Insulin tracer (prepared in house using a standardised chloramine-T iodination technique) at 150000–200000 cpm/100µl was added to each tube as well as to two empty tubes (for total counts) and to two tubes containing 600µl assay buffer only (for non-specific binding). Tubes were vortexed before being incubated for 6 hours at room temperature. Thereafter 500µl of a second antibody mixture, containing goat anti-guinea pig serum IgG at 1:150 dilution (Scottish Antibody Production Unit (SAPU), Lanarkshire, UK) and normal guinea pig serum at 1:500 dilution (SAPU), was added to each tube. Tubes were vortexed again before being incubated overnight at 4^{o}C. The following morning tubes were centrifuged at 3000 rpm (1900g) for 20 minutes at 4^{o}C. The supernatant from each tube was decanted off and the residual pellets were counted on an automatic gamma counter (Wallac Wizard™ 1470, PerkinElmer Inc, Cambridge, UK) for 1 minute. A calibration curve for the assay was produced following logistic transformation. The limit of sensitivity of the assay was 2µU insulin/ml and the intra- and inter-assay coefficients of variation were 6.0% and 9.8%, respectively. The inter-assay coefficient of variation was calculated using quality control (QC) plasma samples (known concentrations of insulin ranging from high to low values) at the beginning and end of each assay. All maternal and fetal samples were analysed in a single assay, whilst the lamb plasma samples were processed across a series of 4 consecutive assays.

2.2.4.3 IGF-1

Insulin-like growth factor 1 (IGF-1) concentrations were determined in duplicate following extraction from maternal, fetal and lamb plasma samples using a radioimmunoassay technique, as previously described by Bruce et al. (1991).

IGF-1 assay buffer was first prepared by dissolving 9.0g NaCl, 7.1g Na_2HPO_4, 3.7g sodium EDTA, 5ml polysorbate (Tween) 20 and 1g sodium azide in 1 litre of d.H_2O, adjusting the pH to 7.5 and storing at 4^{o}C. Neutralising buffer was prepared by dissolving 8.5g Na_2HPO_4 in 1 litre of assay buffer and storing at room temperature. Dummy extract solution was prepared by adding 2ml d.H_2O, 0.5ml 2.4M formic acid and 10ml ethanol to 75ml neutralising buffer and

storing at room temperature. To being the extraction procedure, 50µl of each plasma sample was pipetted into an eppendorf tube, to which was added 12.5µl of 2.4M formic acid followed by 250µl ethanol. Tubes were capped, vortexed and stored at room temperature for 30 minutes. Next they were centrifuged at 2200rpm (1000g) for 30 minutes at 4^{o}C, following which 50µl of each supernatant was transferred to a 5ml assay tube and diluted with 300µl neutralising buffer. Assay tubes were capped, vortexed and stored overnight at 4^{o}C. The following morning, 20µl of each neutralised extract was transferred to a new assay tube and diluted with 80µl dummy extract solution. Seven standard solutions (ranging from 0.0025 to 0.16 pmol/ml) were prepared from a stock solution of IGF-1 (Ref. IP9010, Peninsula Laboratories Europe Ltd, St. Helens, Merseyside, UK). To begin the assay, 300µl of anti-serum, raised in rabbit to human IGF-1 (Ref. M280(1) provided by Dr G. Holder (University Hospitals Birmingham NHS Trust, Birmingham, UK), at 1:2400 initial dilution, was added to each sample tube, to 100µl of each standard solution and to two tubes containing 100µl dummy extract solution only (for total binding). At the same time 300µl of assay buffer was added to a further two tubes containing 100µl dummy extract solution only (for non-specific binding). Tubes were vortexed and incubated at room temperature for 5 hours. Thereafter 100µl of ^{125}I-IGF-1 tracer (prepared in house using a standardised N-bromo-succinimide iodination technique) at 120000–150000 cpm/100µl was added to all tubes as well as to two empty tubes (for total counts). Tubes were vortexed again before being incubated overnight at 4^{o}C. The following day, 100µl of 1% bovine gamma-globulin and 2ml 16.25% polyethylene glycol (PEG) solution (containing 0.01g/ml sodium azide) was added to all tubes except total counts. Tubes were vortexed and incubated at room temperature for 1 hour before being centrifuged at 3000 rpm (1900g) for 30 minutes at 4^{o}C. The supernatant from each tube was decanted off and the residual pellets were counted immediately using an automatic gamma counter (Wallac Wizard™ 1470) for 1 minute each. A calibration curve for the assay was produced following logistic transformation. The limit of sensitivity of the assay was 5 pmol/ml and the intra- and inter-assay coefficients of variation were 8.8% and 7.4%, respectively. The inter-assay coefficient of variation was calculated using four different QC plasma samples (known concentrations of IGF-1) at the beginning and end of each assay. All maternal and fetal samples were analysed in a single assay, whilst serial lamb plasma samples were processed across two consecutive assays.

3.1 Introduction

One of the main objectives of the work reported in this thesis was to determine the effects of gene therapy on fetal growth trajectories as well as the primary outcome measures of uterine blood flow in late gestation and birth weight near to term (see Chapters 4 and 5, respectively). Consequently it was important to validate the methodology used for the ultrasound assessment of ovine fetal growth.

3.1.1 Background

As detailed in Section 1.1.4.3, the most widely used ultrasound measurements for the evaluation of longitudinal fetal growth in human pregnancy are the biparietal diameter (BPD), head circumference (HC), abdominal circumference (AC) and femur length (FL). These biometric parameters are surrogate markers of fetal body weight and in clinical practice are also used singly or in combination, for the point estimation of fetal weight *in utero* using one of a large range of published regression equations, albeit with considerable systematic errors of up to 25%, particularly in cases of FGR or macrosomia (Platz & Newman 2008). In sheep, ultrasound has previously been used to track fetal growth longitudinally by measurement of BPD, AC and FL, as well as TL, thorax height and abdominal diameter (Barbera et al. 1995a; Galan et al. 1999; Parraguez et al. 2005). Direct measurement of the HC using an ellipse is not feasible because, unlike the human fetus, the ovine fetal head is not oval in the transventricular plane. An alternative method of determining the HC in clinical practice is to calculate it from the BPD and occipito-frontal diameter, which are measured at right angles to one another. Although an equivalent anteroposterior head measurement has been described in the sheep (OSL) there are no published regression equations to be able to derive an equivalent of the HC. With respect to the remaining parameters, it has not specifically been established which of these best reflect ovine fetal growth, which has been shown to follow a different pattern compared to the human (Barbera et al. 1995b). It is also generally not known which biometric parameters can be measured most accurately, although it has been shown that the BPD and renal length correlate strongly with equivalent measurements made at post-mortem in fetal sheep (Ward et al. 2006). Regarding the estimation of fetal weight, there are no ovine-specific equations published in the literature. Previous work using ultrasound in the overnourished adolescent paradigm demonstrated that the fetal trunk diameter, renal width and renal length at 116 days gestation were the strongest predictors of fetal body weight

Figure 3.1 – Historical cross-sectional fetal weight data in the overnourished adolescent model

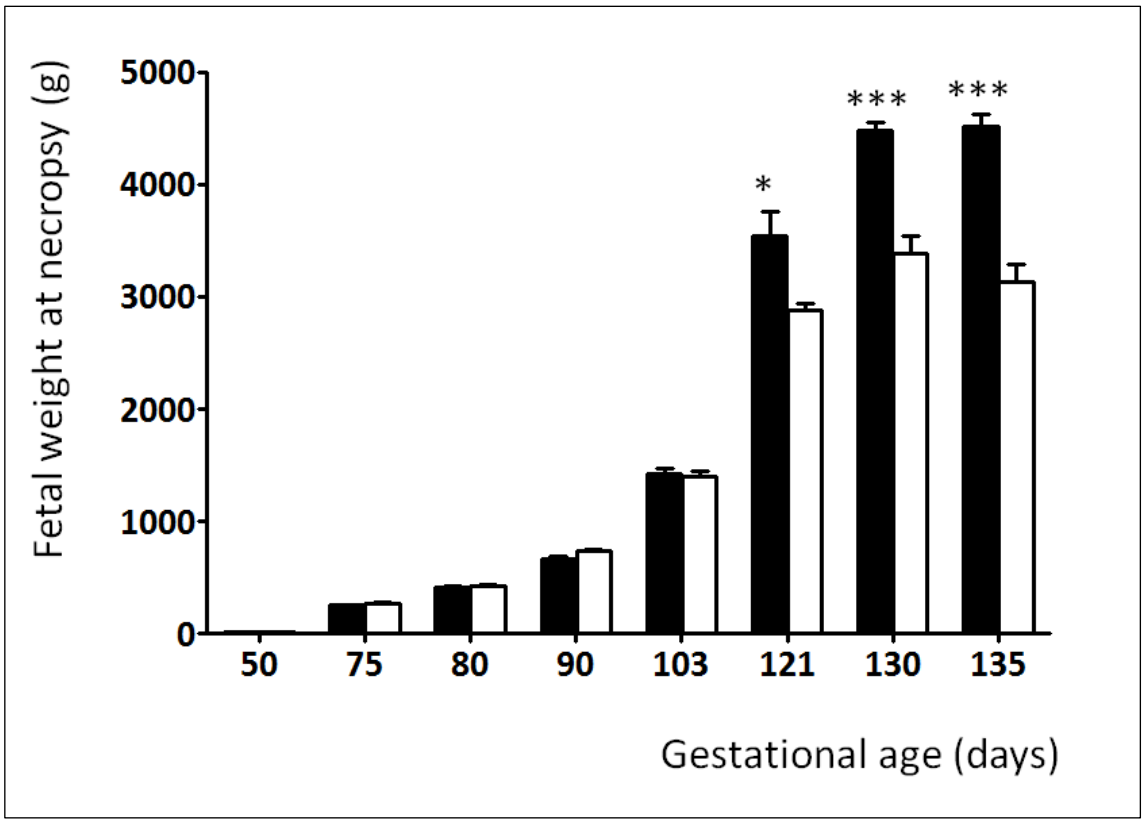

Fetal weight in 236 singleton-bearing adolescent ewes that were fed a control intake (closed bars, n=115) or high intake (open bars, n=121) from the first week of gestation until necropsy (term = 145 days). Data summarised from 6 different studies (Redmer et al. 2005, Redmer et al. 2009, Wallace et al. 2002, Da Silva et al. 2003*, Wallace JM and Aitken RP, unpublished data) * p<0.05, ** p<0.01, *** p<0.001*

---

at 134 days gestation (Bourke et al. 2002). Although renal measurements are not used for the assessment of fetal growth *per se* in clinical practice, these experimental findings implied that an assessment of renal size might be promising for the estimation of ovine fetal weight, hence an evaluation of renal biometry was included here. We planned to extend the previously used two-dimensional measurements (renal width and length) to include the anteroposterior kidney diameter, thus allowing for the additional calculation of renal volume.

Longitudinal fetal growth velocity by means of ultrasound has not been evaluated to date in the overnourished adolescent ewe. Impressions about the timing and pattern of FGR in this model have been derived from cross-sectional data from various studies that were terminated at different stages of gestation (Figure 3.1). These results indicate that the FGR observed

following overnourishment of the growing adolescent is relatively late in its onset, equivalent to the third trimester of human pregnancy. However a major limitation of this type of cross-sectional data is that each time point is derived from a different cohort of pregnancies and it is well recognised that there is a significant degree of year-on-year variation in the birth weights of both normal and experimentally growth-restricted lambs. Ultrasound represents a non-invasive method of repeatedly assessing growth in a single cohort of ongoing pregnancies and might be expected to facilitate detection of more subtle alterations in the longitudinal pattern of fetal growth.

As discussed in Section 1.1.5.2, not all pregnancies of overnourished adolescent ewes result in a significant degree of FGR. Approximately 52% of fetuses are born with a birth weight that falls more than 2SD below the mean birthweight of contemporaneous ewes receiving a control dietary intake (Wallace et al. 2006a). In these markedly FGR pregnancies, both fetal and placental weight are reduced by approximately 48%. Historically the remaining 48% of fetuses are less perturbed, with 23% and 10.5% reductions in placental and fetal weights, respectively. Whilst these represent *statistically* significant deviations from control-intake pregnancies, this is *biologically* much less significant and consequently such pregnancies have been classified as non-FGR (Wallace et al. 2004b). Hence a non-invasive means of distinguishing at an early stage between those pregnancies that are destined to be markedly FGR and non-FGR, respectively, in late gestation would be extremely useful as it would potentially allow putative therapeutic interventions to be evaluated in the most severely compromised pregnancies.

3.1.2 Aims

- To investigate the accuracy of different fetal ultrasound parameters, and determine which:

  (a) can be most accurately measured, i.e. correlate best with fetal measurements with the narrowest limits of agreement

  (b) are the best surrogate markers of fetal weight, i.e. correlate best with fetal body weight at necropsy

- To develop estimated fetal weight equations for the sheep and to evaluate their precision

- To compare measurements of the following between control- and high-intake pregnancies:

  - longitudinal fetal growth velocity - using a range of different biometric parameters
  - UA Doppler indices
  - ultrasound indices of placental size (placentome index)

- ultrasound indices of amniotic fluid volume (deepest vertical pool of liquor)

- To develop reference charts of normal fetal growth for this genotype (for future studies)

- To retrospectively compare the prenatal growth trajectories of fetuses of high-intake ewes eventually categorised as FGR or non-FGR and to determine when these become divergent

3.2 Materials and Methods

A secondary analysis was performed on the ultrasound data collected from sheep pregnancies comprising the control groups for the two main studies detailed within this thesis. Thirty-nine ewes were included from the late gestation study (Chapter 4) and consisted of 12 control- and 27 high-intake pregnancies that were treated with control saline or control vector (Ad.LacZ). It was originally considered that Ad.LacZ might potentially have a detrimental effect of fetal growth, as a consequence of adenoviral infection of the uterine circulation in the absence of a potentially therapeutic transgene. However, a comparison of high-intake pregnancies treated Ad.LacZ versus saline did not reveal any significant differences between these two control treatments (see Section 4.2.7). Therefore it was considered valid to include both Ad.LacZ- and saline-treated ovenourished (FGR) pregnancies for the secondary analyses detailed herein.

Additional ultrasound data was collected from three further control-intake ewes that did not undergo surgery and inclusion into the main cohort, but whose pregnancies were contemporaneously established and nutritionally managed in exactly the same way as their operated counterparts. Thirteen high-intake ewes that received control saline in the postnatal study (Chapter 5) and which underwent full ultrasound evaluation were also included. Pregnancies in either study that received active gene therapy (Ad.VEGF-A_{165}) with the aim of altering fetal growth (n=35) were excluded from this subanalysis.

3.2.1 Establishment of singleton pregnancies and nutritional management

Oestrus synchronisation of adolescent recipient and adult donor ewes was carried out during the mid breeding season (detailed in Section 2.1.1.1). Donor ewes underwent superovulation, laparoscopic intrauterine insemination with semen from a single sire (see Section 2.1.1.2) and embryo recovery four days later (Section 2.1.1.3). Embryos were synchronously transferred into the uteri of the adolescent recipient ewes to generate exclusively singleton pregnancies of precisely known gestational age and maximum genetic homogeneity (see Section 2.1.1.4). Immediately following the embryo transfer and throughout gestation, adolescent recipient ewes received a control- or high-intake of the same complete diet (detailed in Section 2.1.2) to generate normal and compromised placental and fetal growth trajectories, respectively.

3.2.2 Ultrasound and pregnancy outcome data collection

Ewes within the late gestation and postnatal studies underwent serial ultrasound examination at approximately weekly intervals between 79±0.1 and 133±0.1 days, and between 83±0.1 and 126±0.3 days gestation, respectively. The following ultrasound parameters were measured or caculated as described in Section 2.1.3: abdominal circumerence (AC), trunk diameter (TD), biparietal diameter (BPD), occipito-snout length (OSL), renal length (RL), anteroposterior renal diamter (APRD), transverse renal diameter (TRD), renal volume (RV); femur length (FL), tibia length (TL), placentome index, the deepest vertical pool (DVP) of amiotic fluid, and umbilical arterial (UA) maximum (or peak systolic) velocity (Vmax), minimum (or end-diastolic) velocity (Vmin), time-averaged maximum velocity (TAMAX), pulsatility index (PI), resistance index (RI) and systolic to diastolic ratio (SDR). In addition, the BPD:AC and BPD:FL ratios were determined as indices of fetal brain sparing (see Section 1.1.3.4).

3.2.2.1 Necropsy group

The 39 pregnancies from the late gestation study (Chapter 4) were necropsied at 131±0.2 days gestation, as described in Section 4.2.5. Fetuses were dried and weighed. The biparietal head diameter was measured using callipers at the widest point between the two parietal bones. Abdominal girth was measured at the level of the umbilical cord insertion and at right angles to the spine, taking care to reproduce the same plane each time. Girth was also measured at the level of the lowermost rib in an attempt to reproduce the ultrasound AC plane. During fetal dissection the femur and tibia were removed, cleared of overlying tissue and the length of the shaft of each bone was measured using callipers. All major fetal internal organs were weighed. Whole placentomes (fetal cotyledons plus maternal caruncles) were completely dissected from the membranes and their combined weight was recorded. Additional ultrasound data from the extra 3 control-intake ewes was included in this group for the purpose of assessing longitudinal fetal growth velocity however, as these ewes did not undergo necropsy, correlation with post-mortem measurements was limited to the other 39 ewes.

3.2.2.2 Delivery group

The 13 pregnancies in the postnatal study (Chapter 5) were allowed to continue uninterrupted and resulted in spontaneous delivery near term (141±0.4 days gestation). One ewe required an emergency caesarean section due to cervical dystocia. Lambing was managed according to the protocols described in Section 5.2.4. After initial resuscitation (where required), lambs were dried and weighed. The abdominal girth at the level of the umbilicus was measured as described above. Following delivery the placenta was dissected and weighed. Total fetal

Figure 3.2 – Study timeline

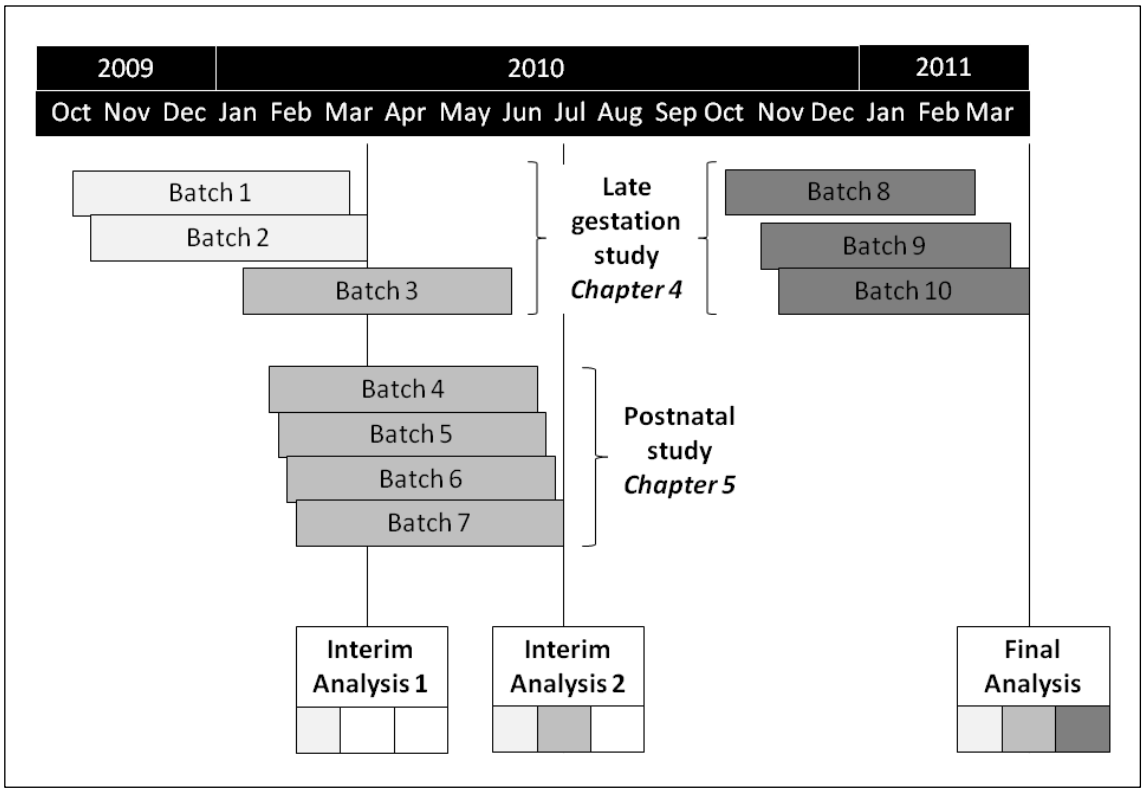

Study timeline showing the chronology and synchronicity of 10 different batches of sheep pregnancies in which fetoplacental growth was evaluated using transabdominal ultrasound. Points at which interim analyses of ultrasound data was performed are indicated.

---

cotyledon weight was determined and the total fetal placental weight calculated as the sum of the fetal cotyledon and residual membrane weights.

3.2.3 Data analysis

Ultrasound data was sequentially analysed at three different stages during the course of the 10 individual batches of pregnancies making up the two main studies for this thesis (Figure 3.2).

3.2.3.1 First interim analysis

An initial interim analysis was performed following completion of the first 2 batches of sheep experiments in March 2010. At this point simultaneous management of a further 5 batches of sheep experiments was about to commence, which meant that the time available for scanning was greatly reduced. Consequently it became clear that it would not be feasible to measure complete fetal biometry during the second study (batches 4 to 7), as to date this had required

approximately 30 minutes per animal per week. Consequently the aim of the first interim analysis was to determine which parameters should continue to be measured and which should be abandoned. In order to decide this the various fetal biometric parameters were ranked on the basis of:

1. The strength of their correlation with relevant physical measurements at necropsy
2. The strength of their correlation with fetal body weight at necropsy
3. The significance level of any differences between control- and high-intake pregnancies

3.2.3.2 Second interim analysis

A second interim analysis was performed after completion of the first 7 experimental batches in June 2010. At this stage ultrasound data was available for 50% of the necropsy group (n=19) and the reference arm of the completed delivery group (n=16), allowing for further correlation of the various parameters with physical measurements and necropsy/birth weight, as well as the generation of estimated fetal weight equations based on data from fetuses and lambs of a wide range of different sizes (range 2622–6260g and 1720–6050g for the necropsy and delivery groups, respectively). Comparisons between control- and high-intake groups were postponed until the final analysis in view of the relatively unbalanced numbers at this stage (n=6 versus n=26, respectively).

3.2.3.3 Third and final analysis

After completion of all 10 experimental batches, ultrasonographic fetal growth velocity, UA Dopplers and indices of placental size and amniotic fluid volume were compared between control-intake and high-intake pregnancies within the necropsy group (n=15 versus n=27, respectively). The high-intake pregnancies were further subcategorised into marked FGR or non-FGR groups based on whether the necropsy weight fell >2SD below the control-intake mean. Ultrasound measurements were compared between marked FGR and non-FGR groups to determine at what stage any significant differences became apparent.

3.2.3.4 Statistical methods

As this was a secondary analysis of data collected during the two gene therapy studies detailed in this thesis, the number of control (untreated) pregnancies available used for these purposes was limited by the power calculations for each primary study, which were based on anticipated changes in UBF and lamb birth weight, respectively (see Sections 4.2.1 and 5.2.1 for details). Nevertheless a retrospective power calculation was made using the parameters which showed

the largest and smallest differences between nutritional treatment (AC and BPD, respectively) based on the maximum variability (SD) at 126 days gestation and the percentage differences observed between control- and high- intake pregnancies at this stage. For the BPD, given the inter-animal variability of 0.99mm, it was calculated that 7 or 9 animals were needed to detect a 3.1% reduction in this measurement (1.7mm) with 80% or 90% power, respectively. For the AC, given the inter-animal variability of 8.25mm, it was estimated that only 4 animals were required to detect a 8.1% reduction in this measurement (23mm) at both 80% and 90% power.

All data are presented as mean ± standard error of the mean (SEM) unless otherwise specified. Analysis was carried out using the Statistical Package for the Social Sciences (SPSS) versions 17.0 to 21.0 (SPSS Inc., Chicago, IL, USA). Due to the variable time interval between the final detailed ultrasound scan and either necropsy or spontaneous delivery (4.6±1.83 and 8.0±2.49 days, respectively) a statistical adjustment was made to the necropsy and birth weight in order to estimate the fetal weight *in utero* on the day of the final ultrasound examination. Fetal weight was adjusted using the following formula, which was derived from serial necropsy studies in late gestation, as previously described (Wallace et al. 2008b):

Adjusted fetal weight (AFW) = weight at necropsy or birth / 1.01305 per day of gestation

Ultrasound measurements were correlated with both AFW and actual necropsy/birth weights (as well as relevant post-mortem measurements of the fetus) using Pearson's product moment test. Limits of agreement were also calculated (where appropriate) by subtracting ultrasound measurements from their respective necropsy measurements, and then determining the 95% confidence intervals for the mean difference. Comparisons were made between the control-intake and high-intake groups and marked FGR and non-FGR subgroups using Student's t test. In order to generate equations for the estimation of fetal weight, AFW values were first logarithmically transformed and plotted against the raw values for each ultrasound parameter as this provided the best fit for the data. All possible combinations of five different biometric parameters (AC, RV, BPD, FL and TL) as well as their quadratic and cubic terms were entered into a multiple parameter model. Stepwise forward and backward regression analyses were used to identify the combination of terms providing the highest R^2 values and lowest standard error of the estimate (SE). The adjusted R^2 value was used to determine whether incorporating additional parameters genuinely improved the model or not. This is because raw R^2 values can be increased by simply adding in more independent variables, without any corresponding improvement in the goodness of fit. By contrast, increases in adjusted R^2 indicate that an additional parameter is adding something extra and refining the model, rather than simply increasing its complexity.

3.3 Results

3.3.1 Evaluation of ultrasonographic fetal biometry

3.3.1.1 Interim analysis 1

Table 3.1 shows the results from the first interim analysis after the completion of the first two batches (13 pregnancies in total). Each biometric parameter was assigned a rank according to the strength of its correlation with relevant post-mortem measurements, its correlation with fetal body weight, and the significance level of the difference between control- and high-intake pregnancies (p value corresponding to the respective t value, with 12 degrees of freedom). The AC, TD and RV were the parameters with the highest overall ranking. On the basis of these preliminary results, the decision was made to omit measurements of BPD, FL and TL for the postnatal study cohort (batches 4 to 7), whilst all fetal biometric parameters continued to be measured for the remaining batches contributing to the late-gestation study (batches 8 to 10).

It should be noted that it was not feasible to include the OSL in this evaluation as, although the measurement was easy to obtain in mid-gestation, it subsequently became very difficult as the pregnancy progressed beyond 0.8 gestation. At 119±0.1 and 126±0.1 days gestation it was not possible to visualise both the occiput and snout in the same plane, hence OSL measurements could not be obtained in 8 (62%) and 11 (85%) pregnancies, respectively. Consequently it was not appropriate to correlate OSL with post-mortem fetal measurements or fetal body weight, or to make any meaningful comparisons between nutritional groups.

3.3.1.2 Interim analysis 2 - correlation with fetal measurements at necropsy/birth

Table 3.2 details the correlation of the various ultrasound indices with their respective physical measurements and organ weights at necropsy (19 pregnancies in total). In addition limits of agreement were determined for ultrasound versus post-mortem fetal measurements where the units of measurement were the same (i.e. BPD, TL, FL and AC/girth). The AC demonstrated the strongest correlation with post-mortem biometry. An attempt to reproduce the ultrasound plane at post-mortem examination when measuring abdominal girth did not improve the level of correlation more than that of girth at the level of the umbilicus, which is ultimately a more reproducible landmark, and the TD correlated less strongly than the AC for all parameters.

Although the ultrasound BPD measurement correlated strongly with fetal brain weight, the correlation between post-mortem and ultrasound BPD measurements was the least strong of all the parameters. The limits of agreement for the BPD included both positive and negative values, indicating that it is possible to both over- and under-estimate the BPD by ultrasound.

Table 3.1 – Comparison of ultrasonographic fetal biometry at 126 days gestation with post mortem fetal biometry at 131 days gestation in the first two experimental batches (interim analysis 1, n=13 pregnancies)

Ultrasound parameter	Correlation with post-mortem measurements		Correlation with fetal weight at necropsy		Difference between control- and high-intake ewes (t-test)		Overall Rank
	r value	Rank	r value	Rank	p value	Rank	
AC	0.660	1	0.682	1	<0.001	1	1
TD	0.618	3	0.604	2	0.001	2	2
RV	0.620	2	0.582	4	0.169	5	3
BPD	0.533	6	0.602	3	0.070	3	4
TL	0.586	4	0.524	5	0.357	6	=5
FL	0.549	5	0.509	6	0.168	4	=5

All correlations shown are statistically significant at p<0.05. Correlations with post-mortem measurements as follows: AC and umbilical girth; TD and umbilical girth; RV and renal weight; BPD and biparietal head diameter; FL and length of femoral shaft; TL and length of tibial shaft. Abbreviations: AC = abdominal circumference; RV = renal volume; BPD = biparietal diameter; TL = tibia length; FL = femur length. Correlations performed using Pearson's product moment test. Control and high-intake comparisons made using Student's t-test.

By contrast, limits of agreement for AC, TL and FL were exclusively positive, which was to be expected given: (1) the time lapse between ultrasound and necropsy (up to 10 days); and (2) that there are systematic differences in the measurements of these parameters on ultrasound versus at post-mortem. Notably all limits of agreement were wide, which likely reflects the relatively small numbers of animals from which these were generated.

In the delivery cohort, AC also correlated well with umbilical girth (r=0.776, n=13, p<0.001). No ultrasound BPD measurements were available for comparison with neonatal biparietal head diameter measurements and it was not feasible to measure femur or tibia length in live lambs.

3.3.1.3 Interim analysis 2 - correlation with fetal body weight at necropsy/birth

Table 3.3 details the correlations between the various fetal ultrasound measurements and

Table 3.2 – Comparison of ultrasonographic fetal biometry at 126 days gestation with post mortem fetal biometry at 131 days gestation in the first three experimental batches (interim analysis 2, n=19 pregnancies)

Ultrasound parameter	Measurement at post-mortem	Correlation coefficient (r)	95% limits of agreement (mm)
AC	Girth (level of umbilicus)	0.833	22.0 – 104.0
AC	Girth (ultrasound plane)	0.827	14.9 – 78.6
AC	Liver weight	0.799	N/A
TD	Girth (level of umbilicus)	0.801	N/A
TD	Girth (ultrasound plane)	0.794	N/A
TD	Liver weight	0.783	N/A
BPD	Brain weight	0.774	N/A
RV	Renal weight	0.754	N/A
FL	Length of femoral bone	0.747	19.3 – 36.3
TL	Length of tibial bone	0.719	15.0 – 36.0
BPD	Biparietal head diameter	0.654	-13.9 – 50.3

All correlations shown are statistically significant at p<0.001. Abbreviations: AC = abdominal circumference; TD = trunk diameter, BPD = biparietal diameter; RV = renal volume; FL = femur length; TL = tibia length. Correlations performed using Pearson's product moment test. Limits of agreement are provided where paired ultrasound and necropsy parameters have the same units of measurement.

---

necropsy/birth weight (both raw and adjusted values) across both cohorts (n=32). Adjustment for time interval marginally improved the correlation for all parameters except the BPD. The AC correlated most strongly with fetal weight, followed by RV, whilst BPD correlated least well.

3.3.2 Estimated fetal weight equations

3.3.2.1 Interim analysis 2 - generation of regression equations

Linear stepwise forward and backward regression was used to generate fetal weight equations based on the following five parameters: AC, RV, BPD, FL and TL. The OSL was not included here given the limitations described above (Section 3.3.1.1) and the TD was excluded in view of its

Table 3.3 – Correlations between ultrasonographic fetal biometry at 126/133 days gestation and necropsy/birth weight at 131/141 days gestation (interim analysis 2, n=32 pregnancies)

Ultrasound parameter	Correlation (r) with necropsy/birth weight	Correlation (r) with adjusted fetal weight
AC	0.809	0.839
RV	0.789	0.800
TD	0.764	0.791
FL	0.761	0.766
TL	0.709	0.714
BPD	0.672	0.659

All correlations shown are statistically significant at p<0.001. Abbreviations: AC = abdominal circumference; RV = renal volume; TD = trunk diameter; FL = femur length; TL = tibia length; BPD = biparietal diameter. Correlations performed using Pearson's product moment test.

Table 3.4 – Strongest estimated fetal equations for each fetal ultrasound parameter, based on final measurements in late gestation (interim analysis 2, n=32 pregnancies)

Ultrasound parameter(s)	Regression equation	R^2	SE	Adjusted R^2
BPD	Log EFW = 1.2 + 0.044 BPD	0.45	0.079	0.41
TL	Log EFW = 2.502 + 0.014 TL	0.54	0.068	0.51
FL	Log EFW = 2.351 + 0.022 FL	0.63	0.061	0.61
RV	Log EFW = 2.568 + 0.18 RV – 0.007 RV^2	0.67	0.072	0.64
AC	Log EFW = – 0.885 + 0.028 AC + 0.00004263 AC^2	0.72	0.067	0.70
AC+RV	**Log EFW = 2.115 + 0.003 AC + 0.12 RV – 0.005 RV^2**	**0.75**	**0.064**	**0.72**

Regression equations generated by linear regression. Abbreviations: SE = standard error of the estimate; BPD = biparietal diameter; EFW = estimated fetal weight; TL = tibia length; FL = femur length; RV = renal volume; AC = abdominal circumference.

similarity to the AC but relatively weaker correlation with fetal weight (Section 3.3.1.3). The AC and RV both demonstrated a quadratic relationship with $\log_{10}$AFW, whilst the BPD, FL and TL demonstrated a linear relationship. Table 3.4 shows the derived formulae and values for each individual biometric parameter as well as the strongest multiple-parameter combination. Mathematically the AC and RV were the best predictors of fetal weight, both independently and in combination with one another. Addition of a third, fourth or fifth biometric parameter did not significantly increase the adjusted R^2 value beyond that of the two-parameter AC+RV model (data not shown).

3.3.2.2 Interim analysis 2 - accuracy of regression equations (internal validation)

The three best equations from Table 3.4 were subsequently applied to each individual fetus within the data set to generate an estimated fetal weight (EFW) value. Each of these estimates was compared with both the raw necropsy/birth weight (NBW) and the AFW to determine the prediction error, both as an absolute value (in g) and as a percentage of actual weight. These results are shown in Table 3.5. Each error was taken as a positive value for the purposes of calculating the mean and SEM. In addition, the proportion of estimates falling within 5, 10, 15, 20 and 25% of the actual values were determined, and the correlation between NBW/AFW and EFW was examined. Prediction error for each equation was compared using one-way ANOVA. There were no statistically significant differences in performance between the three estimated fetal weight equations, although the combined AC+RV equation produced the lowest errors.

The two strongest parameters (AC and RV) were further evaluated by comparing the necropsy and delivery groups, which differed by a week in the gestational age at the final ultrasound examination (126±0.1 and 133±0.1 days gestation, respectively). The correlation between AC/RV, AFW and the absolute prediction error of each regression equation were determined separately for the necropsy and delivery groups and are shown in Table 3.6. The AC demonstrated a stronger correlation with fetal weight at 126±0.1 compared with 133±0.1 days gestation, whilst the RV showed the opposite trend. However differences in absolute prediction error between the three equations were not statistically different between groups.

A further analysis was performed to determine whether or not the prediction error of these equations varied at the extremes of fetal weight. Overall, NBW was weakly correlated with mean prediction error using the AC (r=0.533, p=0.02) but not the RV or AC+RV equations (r=0.095 and 0.147 respectively). Fetuses were stratified into 4 birth weight quartiles according to unadjusted NBW (n=8 each). The mean absolute prediction errors for the AC, RV and AC+RV combined equations were calculated for each group and the results are shown in Figure 3.3.

Table 3.5 – Performance of the three strongest fetal weight estimation equations, based on final ultrasound measurements in late gestation (interim analysis 2, n=32 pregnancies)

Ultrasound parameter(s)	**RV**	**AC**	**AC + RV**
Adjusted fetal weight:			
Mean absolute prediction error (g)	458 ± 54.4	470 ± 63.2	396 ± 53.5
Mean percentage prediction error	13.2 ± 1.8%	12.4 ± 1.4%	11.1 ± 1.4%
Correlation (r) – EFW versus AFW	0.809	0.833	0.856
Estimates within 5%	18.8%	15.6%	28.1%
Estimates within 10%	46.9%	40.6%	50.0%
Estimates within 15%	68.8%	68.8%	71.9%
Estimates within 20%	81.3%	87.5%	84.4%
Estimates within 25%	90.6%	90.6%	96.9%
Necropsy/birth weight:			
Mean absolute prediction error (g)	576 ± 69.4	656 ± 94.4	550 ± 75.6
Mean percentage prediction error	14.1 ± 1.6%	15.4 ± 1.8%	13.2 ± 1.6%
Correlation (r) – EFW versus NBW	0.797	0.802	0.835
Estimates within 5%	18.8%	15.6%	28.1%
Estimates within 10%	37.5%	25.0%	37.5%
Estimates within 15%	53.1%	46.9%	65.6%
Estimates within 20%	75.0%	75.0%	78.1%
Estimates within 25%	87.5%	84.4%	81.3%

Abbreviations: RV = renal volume; AC = abdominal circumference; EFW = estimated fetal weight; AFW = adjusted fetal weight; NBW = necropsy/birth weight. Data presented as mean ± SEM. Correlations performed using Pearson's product moment test.

Table 3.6 – Performance of AC, RV and AC+RV estimated fetal weight equations according to gestational age at ultrasound assessment - necropsy versus delivery cohorts (interim analysis 2, n=32 pregnancies)

Ultrasound Parameter(s)	Correlation coefficient (r)			Absolute Prediction Error (g)		
	Necropsy Group[a]	Delivery Group[b]	All	Necropsy Group[a]	Delivery Group[b]	All
AC	0.852	0.776	0.839	455 ± 63.7	490 ± 128.2	470 ± 63.2
RV	0.725	0.869	0.800	516 ± 68.7	374 ± 86.4	458 ± 54.4
AC+RV				398 ± 63.6	392 ± 96.5	396 ± 53.5

(a) Fetuses in the necropsy group were scanned at ~126 and necropsied at ~131 days gestation. (b) Lambs in the delivery cohort were scanned at ~133 and delivered at ~141 days gestation. Mathematical corrections were made for the interval between the day of ultrasound scan and day of necropsy/birth, as described in Section 3.2.3.4. Abbreviations: AC = abdominal circumference; RV = renal volumes. Data presented as mean ± SEM. Correlations performed using Pearson's product moment test.

Groups were compared using one-way ANOVA. Post-hoc pairwise comparisons (test of LSD) between the highest and lowest quartiles demonstrated a significantly higher error using the AC-only equation in the largest fetuses (670±60.7g versus 300±44.7g, respectively, p=0.036). There were no other significant differences between quartiles and prediction error associated with the RV-only and the AC+RV equations was broadly similar across the full range of NBW.

3.3.2.3 Final analysis - accuracy of regression equations (external validation)

It is well recognised that mathematical models perform significantly better within the dataset from which they are derived and should therefore be externally validated in a separate dataset (Harrell et al. 1984). Accordingly, upon completion of the final 3 batches, performance of the hitherto strongest equation (AC+RV) was examined again in this completely new cohort of 23 pregnancies, comprised of 9 control- and 16 high-intake ewes with necropsy weights ranging from 3190 to 5996g. The resultant prediction errors are presented in Table 3.7 and compared

Figure 3.3 – Performance of AC/RV estimated fetal weight equations by birth weight quartile

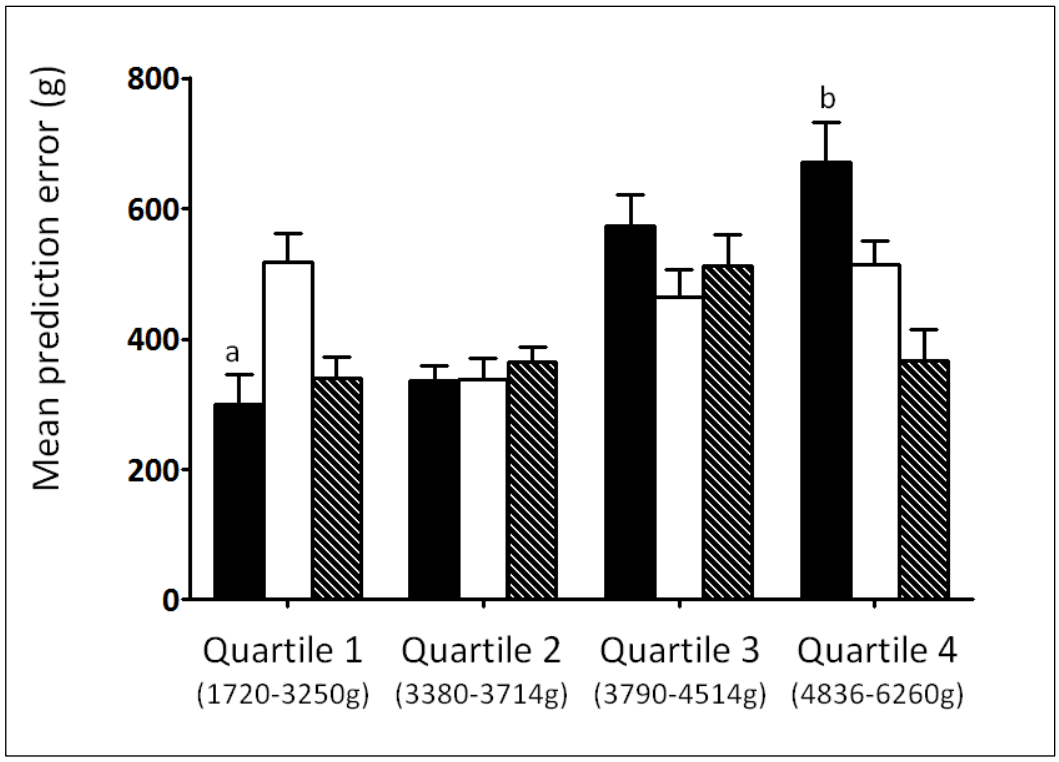

Bar chart comparing the mean prediction errors of 3 different estimated fetal weight equations by necropsy/birth weight quartile for 32 fetuses of singleton-bearing adolescent dams. Equations were derived from the abdominal circumference (AC, closed bars), renal volume (RV, open bars) or AC+RV combined (hatched bars). Mean prediction error was significantly greater for the AC-only equation when comparing the largest (b) versus smallest (a) fetuses (p=0.036).

---

against those from evaluation within the original dataset. There were no statistically significant differences between the degree of precision in the two different datasets and the magnitude of error was broadly similar between them.

3.3.3 Fetal growth velocity

Serial measurements of AC, TD, BPD, OSL, RL, TRD, APRD, RV, TL and FL were plotted against gestational age and compared between control- and high-intake ewes at each time point using Student's t test to characterise the temporal pattern of fetal growth restriction induced by overnourishment of the adolescent ewe.

3.3.3.1 Abdominal circumference and trunk diameter

Figure 3.4A shows serial measurements of the AC between 83±0.1 and 126±0.3 days gestation.

Table 3.7 – Comparison of AC+RV equation performance in 2 different datasets (final analysis, n=55 pregnancies)

Dataset	**Internal Validation Dataset (n=32)**	**External Validation Dataset (n=23)**
Adjusted fetal weight:		
Mean absolute prediction error (g)	396 ± 53.5	449 ± 61.9
Mean percentage prediction error	11.1 ± 1.4%	10.6 ± 1.5%
Correlation (r) – EFW versus AFW	0.856	0.849
Estimates within 5%	28.1%	26.3%
Estimates within 10%	50.0%	47.4%
Estimates within 15%	71.9%	78.9%
Estimates within 20%	84.4%	89.4%
Estimates within 25%	96.9%	100.0%
Necropsy/birth weight:		
Mean absolute prediction error (g)	550 ± 75.6	637 ± 76.5
Mean percentage prediction error	13.2 ± 1.6%	14.4 ± 1.8%
Correlation (r) – EFW versus NW	0.835	0.879
Estimates within 5%	28.1%	10.5%
Estimates within 10%	37.5%	31.6%
Estimates within 15%	65.6%	47.4%
Estimates within 20%	78.1%	68.4%
Estimates within 25%	81.3%	89.4%

Abbreviations: RV = renal volume; AC = abdominal circumference; EFW = estimated fetal weight; AFW = adjusted fetal weight; NW = necropsy/birth weight. Data presented as mean ± SEM. Correlations performed using Pearson's product moment test.

Figure 3.4 – Fetal growth velocity: abdominal circumference and trunk diameter

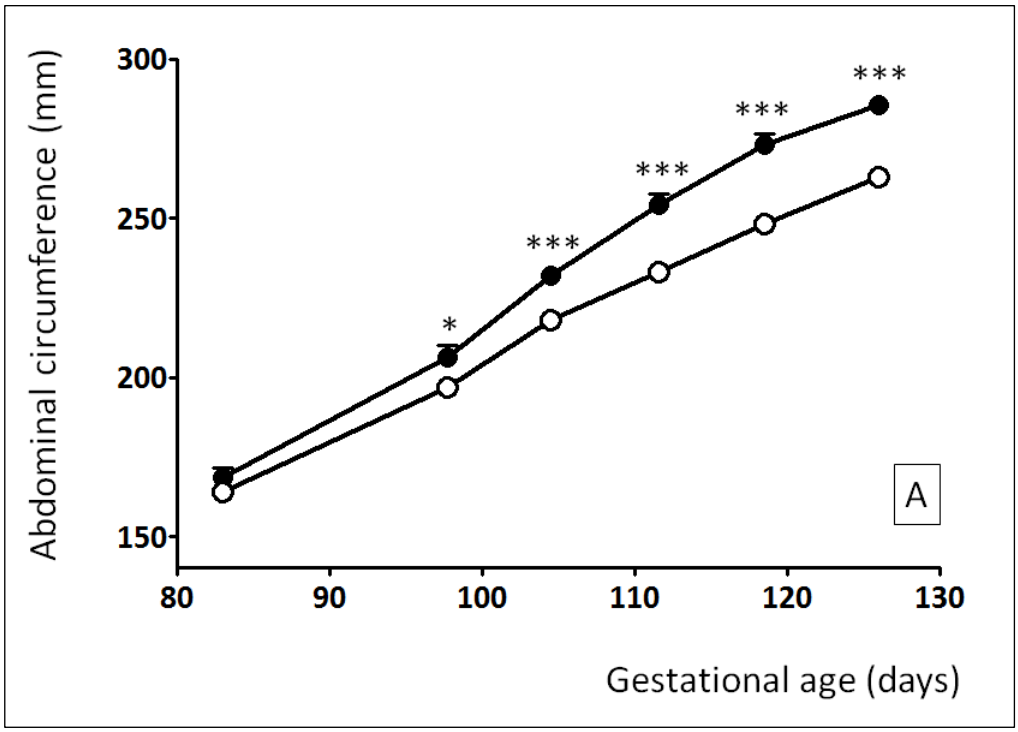

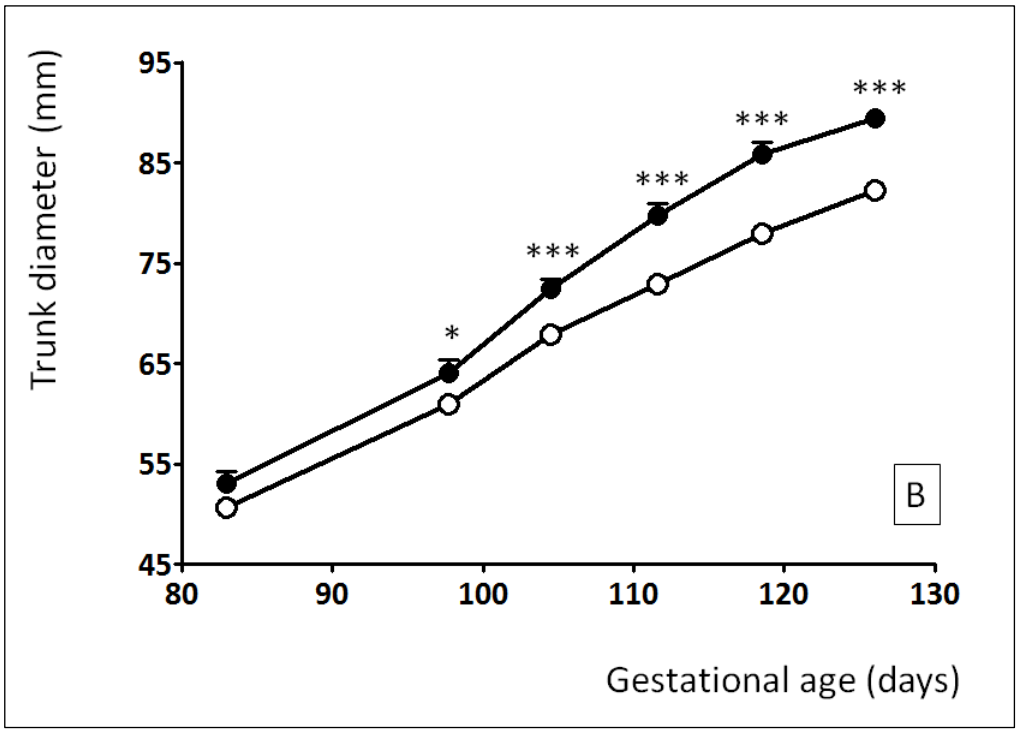

*Serial ultrasonographic measurements of abdominal circumference [A] and trunk diameter [B] (mean ± SEM) from 83±0.1 to 126±0.3 days gestation in singleton-bearing adolescent ewes receiving a control (●, n=15) or high-intake (○, n=27) of the same complete diet. * p<0.05, ** p<0.01, *** p<0.001*

At baseline examination there were no significant differences between nutritional groups. By 98±0.1 days gestation, AC measurements were reduced in high-intake versus control-intake pregnancies (198±2.6mm vs. 206±3.6mm, p=0.035) and remained lower at all subsequent time points (p<0.001). Unsurprisingly the TD followed a similar pattern to the AC, with significant differences observed at the same stages (Figure 3.4B).

3.3.3.2 Biparietal diameter and occipito-snout length

Serial measurements of the BPD between 83±0.1 and 126±0.3 days gestation are illustrated in

Figure 3.5A. Unlike the AC and TD, significant differences between nutritional groups did not become apparent until 112±0.1 days gestation, at which point measurements were lower in high- relative to control-intake groups (48.1±0.26mm vs. 49.4±0.21mm, p=0.002). Differences in the BPD remained significant at 119±0.1 and 126±0.3 days gestation (50.3±0.26mm vs. 52.2±0.30mm, p<0.001, and 53.0±0.40mm vs. 54.5±0.29mm, p=0.008, respectively). Serial measurements of OSL are plotted in Figure 3.5B. Interestingly, differences in OSL by nutritional groups were apparent at an earlier stage than for the BPD - measurements were reduced in high- versus control-intake groups at 105±0.1 days gestation (95.5±0.64mm vs. 98.8±1.07mm, p=0.008) and remained lower at 112±0.1 days gestation (103.0±0.74mm vs. 106.2±0.82mm, p=0.013). Thereafter no significant differences were seen, which is most likely a reflection of incomplete data secondary to the technical difficulty obtaining this measurement in late gestation (highlighted in Section 3.3.1.1). It was not possible to measure OSL in 25 (60%) and 33 (79%) of these 42 pregnancies at 112±0.1 and 126±0.3 days gestation, respectively.

3.3.3.3 Renal measurements

Figures 3.6 and 3.7 illustrate serial measurements of the three individual renal dimensions (RL, TRD and APRD) and the calculated values of RV between 83±0.1 and 126±0.3 days gestation. As per the other parameters, at baseline there were no significant differences between control- and high-intake pregnancies. RV was reduced at 105±0.1 days gestation in fetuses of high-intake compared to control-intake ewes (4.4±0.18cm^3 vs. 5.2±0.15cm^3, p=0.01) and measurements remained lower at all subsequent time points (p<0.001) (Figure 3.7B). These differences were mirrored in each of the individual parameters contributing to the calculation of RV (Figures 3.6A, 3.6B and 3.7A).

3.3.3.4 Femur length and tibia length

Serial measurements of the FL and TL from 83±0.1 until 126±0.3 days gestation are shown in Figure 3.8. There were no significant differences between nutritional groups at baseline for

Figure 3.5 – Fetal growth velocity: biparietal diameter and occipto-snout length

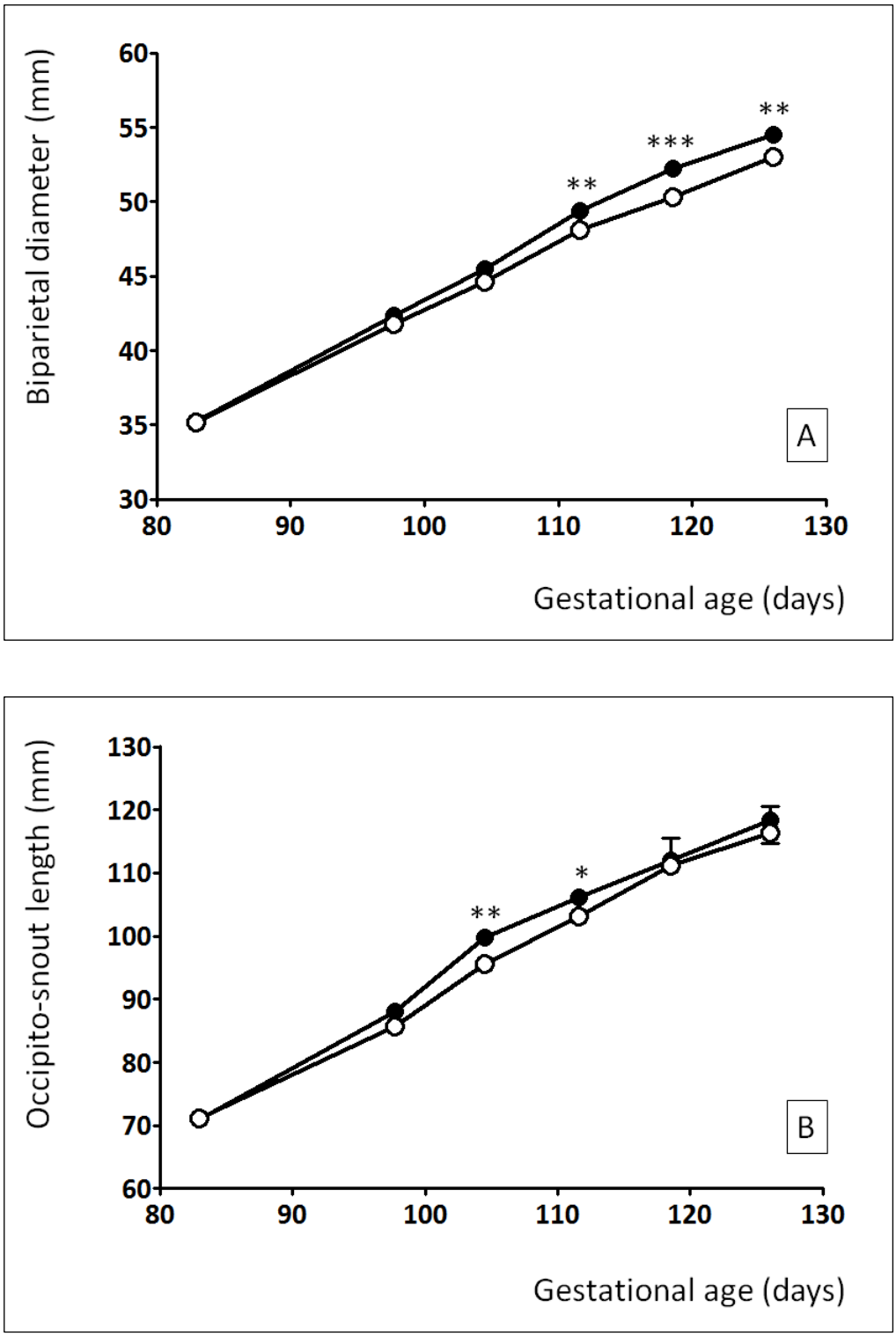

*Serial ultrasonographic measurements of biparietal diameter [A] and occipito-snout length [B] (mean ± SEM) from 83±0.1 to 126±0.3 days gestation in singleton-bearing adolescent ewes receiving a control (●, n=15) or high-intake (○, n=27) of the same complete diet. * p<0.05, ** p<0.01, *** p<0.001*

Figure 3.6 – Fetal growth velocity: renal length and transverse renal diameter

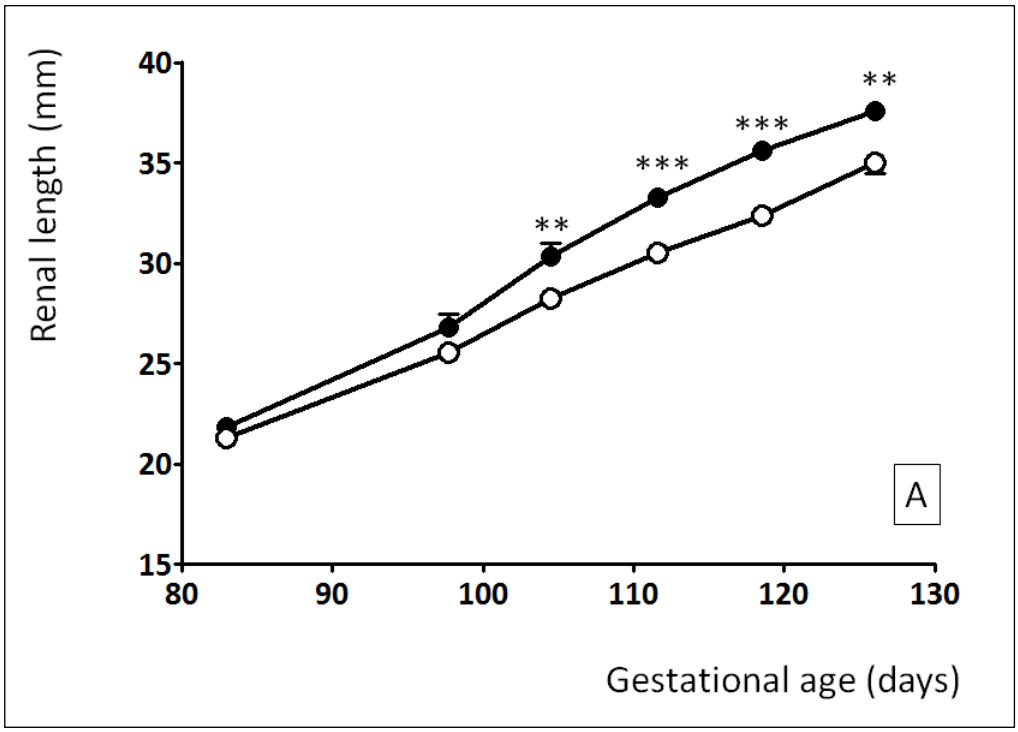

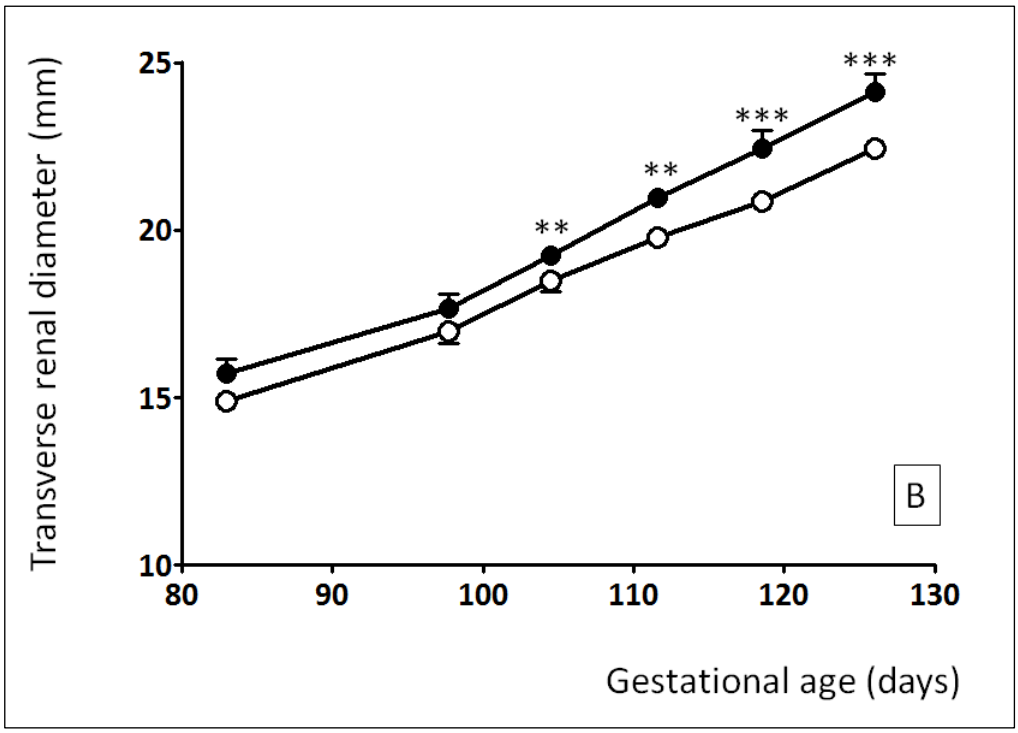

*Serial ultrasonographic measurements of renal length [A], transverse renal diameter [B] (mean ± SEM) from 83±0.1 to 126±0.3 days gestation in singleton-bearing adolescent ewes receiving a control (●, n=15) or high-intake (○, n=27) of the same complete diet. ** p<0.01, *** p<0.001*

Figure 3.7 – Fetal growth velocity: anteroposterior renal diameter and renal volume

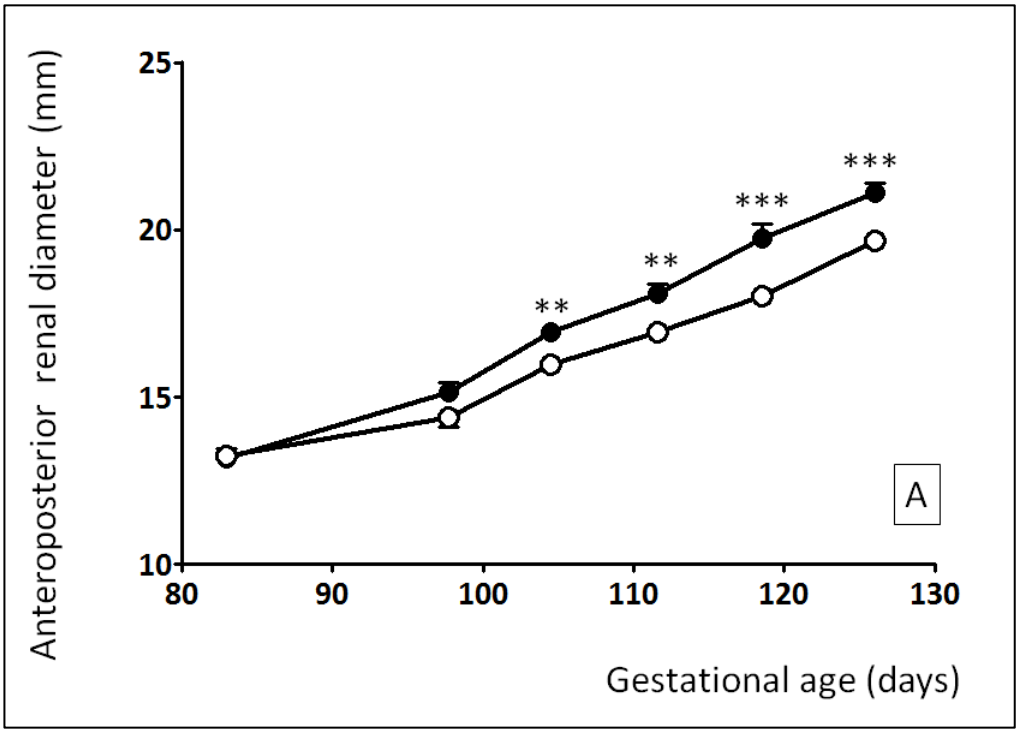

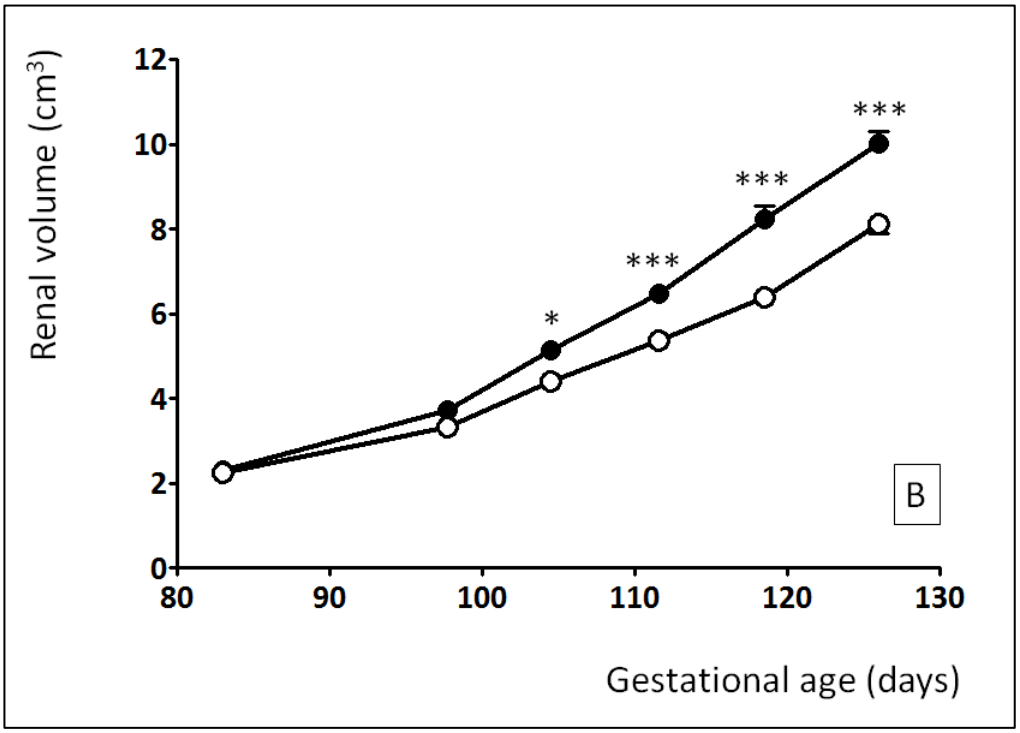

*Serial ultrasonographic measurements of anteroposterior renal diameter [A] and renal volume [B] (mean ± SEM) from 83±0.1 to 126±0.3 days gestation in singleton-bearing adolescent ewes receiving a control (●, n=15) or high-intake (○, n=27) of the same complete diet. * p<0.05, ** p<0.01, *** p<0.001*

Figure 3.8 – Fetal growth velocity: femur length and tibia length

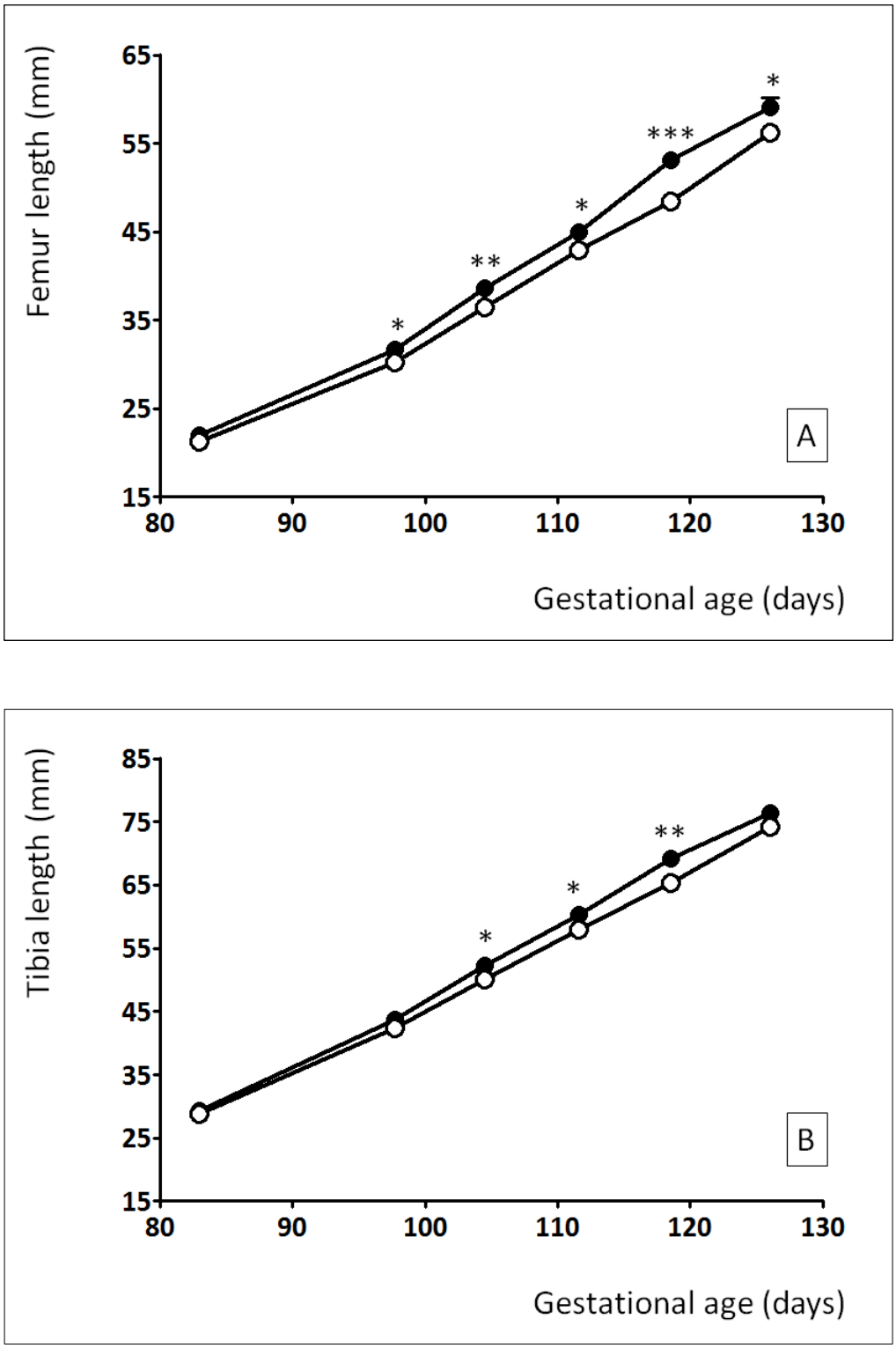

*Serial ultrasonographic measurements of femur length [A] and tibia length [B] (mean ± SEM) from 83±0.1 to 126±0.3 days gestation in singleton-bearing adolescent ewes receiving a control (●, n=15) or high-intake (○, n=27) of the same complete diet. * p<0.05, ** p<0.01, *** p<0.001*

either parameter. Thereafter FL measurements were the first to show a divergence, and were lower in high- relative to control-intake pregnancies at 98±0.1 days (30.2±0.38mm vs. 31.7±0.51mm, p=0.029). Differences in FL remained significant at all further examinations (p<0.001–0.038). By contrast, differences in TL did not become apparent until 105±0.1 days gestation (50.1±0.54mm vs. 52.3±0.70mm, p=0.016). Whilst measurements remained lower at 112±0.1 and 119±0.1 days gestation (p=0.012 and p=0.003, respectively), at 126±0.3 days gestation the difference between nutritional groups was no longer detectable (p=0.117). Measurement of TL technically became more challenging in late gestation as it required visualisation of the full length of an increasingly large bone (maximum 84.6mm) in a single plane. However, unlike the OSL, measurements of TL were still achievable in 100% of pregnancies at 126±0.3 days gestation.

3.3.4 Ultrasound indices of fetal brain sparing

Figure 3.9 shows serial measurements of BPD:AC ratios and BPD:FL ratios (calculated from the parameters above) from 83±0.1 until 126±0.3 days gestation. These indices reflect the size of the fetal head (largely determined by fetal brain growth) relative to the size of the fetal body, the AC being representative of abdominal fat and liver glycogen stores and the FL representing skeletal growth and development. In normally developing control-intake pregnancies, BPD:AC and BPD:FL progressively fell with advancing gestation, which likely reflects the relatively rapid growth of the AC and FL compared to that of the BPD (Figures 3.4A, 3.5A and 3.8A). BPD:AC and BPD:FL ratios also fell with increasing gestational age in high-intake pregnancies but were seen to lag behind, such that they were significantly higher compared with the control-intake group at 105±0.1 days gestation (0.206±0.0016 vs. 0.196±0.0022, p=0.001; and 1.23±0.015 vs. 1.18±0.013, p=0.001, respectively). With the single exception of the BPD:FL ratio at 112±0.1 days gestation, both parameters remained elevated in high- relative to control-intake groups at all subsequent time-points (p<0.001 to p=0.049).

3.3.5 Ultrasound indices of placental size and amniotic fluid volume

Serial measurements of placentome index from 83±0.1 until 126±0.3 days gestation are shown in Figure 3.10A. At baseline examination the placentome index was already reduced in high- versus control-intake groups (4.0±0.17cm^2 vs. 5.2±0.25cm^2, p=0.001) and remained lower at all subsequent examinations (p<0.001). Measurements of placentome index progressively fell with advancing gestation in both groups, in a parallel fashion. Consequently the lines of best fit were similar in slope and differed significantly only in their intercept ($y=15.3+0.17x+0.0006x^2$ and $y=12.2+0.14x+0.0005x^2$ for the high-intake and control-intake pregnancies, respectively).

Figure 3.9 – Ultrasound indices of fetal brain sparing

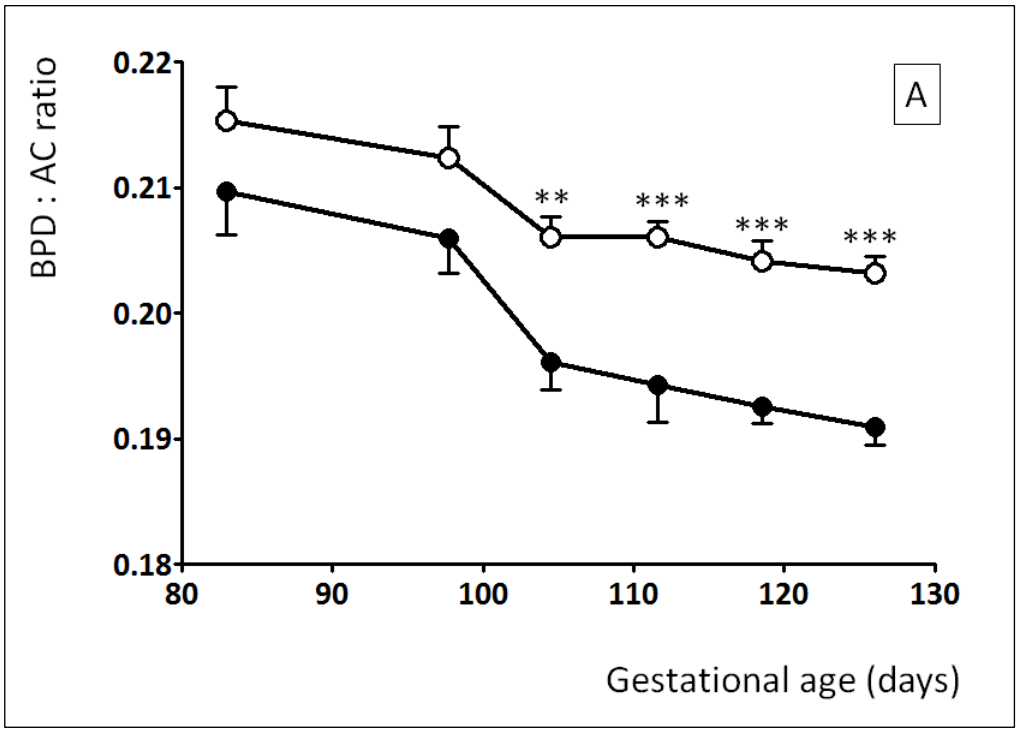

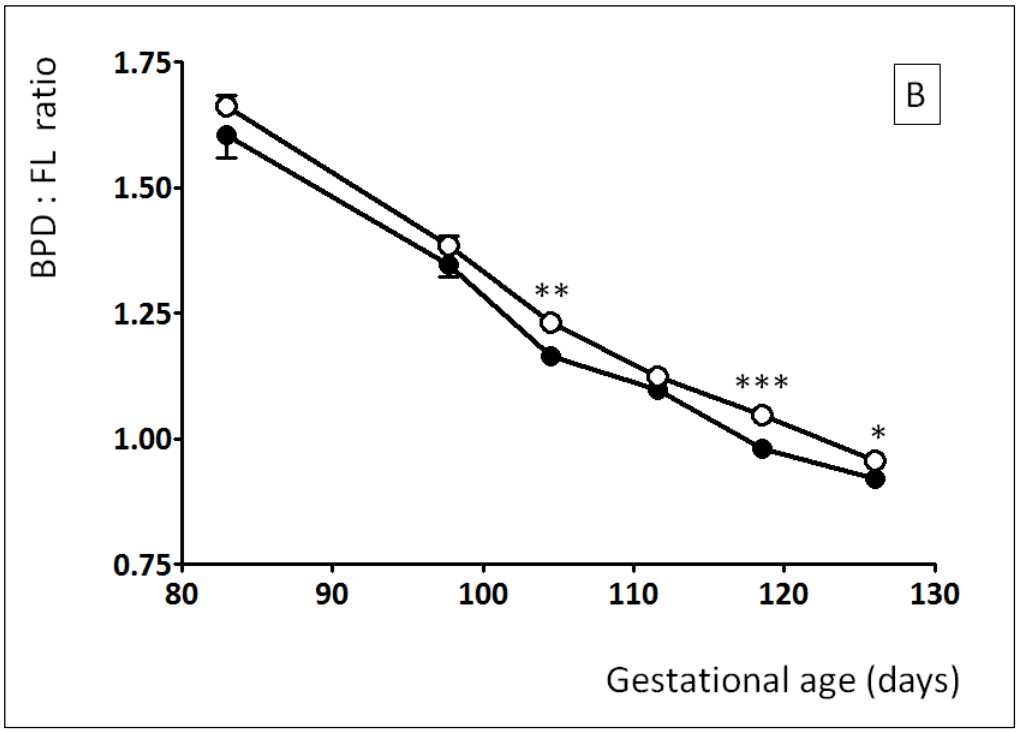

*Biparietal diameter (BPD) : abdominal circumference (AC) ratios [A] and BPD : femur length (FL) ratios [B] (mean ± SEM) as measured by serial ultrasound from 83±0.1 to 126±0.3 days gestation in singleton-bearing adolescent ewes receiving a control (●, n=15) or high-intake (○, n=27) of the same complete diet. * p<0.05, ** p<0.01, *** p<0.001*

Figure 3.10 – Ultrasound indices of placental size and amniotic fluid volume

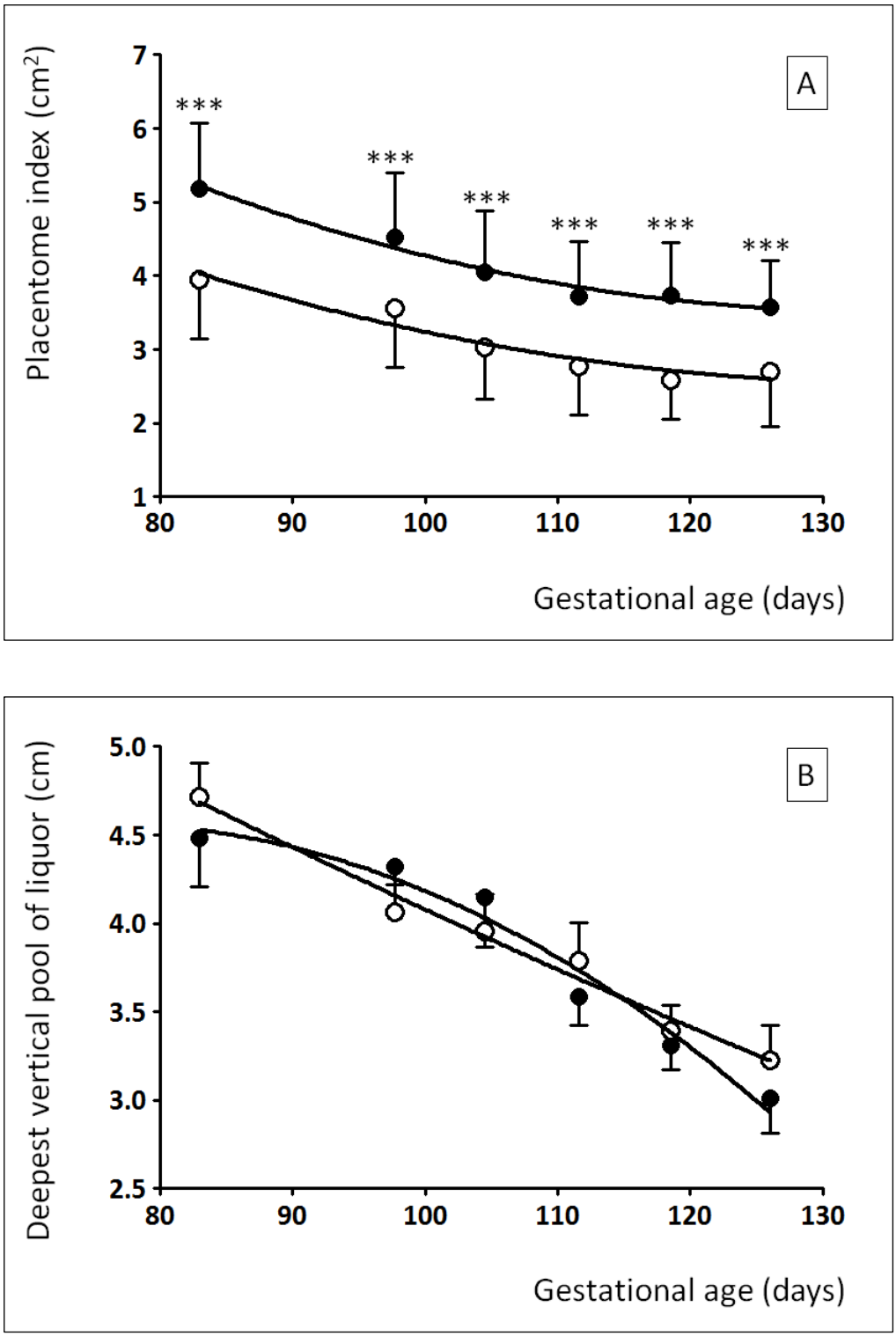

*Serial ultrasonographic measurements of placentome index [A] and deepest vertical pool of amniotic fluid [B] (mean ± SEM) from 83±0.1 to 126±0.3 days gestation in singleton-bearing adolescent ewes receiving a control (●, n=15) or high-intake (○, n=27) of the same complete diet. * p<0.05, ** p<0.01, *** p<0.001*

At necropsy at 131±0.3 days gestation, placentome index at 126±0.1 days gestation correlated reasonably well with total placentome weight in the high- but not in the control-intake group (r=0.685, n=27, p<0.001; and r=-0.201, n=15, p=0.531, respectively). In the high-intake group baseline placentome index at 83±0.1 days gestation also correlated, albeit weakly, with total placentome weight at 131±0.3 days gestation (r=0.501, n=27, p=0.018).

Conversely, in the delivery group, total fetal cotyledon weight and total fetal placental weight following spontaneous birth near term (141±0.4 days gestation) demonstrated a correlation with ultrasound measurements of placentome index at 79±0.1 days gestation (r=0.637, n=13, p=0.026; and r=0.626, n=13, p=0.022, respectively) but not thereafter. Unlike in the necropsy group, there was no obvious relationship between final measurements of placentome index at 133±0.1 days gestation and either total fetal cotyledon weight (r=0.218, n=13, p=0.520) or total fetal placental weight (r=0.295, n=13, p=0.378) at birth. Placentome index also demonstrated strong correlations with necropsy/birth weight. In the delivery group, placentome index at 79±0.1 days gestation showed a positive correlation with eventual lamb birth weight (r=0.642, n=13 p=0.013) and, whilst the correlation with eventual placental weight was lost with advancing gestation, positive correlations with birthweight were maintained throughout pregnancy (r=0.660–0.712, n=13, p=0.004–0.011). Likewise within the necropsy group, placentome index also correlated with eventual fetal weight at 131±0.3 days gestation at all stages of gestation (r=0.481–0.627, n=42, p<0.001–0.009).

Serial measurements of the deepest vertical pool of amniotic fluid in the necropsy group are illustrated in Figure 3.10B. The amount of amniotic fluid decreased with advancing gestation. There were no significant differences according to the nutritional allocation at any stage and no significant correlations with any other fetal or placental ultrasound parameters were seen. In the delivery group, measurements of DVP similarly decreased as pregnancy advanced, from 3.9±0.11cm at 79±0.1 days gestation to 2.6±0.19cm at 133±0.1 days gestation (p<0.001).

3.3.6 Umbilical artery Doppler indices

Figures 3.11 to 3.13 illustrate serial measurements of the UA Doppler indices and the different velocities used to calculate them between 83±0.1 and 126±0.3 days gestation. At baseline examination UA PI, RI and SDR were already found to be higher in high- versus control-intake groups (1.46±0.039 vs. 1.30±0.063, p=0.027; 0.80±0.008 vs. 0.73±0.021, p=0.001; and 5.17±0.295 vs. 3.72±0.263, p=0.002, respectively, Figures 3.12B, 3.13A and 3.13B). All three indices decreased with advancing gestation, however highly significant differences remained between nutritional treatments at all subsequent time points (p<0.001–0.004). Examining the

Figure 3.11 – Umbilical artery Doppler maximum (peak systolic) and minimum (end-diastolic) velocities

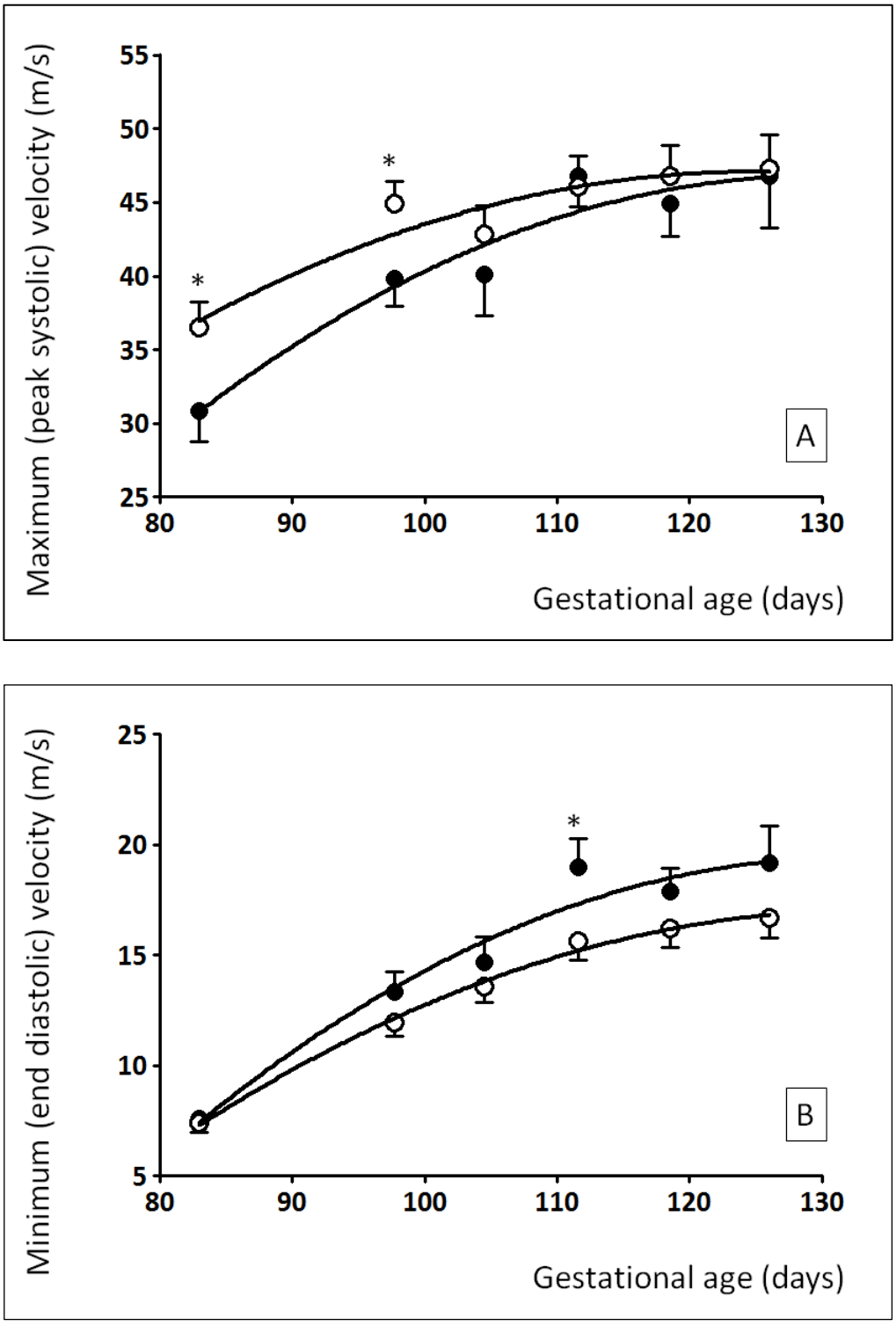

*Serial ultrasonographic measurements of umbilical artery maximum (peak systolic) velocity [A] and minimum (end diastolic) velocity [B] (mean ± SEM) from 83±0.1 to 126±0.3 days gestation in singleton-bearing adolescent ewes receiving a control (●, n=15) or high-intake (○, n=27) of the same complete diet. * p<0.05*

Figure 3.12 – Umbilical artery Doppler time-averaged maximum velocity and systolic to diastolic ratios

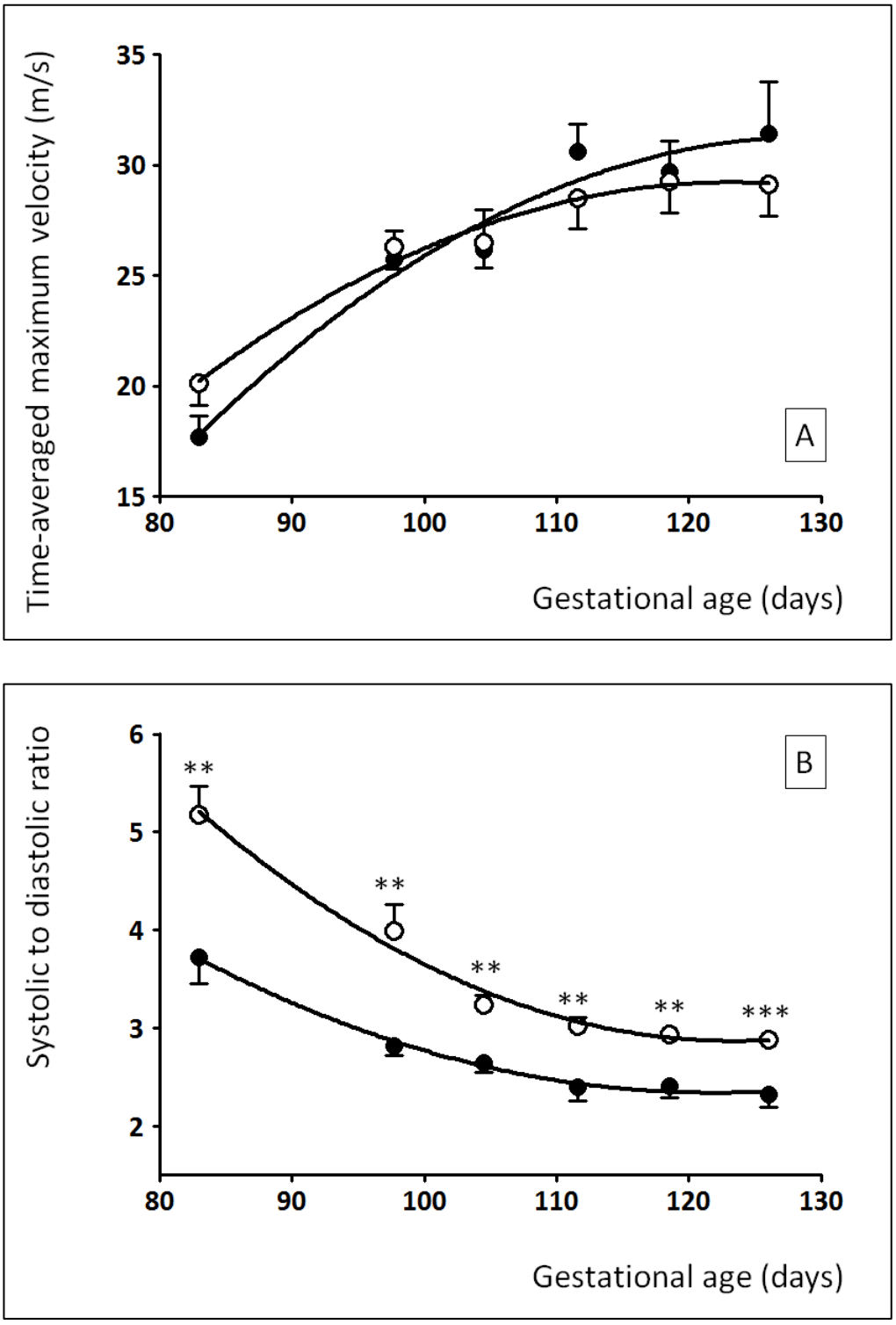

*Serial ultrasonographic measurements of umbilical artery time-averaged maximum velocity [A] and systolic to diastolic ratio [B] (mean ± SEM) from 83±0.1 to 126±0.3 days gestation in singleton-bearing adolescent ewes receiving a control (●, n=15) or high-intake (○, n=27) of the same complete diet. ** p<0.01, *** p<0.001*

Figure 3.13 – Umbilical artery Doppler pulsatility index and resistance index

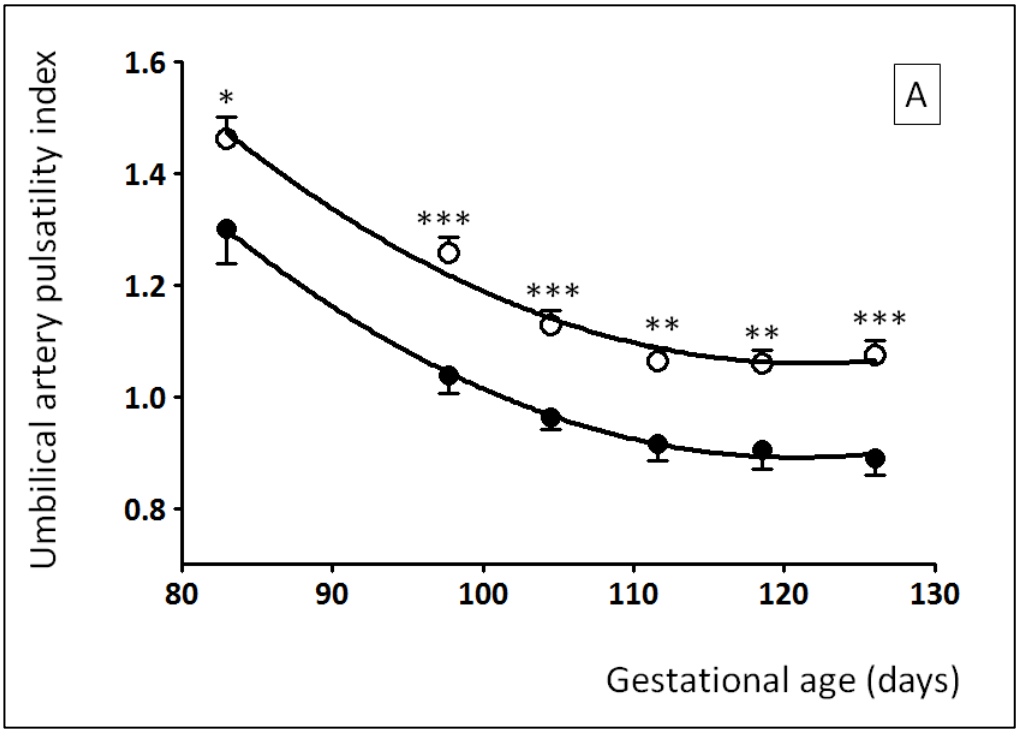

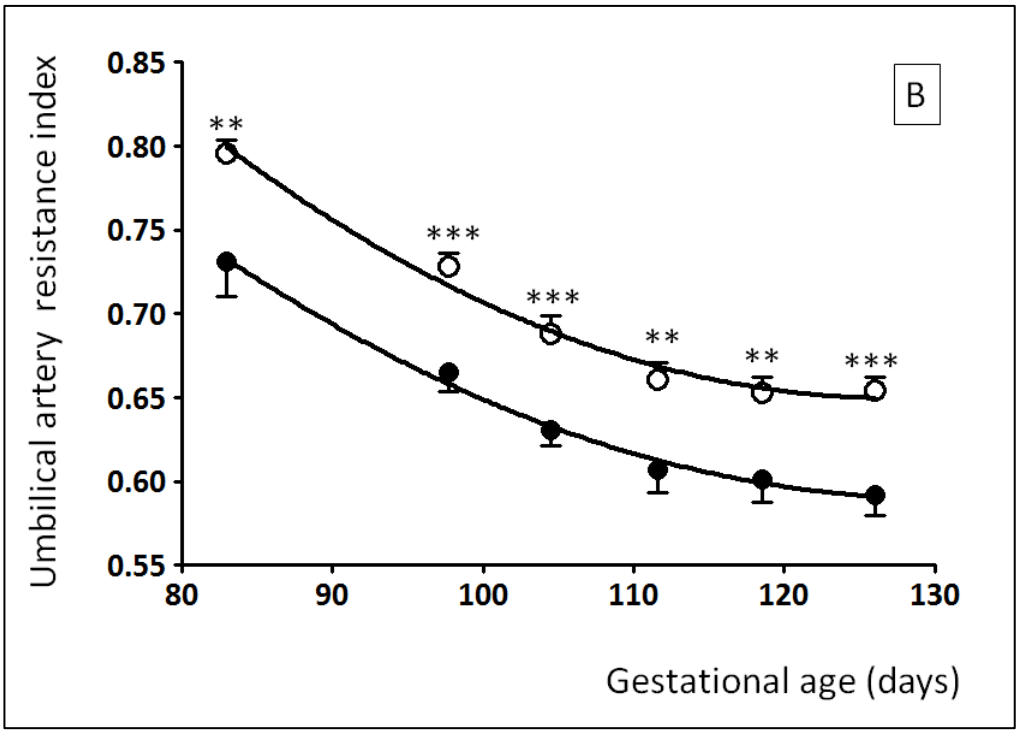

*Serial ultrasonographic measurements of umbilical artery pulsatility index [A] and resistance index [B] (mean ± SEM) from 83±0.1 to 126±0.3 days gestation in singleton-bearing adolescent ewes receiving a control (●, n=15) or high-intake (○, n=27) of the same complete diet. * p<0.05, ** p<0.01, *** p<0.001*

individual velocities, Vmax was higher at 83±0.1 and 98±0.1 days gestation in high- versus control-intake pregnancies (36.5±1.70 vs. 30.8±2.09 m/s, p=0.046, and 44.9±1.50 vs. 39.8±1.89 m/s, p=0.044, respectively, Figure 3.11A). As there were no corresponding differences in Vmin or TAMAX at these points (Figures 3.11B and 3.12A), this increase in peak systolic velocity is likely to have been responsible for the elevated UA, PI and SDR values. There were no significant differences in TAMAX between nutritional groups at any stage (Figure 3.12A) and, although Vmin was found to be higher at 112±0.1 days gestation in the control- relative to the high-intake group (19.0±1.29 vs. 15.7±0.88 m/s, p=0.035, Figure 3.11B), this observation appeared to be out of sync with the general pattern and is likely to be artefactual in nature.

UA Doppler indices were also inversely related to necropsy/birth weight and placental weight. In the delivery group, PI demonstrated a strong negative correlation with eventual lamb birth weight (r=-0.812, n=13, p=0.014) and total fetal placental weight (r=-0.820, n=13, p=0.001) at 95.±0.1 and 101±0.1 days gestation, respectively, and these correlations were maintained at all subsequent time points (r=-0.606–0.847, p=<0.001–0.022). The equivalent correlations for RI and SDR were similar to those seen with the PI (r=-0.737–0.868 and 0.584–0.842, respectively). In the necropsy group, UA PI demonstrated a much weaker negative correlation with eventual fetal weight in late gestation that was significant only from 83±0.1 until 105±0.1 days gestation (r=-0.399–0.420, n=39, p=0.011–0.029). Total placentome and placental weights at necropsy also showed a weak inverse relationship with PI at all time points from 98±0.1 days gestation onwards (r=-0.316–0.449, n=39, p=0.004–0.048).

3.3.7 Fetal growth curve modeling

To further compare the longitudinal fetal growth trajctories between control- and high- intake pregnancies, mean and SD measurements of the most important ultrasound parameters (BPD, AC, RV, FL, TL, UA PI and placentome index) were plotted against gestational age and subjected to mathematical curve analyis using Graphpad Prism® version 5.04 (GraphPad Software Inc., La Jolla, CA, USA) to determine the line of best fit for each individual parameter. Curves for high- and control-intake pregnancies were tested separately. The regression line with the strongest adjusted R^2 value in every case was a quadratic equation of the form: $y = a + b(x) + c(x^2)$, where y is the ultrasound parameter under investigation, x is the gestational age, a is the y intercept, b is the linear coefficient and c is the quadratic coefficient. The mean and SD of the values for a, b and c were calculated and compared between groups. The results are presented in Table 3.8. Y intercepts (values of a) for all fetal parameters except FL/RV were significantly greater in high- versus control-intake pregnancies, however it must be remembered that this is a mathematical extrapolation as the real value of all these measurements at 0 days gestation

Table 3.8 – Modeling of fetal growth curves - analysis of regression lines of best fit

Ultrasound parameter	**Coefficient**	**Control Intake (n=15)**	**High Intake (n=27)**	**P Value**
Biparietal diameter (BPD)	a	-22.1 ± 1.97	-16.1 ± 1.34	**0.014**
	b	0.84 ± 0.038	0.75 ± 0.026	**0.052**
	c	-0.00182 ± 0.000182	-0.00159 ± 0.000125	**0.290**
Abdominal circumference (AC)	a	-156.7 ± 20.29	-34.1 ± 16.46	**<0.001**
	b	4.59 ± 0.393	2.24 ± 0.321	**<0.001**
	c	-0.00835 ± 0.001878	0.00140 ± 0.001523	**<0.001**
Renal volume (RV)	a	12.1 ± 1.21	10.8 ± 0.76	**0.344**
	b	0.32 ± 0.023	0.26 ± 0.015	**0.029**
	c	0.00240 ± 0.000112	0.00190 ± 0.000070	**<0.001**
Femur length (FL)	a	0.2 ± 4.00	8.0 ± 2.21	**0.070**
	b	0.15 ± 0.078	0.28 ± 0.043	**0.120**
	c	0.00498 ± 0.000371	0.00526 ± 0.000205	**0.476**
Tibia length (TL)	a	-43.0 ± 5.09	-22.6 ± 2.55	**0.003**
	b	0.71 ± 0.099	0.33 ± 0.049	**0.004**
	c	0.00196 ± 0.000471	0.00348 ± 0.000236	**0.638**
Umbilical artery pulsatility index (UA PI)	a	5.1 ± 0.22	5.2 ± 0.13	**0.678**
	b	-0.07 ± 0.004	-0.07 ± 0.002	**1.000**
	c	0.00028 ± 0.000020	0.00028 ± 0.000012	**1.000**
Placentome Index	a	15.3 ± 1.22	12.2 ± 0.63	**0.017**
	b	-0.18 ± 0.023	-0.14 ± 0.012	**0.096**
	c	0.00065 ± 0.000112	0.00051 ± 0.000058	**0.226**

All data are presented as mean ± SEM. *Abbreviations: a = y intercept; b = linear coefficient; c = quadratic coefficient (of quadatric best fit lines for each ultrasound parameter)*

would of course be zero in both groups. However the fact that the intercepts differed between nutritional treatment reflects variations in the linear and quadratic components of growth (indicated by the b and c values, respectively) and also implies that fetuses of high-intake ewes might already be on a slower growth trajectory in mid-gestation, even though no significant differences were seen in any parameters when compared by Student's t test at this stage. The linear coefficients (values of b) for all fetal parameters except FL were greater in control-intake pregnancies, reflecting increased overall growth velocity. Meanwhile the quadratic coefficients (values of c) varied between parameters. For BPD, TL and FL values were positive, suggestive of a relative acceleration of growth with advancing gestation, and did not differ between control- and high-intake pregnancies, implying that retardation of head and long bone growth results from a pertubation of linear growth only. C values were also positive for RV, commensurate with acceleration of growth, however they were significantly reduced in high- versus control-intake implying a relative failure of this acceleration of growth in late gestation in addition to compromised linear growth. Interestingly, the AC curve for the control-intake pregnancies was characterised by negative c values, suggesting a tailing off of growth (or deceleration) towards term. This may reflect the fact that these fetuses are probably growing at the maximum rate and may become relatively constrained by nutrient supply or uterine capacity in late gestation. By comparison, c values for the AC curve in high-intake pregnancies was positive, suggesting a relatively more sustained pattern in fetal growth (albeit at a reduced linear rate) without this apparent element of constraint. Clearly however these fetuses do not catch up to the normally growing controls given the striking differences in ultrasonographic AC measurements and post mortem measurements of umbilical girth that are observed between nutritional treatment at 126 to 131 days gestation.

3.3.8 Reference charts for fetal growth

For use in future experiments, normative growth charts were produced for this genotype (Scottish Greyface x Dorset Horn) from the serial ultrasound data derived from the 15 normally developing (control-intake) pregnancies included herein. The charts were created based on the strongest performing abdominal, renal, head and long bone measurements as assessed above: AC, RV, BPD and FL, respectively. Regression lines were fitted to sequential values of the mean ± 2SD for each stage of gestation in order to estimate the reference range in which ~95% of normally growing fetuses would be expected to lie. For the AC, BPD and FL the lines of best fit were linear, whilst for the RV a quadratic curve was more appropriate. The resultant charts are available in Appendices 1 and 2, and are also presented in Figures 3.14 and 3.15, in which the prenatal growth trajectory of a single growth-restricted fetus has been plotted to illustrate the

Figure 3.14 – Reference charts for normal ovine fetal growth: abdominal circumference and biparietal diameter

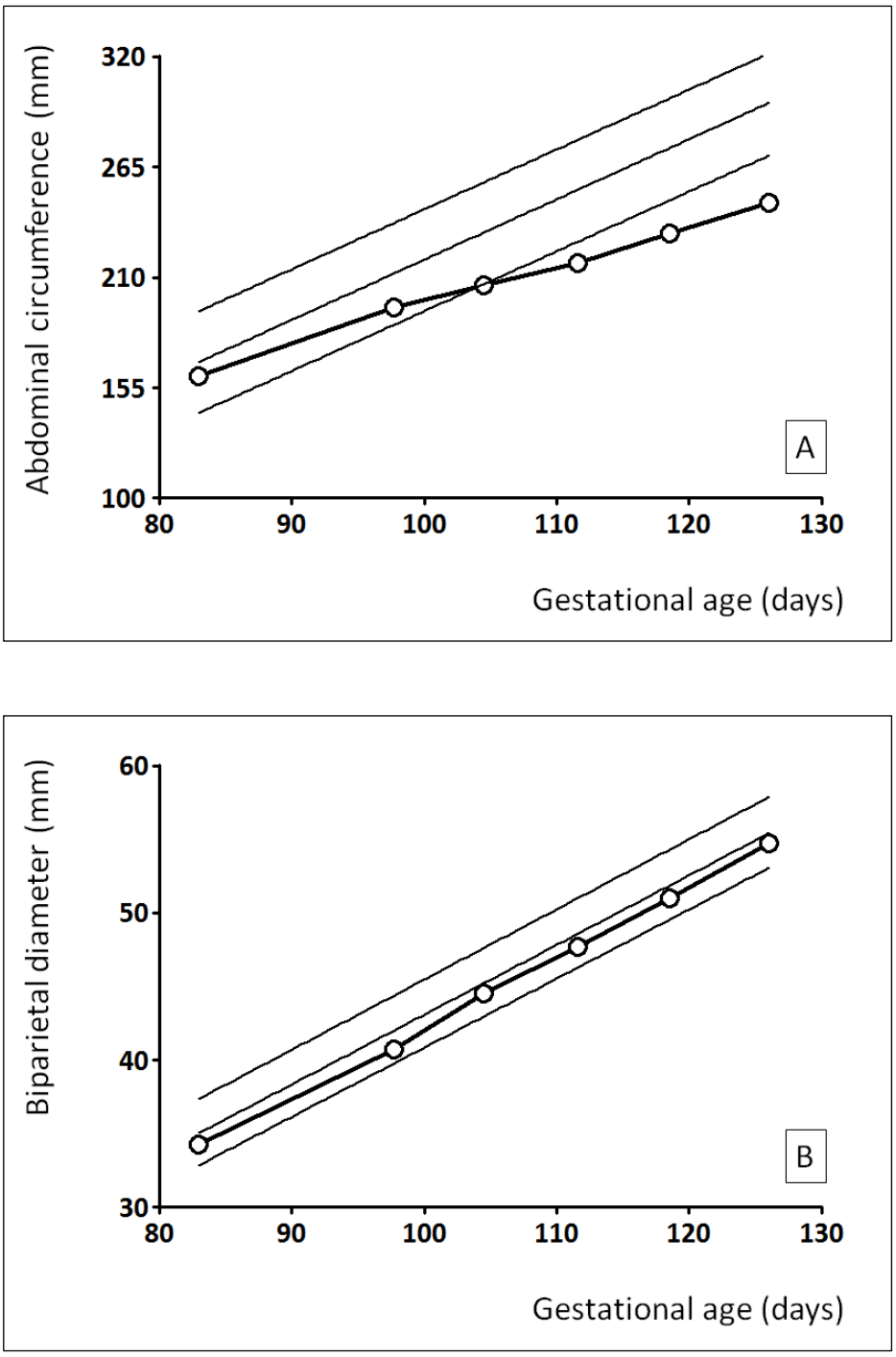

Reference charts for normal fetal growth derived from ultrasound measurements of abdominal circumference [A] and biparietal diameter [B] from 83±0.1 to 126±0.3 days gestation in 15 singleton-bearing adolescent ewes receiving a control intake. Lines indicate mean ± 2SD. For illustration, the individual growth trajectory of a single growth-restricted fetus, induced by overnourishment of its adolescent mother, is plotted (open circles).

Figure 3.15 – Reference charts for normal ovine fetal growth: renal volume and femur length

Reference charts for normal fetal growth derived from ultrasound measurements of the renal volume [A] and femur length [B] from 83±0.1 to 126±0.3 days gestation in 15 singleton-bearing adolescent ewes receiving a control intake. Lines indicate mean ± 2SD. For illustration, the individual growth trajectory of a single growth-restricted fetus, induced by overnourishment of its adolescent mother, is plotted (open circles).

practical utility of such charts. The progressive reduction in the growth velocity of this particular fetus can be clearly seen. Despite starting with baseline measurements around the 50th percentile for gestational age at 83 days gestation, forward growth of the AC, RV and FL can be seen to diminish resulting in a crossing of centiles. Subsequent measurements of AC and RV consistently plotted below the 3rd percentile from ~105 days gestation onwards (Figures 3.14A and 3.15A) followed by FL from ~119 days gestation (Figure 3.15B). By contrast, growth of the fetal BPD was maintained within the normal range throughout gestation (Figure 3.14B), commensurate with fetal brain sparing.

3.3.9 Marked FGR versus non-FGR high-intake pregnancies

The 27 high-intake pregnancies in the necropsy group were further subcategorised into marked FGR (n=17, 63%) and non-FGR (n=10, 37%) groups based on a –2SD cut-off relative to the mean fetal body weight in the control-intake group (<4222g). Pregnancies classified as non-FGR did not differ significantly from control-intake pregnancies here with respect to fetal weight (4824±208g vs. 5084±124g, p=0.248) although total placentome weight was reduced by 22% (406±26.9g vs. 521±23.8g, p=0.005). By comparison, the markedly FGR group exhibited a 28% reduction in fetal weight (3639±117g vs. 5084±124g, p=<0.001) as well as a 37% reduction in total placentome weight (330±23.8g vs. 521±23.8g, p=<0.001) relative to the control group at 131±0.3 days gestation. Ultrasound measurements from each time point in gestation were retrospectively compared across all three groups using one-way ANOVA and post-hoc test of LSD. There were no significant differences between marked FGR and non-FGR groups in placentome index or UA Doppler indices at any stage and no significant differences in fetal biometry between groups between 83±0.3 days and 119±0.1 days gestation. However at 126±0.3 days gestation a number of differences between the two groups were apparent, and are summarised in Table 3.9. Measurements of AC, RV, FL and TL were all reduced in marked FGR versus non-FGR high-intake groups at this stage (p=0.017, p=0.031, p=0.002 and p=0.038, respectively for individual comparisons). Serial measurements of AC in non-FGR high-intake relative to control-intake and marked FGR high-intake pregnancies are illustrated in Figure 3.16 to exemplify the relatively late emergence of measurable differences between these two groups of overnourished pregnancies .

Given that the AC demonstrated the strongest correlation with fetal body weight (see Section 3.3.1.3) we tested the ability of a –2SD ultrasound cut-off for the AC (approximately equivalent to the 3rd percentile and illustrated graphically by the lowermost line on the fetal growth chart in Figure 3.14A) to identify fetuses of high-intake ewes destined for the FGR group. By 126±0.1 days gestation, 15 of 17 fetuses in the marked FGR high-intake group had an AC measurement

Table 3.9 – Late gestation fetal biometry in marked versus mild FGR high-intake pregnancies (final analysis, n=42 pregnancies)

Ultrasound parameter	Control-intake (n=15)	High-intake Non-FGR (n=10)	High-intake FGR (n=17)	P value
AC (mm)	286 ± 2.1[a]	270 ± 4.4[b]	259 ± 2.5[c]	<0.001
TD (mm)	89.9 ± 0.70[a]	84.4 ± 1.56[b]	81.0 ± 0.81[c]	<0.001
RV (cm^3)	10.0 ± 0.28[a]	8.8 ± 0.51[b]	7.7 ± 0.2[c]	<0.001
FL (mm)	59.1 ± 1.07[a]	59.3 ± 1.26[a]	54.4 ± 0.69[b]	0.001
TL (mm)	76.5 ± 1.10[a]	76.4 ± 1.23[a]	72.8 ± 1.11[b]	0.034
BPD (mm)	54.5 ± 0.29[a]	53.9 ± 0.76[ab]	52.5 ± 0.43[b]	0.005

Abbreviations: AC = abdominal circumference; TD = trunk diameter; BPD = biparietal diameter; RV = renal volume; FL = femur length; TL = tibia length. Mean values within are row with unlike superscripts are significantly different (p>0.05). P value shown is for overall ANOVA. Significant post-hoc pairwise comparisons are detailed in the text.

---

below this threshold, giving a sensitivity of 88%. However 5 of 10 the non-FGR overnourished pregnancies were also found to have a fetal AC measurement >2SD below the control-intake mean, suggesting a relatively poor specificity of just 50%.

3.4 Discussion

Firstly, from a practical point of view, this work has demonstrated that it is entirely feasible to assess fetal biometry in the fully awake and upright sheep, without having to resort to turning the animal supine, as is widely practised in biomedical research settings. It is also notable that, due to the nature of this model, overnourished sheep dams became relatively obese as the study progressed (see Section 4.3.1.1). This change in body habitus negatively affected the quality of the views obtained in proportion with the increasing thickness of the subcutaneous fat layer, although it remained feasible to measure complete fetal biometry (excluding OSL) in the majority of cases. Ultrasound examination of control-intake ewes was notably much easier and required far less vertical pressure on the maternal abdomen to ensure an adequate view of the fetus/placenta.

Figure 3.16 – Late gestation fetal biometry in marked versus mild FGR high-intake pregnancies (final analysis, n=42 pregnancies)

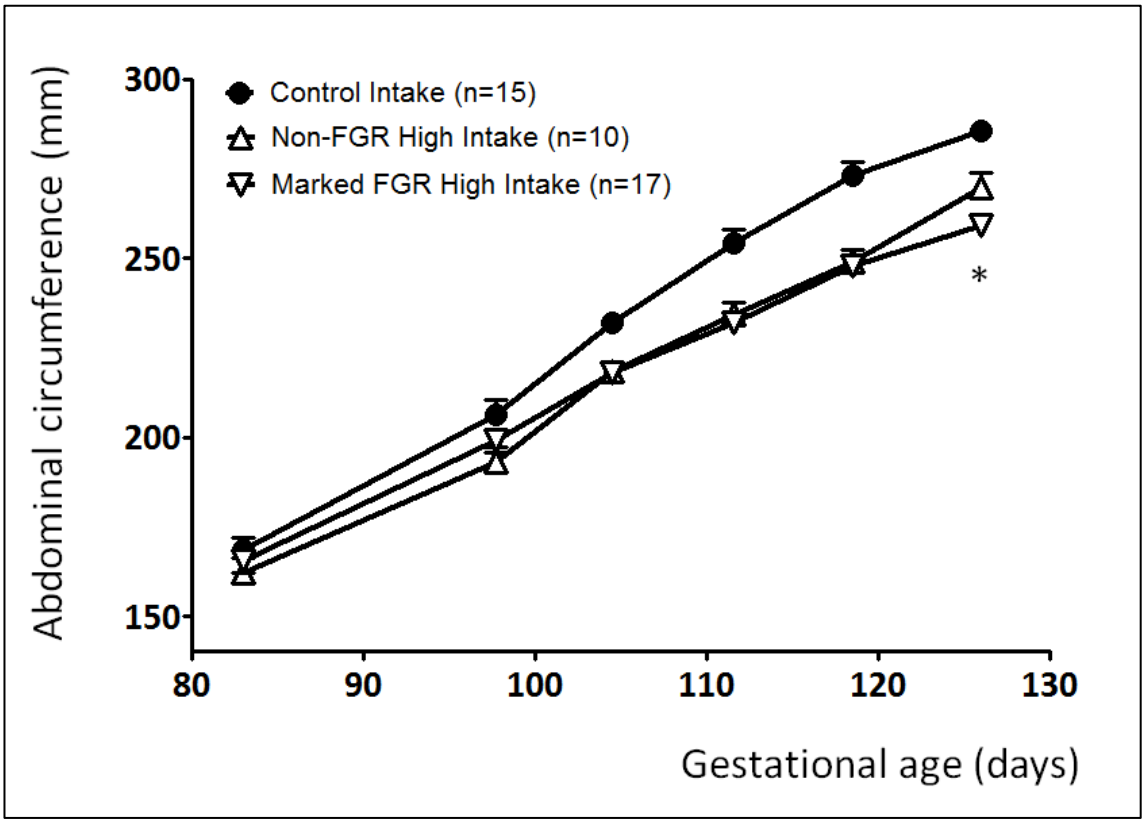

*Serial ultrasonographic measurements of abdominal circumference (mean ± SEM) from 83±0.1 to 126±0.3 days gestation in singleton-bearing adolescent ewes receiving a control (closed circles, n=15) or high-intake (open triangles, n=27) of the same complete diet. The latter group was subdivided into those culminating in markedly growth-restricted (inverted triangles, n=17, defined as fetal weight >2SD below control mean) versus non growth-restricted fetuses (upright triangles, n=10). There were no significant differences in AC between marked FGR and non-FGR pregnancies except where indicated by the asterix. * p<0.05*

3.4.1 Fetal biometry

Longitudinal ultrasound assessment of control- and high-intake adolescent sheep pregnancies has provided novel insights into both the timing and the pattern of FGR in this experimental paradigm. Despite the early differences in placentome index and UA Doppler indices, the first evidence of compromised fetal growth *per se* was a reduction in the AC and FL at 98 days gestation, followed by deviations in RV and TL at 105 days gestation. Meanwhile growth of the

fetal BPD was relatively well preserved until 112 days gestation, commensurate with fetal brain sparing (see Section 1.1.3.4).

3.4.1.1 Abdominal circumference

Overall our findings indicate that the AC is the strongest individual parameter amongst those investigated. In obstetric practice the AC is widely considered to be the most useful individual marker of fetal growth (Degani 2001) and it would appear that the same is true for the sheep, at least in late gestation. The AC is generally considered to be the parameter that best reflects fetal nutritional status as it is measured at the level of the intrahepatic portion of the umbilical vein and hence it potentially represents both subcutaneous fat and liver glycogen stores. The latter assumption is supported by the strong correlation seen here between the AC and fetal liver weight ($p<0.001$). The AC was the parameter that correlated most strongly with physical measurements of abdominal girth taken from fetuses at late gestation necropsy and at birth from live lambs. Measurements of girth at the level of the umbilicus or the lowermost rib were consistently greater than their respective ultrasound AC measurement, possibly due in part to lung inflation. The AC also correlated strongly with necropsy/birth weight ($r=0.81–0.84$) to a degree that is similar to that observed in humans, as illustrated by a clinical validation study (Nahum & Stanislaw 2003) which demonstrated that the correlation between birth weight and AC ($r=0.78$) was stronger than the HC, BPD and FL ($r=0.65$, 0.58 and 0.52, respectively).

The AC was also the first parameter (together with the FL) to exhibit significant differences between control- and high-intake pregnancies, which were manifest from 98 days gestation onwards. Ultrasound studies of longitudinal fetal growth velocity in the hyperthermia sheep model of FGR also found the AC to be the first parameter to be reduced relative to normally growing controls, from as early as 73 days gestation (Barbera et al. 1995a; Galan et al. 1999).

3.4.1.2 Renal volume

In this thesis renal volume has been introduced as a promising marker of fetal growth in the sheep. Previous work using ultrasound at a single time point in this model of FGR demonstrated that renal length x width correlated well with renal weight ($r=0.71$) and fetal body weight ($r=0.77$) at 0.9 gestation (Bourke et al. 2002). The addition of a third renal dimension, thereby allowing the calculation of renal volume, has further improved the correlations with both renal weight ($r=0.75$) and fetal body weight ($r=0.79$). It is notable that renal weight correlates strongly with fetal body weight in both control-intake and high-intake pregnancies ($r=0.90$, $p<0.001$). This is a reflection of the fact that the ratio of renal weight to fetal body weight is not altered by the degree of growth restriction in this FGR paradigm, such

that relative renal weight (per kg fetus) is unchanged (Wallace et al. 2000). Furthermore, serial slaughter studies in this model have shown that relative renal weight remains constant throughout the second half of pregnancy, irrespective of nutritional manipulation (10.41g/kg at 0.5, 10.38g/kg at 0.6 and 10.71g/kg at 0.7 gestation, n=22 per stage, JM Wallace and RP Aitken, unpublished data). Reductions in renal weight are similarly proportionate to overall body weight in the carunclectomy, hyperthermia, umbilico-placental embolisation and single umbilical artery ligation sheep models of FGR (Williams et al. 2002; Mitchell et al. 2004; Limesand et al. 2006; Supramaniam et al. 2006). These observations suggest that the RV might be a good surrogate marker of fetal weight at earlier gestations and lends it credibility as a parameter to track longitudinal fetal growth. The same may not be true in human FGR, as there is some evidence that growth-restricted fetuses have proportionately smaller kidneys than appropriate-for-gestational-age fetuses (Silver et al. 2003). However it has been demonstrated in human fetuses that the ratio of the renal volume to estimated fetal weight (calculated using AC, BPD and FL measurements) remains constant throughout gestation (Gloor et al. 1997).

Differences in RV between nutritional groups did not become apparent until slightly later than the AC, from 105 days gestation. This may be due in part to the greater variability associated with this particular measurement, given its cubic (as opposed to linear) nature. Furthermore intuitively reductions in RV would not be expected to manifest until there had been a degree of substrate deficiency severe enough to impact the growth and development of the major internal organs. This potentially renders it slightly less sensitive than the AC as a longitudinal marker of growth, although it may have a complementary role as a predictor of fetal weight (see Section 3.4.2). We have not strictly validated the use of renal measurements as markers of fetal growth prior to mid-gestation here, however the ovine fetal kidney is identifiable on ultrasound from as early as 40 days gestation, and the ovine renal length demonstrates a linear growth pattern (Ward et al. 2006). By contrast, human renal length and renal volume both demonstrate a logarithmic pattern of growth according to published growth charts of the fetal kidney during normal pregnancy (Chitty & Altman 2003). However, as already mentioned, measurement of the renal volume in human fetuses is usually carried out during the assessment of suspected renal pathology rather than to evaluate fetal growth *per se* in current clinical practice.

3.4.1.3 Femur/tibia length

It has previously been suggested that TL might be a better marker of longitudinal fetal growth in fetal sheep than FL because it demonstrates a greater acceleration in growth with advancing

gestation (Barbera et al. 1995b). However we consistently found that FL performed better than TL as a marker of fetal growth. In late gestation FL correlated better with necropsy measurements and fetal body weight than TL. With respect to longitudinal fetal growth velocity, FL was impacted by prenatal nutrition at an earlier stage than TL, being significantly reduced in the fetuses of high-intake ewes from 98 days gestation, whilst TL measurements did not differ significantly until 105 days gestation. Furthermore TL was the only parameter for which significant differences did not remain at 126 days gestation. The latter is likely to reflect difficulties in measuring TL in late pregnancy rather than an acceleration in growth because subsequent necropsy measurements of the tibial shaft differed significantly between treatment groups ($p=0.003$). In late gestation the tibia was technically more difficult to identify and measure than its proximal counterpart. Often the fetal legs were tucked under the abdomen, making it harder and more time-consuming to identify the tibia than the femur, the proximal end of which could systematically be located via the fetal bladder and pelvic girdle. In addition the tibia is a longer bone than the femur and can measure over 100mm in length at term (Barbera et al. 1995b). It became increasingly difficult as pregnancy progressed to confidently visualise the entire bony shaft in a single plane to ensure accurate measurement. Post-mortem measurements of FL and TL were consistently greater than their respective ultrasound measurements, which is unsurprising because only the calcified shaft of each bone is visualised on ultrasound, whereas the necropsy measurements include additional bony and cartilaginous elements.

3.4.1.4 Head measurements

Although it was possible to measure OSL in mid-pregnancy, by late gestation it was extremely difficult to visualise both the occiput and snout in the same plane and consequently it was not possible to obtain this measurement for the majority of examinations. Although quantification of BPD was relatively feasible, this measurement demonstrated the poorest overall correlation with post-mortem biometry. This would initially seem to contradict the findings of an earlier study that demonstrated a very strong correlation ($r=0.99$) between ultrasound and necropsy measurements of the BPD (Ward et al. 2006). However this group included specimens covering a wide range of gestational ages (40–140 days gestation), whereas here we have investigated variability in fetal size at a single point of gestation. Moreover 60% of the pregnancies studied by Ward et al. (2006) were twin gestations, which are more likely to be associated with smaller fetuses and greater variation in fetal lie relative to the cervix. The latter is relevant because satisfactory views were harder to obtain for the BPD than the other parameters when the fetal head was low in the pelvis. Conversely, with the fetus in breech presentation it was relatively

easy to obtain the BPD measurement, but more difficult to visualise the lower limbs.

Limits of agreement indicated that ultrasound could both over- and under-estimate the BPD. Unlike TL, FL and AC, which are systematically greater at necropsy than on the ultrasound scan, ultrasonographic BPD measurements should theoretically differ from necropsy measurements only by the thickness of the periosteum and overlying skin. The difficulties in measurement of the BPD in late gestation with a cephalic presentation (described above) may have affected its accuracy. It is known that variable extrinsic compression of the fetal head can distort the human BPD measurement and for this reason it is not recommended as a marker of fetal growth in UK obstetric practice, the HC being preferred (Loughna et al. 2009).

3.4.1.5 Fetal brain sparing effect

As discussed in Section 1.1.3.4, FGR secondary to uteroplacental insufficiency is characterised by fetal brain sparing, a phenomenon in which fetal brain growth is prioritised at the expense of fetal body growth. This usually indicates an adaptive response to reduced substrate supply, and results in an asymmetrical growth pattern (Halliday 2009). The fetuses of overnourished adolescent dams demonstrate increased ratios of biparietal head diameter to umbilical girth and higher fetal weight specific brain weights (Wallace et al. 2000; Wallace et al. 2002), commensurate with fetal brain sparing. Serial ultrasound has further characterised the pattern of asymmetrical growth in this paradigm of FGR. Indices of fetal body growth (AC and FL) were diminished from 98 days gestation onwards in high-intake versus control-intake pregnancies, whilst growth of the BPD was maintained until 112 days gestation. Consequently ultrasound markers of fetal brain sparing (BPD:AC and BPD:FL ratios) were significantly increased in the overnourished pregnancies.

3.4.2 Fetal weight estimation

A number of novel estimated fetal weight equations for sheep pregnancy have been presented and validated (both internally and externally) in this chapter. The three strongest equations were derived from the AC and RV (separately and in combination), which also happened to be the most accurately measured and sensitive longitudinal biometric parameters (Section 3.4.1).

In clinical practice, the AC is widely considered to be the best single predictor of fetal weight (Smith et al. 1997; Kiserud & Johnsen 2009). We also found that the RV performed well in the estimation of fetal weight, both independently and in combination with the AC. However, incorporation of additional biometric parameters (FL, TL and BPD) did not improve the model any further. Although no further increase adjusted R^2 values was achieved, interestingly

addition of FL increased unadjusted R^2 values more than TL in all instances, providing further evidence that FL is indeed the better marker of fetal growth. Furthermore these two long bone measurements were not synergistic in this respect, as addition of both to the regression model actually decreased the unadjusted R^2 values. BPD also performed poorly in the estimation of fetal weight. This is unsurprising because growth of the fetal head is relatively well preserved due to fetal brain sparing, which would be expected to distort the normal biological relationship between BPD and fetal weight.

For the purposes of fetal weight prediction, comparison of the AC and RV equations suggested that these parameters may have relative advantages and disadvantages depending on overall fetal size and gestational age. In humans the absolute prediction error of the AC is known to increase with advancing gestation and fetal weight, whilst the percentage error remains fairly constant across a wide range of birth weights (Campbell & Wilkin 1975). In practice this means that inaccuracies in weight estimation are greatest in larger babies. After stratifying our data into weight quartiles we demonstrated a similar pattern for the AC in these sheep, specifically a trend towards increased error with higher birth weight and a significant difference in mean error between the highest and lowest quartiles ($p=0.036$). Meanwhile the mean error using the RV equation was relatively consistent across the full range of birth weights. With respect to gestational age, subgroup analysis at 126±0.1 versus 133±0.1 days gestation revealed that AC correlated better with fetal weight at the earlier time point, whilst RV correlated better at the later time point. We observed that resolution of the kidney generally improved with advancing gestation, possibly as a result of increasing perirenal fat deposition providing a better contrast. Consequently by late pregnancy the RV was both technically easier to measure and less prone to orientation error than the AC, which tended to become less circular due to external forces on the fetal body and was influenced by a variable degree of rumen distension approaching term. This may partially explain why the RV appears to be a better predictor of weight in larger fetuses and closer to full term. Realistically no definitive conclusions can be made from these observations in such a small number of pregnancies, and ultimately there were no statistically significant differences in mean prediction error between equations including one (AC or RV) or two (AC+RV) parameters. However it would seem appropriate to include both AC and RV in the estimation of fetal weight using the combined equation as this potentially takes the above trends into account. The mean prediction error using the AC+RV equation was equivalent at both 126±0.1 and 133±0.1 days gestation (398 and 392g, respectively) and in both the highest and lowest weight quartiles (367 and 339g, respectively).

The estimated fetal weight equations presented herein are the first of their kind for sheep

pregnancy. Equivalent formulae for clinical use in the human are usually generated using verylarge populations to ensure adequate precision. Nevertheless, despite being derived from a relatively small number of sheep pregnancies, the correlations with necropsy or birth weight and the prediction errors of these sheep-specific equations were remarkably similar between the internal and external validation datasets. The high level of maternal genetic homogeneity within each of these datasets and the identical paternal genetics across both (single sire) may have had an impact here, and it would be informative to test out these equations in a more genetically diverse group of fetuses and/or different sheep breed. Incidentally the correlations with fetal weight and mean prediction errors of the three strongest equations (r=0.80–0.90 and 362–656g, respectively) are similar in magnitude to those reported in a clinical study by Nahum and Stanislaw (2003) that evaluated the performance of 25 different fetal weight equations (r=0.76–0.79 and 263–646g). This suggests that the inevitable degree of inaccuracy associated with fetal weight estimation is broadly similar between the sheep and the human. It is of interest that, of the 25 equations evaluated, 24 included the AC as a parameter and they also failed to demonstrate any significant differences in performance between those equations incorporating multiple parameters and those derived from the AC alone.

3.4.3 Assessment of placentation

Despite the lack of significant differences in fetal biometry at baseline ultrasound examination, we found that ultrasound indices of placental size were already attenuated at the point of the first ultrasound examination (83 days gestation) between control- and high-intake ewes. This observation was unexpected, as previous studies in which pregnancies were terminated at 80 to 90 days gestation have not shown any differences in total placentome wet weight by this stage (Redmer et al. 2005; Redmer et al. 2009). However there is certainly evidence of altered placental vascular development and secretory function by mid-pregnancy (see Section 1.1.5.2) in overnourished adolescent pregnancies. Putative alterations in placental density, possibly due to compensatory changes in placental vascularity or differences in carbohydrate metabolism and water content (Redmer et al. 2009), might explain the lack of a difference in weight *per se* despite obvious differences in ultrasonographic appearances and indices of size mid-gestation.

To date very few other studies have assessed ovine ultrasonographic placental biometry. Doize et al. (1997) evaluated transrectal measurements of the placentome diameter as a method of pregnancy dating in sheep and goats. Selecting between 2 and 5 average-sized placentomes, they demonstrated a rapid increase in placentome diameter up until 70–90 days gestation. Placentome measurements correlated with gestational age in does but not ewes and the

authors concluded that placental biometry was unsuitable for dating sheep pregnancies. Kaulfuss et al. (1998) used transrectal ultrasound to measure the maximum diameter of 10 representative placentomes in four different breeds of sheep. They similarly observed that placentome dimensions reached a peak in mid-gestation and declined thereafter. This is consistent with the trends seen herein in both control- and high-intake ewes as well as the findings of serial slaughter studies in normal sheep pregnancy which indicate that placental weight peaks at around 80 days gestation (Robinson et al. 1977), shortly following the apex of placental proliferation at 77 days gestation (Ehrhardt & Bell 1995). The positive correlations between ultrasonographic placentome index from mid-gestation and total placentome weight in late gestation suggest that the early identification of compromised placentae by ultrasound is feasible. Moreover the positive correlation between placentome index at various stages and eventual fetal weight reinforces the observation that it is placental size *per se* which provides the major constraint to fetal growth in overnourished adolescent ewes (Wallace et al. 2006a). In keeping with this assumption, necropsy/birth weight was strongly correlated with placental weight, irrespective of nutritional manipulation ($r=0.901$, $n=55$, $p<0.001$).

3.4.4 Umbilical artery Dopplers

We observed that UA Doppler indices were already significantly increased by 83 days gestation in high-intake versus control-intake pregnancies and remained so through to late gestation. In normally developing sheep pregnancies UA Doppler indices decline with advancing gestation, with the most rapid fall in values between 66 and 109 days gestation (Newnham et al. 1987). Between 109 and 139 days gestation, earlier studies in chronically instrumented normal sheep pregnancy have shown that UA PI, RI and SDR continue to fall progressively and that all three correlate positively with directly measured umbilical vascular resistance and negatively with both umbilical and placental blood flow (Irion & Clark 1990a; Acharya et al. 2004). At ~133 days gestation, growth-restricted pregnancies of overnourished adolescent ewes are characterised by a 37% reduction in umbilical blood flow, measured directly using the Fick principle (Wallace et al. 2002). It seems logical that the observed UA Doppler changes reflect either this reduction in absolute blood flow and/or putatively increased downstream vascular impedance to blood flow. Although umbilical blood flow has not been directly assessed using the same method in mid-gestation, measurement of uterine blood flow using indwelling flow probes has shown a 42% reduction relative to control-intake pregnancies as early as 88 days gestation (Wallace et al. 2008b). As umbilical and uterine blood flows are generally closely matched, at least in late gestation (Wallace et al. 2002), it is likely that a corresponding reduction in umbilical flow does exist in mid-gestation in the overnourished dams, especially

given the striking differences in UA Doppler indices seen here at 83 days gestation. One means of further investigating this non-invasively would be to measure vessel diameter and absolute velocities (requiring correction for the angle of insonation) in order to calculate volume blood flow, although the precision of this method has been questioned, at least with respect to uterine artery Doppler blood flow assessment (Abi-Nader et al. 2010). UA Doppler indices have been measured previously in two other established sheep models of FGR. Indices were found to be increased from 80 to 135 days gestation following maternal hyperthermia (Galan et al. 1998; Galan et al. 2005; Barry et al. 2006), an intervention which has been shown to reduce absolute umbilical blood flow in late pregnancy (Thureen et al. 1992). By contrast, Doppler indices were not influenced by premating carunclectomy (Giles et al. 1989), which appears to restrict fetal growth via a reduction in total placentome number in the absence of specific effects on the fetoplacental circulation.

Numerous other research groups have evaluated UA Dopplers in ovine pregnancies using internal or external Doppler probes or the inbuilt Doppler functionality of modern ultrasound machines. Correlations between UA Doppler indices, blood flow and resistance are maintained following maternal phenylephrine infusion (Acharya et al. 2004), progressive downstream UA constriction with ligatures (Maulik et al. 1989) and both acute and chronic placental embolization (Nimrod et al. 1989; Adamson et al. 1990; Muijsers et al. 1990; Gagnon et al. 1994; Acharya et al. 2004). Terminal placental embolization studies in the sheep illustrate a progressive reduction in end-diastolic blood flow (reflected by increasing UA Doppler indices) following by absent and finally reversed end-diastolic flow shortly prior to fetal demise (Morrow et al. 1989). A similar sequence of changes is observed in human FGR (Baschat 2010).

Both increased UA PI and reversed end-diastolic flow can also be experimentally induced by progressive umbilical venous compression (Fouron et al. 1991), an effect which is not ameliorated by maternal oxygen administration (Sonesson et al. 1993). Hence whilst there is strong evidence that UA Doppler indices reflect both umbilical blood flow and downstream fetal placental resistance, whether they additionally indicate fetal hypoxaemia is less clear. Indeed hypoxia induced by occlusion of the maternal common iliac artery (Muijsers et al. 1990), epidural-induced maternal hypotension (Erkinaro et al. 2006) and reducing the oxygen content of inspired air (Morrow et al. 1990) have no effect on the UA waveform in spite of a slight increase in placental vascular resistance following the latter (van Huisseling et al. 1991b). By contrast, (Downing et al. 1991) demonstrated an increase in UA SDR, PI and RI during periods of hypoxaemia but concluded these changes may have been primarily due to effects on the fetal heart rate.

It is also less clear whether pharmacologically induced changes in fetal haemodynamics have significant effects on UA Doppler indices. No changes were demonstrated following increases in umbilical artery resistance (Adamson et al. 1990) using angiotensin II infusion or in fetal arterial hypertension induced by norepinephrine delivery (van Huisseling et al. 1991a), whereas infusion of the nitric oxide synthase inhibitor N-omega-nitro-D-arginine (Giles et al. 1997) or the thromboxane analogue U-46619 (Trudinger et al. 1989; Irion and Clark 1990b), and maternal nicotine administration (Arbeille et al. 1992) increase UA PI, SDR and RI, respectively. In addition, UA Doppler indices are increased in ovine pregnancy-induced hypertension (Keith et al. 1992) and in fetal hypovolaemia but not fetal hypervolaemia (van Huisseling et al. 1992) or following isovolumic increases in red cell mass (Teyssier et al. 1998). The variable responses to a range of different biological conditions clearly illustrate the highly dynamic nature of UA Doppler indices as measurements, and this should be borne in mind when interpreting results.

It is interesting that we observed a close negative correlation between UA Doppler indices in mid-pregnancy and eventual fetal and placental weights in late gestation. In contemporary obstetric practice umbilical artery Dopplers are widely used as the primary surveillance tool for pregnancies complicated by FGR (Baschat 2010), however a correlation with birth weight *per se* has not to my knowledge been reported in either humans or animals. In combination with similar findings for the placentome index (see Section 3.4.3), this suggests that ultrasound may have a role in identifying poor placentation and/or high resistance to fetoplacental blood flow as antecedents of the reduction in fetal growth velocity during the final third of gestation.

3.4.5 Prediction of marked FGR

Despite the promising correlations between mid-gestation placental biometry and UA Dopplers and eventual fetal weight described above, attempts at early identification of fetuses destined to become markedly FGR in late gestation using ultrasound markers was relatively disappointing. Markedly FGR and non-FGR high-intake pregnancies did not differ from one another with respect to placental biometry or UA Doppler indices at any stage of pregnancy. Furthermore no differences in fetal biometry between these two groups were detected between 83 and 119 days gestation. Rather it was only when examined at 126 days gestation that significant differences in any fetal measurements became apparent. This is perhaps unsurprising as by 121 days gestation the fetus has only achieved ~70% of its final weight (Figure 3.1), irrespective of nutritional group. Hence whilst differences between control- and high-intake pregnancies begin to emerge at 98 days gestation, more subtle differences within the overnourished group would intuitively be harder to detect. It appears that despite an initial

reduction in placental biometry and increased UA Doppler indices relative to control-intake pregnancies, non growth-restricted fetuses of high-intake ewes are subsequently subjected to a lesser degree of placental constraint during the exponential period of fetal growth compared with their FGR counterparts. This assumption is reinforced by the significant differences between the two groups in total placentome weight observed at 131 days gestation. Given their significantly greater placental mass it is likely that overall placental transport capacity is relatively preserved in the late gestation mildly growth-restricted high-intake pregnancy at a time when the supply of nutrients from the maternal circulation is plentiful secondary to overnutrition, which consequently allows the fetus to thrive. The placenta has a certain intrinsic reserve capacity, and we have consistently observed that placental growth needs to be restricted by >20% before it significantly impacts fetal growth (Wallace et al. 2004b); JM Wallace, unpublished data) and this is consistent with estimates derived from experiments involving mid-pregnancy placentome ablation (Mellor et al. 1977). In spite of the lack of early differences between marked FGR and non-FGR high-intake pregnancies, fetal biometry nonetheless performed well in the identification of the most compromised pregnancies in late gestation, as an AC >2SD below the control-intake mean had a sensitivity of 88.2% to predict a markedly FGR fetus.

3.5 Conclusions

In summary, it has been shown that the AC and RV are the most accurately measured markers of fetal growth in sheep pregnancy and that they correlate best with fetal weight in late gestation and birth weight at term. Serial assessment of fetal growth velocity in high-intake pregnancies revealed a reduction in AC and FL from 98 days, RV and TL from 105 days and BPD from 112 days gestation, respectively. This asymmetrical pattern of growth resulted in elevated BPD:AC and BPD:FL ratios indicative of fetal brain sparing.

Estimation of fetal weight using regression equations is feasible in the sheep and is subject to similar degrees of inaccuracy as human fetal weight estimation. Use of an equation derived from both AC and RV measurements is recommended, as these particular parameters may complement each other across a wide range of fetal size and gestational ages. Although there were no significant differences between nutritional groups in fetal biometry at mid-gestation, placentome index was reduced ($p<0.001$) and UA Doppler indices increased ($p<0.01$-0.05) in overnourished pregnancies from 83 days gestation onwards. These ultrasound parameters were correlated with necropsy/birth weight and placental weight, indicating that placental size and fetoplacental blood flow are important determinants of eventual fetal size in these compromised pregnancies.

4.1 Introduction

This chapter details the first of two studies aimed at evaluating the efficacy, safety and mechanism of action of Ad.VEGF gene therapy treatment in an ovine paradigm of FGR.

4.1.1 Background

Previous work evaluating the effects of Ad.VEGF in normal adult sheep pregnancy showed that local adenovirus-mediated over-expression of VEGF-A_{165} in the uterine arteries significantly increased UBF compared to transduction with a non-vasoreactive control vector (Ad.LacZ). This increase in UBF became significant as early as 7 days post-injection and was maintained for at least 28 days, at which point it reached a 37% increase over baseline compared to 20% on the Ad.LacZ injected side (Mehta et al. 2011). Vessels harvested at 4 to 7 days post-injection demonstrated altered vascular reactivity, more specifically a reduced vasoconstrictor response to phenylephrine and an enhanced vasorelaxation response to bradykinin (David et al. 2008), as well as an upregulation of eNOS and both VEGF receptors (FLT1 and KDR), measured by ELISA and immunohistochemistry, respectively (Mehta et al. 2011). Subsequently near to term (28 days following vector injection) eNOS expression was equivalent in Ad.VEGF-A_{165} and Ad.LacZ-transduced vessels. Vasorelaxation was also equivalent but vessels still contracted significantly less strongly. In addition there was a significant increase in neovascularization within the perivascular adventitia and reduced intima-to-media ratios. Additional experiments using endothelial cells isolated from the uterine arteries during mid-gestation sheep pregnancy and transfected with adenovirus vectors *in vitro* showed that Ad.VEGF-A_{165} upregulated levels of eNOS, iNOS and the phosphorylated (activated) form of eNOS, providing further evidence that VEGF over-expression increases the concentration of endogenous vasodilator substances. Whilst all of this is commensurate with a potentially beneficial effect of Ad.VEGF on fetal nutrient supply, the effect clearly needed to be evaluated in pregnancies complicated by FGR.

It has been repeatedly shown that overnourishing the pregnant adolescent ewe, which is itself still growing during pregnancy, results in accelerated maternal tissue deposition and nutrient partitioning away from the gravid uterus at the expense of the pregnancy. This results in a major degree of placental followed by fetal growth restriction relative to the normally developing pregnancies of adolescent ewes receiving a moderate (control) dietary intake (Wallace et al. 2006a). This ovine paradigm is ideally suited for the evaluation of the effects of

Ad.VEGF in FGR pregnancy as it is replicates many of the key features of human FGR secondary to uteroplacental insufficiency without the need for any interference at a vascular or placental level (Wallace et al. 2005b). There is a major (42%) reduction in UBF that is manifest by mid-gestation (Wallace et al. 2008b), which is associated with reduced placental vascularity, secretory function and mRNA expression of key angiogenic factors and receptors including VEGF and FLT1 (Redmer et al. 2005; Lea et al. 2007; Redmer et al. 2009).

4.1.1 Aims

The aims of this first study were to assess the effect of prenatal Ad.VEGF gene therapy on:

- Uterine blood flow (measured using indwelling flow probes)
- Fetal growth velocity (measured by ultrasound)
- Fetal weight in late gestation
- Fetal body composition, organ weights and gross organ morphology
- Uterine artery vascular reactivity, IMR and adventitial neovascularisation
- Placental mRNA expression of important angiogenic factors and receptors

4.2 Materials and Methods

4.2.1 Experimental design

The primary outcome for this study was serial changes in UBF, measured using indwelling flow probes, from mid to late gestation. Secondary outcomes are detailed above. An endpoint in late pregnancy was chosen in order to quantify the maximum treatment effect following mid-gestation vector delivery, to sample the placenta and to harvest the maternal uterine arteries for *in vitro* tests of vascular reactivity. This had to be achieved prior to delivery which can occur as early as day 135 of gestation in the FGR pregnancies. Tissues were subsequently utilised to investigate putative downstream effects of Ad.VEGF on the uteroplacental circulation.

A sample size calculation was performed based on preliminary data showing a 40% increase in UBF following Ad.VEGF delivery in normal adult sheep pregnancy (David et al. 2008) and prior evaluation of UBF in the overnourished adolescent model (Wallace et al. 2008b). Assuming inter-animal variability of 143ml/min, it was estimated that 11 animals per group would be required to detect a 50% increase in UBF (212ml/min) with 90% power.

To investigate the efficacy of Ad.VEGF it was important to assess fetal growth relative to both normally growing fetuses and growth-restricted fetuses receiving inactive control treatments.

Therefore a contemporaneous control group of pregnant adolescent ewes fed a control dietary intake to promote normal maternal and fetal growth was included in order to account for the yearly variation in fetal growth observed in sheep. Two separate overnourished comparator groups were used to control for different aspects of the surgery to administer the gene therapy (Section 2.1.4.2). The first group received bilateral UtA injections of normal saline to control for the laparotomy, injection procedure and subsequent 5 minute occlusion of each UtA during vector administration (H+Saline group). The second group received bilateral UtA injections of $5x10^{11}$ particles of a control vector Ad.LacZ (adenovirus encoding the reporter gene LacZ) to control for any additional effects of adenovirus vector infection in compromised sheep pregnancy (H+Ad.LacZ group). Control-intake ewes also received saline in order to control for the surgical intervention (C+Saline group).

4.2.2 Establishment of singleton pregnancies and nutritional management

Oestrus cycles were synchronised in 108 potential adolescent recipients and 27 potential adult donor ewes in the lead up to 6 separate embryo recovery and transfer days in the mid breeding season (Section 2.1.1.1). Adolescent recipients weighed 44.5±0.22 kg (mean ± SEM) and had an initial body condition score (BCS) of 2.3±0.01. Donor ewes weighed 65.9±0.87 kg with a BCS of 2.3±0.02 and were superovulated prior to undergoing laparoscopic intrauterine insemination (Section 2.1.1.2) and embryo recovery (Section 2.1.1.3). Thirteen donors in total required to be flushed to provide sufficient embryos for transfer into 86 adolescent recipients (Section 2.1.1.4).

Immediately following embryo transfer and throughout gestation, adolescent ewes were fed a control-intake (n=21) or high-intake (n=65) of the same complete diet, as described in Section 2.1.2. Adolescent ewes were evenly allocated to nutritional groups on the basis of initial live weight and BCS, recipient ovulation rate and, where possible, donor source. Pregnancy diagnosis was carried out by ultrasound at 45 days gestation (Section 2.1.1.5) and confirmed viable pregnancies in 17 of 21 control-intake and 55 of 65 overnourished ewes, giving overall pregnancy rates of 81.0 and 84.6%, respectively.

4.2.3 Ultrasound examination and gene therapy administration

At 83±0.1 days gestation all ewes underwent ultrasound examination and measurement of fetal and placental biometry and umbilical artery Doppler indices, as described in Section 2.1.3. Subsequently, at 89±0.2 days gestation, 60 ewes underwent a midline laparotomy as described in Section 2.1.4.2, and administration of Ad.VEGF gene therapy or a control treatment (saline or Ad.LacZ). At induction of anaesthesia, a venous blood sample was taken into a 5ml syringe,

placed into an incubator at 37^{o}C and allowed to clot. Subsequently at surgery, an ultrasonic perivascular flow probe was placed around the uterine artery supplying the gravid horn (see Section 4.2.4.1) and this blood clot was used to fill the dead space between the vessel and the probe, to improve transmission of the ultrasound signal. After fitting the flow probe, both uterine arteries were injected with either the active gene therapy (Ad.VEGF), control vector (Ad.LacZ) or control saline, as per the experimental design (described in Section 2.1.4.2). All control-intake ewes received saline (C+Saline group), whilst high-intake ewes were evenly allocated to one of three groups (H+Ad.VEGF, H+Saline or H+Ad.LacZ) on the basis of estimated fetal and placental size (values of TD, AC, RV and placentome index), the BPD:AC ratio (an index of fetal brain sparing) and the daily maternal live weight gain between embryo transfer and surgery. After allowing a full week's postoperative recovery for all ewes, serial scans were performed at approximately weekly intervals from 98±0.1 until 126±0.3 days gestation. Abdominal wounds were inspected for signs of infection or dehiscence prior to each ultrasound examination and care was taken to minimise pressure from the transducer. All scans were carried out by a single operator (David Carr) accredited in advanced obstetric ultrasound who was kept blind to the treatment administered at surgery in order to avoid any bias in the ultrasound evaluation of fetal growth.

4.2.4 Measurement of uterine blood flow

4.2.4.1 Placement of uterine artery flow probes

At laparotomy for gene therapy administration, each ewe had an ultrasonic perivascular flow probe (PSS Series, Transonic® Systems Inc., Ithaca, NY, USA) fitted around the uterine artery supplying the gravid uterine horn prior to injection of that artery. A straight section of the vessel was chosen, proximal to the first bifurcation and distal to the planned site of injection. At this location the visceral peritoneum was opened with fine scissors and the vessel was mobilised free from the underlying tissue. Either a 4mm or 6mm sized probe was selected depending on the size of the vessel, aiming for it to fill 75 to 95% of the space between the two lateral reflector brackets as per the manufacturer's recommendations. To fit the probe, the screw securing the adjustable reflector bracket was first loosened, allowing the bracket to be displaced upwards. The reflective plate was then hooked underneath the vessel, the bracket slid back into its original position and the screw tightened, leaving the flow probe securely positioned around the vessel with a non-constrictive fit (Figure 4.1A).

An autologous blood clot was used to fill the space between vessel and probe if necessary (see above). The flow probe unit was loosely anchored onto the adjacent peritoneum using

Figure 4.1 – Placement and exteriorisation of uterine artery flow probes

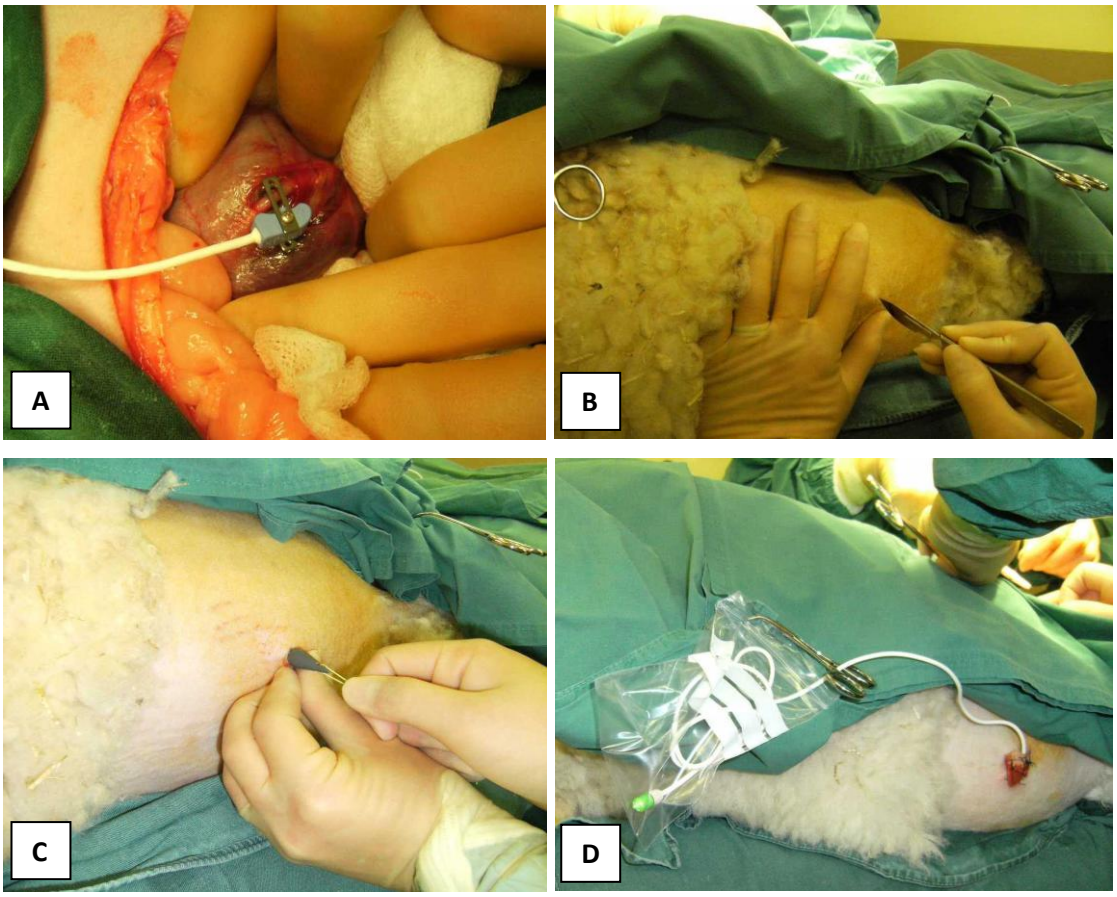

A *Transonic® flow probe was fitted around the uterine artery supplying the gravid horn [A] during laparotomy. The flow probe cable was delivered through an incision in the right flank [B] using a custom-designed exteriorising device [C] and loosely secured to the adjacent skin [D].*

---

nonabsorbable braided silk (3.0 Mersilk®, W192, Ethicon). Thereafter the connector at the far end of the probe cable was inserted into a custom-made exteriorising device, consisting of a hollowed out plastic cone with two small holes near its tip to accommodate a length of string for traction. The device was carefully slid along the lateral internal wall of the body cavity, with the tip guarded by the operator's palm, until it reached a location corresponding to the desired exit point on the right flank, which had been shaven and cleaned in preparation. Controlled pressure was applied to pass the device through the body wall and into a 1.5cm skin incision made externally on the flank by a second operator (Figure 4.1B). Great care was taken to ensure that there was no omentum or bowel between the device and the parietal peritoneum during exteriorisation. Once the tip of the device had passed through the muscle and fat, the

tip was grasped externally and string was threaded through the custom-made holes. Gentle traction was then applied to deliver the device (and the flow probe cable) out through the incision (Figure 4.1C). A generous loop of cabling was left inside the body cavity to allow for subsequent gravid uterine growth. The flank incision was closed with interrupted braided absorbable polyglactin (2.0 Vicryl®, W9463, Ethicon). A "flag" made from surgical tape was attached to the flow probe cable at its exit point and loosely secured to the adjacent skin with 2.0 Vicryl® to prevent any slack cabling inadvertently being pulled out (Figure 4.1D). Opsite® liquid spray dressing was applied to the wound and a custom-made fabric pouch (to house the flow probe cable and connector) was glued onto the skin using Kamar® adhesive (Kamar Inc., Steamboat Springs, CO, USA).

4.2.4.2 Telemetric monitoring of uterine blood flow

UBF was monitored on alternate days, beginning on the third post-operative day (92±0.2 days gestation) and ending with a final recording on the day prior to necropsy (130±0.2 days gestation). Ewes were monitored for 45 minutes each time. On the first occasion, UBF was recorded during the late afternoon in order to allow each ewe a full 72 hours post-operative recovery. Thereafter each individual animal was monitored at approximately the same time each day to minimise any confounding by potential circadian variation in UBF. Monitoring was also avoided at feeding times. During telemetric monitoring periods, ewes wore a custom-made fabric back-pack housing a PhysioMeter™ PGPM110 unit and Intelligent battery pack containing 2 rechargeable V286 7.2 lithium-ion batteries (PhysioGear®I, Transonic® Systems Inc.). To begin monitoring, the 4-pin flow probe connector was removed from the pouch on the animal's flank and connected to the PhysioMeter™ unit via a 4-pin AET8-4 interface cable. The backpack and any loose cabling were tucked away under the Tubigrip® bandage around the maternal abdomen (Figure 4.2A). Ewes were unrestrained and hence allowed to behave normally during monitoring. Real-time measurements of UBF (at a frequency of 128 per second) were transmitted to a trolley-mounted PC via a Bluetooth® connection (Figure 4.2B) and recorded using PhysioView™ P1U software (Transonic® Systems Inc., Figure 4.2C). Data was subsequently exported in *txt format and analysed using AcqKnowledge 3.9.1 software (BIOPAC Systems Inc., Goleta, CA, USA) to determine the mean and standard deviation.

Previous studies using indwelling Transonic® flow probes to monitor UBF in normal sheep pregnancy (Mehta et al. 2011) and in overnourished adolescent dams (Wallace et al. 2008b) had used recording times of 1 and 2 hours, respectively. In view of the large number of ewes undergoing UBF monitoring at any given point in the present study (up to 25 animals), it was

Figure 4.2 – Telemetric monitoring of uterine blood flow

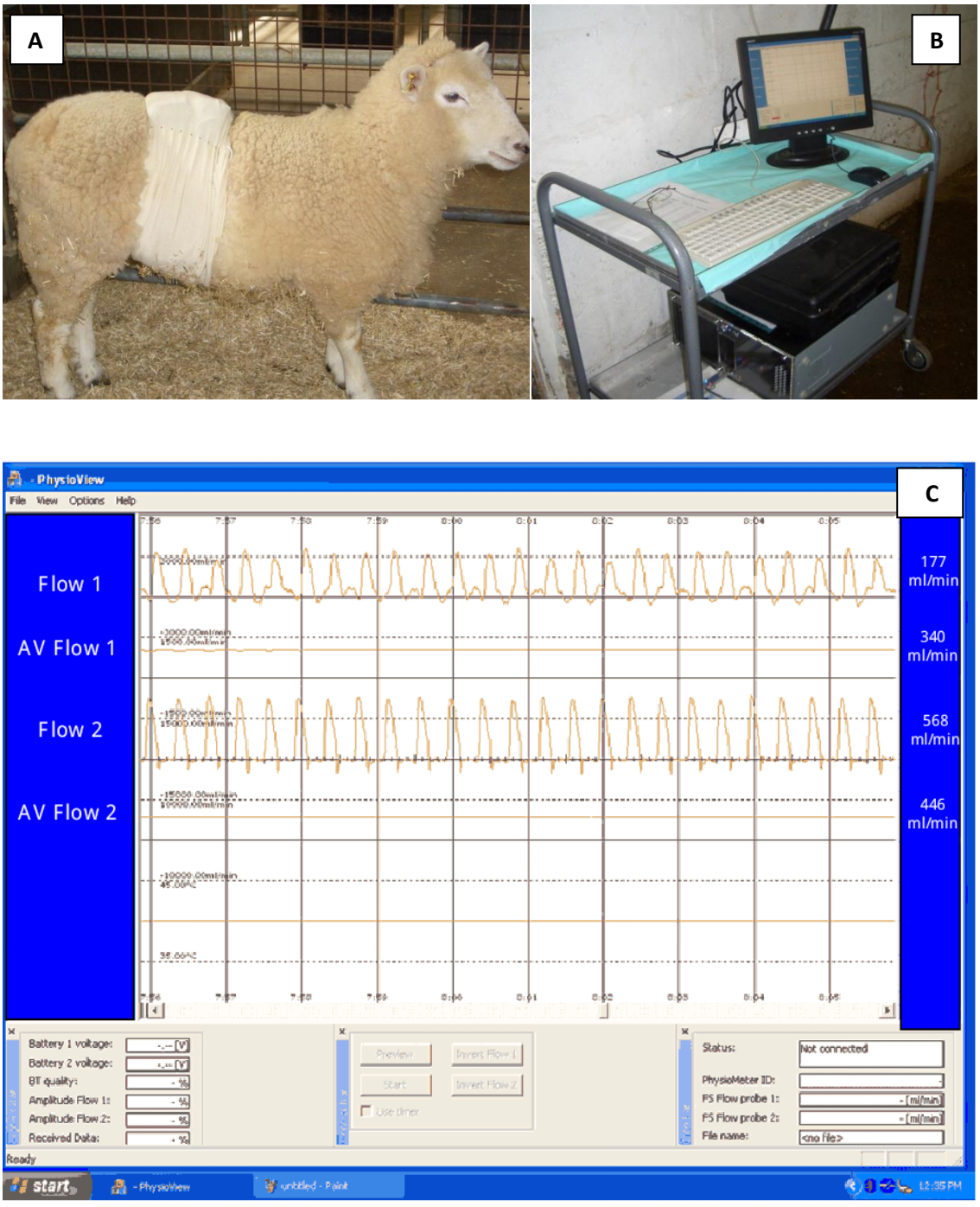

Photograph of a pregnant ewe undergoing telemetric monitoring of uterine blood flow (UBF): the ewe is unrestrained with the wireless Physiogear® system tucked away in a pouch under an abdominal bandage [A]. Real-time measurements of volume flow (ml/min) are transmitted to a nearby PC via Bluetooth® [B]. The data acquisition screen shows measurements of UBF and records values at a rate of 128 per second [C].

necessary to reduce recording times to 45 minutes. In order to validate 45-minute recording times against longer periods of monitoring, UBF was recorded in 21 ewes for 2-hour periods on a total of 35 occasions. A representative blood flow profile, showing the typical variation in an individual ewe over a 2-hour period, is shown in Figure 4.3. From these 35 recordings, mean UBF was determined on a minute-by-minute basis and used to calculate the overall mean and standard deviation for periods of 45, 60 and 120 minutes. These values were subsequently compared by one-way analysis of variance (ANOVA). There were no statistically significant differences between average flows over 45, 60 and 120 minutes. Mean differences in absolute UBF were ±7.6 ml/min for 45 versus 60 minutes and ±17.8 ml/min for 45 versus 120 minutes. Coefficients of variation were 1.5% and 3.2%, respectively.

Figure 4.3 – Representative uterine blood flow profile for an individual ewe over 2 hours

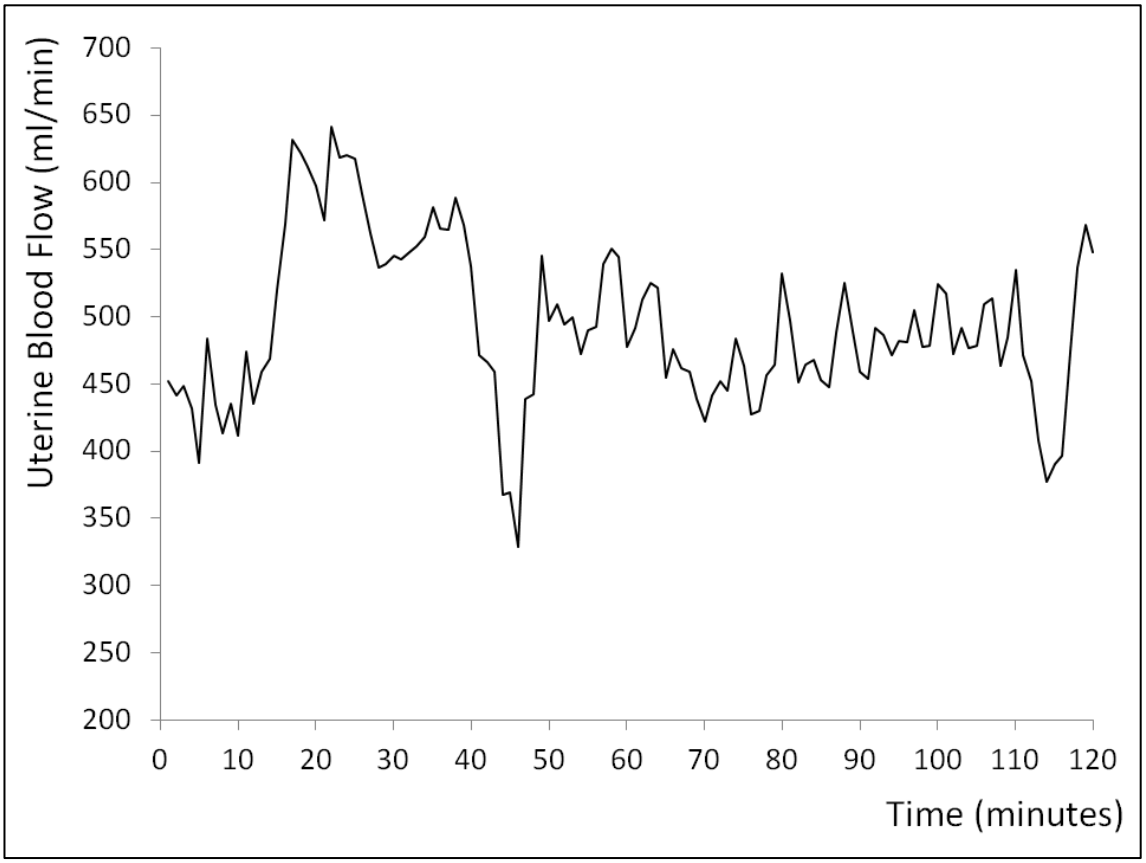

Example of a typical uterine blood flow profile in an individual ewe over 2 hours at 130 days gestation, demonstrating the physiological variation in flow (mean 493ml/min, standard deviation 10.9ml/min)

4.2.5 Necropsy procedures

4.2.5.1 Euthanasia

At 131±0.3 days gestation ewes were humanely killed using an overdose of 20-40ml pentobarbital sodium (Euthatal®, Merial Animal Health Ltd, Harlow, UK) administered by i.v. injection into the jugular vein. Death was confirmed by the absence of corneal reflexes. Thereafter the animal was suspended by the back legs using a ceiling mounted electric hoist. A large midline abdominal incision was made, taking care not to traumatise the rumen or cut the flow probe cable along its course from the flank to the pelvis. The abdominal cavity was opened and the gravid uterus was delivered and held by an assistant. The main trunk of the UtA supplying the gravid horn was clamped just distal to the flow probe and bowel clamps were placed across the cervix and paracervical ligament, which were then cut, allowing the entire reproductive tract to be removed *en bloc* without the flow probes attached, and weighed. The ewe was subsequently exsanguinated by severing the main vessels of the neck and maternal blood was collected in a bucket and subsequently weighed. The uterus was opened at the tip of the gravid horn, as per veterinary caesarean section. After sampling amniotic fluid into a 50ml syringe, the fetus was delivered out of the tip of the horn. A fetal blood sample was taken by cardiac puncture into a 10ml K2-EDTA tube immediately prior to the administration of 5–10ml pentobarbital sodium via a three-way tap. Blood samples were kept on ice before being processed as described in Section 2.2.1.

4.2.5.2 Fetal dissection

Once death had been confirmed, the fetus was dried with a cotton towel, weighed and transferred to a dedicated station for dissection and sampling. Fetal sex was recorded. The biparietal head diameter was measured using callipers at the widest point between the two parietal bones. Abdominal girth at the level of the umbilicus was determined using a piece of string, which was wrapped around the lamb's mid-section at the level of the cord insertion and at right angles to the spine, marked and subsequently measured against a ruler. Care was taken to reproduce the same plane each time. In addition, abdominal girth at the level of the lowermost rib was measured in an attempt to reproduce the level of the ultrasound AC plane.

Next the fetus underwent a systematic post-mortem examination with careful documentation of any gross abnormalities. A sample fetal record sheet is shown in Appendix 3, including a checklist of samples to be snap-frozen and/or immersion fixed. All samples for freezing were placed into liquid nitrogen chilled isopentane until frozen through and then stored on dry ice until the end of each necropsy, when they were transferred to -80^{o}C storage. All samples for

fixing were immersed in approximately 10 times their volume of neutral-buffered formalin (NBF) or Carnoy's solution, prepared as described in Section 2.2.2. Fixed tissues were subsequently processed to the wax block stage as described in Section 2.2.3. Widespread tissue sampling was carried out as described below, mainly as a precautionary measure. If Ad.VEGF treatment were to have any unexpected effects on gross organ morphology then a large tissue bank would be available for histopathological examination and additional analyses.

To begin the dissection, the fetal head was removed and the skull opened using a hacksaw. The fetal brain was carefully extracted and snap-frozen whole. The pituitary gland was removed from the sella turcica and placed into Tissue-Tek® O.C.T. compound (Ted Sella Inc., Redding, CA, USA) prior to freezing. Before opening the abdomen, a sample of umbilical cord was taken for freezing. The abdominal wall was then incised and the peritoneal cavity entered. Firstly the pancreas was dissected off, weighed complete and separately sampled at its hepatic and splenic poles for freezing and fixing, respectively.

Following removal en bloc, the complete gastrointestinal tract was placed into warm PBS (at 39^{o}C). Thereafter a length of fetal small intestine was selected for sampling and perfusion. Beginning at a location three mesenteric vein branches distal from the mesenteric-ileocaecal venous junction, a portion of fetal jejunum approximately 100cm in length was carefully excised together with its associated mesenteric vasculature. From the cranial end of this sample, a number of sections were taken and separately immersion-fixed in NBF and Carnoy's solution. The remaining length of fetal jejunum was subsequently perfuse-fixed with Carnoy's solution following cannulation of the mesenteric vascular arcade (see Figure 4.4). Sections of perfused jejunal tissue were then immersed in Carnoy's solution. Next the stomach complex, small intestine and large intestine were stripped off the mesentery and the bowel contents were extruded. The weight of the stomach complex was recorded before the mid-abomasum was sampled for freezing, halfway between the pyloric valve and the junction of the abomasum and omasum. The small intestine was weighed and sampled for freezing at the third branch of the mesenteric vein, distal to the portal-mesenteric venous intersection. A further 100cm section of fetal small intestine was removed, separately weighed and added to the small intestine weight to account for lost mass due to sampling and perfusion. Finally the large intestine was weighed and the proximal colon was sampled for freezing.

Next the liver was removed and weighed. A sample was taken from the right lobe for fixing, followed by generous samples from both lobes for freezing. The spleen was removed, weighed and sampled for fixing and freezing. Both kidneys were removed together with all perirenal fat,

Figure 4.4 – Perfusion-fixation of the fetal gastrointestinal tract

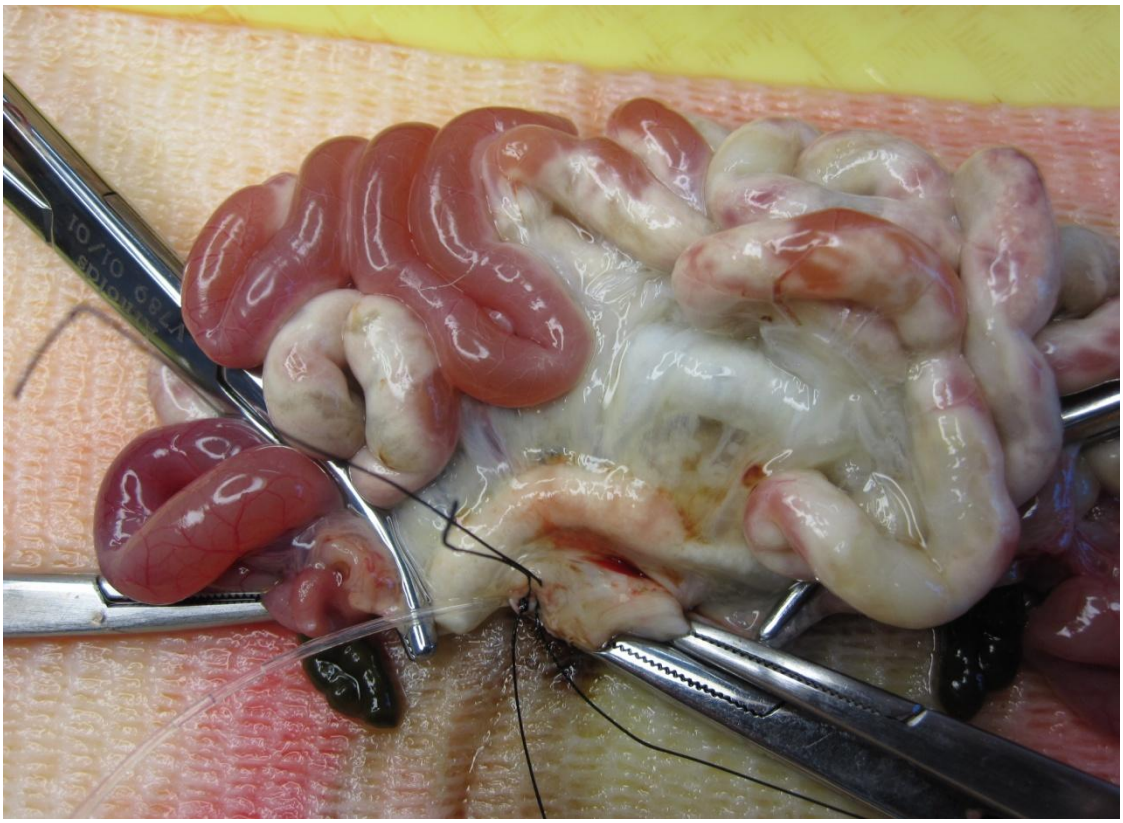

Image showing cannula threaded into mesenteric vessels and used to perfuse the mesenteric circulation with Carnoy's solution - note the whitish appearance of perfused-fixed jejunal tissue.

---

which was subsequently stripped off, weighed and sampled for fixing and freezing. The kidneys were then cut transversely and mid-section slices were fixed and frozen. The adrenal glands were removed and cut in half, one transversely and one longitudinally. Half of each adrenal was fixed and the other half frozen. A sample of skin was taken from the anterior thigh for freezing and the underlying quadriceps muscle was sampled for fixing and freezing. Next the fetal chest was opened and the heart removed and weighed. A transverse cross-sectional slice was taken for fixing, which included both ventricular walls and the interventricular septum. The remaining right and left ventricular tissue was separately frozen. The lungs were disconnected from the trachea, removed and weighed. The right lower lobe was sampled for fixing and freezing by cutting perpendicularly to the main bronchus approximately 3cm above the inferior border of the lobe. The thymus was removed, weighed and sampled for fixing and freezing, followed by the thyroid gland, which was cut in half for fixing and freezing. Next the

gonads were also weighed and sampled. For female fetuses the entire reproductive tract was removed and the ovaries were trimmed off. One was fixed and one was frozen in Tissue-Tek®. For male fetuses the tip of the scrotal sac was cut off and the testes displaced out of the cut end. The pampiniform venous plexus and the head, body and tail of the epididymis were trimmed off and each testicle cut into two halves in cross-section. One half of each testis was fixed and the other frozen in Tissue-Tek®. Next the femur was dissected out and cleared of all associated muscles and ligaments. The length of the bony shaft was measured using callipers. The bone was subsequently cut in half and a sample of bone marrow extracted for freezing. The tibia was then dissected clean and its length measured in the same manner as the femur. The fetal eyes were removed from the skull and each one cut in half in coronal section. Each half was cut in two again to produce semicircular samples, and one of each (i.e. one from the anterior and one from the posterior half of the eyeball) were fixed. Retinal tissue was carefully scraped off the inner surface of the remaining posterior eyeball for freezing. Finally, the fetal carcass was weighed and stored at -20^{o}C pending body composition analysis (Section 4.2.6.2).

4.2.5.3 Uteroplacental dissection

Following delivery of the fetus, the reproductive tract was moved to a dedicated dissection station where sampling of the uterine arteries was commenced immediately and in parallel with the fetal dissection described above. The uterine artery dissections were carried out as swiftly but carefully as possible to ensure that the vessels were in the best possible condition when subsequently examined in the organ bath (see Section 4.2.6.3). In particular, care was taken to avoid placing excessive tension on the vessels to ensure that the myofibres remained unstretched. Firstly the uterus was laid out on a tray and the visceral peritoneum was opened up with fine scissors to visualise the entire vascular tree, with its sequential branching pattern. Four reproducible levels of arterial branching were identified: the main UA trunk (UtA1); first branches (UtA2) and second branches (UtA3) at the level where the vessels entered the myometrium (see Figure 4.5). Starting with the gravid horn, samples of all these UtA branches were harvested. Each vessel was gently elevated using non-toothed tissue forceps and carefully separated off the underlying uterine tissue using Metzenbaum scissors. From all four branches (UtA1–4), two straight sections >1cm in length were taken and immersion fixed in NBF. In a subset of 22 animals, from branches UtA2 and UtA3 only, two straight sections 4cm in length were taken and placed into cold Krebs Ringer buffer (Ref. K0507, Sigma Aldrich) for subsequent organ bath analysis (see Section 4.2.6.3). All remaining samples from branches UtA1–4 were carefully cleared of associated connective tissue and blood before being frozen separately. Thereafter, the same dissection and sampling was repeated on the non-gravid side.

Figure 4.5 – Branching pattern of the uterine artery

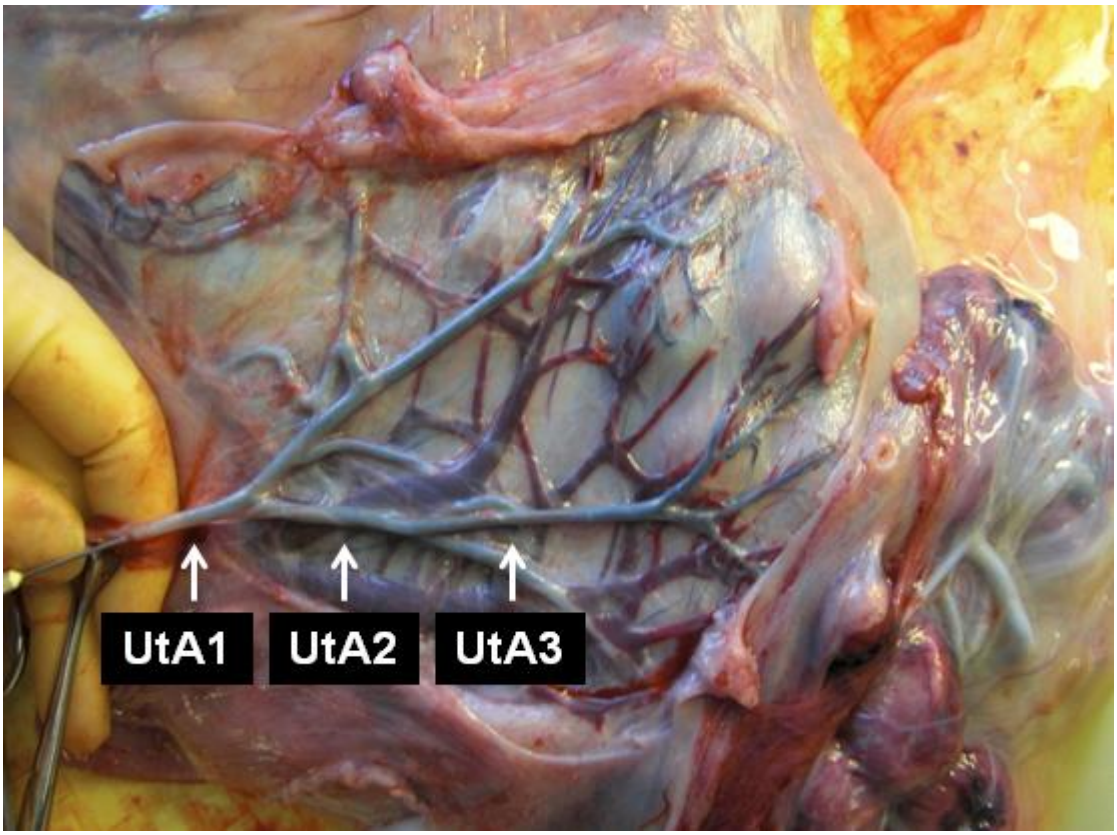

Uterine arterial tree (supplying the gravid uterine horn) perfused with Evans Blue dye in order to demonstrate the sequential branching pattern of the uterine artery (UtA) - the main trunk is designated UtA1, the first branches UtA2 and the second branches UtA3

Once the uterine artery dissection and sampling was complete, 10 representative placentomes from the gravid uterine horn were cut off the membranes, weighed and categorised by their morphological appearance (see Figure 4.6) into subtypes (A to D) according to the classification of Vatnick et al. (1991). Two placentomes were snap frozen whole, whilst a further two were separated into fetal cotyledonary and maternal caruncular portions and frozen separately. The remaining placentomes were each cut into 5mm slices, following which half the slices were immersion fixed in NBF and half in Carnoy's solution (prepared as described in Section 2.2.2). Finally, all remaining placentomes were removed from the membranes and separated into four groups according to their size (>5cm, 2–5cm, 1–2cm and <1cm). Placentomes were weighed by groups and individually subtyped. Weights and subtypes of the fixed, frozen and perfused placentomes (see above) were added in to complete these datasets. A sample

Figure 4.6 – Morphological classification of ovine placentomes

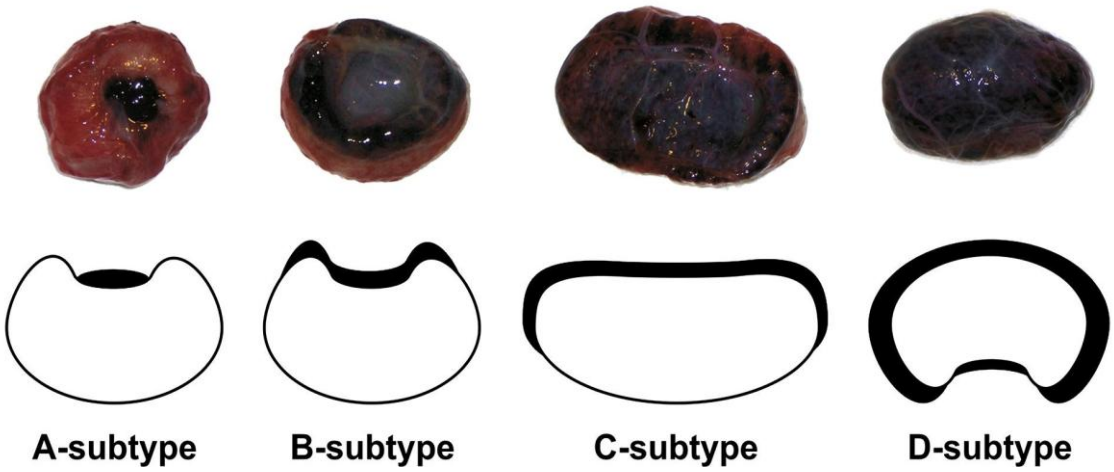

Subtypes of sheep placentome according to the classification of Vatnick et al. (1991) illustrating increasing surface area for maternofetal exchange with conversion from A through D subtypes. Figure reproduced with permission from Braun et al. (2011)

---

placental record sheet is shown in Appendix 4. The residual membranes were weighed and added to the total placentome weight to give the total placental weight. The residual uterus was also weighed, following which a sample of uterine wall was taken for freezing.

4.2.5.4 Maternal dissection

The weight of maternal blood collected in a bucket following exsanguination was recorded as an index of blood volume and the liver and perirenal fat depots were removed and weighed. The flow probe was recovered by carefully dissecting back from its exteriorisation point in the flank to its position around the transected uterine artery in the maternal pelvis. It was cleared of all adherent tissue and cleaned for subsequent retesting, sterilisation and reuse. The weight of the residual carcass was recorded. A sample maternal record sheet is shown in Appendix 5.

4.2.6 Laboratory techniques

For all the following analyses the individual investigator was blinded to the treatment group (both control versus high-intake and Ad.VEGF versus Saline/Ad.LacZ treatment) by means of block and sample coding until the analysis was complete.

4.2.6.1 Measurement of nutrients and metabolic hormones

Glucose, insulin and insulin-like growth factor 1 (IGF-1) concentrations were determined in duplicate in fetal and pre-necropsy maternal plasma samples, as described in Section 2.2.4. Glucose was also measured in amniotic fluid samples using the same method.

4.2.6.2 Fetal body composition analysis

Fetal carcasses were initially stored at -20^{o}C following necropsy. Subsequently each carcass was individually thawed out, weighed and cut into pieces of approximately 1kg. Each piece was processed through a mincer (Wolfking®, Slagelse, Denmark) before being combined in a bakers mixer for 5 minutes. After mixing thoroughly, three sub-samples of the homogenate (approximately 250g) were taken. After determining their exact weights, samples were placed onto aluminium trays and freeze-dried. Thereafter they were reweighed, ground using a coffee grinder and submitted to the Rowett Institute's Analytical Department for the determination of ash, protein and fat content. The residual moisture content of the remaining fetal carcass following freeze- drying was also determined by drying to constant weight at 100^{o}C. Ash content was determined by ashing at 600^{o}C to constant weight, protein content (nitrogen x 6.25) by the Kjeldahl procedure (Davidson et al. 1970) and fat content by the chloroform-methanol technique, as previously described (Atkinson et al. 1972).

4.2.6.3 Organ bath experiments

In 22 animals, two samples of uterine artery branches UtA2 and UtA3 from both the gravid and non-gravid sides (four samples in total) were stored in cold Krebs Ringer buffer and couriered overnight from Aberdeen to London for analysis in an organ bath the following day by Vedanta Mehta. Vascular reactivity was assessed by generating dose response curves to phenylephrine and bradykinin, as previously described (David et al. 2008; Mehta et al. 2011). The set-up for these experiments is illustrated in Figure 4.7. There was no suitable organ bath equipment available locally, hence the need to transport the vessels to the Rayne Institute at UCL for analysis using previously validated techniques. To evaluate the suitability of overnight transfer, an intact rat aorta was shipped from Aberdeen to UCL under similar transportation conditions, and analysed in the organ bath to test its response 24 hours after harvest. It was noted that the aortic segments reacted to potassium chloride, phenylephrine and acetylcholine, although the magnitude of responses recorded was 15-20% less than fresh vessels.

On arrival the vessels were prepared by carefully clearing them of any residual connective tissue under a dissecting microscope. Thereafter each vessel was cut into 3mm ring segments.

Figure 4.7 – Schematic of organ bath equipment set-up

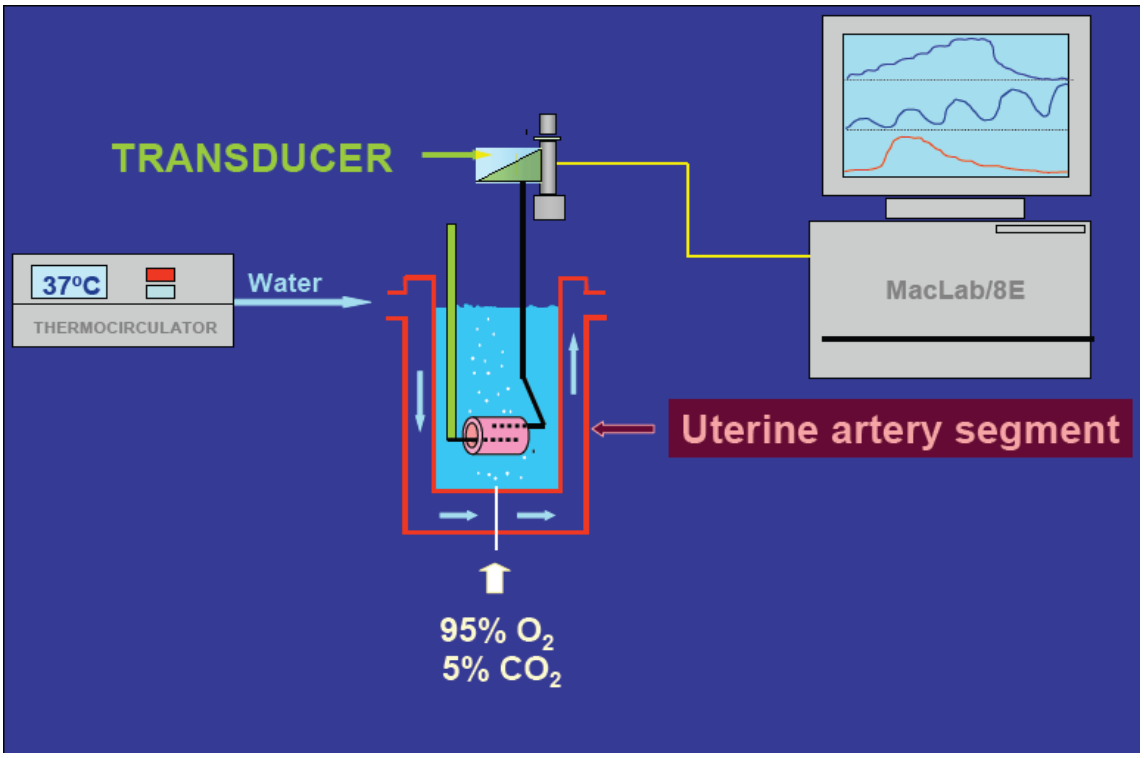

Schematic diagram illustrating the organ bath set-up. A section of uterine artery is suspended between two pins in a chamber filled with Krebs buffer, maintained at 37°C using a thermocirculator. Increasing concentrations of agonists are added to the chamber to induce vasoconstriction/vasorelaxation, which is recorded in real time by a transducer linked to a PC. Figure reproduced with permission from the thesis of Dr Vedanta Mehta (PhD awarded 2011).

Sixteen 25ml organ bath chambers were filled with Krebs Ringer buffer, to which 2.5mM calcium chloride ($CaCl_2$) was added. Channels were calibrated using a 5g weight. A water thermocirculator was used to maintain the temperature within the chambers at 37°C and carbogen (95% oxygen, 5% carbon dioxide) gas was bubbled in to maintain the pH at a physiological level (7.3–7.4). Eight ring segments were mounted between vertically opposed pins in the series of chambers (taking care not to damage the vessel endothelium) and kept under gentle holding tension whilst being allowed to equilibrate. Subsequently the tension was increased gradually to 0.3g, 0.5g and 1.0g, at intervals of 5–10 minutes. Vessel segments were washed in between each increase in tension by flushing the chambers and refilling them with fresh Krebs Ringer buffer (+$CaCl_2$). Next a viability check was performed by adding 0.3ml 4M

KCl solution to achieve a concentration of 48mM within each organ bath. The resultant increase in measured tension was allowed to plateau, at which point maximum contractility was recorded. Vessel segments were then washed repeatedly until tension returned to baseline. After waiting for a minimum of 10 minutes, the KCl challenge was repeated until maximum contractility no longer exceeded the previous measurement. Thereafter vessel segments were repeatedly washed to remove all KCl and allowed to recover for >30 minutes.

To assess vascular contractility, a dose-response curve to phenylephrine (PE) was generated by adding sequential doses of PE at increasing concentrations to achieve 9 stepwise semi-logarithmic concentrations within the organ bath (10^{-9}, $3x10^{-9}$, 10^{-8}, $3x10^{-8}$, 10^{-7}, $3x10^{-7}$, 10^{-6}, $3x10^{-6}$ and 10^{-5}). After each addition of PE the contractile response was allowed to plateau before the next dose was added. At the end, vessel segments were repeatedly washed and allowed to recover for at least 30 minutes. To assess vasorelaxation, a dose-response curve to bradykinin (BK) was generated by adding sequential doses of BK at increasing concentrations to achieve 9 concentrations within each bath (10^{-11}, $3x10^{-11}$, 10^{-10}, $3x10^{-10}$, 10^{-9}, $3x10^{-9}$, 10^{-8}, $3x10^{-8}$ and 10^{-7}). Prior to adding any BK, vessel segments were pre-contracted using PE. From the PE dose-response curve the degree of tension equivalent to 10-15% of maximum contractility to KCl (typically 2–3g) was calculated and the corresponding volume and concentration of PE to achieve this tension was added to the bath. The contraction was allowed to stabilise before adding BK. After each dose of BK the relaxation response was allowed to plateau before adding the next.

4.2.6.4 Uterine artery sectioning, H&E staining, anti-vWF immunohistochemistry

Duplicate paraffin-embedded sections of uterine artery at three levels of branching (UtA1 to 3) were cut into ribbons of three micron thickness using a microtome. Ribbons were floated in water heated to 37^{o}C until completely stretched out, transferred in duplicate onto glass slides coated with polylysine (Ref. 631-0107, VWR, Leuven, Germany) to prevent undesired slippage of the tissue during subsequent processing, and allowed to air dry.

One slide from each pair was stained with haematoxylin and eosin (H&E) at the Barts Cancer Institute, Queen Mary University London using a Leica ST5010 Autostainer XL coupled with a CV5030 automated glass coverslipper (Leica Microsystems). During this process the slides were immersed in haemotoxylin in PBS at pH 7.2 for 5 minutes and washed three times with fresh PBS before being transferred into 1% eosin in PBS (also at pH 7.2) for 5 seconds and washed again three times in PBS. The slides were then passed through an ascending alcohol gradient into xylene, mounted in di-n-butylphthalate in xylene (DPX), covered with glass slips and dried.

The second slide from each pair was immunostained using the endothelial marker anti-VWF in order to identify and count the small vessels within the perivascular adventitia, as previously described (Mehta et al. 2011). This particular technique was adapted from the methodology of (Bobryshev et al. 2001) but used trypsin digestion in place of proteinase K for the purpose of antigen retrieval. The aim of staining endothelial cells was to differentiate blood vessels from other structures that can appears similar on histology e.g. nerve fibres and lymph vessels.

Prior to starting the immunohistochemistry, a 5mM Tris- (tris[hydroxymethyl]aminomethane, molecular weight = 121g) buffered saline solution was prepared by adding 0.3g Trizma® base (Ref. T-6066, Sigma Aldrich) to each 500ml distilled water and adjusting the pH to 7.8 with 1M hydrochloric acid. PBS solution (10mM sodium phosphate, pH 7.5, 0.9% saline) was prepared by dissolving 1 Gibco® PBS tablet (Ref. 18912-014, Invitrogen, Paisley, UK) per 500ml distilled water. In addition a 0.1% PBS/BSA solution was prepared by gently dissolving 0.1g bovine serum albumin (Ref. B-4287, Sigma Aldrich) per 100ml PBS solution. PBS and Tris-buffered saline were stored at room temperature, and PBS/BSA stored at 4°C pending use. To begin, the paraffin-embedded sections of UtA mounted on slides were dewaxed and hydrated by passing them sequentially through the following solutions:

- Xylene 5 min
- Xylene 5 min
- 100% ethanol 5 min
- 100% ethanol 5 min
- 95% ethanol 3 min
- 80% ethanol 2 min
- Distilled water 5 min
- Distilled water 5 min

A 0.6% solution of hydrogen peroxide was prepared immediately before use by 1:50 dilution of a 30% stock solution (Ref. 216763, Sigma Aldrich) with distilled water. Slides were immersed for 15 minutes in order to block endogenous peroxidase activity and then rinsed in tap water. Each slide in turn was gently dried before a PAP (peroxidase-antiperoxidase) pen (Dako, Glostrup, Denmark) was used to draw a hydrophobic boundary around the vessel. Slides were returned to tap water pending the subsequent antigen retrieval step. Immediately before use, a 0.1% solution of trypsin (Difco Trypsin-250, 215240, Scientific Laboratory Supplies (SLS), Nottingham) and calcium chloride (Ref. C-7902, Sigma Aldrich) was prepared by gently

dissolving 50mg of each in 50ml 5mM Tris-buffered saline. Next 200µl of this solution was pipetted onto each slide and placed into an incubator for 10 minutes at 37°C. After incubation, slides were washed three times with PBS, for three minutes each. Meanwhile a 5% solution of non-immune goat serum was prepared by diluting a stock solution (Ref. X0907, Dako) 50-fold with PBS. Each slide was dried to remove any excess buffer then 200µl of serum was pipetted onto each slide and allowed to incubate for 30 minutes at room temperature to prevent non-specific binding of antibody to proteins in tissue. Meanwhile the primary antibody, rabbit anti-human vWF (A0082, Dako), was diluted with PBS/BSA, initially at varying concentrations (1:50, 1:100, 1:200, 1:400 and 1:800) and subsequently at the optimum concentration of 1:200. 200µl of solution was pipetted onto each slide. A negative control was included here by omitting the incubation with primary antibody i.e. pipetting on 200µl PBS/BSA only. Slides were incubated overnight in a humidified chamber at 4°C.

The following morning, slides were washed three times with PBS/BSA for three minutes each time. Meanwhile the secondary antibody, goat anti-rabbit biotinylated IgG (E0432, Dako), was diluted 100-fold with PBS/BSA. Each slide was gently dried to removed excess PBS/BSA before 200µl of solution was pipetted onto each vessel section and slides were incubated for 60 minutes at room temperature. Thirty minutes into the incubation step 5ml of avidin-biotin complex (ABC) solution was prepared by adding one drop (50µl) of solutions "A" and "B" (VECTASTAIN® Standard Kit, Ref. PK-4000, Vector Laboratories, Peterborough, UK) into 5ml PBS, as per the manufacturer's protocol. The solution was allowed to stand at room temperature for at least 30 minutes before use. Following the incubation step, slides were washed once with PBS/BSA and twice with PBS for three minutes each time. After gently drying off any excess buffer 200µl of ABC solution was pipetted onto each vessel section and slides were incubated for 60 minutes. Forty-five minutes into the incubation step, a 3,3'-diaminobenzidine tetrahydrochloride (DAB) substrate solution (D5905, Sigma Aldrich) was prepared by adding 25mg (2½ tablets) DAB per 50ml of PBS in a Falcon tube, which was then vigorously vortexed until complete dissolution and kept in the dark pending use. Following the incubation step, slides were washed three times with PBS for three minutes each time. Immediately prior to use, 16.7µl of 30% hydrogen peroxide (Ref. 216763, Sigma Aldrich) was added for each 50ml of DAB solution required, vortexed and transferred into a cuvette. Slides were transferred into the solution and allowed to stain for 10 minutes. Thereafter the reaction was stopped by transferring the slides into distilled water. Sections were counterstained by immersing them in Mayer's haematoxylin solution (Ref. 51275, Sigma Aldrich) for 2 minutes then transferring into tap water. Finally, slides were dehydrated by passing them sequentially through the following solutions:

- 80% ethanol 2 min
- 95% ethanol 3 min
- 100% ethanol 5 min
- 100% ethanol 5 min
- Xylene 5 min
- Xylene 5 min

Slides were mounted in DPX (Ref. 360294H, VWR International) and 50x20mm glass cover slips were manually applied (SLS Ltd, Nottingham). Slides were allowed to dry for 24 hours before the vessel counting and image analysis was performed (see below). Figure 4.8 illustrates two different sections of the same vessel stained with H&E and anti-vWF antibodies, respectively.

4.2.6.5 Uterine artery image analysis

To assess neovascularisation within the perivascular adventitia, anti-vWF stained sections were first examined under the microscope (Nikon Eclipse E600, Amstelveen, Netherlands) at x20 magnification for vessel counting. All positively stained structures with a distinct lumen within the adventitia were counted in duplicate, as previously described (Mehta et al. 2011). An example of such a positively stained structure is provided in Figure 4.9A. Subsequently a photograph of the entire vessel (x2 magnification) was taken for image analysis in order to quantify the adventitial area. This extension of the previously described methodology aimed to give some indication of vessel density. Each image was analysed using Motic Images 2.0 (Motic China Group Co Ltd, Indusxiamen, China) by manually tracing around the following three areas:

- Total vessel area (TVA) (Figure 4.9B)
- Intima + media + lumen area (IMLA) (Figure 4.9C)
- Lumen area (LA) (Figure 4.9D)

which allowed for the calculation of the following additional parameters:

- Adventitial area (AA) = TVA – IMLA
- Intima + media area (IMA) = IMLA – LA

The number of vessels in the perivascular adventitia was subsequently compared in absolute terms and expressed per unit adventitial area.

To assess intima-to-media ratios (IMR), H&E stained sections were examined in duplicate at

Figure 4.8 – Uterine artery sections stained with H&E and anti-vWF antibodies

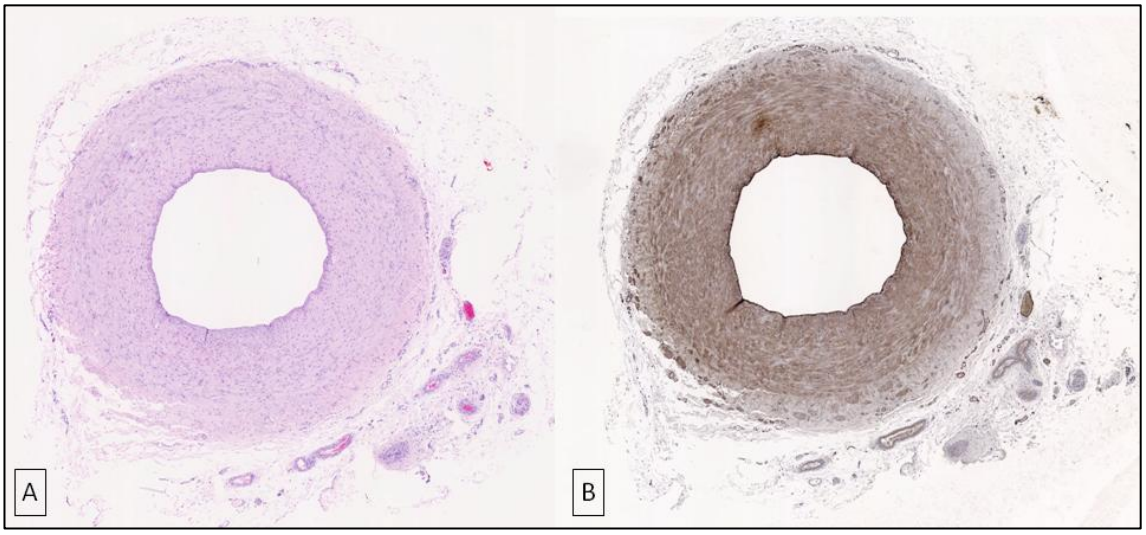

Sections of the main trunk of the uterine artery stained with: [A] haematoxylin and eosin; and [B] anti- von Willebrand factor antibodies (an endothelial cell marker); for the measurement of intima-to-media ratios and the asssessment neovascularisation in the perivascular adventitia.

---

x20 magnification and photographs were taken of the vessel wall at the 3, 6, 9 and 12 o'clock positions, taking care that the borders between the intima and media, and the media and adventitia, were both clearly visible. Image J software (National Institutes of Health, Bethesda, MD, USA) was used to measure the thickness of a representative portion of the intima and media, immediately parallel to one another in a radial fashion, in each of the four images per vessel section (Figure 4.10). The coefficient of variation was calculated and any outlying measurements were repeated where this exceeded 10%. Finally the mean intimal and medial thickness and IMR were calculated for each duplicate section and averaged again.

4.2.6.6 RNA extraction

Separately frozen caruncular and cotyledonary tissues were powdered and 50mg of each sample transferred into 0.5ml Tri-Reagent (Sigma Aldrich Co. Ltd) in a 2ml microcentrifuge tube. Samples were kept on ice and processed using an Ultraturrex tissue homogeniser. After homogenisation tubes were allowed to stand for 5 minutes prior to the addition of 0.1ml chloroform. Tubes were shaken manually for 15 seconds, left to stand again for 5 minutes and then centrifuged at 12000g for 15 minutes at 4°C (Jouan KR422). Taking care to avoid the

Figure 4.9 – Vessel enumeration and determination of adventitial area

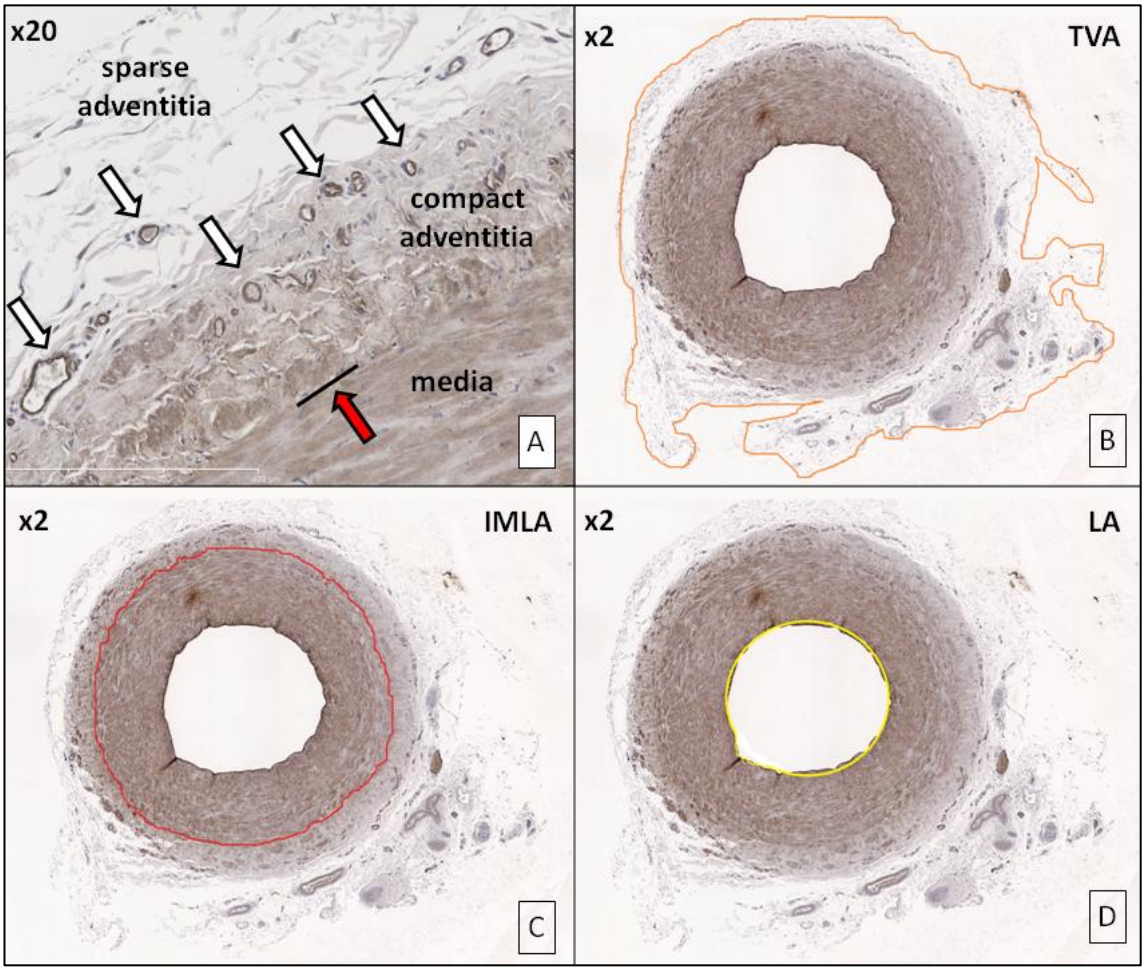

[A] View of perivascular adventitia at x20 magnification illustrating structures with a distinct lumen (some examples are indicated by the white arrows) that have been positively stained with the endothelial cell marker anti- von Willebrand factor - these represent adventitial blood vessels. The red arrow indicates the medial/adventitial border, which separates the muscular layer of the blood vessel from the compact adventitia. [B/C/D] Determination of adventitial area (AA) and intima+media area (IMA) by separate calculation of: [A] total vessel area (TVA); [B] intima+media+lumen area (IMLA); and [C] lumen area (LA) and subtraction as follows: AA = TVA – IMLA; IMA = IMLA – LA

---

interphase, the upper aqueous phase was transferred into a 1.5ml microcentrifuge tube, to which was added 0.25ml isopropanol. After inverting several times to gently mix, tubes were left at room temperature for 10 minutes before being centrifuged again at 12000g for 10

Figure 4.10 – Measurement of intima-to-media ratios

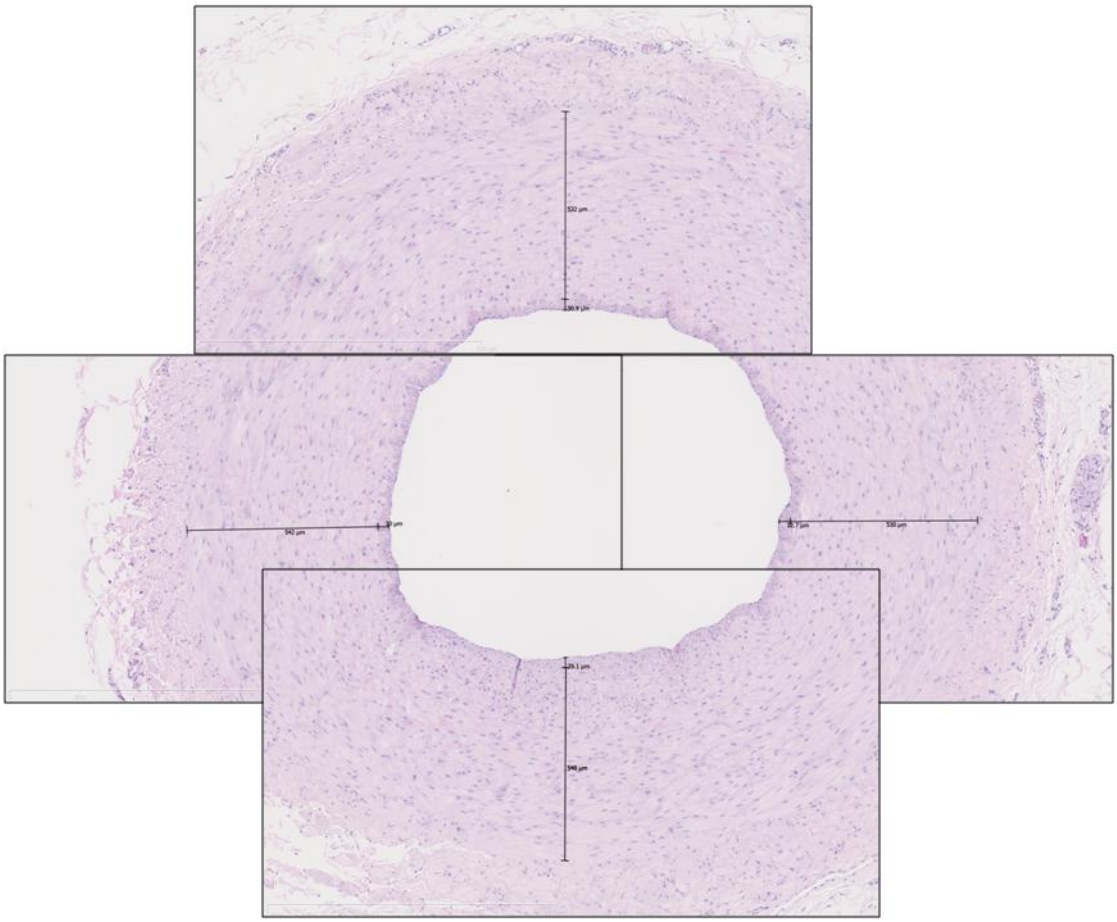

Series of four photographs taken at 3, 6, 9 and 12 o'clock demonstrating the measurement of intimal and medial thickness and calculation of intima-to-media-ratios. The mean of the four measurements was determined in duplicate for each vessel.

---

minutes at 4°C (Jouan KR422). The supernatant was discarded and the resultant pellet was washed in 0.5ml cold 70% ethanol, vortexed and centrifuged for a third time at 7500g for 5 minutes at 4°C (Jouan KR422). The supernatant was again discarded and pellets allowed to air dry for a short period, taking care not to allow them to dry out completely. Pellets were resuspended by vortexing in 40µl Ultrapure™ diethylpyrocarbonate (DEPC) treated water. A subsample of 1µl was added to 9µl in a 1.5ml microcentrifuge tube and used to determine the quality and quantity of total RNA by capillary electrophoresis using an Agilent 2100 Bioanalyser (Agilent Technologies, Wilmington, DE, USA). The remaining sample was stored at -80^{o}C pending quantitative reverse transcription polymerase chain reaction (qRT-PCR).

4.2.6.7 Quantitative real-time reverse transcription polymerase chain reaction

Extracted RNA was subsequently reverse transcribed in triplicate using Taqman Reverse Transcription reagents and Multiscribe Reverse Transcriptase (Applied Biosystems, Warrington, Cheshire).

To reverse transcribe the extracted RNA, 23.1µl (~90ng) of each diluted sample was transferred to a 96-well plate. To each well was added 36.9µl RT Mastermix (Applied Biosystems). Samples were mixed, then 18µl of each was transferred into a new 96-well plate. Plates were processed through a 4-block thermal cycler (Techgene). Samples were initially heated to 25^{o}C for 10 minutes, followed by 48^{o}C for 30 minutes and 95^{o}C for 5 minutes, and then held at 4^{o}C. The RT plate was subsequently diluted 5-fold by adding 72µl nano water (ultrapure water prepared with an ELGASTAT UHQ PS water purification system) to each 18µl sample. This plate (termed "GOI RT-Prep") was used for the gene of interest determinations. Next 5µl of each diluted sample was transferred into a new 96-well plate and diluted 20-fold by adding 95µl nano water. This plate (termed "18s RT Prep") was used for the housekeeping gene determinations. Both plates were stored at -20^{o}C pending the subsequent PCR step.

A set of standards was prepared using RNA pooled from placentomes sampled from control-intake ewes at 130 days gestation (consisting of 6 cotyledon and 6 caruncular samples, respectively). To begin, 123µl RT Mastermix was added to 77µl of standard at 3.9ng/µl dilution in a 0.5ml thin-walled PCR eppendorf tube and then processed through the thermal cycler exactly as described above. Following the reaction the standard was diluted five-fold by combining it with 800µl nano water in a fresh 1.5ml eppendorf tube. A 100µl aliquot of this top standard was then double diluted down six times (in 50µl nanowater each time) to produce a set of seven standards for the GOI RT Prep plate. A further 5µl aliquot was combined with 95µl nano water and similarly double diluted to produce seven standards for the 18s RT Prep plate.

The real-time PCR step utilised custom-designed Taqman probes and primers that had been designed for ovine-specific gene sequences using Primer Express (Applied Biosystems), and validated in previous experiments (Wallace et al. 2004a; Redmer et al. 2005). Table 4.1 details the sequences for the forward and reverse primers and FAM-labelled probes for the following 11 genes of interest (Genbank accession numbers are given in parentheses, where available):

- Vascular endothelial growth factor A –VEGFA (X89506)
- Fms-related tyrosine kinase 1 –FLT1 (AF488351)
- Kinase insert domain receptor – KDR (AF233076)

- Nitric oxide synthase – NOS3 (AF201926)
- Fibroblast growth factor 2 – FGF2 (L36136)
- Angiopoietin 1 – ANGPT1
- Angiopoietin 2 – ANGPT2
- Endothelial tyrosine kinase – TEK (AY288926)
- Soluble guanylate cyclase – GUCY1B3 (AF486295)
- Glucose transporter 1 – GLUT1 (U89029)
- Glucose transporter 3 – GLUT3 (L39214)

For the PCR, 5µl of each sample from the GOI RT Prep and 18s RT Prep plates and 5µl of each standard was added to a 96-well plate using an 8-channel pipette and mixed well with 20µl of PCR Mastermix (Applied Biosystems). The volume of each forward/reverse primer and FAM-labelled probe required to give a final concentration of 900nM (1.125µl per 12.5µl reaction) and 250nM (1.125µl per 12.5µl reaction), respectively, was calculated and the working stocks of 10µM were diluted accordingly. Finally, 10µl of each sample/standard (with PCR Mastermix) was transferred in duplicate into a new 96-well PCR plate, to which was added the necessary volume of each primer and probe. Polymerization and amplification reactions were carried out for 40 cycles of 95^{o}C for 15 seconds and 60^{o}C for 1 minute using an ABI 7500 Fast Real-Time PCR system (Applied Biosystems). mRNA expression was quantified by generating a relative standard curve from the serially diluted standard. Individual sample mRNA expression for each gene of interest was expressed relative to the sample's own internal 18S RNA using 18S PDAR kit reagents (Applied Biosystems).

4.2.6.8 Assessment of small intestinal crypt cell proliferation

To assess small intestinal crypt cell proliferation, paraffin-embedded sections of perfuse-fixed jejunal tissues were sectioned and immunostained for proliferating cell nuclear antigen (Ki-67) at North Dakota State University. Tissue sections were initially treated with a blocking buffer consisting of PBS and 1.5% by volume normal horse serum (Vector Laboratories, Burlingame, CA, USA) for 20 minutes before being incubated with primary mouse monoclonal anti-Ki-67 antibody 1:100 concentration (Clone MM1, Vector Laboratories). Following treatment with the secondary antibody (ImmPress™ anti-mouse immunoglobulin (peroxidase) polymer detection kit, Ref. MP7402, Vector Laboratories) and DAB substrate, tissue sections were counterstained with hematoxylin. From each animal five tissue sections were photographed and subjected to image analysis using Image Pro Plus 5.0 software (MediaCybernetics, Inc., Silver Spring, MD).

Table 4.1 - Forward/reverse primers and probes for placental RT-PCR analyses

Oligonucleotide	**Nucleotide sequence**
VEGFA forward primer	5'-GGA TGT CTA CCA GCG CAG C-3'
VEGFA reverse primer	5'-TCT GGG TAC TCC TGG AAG ATG TC-3'
VEGFA probe	5'(6FAM)-TCT GCC GTC CCA TTG AGA CCC TG-(TAMRA)3'
FLT1 forward primer	5-TGG ATT TCA GGT GAG CTT GGA-3'
FLT1 reverse primer	5'-TCA CCG TGC AAG ACA GCT TC-3'
FLT1 probe	5' (6FAM)-AAA ATG CCT GCG GAA GGA GAG GAC C-(TAMRA)3'
KDR forward primer	5'-CTT CCA GTG GGC TGA TGA CC-3'
KDR reverse primer	5'-GCA ACA AAC GGC TTT TCA TGT-3'
KDR probe	5'(6FAM)-AGA AGA ACA GCA CGT TCG TCC GGG-(TAMRA)3'
NOS3 forward primer	5'-CAG CGG CTG GTA CAT GAG C-3'
NOS3 reverse primer	5'-TTG TAG CGG TGA GGG TCA CA-3'
NOS3 probe	5'(6FAM)-CGG AGA TTG GCA CGC GGA ACC-(TAMRA)3'
FGF2 forward primer	5'-CGA CGG CCG AGT GGA C-3'
FGF2 reverse primer	5'-CTC TCT TCT GCT TGA AGT TGT AGT TTG-3'
FGF2 probe	5'(6FAM)-TCC GCG AGA AGA GCG ACC CTC AC-(TAMRA)3'
ANGPT1 forward primer	5'-AAA TGA AAA GCA GAA CTA CAG GTT GTA T-3'
ANGPT1 reverse primer	5'-GCA AGA TCA GGC TGC TCT GTT-3'
ANGPT1 probe	5'(6FAM)-TGA AGG GTC ACA CTG GGA CAG CAG G-(TAMRA)3'
ANGPT2 forward primer	5'-AAA TAG GGA CCA ACC TGC TCA A-3'
ANGPT2 reverse primer	5'-TGT TGT CTG ATT TAA TAC TTG GGC TT-3'
ANGPT2 probe	5'(6FAM)-CTG CAG AGC AGA TCC GGA AGT TAA CAG ATG T-(TAMRA)3'
TEK forward primer	5'-CCT CGG AGG CAG GAA GAT G-3'
TEK reverse primer	5'-TCA GGC AGG TCA TTC CCG-3'
TEK probe	5'(6FAM)-TGC TTA TCG CCA TCC TCG GCT CA-(TAMRA)3'
GUCY1B3 forward primer	5'-CCG AGC CGT GCA TCC A-3'
GUCY1B3 reverse primer	5'-ATC TCC ATC ATG TCC AAG GCC -3'
GUCY1B3 probe	5'(6FAM)-CAT GCA CGG TCC ATC TGC CAC C-(TAMRA)3'
GLUT1 forward primer	5’-TGC TCA TTA ACC GCA ACG AG -3’
GLUT1 reverse primer	5’-GGT CCC ACG CAG CTT CTT C-3’
GLUT1 probe	5’(6FAM)-AGA ACC GGG CCA AGA GCG TGC-(TAMRA)3’
GLUT3 forward primer	5’-TTT GGA AGA ACG GTC AGA AAC A-3’
GLUT3 reverse primer	5’-CAG ACA AGG ACC ACA GGG ATG-3’
GLUT3 probe	5’(6FAM)-CCC CGT CCA GCG TGC TCC TC-(TAMRA)3’

The number of proliferating and non-proliferating epithelial cells was counted and the labelling index was determined as the proportion of proliferating cells, expressed per unit of tissue area. Representative images from two individual fetuses selected from the H+Ad.VEGF and C+Saline groups are in presented in Figure 4.11.

4.2.7 Statistical analyses

After testing for normality of the data and equality of variance using Q-Q plots and Levene's test, respectively, comparisons were made between the two nutritional regimes (prior to the allocation of high-intake ewes to H+Ad.VEGF, H+Saline and H+Ad.LacZ groups) using Student's t test. Subsequently, comparisons between the four main study groups were made using one-way ANOVA. Following any significant F-test result ($p<0.05$) post-hoc pairwise comparisons were performed using the test of least significant difference (LSD). Post-hoc tests were also performed where F values tended towards significance ($p<0.1$). Correlations were assessed using Pearson's product moment test. For the UtA analyses, General Linear Model was used to assess differences between study groups whilst taking into account the level of branching (UtA1-3) and uterine horn (gravid/non-gravid). All data are presented as mean ± standard error of the mean (SEM) unless otherwise stated. Formal statistical significance was considered to have been reached where $p <0.05$ and a tendency towards significance was defined as $p<0.1$.

4.3 Results

Full datasets (comprising UBF, serial ultrasound and necropsy data) were collected in 57 of 60 animals. One ewe in the H+Saline group was euthanased on welfare grounds on post-operative day 3 following persistent inappetance and signs of distress. At post-mortem examination there was found to have been trauma to an avascular area of the bowel mesentery during exteriorisation of the flow probe. Another ewe in the H+Saline group (and carrying a very large fetus) developed a hernia as a late complication of surgery 4 weeks post-op. A decision was made to omit her fifth time point ultrasound scan (119 days gestation) due to the risk of bowel strangulation, however she remained well and a final ultrasound examination was performed on the day prior to necropsy (131 days gestation). At post-mortem a paramedian defect in the rectus sheath was identified, through which the abdominal viscera had herniated. The suture line remained intact. Finally, one ewe in the H+Ad.VEGF group was fitted with a flow probe which subsequently failed to function *in vivo*. Therefore UBF data in the latter group was limited to 17 of 18 animals.

In addition, two animals were excluded from further analysis. One ewe in the H+Saline group was identified as an extreme outlier with respect to UBF measurements (756ml/min at

Figure 4.11 – Evaluation of small intestinal crypt cell proliferation by immunhistochemistry

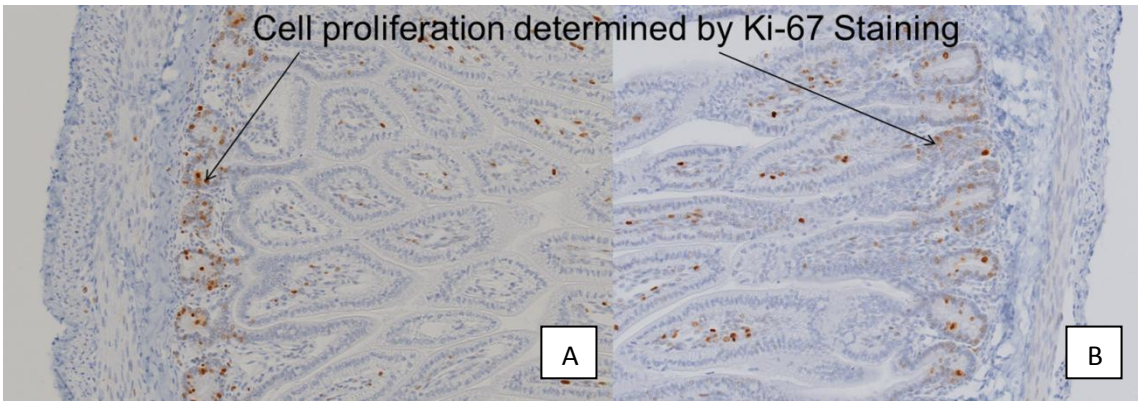

Sections of fetal jejunum immunostained with anti Ki-67 antibodies to determine the number of proliferating cells within the small intestinal crypts by image analysis. A = example taken from the growth-restricted fetus of a high-intake ewe treated with Ad.VEGF. B = example taken from a non-growth restricted fetus of a control-intake ewe treated with Saline. There were no significant differences between study groups for any indices.

---

baseline in mid-pregnancy; >4 standard deviations above the mean of 324ml/min). A Q-Q plot demonstrated that her measurements lay well outside the normal distribution. A second ewe, also in the H+Saline group, was excluded after she was found to have a congenital abnormality of the reproductive tract (uterus didelphys) resulting in restriction of her pregnancy to a single uterine horn (see Section 4.3.4.6 for a full description). Data from all remaining pregnancies in the H+Saline (n=13), H+Ad.LacZ (n=14), H+Ad.VEGF (n=18) and C+Saline groups (n=14) is presented below. All data are reported as mean ± SEM unless otherwise specified.

4.3.1 Baseline characteristics prior to gene therapy administration

4.3.1.1 Maternal weight and adiposity

Table 4.2 shows baseline characteristics in the four experimental groups at the time of embryo transfer, summarised retrospectively. Despite randomisation for live weight and BCS (adiposity) of adolescent recipients following embryo transfer, those actually conceiving after allocation to a control diet were initially heavier than those conceiving after allocation to a high intake diet (46.5±0.43 vs. 44.2±0.28 kg, $p<0.001$). All ewes had an initial BCS score of either 2¼ or 2½ and there were no significant differences in these proportions between study

Table 4.2 – Baseline maternal characteristics at the time of embryo transfer and donor source

A	C+Saline (n=12)	H+Ad.VEGF (n=18)	H+Saline (n=13)	H+Ad.LacZ (n=14)	P Value
Live weight (kg)	46.5 ± 0.43[a]	44.2 ± 0.45[b]	44.3 ± 0.60[b]	44.2 ± 0.45[b]	**0.005**
BCS (units)	2 ± 0.04	2 ± 0.01	2 ± 0.02	2 ± 0.00	0.692
Ovulation rate	2 ± 0.4	2 ± 0.3	2 ± 0.3	2 ± 0.1	0.701

	Embryo Donor ID												
B	**1**	**2**	**3**	**4**	**5**	**6**	**7**	**8**	**9**	**10**	**11**	**12**	**13**
C+Saline	1	1		1	1	2	2				2	1	1
H+Ad.VEGF	2	1		1	2	3	2		1	1	2		3
H+Saline	2		1		1	3	1	2		1	1		1
H+Ad.LacZ	2	1	1	1		2	1		1		3	1	1

BCS values were compared using Chi square test. Remaining P values shown in Table A are for overall ANOVA. Mean values within a row with unlike superscripts are significantly different (p=<0.05 for individual comparisons, see text for details).

---

groups. Despite these initial live weight differences, overnourished ewes soon overtook control-intake ewes in terms of body weight and adiposity, as per the experimental design (Figure 4.12). Thus, maternal live weight and adiposity score were greater in overnourished relative to control-intake ewes from ~42 days gestation (54.8±0.50 vs. 52.3±1.23 kg, p=0.037 and 2.5±0.02 vs. 2.3±0.04, p<0.001, respectively).

There were no significant differences in initial live weight or BCS at the time of embryo transfer between overnourished ewes subsequently allocated to H+Ad.VEGF, H+Saline or H+Ad.LacZ groups. With respect to maternal genetics, embryos derived from 9 of 13 adult donor ewes were represented in the animals that conceived in both control-intake and overnourished cohorts, and there was a reasonably even spread in embryo source across the H+Ad.VEGF, H+Saline and H+Ad.LacZ groups. Finally, recipient ovulation rate was evenly matched across all four groups.

At the last time point prior to gene therapy administration at 89±0.2 days gestation, maternal live weight and BCS remained significantly greater in overnourished versus control-intake ewes

Figure 4.12 – Changes in maternal live weight and adiposity prior to gene therapy surgery

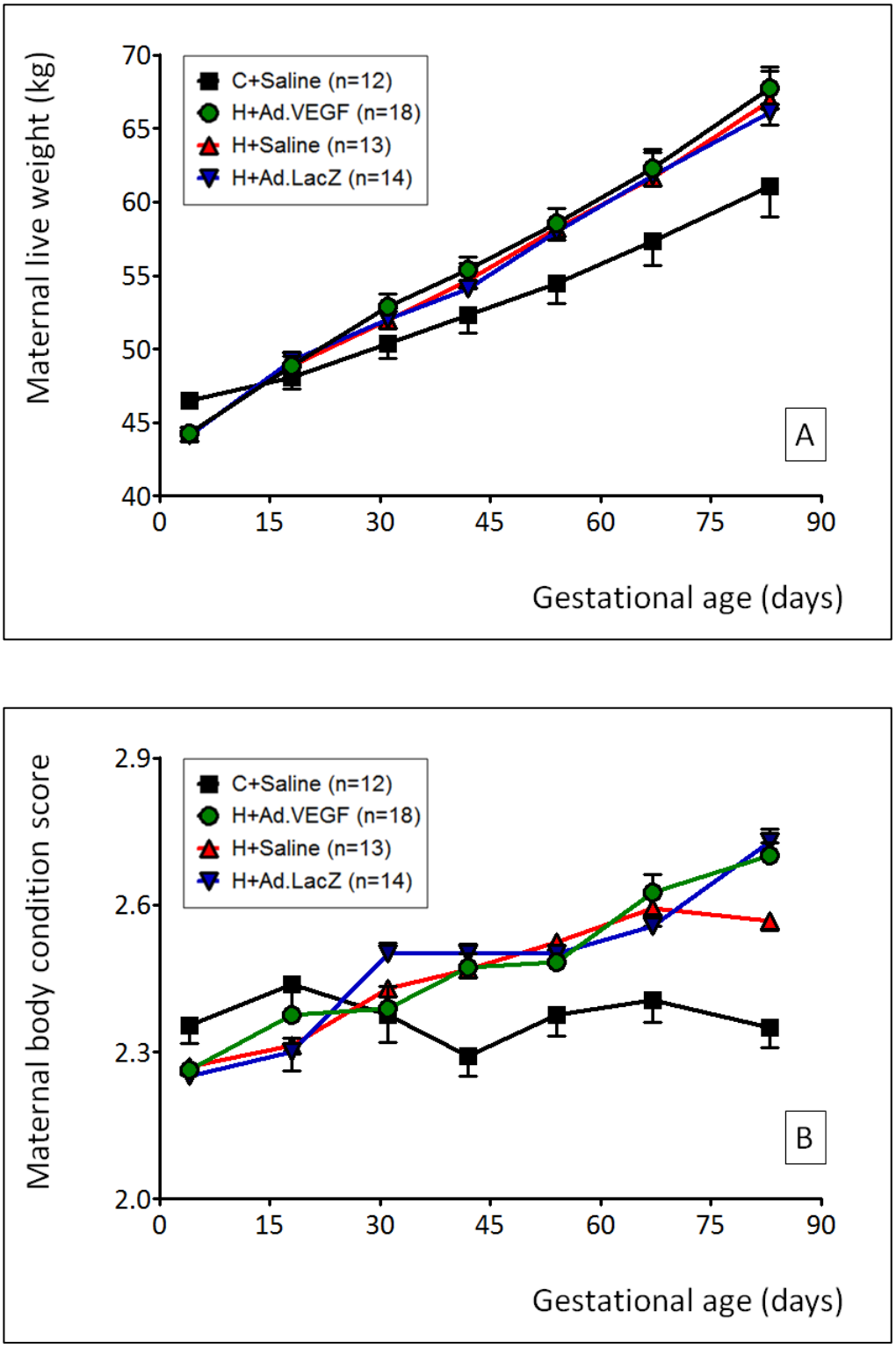

Changes in maternal live weight [A] and body condition score [B] between embryo transfer and mid-gestation in singleton-bearing adolescent dams offered a control-intake (C) or high-intake (H) diet to generate normal or compromised fetoplacental growth, respectively, and subsequently receiving bilateral uterine artery injections of Ad.VEGF, Ad.LacZ or saline.

(67.0±0.89 vs. 61.0±2.03 kg, p=0.005 and 2.7±0.19 vs. 2.4±0.04, p<0.001, respectively). Maternal live weight was not significantly different between overnourished ewes subsequently allocated to H+Ad.VEGF, H+Saline or H+Ad.LacZ groups, however BCS was marginally lower in H+Saline compared to H+Ad.VEGF and H+Ad.LacZ groups at this stage (2.6±0.02 vs. 2.7±0.03 and 2.7±0.03; p<0.001).

4.3.1.2 Maternal live weight gain and baseline ultrasound parameters

Table 4.3 shows the maternal live weight gain (in g/day) between embryo transfer and baseline ultrasound measurements (taken at 83±0.1 days gestation) prior to gene therapy by experimental group. Following even allocation of overnourished ewes to H+Ad.VEGF, H+Saline and H+Ad.LacZ groups on the basis of fetal trunk diameter (TD), abdominal circumference (AC), renal volume (RV), placentome index, biparietal diameter (BPD):AC ratio and maternal live weight gain, there were unsurprisingly no significant differences between the three groups in any of these parameters. There were also no significant differences in any of the other fetal biometric parameters (BPD, occipito-snout length (OSL), femur length (FL) or tibia length (TL)), deepest vertical pool (DVP) of amniotic fluid or umbilical cord diameter (UCD) between the H+Ad.VEGF, H+Saline and H+Ad.LacZ groups. In addition there were no differences in fetal biometry between overnourished and control-intake pregnancies. Thus at this stage of gestation mean fetal size was equivalent between all four groups. In contrast, placentome index was lower in H+Ad.VEGF, H+Saline and H+Ad.LacZ relative to C+Saline groups (p=0.001, p=0.0001 and p<0.001, respectively). Overall, prior to gene therapy administration, overnourished ewes had higher values of UA PI, RI and SDR than control-intake ewes (1.45±0.03 vs. 1.32±0.072, p=0.038; 0.79±0.006 vs. 0.74±0.025, p=0.002; and 4.96±0.195 vs. 3.75±0.312, p=0.005, respectively). The significance levels for individual comparisons of H+Ad.VEGF, H+Saline and H+Ad.LacZ groups against the C+Saline group varied between indices (see Table 4.3) however importantly there were no significant differences between H+Ad.VEGF, H+Saline and H+Ad.LacZ groups in any of the UA Doppler indices measured.

4.3.2 Uterine blood flow

4.13A illustrates serial measurements of UBF through the artery supplying the gravid uterine horn by experimental group, from baseline values (92±0.2 days gestation; post-operative day 3) until final determinations on the day prior to necropsy (130±0.2 days gestation; post-operative day 41). Significant differences between groups were observed at 94±0.1 and 96±0.1 days gestation only (overall ANOVA: p=0.045 and p=0.047, respectively). Subsequently there were no significant differences between any of the four groups. At 94±0.1 days gestation,

Table 4.3 – Maternal live weight gain following embryo transfer and baseline ultrasound measurements in mid-gestation prior to gene therapy administration

	C+Saline (n=12)	**H+Ad.VEGF (n=18)**	**H+Saline (n=13)**	**H+Ad.LacZ (n=14)**	**P value**
Live weight gain (g/day)	184 ± 24.3[a]	297 ± 17.8[b]	286 ± 26.5[b]	278 ± 11.7[b]	**<0.001**
BPD (mm)	35.3 ± 0.29	35.4 ± 0.30	34.8 ± 0.28	35.6 ± 0.29	0.299
OSL (mm)	71.0 ± 0.92	70.5 ± 0.85	70.8 ± 0.73	71.3 ± 0.56	0.898
TD (mm)	53.0 ± 1.21	51.2 ± 0.98	50.3 ± 1.47	51.2 ± 1.00	0.462
AC (mm)	171 ± 3.4	166 ± 3.2	161 ± 4.0	167 ± 3.1	0.251
FL (mm)	22.2 ± 0.79	21.7 ± 0.38	21.0 ± 0.36	21.4 ± 0.33	0.375
TL (mm)	29.2 ± 0.79	29.7 ± 0.45	28.3 ± 0.42	29.4 ± 0.43	0.277
RV (cm^3)	2.38 ± 0.120	2.23 ± 0.129	2.10 ± 0.174	2.36 ± 0.124	0.499
UA PI	1.32 ± 0.072[a]	1.43 ± 0.032[ab]	1.40 ± 0.048[ab]	1.52 ± 0.059[b]	0.074
UA RI	0.74 ± 0.025[a]	0.78 ± 0.008[b]	0.79 ± 0.012[b]	0.78 ± 0.011[b]	**0.014**
UA SDR	3.75 ± 0.312[a]	4.64 ± 0.189[ab]	4.92 ± 0.274[b]	4.70 ± 0.513[b]	**0.014**
BPD:AC ratio	0.21 ± 0.003	0.22 ± 0.004	0.22 ± 0.004	0.21 ± 0.002	0.341
DVP (cm)	4.61 ± 0.332	4.71 ± 0.256	4.88 ± 0.250	4.55 ± 0.294	0.866
UCD (mm)	12.7 ± 0.24	12.9 ± 0.25	12.2 ± 0.33	12.7 ± 0.36	0.312
Plac. index (cm^2)	5.43 ± 0.256[a]	4.24 ± 0.233[b]	4.14 ± 0.246[b]	3.75 ± 0.229[b]	**<0.001**

Maternal live weight gain (g/day) between embryo transfer and 83±0.2 days gestation and baseline ultrasound measurements prior to gene therapy administration. P values shown in the table are for overall ANOVA. Mean values within a row with unlike superscripts are significantly different (p=<0.05 for individual comparisons, see text for details).

---

relative to the C+Saline group, UBF was significantly reduced in the H+Ad.LacZ group (401±27.9 vs. 291±16.3 ml/min, p=0.006) and tended to be reduced in the H+Saline group (401±27.9 vs. 324±32.9 ml/min, p=0.053). UBF was reduced in both H+Saline and H+Ad.LacZ versus C+Saline groups at 96±0.1 days gestation (339±30.8 and 310±19.7 vs. 426±29.5 ml/min, p=0.042 and p=0.007, respectively).

As there were no significant differences between the H+Ad.Saline and H+Ad.LacZ groups at any

Figure 4.13 – Uterine blood flow

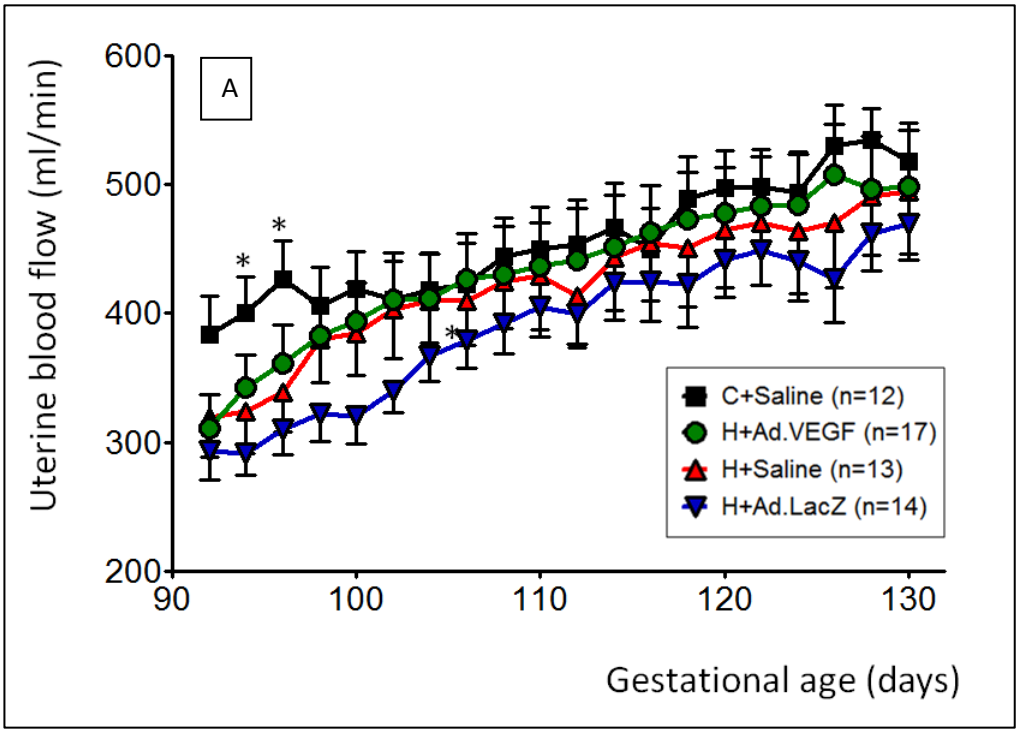

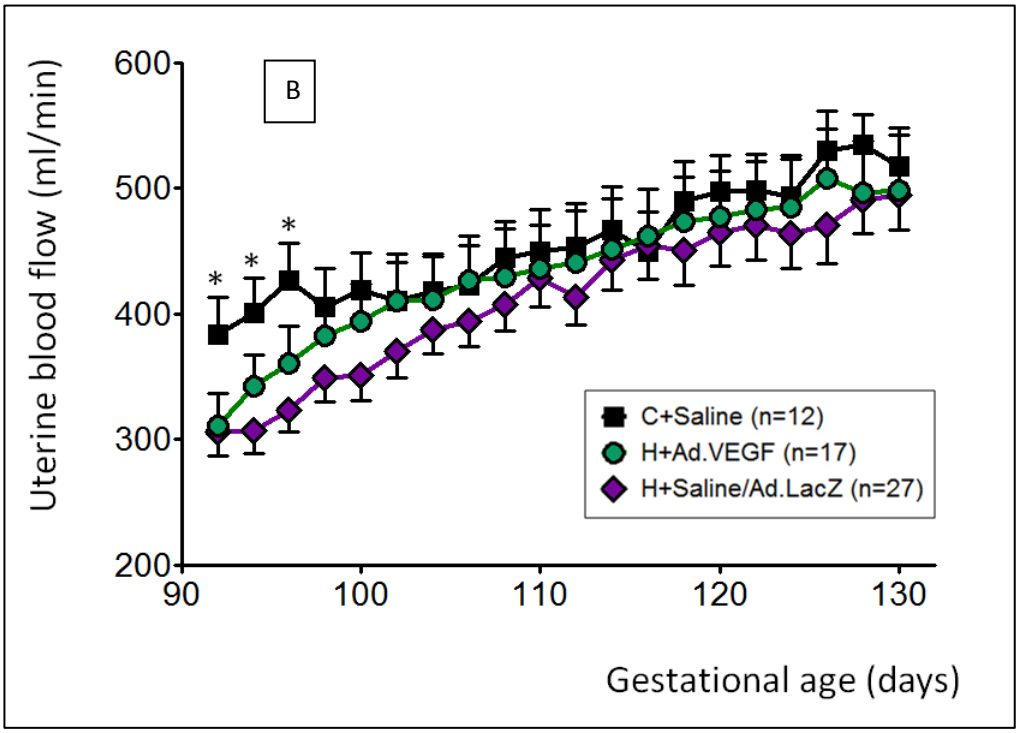

*Serial measurements of uterine blood flow from 92±0.2 days until 130±0.2 days gestation in singleton-bearing adolescent dams offered a control-intake (C) or high-intake (H) diet and receiving bilateral uterine artery injections of Ad.VEGF, Ad.LacZ or saline. * p<0.05. P values shown are for overall ANOVA - see text for significance levels of individual comparisons.*

stage, these were combined into one group (H+Saline/Ad.LacZ) for comparison with C+Saline and H+Ad.VEGF groups (Figure 4.13B). This approach revealed a tendency towards an additional difference at 92±0.2 days gestation (overall ANOVA: p=0.081) and post-hoc testing demonstrated a significant reduction in UBF in the H+Saline/Ad.LacZ group relative to the C+Saline group at this stage (306±18.9 vs. 384±29.4 ml/min, p=0.032). UBF was also reduced in H+Saline/Ad.LacZ versus C+Saline groups at 94±0.1 and 96±0.1 days gestation (p=0.007 each). UBF in the H+Ad.VEGF group was not significantly different to any other group at any stage of gestation (using either approach).

UBF at all time points was weakly correlated with eventual fetal and placental weight at late-gestation necropsy (r=0.358–0.526, n=56, p<0.001–0.007; and r=0.321–0.526, n=56, p<0.001–0.009, respectively). Average UBF from 92±0.2 to 130±0.2 days gestation was not significantly different between C+Saline, H+Ad.VEGF, H+Saline and H+Ad.LacZ groups (456±27.4, 434±34.1, 435±41.1 and 389±22.4 ml/min, respectively) and was also correlated with fetal and placental weight (r=0.453, n=56, p=0.001; and r=0.438, n=56, p=0.001, respectively). Mean change in UBF from 92 to 130 days gestation was not different between C+Saline, H+Ad.VEGF, H+Saline and H+Ad.LacZ groups (134±96.3, 188±100.6, 201±115.1 and 176±78.6 ml/min, representing fold changes of 0.35, 0.61, 0.63 and 0.60, respectively) and was not correlated with subsequent fetal or placental weight. Neither individual or summary measurements of UBF demonstrated any significant correlation with umbilical arterial Doppler indices (reported in Sections 4.3.3.6 and 4.3.3.7) or measures of vascular reactivity from the organ bath analysis of harvested uterine arteries (see Section 4.3.5.4).

4.3.3 Ultrasound parameters

The following sections report the serial changes in the various ultrasound markers throughout the second half of gestation.

4.3.3.1 Abdominal circumference

Figure 4.14 shows serial measurements of abdominal circumference by experimental group. AC measurements were reduced in all three overnourished groups (H+Ad.VEGF, H+Saline and H+Ad.LacZ) relative to the C+Saline group at 105±0.1 days (223±2.9, 217±2.7 and 219±2.9 vs. 235±2.3 mm, p=0.003, p<0.001 and p<0.001, respectively), 112±0.1 days (241±2.8, 233±2.3 and 233±2.5 vs. 257±3.9 mm; p<0.001), 119±0.1 days (258±3.1, 249±2.3 and 248±2.8 vs. 274±3.3 mm; p<0.001) and 126±0.3 days gestation (272±4.3, 262±1.8 and 264±4.5 vs. 286±2.4 mm, p=0.011, p<0.001 and p<0.001, respectively). AC measurements were increased in H+Ad.VEGF relative to H+Saline and H+Ad.LacZ groups at 112 (p=0.031 and p=0.047,

Figure 4.14 – Fetal abdominal circumference

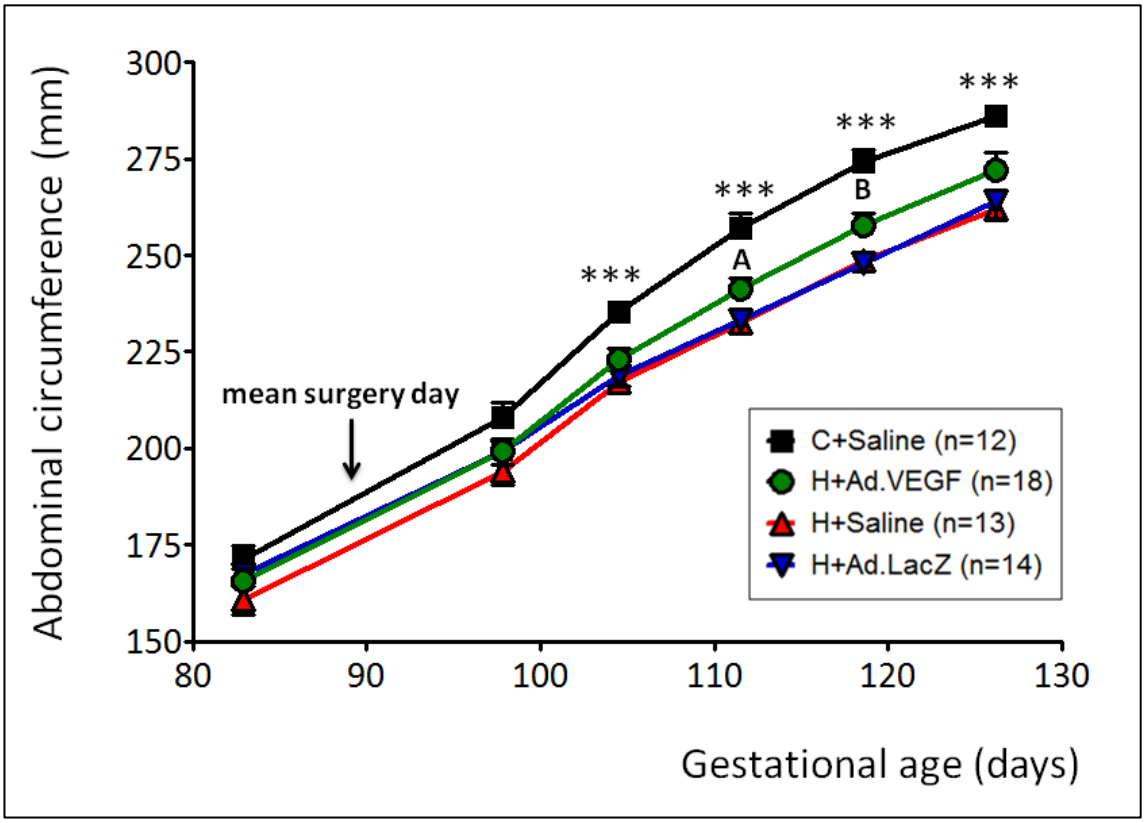

*Serial ultrasound measurements of fetal abdominal circumference at weekly intervals between 83±0.1 days and 126±0.3 days gestation in singleton-bearing adolescent dams offered a control-intake (C) or high-intake (H) diet and receiving bilateral uterine artery injections of Ad.VEGF, Ad.LacZ or saline. *** p<0.001. P values shown are for overall ANOVA - see text for significance levels of individual comparisons. Letters A and B indicate time points at which measurements in H+Ad.VEGF group > H+Saline / H+Ad.LacZ groups (p=<0.05)*

---

respectively) and 119 days gestation (p=0.032 and p=0.016, respectively), which corresponds to 22±0.2 and 29±0.2 days post therapy, respectively.

4.3.3.2 Biparietal diameter

Serial measurements of biparietal diameter by experimental group are detailed in Figure 4.15A. There were increasing tendencies towards overall differences between groups at 112, 119and 126 days gestation (overall ANOVA: p=0.081, p=0.071 and p=0.051, respectively) and post-hoc testing revealed a number of significant differences between overnourished and

Figure 4.15 – Fetal biparietal diameter and BPD:AC ratios

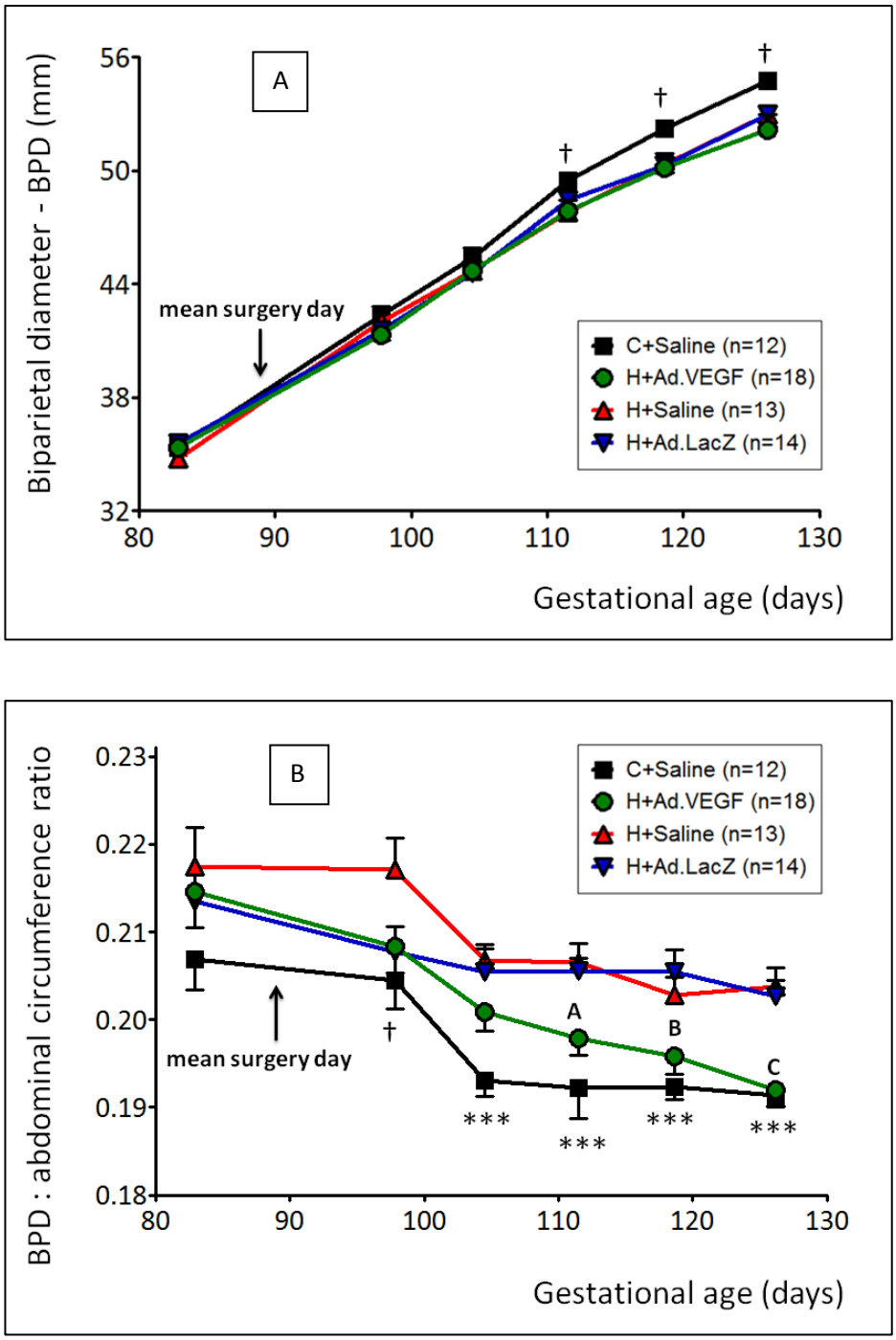

*Serial ultrasound measurements of biparietal diameter [A] and BPD:AC ratios [B] at weekly intervals between 83±0.1 days and 126±0.3 days gestation in singleton-bearing adolescent dams offered a control-intake (C) or high-intake (H) diet and receiving bilateral uterine artery injections of Ad.VEGF, Ad.LacZ or saline. † p=0.05-0.1, *** p<0.001. P values shown are for overall ANOVA - see text for significance levels of individual comparisons. Letters A, B and C indicate points at which measurements in H+Ad.VEGF > H+Saline / H+Ad.LacZ groups (p=<0.05)*

control-intake fetuses at these time points. At 112 days gestation, BPD was reduced in H+Ad.VEGF and H+Saline groups versus the C+Saline group (47.9±0.61 and 47.8±0.27 vs. 49.5±0.22 mm; p=0.021 and p=0.025, respectively). At 119 days gestation, BPD was reduced in all three overnourished groups (H+Ad.VEGF, H+Saline and H+Ad.LacZ) relative to the C+Saline group (50.2±0.76, 50.3±0.29 and 50.3±0.44 vs. 52.2±0.33 mm; p=0.016, p=0.037 and p=0.034, respectively). At 126 days gestation, BPD was reduced only in H+Ad.VEGF relative to C+Saline groups (52.2±0.81 vs. 54.7±0.29 mm, p=0.006). BPD measurements in the H+Ad.VEGF group were not significantly different to the H+Saline or H+Ad.LacZ groups at any stage.

4.3.3.3 BPD : AC ratio

From the above measurements, the BPD to AC ratio was calculated at each gestational time point (Figure 4.15B). BPD:AC ratios were increased in H+Ad.VEGF, H+Saline and H+Ad.LacZ groups relative to C+Saline groups at 105 days gestation (0.20±0.002, 0.21±0.002 and 0.21±0.003 vs. 0.19±0.002; p=0.012, p<0.001 and p<0.001, respectively). Subsequently only H+Saline and H+Ad.LacZ groups differed from the C+Saline group and were increased at 112 (0.21±0.002 and 0.21±0.001 vs. 0.19±0.003; p<0.001), 119 (0.20±0.002 and 0.21±0.003 vs. 0.19±0.001; p=0.002 and p<0.001, respectively) and at 126 days gestation (0.20±0.002 and 0.20±0.002 vs. 0.19±0.001; p<0.001). BPD:AC ratios were attenuated in H+Ad.VEGF relative to H+Saline and H+Ad.LacZ groups at 112 (p=0.007 and p=0.016, respectively), 119 (p=0.016 and p<0.001, respectively) and 126 days gestation (p<0.001).

4.3.3.4 Renal volume

Figure 4.16 depicts serial measurements of renal volume by experimental group. At 105 days gestation there was a tendency towards an overall difference between groups (p=0.076) and post-hoc testing revealed a significant difference between H+Saline and C+Saline groups only (4.3±0.24 vs. 5.2±0.19 cm^3, p=0.012). Subsequently RV measurements were reduced in all three overnourished groups (H+Ad.VEGF, H+Saline and H+Ad.LacZ) relative to the C+Saline group at 112 (5.9±0.28, 5.4±0.22 and 5.3±0.21 vs. 6.6±0.16 cm^3; p=0.038, p=0.002 and p=0.001, respectively), 119 (7.0±0.33, 6.3±0.24 and 6.4±0.24 vs. 8.3±0.39 cm^3; p=0.003, p<0.001 and p<0.001, respectively) and at 126 days gestation (8.7±0.47, 8.2±0.24 and 8.1±0.42 vs. 10.0±0.35 cm^3; p=0.027, p=0.004 and p=0.002, respectively). RV values in the H+Ad.VEGF group were not significantly different to the H+Saline or H+Ad.LacZ groups at any stage.

4.3.3.5 Femur length and tibia length

Serial ultrasound measurements of femur length by experimental group are shown in Figure

Figure 4.16 – Fetal renal volume

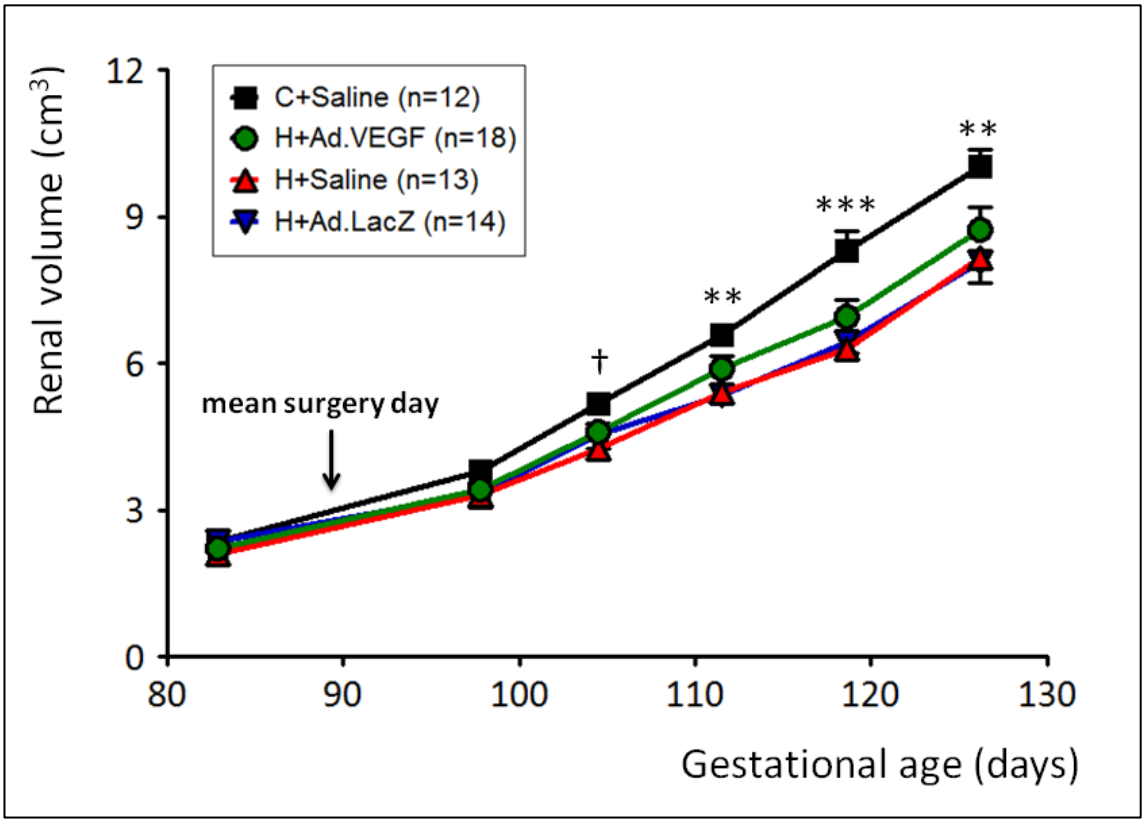

*Serial ultrasound measurements of renal volume at weekly intervals between 83±0.1 days and 126±0.3 days gestation in singleton-bearing adolescent dams offered a control-intake (C) or high-intake (H) diet and receiving bilateral uterine artery injections of Ad.VEGF, Ad.LacZ or saline. † p=0.05-0.1, ** p<0.01, *** p<0.001. P values shown are for overall ANOVA - see text for significance levels of individual comparisons.*

4.17A. At 98 days gestation there was a tendency towards a difference between groups (overall ANOVA p=0.07). Post-hoc testing revealed a significant difference between H+Saline and C+Saline groups (29.5±0.54 vs. 31.6±0.62 mm, p=0.017). FL measurements also tended to be reduced in H+Ad.VEGF versus C+Saline groups (30.0±0.55 vs. 31.6±0.62 mm, p=0.056). Subsequently FL measurements were reduced in all overnourished (H+Ad.VEGF, H+Saline and H+Ad.LacZ) groups relative to C+Saline groups at 105 (36.2±0.73, 36.1±0.55 and 36.8±0.50 vs. 39.0±0.46 mm; p=0.002, p=0.003 and p=0.019, respectively) and 119 days (49.3±0.68, 47.8±0.75 and 49.0±0.79 vs. 53.6±0.69 mm; p<0.001) but not at 112 or 126 days gestation. FL measurements in the H+Ad.VEGF group were not significantly different to the H+Saline or H+Ad.LacZ groups at any stage.

Figure 4.17 – Fetal femur and tibia lengths

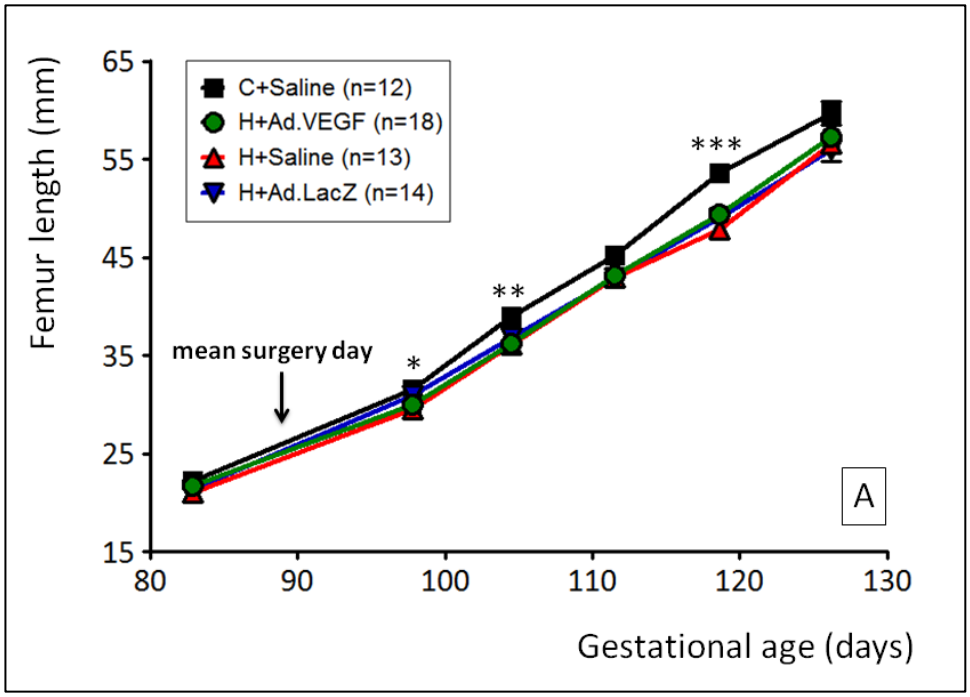

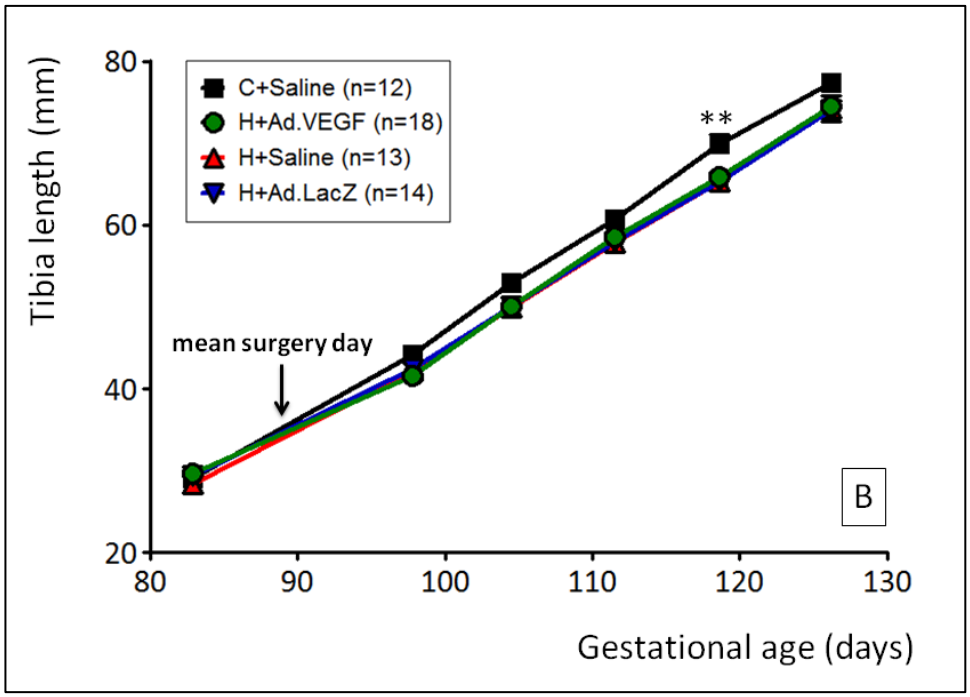

*Serial ultrasound measurements of femur length [A] and tibia length [B] at weekly intervals between 83±0.1 days and 126±0.3 days gestation in singleton-bearing adolescent dams offered a control-intake (C) or high-intake (H) diet and receiving bilateral uterine artery injections of Ad.VEGF, Ad.LacZ or saline. * p<0.05, ** p<0.01, *** p<0.001. P values shown are for overall ANOVA - see text for significance levels of individual comparisons.*

Figure 4.17B details serial ultrasound measurements of tibia length by experimental group. TL measurements were reduced in H+Ad.VEGF, H+Saline and H+Ad.LacZ groups relative to C+Saline groups at 119±0.1 days gestation only (65.9±1.00, 65.2±0.63 and 65.3±1.08 vs. 69.9±1.23 mm; p=0.009, p=0.005 and p=0.004, respectively). TL values in the H+Ad.VEGF group were not significantly different to the H+Saline or H+Ad.LacZ groups at any stage.

4.3.3.6 Umbilical artery Doppler indices

Values of all umbilical artery Doppler indices decreased progressively with advancing gestation. Variability within groups was greater for Doppler indices than for fetal biometry.

Figure 4.18A shows serial ultrasound measurements of umbilical artery pulsatility index by experimental group. UA PI was higher in H+Ad.VEGF, H+Ad.Saline and H+Ad.LacZ groups relative to C+Saline groups at 98 (1.26±0.029, 1.25±0.048 and 1.26±0.034 vs. 1.03±0.039; p<0.001), 119 (1.07±0.046, 1.03±0.038 and 1.08±0.033 vs. 0.90±0.033; p=0.003, p=0.033 and p=0.002, respectively) and 126days gestation (1.07±0.045, 1.10±0.038 and 1.06±0.033 vs. 0.89±0.037; p=0.002, p=0.001 and p=0.006, respectively). At 105 days gestation there was a tendency towards a difference between groups (overall ANOVA p=0.068) and post-hoc testing revealed significant differences in H+Ad.VEGF and H+Ad.LacZ versus C+Saline groups (1.17±0.081 and 1.15±0.038 vs. 0.96±0.026; p=0.012 and p=0.031). UA PI measurements also tended to be increased in H+Saline versus C+Saline groups (1.11±0.040 vs. 0.96±0.026; p=0.098). UA PI measurements in the H+Ad.VEGF group were not different to the H+Saline or H+Ad.LacZ groups at any stage.

Serial ultrasound measurements of umbilical artery resistance index by experimental group are illustrated in Figure 4.18B. UA RI was increased in H+Ad.VEGF, H+Ad.Saline and H+Ad.LacZ groups relative to C+Saline groups at 98 (0.72±0.008, 0.73±0.013 and 0.73±0.011 vs. 0.66±0.014; p<0.001), 105 (0.70±0.018, 0.68±0.016 and 0.70±0.013 vs. 0.63±0.011; p=0.003, p=0.039 and p=0.004, respectively) and 126 days gestation (0.65±0.014, 0.66±0.013 and 0.65±0.012 vs. 0.59±0.015; p=0.003, p=0.001 and p=0.006, respectively). At 112 days gestation, UA RI was increased in H+Ad.VEGF and H+Ad.LacZ groups only relative to the C+Saline groups (0.69±0.020 and 0.67±0.012 vs. 0.61±0.016; p=0.002 and p=0.016, respectively). At 119 days gestation, UA RI was significantly higher in H+Ad.VEGF and H+Ad.LacZ relative to C+Saline groups (0.65±0.015 and 0.67±0.012 vs. 0.60±0.015; p=0.009 and p=0.002) and there was a tendency towards increased UA PI in H+Saline versus C+Saline groups (0.64±0.015 and vs. 0.60±0.015; p=0.081). UA RI measurements in the H+Ad.VEGF group were not different to the H+Saline or H+Ad.LacZ groups at any stage.

Figure 4.18 – Umbilical artery pulsatility index and resistance index

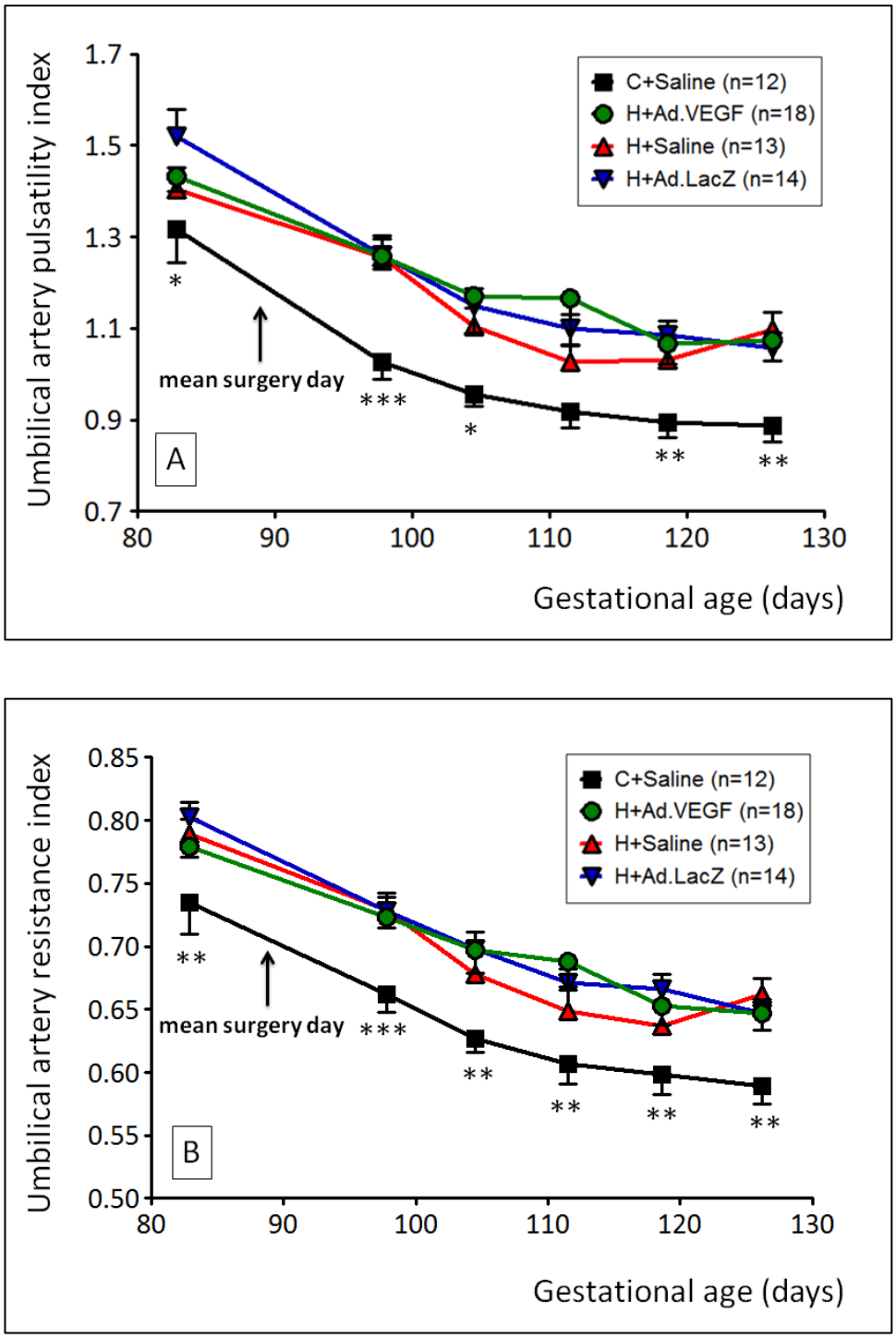

*Serial ultrasound measurements of umbilical arterial pulsatility index [A] and resistance index [B] at weekly intervals between 83±0.1 days and 126±0.3 days gestation in 57 singleton-bearing adolescent dams offered a control-intake (C) or high-intake (H) diet and receiving bilateral uterine artery injections of Ad.VEGF, Ad.LacZ or saline. * p<0.05, ** p<0.01, *** p<0.001. P values shown are for overall ANOVA - see text for significance levels of individual comparisons.*

Figure 4.19A shows serial ultrasound derived measurements of umbilical arterial systolic to diastolic ratio by experimental group. UA SDR was increased in H+Ad.VEGF, H+Saline and H+Ad.LacZ groups relative to C+Saline groups at 98 (3.66±0.117, 4.28±0.526 and 3.73±0.143 vs. 2.74±0.202; p=0.021, p<0.001 and p=0.018, respectively) and 126 days (2.92±0.122, 3.00±0.117 and 2.78±0.106 vs. 2.28±0.161; p=0.001, p<0.001 and p=0.011, respectively). At 119 days gestation, UA SDR was increased in H+Ad.VEGF and H+Ad.LacZ versus C+Saline groups (3.01±0.189 and 3.05±0.111 vs. 2.35±0.129; p=0.003) and there was a tendency towards increased UA PI in H+Saline versus C+Saline groups (2.81±0.121 and vs. 2.35±0.129; p=0.055). UA SDR measurements in the H+Ad.VEGF group were not different to the H+Saline or H+Ad.LacZ groups at any stage.

4.3.3.7 Umbilical cord diameter

Serial ultrasound measurements of umbilical cord diameter by experimental group are shown in Figure 4.19B. UCD was reduced in H+Saline and H+Ad.LacZ groups relative to the C+Saline group at 98 (14.3±0.32 and 14.8±0.24 vs. 15.8±0.33 mm, p=0.002 and p=0.031, respectively), 105 (15.7±0.25 and 16.3±0.25 vs. 17.6±0.39 mm, p<0.001 and p=0.01, respectively) and 112 days gestation (17.2±0.28 and 17.7±0.33 vs. 19.1±0.47 mm, p=0.001 and p=0.012, respectively). At these time points, UCD measurements also tended to be reduced in H+Ad.VEGF versus C+Saline groups (p=0.064, p=0.097 and p=0.05, respectively). Subsequently UCD was decreased in all overnourished (H+Ad.VEGF, H+Saline and H+Ad.LacZ) groups relative to the C+Saline group, at 119 (19.8±0.42, 18.7±0.34 and 19.5±0.30 vs. 21.2±0.39 mm; p=0.012, p<0.001 and p=0.007, respectively) and at 126 days gestation (21.2±0.51, 20.2±0.29 and 20.6±0.46 vs. 22.9±0.42 mm; p=0.009, p<0.001 and p=0.001, respectively). UCD was increased in the H+Ad.VEGF group relative to the H+Saline (but not H+Ad.LacZ) group at 105 and 119 days gestation (p=0.02 and p=0.049).

4.3.3.8 Placentome index

Figure 4.20A shows serial ultrasound measurements of placentome index by group. Mean placentome index progressively decreased with advancing gestation between mid and late pregnancy and was reduced in all overnourished (H+Ad.VEGF, H+Saline and H+Ad.LacZ) groups relative to the C+Saline group at 98 (3.85±0.230, 3.54±0.231 and 3.58±0.201 vs. 4.71±0.243 cm^2; p=0.011, p=0.001 and p=0.002, respectively), 105 (3.23±0.200, 3.01±0.225 and 3.04±0.161 vs. 4.25±0.230 cm^2; p=0.001, p<0.001 and p<0.001, respectively), 112 (3.00±0.181, 2.81±0.235 and 2.74±0.123 vs. 3.86±0.218 cm^2; p=0.002, p=0.001 and p<0.001, respectively), 119 (2.86±0.180, 2.66±0.209 and 2.53±0.087 vs. 3.82±0.204 cm^2, all p<0.001) and 126 days

Figure 4.19 – Umbilical artery systolic to diastolic ratio and umbilical cord diameter

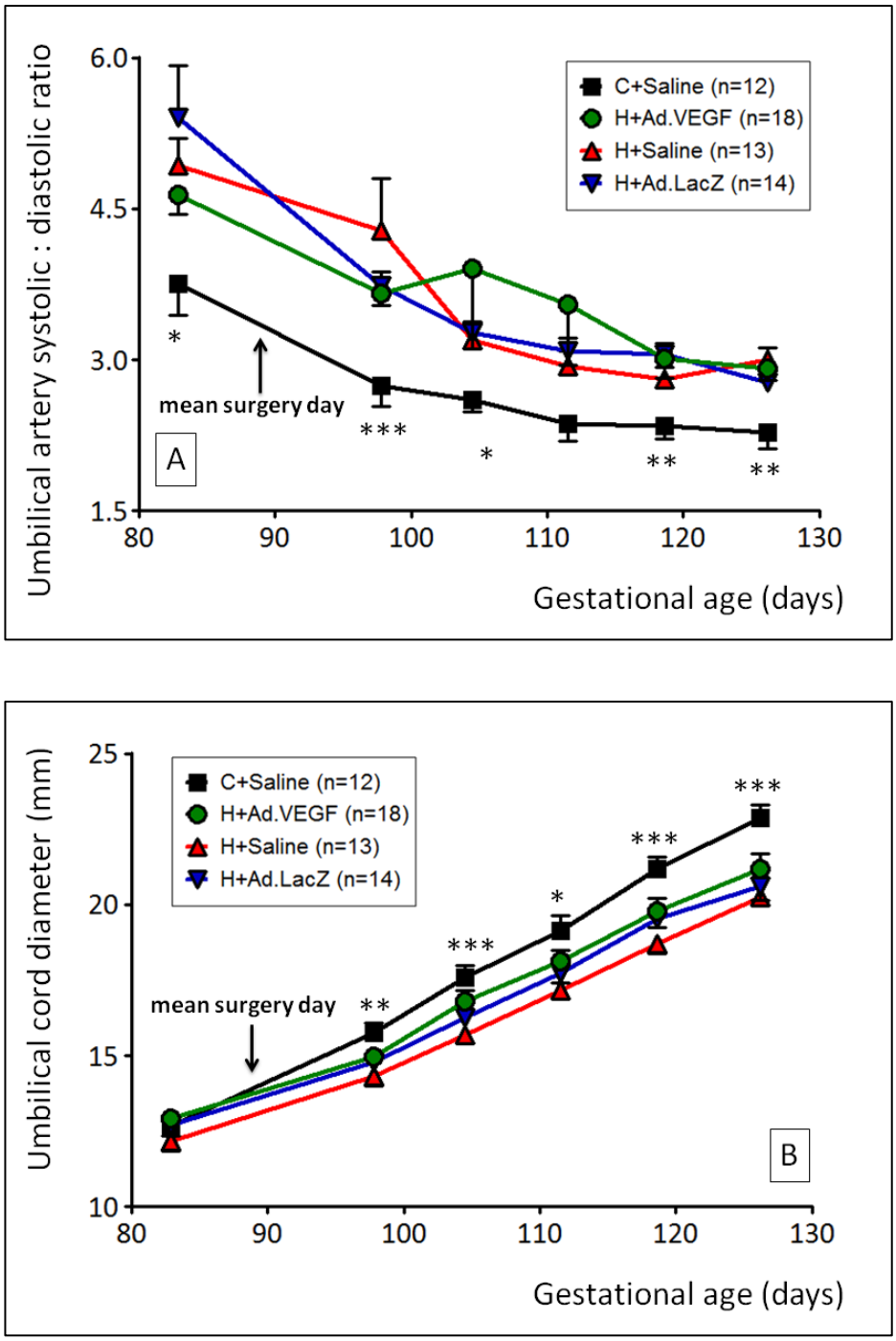

*Serial ultrasound measurements of umbilical artery systolic to diastolic ratios [A] and umbilical cord diameter [B] at weekly intervals between 83±0.1 days and 126±0.3 days gestation in 57 singleton-bearing adolescent dams offered a control-intake (C) or high-intake (H) diet and receiving bilateral uterine artery injections of Ad.VEGF, Ad.LacZ or saline. * p<0.05, ** p<0.01, *** p<0.001. P values shown are for overall ANOVA - see text for significance levels of individual comparisons.*

Figure 4.20 – Placentome index and deepest vertical pool of amniotic fluid

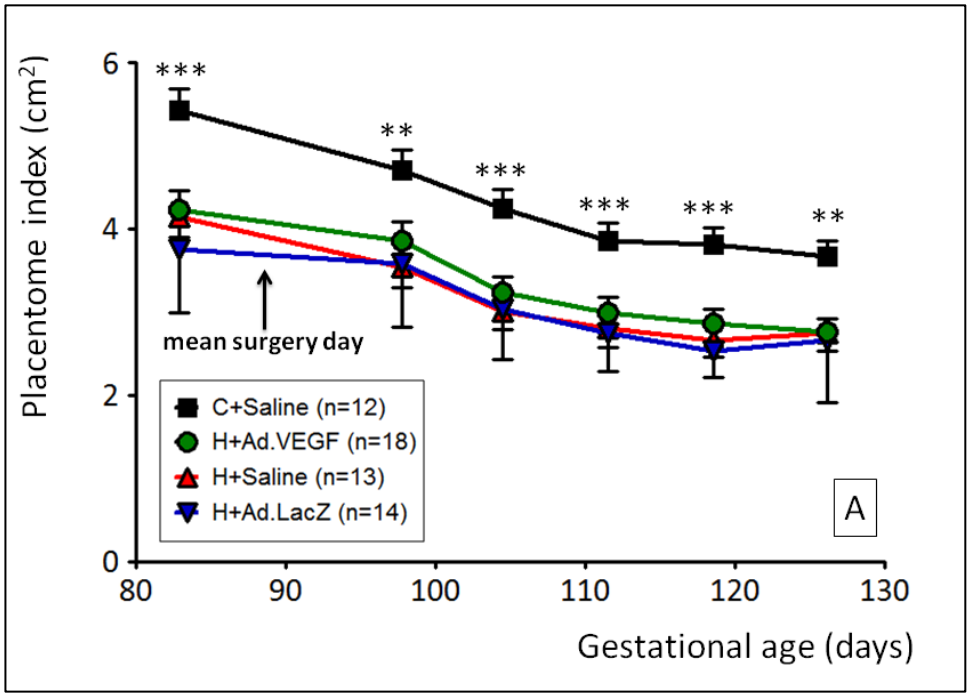

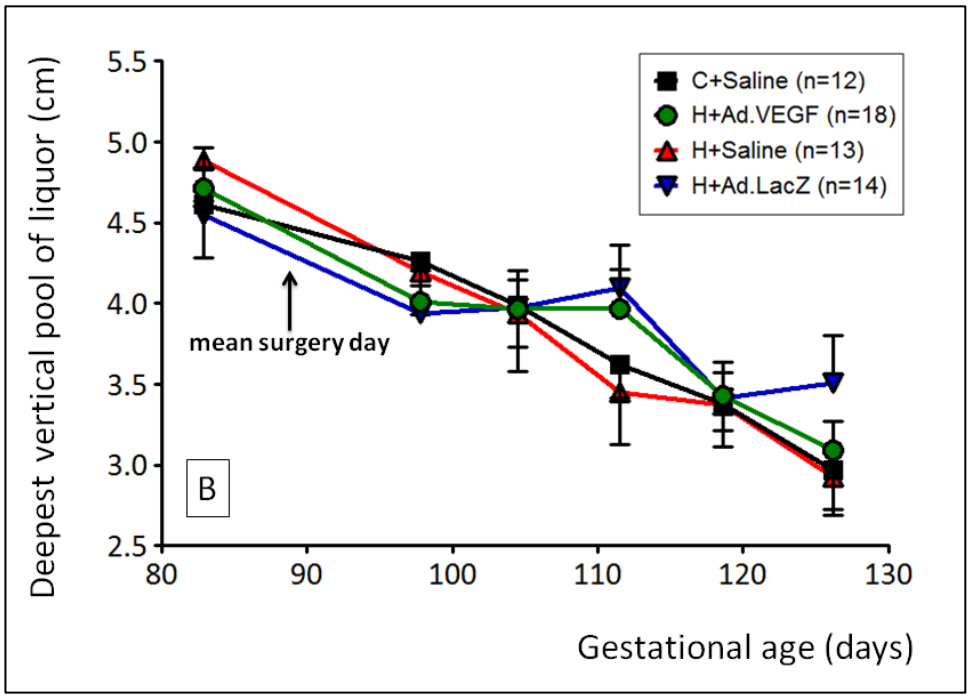

*Serial ultrasound measurements of placentome index [A] and deepest vertical pool of liquor [B] at weekly intervals between 83±0.1 days and 126±0.3 days gestation in singleton-bearing adolescent dams offered a control-intake (C) or high-intake (H) diet and receiving bilateral uterine artery injections of Ad.VEGF, Ad.LacZ or saline. ** p<0.01, *** p<0.001. P values shown are for overall ANOVA - see text for significance levels of individual comparisons.*

gestation (2.76±0.163, 2.75±0.219 and 2.66±0.200 vs. 3.67±0.181 cm^2; p=0.001, p=0.002 and p=0.001, respectively). Measurements of placentome index in the H+Ad.VEGF group were not significantly different to the H+Saline or H+Ad.LacZ groups at any stage. Placentome index at the final time point (126 days gestation) correlated with total placental weight at necropsy irrespective of treatment group (r=0.672, n=57, p<0.001), and in H+Ad.VEGF (r=0.681, n=18, p=0.002), H+Saline (r=0.708, n=13, p=0.007) and H+Ad.LacZ (r=0.698, n=18, p=0.006) but not C+Saline groups (r=–0.175, n=12, p=0.587).

4.3.3.9 Deepest vertical pool of liquor

Serial ultrasound measurements of DVP by experimental group are illustrated in Figure 4.20B. DVP progressively decreased with advancing gestation. There were no differences between any of the four groups at any stage.

4.3.4 Necropsy parameters

4.3.4.1 Maternal characteristics

Table 4.4 summarises maternal parameters at the time of necropsy. Maternal weight, BCS and weight of the liver, perirenal fat depots and residual carcass were all significantly increased in H+Ad.VEGF, H+Saline and H+Ad.LacZ groups relative to the C+Saline group (p<0.001 for all individual comparisons). There were no differences in the absolute weight of maternal blood (an index of maternal blood volume) or uterine weight (either before or after removal of the fetus and placenta). However, the relative weight of maternal blood (expressed per kg live weight) was significantly lower in all three overnourished groups compared to the control-intake group. There were no differences in any maternal parameters between the H+Ad.VEGF, H+Saline and H+Ad.LacZ groups.

4.3.4.2 Fetal and placental weight

Fetal weight at necropsy (131±0.2 days gestation) was reduced in all overnourished groups relative to the C+Saline group (Figure 4.21). Total placental weight was also reduced in H+Ad.VEGF, H+Saline and H+Ad.LacZ (see Table 4.5) compared to C+Saline groups (p<0.001, p=0.001 and p<0.001, respectively). There were no significant differences in fetal or placental weight between H+Ad.VEGF, H+Saline and H+Ad.LacZ groups. Fetal to placental weight ratio was highest in the H+Ad.VEGF group and was increased relative to the C+Saline group (p=0.009). Fetal to placental weight ratios were intermediate in H+Saline and H+Ad.LacZ groups (i.e. not significantly different to either H+Ad.VEGF or C+Saline groups).

Table 4.4 – Maternal live weight, body condition score and internal organ weights at point of necropsy in late gestation

	C+Saline (n=12)	H+Ad.VEGF (n=18)	H+Saline (n=13)	H+Ad.LacZ (n=14)	P Value
Live weight (kg)	65.74 ± 0.58[a]	81.36 ± 1.11[b]	80.54 ± 1.33[b]	81.17 ± 1.19[b]	**<0.001**
BCS (units)	2.35 ± 0.037[a]	2.93 ± 0.027[b]	2.90 ± 0.035[b]	2.95 ± 0.028[b]	**<0.001**
Perirenal fat weight (kg)	543 ± 51.9[a]	1407 ± 83.7[b]	1308 ± 105.1[b]	1286 ± 78.0[b]	**<0.001**
Liver weight (kg)	854 ± 21.6[a]	1183 ± 34.1[b]	1183 ± 36.5[b]	1177 ± 46.7[b]	**<0.001**
Gravid tract weight (g)	8404 ± 332.9	7670 ± 247.2	7452 ± 396.7	7114 ± 428.2	0.098
Residual uterus weight (g)	686.2 ± 29.95	624.7 ± 25.84	603.7 ± 23.02	604.6 ± 33.92	0.193
Blood weight (g)	1984 ± 72.9	2175 ± 78.5	2028 ± 120.2	2082 ± 123.8	0.540
Carcass (kg)	39.09 ± 0.74[a]	51.19 ± 0.58[b]	51.25 ± 0.76[b]	50.5 ± 0.76[b]	**<0.001**
Fat / live weight (g/kg)	8.3 ± 0.78[a]	17.3 ± 1.10[b]	16.2 ± 1.19[b]	15.8 ± 0.91[b]	**<0.001**
Liver / live weight (g/kg)	13.0 ± 0.32[a]	14.5 ± 0.35[b]	14.7 ± 0.37[b]	14.5 ± 0.45[b]	**0.016**
Blood / live weight (g/kg)	30.1 ± 0.97[a]	26.7 ± 0.79[b]	25.3 ± 1.43[b]	25.6 ± 1.50[b]	**0.033**

P values shown in the table are for overall ANOVA. Mean values within a row with unlike superscripts are significantly different (p=<0.05 for individual comparisons, see text for details).

For the three overnourished groups, the number of fetuses falling more than two standard deviations below the control-intake group mean was determined as an indicator of the incidence of "marked" FGR. In the present study, the mean weight in the C+Saline group was 5084g and the standard deviation was 431g, therefore the threshold for diagnosis of marked FGR was <4222g. Proportions of fetuses above and below this cut-off in the H+Ad.VEGF, H+Saline and H+Ad.LacZ groups are presented in Figure 4.22. For the purpose of statistical analysis, in view of the presence of frequency < 5 in one of the cells in the 2 x 3 contingency table and the fact that there were no statistically significant difference between H+Saline and H+Ad.LacZ groups, these two groups were combined as one group (H+Saline/Ad.LacZ) to

Figure 4.21 – Fetal weight at necropsy

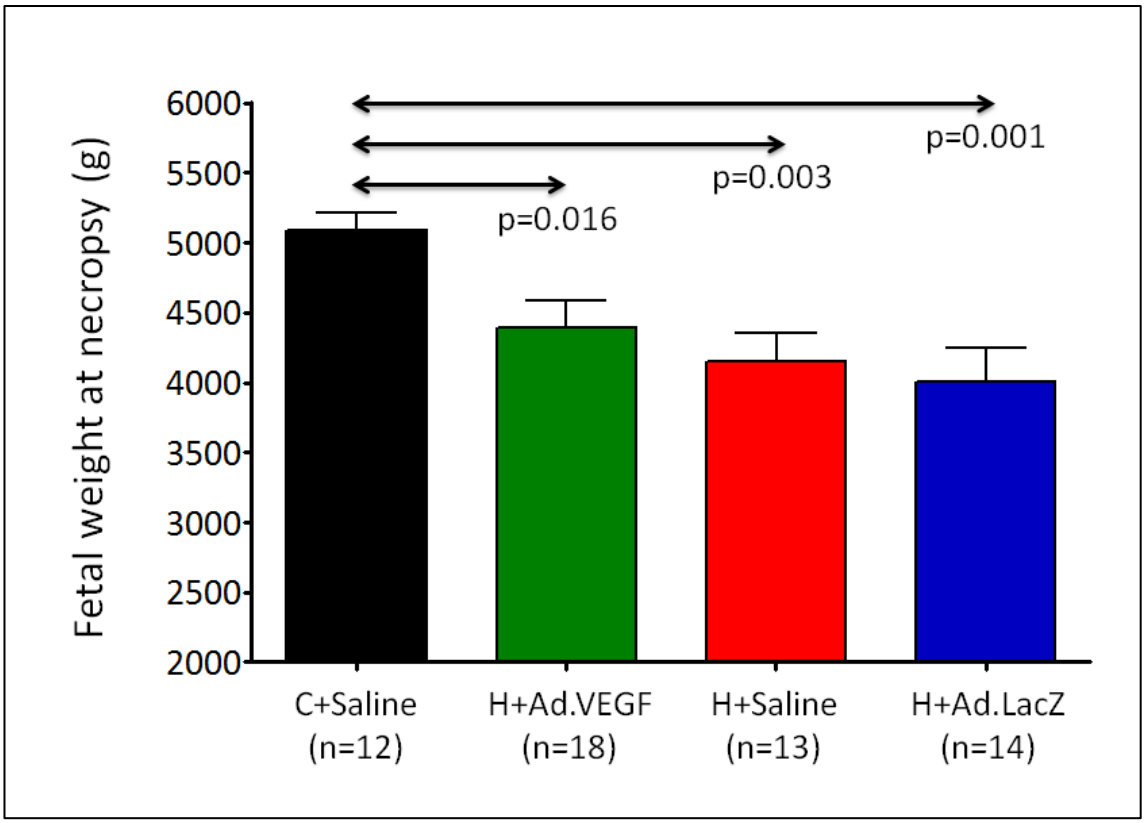

*Fetal weight at late gestation necropsy (*131±0.2 days gestation*) in singleton pregnancies in adolescent dams offered a control-intake (C) or high-intake (H) diet and receiving bilateral uterine artery injections of Ad.VEGF, Ad.LacZ or saline. P values shown are for individual post-hoc comparisons using the test of least significant difference (overall ANOVA p<0.001).*

Table 4.5 – Fetal and placental weights and weight ratio (placental efficiency) at necropsy

	C+Saline (n=12)	**H+Ad.VEGF (n=18)**	**H+Saline (n=13)**	**H+Ad.LacZ (n=14)**	**P Value**
Fetal weight (g)	5084 ± 124[a]	4395 ± 188[b]	4153 ± 202[b]	4008 ± 234[b]	**0.003**
Placental weight (g)	802 ± 36.1[a]	594 ± 33.5[b]	595 ± 42.4[b]	570 ± 37.2[b]	**<0.001**
Fetal : placental wt ratio	6.45 ± 0.27[a]	7.52 ± 0.25[b]	7.16 ± 0.25[ab]	7.21 ± 0.34[ab]	**0.018**

P values shown in the table are for overall ANOVA. Mean values within a row with unlike superscripts are significantly different (p=<0.05 for individual comparisons, see text for details).

Figure 4.22 – Proportions of fetuses categorised as markedly growth-restricted

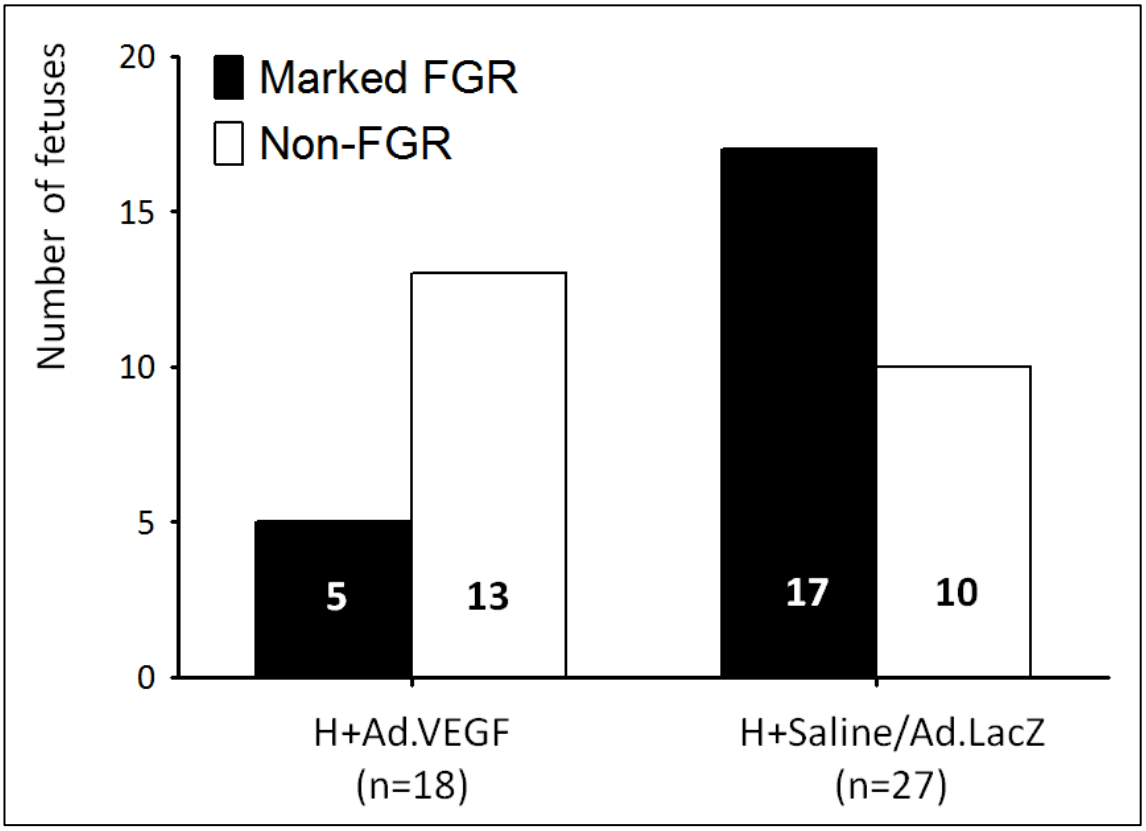

Numbers of fetuses from overnourished singleton-bearing adolescent dams categorised as markedly FGR at late gestation necropsy (131±0.2 days gestation). Marked FGR was defined as a fetal weight more than 2 standard deviations below the mean fetal weight of the normally grown fetuses of 12 contemporaneous control-intake ewes (<4222g). Fetuses with weights >4222g were of similar weight to normally grown controls and therefore termed "non-FGR". In mid-gestation ewes received bilateral uterine artery injections of Ad.VEGF or inactive control treatment (Ad.LacZ/Saline).

---

produce a 2 x 2 contingency table. The proportion of fetuses demonstrating marked FGR was significantly reduced in H+Ad.VEGF vs. H+Saline/Ad.LacZ groups (p=0.033; Fisher's exact test).

Table 4.6 shows the breakdown of total placental weight into its component parts (placentome and membrane weight) as well as the total placentome number and its breakdown into categories by morphological type and size. Total placentome weight and membrane weight were reduced in all overnourished (H+Ad.VEGF, H+Saline and H+Ad.LacZ) groups relative to the C+Saline group (all p<0.001; and p=0.01, p=0.009 and p=0.11, respectively). Placentome number and mean placentome weight were also reduced in H+Ad.VEGF, H+Saline and

Table 4.6 – Indices of placental weight, size and morphology at late gestation necropsy

	C+Saline (n=12)	H+Ad.VEGF (n=18)	H+Saline (n=13)	H+Ad.LacZ (n=14)	P Value
Total placental weight (g)	802 ± 36.1[a]	594 ± 33.5[b]	595 ± 42.4[b]	570 ± 37.2[b]	**<0.001**
Membrane weight (g)	280 ± 15.9[a]	228 ± 12.9[b]	223 ± 14.0[b]	225 ± 13.9[b]	**0.024**
Placentome weight (g)	521 ± 23.8[a]	367 ± 22.8[b]	372 ± 29.6[b]	345 ± 25.0[b]	**<0.001**
Placentome number	113 ± 5.2[a]	99 ± 3.6[b]	99 ± 3.2[b]	97 ± 5.4[b]	**0.078**
Mean placentome weight (g)	4.7 ± 0.21[a]	3.7 ± 0.22[b]	3.8 ± 0.27[b]	3.6 ± 0.16[b]	**0.005**
Type A (%)	41.6 ± 11.46	51.2 ± 8.89	50.9 ± 9.23	50.7 ± 8.10	0.612
Type B (%)	34.8 ± 6.18	35.4 ± 6.21	39.6 ± 7.69	29.7 ± 7.17	0.803
Type C (%)	7.4 ± 2.79	4.5 ± 1.82	1.1 ± 0.45	2.2 ± 1.04	0.119
Type D (%)	16.2 ± 3.86	8.9 ± 2.32	8.5 ± 4.08	17.3 ± 9.35	0.532
Size > 5cm (%)	2.0 ± 3.51	1.0 ±2.21	0.9 ± 3.79	1.4 ± 9.01	0.234
Size 2-5cm (%)	63.8 ± 0.49	62.5 ± 0.43	63.4 ± 0.48	63.3 ± 0.45	0.459
Size 1-2cm (%)	15.6 ± 4.25	23.5 ± 4.60	20.7 ± 4.54	20.6 ± 4.41	0.477
Size < 1cm (%)	18.6 ±2.15	13.0 ± 3.29	15.0 ± 2.41	14.7 ± 1.98	0.470

P values shown in the table are for overall ANOVA. Mean values within a row with unlike superscripts are significantly different (p=<0.05 for individual comparisons, see text for details).

H+Ad.LacZ versus C+Saline groups (p=0.032, p=0.043 and p=0.02; and p=0.003, p=0.006 and p=0.001, respectively). There were no significant differences between the three overnourished groups for any placental parameters. There were no significant differences between any of the four groups with respect to the proportions (% by number) of placentomes of each morphological type or in each category of size. Irrespective of treatment group, fetal weight was strongly correlated with total placental weight (r=0.776, n=57, p<0.001), placentome weight (r=0.735, n=57, p<0.001) and membrane weight (r=0.753, n=57, p<0.001).

4.3.4.3 Fetal anthropometric measurements and gender distribution

There were no significant differences in the male to female fetal sex ratio between the four experimental groups (see Table 4.7). Post-mortem measurements of biparietal diameter and girth at the level of the lowermost rib (ultrasound plane) were reduced in both H+Ad.Saline

Table 4.7 – Fetal gender distribution and post-mortem physical measurements following late gestation necropsy

	C+Saline (n=12)	H+Ad.VEGF (n=18)	H+Saline (n=13)	H+Ad.LacZ (n=14)	Total (n=57)
Male	7	8	4	7	26
Female	5	10	9	7	31

	C+Saline (n=12)	H+Ad.VEGF (n=18)	H+Saline (n=13)	H+Ad.LacZ (n=14)	P Value
Biparietal head diameter	71.0 ± 0.78[a]	68.6 ± 1.28[ab]	66.6 ± 1.12[b]	66.8 ± 1.00[b]	**0.043**
Girth (level of umbilicus)	363 ± 4.9[a]	340 ± 6.2[b]	336 ± 7.2[b]	328 ± 7.0[b]	**0.006**
Girth (ultrasound plane)	340 ± 5.6[a]	327 ± 6.4[ab]	320 ± 5.6[b]	314 ± 5.9[b]	**0.038**
Length of femoral bone	89.8 ± 1.00[a]	85.9 ± 1.42[b]	84.4 ± 1.11[b]	83.9 ± 1.56[b]	**0.024**
Length of tibial bone	107 ± 1.2[a]	102 ± 1.9[ab]	101 ± 1.4[b]	100 ± 1.9[b]	0.070

P values shown in the table are for overall ANOVA. Mean values within a row with unlike superscripts are significantly different (p=<0.05 for individual comparisons, see text for details).

---

and H+Ad.LacZ (but not H+Ad.VEGF) relative to C+Saline groups (p=0.013 and p=0.015; p=0.04 and p=0.006, respectively). There was a tendency towards an overall difference in post-mortem measurements of tibia length, with post-hoc testing demonstrating a significant reduction in H+Saline and H+Ad.LacZ relative to C+Saline groups (p=0.026 and p=0.016) and a tendency towards a reduction in the H+Ad.VEGF group (p=0.087). Post-mortem measurements of femur length and umbilical girth were reduced in all three overnourished (H+Ad.VEGF, H+Saline and H+Ad.LacZ) groups relative to C+Saline groups (p=0.044, p=0.01 and p=0.005; and p=0.015, p=0.009 and p=0.001, respectively). There were no statistically significant differences for any measurements in the H+Ad.VEGF group relative to the H+Saline or H+Ad.LacZ groups.

4.3.4.4 Absolute fetal organ weights

Absolute weights of the fetal internal organs and the weight of the residual carcass, as determined at late gestation necropsy are presented in Table 4.8. Weights of the fetal kidneys,

Table 4.8 – Weights of the major internal organs of the fetus in absolute terms at late gestation necropsy

	C+Saline (n=12)	H+Ad.VEGF (n=18)	H+Saline (n=13)	H+Ad.LacZ (n=14)	P Value
Brain	47.0 ± 0.95	44.1 ± 1.58	44.8 ± 0.79	44.5 ± 1.10	0.431
Pituitary	0.16 ± 0.014	0.14 ± 0.009	0.14 ± 0.007	0.12 ± 0.006	0.133
Adrenals	0.50 ± 0.023	0.46 ± 0.022	0.47 ± 0.027	0.50 ± 0.032	0.666
Pancreas	3.93 ± 0.134	3.75 ± 0.197	3.63 ± 0.287	3.51 ± 0.182	0.582
Gut (full)	302.5 ± 17.20	271.3 ± 16.44	267.3 ± 15.77	248.4 ± 19.43	0.230
Stomach	32.64 ± 1.460	30.16 ± 1.207	30.55 ± 0.846	28.52 ± 1.264	0.171
Small intestine	50.85 ± 2.741	44.59 ± 2.327	48.12 ± 2.450	42.68 ± 2.117	0.109
Large intestine	14.50 ± 1.084	12.93 ± 0.485	13.31 ± 0.592	12.43 ± 0.754	0.261
Liver	161.3 ± 6.99^{a}	134.1 ± 6.31^{b}	131.6 ± 7.80^{b}	120.8 ± 9.32^{b}	**0.007**
Spleen	9.03 ± 0.415	8.10 ± 0.444	8.16 ± 0.736	7.57 ± 0.598	0.374
Perirenal fat	21.11 ± 0.575^{a}	18.23 ± 0.925^{b}	18.86 ± 1.047^{ab}	17.20 ± 1.088^{b}	0.055
Kidneys	27.49 ± 0.766^{a}	25.11 ± 1.171^{ab}	23.37 ± 1.136^{b}	21.99 ± 1.429^{b}	**0.019**
Heart	36.71 ± 1.199^{a}	33.55 ± 1.475^{ab}	30.89 ± 1.289^{b}	29.57 ± 1.454^{b}	**0.007**
Lungs	171.6 ± 10.85^{a}	157.9 ± 8.47^{ab}	142.3 ± 8.67^{b}	128.4 ± 10.78^{b}	**0.021**
Thymus	7.15 ± 0.447	6.72 ± 0.489	5.95 ± 0.581	6.10 ± 0.661	0.472
Thyroid	0.97 ± 0.021^{a}	0.77 ± 0.069^{b}	0.80 ± 0.044^{b}	0.74 ± 0.048^{b}	**0.025**
Testes*	1.84 ± 0.074	1.69 ± 0.121	2.03 ± 0.092	1.98 ± 1.402	0.855
Ovaries*	0.11 ± 0.014	0.09 ± 0.008	0.12 ± 0.022	0.10 ± 0.012	0.373
Carcass	3289 ± 92.2^{a}	2847 ± 134.7^{b}	2779 ± 132.6^{b}	2669 ± 157.7^{b}	**<0.001**

*P values shown in the table are for overall ANOVA. Mean values within a row with unlike superscripts are significantly different (p=<0.05 for individual comparisons, see text for details). * Gender distribution between groups = C+Saline: 7 male, 5 female. H+Ad.VEGF: 8 male, 10 female. H+Saline: 4 male, 9 female. H+Ad.LacZ: 7 male, 7 female.*

---

heart and lungs were reduced in H+Saline and H+Ad.LacZ (but not H+Ad.VEGF) versus C+Saline groups (p=0.026 and p=0.003; p=0.008 and p=0.001; p=0.049 and p=0.004, respectively).

Weights of the fetal liver, thyroid and carcass were reduced in all three overnourished (H+Ad.VEGF, H+Saline and H+Ad.LacZ) groups compared to the C+Saline group (p=0.014, p=0.013 and p=0.001 for liver; p=0.01, p=0.044 and p=0.005 for thyroid and p=0.025, p=0.016 and p=0.003 for carcass, respectively). The weight of the perirenal fat depot was significantly reduced in H+Ad.VEGF and H+Ad.LacZ (but not H+Saline) relative to C+Saline groups (p=0.037 and p=0.008, respectively). Irrespective of treatment group all fetal organ weights (except gonads) correlated with fetal body weight. The weakest correlation was demonstrated for the adrenals (r=0.449, n=57 p<0.001) and the strongest for the kidneys (r=0.902, n=57 p<0.001).

4.3.4.5 Relative fetal organ weights

Table 4.9 summarises the relative weights of the fetal internal organs, expressed per kg fetus together with the liver to brain weight ratio. Relative brain weight was increased in H+Saline and H+Ad.LacZ relative to C+Saline groups (p=0.002 and p=<0.0001, respectively) with a tendency towards an increase in the H+Ad.VEGF group (p=0.079). Relative brain weight was lower in the H+Ad.VEGF group compared with the H+Ad.LacZ group (p=0.008) and also tended to be lower in H+Ad.VEGF versus H+Saline groups (p=0.077). Relative adrenal weight was increased in H+Ad.LacZ versus C+Saline groups (p=0.005) with tended to be higher in H+Saline versus C+Saline groups (p=0.053). Relative adrenal weight was lower in H+Ad.VEGF compared to H+Ad.LacZ groups (p=0.038) but was not significantly different to the C+Saline or H+Saline group. Relative stomach weight was increased in H+Saline versus C+Saline groups (p=0.006) but was not significantly different to H+Ad.VEGF or H+Ad.LacZ groups. Relative small intestine weight was increased in H+Saline versus both C+Saline and H+Ad.VEGF groups (p=0.003 and p=0.002, respectively) but was not significantly different to the H+Ad.LacZ group. Liver to brain weight ratios were significantly increased in H+Saline and H+Ad.LacZ relative to C+Saline groups (p=0.018 and p<0.001, respectively) and tended to be increased in H+Ad.VEGF versus C+Saline groups (p=0.093). Liver to brain weight ratios were also significantly lower in H+Ad.VEGF versus H+Ad.LacZ (but not H+Ad.Saline) groups (p=0.015).

As there were no significant differences in fetal weight specific organ weights between the H+Saline and H+Ad.LacZ groups for any organ, these two groups were once again combined (H+Saline/Ad.LacZ) to facilitate further comparisons with the H+Ad.VEGF and C+Saline groups. This approach revealed significant differences between the H+Ad.VEGF and H+Saline/Ad.LacZ groups in relative brain weight (see Figure 4.23A), brain to liver weight ratio (see Figure 4.23B) and relative small intestine weight (see Figure 4.24A), as well as a tendency towards a difference in relative adrenal weight (see Figure 4.24B). Significance levels for individual group comparisons are indicated in the figures.

Table 4.9 – Relative weights of the major internal organs (expressed in g per kg fetus) at late gestation necropsy, and brain to liver weight ratios

	C+Saline (n=12)	H+Ad.VEGF (n=18)	H+Saline (n=13)	H+Ad.LacZ (n=14)	P Value
Brain	9.27 ± 0.239[a]	10.15 ± 0.259[ab]	11.00 ± 0.400[bc]	11.43 ± 0.451[c]	**<0.001**
Pituitary	0.03 ± 0.002	0.03 ± 0.002	0.03 ± 0.002	0.03 ± 0.002	0.817
Adrenals	0.10 ± 0.004[a]	0.11 ± 0.004[a]	0.12 ± 0.008[ab]	0.12 ± 0.007[b]	**0.029**
Pancreas	0.78 ± 0.027	0.85 ± 0.018	0.87 ± 0.051	0.87 ± 0.051	0.285
Gut (full)	59.50 ± 3.042	61.59 ± 2.769	64.67 ± 3.227	60.84 ± 3.882	0.748
Stomach	6.41 ± 0.208[a]	6.93 ± 0.618[ab]	7.47 ± 0.252[b]	7.09 ± 0.337[ab]	**0.047**
Small intestine	9.95 ± 0.345[a]	10.13 ± 0.313[a]	11.65 ± 0.457[b]	10.71 ± 0.400[ab]	**0.011**
Large intestine	2.84 ± 0.175	2.99 ± 0.100	3.22 ± 0.091	3.06 ± 0.138	0.238
Liver	31.70 ± 1.089	30.53 ± 0.707	31.79 ± 1.490	29.30 ± 1.266	0.388
Spleen	1.77 ± 0.053	1.84 ± 0.059	1.94 ± 0.122	1.84 ± 0.092	0.594
Perirenal fat	4.18 ± 0.144	4.15 ± 0.152	4.54 ± 0.126	4.24 ± 0.216	0.363
Kidneys	5.42 ± 0.118	5.70 ± 0.079	5.64 ± 0.140	5.37 ± 0.170	0.164
Heart	7.24 ± 0.230	7.68 ± 0.187	7.50 ± 0.214	7.27 ± 0.241	0.426
Lungs	33.60 ± 1.607	35.95 ± 1.473	34.19 ± 1.254	31.09 ± 1.895	0.169
Thymus	1.41 ± 0.084	1.52 ± 0.070	1.41 ± 0.105	1.46 ± 0.111	0.810
Thyroid	0.19 ± 0.005	0.17 ± 0.012	0.20 ± 0.009	0.18 ± 0.013	0.364
Testes*	0.35 ± 0.015	0.36 ± 0.016	0.44 ± 0.039	0.55 ± 0.026	0.488
Ovaries*	0.02 ± 0.003	0.02 ± 0.002	0.03 ± 0.005	0.03 ± 0.004	0.094
Brain: liver weight ratio	0.29 ± 0.042[a]	0.33 ± 0.038[ab]	0.35 ± 0.074[bc]	0.39 ± 0.077[c]	**0.003**

*P values shown in the table are for overall ANOVA. Mean values within a row with unlike superscripts are significantly different (p=<0.05 for individual comparisons, see text for details). * Gender distribution between groups = C+Saline: 7 male, 5 female. H+Ad.VEGF: 8 male, 10 female. H+Saline: 4 male, 9 female. H+Ad.LacZ: 7 male, 7 female.*

Figure 4.23 – Indices of fetal brain sparing at necropsy

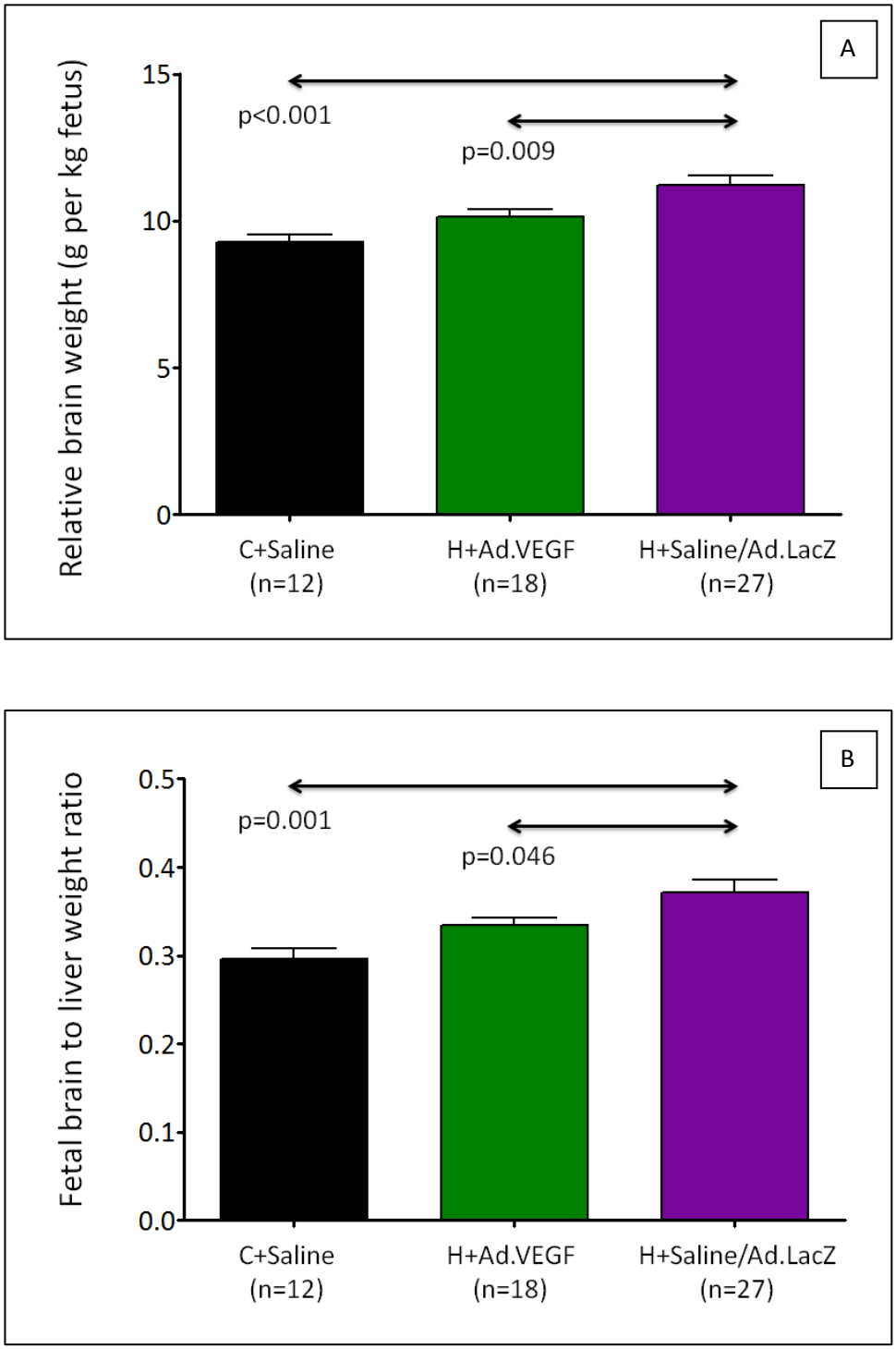

*Relative fetal brain weights [A] and brain to liver weight ratios [B] at late gestation necropsy (*131±0.2 days gestation*) in singleton pregnancies in adolescent ewes offered a control-intake (C) or high-intake (H) diet and receiving bilateral uterine artery injections of Ad.VEGF, Ad.LacZ or saline. P values shown are for individual post-hoc comparisons using the test of least significant difference (overall ANOVA p<0.001 and p=0.002 for figures A and B, respectively).*

Figure 4.24 – Small intestine and adrenal weights per kg fetus

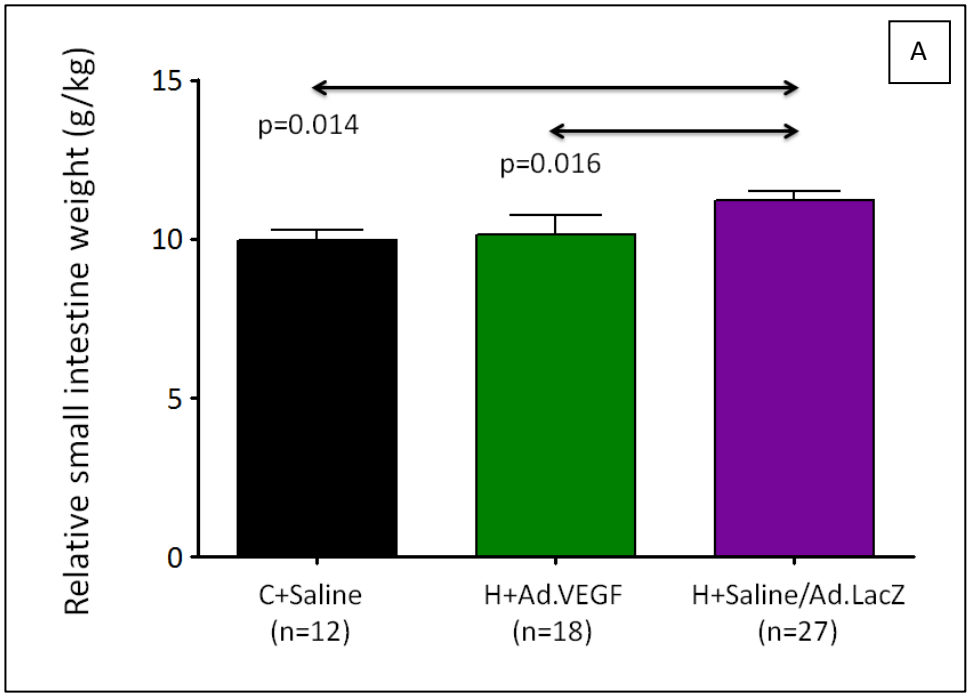

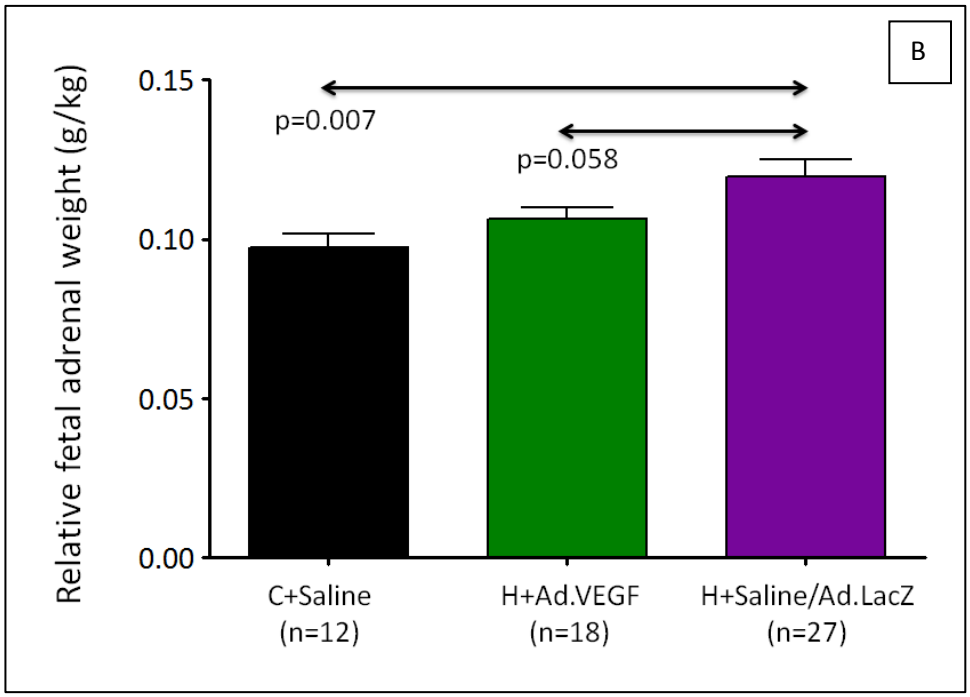

*Relative fetal small intestine weights [A] and adrenal weights [B] at late gestation necropsy (*131±0.2 days gestation*) in singleton pregnancies in adolescent ewes offered a control-intake (C) or high-intake (H) diet and receiving bilateral uterine artery injections of Ad.VEGF, Ad.LacZ or saline. P values shown are for individual post-hoc comparisons using the test of least significant difference (overall ANOVA p<0.013 and p=0.016 for figures A and B, respectively).*

4.3.4.6 Gross abnormalities

A number of anomalies were found during the course of the fetal dissections. One fetus in the H+Ad.LacZ group had an undescended right testicle and a hydrocoele of the left testicle. One fetus in the H+Saline group was found to have a mass arising from the right atrium of the heart (see Figure 4.25A). Histology revealed this to be an extension of the myocardial tissue of generally normal appearances, but with several small foci of myofibre hypereosinophilia and nuclear pyknosis. One fetus in the H+Ad.VEGF group had discordant kidneys, the right one weighing 50% more than the left. A second fetus in the H+Ad.VEGF group was found to have a mass adjacent to the small bowel mesentery (see Figure 4.25B). Histology revealed this to be a lymph node with normal internal architecture and no evidence of hyperplasia or abnormal cellular infiltrates. A third fetus in the H+Ad.VEGF group had a similar finding of a discrete mass arising from the lymphoid tissue of the gut. Only one abnormality of note was found during the course of the maternal dissections. The ewe in question (allocated to the H+Saline group) did not have a flow probe fitted and received only a unilateral UtA injection due to major difficulty in locating and hence visualising the uterine horn and vessels on the left side at the time of surgery. On the right the main UtA was noted to be tortuous and enlarged. The impression at the time was that there was a possible partial uterine torsion or adhesion due to the prior embryo transfer surgery compromising access to the left hand side. While enlarging the mid-line incision would have been possible it was considered that the ewe would be vulnerable to subsequent herniation. As she was allocated to receive saline only the decision was taken to inject on one side only. The ewe was observed closely during the post-op period but recovered normally and fetal growth and wellbeing at weekly ultrasound examination were unremarkable thereafter. At necropsy, the ewe was discovered to have uterus didelphys, a rare congenital abnormality of the reproductive tract. The gravid (right) horn was completed separated from the non-gravid (left) horn, and each horn had its own cervix (see Figure 4.25C). The pregnancy was located in the right uterine horn, the site of the original embryo transfer. Placentome number in this gravid horn was 54 compared to an average of 98 amongst the overnourished pregnancies of the present study, in which both horns were utilised (representing a 45% reduction in caruncle occupancy). There was evidence of compensatory placentome growth in the gravid horn (mean placentome weight was 7.2g compared with an average of 3.8g for the other animals in the H+Saline group). The left uterine horn was filled with clear fluid only (hydrometra). There had still been considerable development of the uterine arterial vasculature, presumably an effect of the circulating reproductive steroids. In view of this significant abnormality, data from this ewe was excluded from further analysis.

Figure 4.25 – Fetal and maternal abnormalities encountered at necropsy

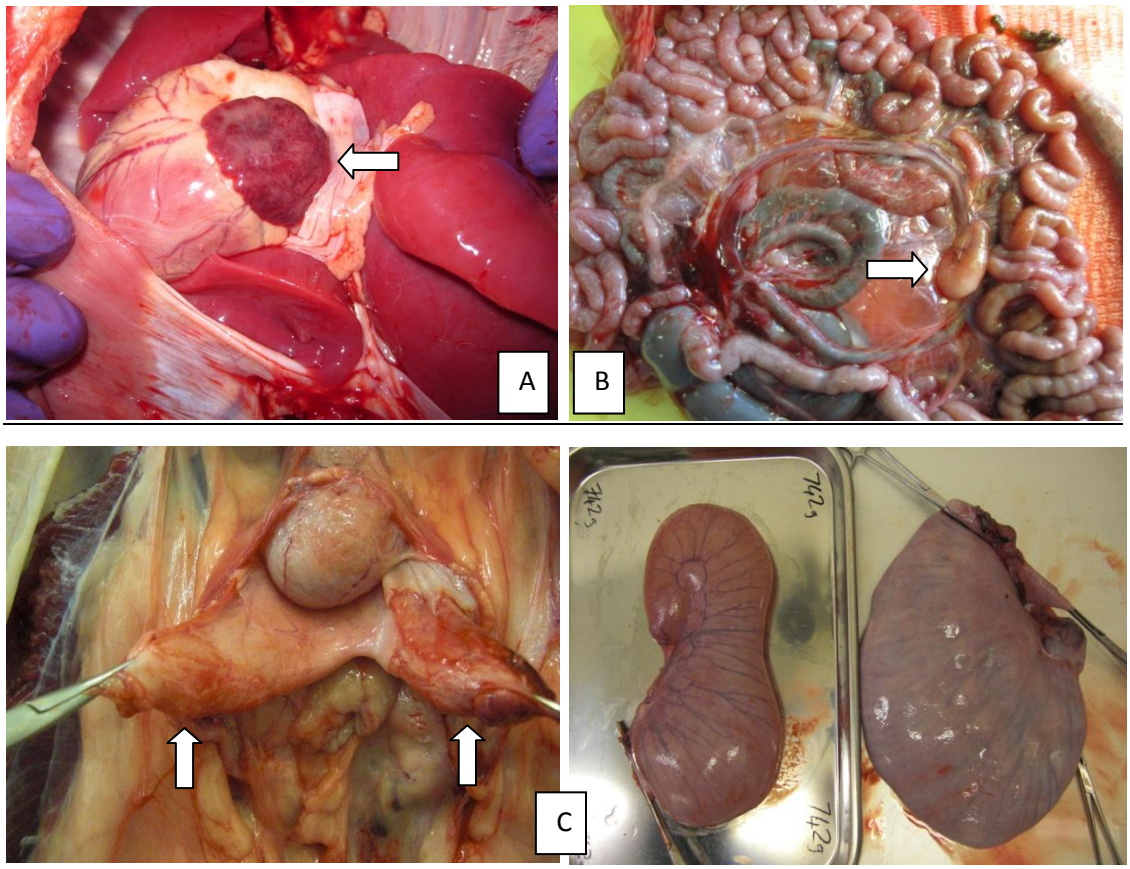

Fetal abnormalities included a right atrial appendage, composed of normal myocardial tissue [A] and a mass arising from small bowel mesentery [B], histology of which demonstrated a normal lymph node. One ewe was found to have uterus didelphys [C] with two cervices (indicated by white arrows) and completely separate uterine horns: gravid (right, with fetus removed) and non-gravid (left) containing only fluid and completely devoid of placentomes.

4.3.5 Laboratory analyses

4.3.5.1 Nutrients and metabolic hormones

Table 4.10 shows the concentration of nutrients and metabolic hormones in maternal and fetal plasma on the day before and on the day of necropsy, respectively. Concentrations of glucose, insulin and IGF-1 in the maternal circulation were all increased in overnourished (H+Ad.VEGF, H+Saline and H+Ad.LacZ) versus the C+Saline group ($p=0.012$, $p=0.002$ and $p=0.004$; $p<0.001$, $p=0.001$ and $p<0.001$; $p<0.001$, $p=0.005$ and $p=0.002$, respectively). There were no significant

Table 4.10 – Concentrations of selected nutrients and metabolic hormones in maternal and fetal plasma and in the amniotic fluid

	C+Saline (n=12)	H+Ad.VEGF (n=18)	H+Saline (n=13)	H+Ad.LacZ (n=14)	P Value
Maternal glucose (mg/dl)	62.3 ± 1.44[a]	67.8 ± 1.44[b]	69.6 ± 1.21[b]	67.4 ± 2.08[b]	**0.009**
Maternal insulin (ng/ml)	1.13 ± 0.157[a]	2.17 ± 0.185[b]	2.08 ± 0.164[b]	1.97 ± 0.208[b]	**<0.001**
Maternal IGF-1 (ng/ml)	0.36 ± 0.022[a]	0.49 ± 0.019[b]	0.46 ± 0.028[b]	0.47 ± 0.024[b]	**0.001**
Fetal glucose (mg/dl)	19.8 ± 2.54	19.4 ± 2.25	24.1 ± 4.12	22.7 ± 3.98	0.992
Fetal insulin (ng/ml)	0.55 ± 0.038	0.53 ± 0.050	0.39 ± 0.029	0.52 ± 0.043	0.060
Fetal IGF-1 (ng/ml)	0.21 ± 0.018	0.18 ± 0.014	0.19 ± 0.014	0.18 ± 0.014	0.423
Fetal lactate (mmol/l)	8.8 ± 0.40	8.1 ± 0.29	8.4 ± 0.36	8.5 ± 0.41	0.370
Amniotic fluid glucose (mg/dl)	19.8 ± 2.54	19.4 ± 2.25	24.1 ± 4.12	21.4 ± 3.98	0.700

Concentrations of glucose, insulin and IGF-1 in late-gestation maternal and fetal plasma, fetal lactate and amniotic fluid glucose concentrations. P values shown in the table are for overall ANOVA. Mean values within a row with unlike superscripts are significantly different (p=<0.05 for individual comparisons, see text for details).

---

differences between the three overnourished groups for any of the above parameters. With respect to the fetal blood results, there were no significant differences between any of the four groups in glucose, insulin, IGF-1 or lactate. There were also no differences between groups in amniotic fluid glucose concentrations. Fetal IGF-1 (but not insulin, glucose or lactate) concentrations were correlated with fetal weight ($r=0.528$, $n=57$, $p<0.001$).

4.3.5.2 Small intestinal crypt cell proliferation

Figure 4.26 illustrates the absolute numbers of proliferating cells within the crypts of the small intestine as well as the labelling index (proportion of proliferating cells per unit tissue area) by study group. There were no differences between groups for either parameter (p=0.716 and p=0.915, respectively). Despite the significant effects of FGR and Ad.VEGF gene therapy on the relative small intestinal weights (see Figure 4.24A), there were no differences in the total cell number between C+Saline, H+Ad.VEGF, H+Saline and H+Ad.LacZ groups (1158±288, 1176±571, 1284±663 and 1054±250, respectively, overall ANOVA p=0.680). No significant correlalations were seen between these parameters and fetoplacental weight or absolute/relative weights of the various components of the gastrointestinal tract, including the small intestine.

4.3.5.3 Body composition analysis

The results of the fetal carcass analysis are shown in Table 4.11. Prior to mincing, the weight of the thawed-out carcasses was significantly reduced in all three overnourished groups (H+Ad.VEGF, H+Saline and H+Ad.LacZ) relative to the C+Saline group (p=0.045, p=0.046 and p=0.12, respectively) in keeping with the group differences previously observed at necropsy, prior to freezing (see Table 4.8). Absolute carcass dry matter weight (in grams) was lower in H+Ad.LacZ versus C+Saline groups (p=0.013) and carcass ash content (in grams) was lower in both H+Ad.LacZ and H+Ad.VEGF relative to C+Saline groups (p=0.049 and p=0.015, respectively). However percentage dry matter was equivalent between groups and similarly the ash, protein and fat contents of the fetal carcass were equivalent between groups when expressed as a percentage of dry matter and per kg “wet” carcass. Thus no alteration in chemical carcass composition was demonstrated.

4.3.5.4 Vascular reactivity

Figure 4.27A shows the vasoconstriction response of UtA2/UtA3 vessel segments to increasing concentrations of phenylephrine in the organ bath when examined on the day after necropsy. Satisfactory dose response curves were achieved in 76 of 78 vessels examined from a subset of 22 animals. For these vessels the degree of contraction was greater in H+Ad.VEGF relative to H+Ad.LacZ/Saline groups at phenylephrine concentrations of -6.0 logM (87±7.2% vs. 71±3.6%, p=0.043), -5.5 logM (140±13.1% vs. 112±2.8%, p=0.007), -5.0 logM (168±15.7% vs. 133±3.1%, p=0.005) and -4.5 logM (174±16.7% vs. 136±3.2%, p=0.004). Contraction of Ad.VEGF tranduced vessels was not significantly different to the C+Saline group at any point. Maximum contractile response (E_{max}) was also increased in H+Ad.VEGF versus H+Saline/Ad.LacZ groups (190±18.5 vs. 148±3.2%, p=0.04) and was not significantly different to the C+Saline group (p=0.718).

Figure 4.26 – Fetal small intestinal crypt cell proliferation

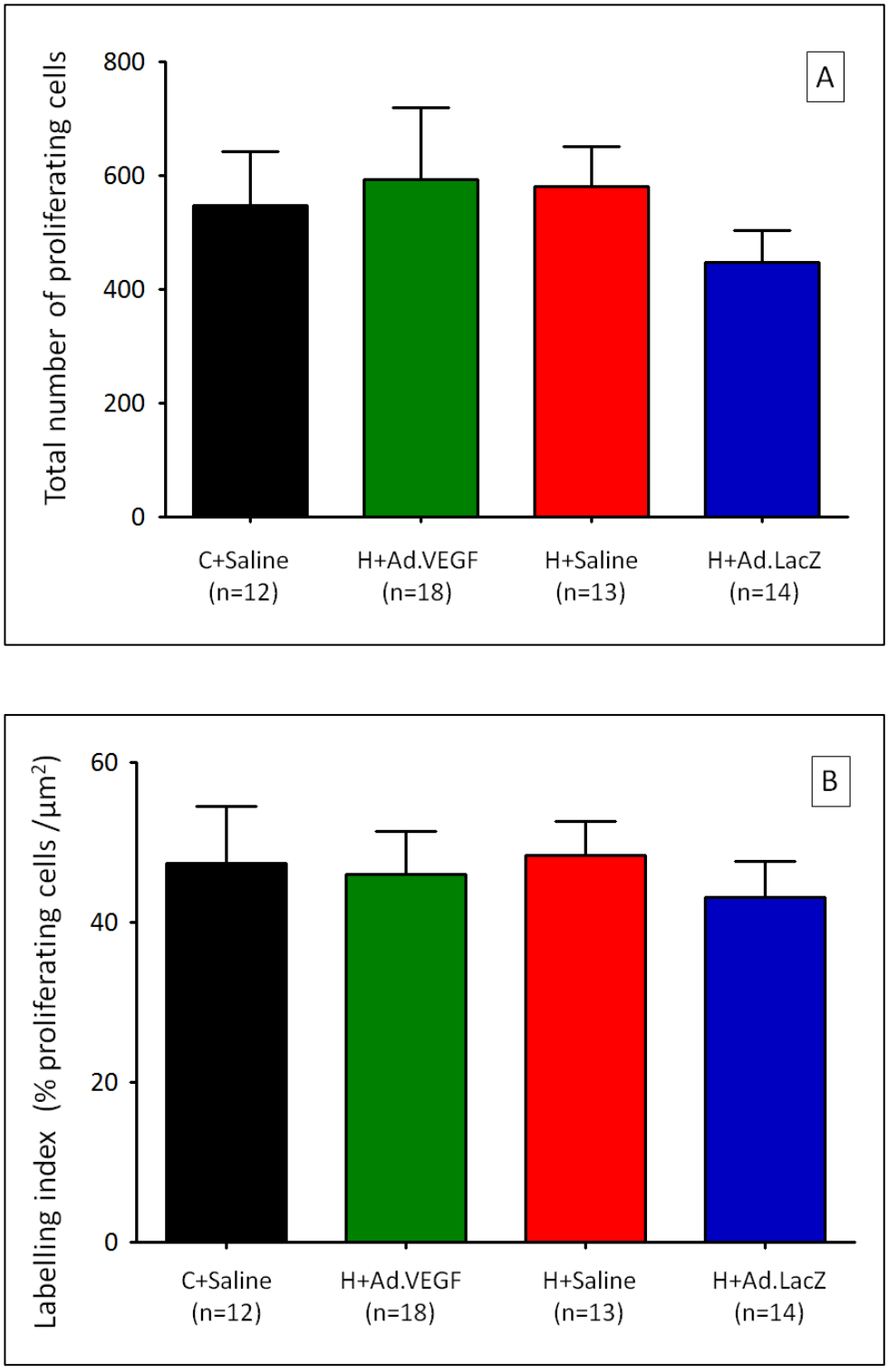

Crypt cell proliferation assessed by anti-Ki-67 immunohistochemistry and image analysis of fetal jejunum perfuse-fixed at 131±0.2 days gestation in singleton pregnancies in adolescent ewes offered a control-intake (C) or high-intake (H) diet and receiving bilateral uterine artery injections of Ad.VEGF, Ad.LacZ or saline. There were no differences between groups (p>0.05).

Table 4.11 – Fetal body composition analysis by chemical determination of the dry matter, ash, protein and fat contents of the fetal carcass

	C+Saline (n=12)	H+Ad.VEGF (n=18)	H+Saline (n=13)	H+Ad.LacZ (n=14)	P Value
Pre-mince weight (g)	3591 ± 101[a]	3159 ± 147[b]	3129 ± 156[b]	3010 ± 169[b]	0.067
Wet weight (g)	272 ± 12.8	267 ± 10.3	272 ± 12.2	269 ± 11.5	0.992
Dry weight (g)	66.6 ± 3.65	65.7 ± 2.74	67.9 ± 3.32	66.3 ± 3.17	0.966
Dry matter (g)	878 ± 28.7[a]	776 ± 36.8[ab]	780 ± 38.3[ab]	737 ± 38.2[b]	0.080
Dry matter (%)	24.4 ± 0.22	24.5 ± 0.16	25.0 ± 0.18	24.6 ± 0.21	0.247
Ash (g)	145 ± 5.8[a]	125 ± 6.5[b]	134 ± 7.9[ab]	119 ± 7.4[b]	0.076
Ash (%)	16.6 ± 0.43	16.1 ± 0.34	17.1 ± 0.41	16.1 ± 0.49	0.318
Ash (g/kg)	40.4 ± 1.21	39.6 ± 0.95	42.7 ± 1.17	39.6 ± 1.31	0.209
Protein (g)	588 ± 21.0	518 ± 25.2	519 ± 25.9	495 ± 28.0	0.102
Nitrogen (%)	10.7 ± 0.08	10.7 ± 0.07	10.6 ± 0.08	10.7 ± 0.09	0.870
Protein (g/kg)	164 ± 2.1	163 ± 1.6	166 ± 1.7	164 ± 1.0	0.670
Fat (g)	103 ± 3.8	95 ± 4.4	95 ± 5.4	91 ± 4.5	0.400
Fat (%)	11.8 ± 0.30	12.3 ± 0.24	12.2 ± 0.34	12.5 ± 0.47	0.509
Fat (g/kg)	28.7 ± 0.77	30.2 ± 0.64	30.5 ± 0.75	30.8 ± 1.38	0.445

Post-mortem fetal carcass analysis, detailing body composition in absolute terms (in grams) and relative terms as follows. Fat percentage was expressed relative to dry matter content and relative fat weight (g/kg) was expressed as a proportion of wet weight. All other parameters were expressed relative to the pre-mince weight. P values shown in the table are for overall ANOVA. Mean values within a row with unlike superscripts are significantly different (p=<0.05 for individual comparisons, see text for details).

Figure 4.27B illustrates the relaxation response of the same set of vessels to increasing doses of bradykinin within the organ bath. The relaxation response to bradykinin was insufficient for analysis in 3 out of 14 vessel segments (27.3%) in C+Saline, 7 of 24 (29.2%) in H+Ad.VEGF, and 13 of 38 (34.2%) in H+Saline/Ad.LacZ groups, respectively. Consequently no data was available from these particular vessels. For the remaining vessels, vasorelaxation was markedly greater

Figure 4.27 – Vascular reactivity of uterine artery segments examined in the organ bath

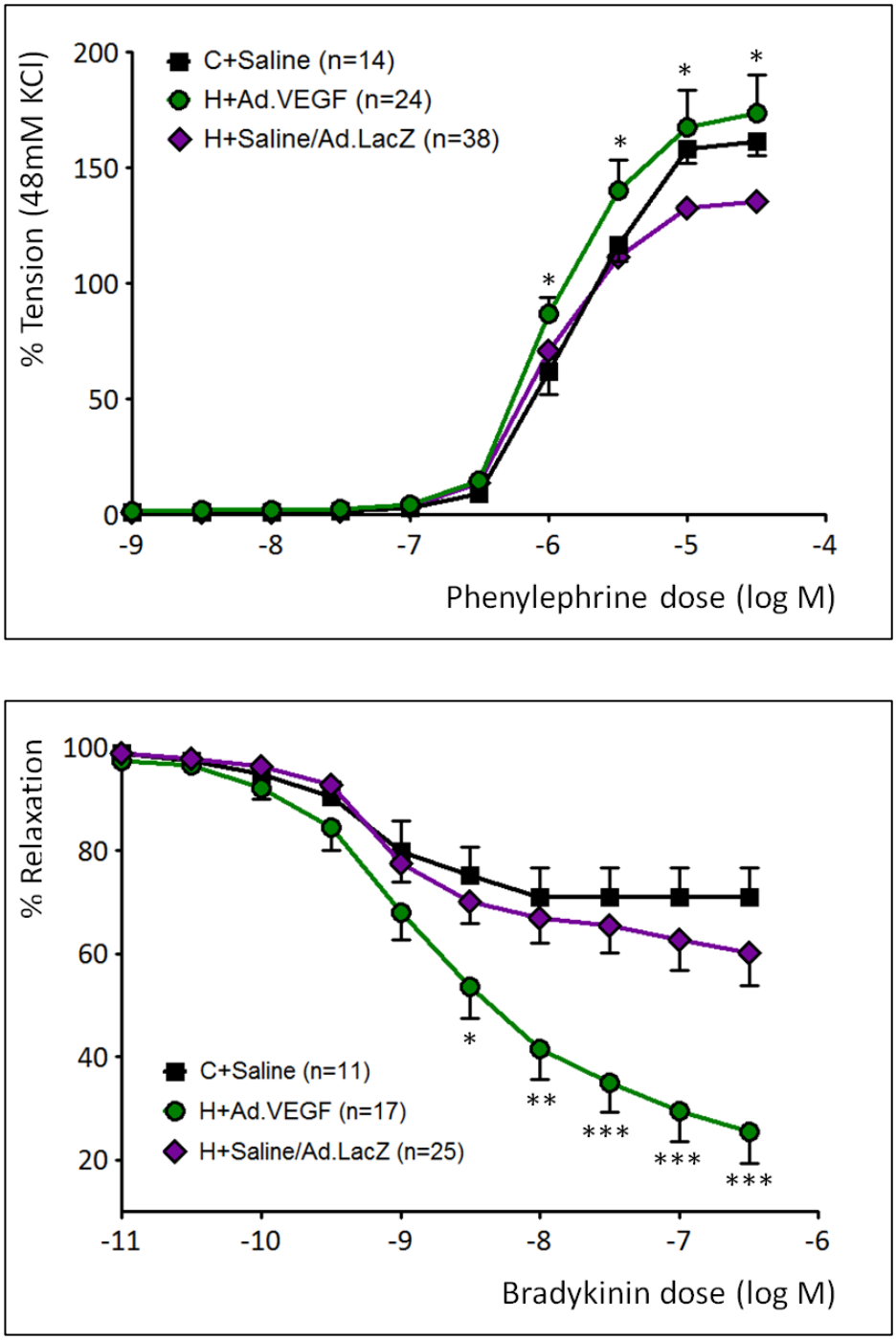

*Dose response curves to phenylephrine [A] and bradykinin [B] assessing vascular contraction and relaxation, respectively, of uterine artery (UtA) segments examined in an organ bath the day after late gestation necropsy (131±.0.2 days gestation). Uterine arteries were injected mid-pregnancy with Ad.VEGF, Ad.LacZ or saline in 22 singleton-bearing adolescent dams receiving a control-intake (C) or high-intake (H) of a complete diet. * p<0.05, ** p<0.01, *** p<0.001. P values shown are for overall ANOVA - see text for significance levels of individual comparisons.*

in H+Ad.VEGF relative to H+Saline/Ad.LacZ and C+Saline groups at bradykinin concentrations of -8.5 logM (46±6.1 vs. 30±4.3% and 25±5.4%, p=0.021 and p=0.015, respectively), -8.0 logM (58±6.0 vs. 33±4.9% and 29±5.7%, p=0.001 and p=0.002, respectively), -7.5 logM (65±5.7 vs. 34±5.4% and 29±5.7%, p<0.001 each), -7.0 logM (70±5.9 vs. 37±5.8% and 29±5.7%, p<0.001 each) and -6.5 logM (74±6.3 vs. 40±6.2% and 29±5.7%, p<0.001 each). Relaxation of UtA from control-intake pregnancies were noted to plateau at concentrations of -8.0 logM upwards. The maximum relaxation (E_{max}) was higher in H+Ad.VEGF (75±6.2%) versus both H+Saline/Ad.LacZ (41±6.1%, p<0.001) and C+Saline (30±6.0%, p<0.001) groups. There were no significant differences in the half maximal effective concentration (EC_{50}) of bradykinin between C+Saline, H+Ad.VEGF and H+Saline/Ad.LacZ groups (9.3±3.68 x 10^{-10}, 6.4±2.72 x 10^{-9} and 4.0±4.02 x 10^{-9}, respectively, p=0.483).

There were no significant differences in any indices of vascular contractility or relaxation between branches UtA2 and UtA3 (p=0.984 and p=0.655, respectively) or between those from the gravid versus non-gravid horns (p=0.156; p=0.562). There were also no interactions between these factors and treatment group (p=0.386–0.855; p=0.129–0.778).

4.3.5.5 Intima to media ratios

Table 4.12 shows the intimal and medial thicknesses and IMR for each UtA branch. Significant differences were observed between the three different levels of branching (UtA1, 2 and 3) for all of these parameters. Whilst, unsurprisingly, the absolute vessel dimensions decreased with successive branching, values of IMR increased significantly with progression from UtA1 to UtA3 (p<0.001). The dimensions of the vessels supplying the gravid and non-gravid horn were equivalent. Although there were no differences between study groups when analysing each branch separately, comparisons across all vessel segments showed that the intima was thicker in C+Saline compared with H+Ad.VEGF and H+Ad.LacZ/Saline groups (96±4.4 vs. 86±3.4 and 80±2.6 p=0.001 and p=0.038, respectively) and that the media was thicker in C+Saline versus H+Saline/LacZ groups only (500±20.6 versus 417±30.9µm, p=0.024). There were no differences in IMR between any of the groups, neither was there any demonstrable effect of Ad.VEGF on any of these vessel parameters.

4.3.5.6 Neovascularisation in perivascular adventitia

Table 4.13 shows absolute numbers of blood vessels in the perivascular adventitia, adventitial area and vessel density (number of vessels per unit adventitial area) stratified by UtA branch. There were no differences between vessels harvested from the gravid and non-gravid horns

Table 4.12 – Intima to media ratios in the uterine arteries at three different levels of branching

Parameter	UtA Branch	C+Saline (n=24)	H+Ad.VEGF (n=36)	H+Saline/Ad.LacZ (n=54)	P Value
Intimal thickness (µm)	UtA1	108 ± 9.4	99 ± 7.3	90 ± 4.7	0.191
	UtA2	95 ± 6.3	82 ± 4.9	78 ± 4.5	0.103
	UtA3	88 ± 6.5	75 ± 4.1	74 ± 4.2	0.151
Medial thickness (µm)	UtA1	658 ± 56.7	562 ± 47.1	563 ± 40.4	0.366
	UtA2	496 ± 46.7	411 ± 39.6	396 ± 30.8	0.200
	UtA3	347 ± 36.4	344 ± 31.2	293 ± 24.3	0.319
Intima to media ratio	UtA1	0.083 ± 0.0037	0.097 ± 0.0065	0.088 ± 0.0038	0.172
	UtA2	0.104 ± 0.0059	0.116 ± 0.0073	0.109 ± 0.0045	0.408
	UtA3	0.144 ± 0.0009	0.128 ± 0.0010	0.145 ± 0.0067	0.295

P values shown in the table are for overall ANOVA. As there were no significant differences between groups, no post-hoc tests were performed.

---

therefore data were combined. Although there were no significant differences in the absolute vessel numbers between study groups when looking at individual levels of branching, overall there were more vessels per section in H+Ad.VEGF and H+Ad.LacZ/Saline versus C+Saline groups (142±7.2 and 138±11.0 vs. 105±7.0, p=0.006 and p=0.024, respectively). As there were no significant differences between groups in adventitial area (p=0.846), this translated into a significant increase in vessel density in high-intake relative to control-intake pregnancies, both overall and at each individual level of branching (p<0.001). There was no correlation between these the degree of neovascularisation and fetal to placental weight ratio. Notably both vessel number and adventitial area decreased with successive branching (p<0.001) and consequently there were no differences in vessel density between branches UtA1, 2 and 3 (p=0.113). There was no demonstrable effect of Ad.VEGF on any of these parameters.

In UtA2 branches, lumen area was increased in H+Ad.VEGF relative to both H+Saline/Ad.LacZ and C+Saline groups (p=0.023 and p=0.046, respectively). Intima+media area was also greater

Table 4.13 – Neovascularisation within the perivascular adventitia of the uterine arteries at three different levels of branching

Parameter	UtA Branch	C+Saline (n=24)	H+Ad.VEGF (n=36)	H+Saline/Ad.LacZ (n=54)	P Value
Total vesssel area (mm^2)	UtA1	15.7 ± 1.42	15.7 ± 1.36	16.0 ± 1.25	0.762
	UtA2	9.4 ± 0.81	11.3 ± 1.23	10.4 ± 0.86	0.493
	UtA3	7.0 ± 0.94	7.1 ± 0.95	5.7 ± 0.46	0.243
Intima+media+lumen area (mm^2)	UtA1	5.2 ± 0.47	5.2 ± 0.38	5.4 ± 0.30	0.884
	UtA2	3.0 ± 0.31	3.6 ± 0.37	3.0 ± 0.27	0.323
	UtA3	1.5 ± 0.23	2.0 ± 0.26	1.4 ± 0.14	0.134
Lumen area (mm^2)	UtA1	2.0 ± 0.26	2.3 ± 0.31	1.9 ± 0.16	0.495
	UtA2	1.0 ± 0.14[a]	1.7 ± 0.30[b]	1.1 ± 0.14[a]	**0.049**
	UtA3	0.4 ± 0.08[a]	0.9 ± 0.21[b]	0.4 ± 0.05[a]	**0.019**
Intima+media area (mm^2)	UtA1	3.2 ± 0.25	3.4 ± 0.24	3.6 ± 0.19	0.431
	UtA2	1.9 ± 0.20[a]	2.8 ± 0.36[b]	2.0 ± 0.16[a]	**0.021**
	UtA3	1.0 ± 0.17[ab]	1.5 ± 0.26[b]	1.0 ± 0.09[a]	0.058
Adventitial area (mm^2)	UtA1	10.5 ± 1.09	10.5 ± 1.05	11.7 ± 1.03	0.621
	UtA2	6.5 ± 0.62	7.7 ± 0.92	7.6 ± 0.69	0.539
	UtA3	5.5 ± 0.77	5.1 ± 0.71	4.2 ± 0.36	0.224
No. of blood vessels in perivascular adventitia	UtA1	144 ± 13.2	190 ± 26.5	190 ± 14.0	0.256
	UtA2	105 ± 10.2[a]	137 ± 12.1[ab]	150 ± 11.4[b]	0.058
	UtA3	67 ± 6.9	85 ± 9.4	85 ± 6.1	0.257
Blood vessels per unit adventitial area (mm^{-2})	UtA1	13.1 ± 1.73[a]	21.0 ± 2.62[b]	19.7 ± 1.21[b]	**0.026**
	UtA2	17.1 ± 2.13[a]	24.2 ± 2.46[b]	23.8 ± 1.48[b]	**0.049**
	UtA3	15.6 ± 2.40[a]	20.5 ± 2.93[ab]	24.5 ± 1.83[b]	**0.044**

(p=0.012 and p=0.02, respectively). In UtA2 vessel number was significantly greater in H+Saline/Ad.LacZ versus C+Saline (p=0.017), Ad.VEGF being intermediate. In UtA3 branches, lumen area was increased in H+Ad.VEGF relative to both H+Saline/Ad.LacZ and C+Saline groups (p=0.008 and p=0.03, respectively). Intima+media area was also greater relative to H+Saline/Ad.LacZ (p= 0.021) and tended to be greater versus C+Saline (p=0.084).

4.3.5.7 Expression of placental angiogenic factors and receptors

Table 4.14 details the placental mRNA expression of nine different angiogenic factors and their receptors, quantified separately in caruncular and cotyledonary tissues. In the carcuncle, mRNA expression of endogenous VEGFA as well as its two main receptors (FLT1 and KDR) was reduced in H+Ad.LacZ/Saline relative to C+Saline groups (p=0.012, p=0.031 and p=0.039, respectively). Although endogenous ovine VEGFA expression was not significantly influenced by Ad.VEGF treatment, expression of both FLT1 and KDR was increased in H+Ad.VEGF versus H+Ad.LacZ/Saline groups (p=0.028 and p=0.034, respectively) and was similar in magnitude to control-intake pregnancies. In fetal cotyledonary tissues, mRNA expression of ANGPT2 and TEK were significantly increased in both H+Ad.VEGF and H+Ad.LacZ/Saline compared with C+Saline groups (ANGPT2: p=0.032 and p=0.003; and TEK: p=0.018 and p=0.045, respectively), commensurate with an effect of maternal nutrition *per se*. There was no significant effect of Ad.VEGF on expression of any angiogenic factors or receptors measured in the fetal placental compartment.

Unsurprising there were also some clear correlations between the various angiogenic factors and receptors, both within and across groups. The correlations between VEGFA, FLT1, KDR and NOS3 were particularly reproducible and are detailed in Table 4.15 (n=57, p<0.001–0.037). In the fetal cotyledon, these four parameters were correlated irrespective of treatment group. The equivalent correlations for the maternal caruncle were consistently weaker and, with the exception of KDR's relationship with VEGFA and FLT1, were restricted to one or more groups.

4.3.5.8 Expression of placental glucose transporters

Placental mRNA expression of GLUT1 and GLUT3, measured separately in maternal caruncular and fetal cotyledonary tissues, is illustrated in Figure 4.28. Caruncular GLUT3 expression was reduced in both H+Ad.VEGF and H+Saline/Ad.LacZ relative to C+Saline groups (p=0.011 and p<0.001, respectively, see Figure 4.28A). Caruncular GLUT1 expression tended to be greater in both H+Ad.VEGF and C+Saline compared with H+Saline/Ad.LacZ groups (p=0.065 and p=0.085, respectively, see Figure 4.28B). Irrespective of treatment group, GLUT1 correlated with GLUT3 (r=0.735, n=57, p<0.001) within the fetal cotyledon (Figure 4.29A), however a corresponding correlation between GLUT1 and GLUT3 in the caruncle was observed for high-intake (r=0.699, n=45, p<0.001) but not for control-intake (r=0.211, n=12, p=0.511) pregnancies (Figure 4.29B). In the H+Saline/Ad.LacZ group, fetal plasma glucose concentrations at the time of necropsy demonstrated a weak negative correlation with cotyledonary GLUT1 and GLUT3 expression (r=-0.386, p=0.047; and r=-0.428, p=0.026, respectively; n=27 each). Similarly maternal plasma

glucose concentrations correlated inversely with caruncular GLUT1 (but not GLUT3) expression only in the H+Saline/Ad.LacZ group (r=-0.400, n=27, p=0.039). Of the four variables measured, only caruncular GLUT1 correlated significantly with fetal and placental weights, once again only in high-intake pregnancies treated with saline or Ad.LacZ (r=0.479, p=0.011; and r=0.462, p=0.015, respectively; n=27 each).

Table 4.14 – Placental mRNA expression of various important angiogenic factors and receptors measured separately in maternal caruncular and fetal cotyledonary tissues

Placental Compartment and Gene of Interest		**C+Saline (n=12)**	**H+Ad.VEGF (n=18)**	**H+Saline/Ad.LacZ (n=27)**	**P Value**
MATERNAL CARUNCLE (GOI: 18S)	VEGFA	27.3 ± 3.04[a]	23.7 ± 1.75[ab]	20.3 ± 1.26[b]	**0.036**
	FLT1	18.8 ± 2.26[a]	18.1 ± 2.36[a]	12.5 ± 1.36[b]	**0.031**
	KDR	23.8 ± 2.40[a]	23.2 ± 2.52[a]	17.4 ± 1.43[b]	**0.040**
	NOS3	28.6 ± 2.82	37.6 ± 3.25	33.5 ± 2.65	0.185
	FGF2	15.7 ± 1.54	13.8 ± 1.28	12.5 ± 1.15	0.280
	ANGPT1	24.0 ± 1.62	21.1 ± 1.65	20.1 ± 1.48	0.291
	ANGPT2	14.0 ± 1.17	14.7 ± 0.85	12.4 ± 0.69	0.110
	TEK	21.6 ± 2.63	22.9 ± 1.51	19.8 ± 1.33	0.370
	GUCY1B3	16.5 ± 1.52	16.2 ± 1.15	13.6 ± 0.96	0.138
FETAL COTYLEDON (GOI: 18S)	VEGFA	26.5 ± 3.53	30.6 ± 2.67	30.9 ± 2.59	0.579
	FLT1	15.1 ± 2.42	13.0 ± 1.50	14.6 ± 1.44	0.699
	KDR	17.0 ± 2.44	17.6 ± 1.59	18.4 ± 1.80	0.877
	NOS3	16.1 ± 2.17	21.5 ± 3.01	19.6 ± 1.87	0.383
	FGF2	9.9 ± 1.07	10.6 ± 0.58	11.3 ± 0.69	0.430
	ANGPT1	21.9 ± 1.64	20.9 ± 0.94	23.1 ± 0.90	0.312
	ANGPT2	13.0 ± 0.79[a]	16.0 ± 0.73[b]	16.9 ± 0.80[b]	**0.010**
	TEK	14.0 ± 0.79[a]	16.8 ± 0.71[b]	16.2 ± 0.61[b]	**0.049**
	GUCY1B3	8.9 ± 0.90	9.3 ± 0.81	8.3 ± 0.40	0.517

Abbreviations: GOI = gene of interest

Figure 4.28 – Placental expression of glucose transporters

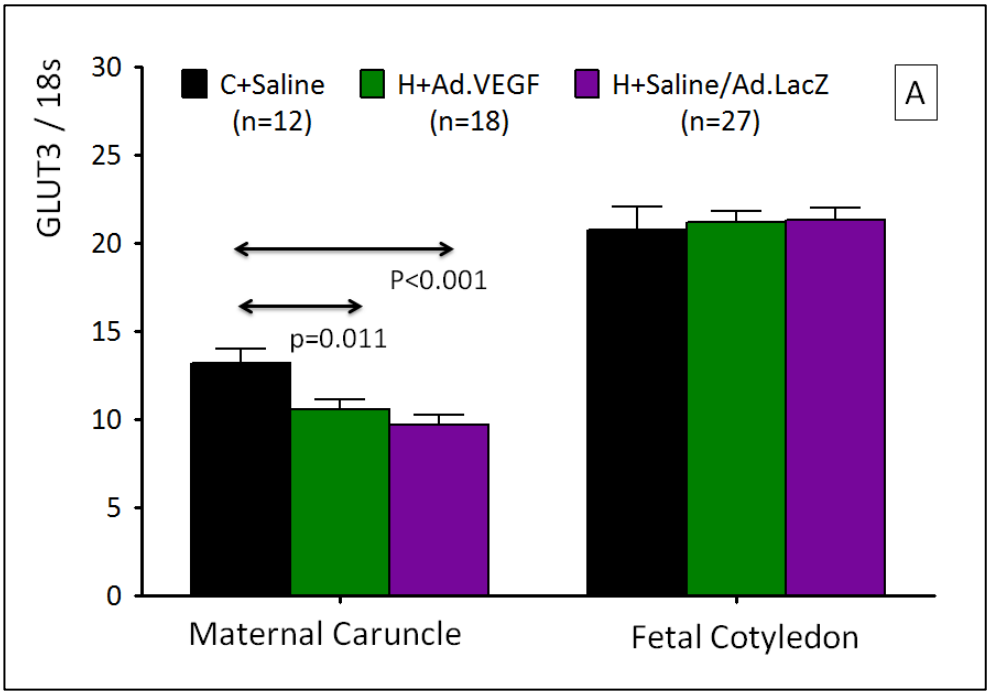

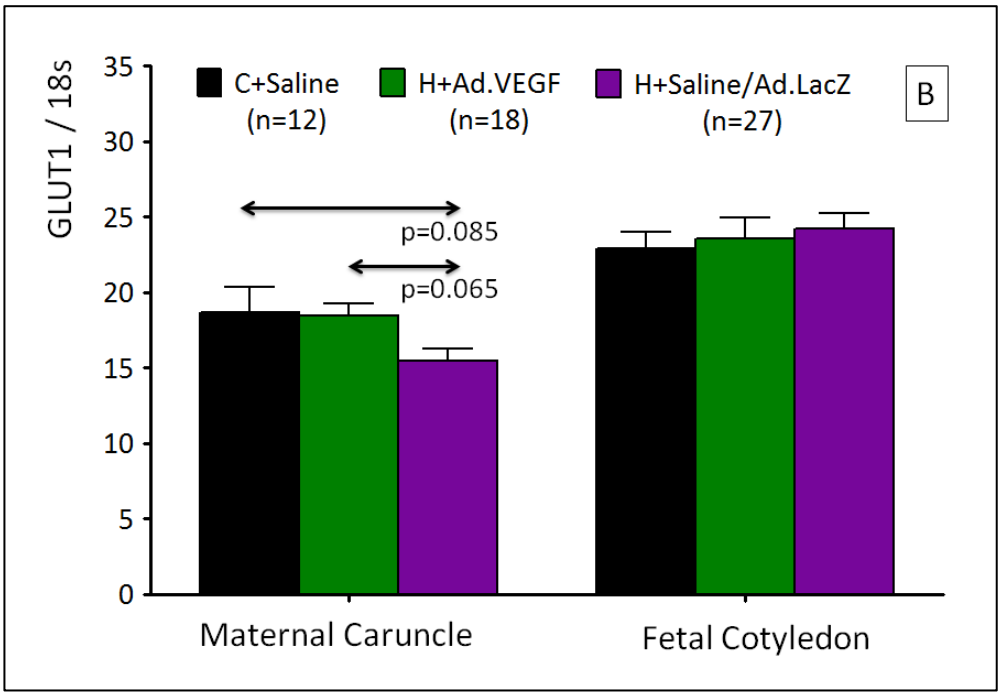

*mRNA expression of GLUT3 [A] and GLUT1 [B], measured by qRT-PCR and quantified relative to 18s content, in maternal caruncular and fetal cotyledonary tissues from late gestation necropsy (*131±0.2 days gestation*) in singleton pregnancies in adolescent ewes offered a control-intake (C) or high-intake (H) diet and receiving bilateral uterine artery injections of Ad.VEGF, Ad.LacZ or saline. P values shown are for individual post-hoc comparisons using the test of least significant difference (overall ANOVA p=0.002 and p=0.095 for figures A and B, respectively).*

Figure 4.29 – Correlations between placental mRNA expression of GLUT1 and GLUT3

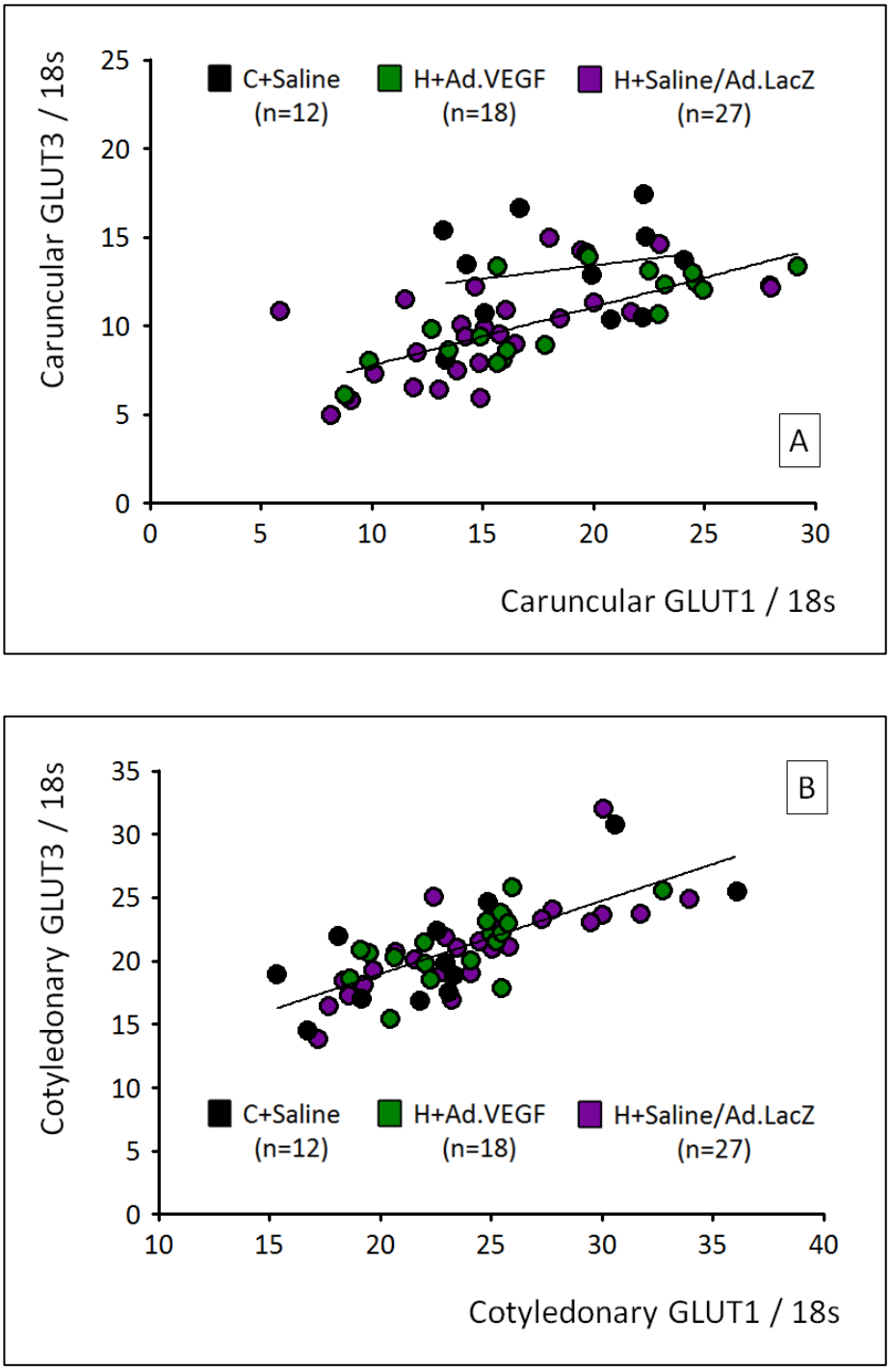

*Correlations between mRNA expression of GLUT1 and GLUT3, measured by qRT-PCR and quantified relative to 18s content, in maternal caruncular [A] and fetal cotyledonary [B] tissues from late gestation necropsy (*131±0.2 days gestation*) in singleton pregnancies in adolescent ewes offered a control-intake (C) or high-intake (H) diet and receiving bilateral uterine artery injections of Ad.VEGF, Ad.LacZ or saline. Within the caruncle, the correlation was significant in high-intake (long regression line) but not control-intake (short regression line) pregnancies.*

Table 4.15 – Correlations between four key placental angiogenic factors and receptors in the maternal caruncule and fetal cotyledon

FETAL COTYLEDON **MATERNAL CARUNCLE**

	VEGFA	FLT1	KDR		VEGFA	FLT1	KDR
VEGFA				VEGFA			
FLT1	**0.839**[a]			FLT1	**0.722**[b]		
KDR	**0.933**[a]	**0.915**[a]		KDR	**0.822**[a]	**0.803**[a]	
NOS3	**0.660**[a]	**0.461**[a]	**0.558**[a]	NOS3	**0.494**[c]	**0.402**[c]	**0.452**[c]

*Co-efficients of correlation (r values) between mRNA expression of VEGFA, FLT1, KDR and NOS3 genes measured by qRT-PCR and quantified relative to 18s content in maternal caruncular and fetal cotyledonary tissues at late gestation necropsy (*131±0.2 days gestation) *of 57 adolescent ewes offered a control-intake (C) or high-intake (H) diet and receiving bilateral uterine artery injections of Ad.VEGF, Ad.LacZ or saline in mid-pregnancy. a = correlated in every group (n=57); b = only correlated within H+Ad.VEGF and H+Saline/Ad.LacZ groups (n=45); c = only correlated in the H+Saline/Ad.LacZ group (n=27). R values for latter two are n=45 and n=27, respectively.*

4.4 Discussion

4.4.1 Ad.VEGF increased fetal growth velocity

The most important finding of this study was that Ad.VEGF treatment mid-pregnancy improves fetal growth velocity in this well-characterised ovine paradigm of FGR. This was apparent from the greater AC measurements at 3 and 4 weeks following Ad.VEGF treatment compared with inactive treatments controlling for surgical intervention ± adenoviral infection in the putatively FGR pregnancies. As explained in Chapter 3, the AC is the most sensitive ultrasound marker of longitudinal fetal growth in human and sheep pregnancies. Fetal growth was not completely normalised, given that the growth trajectories of Ad.VEGF- treated growth-restricted fetuses remained significantly below those of the normally-growing fetuses of the contemporaneous control-intake ewes. However complete normalisation of growth is: (a) likely to be unrealistic; and (b) unlikely to be necessary to achieve a significant clinical benefit (discussed in Chapter 7).

4.4.2 Ad.VEGF mitigated fetal brain sparing

As discussed in Section 1.1.3.4, uteroplacental insufficiency tends to produce an asymmetrical pattern of FGR (Cox & Marton 2009). Faced with a reduced substrate supply, the compromised fetus adapts to its poor uterine environment using a wide range of compensatory mechanisms (Peebles 2004) that serve to prioritise growth and development of important organ systems, such as the heart and brain. This so-called brain sparing effect results in a higher ultrasound BPD:AC ratio, a higher brain to liver weight ratio and a progressive redistribution of blood flow to the cerebral circulation (Mari & Deter 1992; Mari 2009). Brain sparing has generally been regarded as a benign, beneficial adaptive response mounted by the fetus to ensure adequate cerebral perfusion (Scherjon et al. 1993; Scherjon et al. 1998). However there is now a growing body of evidence that this phenomenon may actually confer an increased risk of brain injury since it is an imperfect compensation. Children born following brain sparing, reflected by an increased ratio of UA to middle cerebral artery PI, have recently been shown to have poorer neurobehavioural outcomes at 40 weeks corrected gestational age (Figueras et al. 2011) and 18 months of age (Roza et al. 2008), as well as poorer cognitive outcomes at 5 years of age (Scherjon et al. 2000). Recent studies also show that FGR fetuses with normal blood flow in the umbilical artery may have cerebral vasodilatation, and these fetuses are also at increased risk of abnormal neurodevelopment after birth (Benavides-Serralde et al. 2011). Even in mild FGR there is increased perfusion of all cerebral regions with a preferential flow to the frontal lobe, which is associated with altered neurodevelopment after birth (Cruz-Martinez et al. 2009).

In the present study, the degree of fetal brain sparing was attenuated in H+Ad.VEGF compared with H+Saline/Ad.LacZ groups, indicated by both ultrasonographic (BPD to AC ratios) and post-mortem findings. Importantly BPD measurements were not reduced, rather it was the AC that caught up to produce the fall in BPD to AC ratio. These findings suggest that the need for fetal adaptation to poor nutrient supply was reduced following Ad.VEGF treatment. Although fetal oxygenation was not measured in these sheep studies (other than venous oxygen content at birth), it might be hypothesised that oxygen delivery was improved following Ad.VEGF therapy, as hypoxia is predominantly responsible for the cardiovascular changes resulting in fetal brain sparing (Giussani et al. 2012). Accordingly, attenuated brain sparing may imply less hypoxia.

4.4.3 Ad.VEGF reduced the incidence of marked FGR

Despite the improvements in fetal growth velocity, fetal weight *per se* on a group basis was not significantly increased in Ad.VEGF-treated compared with Ad.Saline/LacZ-treated high-intake pregnancies. This likely reflects the heterogeneous response to nutritional manipulation that

occurs in this and many other sheep models of FGR. Consistently in the overnourished adolescent paradigm approximately 52% of high-intake pregnancies result in marked FGR, an accepted definition of which is a birthweight more than two standard deviations (SD) below the genetic potential (Robinson et al. 1979), which can be estimated from the contemporaneous control-intake group on a study-by-study basis. In these pregnancies fetal and placental weights are reduced by approximately 48%, whilst the remaining high-intake pregnancies (48%) produce fetuses that may be considered "non-FGR" (Wallace et al. 2004b). In the present study significantly fewer fetuses were categorised as markedly growth-restricted at necropsy following Ad.VEGF treatment ($p=0.033$) and the incidence of marked FGR in this group (28%) was considerably lower than the historical average for overnourished adolescents delivering near to term (52%).

4.4.4 Ad.VEGF attenuated disproportionate organ growth

In the present study, the restriction of fetal size induced by overnourishment of the adolescent mother was largely proportionate, as evidenced by the lack of significant differences in the relative weights of most fetal organs as well as the fetal carcass composition analysis. There were however two exceptions to this observation, namely relative fetal small intestine weight and relative fetal adrenal weight, which were both significantly increased in Saline/Ad.LacZ treated high-intake pregnancies relative to control-intake pregnancies. These findings are not new as relative weights of the adrenal glands and the empty gut have previously been shown to be higher at 134 and 128 days gestation, respectively, in fetuses of overnourished versus control-fed dams (Wallace et al. 2000; Wallace et al. 2002).

The biological significance of increased relative adrenal weight unfortunately remains unclear. Theoretically accelerated adrenal maturation in growth-restricted fetuses might be expected to result in higher levels of adrenal hormones, which help promote maturation of the fetal lung, liver and gut, and might also play a role in the initiation of parturition. However the literature in this area is conflicting and in this particular model no significant differences in fetal plasma cortisol have been measured at ~130 days gestation between high- and control-intake pregnancies (Wallace et al. 2005a) in spite of a robust reduction in gestation length in all overnourished pregnancies allowed to proceed to delivery (Wallace et al. 2006a). Furthermore when function of the hypothalamic-pituitary-adrenal axis was examined *in vivo* at various stages during postnatal life (in lambs at 9, 18 and 24 months of age) there was no obvious relationship with prenatal growth (Wallace et al. 2011). A similar increase in relative adrenal weight is observed in ovine FGR induced by single umbilical artery ligation (Supramaniam et al. 2006), uteroplacental embolisation (Murotsuki et al. 1996) and pre-mating carunclectomy

(Phillips 1996). The latter is also associated with reduced adrenal expression of phenylethanolamine *N*-methyltransferase (Adams et al. 1998) and steroidogenic acute regulatory protein (Coulter et al. 2002). With respect to the small intestine, it is well documented that relative immaturity of the gut in growth-restricted neonates places them at increased risk of necrotising enterocolitis (Halliday 2009), however it is not immediately clear what the relationship between higher relative gut weight and gut function might be in the paradigm used herein. This was the rationale behind examining for putative differences in small intestinal crypt cell proliferation in the small intestine in the present study. Notably there were no differences between control- and high-intake pregnancies in these parameters. Future work will include examination of the tissues sampled in this study for evidence of any differences in indices of mesenteric vascularity.

The novel finding herein was that Ad.VEGF treatment resulted in a significant attenuation of the disproportionate small intestine growth and tended also to mitigate the disproportionate adrenal growth seen in this model, indicated by the reduction in relative small intestine and adrenal weights in H+Ad.VEGF- versus Ad.Saline/LacZ-treated fetuses ($p=0.016$ and $p=0.058$, respectively). As these pregnancies were terminated in late gestation it is not known whether there would have been any significant correlation between relative adrenal weights and gestation length. It is also not known whether there were associated changes in the adrenal hormone levels, however given the lack of any baseline differences in cortisol by nutritional group measured previously, this appears unlikely. There was also no effect of Ad.VEGF on crypt cell proliferation.

4.4.5 Ad.VEGF increased uterine artery vascular reactivity

In the subset of animals whose UtA were examined in the organ bath, there was clear evidence of effects on *in vitro* vascular reactivity following Ad.VEGF treatment. Ad.VEGF transduced vessels demonstrated an enhanced contractile response to phenylephrine relative to Ad.LacZ/Saline treated vessels that was very similar in magnitude to vessels harvested from control-intake pregnancies. There was also a strikingly enhanced relaxation response to bradykinin relative to all other groups (David et al. 2008; Mehta et al. 2011). These results contrast with the previous work in normal sheep pregnancy in which Ad.VEGF UtA segments from normal sheep pregnancies were examined at short and long term time points: 4–7 days and 30–45 days post injection, respectively. Previously a reduced contractile response was observed in Ad.VEGF- versus Ad.LacZ-transduced vessels at both stages, whilst enhanced relaxation was apparent only in the short term. Although the interval between vector injection and analysis was similar in the long term cohort to the present study, the studies are otherwise

not directly comparable with respect to maternal genotype, age or nutritional treatment. An additional problem here was the unavoidable delay between harvesting and analysing the vessels, as the tissues had to be couriered overnight from Aberdeen, where the FGR model was based, to London, where the organ bath equipment was available. Unfortunately no suitable equipment of sufficient quality or channel size could be found in Aberdeen in order to perform the analyses locally. Samples were shipped in chilled Krebs buffer and the viability of the endothelium was checked prior to analysis in the organ bath. Nevertheless, more subtle changes in the condition of the vessel may have occurred and might have impacted the results.

The observation herein that Ad.VEGF enhanced both vasoconstriction and vasorelaxation in the organ bath would initially appear difficult to explain, and there is to my knowledge no published evidence that an intervention can have apparently opposite effects on vascular reactivity. However the fact that VEGF is believed to have a vascular protective effect and can induce prolonged endothelial cell survival (Zachary et al. 2000) may help to explain these apparently contradictory findings. The observation that Ad.VEGF-transduced vessels were significantly more contractile than Saline/Ad.LacZ-treated vessels may appear to contradict the initial hypothesis, however it is possible that this merely reflects an improvement in overall vascular function as a hangover effect of VEGF-A_{165} over-expression. The dramatically enhanced vasorelaxation that was observed is on the face of it more in keeping with the original hypothesis. The fact that no significant differences were seen between C+Saline and H+Saline/Ad.LacZ groups in relaxation may again reflect relative degradation of the vessels, particularly the endothelium, in the absence of Ad.VEGF transduction. This could have further magnified the differences seen in the H+Ad.VEGF relative to all other study groups in terms of vascular relaxation responses.

4.4.6 Ad.VEGF increased caruncular expression of VEGF receptors

At necropsy in late gestation, placental nutrient transport efficiency, as inferred from the fetal : placental weight ratio, was noted to be highest in the H+Ad.VEGF group, and was significantly greater than in the C+Saline group. There was also a significant upregulation of both VEGF receptors (FLT1 and KDR) in caruncular but not cotyledonary tissues in Ad.VEGF- versus Saline/Ad.LacZ-treated high-intake pregnancies. FLT1 and KDR are both important for vasculogenesis and angiogenesis throughout pregnancy. mRNA expression of FLT1 and KDR increases dramatically in the maternal caruncle during early sheep pregnancy (up to 30 days gestation) without any concurrent increase in VEGF expression (Grazul-Bilska et al. 2010). Endogenous VEGF expression steadily increases from 50 to 110 days gestation, after which it remains fairly static (Borowicz et al. 2007). KDR expression also peaks at 110 days gestation

but declines thereafter, whilst FLT1 expression increases progressively to 140 days gestation. The upregulation of FLT1 and KDR expression seen here was not associated with any significant change in VEGFA expression, however this is relatively unsurprising as the RT-PCR was specific for endogenous (ovine) VEGF and would not have detected any transcripts from the transgenic (human) VEGF gene. Consequently over-expression of human VEGF-A_{165} might well have led to an upregulation of FLT1 and KDR without any shift in endogenous VEGF-A. It did not seem that human VEGF down-regulated ovine VEGF however, as mean mRNA levels were intermediate in the H+Ad.VEGF group. The lack of significant changes in placental angiogenic factor/receptor expression on the fetal side of the placenta is in keeping with the absence of any effect on UA Doppler indices, which reflect fetoplacental vascular resistance. Furthermore, previous work in normal adult sheep pregnancies showed that expression of transgenic VEGF (measured using RT-PCR with primers spanning the vector-transgene boundary) was not detectable in any fetal tissues, suggesting that the adenovirus vector does not traverse the ovine placental barrier. In addition VEGF itself (the transgenic protein) is relatively large and therefore unlikely to cross the epitheliochorial placenta (Vonnahme et al. 2005).

In the present study, mRNA expression of VEGF-A, FLT1 and KDR were all reduced in untreated high- versus control-intake pregnancies. VEGF-A and FLT1 have previously been shown to be attenuated in overnourished adolescent pregnancies when measured in whole placentomes at 81 days gestation, along with ANGPT1, ANGPT2 and NOS3. The finding of reduced expression of KDR herein is novel but perhaps unsurprising given that VEGF-A, FLT1 and KDR correlated strongly with each other, irrespective of treatment group. A reduction in KDR expression may be a relatively late feature of placental vascular compromise in this paradigm. No significant differences in caruncular ANGPT1, ANGPT2 and NOS3 expression were seen herein. The lack of a persistent reduction in NOS3 expression between nutritional groups might reflect adaptative changes occurring in late pregnancy. eNOS protein expression is actually increased relative to normal controls in the near term placentae of growth-restricted sheep pregnancies induced by maternal hyperthermic exposure (Arroyo et al. 2006). Increased eNOS protein expression is also detected in the trophoblast cells of human placentae from term pregnancies complicated by FGR and pre-eclampsia (Barut et al. 2010a; Barut et al. 2010b). In addition, in the previous work in normal adult sheep pregnancies it was not considered possible to demonstrate any additional effect of Ad.VEGF on term eNOS protein levels (measured by Western blot) as expression already appeared to be maximal by this stage (Mehta et al. 2011).

In the fetal cotyledon there was an upregulation of ANGPT2 and its receptor TEK in late gestation. In a previous late gestation study using the overnourished adolescent model, there

were no significant differences between high- and control-intake pregnancies in cotyledonary mRNA expression of any angiogenic factors or receptors, although switching from a high- to a low-intake diet from 90 days gestation to induce a severe catabolic state was associated with an upregulation of cotyledonary ANGPT1, TEK, VEGFA, neuropilin 1 and hypoxia inducible factor 1 alpha subunit expression. In both situations upregulation of ANGPT and TEK probably reflects fetoplacental adaptation to an adverse intrauterine environment i.e. uteroplacental insufficiency ± metabolic stress. Like VEGF, the angiopoietins are important growth factors for physiological vasculogenesis and angiogenesis in pregnancy and are similarly upregulated during the first 28 days of ovine pregnancy (Grazul-Bilska et al. 2010; Grazul-Bilska et al. 2011). Thereafter ANGPT1 and ANGPT2 increase approximately five-fold and ten-fold, respectively, from 50 to 140 days gestation (Borowicz et al. 2007). ANGPT1 mRNA expression is consistently higher in cotyledonary compared with caruncular tissues, but the opposite is true for ANGPT2. During the course of primate pregnancy, ANGPT2 levels increase whilst ANGPT1 remain static or decrease, resulting in a lower ANGPT1:2 ratio (Babischkin et al. 2007; Hurliman et al. 2010). ANGPT2 expression appears to be sensitive to various gestational insults but the direction of shift is variable. For example, ANGPT2 expression has been shown to be increased by hypoxia in human placental explants (Zhang et al. 2001) but is decreased in the fetal cotyledon at 135 days gestation following hyperthermia-induced ovine FGR (Hagen et al. 2005). Similarly serum levels of angiopoietin-2 protein during the first trimester have been shown to be increased in pregnancies later developing pre-eclampsia (Leinonen et al. 2010) and yet decreased in those subsequently complicated by severe FGR (Wang et al. 2007). TEK expression is reduced at 135 days gestation following hyperthermic exposure in ewes (Regnault et al. 2002) and soluble TEK protein levels are reduced in human pregnancies affected by pre-eclampsia (Sung et al. 2011).

4.4.7 Ad.VEGF tended to increase caruncular expression of GLUT1

In view of the significant effect of Ad.VEGF therapy on placental FLT1/KDR mRNA expression and evidence of increased placental efficiency, expression of the glucose transporters GLUT1 and GLUT3 was evaluated separately in the maternal caruncle and fetal cotyledon to examine whether there might have been an increase in placental glucose transport capacity secondary to prenatal Ad.VEGF treatment. Caruncular GLUT1 (but not GLUT3) expression tended to be increased in Ad.VEGF- versus Ad.Lacz/Saline-treated high-intake pregnancies and was similar in magnitude to control-intake pregnancies with normally grown placentae. As for the angiogenic factors and receptors detailed above, the absence of an effect of Ad.VEGF in the fetal placental compartment is in keeping with the lack of evidence that Ad.VEGF crosses the ovine placenta.

The fact that the effects are limited to the maternal caruncle suggests downstream effects of UtA transduction on placental function with a potential increase in placental glucose transfer.

Previously no significant differences in GLUT1/GLUT3 expression were seen in high- versus control-intake pregnancies at 81 or 133 days gestation (Wallace et al. 2004a; Wallace et al. 2004b). Expression of both these transporters increases several fold between mid- and late-gestation, and is associated with a five-fold increase in placental glucose transport capacity (Molina et al. 1991). The results of the present study differed in that there was a reduction in caruncular GLUT3 expression in the overnourished dams with growth-restricted placentae and a tendency towards a similar reduction in GLUT1 in late gestation. Notably the previous experiment at 133 days gestation in this FGR model measured GLUT1/GLUT3 in whole rather than in separated placentomes, which might explain this apparent discrepancy. Currie et al. (1997) also measured these transporters in whole placentomes from normal ovine pregnancies and found that GLUT1 expression peaked around 120 days gestation, whilst GLUT3 continued to increase significantly until term. By contrast, in human pregnancy, GLUT1 expression rises steadily throughout gestation (Sakata et al. 1995) whilst GLUT3 appears to be maximal in the first trimester and declines thereafter (Brown et al. 2011). GLUT1 is reduced in high altitude pregnancies (Zamudio et al. 2006) and GLUT3 mutations are associated with FGR (Ganguly et al. 2007). Both glucose transporters are down-regulated by glucocorticoid exposure (Hahn et al. 1999), which may partially explain the detrimental effect of repeated antenatal steroids on fetal growth. GLUT1 and GLUT3 are also upregulated by moderate maternal undernutrition in ewes (Bell et al. 1999; Ma et al. 2011). This presumably represents a form of compensation for reduced maternal substrate concentrations in the maternal blood.

4.4.8 Ad.VEGF had no measurable effect on uterine blood flow

The original hypothesis for this programme of work was that increased fetal growth would occur secondary to a therapeutic increase in UBF. Surprisingly, however, in this study no impact of Ad.VEGF on UBF was detectable in the growth-restricted pregnancies despite quite obvious effects on fetal growth velocity, incidence of marked FGR and vascular reactivity, as detailed above. There are broadly speaking two possible explanations for this lack of a measurable effect on UBF. On one hand, it may be that Ad.VEGF treatment was unable to restore the putative reduction in UBF characteristic of this model and that other effects of the therapy, possibly mediated downstream at the level of the placenta, were actually responsible for the beneficial impact on fetal growth. The upregulation of VEGF receptors on the maternal side of the placenta (as discussed above) lends further credibility to this particular hypothesis. On the other hand, it may be that there was a genuine increase in UBF following Ad.VEGF

treatment but that for one or more reasons this was not detected by the telemetric monitoring system used herein. Personally I would speculate that both factors may have contributed, but on balance the telemetric flow probe system was probably not functioning optimally for a number of reasons, as detailed below.

Firstly, the fact that Ad.VEGF-transduced vessels demonstrated strikingly enhanced relaxation responses to bradykinin relative to all other groups and increased contraction relative to the H+Saline/Ad.LacZ group, perhaps due to the vasoprotective effects of VEGF, suggests that Ad.VEGF did indeed exert some effects on the function of the uterine artery, as anticipated. Secondly, the apparent variability in baseline UBF amongst the high-intake ewes in this study was 98ml/min, which is well below the 212ml/min derived from our original study and used for the power calculation. Thirdly, and most importantly, it is perhaps quite telling that, other than for a transient reduction between 94 and 96 days gestation, there were no significant differences in UBF between high- and control-intake pregnancies. This is particularly surprising given the fact that all other parameters, including fetal and placental weights, were reduced to the degree that one would expect from historical observations in this ovine paradigm of FGR. In this study we also demonstrated highly significant differences between overnourished and control-intake pregnancies in UA Doppler indices, which can be considered a reflection of resistance to umbilical blood flow. Although for technical reasons umbilical blood flow has not been directly measured at mid-gestation in this paradigm, one would expect it to be strongly correlated with UBF, as is the case in late gestation (Wallace et al. 2002). Previous studies in the overnourished adolescent paradigm have shown highly significant reductions in UBF relative to control-intake pregnancies using two different methods of measurement. When quantified using flow probes linked directly (i.e. non-telemetrically) to a flow meter, UBF was found to be reduced by 42% as early as 88 days gestation and remained reduced by 30% on average during the subsequent 50 day period (Wallace et al. 2008b). When determined using the Fick principle in chronically instrumented pregnancies at 130 days gestation (via fetal infusion of blood flow indicators and simultaneous blood sampling under steady state conditions), UBF and umbilical blood flow were attenuated by 36 and 37%, respectively, in high-intake versus control-intake pregnancies (Wallace et al. 2002). The reason for the apparent discrepancy in a key feature of this experimental paradigm is therefore unclear. Notably, the increase in flow from mid to late gestation within the normally developing control- intake pregnancies (41%) in the present study was markedly lower than the 2-fold increase reported previously in this genotype (Wallace et al. 2008b) and the 2.5- to 4.5-fold increase found by other studies in sheep (Meschia 1983), other mammals (Reynolds et al. 1986; Reynolds & Redmer 1995) and indeed in human pregnancies (Konje et al. 2003).

Taken overall, these observations imply that the telemetric system used for the present study might have lacked the required sensitivity to detect both the expected differences between nutritional groups and the impact of Ad.VEGF treatment. It was with good intention that a telemetric system was chosen for this study. Indwelling transit time flow probes are widely considered to be the gold standard for blood flow determination and have been successfully used to quantify differences between nutritional treatments in this paradigm (Wallace et al. 2008b) and to measure changes in UBF acutely following sildenafil citrate (Miller et al. 2009) and long term following Ad.VEGF administration in sheep (Mehta et al. 2011). The previous experiments assessing the short term effects of Ad.VEGF used Doppler ultrasonography to measure UBF (David et al. 2008). However, although Doppler and flow probe measurements do correlate with one another in mid-gestation sheep pregnancies (Acharya et al. 2007), this method lacks precision and can also be technically challenging (Abi-Nader et al. 2010). The use of a telemetric system was considered an advantage as it allows the ewe to behave normally during monitoring, rather than being restrained. This also constituted a refinement under the principle of the three "R"s, as promoted by the UK Home Office (Robinson 2005). However, retrospectively, this may have introduced an additional level of complexity that could have contributed to the lack of precision, although it remains unclear at which point any technical error might have been introduced. In addition to potential problems with the wireless transfer data, other possibilities include problems with data acquisition at the level of the flow probe within the animal or with the analysis. With respect to the latter, in the present study a mathematical adjustment had to be made to the raw UBF values for the majority of the animals as the equipment was not completely fit for purpose. The flow probe system used was designed to monitor up to two animals at once and each flow probe had its own 3-pin erasable programmable read only memory (EPROM) key, which was housed within the Physiogear unit. Consequently to gain accurate flow readings the unit would have had to be have been opened up and the EPROM key changed prior to each monitoring episode i.e. around 10 times per day. As the pins were extremely fragile this was not done in view of the risk of irreparably damaging the equipment. Consequently a single EPROM key was used and a mathematical conversion factor was calculated based on the calibration information for each individual flow probe following discussion with the manufacturer.

It also possible that this study lacked power, although it would not explain the lack of control- versus high-intake pregnancy differences. The assumption of a 50% increase in UBF following Ad.VEGF treatment for the purpose of sample size calculation (Section 4.2.1) was based on a previous study with a distinctly different experimental design, having compared the effects of Ad.VEGF injection into one UtA with Ad.LacZ injection into the opposite UtA of the same

animal (Mehta et al. 2011). Moreover, changes in UBF were also expressed as a percentage change from baseline values measured within the same animal using flow probes, which had been determined over 4-7 days prior to gene therapy administration. Comparing UBF with a pre-intervention baseline in this way controls for some of the inter-animal variability seen in uterine blood flow (which is known to be high) and this has been done previously (Miller et al. 1999; Miller et al. 2009). By contrast, the present study compared UBF between animals and in absolute terms. UBF was not measured in the first few days after probe placement because of the need to recover the ewes from surgery and the fact that these animals had already gone a laparotomy for embryo transfer. Adding in a third laparotomy to fit the flow probes earlier in order to measure baseline blood flow was considered excessive by the investigators and the Home Office. In addition the 50% estimation was derived from injection of both gravid and non-gravid UtA, and it has been reported that Ad.VEGF-induced increases in UBF are more dramatic within the non-gravid UtA (Mehta et al. 2011), possibly because it has undergone less vascular remodeling (Osol & Mandala 2009). In the present study flow probes were only placed around the gravid UtA in view of the cost implications of monitoring large numbers of animals concurrently, hence a potentially larger effect on the contralateral side may have been missed.

Unfortunately it was not possible to perform a retrospective power calculation based on the primary outcome measure of UBF because the baseline values and gestational increase were not believable compared with previous investigations. As detailed above the variability in UBF seen in the present study was in keeping with the assumptions of the initial power calculation, suggesting the study was not underpowered (assuming a 50% increase following UBF), hence it appears more likely that the telemetric equipment used was not working correctly. However it could also be argued that only a ~20% increase in UBF could be directly attributed to Ad.VEGF treatment in the previous experiments in normal sheep pregnancy, as the apparent doubling was relative to baseline values and not absolute blood flow (Mehta et al. 2011). In this case, based on the inter-animal variability in the present study of 98ml/min, 45 or 60 pregnancies per group would have been required to detect a 20% increase in UBF (61.2ml/min) with 80% or 90% power, respectively. With respect to the effects of Ad.VEGF on fetal growth, the sample size for the present study appears to have been sufficient when a retrospective power calculation is performed based on the secondary outcome measure of fetal weight. Based on the inter-animal variability seen in the present study of 728g, 12 to 16 animals per group were required to show a 20% increase in fetal weight (831g) with 80% or 90% power, respectively.

4.4.9 Ad.VEGF had no measurable effect on intima-to-media ratios

In the present study there was also no detectable effect of Ad.VEGF on intima-to media ratios.

This contrasted with the previous studies in normal adult sheep pregnancy, which demonstrated a reduction in IMR in Ad.VEGF- versus Ad.LacZ-transduced vessels at 30 days post-injection. This previous work differed somewhat, in that it involved comparison of one UtA with the other within the same animal, and in twin pregnancies only. Consequently the degree of variability was markedly less.

Interest in the IMR and a related parameter, intima-media thickness (IMT), largely comes from the field of cardiovascular biology and medicine. Increases in IMT occur in vasoproliferative disorders characterised by neointima formation, such as atherosclerosis. IMT can be easily measured in the carotid artery by ultrasound, in which it helps to stratify cardiovascular risk (Simon et al. 2002), although recent meta-analyses have challenged its use as a surrogate endpoint in randomised clinical trials (Goldberger et al. 2010) in favour of direct ultrasound evaluation of carotid plaque (Simon et al. 2010; Inaba et al. 2012). Atherosclerosis also occurs in the UtA and appears to reflect the degree of atherosclerosis in other critical vascular beds such as the coronary and carotid arteries. UtA IMR increases with advancing age and is associated with electrocardiographic abnormalities and elevated markers of cardiovascular risk including hypercholesterolaemia (Crawford et al. 1997). Various studies have associated intimal hyperplasia and/or increased IMR with reduced NO action via different mechanisms. Premenopausal women with intimal hyperplasia and increased IMR have been shown to have impaired cGMP production and increased arginase activity, which reduces the availability of L-arginine to NOS (Marinova et al. 2008). Increased IMR has also been linked to increased levels of endothelin-1, a potent vasoconstrictor, to higher levels of endogenous NOS inhibitors in endothelial cells (Beppu et al. 2002; Loyaga-Rendon et al. 2005), and to impaired synergism between prostaglandin I2 and NO (Obayashi et al. 1996). One study of UtA vascular reactivity in perimenopausal women found that an abnormally high IMR was associated with the failure of 17β-estradiol to augment endothelium-dependent relaxation and cAMP/cGMP production in the UtA, an effect that did occur in vessels with a normal IMR (Obayashi et al. 2001). Overall the literature would suggest that a high IMR is associated with endothelial dysfunction and an adverse cardiovascular profile. It is however unclear whether any putative arterioprotective reduction in IMR secondary to Ad.VEGF gene therapy would have any impact on long-term cardiovascular risk. It is well known that there is an association between FGR and maternal cardiovascular disease (Smith et al. 2001; Manten et al. 2007), although to what degree this represents cause and effect still remains unclear. In the present study, control-fed ewes had significantly greater intimal and medial thicknesses (with no significant change in IMR) and increased intima+media areas on image analysis when compared to overnourished animals.

This likely reflects a lack of appropriate vascular development during pregnancy in the latter group, commensurate with reduced UBF and levels of circulating sex steroids, resulting in (proportionately) smaller vessels. It seems particularly unlikely that a thicker intima in this scenario reflects any pathological process, particularly as these were adolescent ewes in good cardiovascular health prior to pregnancy.

4.4.10 Ad.VEGF had no measurable effect on adventitial neovascularisation

Previous work in normal sheep pregnancy suggested that the increase in UBF was likely to be mediated in the longer term through neovascularisation within the perivascular adventitia, as there was a significant increase in the number of positively-stained peripheral small vessels in Ad.VEGF- versus Ad.LacZ-transduced vessels (Mehta et al. 2011). This was believed to reflect a proliferation of the vasa vasorum, a network of small blood vessels that supplies oxygen and nutrients to the tunica adventitia and peripheral tunica media of larger blood vessels (Heistad et al. 1981), such as the uterine or ovarian arteries. It has been suggested that the vasa vasora might play a role in mediating increases in ovarian and uterine blood flows during the oestrus cycle and pregnancy, respectively (Zezula-Szpyra et al. 1997). The neovascularisation observed following Ad.VEGF treatment may represent a migration and reorganisation of endothelial cells into new blood vessels, as previous work using the VEGF-D isoform in normal pregnancy demonstrated a significant increase in adventitial endothelial cell proliferation at 4–7 days but not at 30 days post-injection (Mehta et al. 2013), i.e. preceding the increase in vessel numbers.

In the present study there was no significant effect of Ad.VEGF on neovascularisation within the perivascular adventitia, expressed either in absolute numbers or per unit adventitial area. Notably however there was increased neovascularisation in all three high-intake groups versus the control-intake pregnancies. This might represent an adaptive response aimed at optimising blood flow in these compromised pregnancies. This would be in keeping with the greater fetal to placental weight ratios and increased expression of TEK and ANGPT2 in the fetal compartment of the placenta (see Section 4.4.6 above) in the overnourished pregnancies. Further evidence of adaptation is provided by the previous observation that capillary number within the fetal cotyledon was increased in high- versus control-intake pregnancies when examined at 90 days (but not at 130 days) gestation (Redmer et al. 2009). Irrespective, on a background of enhanced neovascularisation secondary to a high nutritional intake it would seem intuitive that any additional effect owing to Ad.VEGF delivery might be more difficult to detect. Alternatively other mechanisms may be more important in mediating the effects of Ad.VEGF on fetal growth, such as downstream effects at the level of the placenta, possibly affecting placental vascularity or nutrient transport capacity.

4.5 Conclusions

Mid-gestation delivery of Ad.VEGF gene therapy in FGR pregnancies induced by overnourishing adolescent sheep dams resulted in a significant increase in fetal growth velocity at 3 and 4 weeks post-treatment. Despite no significant differences in overall final fetal weight, fewer fetuses exhibited marked FGR in late gestation following Ad.VEGF treatment. Moreover fetal brain sparing and disproportionate growth of the fetal adrenal and small intestine were mitigated. Ad.VEGF-transduced UtA demonstrated both increased vasoconstriction and strikingly enhanced vasorelaxation, however there was no measurable effect of Ad.VEGF on UBF, IMR or neovascularisation in the perivascular adventitia. There was however an upregulation of both VEGF receptors (FLT1 and KDR) in the maternal placental compartment, suggesting downstream effects on placental function.

5.1 Introduction

This chapter details the second of two studies aimed at evaluating the efficacy, safety and mechanism of action of Ad.VEGF gene therapy treatment in an ovine paradigm of FGR.

5.1.1 Background

During the course of the previous study a beneficial effect of Ad.VEGF on fetal growth velocity had been observed and a number of different mechanisms of action were explored. However as the pregnancies had been terminated in late gestation it was not possible to say what impact Ad.VEGF might have had on neonatal mortality and morbidity had they continued until delivery. As discussed in Section 1.1.3.6, growth-restricted neonates are at risk of a wide range of medical complications as a result of a combination of prenatal starvation, hypoxia and acidaemia, small size at birth, prematurity and the negative consequences of adaptations designed to maximise *in utero* survival at the potential expense of *ex utero* wellbeing (Halliday 2009). Consequently it was important to investigate whether prenatal Ad.VEGF treatment could mitigate such effects.

In the overnourished adolescent paradigm, lambs can be born alive from as early as 135 days gestation. Accordingly, as sheep tolerate premature delivery poorly, a significant amount of neonatal care is required to ensure survival. While the mean gestation length in the 52% of pregnancies that historically result in marked FGR is significantly shorter than the remaining 48% of overnourished pregnancies: 141.2 ±0.44 vs. 142.7±0.30 days gestation, $p<0.01$, respectively, both groups are delivered prematurely as term = 145 days gestation (Wallace et al. 2006a). In addition to the problems of prematurity, overnourishment of the adolescent ewe is associated with a ~62% reduction in colostrum yield and total immunoglobulin G (IgG) supply (Wallace et al. 2001), which is the main determinant of neonatal immunity (Hunter et al. 1977). Unlike in the human, IgG does not cross the placenta in ruminants and therefore lambs must acquire all their passive immunity via the maternal colostrum (Larson et al. 1980). It has been established that newborn lambs require 50ml good quality colostrum per kg of their body weight at birth (Logan et al. 1978), and this requirement is not met by many overnourished adolescent dams due to suboptimal mammary development. This in turn is probably related to reduced circulating oestradiol-17β levels as well as attenuated secretion of other lactogenic hormones such as placental lactogen, growth hormone and progesterone (Wallace et al.

1997a; Wallace et al. 1997b; Lea et al. 2007; Wallace et al. 2008a). Consequently, without colostrum supplementation and other supportive care measures, neonatal mortality is high. In the earliest study using this paradigm of FGR, the neonatal mortality rate was 62% (Wallace et al. 1996). In addition to assessing the impact of Ad.VEGF on the delivery process *per se* and neonatal outcomes, a second reason for including a term study with early post-natal follow-up was that, although there had been no obvious maternal or fetal adverse effects of gene therapy treatment between mid and late gestation in the previous study (see Chapter 4), it was considered necessary to follow up both mother and offspring for an extended period to exclude any indications of longer term problems. In particular it was considered that putative effects of Ad.VEGF on uterine blood flow and angiogenesis within the uteroplacental bed might confer an increased risk of post-partum haemorrhage. Consequently assessment of safety was a key aspect of this study.

As discussed in Section 1.1.3.8, there is a growing body of epidemiological and experimental evidence that FGR predisposes to a number of different metabolic diseases in later life. It is likely that this results from a combination of changes occurring *in utero* as a consequence of FGR (intrauterine programming effects) and a mismatch between the prenatal and postnatal environments (Godfrey et al. 2007), as there is considerable developmental plasticity in both fetal and neonatal life. Various factors may contribute to mismatch including the release of the fetus from the constraint of poor nutrient supply secondary to uteroplacental insufficiency at birth, programmed hyperphagia (Vickers et al. 2000) and relative calorie excess secondary to maternal lifestyle factors and/or formula feeding, which is more prevalent in growth-restricted and premature babies. Irrespective, a mismatch between the prenatal and postnatal nutrient environment is an important risk factor for metabolic disease in the human, in that catch-up growth in early postnatal life is associated with adiposity (Ibanez et al. 2008), insulin resistance (Jaquet et al. 2000) and an increased risk of cardiovascular disease (Barker et al. 2005) in later life. The early postnatal period presents an opportunity for interventions aimed at preventing the long-term morbidity associated with FGR (Hanson & Gluckman 2011).

In the overnourished adolescent sheep paradigm, the impact of the resultant FGR on postnatal growth and metabolism has been studied in young lambs up to three months of age, relative to the normally grown lambs of control-intake ewes. Following prenatal growth restriction lambs exhibit rapid catch-up growth with increased fractional growth rates to weaning, at which stage there is evidence of increased adiposity and reduced bone mineral density (BMD) measured using dual energy X-ray absorptiometry (DEXA) (Wallace et al. 2010a; Wallace et al. 2010b). At 6 weeks of age, there is an exaggerated immune response to routine vaccination, as

indicated by higher levels of the acute phase reactant serum amyloid A 24 and 48 hours later (Carr et al. 2012). At 7 weeks of age, fasting plasma levels of glucose, insulin, non-esterified fatty acids (NEFA) and glycerol are increased and plasma urea levels are decreased (Wallace et al. 2010b). For glucose, insulin and urea these represent reversals of the patterns observed in late gestation, when growth-restricted fetuses are hypoglycaemic, hypoinsulinaemic and hyperuraemic relative to normally growing fetuses (Wallace et al. 2000). Glucose-stimulated insulin secretion, given by the area under the curve (AUC) of plasma insulin over time following an intravenous glucose bolus, is increased at 7 weeks postnatal age in the prenatally growth-restricted lambs and accompanied by alterations in protein and fat metabolism, specifically increased NEFA AUC and glycerol AUC, and decreased urea AUC, respectively (Wallace et al. 2010b). Insulin AUC : glucose AUC ratios and fasting insulin : glucose ratios are both increased, suggesting relative insulin resistance (Wallace et al. 2010a). Aspects of altered metabolism and body composition, including relative obesity, persist into adulthood (JM Wallace, unpublished data) in keeping with the developmental origins of adult disease concept. It was hypothesised that prenatal Ad.VEGF gene therapy, by mitigating the degree of FGR, would reduce neonatal catch-up growth and thereby improve the metabolic profile and body composition of lambs in early postnatal life.

5.1.2 Aims

The aims of this second study were to assess the effect of prenatal Ad.VEGF gene therapy on:

- Fetal growth velocity (measured by ultrasound)
- Gestation length and the delivery process
- Lamb birth weight
- Neonatal mortality and morbidity
- Postnatal growth rates to weaning
- Inflammatory response to routine vaccination
- Metabolic responses to a standardised glucose tolerance test
- Body composition (*in vivo* using DEXA and subsequently at necropsy)

5.2 Materials and Methods

5.2.1 Experimental design

This study was predominantly designed to provide information about the efficacy and safety of Ad.VEGF as a therapy for FGR. The main outcome measure was lamb birth weight following

spontaneous delivery at term and important secondary outcome measures included assessments of fetal growth velocity (determined by serial ultrasound examination) and neonatal growth and development. A sample size calculation was performed based on a target increase in lamb birth weight of 20% following Ad.VEGF delivery in the putatively growth-restricted sheep. Assuming inter-animal variability of 607g, it was estimated that 16 animals per group would be required to detect a 20% increase in birth weight (719g) with 90% power.

Given that patterns of fetal growth following Ad.VEGF treatment relative to normally growing fetuses of control-intake ewes had been investigated in the previous study terminated in late gestation (see Chapter 4), a contemporaneous group of control-intake ewes was not included in the present experiment. A second reason for not including a non-FGR control group was that previous studies have shown that their lambs do not suffer any significant neonatal morbidity (Wallace et al. 2010). Thus in order to investigate the rate of neonatal complications or need for intervention, a direct comparison between treated and untreated FGR lambs was prioritised. As there had been no significant differences between saline- and Ad.LacZ-treated fetuses in the previous study, a single FGR control group was chosen for the present experiment (receiving saline only) to control for the effects of the laparotomy and injection procedure. Hence all ewes herein were overnourished and were allocated in mid-gestation to one of two study groups: Ad.VEGF or Saline.

5.2.2 Establishment of singleton pregnancies and nutritional management

Oestrus cycles were synchronised in 69 potential adolescent recipients and 13 potential adult donor ewes in the lead up to four separate embryo recovery and transfer days in the mid breeding season (Section 2.1.1.1). Adolescent recipients weighed 44.1±0.32 kg (mean ± SEM) and had an initial body condition score (BCS) of 2.3±0.01. Donor ewes weighed 67.7±2.20 kg with a BCS of 2.4±0.04 and were superovulated prior to undergoing laparoscopic intrauterine insemination (Section 2.1.1.2) and embryo recovery (see Section 2.1.1.3). Seven donors in total required to be flushed to provide sufficient embryos for singleton transfer into 56 recipient ewes (see Section 2.1.1.4).

Immediately following embryo transfer and throughout gestation, all adolescent ewes were overnourished (see Section 2.1.2) as per the study design. Pregnancy diagnosis was carried out by ultrasound at 45 days gestation (Section 2.1.1.5) and initially confirmed viable pregnancies in 42 of 56 ewes (overall pregnancy rate 75.0%). Two ewes subsequently reabsorbed their fetuses between day 45 and mid-gestation. The 40 ewes with ongoing pregnancies had serial venous blood samples taken at 55, 70, 85, 100, 114, 128 and 136 days gestation for

subsequent placental hormone analyses. Blood samples were taken into 10ml lithium-heparin tubes and processed as described in Section 2.2.1.

5.2.3 Ultrasound examination and gene therapy administration

At 79±0.1 days gestation all ewes underwent a baseline ultrasound examination, as described in Section 2.1.3. For the present study the following ultrasound parameters were measured: abdominal circumference (AC), renal volume (RV), deepest vertical pool (DVP) of amniotic fluid, umbilical cord diameter (UCD), placentome index and umbilical arterial (UA) Doppler indices. Head and long bone measurements (biparietal diameter (BPD), occipito-snout length (OSL), femur length (FL) and tibia length (TL)) were omitted in this cohort due to the large number of animals being scanned on any given day. Interim analysis of ultrasound data had indicated that AC and RV were the strongest markers of fetal growth (see Chapter 3 for a detailed discussion) and therefore these parameters were prioritised.

At 88±0.7 days gestation, 33 ewes underwent a midline laparotomy (as described in Section 2.1.4.2) and received bilateral uterine artery (UtA) injections of $1x10^{12}$ particles Ad.VEGF (n=17) or 10ml saline only (n=16) over 1 minute, following which each UtA was occluded for a further 4 minutes. Ewes were evenly allocated to Ad.VEGF and Saline groups on the basis of estimated fetal and placental size (values of AC, RV and placentome index) and the maternal live weight gain between embryo transfer and surgery. After allowing a full week's postoperative recovery for all ewes, serial scans were performed at approximately weekly intervals from 101±0.1 until 133±0.1 days gestation. Wounds were inspected for signs of infection or dehiscence prior to each scan and care was taken to minimise pressure from the transducer. All examinations were carried out by a single operator (David Carr), who was kept blind to the treatment administered in order to avoid any bias in the ultrasound evaluation of fetal growth.

5.2.4 Lambing

Ewes were supervised 24 hours a day 7 days a week from 135 days gestation (the earliest gestational age commensurate with live births in this FGR model) until 72 hours after the birth of the final lamb (17 days in total). Lambing was managed as per local husbandry procedures. All the lambs were delivered by one of three experienced lambers: Jacqueline Wallace, Raymond Aitken or John Milne and the rota was organised in the form of three overlapping shifts (7am to 5pm, 4pm to midnight and 10pm to 8am). David Carr assisted in a variety of roles, predominantly in the provision of neonatal care and monitoring, and assumed overall responsibility for data collection. All the team members except Jacqueline Wallace were blind to the treatment allocated at the time of surgery in order to minimise any bias in the provision

of perinatal care. An extensive protocol to maximise neonatal survival was used (see below) in view of the fact that neonatal morbidity and mortality is otherwise very high amongst lambs born to overnourished adolescent dams, particularly in relation to inadequate colostrum production, as discussed above (Wallace et al. 1996). The protocol was further developed to capture information on the interventions performed so as to provide an assessment of the degree of neonatal care needed.

5.2.4.1 Management of delivery

Ewes were regularly observed for signs of labour, which usually presented as a slowing of voluntary feed intake on the day of parturition, followed by signs of discomfort (raising of head, bleating, pawing ground etc.) with or without a show (mucus) or small vaginal bleed. Once labour was established and the cervix dilated, a digital vaginal examination was usually performed to establish fetal presentation, exclude obstruction and assess the need for assisted delivery (which is very common in primigravid and obese adolescent ewes that have been housed indoors throughout pregnancy). Malpresentation was corrected if present and appropriate traction was applied to facilitate safe delivery of the lamb. If assisted vaginal delivery was necessary, the degree of intervention was detailed in narrative form and the overall delivery was categorised as easy, average or difficult. Persistent failure of cervical dilatation or severe dystocia incompatible with vaginal delivery prompted review by a licensed veterinary surgeon, with recourse to caesarean section. Following completion of the third stage (typically 2–12 hours following birth of lamb), the placenta was carefully examined to ensure that it was complete and to identify any abnormalities such as stigmata of intrauterine infection, abnormal cotyledonary tissue or abnormal vasculature. All fetal cotyledons were dissected off the membranes, counted and weighed. The residual membrane weight was then determined and added to the cotyledon weight to give the total fetal placental weight. The degree of blood loss at delivery was assessed and categorised as average or excessive. In the event of a post-partum haemorrhage, the suspected cause (e.g. uterine atony, vaginal trauma) and any measures required to control it (e.g. use of oxytocin) were recorded. Following a difficult assisted vaginal delivery or caesarean section, maternal antibiotics (i.m. Duphapen®+Strep for at least 3 days) and analgesia in the form of flunixin (Finadyne®, Schering-Plough Animal Health) were provided.

5.2.4.2 Neonatal resuscitation

Initial condition at birth was assessed using an ABC (airway, breathing, circulation) approach. Firstly, any requirement for suctioning in order to establish a functional airway was recorded.

In particular a distinction was made between “routine” suctioning to clear maternal secretions in an otherwise potentially vigorous lamb and “extensive” suctioning to stimulate respiration and/or clear a non-patent airway in a compromised lamb. Secondly, a subjective assessment was made of breathing, which was categorised as normal or abnormally fast, slow or laboured. Thirdly, the circulation was assessed by observing the colour of the mucous membranes and palpating the anterior chest for the cardiac impulse, which was documented either as normal or obviously slow. In addition, an initial assessment of tone was made. Tone was categorised as normal, decreased (floppy) or increased (stiff, extended neck). Any additional resuscitation measures required were detailed in narrative form, e.g. mouth-to-mouth ventilation, cardiac compressions, supplementary oxygen therapy or use of respiratory stimulants such as doxapram (Dopram-V® Drops, Fort Dodge Animal Health) or etamiphylline (Millophylline-V®, Dechra Veterinary Products, Shrewsbury, Shropshire, UK).

5.2.4.3 Routine neonatal care

Once stabilised, each lamb was dried thoroughly with a warm cotton towel before being placed onto a set of scales (D-7470, Sauter, Ebingen, Germany) to measure birth weight (see Figure 5.1A). Sex and gestational age at delivery were recorded. The biparietal head diameter and abdominal girth at the level of the umbilicus were measured as described in Section 4.2.5.2. Within 10 minutes of delivery and with the lamb remaining in its mother's pen, the wool on the lamb’s neck was shaved to expose the jugular vein, from which a sample of venous blood was taken into a 2.5ml heparinised syringe using a 21 gauge needle. Fetal haemoglobin and venous blood gas parameters were determined immediately using an OSM™ 3 Hemoximeter™ (Radiometer Medical A/S, Copenhagen, Denmark). A small amount of blood was transferred into a pair of glass capillary tubes, which were subsequently sealed with non-dry putty (Brand GMBH, Wertheim, Germany) before being spun at 12000 rpm for 3 minutes in a haematocrit centrifuge (Micro Haematocrit MK-IV, Hawksley and Sons Ltd, Lancing, Sussex, UK). The haematocrit was then determined in duplicate using a tube reader. The remaining blood sample was transferred into a 5ml glass tube and processed as described in Section 2.2.1. The resultant plasma was analysed immediately for glucose and lactate (as described in Section 2.2.4.1) and then stored at –20^{o}C pending further analyses. Lambs routinely received i.m. vitamin E and selenium supplementation (0.5ml Vitesel® (Norbrook Laboratories, Newry, Co. Down, Northern Ireland, UK) and prophylactic antibiotics in the form of 0.1mg/kg s.c. enrofloxacin (Baytril®, Bayer Ltd, Newbury, Berks, UK) for a total of 5 days. The lamb’s navel was dipped in iodine to reduce the risk of infection (at birth and repeated within 12 hours).

Figure 5.1 – Routine neonatal care measures

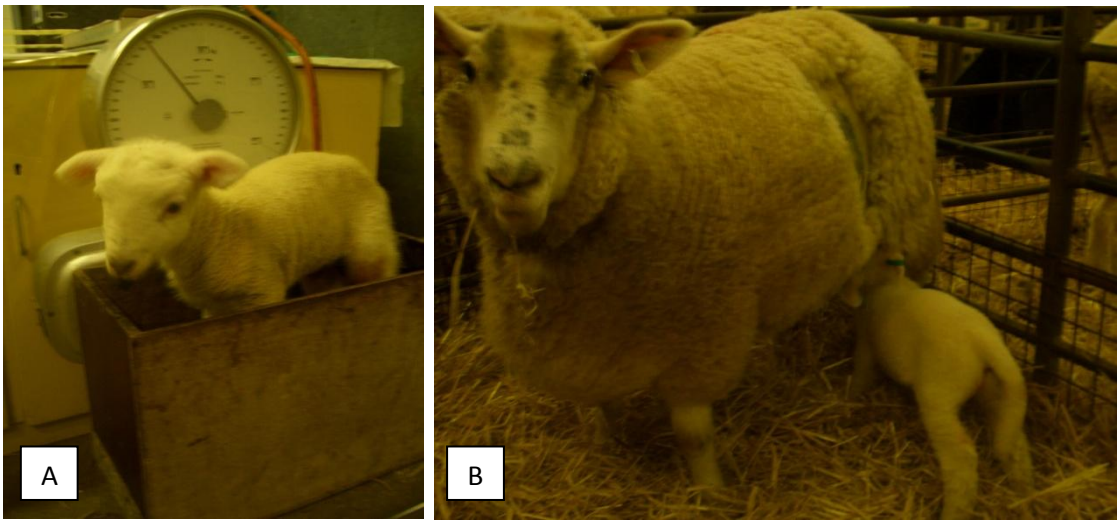

[A] Young lamb being weighed on a set of scales - this was done at regular intervals to ensure appropriate weight gain and to identify lambs requiring supplementary feeding. [B] A lamb suckling spontaneously from its mother.

Shortly after delivery 10 IU oxytocin i.v. or i.m. (Oxytocin-S®, Intervet UK Ltd) was administered to the ewe to induce milk let-down, following which the udder was completely stripped of all colostrum by hand. Colostrum was collected in a measuring jug and weighed to determine the total colostrum yield. After freezing a 40ml sample for subsequent IgG and nutrient composition analyses (see Sections 5.2.7.2 to 5.2.7.5), the remaining colostrum was filtered through a gauze to remove any obvious dirt and then fed back to the lamb at a dose of 50ml/kg using a sterilised baby bottle. A lamb feeding tube (William Daniels UK Ltd, Withernsea, East Yorkshire, UK) was used if the bottle was not tolerated (rare). Lambs born to ewes producing insufficient colostrum to meet this basic requirement were supplemented with donor colostrum, which had been collected previously and stored frozen. Donor colostrum was sourced from healthy multiparous adult ewes and pooled ahead of this study in order to standardize its nutrient and IgG content (105mg/ml). Following this initial feed, lambs were encouraged to suckle their mothers (see Figure 5.1B) and to establish demand feeding.

At one hour of age, once vital signs had stabilised following birth, a set of routine observations was performed on all lambs. The respiratory rate per minute was determined by counting the number of outward chest movements in a 15 second period and multiplying by four. The heart

rate per minute was determined by palpation of the left anterior chest over a 15 second period and multiplying by four. Core temperature was measured using a rectal thermometer (Becton Dickinson) and prior to the use of a heating lamp if this was deemed necessary (see Section 5.2.4.4). Lambs were observed at frequent intervals until they were seen to be standing independently on all four legs, at which point time to standing was documented.

Routine reviews of wellbeing for uncomplicated neonates were performed every 4 hours until 48 hours of age, and subsequently every 6 hours until 72 hours of age. Lambs were weighed at each review to confirm weight gain, an (indirect) indicator of appropriate lactation and suckling technique**.** If sleeping or lying down prior to being weighed, lambs were gently stimulated, encouraged to stand and observed for a stretch response, which is a reassuring sign of wellbeing. On returning to their mothers, lambs' suckling behaviour was observed as a further sign of appropriate establishment and functioning of the ewe lamb bond. At 24 hours of age, shoulder height was measured using a horse height measuring stick with an extending stem, folding arm and spirit level. Lambs were encouraged to stand still and in a neutral position without excessive extension or flexion of the back. Measurements were taken at the anterior shoulder and were repeated several times for accuracy. A proforma for routine lamb data collection is shown in Appendix 6. At the same time, paired maternal and lamb venous blood samples were taken into heparinised tubes and processed as described in Section 2.2.1. The resultant plasma was subsequently analysed for IgG, as described in Section 5.2.7.2.

5.2.4.4 Additional neonatal care

Any deviation from the routine schedule of care was documented in detail in narrative form, with particular care taken to document specific concerns and justification for any interventions. Lamb weight was used as the primary surveillance tool for neonatal wellbeing. Weight loss or failure of the lamb to gain weight over an 8 hour period prompted a careful review of feeding as well as consideration of other complications such as hypothermia or infection. Lambs with inadequate suckling technique, or for whom maternal milk production was insufficient, had supplementary feeding. If this was required during the first 24 hours of life, further colostrum was provided. Thereafter milk was used for all supplementary feeds and was ideally sourced by hand milking the lamb's own mother, provided lactation was adequate. Further doses of oxytocin were given if necessary to enhance milk let down and supply. If insufficient, donor milk was obtained from neighbouring ewes with milk supply in excess of their own lambs' requirements or from a commercial flock of adult ewes. As a last resort, lamb milk replacer was occasionally used to supplement feeds (SCA Shepherdess®, SCA NuTec, Dalton, North Yorkshire, UK). This formula milk consisted of 23% protein, 23% oil, 7% ash and

0.05% fibre, and provided 45000 IU vitamin A, 4000 IU vitamin D3 and 150 IU vitamin E (alpha-tocopherol) per kg. Supplementary feeds were continued for as long as necessary until the ewe lamb bond and appropriate lactation and suckling technique had been established. The number and frequency of supplementary feeds per lamb were recorded. All feeds were given by bottle unless this was not tolerated, in which case a nasogastric route was used (rare). For lambs with specific concerns, such as prematurity or poor urine output, supplementary colostrum or milk was mixed 50:50 with Energaid® (Elanco Animal Health, Basingstoke, Hampshire, UK) in order to provide energy without overloading the neonatal gut (and ultimately also the kidneys) with relatively high concentrations of fat and protein.

The most common intervention was the use of heating lamps, which were set up for a wide range of indications including concerns prior to delivery (e.g. initiation of labour at an early gestational age, very low estimated fetal weight by ultrasound) as well as neonatal concerns (e.g. poor condition at birth or evidence of hypothermia). In addition lamps were often put up in response to boisterous maternal behaviour, when the lamb was considered to be at risk of crush injury. In this specific context warmth from the heat lamp encouraged the lamb to lie in the corner of the pen, which was then wired off (see Figure 5.2A) to provide an area of relative safety. Cotton towels were provided where necessary for comfort and to confirm meconium throughput and urine output. Lambs with respiratory difficulty requiring supplementary oxygen were transferred to an intensive care area in a heated surgery, where ambient oxygen was provided from a cylinder via a face mask (see Figure 5.2B) and oxygen saturations were monitored using a portable hemoximeter unit, with the probe attached to the lamb's ear. Rectal temperature was regularly checked in any unwell lambs. Further medications were given as necessary, as dictated by the clinical condition e.g. further antibiotics (Duphapen®+Strep and/or marbofloxacin (Marbocyl®, Vetoquinol UK Ltd, Buckingham, UK)), analgesia (meloxicam or buprenorphine) and dexamethasone (Dexadreson®, Intervet UK Ltd). In the event of any persistent concerns about neonatal health, individualised advice was sought from the named veterinary surgeon.

5.2.5 Postnatal investigations

At the end of the intensive neonatal monitoring period (minimum 72 hours per lamb), lambs were weighed using CW-11 scales (Ohaus Corporation, Pine Brook, NJ, USA) initially at daily and then at weekly intervals to determine absolute and fractional postnatal growth velocity. Fractional growth velocity to weaning (%/day) were calculated by expressing the live weight gain between birth and necropsy as a proportion of lamb birth weight and dividing by the interval between birth and necropsy. Measurements of umbilical girth and shoulder height

Figure 5.2 – Additional neonatal care measures

[A] Wired off pen corner beneath a heat lamp, providing a safe area for the lamb. [B] Provision of supplementary oxygen to a lamb experiencing respiratory difficulties following a protracted labour which eventually necessitated a caesarean section.

---

were also repeated weekly. Serial blood samples were taken by jugular venepuncture into 5ml heparinised assay tubes at 7, 14, 21, 28, 35, 42, 49, 56, 63, 70 and 77 days of age for subsequent insulin and IGF1 analyses (see Section 2.2.4). An additional venous blood sample was taken into a plain (serum) tube on day 8. All samples were processed as described in Section 2.2.1. Day 8 serum samples were sent to the laboratories at the Royal Veterinary College, North Mimms, Hertfordshire, where they were analysed for serum biochemistry and liver function. The parameters reported included sodium, potassium, chloride, urea, creatinine, albumin, alanine transaminase (ALT), aspartate aminotransferase (AST), gamma-glutamyl transferase (GGT), glutamate dehydrogenase (GLDH) and alkaline phosphatase (ALP).

5.2.5.1 Immune challenge

At 58±0.4 days postnatal age, all lambs underwent routine vaccination with 2ml i.m. Heptavac P Plus® 8 in 1 Clostridial and pasteurella vaccine for sheep (Intervet UK Ltd). Venous blood was sampled into K2-EDTA (plasma) tubes immediately prior to vaccination (day 0) and at exactly 24 hours (day 1) and 48 hours (day 2) post-vaccination by jugular venepuncture and processed as described in Section 2.2.1. Individual immune responses to vaccination were investigated by measurement of the concentrations of serum amyloid A (San acute phase reactant) in these samples (see Section 5.2.7.6).

5.2.5.2 Metabolic challenge

At 68±0.5 days postnatal age, metabolic function was assessed by the measurement of various metabolite responses to a body weight specific glucose bolus, as described (Wallace et al. 2010a). By this age lambs had been handled frequently and hence were exceptionally docile. They remained with their mothers during the glucose challenge, were observed throughout and did not display any overt signs of stress or discomfort.

Glucose tolerance tests were performed in groups of three lambs per day across a seven day period. Maternal udder covers (custom-made cloth slings) were applied three hours before glucose infusion in order to prevent suckling and thereby fast the lambs. Lambs were weighed at the time of application of the udder covers. After shaving the neck fleece on both sides and cleaning the skin thoroughly with a mixture of HibiTANE® and ethanol, a 16-gauge short intravenous cannulae (Vygon, Ecouen, France) was inserted into the jugular vein on each side of the neck and secured using nonabsorbable braided silk (2.0 Mersilk®, W327H, Ethicon). Patency of the cannulae was checked bilaterally during the withdrawal of baseline blood samples at –20 and –10 minutes relative to glucose administration. Thereafter one side was designated for sampling and the other for infusion. At 0 minutes a third and final baseline sample was taken from the sampling cannula, immediately prior to the administration of 0.25mg/kg (=0.5ml/kg) sterile 50% glucose solution (Baxter Healthcare Corporation, Deerfield, IL, USA). The infusion was given steadily (at a rate of approximately 1ml every 5 seconds) and was synchronised between the 3 lambs in each group. The infusion was followed by a 5ml sterile normal saline flush. Thereafter further venous blood samples were collected at +5, +10, +15, +20, +25, +30, +45, +60, +90 and +120 minutes relative to the glucose bolus. All blood samples were taken into heparinised 5ml assay tubes and were kept on ice and processed as quickly as possible, as described in Section 2.2.1. The resultant plasma was stored at –20°C for subsequent measurement of serial concentrations of glucose (see Section 2.2.4.1), insulin (see Section 2.2.4.2), non-esterified fatty acids, glycerol and urea (Section 5.2.7.8). Udder covers were removed after the final sample was collected and a post-fasting weight was taken 15 minutes later to give an index of appetite following a total fasting period of around 5 hours.

5.2.5.3 Body composition analysis

At 74±0.4 days postnatal age, all lambs underwent a non-invasive assessment of body composition using dual-energy X-ray absorptiometry (DEXA). Lambs (and their cohabiting mothers) had their feed withheld on the morning of DEXA examination. General anaesthesia was induced and maintained using isoflurane in a mixture of oxygen and nitrous oxide. Lambs

were temporarily removed from their mothers and transported a short distance to the scanning facility on site. Lambs were then positioned prone (see Figure 5.3A) in a Norland XR-26 Mark II analyser (Norland Corporation, Fort Atkinson, WI, USA). DEXA images (see Figure 5.3B) were analysed by computer to determine bone mineral density, bone mineral content, lean mass, fat mass and percentage body fat. Three replicate scan analyses were averaged for the final results. Coefficients of variation for DEXA measurements of total body fat, lean mass and bone mineral content were 3.6%, 3.2% and 1.5%, respectively.

Figure 5.3 – Dual energy X-ray absorptiometry

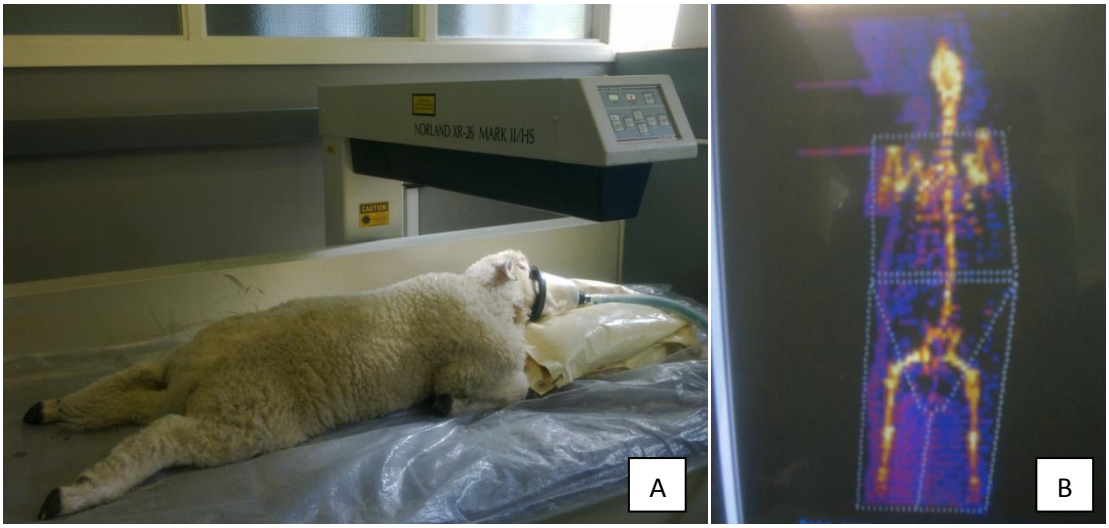

[B] Lamb anaesthetised and undergoing DEXA analysis at 11 weeks of age. [B] Representative DEXA scan image.

5.2.6 Necropsy procedures

At 83±0.2 days postnatal age, lambs were sacrificed for post-mortem analysis. On the day prior to necropsy final measurements of live weight, shoulder height and umbilical girth were made and a venous blood sample was taken for measurement of leptin (described in Section 5.2.7.7), haematocrit and haemoglobin (see Section 5.2.4.3). The following day, lambs were humanely killed using an overdose of 20ml pentobarbital sodium administered by i.v. injection into the jugular vein. Death was confirmed by the absence of corneal reflexes. Thereafter lambs were suspended by the back legs using a ceiling mounted electric hoist and exsanguinated by severing the main vessels of the neck. Blood was collected into a bucket and subsequently

weighed. Each lamb underwent a systematic post-mortem examination with careful documentation of any gross abnormalities. Samples for freezing were placed into liquid nitrogen chilled isopentane until frozen through and then stored on dry ice until the end of each necropsy, when they were transferred to –80^{o}C storage. Samples for fixing were immersed in approximately 10 times their volume of NBF or Carnoy's solution, prepared as described in Section 2.2.2. Fixed tissues were subsequently processed to the wax block stage as detailed in Section 2.2.3. A sample lamb necropsy record sheet is shown in Appendix 7. Widespread tissue sampling was carried out as described below, mainly as a precautionary measure. If Ad.VEGF treatment were to have any unexpected effects on gross organ morphology then a large tissue bank would be available for histopathological examination and additional analyses.

Firstly, the lamb's head was removed and placed into a vice by one member of the team. The skull was opened up using a saw and chisel and the brain was removed and snap-frozen whole. The underlying pituitary gland was dissected from the sella turcica and frozen in Tissue-Tek®, following which the residual head was weighed. In parallel another team member sampled the longissimus dorsi muscle for fixing and freezing. At the same time the abdomen was opened by a third team member and the pancreas was dissected out as swiftly as possible. It was weighed before being separately sampled at its hepatic and splenic ends for freezing and fixing, respectively. Next, the gastrointestinal tract was dissected out whole and laid out so that the vascular mesenteric arcade was clearly visible. The intersection of the mesenteric and ileocaecal veins was identified. From this landmark, moving in a direction away from the liver, the third mesenteric branch up the arcade was located and followed down to the intestinal wall. At this site, multiple "rings" of jejunum were excised and snap frozen. Further jejunal samples in the form of rings and rolls (rings cut along the mesenteric seem and opened up) were obtained for fixing. Half of these were immersed in NBF and half in Carnoy's solution. Next the liver was removed and weighed. A sample was taken from the right lobe for fixing, followed by generous samples from both lobes for freezing. The spleen was removed, weighed and sampled for fixing and freezing. Both kidneys were removed together with all perirenal fat, which was subsequently stripped off, weighed and sampled for fixing and freezing. The kidneys were then cut transversely and mid-section slices were fixed and frozen. The adrenal glands were removed and cut in half, one transversely and one longitudinally. Half of each adrenal was fixed and the other half frozen.

Next the fetal chest was opened and the heart was removed and weighed. The lungs were disconnected from the trachea, removed and weighed. The right lower lobe was sampled for

fixing and freezing by cutting perpendicularly to the main bronchus approximately 3cm above the inferior border of the lobe. The thymus and gonads were also removed and weighed. Finally, all four hocks were removed and weighed together. The tibia was dissected out from the front left hock and cleared of connective tissue. The length of the bone was measured using callipers and its weight determined. The residual carcass was then weighed and the weight of the lamb's blood collected in a bucket following exsanguination was recorded as an index of blood volume.

5.2.7 Laboratory measurements

5.2.7.1 Oestradiol-17β

Oestradiol-17β was extracted in duplicate from serial maternal plasma samples and measured using a double antibody radioimmunoassay technique, as described by Johnson et al. (1997).

Assay buffer solutions were first made up as follows and stored at 4°C. Phosphate buffered saline (PBS) was prepared by stirring 1.55g Na_2HPO_4, 0.224g $Na_2H_2PO_4$, 8.183g NaCl and 1.0g NaN_3 into 900ml d.H_2O, adjusting the pH to 7.3 and making up to 1 litre with d.H_20. PBS/Gel was prepared by adding 0.1g gelatin to 100ml PBS, warming and stirring until dissolved. Dextran-coated charcoal solution was prepared by adding 0.625g charcoal (Ref. C-526, Sigma Aldrich) and 0.0625g dextran (Ref. 31390, Fluka Biochemica, Buchs, Switzerland) to 100ml PBS and stirring for 2 hours. 1ml of each plasma sample was placed in a Soveril screw cap extraction tube, to which 4ml benzene (Ref. 12549, Fluka Biochemika) was added. Each tube was capped and vigorously shaken for 4 minutes before being centrifuged for 2 minutes at 1000rpm (225g) at 4°C. Under an extractor hood, the top layer of benzene (containing the extracted oestrogens) was aspirated from each tube and placed into 12x75mm borosilicate glass assay tubes (Fisherbrand®, Fisher Scientific UK Ltd, Loughborough, Leicestershire, UK). Tubes were then placed in an evaporating block (Techne DB-3), gently warmed and the solvent evaporated under a stream of air. Thereafter 100µl of PBS/Gel was added to each tube. A set of 10 standards (ranging from 0.585 to 300pg 17β-oestradiol per tube) was prepared by serial dilution of a stock solution of 17β-oestradiol (Ref. E-8875, Sigma Aldrich) using ethanol. The standard tubes were dried down and reconstituted with PBS/Gel as described above.

To begin the assay, 100µl of diluted antiserum (E2-6 #3 2-19-73, Eli Lilly & Co., Lilly Corporate Center, Indianapolis, IN, USA) at a dilution of 1:20,000 was added to each tube and to two tubes containing 100µl PBS/Gel only (for total binding). Tubes were vortexed before being incubated at 4°C for 30 minutes. Next, 100µl of a tritiated oestradiol tracer solution (NEN 2,4,6,7 3 H(N) Estradiol, Ref. NET317250UC, PerkinElmer Inc), diluted with PBS/Gel to give

12000cpm/100µl, was added to all tubes as well as to 4 additional tubes containing 200µl PBS/Gel only (2 for total counts and 2 for non-specific binding). Tubes were then incubated overnight at 4°C. The following morning 500µl cold PBS with sodium azide was added to the total count tubes, which were then capped. To all remaining tubes was added 500µl cold Dextran-coated charcoal solution, as quickly as possible. The mixture was then incubated for 10 minutes on ice before being centrifuged at 3300rpm (2250g) at 4°C for 15 minutes. The supernatant was decanted into mini scintillation vials, to which 3ml Ultima Gold™ scintillation fluid (PerkinElmer) was added. Vials were capped, shaken well to mix and then left for 3 to 4 hours. Thereafter vials were counted for 5 minutes each on a Tri-Carb 2900TR liquid scintillation analyser (Packard BioScience, Meriden, CT, USA). A calibration curve for the assay was produced following logistic transformation. The limit of sensitivity of the assay was 1pg/ml. Serial maternal plasma samples were analysed during 9 consecutive assays, each comprising samples from four animals matched according to treatment group (i.e. two from Ad.VEGF and two from Saline groups). The inter-assay coefficient of variation was 7.1% and was calculated using QC plasma samples (known concentrations of oestradiol ranging from high to low values) at the start of each assay.

5.2.7.2 Immunoglobulin G

Levels of IgG were determined in triplicate in colostrum and in paired maternal and lamb plasma samples (taken at 24 hours of life) by competitive ELISA, as previously described (Wallace et al. 2006b). A 96-well polysterene microtitre high-protein binding assay plate (Immunolon 4 HBX, Dynex Technologies, Chantilly, VA, USA) was firstly coated with purified stock ovine IgG (0.5µg/ml in a 0.05M bicarbonate buffer, Ref. I-5131, Sigma Chemical Co, St. Louis, MO, USA) and stored at 4°C for 24 hours before being washed 3 times at 2 minute intervals with a 0.05% solution of PBS/Tween (Ref. P1379, Sigma Aldrich) to remove any unbound antibody. 500µl of each colostrum sample was then transferred into an eppendorf tube and centrifuged at 12000rpm (12000g) for 5 minutes at 4°C. Test samples were pipetted from below the fat layer and diluted 1:100000 with PBS/Tween. Maternal and lamb plasma samples were diluted 1:30,000 with PBS/Tween. A set of 10 standard solutions (ranging from 0.025 to 12.5µg IgG/ml) was prepared by serial dilution of a stock solution of IgG (Ref. E-8875, Sigma Aldrich) using PBS/Tween. In a separate 96-well round-bottomed microtitre assay plate, to 120µl of each sample and 120µl of each standard solution was added 120µl of first antibody, raised in rabbit to purified sheep IgG (Ref. S-1265, Sigma Aldrich). At the same time, 240µl of PBS/Tween was added to two blank wells (for zero binding). Plates were incubated overnight at room temperature. The following day, the IgG coated assay plate was washed

three times with PBS before 200µl from each well in the round-bottomed plate was transferred to its corresponding well on the high-protein binding plate. After incubating at room temperature for 2 hours, the assay plate was once again washed three times with fresh PBS. Next 200µl of second antibody (anti-rabbit peroxidase conjugate, Ref. A-0545, Sigma Aldrich) was added to each sample and standard well, whilst 200µl of PBS/Tween was added to the two blank wells. After incubating at room temperature for a further 1 hour, the plate was washed for a final time. Next 200µl of enzyme substrate (2,2'-azino-bis(3-ethylbenzothiazoline-6-sulphonic acid) (ABTS, Ref. A-1888, Sigma Aldrich)–hydrogen peroxide (Ref. H-6520, Sigma Aldrich)) was added to each well and incubated for 30 minutes, following which 100µl 0.4M sodium fluoride (stop solution) was added. At 30 minutes optical density at 405nm was read by a multichannel spectrometer. A calibration curve for the assay was produced following logistic transformation. Intra- and inter-assay coefficients of variation (calculated from two colostrum QC samples included in each plate) were 8.2 and 13.4%, respectively.

5.2.7.3 Fat

Concentrations of butterfat were measured in duplicate in colostrum using the Soxhlet procedure after initial acid hydrolysis. In a conical flask, 2.5 to 5.0g of well-mixed colostrum was accurately weighed before being dissolved in 100ml 4M hydrochloric acid. The flask was placed onto a refluxing hotplate attached to a cold finger condenser and boiled gently for 60 minutes. Thereafter the solution was allowed to cool down to below 40°C beneath an extractor hood. A 22µm ashless filter paper (Whatman® grade 541) was folded and placed into a funnel, to which was added 1g Celite® Hyflo Super-Cel filter aid (Shengzhou Huali Diatomite Products Co. Ltd, Zhejiang, China). The contents of the flask were slowly filtered through and the flask was repeatedly washed to ensure that no residue was left behind. The filter paper was subsequently washed continuously until no acidity was detectable in the washings (using litmus paper). The above steps were repeated for each colostrum sample. Funnels and filter papers were then dried overnight at 50°C in an oven. The following day, filter papers were removed and placed into extraction thimbles. The surface of each funnel was wiped with a piece of petroleum spirit-soaked cotton wool, which was then added to the thimble, to ensure all the fat was transferred. Soxtec™ extraction cups were preheated to 50°C prior to the addition of anti-bumping granules. Thereafter cups were cooled to room temperature in a dessicator and their initial weight was determined. The thimbles (containing sample) were attached to the condensers in a Soxtec™ extraction system (Foss Analytical, Hilleroed, Denmark) and the extraction cups were inserted after addition of 40–45ml fresh petroleum spirit to each. Thimbles were extracted by boiling for 30 minutes and subsequently rinsed for

35 minutes. Thereafter condenser valves were closed to recover the solvent. Air pressure was used to remove the final traces. Extraction cups were dried at 100–103°C in an oven for 30 minutes and then placed into a dessicator to cool. Finally cups were reweighed and the butterfat concentration was calculated as the difference in weight multiplied by 100 and divided by the precise sample weight in grams. Variation between duplicates was less than 5%.

5.2.7.4 Protein

Concentrations of crude protein were measured in duplicate in colostrum using a Vario Max CN analyser. To begin, 0.7 to 0.8g of colostrum was accurately weighed out and placed into nickel crucibles. A sample of lentil peas was used as a standard/quality control. Samples were combusted at high temperatures in an oxygen-rich environment and the liberated gases passed through a series of reduction and absorption tubes by way of a helium-gas carrier. The resultant mixture of helium and nitrogen was channelled through a thermal conductivity detector to determine the volume of nitrogen present in the sample. Crude protein was then calculated by multiplying the volume of nitrogen by 6.38, which is a previously validated constant for ovine colostrum.

5.2.7.5 Lactose

Concentrations of lactose were measured in duplicate in colostrum. Samples of approximately 0.1g were accurately weighed and then made up to a total of 30g with 0.02% Brij® (polyoxyethylene (20) cetyl ether) solution (G Biosciences®, Maryland Heights, MO, USA). To 2.5ml of the diluted sample in a test tube was added 0.2ml 5% zinc sulphate and 0.2ml barium hydroxide. Tubes were centrifuged at 3000rpm for 30 seconds, following which 1ml of each supernatant was transferred to a new test tube. A set of 5 standard solutions was prepared, ranging from 10% to 80% pure lactose. To 1ml of each standard, 1ml of each sample and to 1ml water (blank) was added 2.5ml Teles' reagent (made up of 1 part phenol, 2 parts sodium hydroxide, 2 parts picric acid and 1 part sodium bisulphate). Tubes were capped and placed into a bath of boiling water for 6 minutes, following which they transferred into cold water. A further 9ml Brij® solution was added to each tube before absorbance was read at 520nm using a spectrophotometer. Lactose concentrations were calculated from absorbance readings and sample weights.

5.2.7.6 Serum amyloid A

Serum amyloid A (SAA) levels were determined in three plasma samples per lamb taken prior to and 24 and 48 hours following routine vaccination (Section 5.2.5.1) using a commercial solid

phase sandwich ELISA kit (Phase™ Range Multispecies SAA, Tridelta Development Ltd, Bray, Co. Wicklow, Ireland). 96-well microtitre assay plates coated with monoclonal antibody specific for SAA were used. To begin, 50µl of biotinylated anti-SAA antibody conjugate was added to each well. Plasma samples were diluted 1:5 (baseline samples) or 1:100–2000 (post-vaccination samples) with diluent buffer and a set of 6 standard solutions was prepared by serial dilution of SAA calibrator using diluent buffer. In duplicate, 50µl of each diluted sample or standard was added to each well and the sides of each plate were tapped gently to mix. Plates were covered with a dust cover and incubated for 1 hour at 37°C, following which the reagents were aspirated out of each well. Plates were washed 4 times with a minimum of 400µl diluted wash buffer per well. After the last aspiration, plates were tapped dry on absorbent paper. Subsequently 100µl of streptavidin horse radish peroxidise (HRP) conjugate at 1:4000 dilution was added to each well. Plates were covered again and incubated at room temperature and in the dark for 30 minutes, following which reagents were decanted. Plates were once again washed 4 times with a minimum of 400µl diluted wash buffer per well. After drying, 100µl of tetramethylbenzidine (TMB) substrate was added to each well, plates were covered again and incubated for a further 30 minutes at room temperature in the dark. Finally 50µl of stop solution was added and the absorbance in each well was read at 450nm. A calibration curve for the assay was produced following logistic transformation. Samples were analysed across 4 consecutive plates. The intra- and inter-assay coefficients of variation were both <10%.

5.2.7.7 Leptin

Leptin concentrations were determined in duplicate in pre-necropsy lamb plasma samples using a double antibody radioimmunoassay technique, as described by Marie et al. (2001). Assay buffer was first prepared by adding 0.5% bovine serum albumin to 0.05M phosphate buffer, adjusting the pH to 7.4 and storing at 4°C. Eight standard solutions (ranging from 0.195 to 25.0ng/ml) were prepared from a stock solution of recombinant ovine leptin, produced by the method of Gertler et al. (1998). On day 1 of the assay, 500µl of whole anti-serum (chicken Igγ anti-recombinant ovine leptin, Ref. C35, Genosys, Cambridge, UK) at 1:2000 dilution was added to 100µl of each standard solution or plasma sample, as well as to two tubes containing 100µl assay buffer only (for total binding). Tubes were vortexed before being incubated at room temperature for 48 hours. On day 3, 100µl of ^{125}I-Leptin tracer (prepared in house by chloramine-T iodination of leptin standard followed by purification on a Sephadex G25 column) at 12000 cpm/100µl ml was added to each tube as well as 2 empty tubes (for total counts) and 2 tubes containing 600µl assay buffer only (for non-specific binding). Tubes were vortexed before being incubated overnight at 4°C. On day 4, 500µl of the second antibody

mixture, containing goat anti-chicken whole serum antibody (Ref. A30-109, Bethyl Laboratories, Montgomery, Texas, USA) at 1:50 dilution and chicken Ig-γ, prepared in house using an EGGstract® Ig-γ purification system (Promega), at 1:300 dilution, was added to each tube. Tubes were vortexed again before being incubated for 3 days at 4°C. On day 7, 1ml cold polyethylene glycol solution was added to all tubes except the total counts. Tubes were then centrifuged at 3300 rpm (2250g) for 30 minutes at 4°C. The supernatant from each tube was decanted off and the residual pellets were counted on an automatic gamma counter (Wallac Wizard™ 1470) for 1 minute. A calibration curve for the assay was produced following logistic transformation. All the lamb samples were analysed in a single assay, for which the intra-assay coefficient of variation was 6.2%. The limit of sensitivity of the assay was 0.05ng leptin/ml.

5.2.7.8 Glycerol, urea and non-esterified fatty acids

Concentrations of glycerol, urea and non-esterified fatty acids (NEFA) were measured in 13 serial plasma samples per lamb, collected relative to a glucose bolus (see Section 5.2.5.2). Samples were processed through an automated clinical analyser (KONELAB30) using kits supplied by the manufacturer (LabMedics, Manchester, UK), which were capable of measuring plasma glycerol and NEFA levels in the ranges of 0.1–1.0 mmol/l, 2–20 mmol/l and 0–100 mmol/l, respectively.

Glycerol was first converted by glycerol kinase into glycerol-3-phosphate, which was in turn converted into dihydroxyacetone-phosphate and H_2O_2 by glycerol phosphate oxidase. H_2O_2 subsequently reacted in the presence of 3,5-dichloro-2-hydroxybenzene sulphonic acid and aminophenazone to produce n-(4-antipyrl)-3-chloro-5-sulphonate-p-benzoquinoneimine. A direct colorimetric procedure was used to determine glycerol concentrations. Urea was first hydrolysed to produce ammonia, which reacted with 2-oxyglutarate (catalysed by glutamate dehydrogenase) to form L-glutamate with oxidation of NADH to NAD. Absorbance was read at 340nm to determine urea concentrations. Free NEFA were first converted into coenzyme A (CoA) esters by CoA synthetase. Acyl-CoA was oxidised by acyl-CoA oxidase to produce hydrogen peroxide (H_2O_2), which was subsequently converted by peroxidase (POD) in the presence of 3-methyl-N-ethyl-N-beta-hydroxyethyl-aniline and 4-aminoantipyrine into a purple quinone product. Absorbance was read at 540nm to determine NEFA concentrations.

5.2.8 Statistical analyses

After checking for normality using Q-Q plots and for equality of variance using Levene's test, comparisons between the Ad.VEGF and Saline groups were made using Student's t test. Correlations were assessed using Pearson's product moment test. In postnatal life it is well

known that strong male versus female differences rapidly become apparent in a number of different biological parameters. In view of this, the General Linear Model was used in order to examine for the effect of prenatal Ad.VEGF treatment, gender and their potential interactions for all variables from birth onwards. Where significant gender differences or interactions were detected, results are presented as four groups (Ad.VEGF-M, Ad.VEGF-F, Saline-M and Saline-F) Categorical data were compared between groups using Chi squared tests.

5.3 Results

Serial ultrasound data was collected in 30 of 33 pregnancies following administration of gene therapy or saline. Three ewes (two in the Saline group and one in the Ad.VEGF group) developed hernias of their midline surgical wounds in the first post-operative week and ultrasound examinations were omitted in order to avoid placing pressure on the bowel. They otherwise remained well throughout the study and parturition was unremarkable. There was one intra-uterine death in the study (in the Saline group) which occurred at 132 days gestation in a fetus which had tracked extremely small on serial ultrasound assessment with persistently high UA Doppler indices (>2SD above mean values from 87 days to 116 days gestation). A stillborn lamb was subsequently delivered, weighing only 1496g. Full pregnancy outcome data (including blood parameters) was collected in the remaining 32 ewes, which went on to deliver live lambs between 136 and 145 days gestation. One lamb in the Ad.VEGF group was crushed by its mother and sustained 16 fractured ribs necessitating euthanasia at 27 hours of age. Full postnatal datasets (including growth, immune challenge, glucose tolerance test, DEXA and necropsy data) were collected for the surviving 31 lambs. One lamb in the Ad.VEGF group developed severe pneumonia in the eleventh week of life which required aggressive medical treatment and resulted in an acute and dramatic weight loss (5kg over a three day period). For this reason final live weight and body composition data for this particular lamb were excluded from the relevant analyses. All data are presented as mean ± SEM unless otherwise specified.

5.3.1 Baseline characteristics prior to gene therapy administration

5.3.1.1 Maternal weight and adiposity

Table 5.1 shows baseline characteristics of the two study groups at the time of embryo transfer, summarised retrospectively. There were no significant differences between groups in initial maternal live weight, adiposity score or recipient ovulation rate at the time of embryo transfer. With respect to maternal genetics, embryos derived from 5 of 7 adult donor ewes were represented in both study groups, across which there was a reasonably even spread in embryo source. Figure 5.4 illustrates the serial changes throughout gestation in maternal live

Table 5.1 – Baseline maternal characteristics at the time of embryo transfer

	Saline (n=16)	**Ad.VEGF (n=17)**	**P Value**
Live weight (kg)	43.1 ± 0.55	43.9 ± 0.42	0.239
BCS	2.3 ± 0.02	2.3 ± 0.02	0.331
Ovulation rate	2 ± 0.25	2 ± 0.35	0.330

weight and body condition score, by study group. There were no significant differences between groups in maternal weight or adiposity at any stage.

5.3.1.2 Maternal live weight gain and baseline ultrasound parameters

Table 5.2 shows the maternal live weight gain (in g/day) between embryo transfer and gene therapy administration and baseline ultrasound measurements (taken at 79±0.1 days gestation) by study group. Following even allocation of ewes to Ad.VEGF and Saline groups on the basis of TD, AC, RV, placentome index and maternal live weight gain, there were unsurprisingly no significant differences between groups in any of these parameters. In spite of randomisation for this large number of ultrasound parameters, baseline measurements of UCD and UA PI, but not RI or SDR, were retrospectively found to be significantly higher in Ad.VEGF relative to Saline groups.

5.3.2 Ultrasound parameters

5.3.2.1 Abdominal circumference

Figure 5.5A shows serial changes in fetal AC from mid to late gestation by study group. Abdominal circumference measurements were higher in Ad.VEGF relative to Saline groups at 108±0.1 days and 116±0.1 days gestation (221±2.7 vs. 211±3.5 mm, p=0.021; and 239±2.6 vs. 226±3.9 mm, p=0.013, respectively), corresponding to 21±0.8 and 28±0.7 days post treatment, respectively.

5.3.2.2 Renal volume

Figure 5.5B depicts serial measurements of fetal RV by group. Renal volume was greater in

Figure 5.4 – Changes in maternal live weight and adiposity throughout gestation

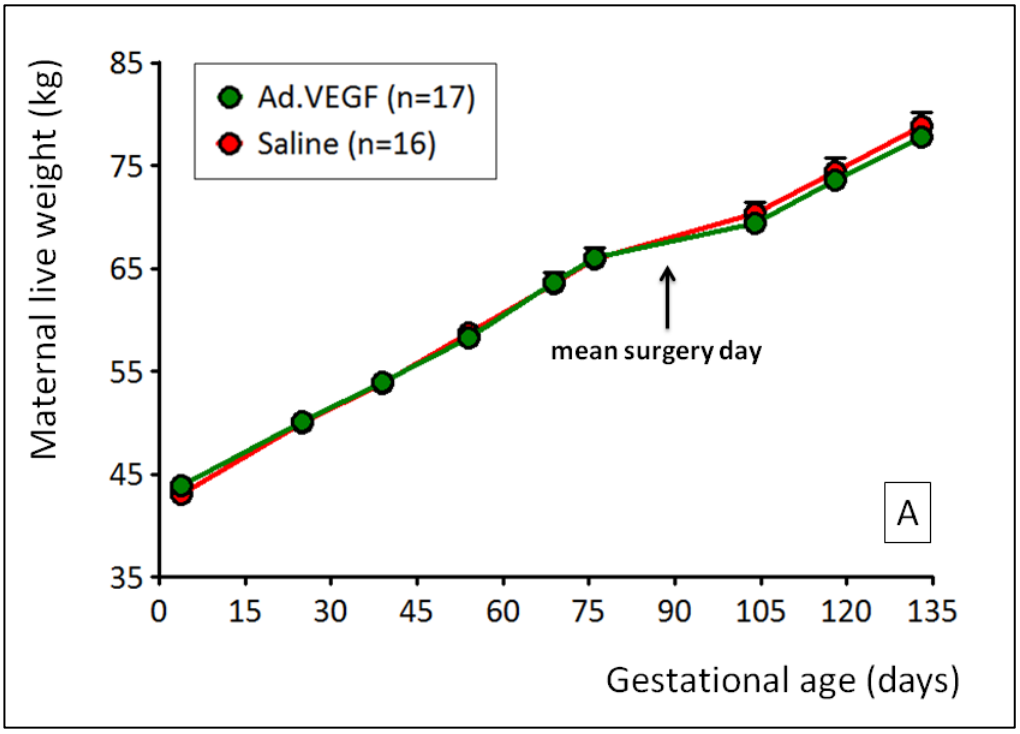

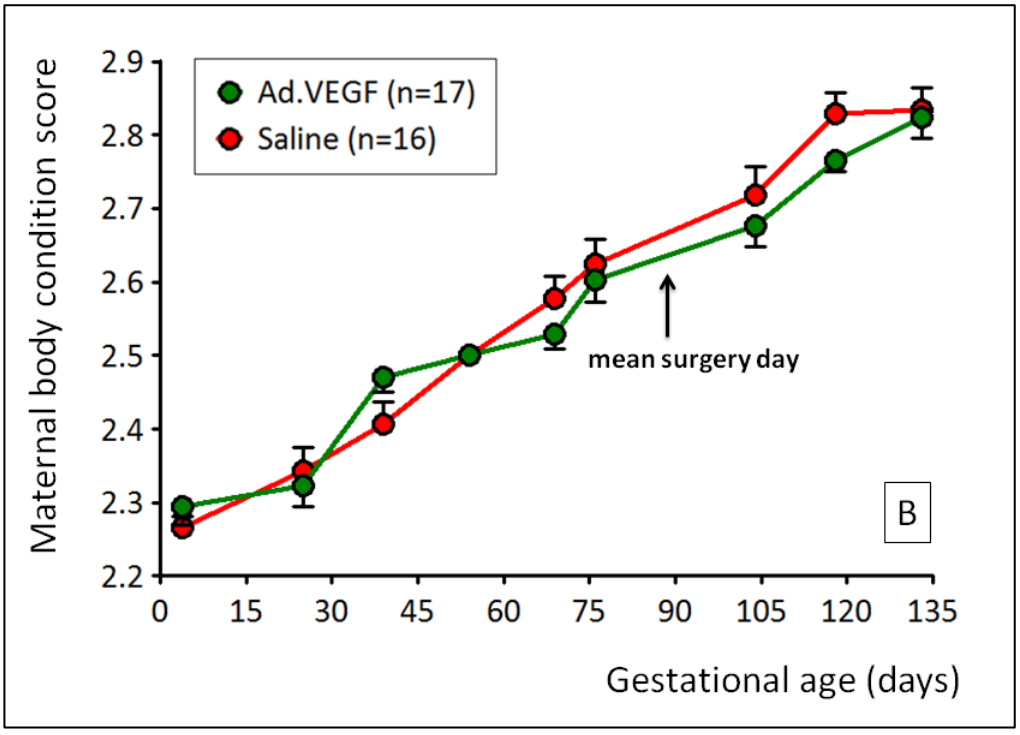

Changes in maternal live weight [A] and body condition score [B] between embryo transfer and mid-gestation in singleton-bearing adolescent dams overnourished to induce fetal growth restriction and subsequently receiving bilateral uterine artery injections of Ad.VEGF or saline.

Table 5.2 – Maternal live weight gain following embryo transfer and baseline ultrasound measurements in mid-gestation prior to gene therapy administration

	Saline (n=16)	**Ad.VEGF (n=17)**	**P Value**
Live weight gain (g/day)	317 ± 11.1	308 ± 9.1	0.495
AC (mm)	145 ± 1.4	145 ± 1.6	0.992
TD (mm)	44.4 ± 0.49	44.4 ± 0.66	0.924
RV (cm^3)	1.29 ± 0.038	1.32 ± 0.035	0.643
UA PI	1.54 ± 0.030	1.45 ± 0.028	**0.032**
UA RI	0.81 ± 0.005	0.79 ± 0.009	0.293
UA SDR	5.21 ± 0.142	4.83 ± 0.293	0.262
DVP (cm)	3.88 ± 0.106	4.23 ± 0.210	0.154
UCD (mm)	11.3 ± 0.15	11.7 ± 0.16	**0.046**
Placentome index (cm^2)	3.70 ± 0.248	3.69 ± 0.217	0.967

Ad.VEGF compared with Saline groups at 108 days and 116 days gestation (5.14±0.193 vs. 4.37±0.165 cm^3, p=0.006; and 6.38±0.224 vs. 5.60±0.280 cm^3, p=0.037, respectively). Furthermore, there remained a tendency towards higher RV in Ad.VEGF versus Saline groups at 133±0.1 days gestation (8.63±0.416 vs. 7.51±0.381 cm^3, p=0.061).

5.3.2.3 Umbilical artery Doppler indices

Figure 5.6A shows serial measurements of UA PI by study group. Values of UA PI progressively fell with advancing gestation and were attenuated in Ad.VEGF versus Saline groups at 79±0.1 days gestation, prior to gene therapy administration (see Table 5.2). Subsequently there were no significant differences except for a tendency towards decreased UA PI in Ad.VEGF relative to Saline groups at 108 days gestation (1.00±0.031 vs. 1.16±0.079, p=0.066). Figure 5.6B illustrates serial measurements of UA RI by study group. UA RI decreased with advancing

Figure 5.5 – Fetal abdominal circumference and renal volume

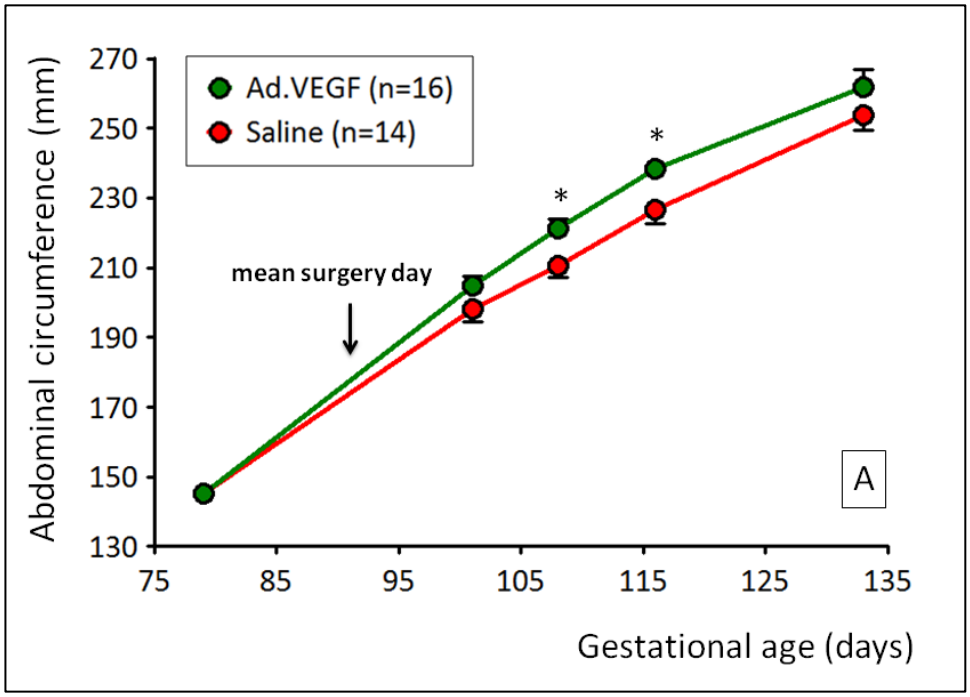

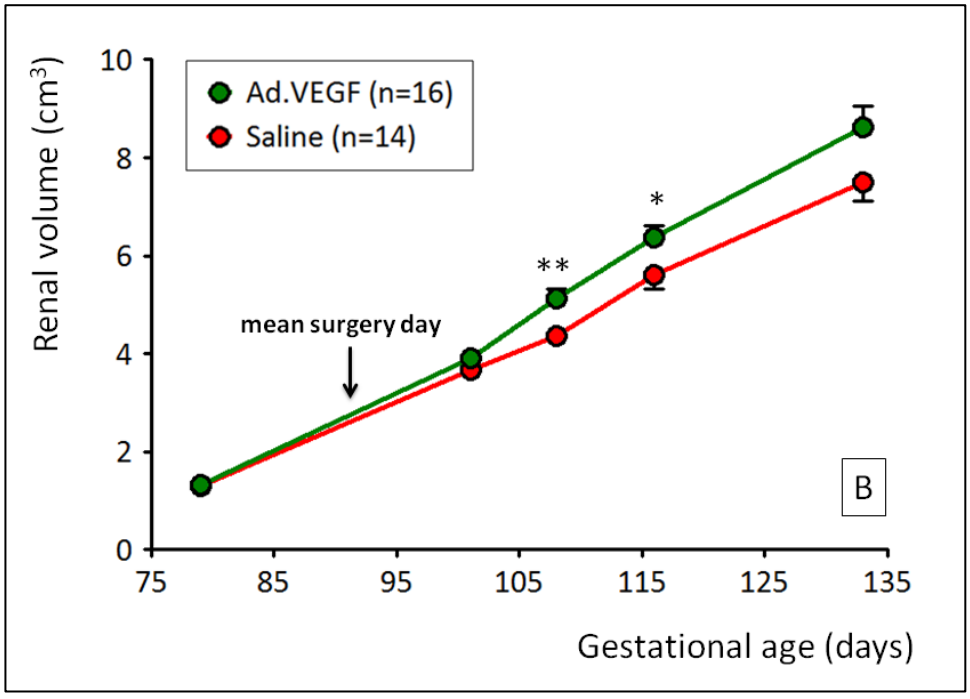

*Serial ultrasound measurements of fetal abdominal circumference [A] and renal volume [B] at regular intervals between 76±0.1 days and 133±0.3 days gestation in singleton-bearing adolescent dams overnourished to induce fetal growth restriction and receiving mid-gestation bilateral uterine artery injections of Ad.VEGF or saline. * p<0.05, ** p<0.01.*

Figure 5.6 – Umbilical artery pulsatility index and resistance index

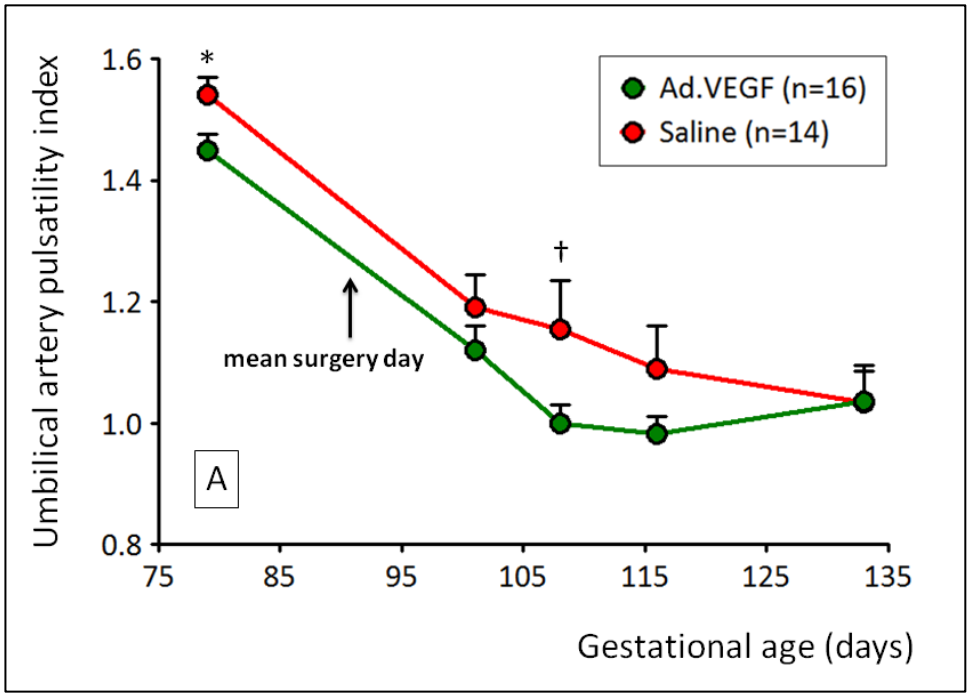

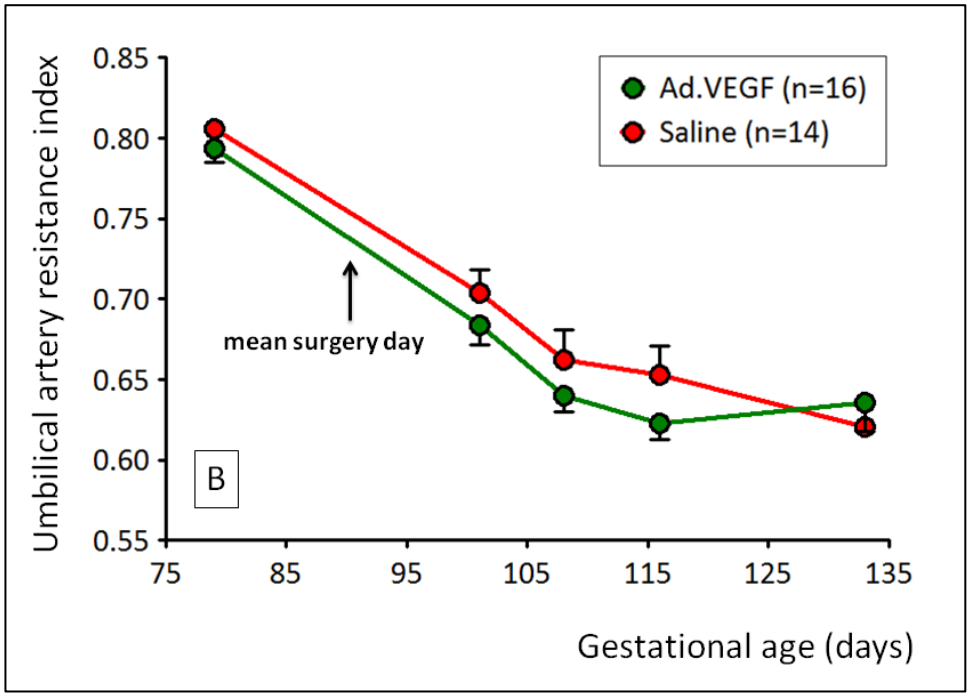

*Serial ultrasound measurements of umbilical arterial pulsatility index [A] and resistance index [B] at regular intervals between 76±0.1 days and 133±0.3 days gestation in singleton-bearing adolescent dams overnourished to induce fetal growth restriction and receiving mid-gestation bilateral uterine artery injections of Ad.VEGF or saline. † p=0.05-0.1 * p<0.05.*

gestation and there were no significant differences between groups at any stage examined. Figure 5.7A shows serial measurements of UA SDR by study group. UA SDR decreased with advancing gestation, as per other UA Doppler indices. There were no significant differences between groups at any stage of gestation. There was a tendency towards decreased UA SDR in Ad.VEGF relative to Saline groups at 108 and 116 days gestation (2.73±0.143 vs. 3.35±0.287, p=0.054; and 2.58±0.135 vs. 3.01±0.202, p=0.078, respectively).

5.3.2.4 Umbilical cord diameter

Figure 5.7B shows serial measurements of UCD by study group. The diameter of the umbilical cord was significantly higher in Ad.VEGF relative to Saline groups at baseline in mid-gestation (see Table 5.2) and at 116 days gestation (18.5±0.35 vs. 17.5±0.33 mm, p=0.042). There was a similar tendency towards an increase in Ad.VEGF versus Saline groups at all other time points, namely 101, 108 and 133 days gestation (16.0±0.33 vs. 15.0±0.33 mm, p=0.052; 17.1±0.37 vs. 16.1±0.34 mm, p=0.08; and 20.1±0.40 vs. 19.2±0.30 mm, p=0.091, respectively).

5.3.2.5 Placentome index

Figure 5.8A shows serial ultrasound assessments of placentome index by study group. Values progressively decreased in both groups with advancing gestation. Variability between animals was greater for measurements of placentome index than for fetal biometric parameters. There were no significant differences between Ad.VEGF and Saline groups at any stage of gestation. Irrespective of treatment, final time point measurements of placentome index correlated with lamb birth weight (r=0.647, n=29, p=<0.001). By contrast, placentome index correlated with total fetal placental weight in Ad.VEGF (r=0.634, n=16, p=0.008) but not Saline groups (0.264, n=11, p=0.433).

5.3.2.6 Deepest vertical pool of liquor

Figure 5.8B depicts serial measurements of DVP by group. The DVP was significantly lower in Saline compared with Ad.VEGF groups at 108 days gestation (3.61±0.226 vs. 4.25±0.185, p=0.036) and also tended to be lower at 133 days gestation in Saline versus Ad.VEGF groups (2.64±0.189 vs. 3.00±0.102, p=0.09).

5.3.3 Maternal oestradiol-17β

Figure 5.9 shows maternal plasma oestradiol-17β concentrations from early to late pregnancy. Peripheral oestradiol-17β concentrations increased with advancing gestation and were not affected by Ad.VEGF treatment. Oestradiol-17β levels tended to correlate with eventual total

Figure 5.7 – Umbilical artery systolic to diastolic ratio and umbilical cord diameter

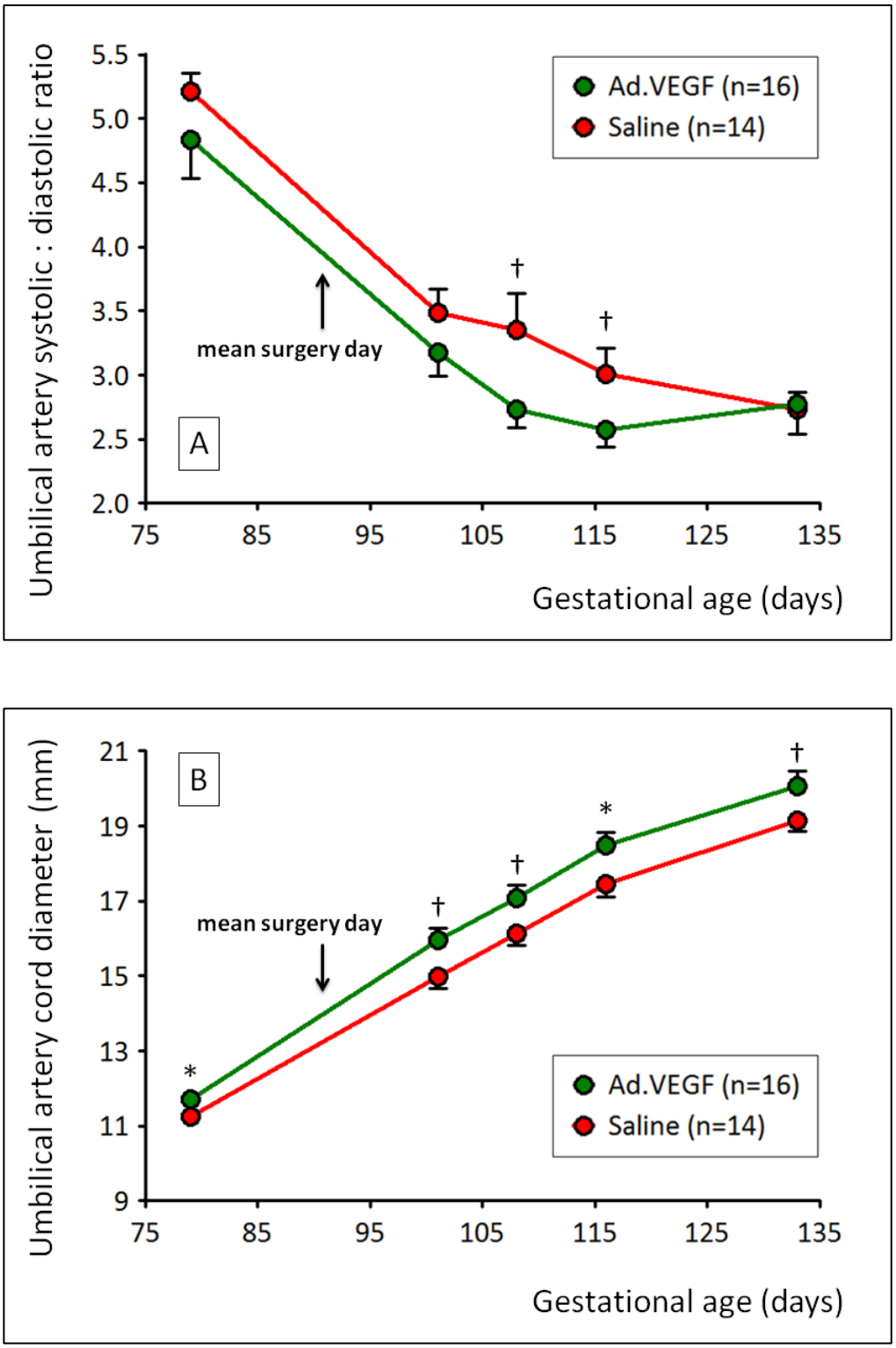

*Serial ultrasound measurements of umbilical arterial systolic to diastolic ratio [A] and umbilical cord diameter [B] at regular intervals from 76±0.1 days to 133±0.3 days gestation in singleton-bearing adolescent dams overnourished to induce fetal growth restriction and receiving mid-gestation bilateral uterine artery injections of Ad.VEGF or saline. † p=0.05-0.1 * p<0.05.*

Figure 5.8 – Placentome index and deepest vertical pool of amniotic fluid

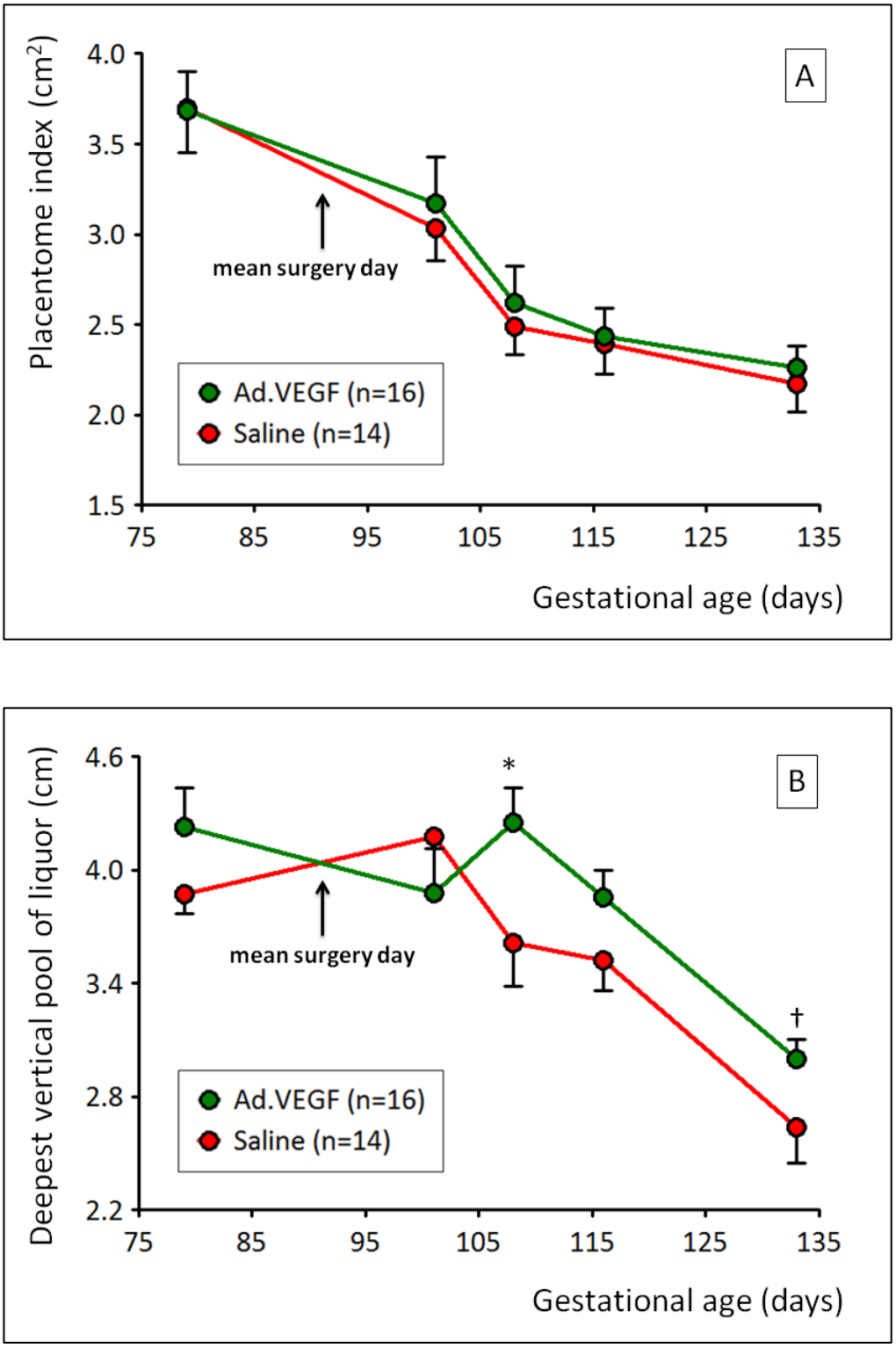

*Serial ultrasound measurements of placentome index [A] and deepest vertical pool of liquor [B] at regular intervals between 76±0.1 days and 133±0.3 days gestation in singleton-bearing adolescent dams overnourished to induce fetal growth restriction and receiving mid-gestation bilateral uterine artery injections of Ad.VEGF or saline. † p=0.05-0.1 * p<0.05*

Figure 5.9 – Oestradiol-17β in maternal plasma

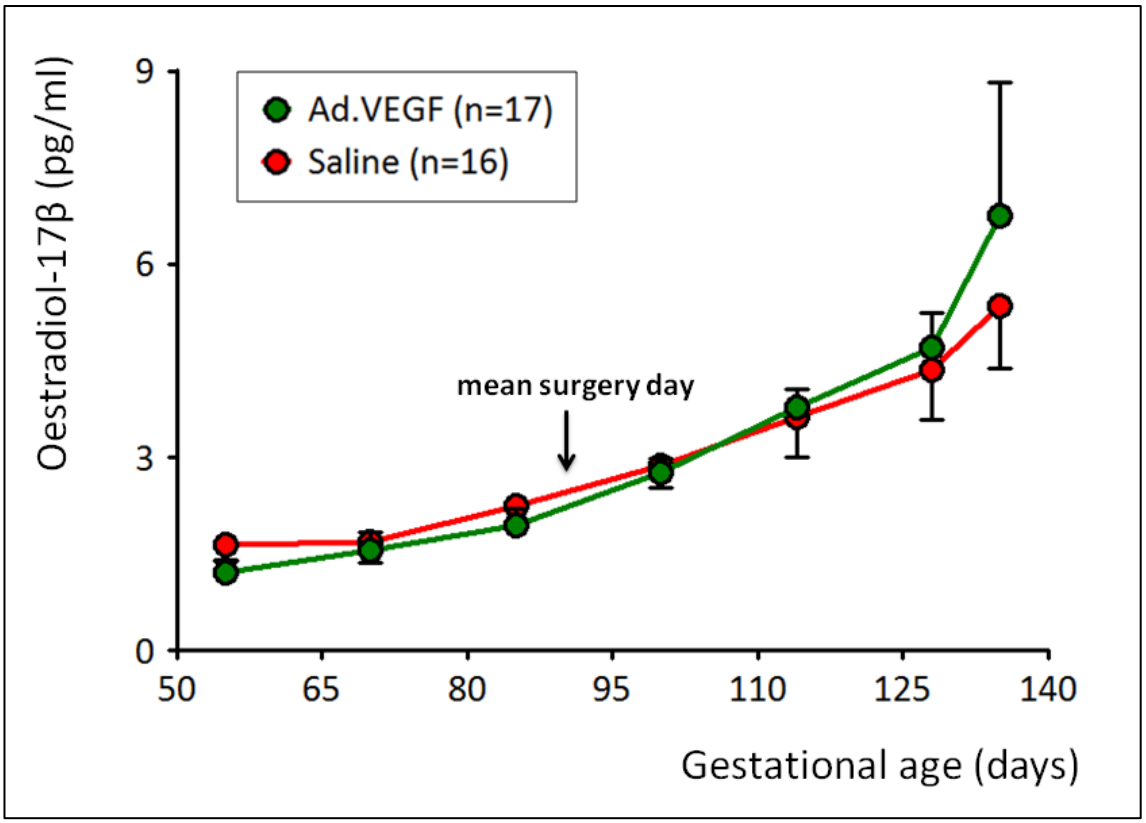

Serial concentrations of oestradiol-17β, measured in maternal plasma by radioimmunoassay, at regular intervals between 55 and 136 days gestation in singleton-bearing adolescent dams overnourished to induce fetal growth restriction and receiving mid-gestation bilateral uterine artery injections of Ad.VEGF or saline.

---

fetal placental weight at delivery from 85 days gestation onwards in the Saline group (r=0.535–0.697, n=16, p=0.012–0.073) however there appeared to be a disassociation of this relationship in the Ad.VEGF group with no significant correlations observed between these parameters. Similarly oestradiol-17β levels at 114 days gestation onwards were strongly correlated with lamb birth weight from 114, 128 and 135 days gestation, once again only in the Saline group (r=0.716-0.770, n=16, p<0.001). Gestation length and colostrum yield did not correlate significantly with oestradiol-17β levels at any stage of gestation.

5.3.4 Pregnancy outcome and early neonatal care

One ewe (in the Ad.VEGF group) had a spontaneous vaginal delivery and 2 ewes (both in the Saline group) required caesarean sections because of failure of cervical dilatation. Interestingly

the two ewes born by caesarean were the two smallest lambs in the study overall, suggesting a functional rather than a mechanical cause for dystocia. Notably the mother of the smallest lamb had a particularly low maternal plasma oestradiol level of 1.41 pg/ml (mean ± SEM = 6.09 ± 1.2 pg/ml) at 135 days gestation. The only ewe to have a lower value than this (0.29 pgl/ml at 128 days gestation) was the one who experienced a stillbirth All the other ewes had assisted vaginal deliveries and there were no differences between groups with respect to the level of difficulty (4 vs. 8 births were categorised as "easy", 12 vs. 3 "average" and 0 vs. 2 "difficult" in Ad.VEGF and Saline groups, respectively). This high frequency of intervention is not unusual when delivering obese primigravid adolescents. Estimated blood loss at all deliveries was categorised as average, with the exception of one ewe (in the Saline group) which sustained excessive blood loss secondary to a vaginal tear. There were no significant differences in the requirement for airway suctioning at delivery between Ad.VEGF and Saline groups (with 7 versus 5 lambs requiring "routine" and 1 versus 3 "extensive" suctioning, respectively). Two lambs (both in the Saline group) were noted to have abnormally slow breathing at birth, one of which also had an initially slow heart rate and poor tone. All other lambs were born in good condition.

5.3.4.1 Birth weight, gestation length and placental weight

Lamb birth weight, gestational age at delivery and placental data are presented in Table 5.3. There was a tendency towards increased birth weight and length of gestation in Ad.VEGF versus Saline groups. The number of lambs delivering on each day of gestation is illustrated as a histogram in Figure 5.10. Individual birth weights were adjusted to term gestation (145 days) using the following formula (as previously described by (Wallace et al. 2008b)): adjusted birth weight = birth weight x 1.01305 per day of gestation. Birth weights were also adjusted to the mean gestational age at delivery for the cohort as a whole, namely 142 days. The tendency towards a difference in birth weight between groups remained following correction for gestation length using either approach and birth weight was on average 18% higher in the Ad.VEGF group. There was virtually an even gender distribution within groups and for the study as a whole (17 males and 16 females in total).

Figure 5.11 shows the individual birth weight values by study group in the form of a dot plot [A] and for all lambs (irrespective of group) as a Q-Q plot [B]. These illustrate clearly that the range of birth weights in the Saline group (1496–6050g) was wider than in the Ad.VEGF group (2620–5540g) but that a normal distribution was maintained across groups. The largest lamb in this study was born to a Saline-treated ewe. It was evident that this lamb had a major impact on the statistical analysis of the birth weight data as its exclusion greatly altered the

Table 5.3 – Lamb birth weight, gestation length, gender distribution and placental weight following spontaneous delivery near term

	Saline (n=16)	**Ad.VEGF (n=17)**	**P Value**
Birth weight (g) (*range*)	3433 ± 303.3 (1496–6050)	4114 ± 230.4 (2620–5540)	0.081
Gestation length (days) (*range*)	140 ± 0.8 (132–144)	142 ± 0.4 (138–145)	0.072
Total fetal placental weight** (g) (*range*)	298 ± 20.2 (186–438)	289 ± 19.2 (164–416)	0.776
Male to female sex ratio	8 : 8	9 : 8	0.866
Membrane weight** (g)	216 ± 13.0	214 ± 13.5	0.919
Cotyledon weight* (g)	78 ± 8.7	76 ± 6.34	0.849
Cotyledon number*	81 ± 4.8	89 ± 3.4	0.203
Mean cotyledon weight (g)	0.86 ± 0.066	0.96 ± 0.100	0.372
Birth weight to placental weight ratio	13.10 ± 0.640	14.46 ± 0.419	0.074
Birth weight adjusted to 142 days (g)	3449 ± 283.6	4083 ± 226.1	0.089
Birth weight adjusted to 145 days (g)	3634 ± 298.1	4300 ± 238.1	0.089

** Total cotyledon weight and number were unavailable for 3 lambs (individual birth weights 1720, 2090 and 3080g) ** Membrane weight and therefore total placental weight were unable for a fourth fetus (1496g) – see text for explanation of missing data*

---

significance level of the birth weight difference between groups from p=0.081 to p=0.02. However, it was not valid to exclude this animal as it did not meet criteria to be an outlier and simply lay at one extreme of the normal distribution in birth weight.

In the late gestation study, the number of fetuses of overnourished mothers whose weight fell more than two standard deviations below their genetic potential was calculated on the basis

Figure 5.10 – Gestation length of pregnancies treated with Ad.VEGF or saline

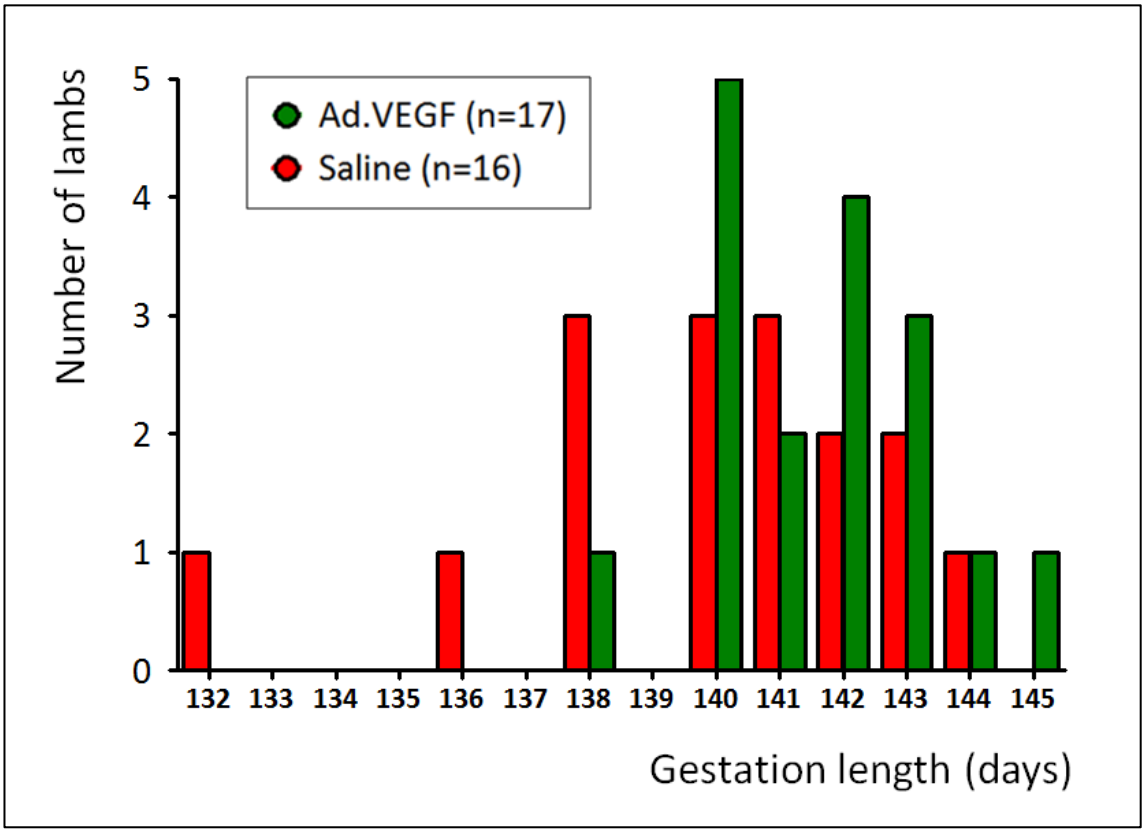

Histogram showing the number of lambs delivering per day of gestation between 132 and 145 days gestation (full term) to singleton-bearing adolescent dams overnourished to induce fetal growth restriction and receiving mid-gestation bilateral uterine artery injections of Ad.VEGF or saline. The single lamb born at 132 days gestation was stillborn and the other 32 were liveborn.

---

of the contemporaneous control-intake group mean, to give an indicator of the incidence of marked FGR. In the present study, no such control group was included. In order to estimate the effect of Ad.VEGF on rates of marked FGR a comparison was made with historical control data. The mean birthweight of 77 normally grown lambs born near term between 2005 and 2009 was 5453g, with a standard deviation of 798g, which gave a -2SD cut-off of 3857g. The proportions of fetuses weighing above and below 3857g within each group are presented in Figure 5.12. Although fewer fetuses were markedly growth-restricted in Ad.VEGF versus Saline groups (35% versus 63%, compared with historical average of 52% (Wallace et al. 2004b), this difference did not reach statistical significance (p=0.118). It is noteworthy that markedly FGR lambs had a significantly shorter gestation length than non-FGR lambs within the Saline group

Figure 5.11 – Lamb birth weight distribution

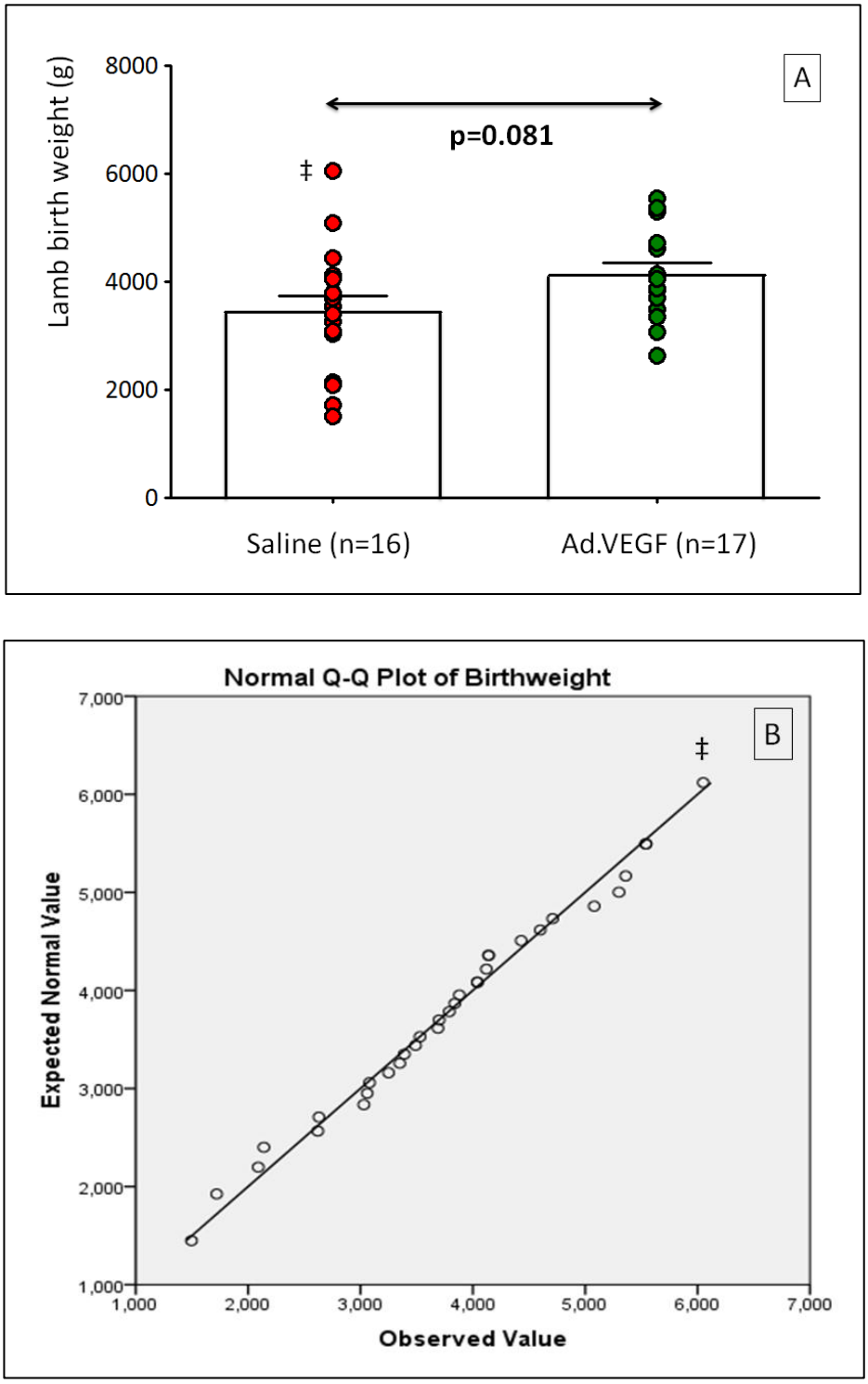

Dot plot showing individual birth weights by group [A] and Q-Q plot for all birth weights demonstrating normality of data [B] in lambs born to singleton-bearing adolescent dams overnourished to induce fetal growth restriction and receiving mid-gestation bilateral uterine artery injections of Ad.VEGF or saline. ‡ indicates a particularly large lamb with a major impact on the statistical analysis - see text for full discussion.

Figure 5.12 – Incidence of marked FGR relative to historical controls

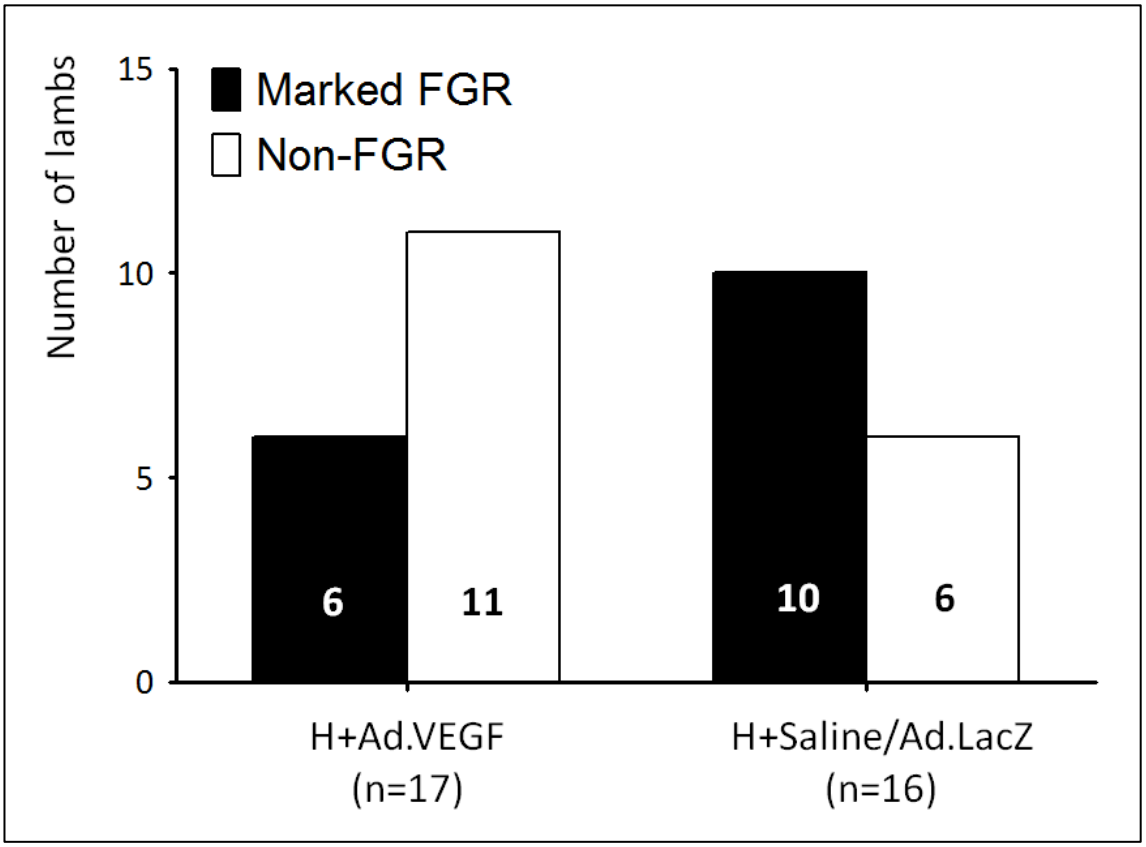

Numbers of lambs from overnourished singleton-bearing adolescent dams categorised as markedly FGR following spontaneous delivery near to term (~141 days gestation). Marked FGR was defined as a birth weight more than 2 standard deviations below the historical mean birth weight of 77 normally grown lambs of control-intake ewes (<3857g). Lambs weighing >3857g were of similar weight to normally grown controls and therefore termed "non-FGR".

(139±0.9 versus 142±0.7 days, p=0.022) but not in the Ad.VEGF group (141±0.9 versus 142±0.4 days, p=0.470) suggesting a dissociation of the usual relationship following Ad.VEGF treatment.

Placental data was unavailable from two ewes in the Saline group which underwent caesarean section (section of placenta retained) and from a third ewe (in the Ad.VEGF group) which had partially eaten her placenta before it was retrieved. Fetal cotyledon weight only was obtained for the stillborn fetus. Total fetal placental weight, its component parts (membrane and cotyledon weights), cotyledon number and mean cotyledon weight were not significantly different between groups. There was a tendency towards increased birth weight to placental

weight ratio in Ad.VEGF versus Saline groups. Irrespective of treatment group, birth weight was strongly correlated with total fetal placental weight (r=0.839, n=30, p=<0.001), membrane weight (r=0.810, n=30, p=<0.001) and cotyledon weight (r=0.812, n=30, p=<0.001). Birth weight was correlated with gestation length in the Saline group (r=0.742, n=16, p=0.001) but not in the Ad.VEGF group (r=0.212, n=17, p=0.413). The relationship between birth weight and total fetal placental weight is illustrated in Figure 5.13A. These two parameters correlated strongly in both Ad.VEGF (r=0.907, n=17, p<0.001) and Saline groups (r=0.780, n=12, p=0.003).

5.3.4.2 Lamb measurements and blood parameters at birth

Table 5.4 summarises physical measurements taken from all lambs and the results of various analyses performed on blood samples taken at birth, by study group. There was a tendency towards increased biparietal head diameter, girth at the level of the umbilicus and glucose concentrations in Ad.VEGF versus Saline groups. There were no significant differences between groups in any hormonal or haematological parameters. Birth weight was positively correlated with biparietal head diameter (r=0.845, n=33, p=<0.001), abdominal girth (r=0.954, n=33, p=<0.001) and plasma IGF-1 at birth (r=0.682, n=32, p=<0.001), irrespective of treatment group. Birth weight was strongly correlated with plasma insulin levels at birth in the Saline group (r=0.828, n=15, p=<0.001) but not in the Ad.VEGF group (r=0.008, n=17, p=0.976). Lamb birth weight and abdominal girth correlated strongly in both Ad.VEGF (r=0.941, n=17, p<0.001) and Saline groups (r=0.960, n=16, p<0.001), as illustrated in Figure 5.13B.

5.3.4.3 Routine observations within the first 24 hours of life

Table 5.5 shows the routine observations made on all lambs at one hour of age as well as time to standing, lamb shoulder height at 24 hours and the concentration of IgG in maternal and lamb blood at 24 hours of age. There were no significant differences between groups in any of these parameters.

5.3.4.4 Colostrum yield, nutrient composition and immunoglobulin G content

The total volume, nutrient and IgG content of colostrum sampled at the time of birth is shown in Table 5.6. There were no differences in colostrum yield, IgG, butterfat, lactose or protein between Ad.VEGF and Saline groups when expressed either as concentration or total content. Energy concentration per ml colostrum was determined from the concentration of butterfat using the equation [E = 32.80 F + 2.5 D + 2303.3] as previously described by Brett et al. (1972) where E = energy concentration (kJ/kg), F = butterfat concentration (g/kg) and D = day of lactation (=1 for all colostrum samples). Total energy concentration and total energy content

Figure 5.13 – Birth weight versus placental weight and abdominal girth

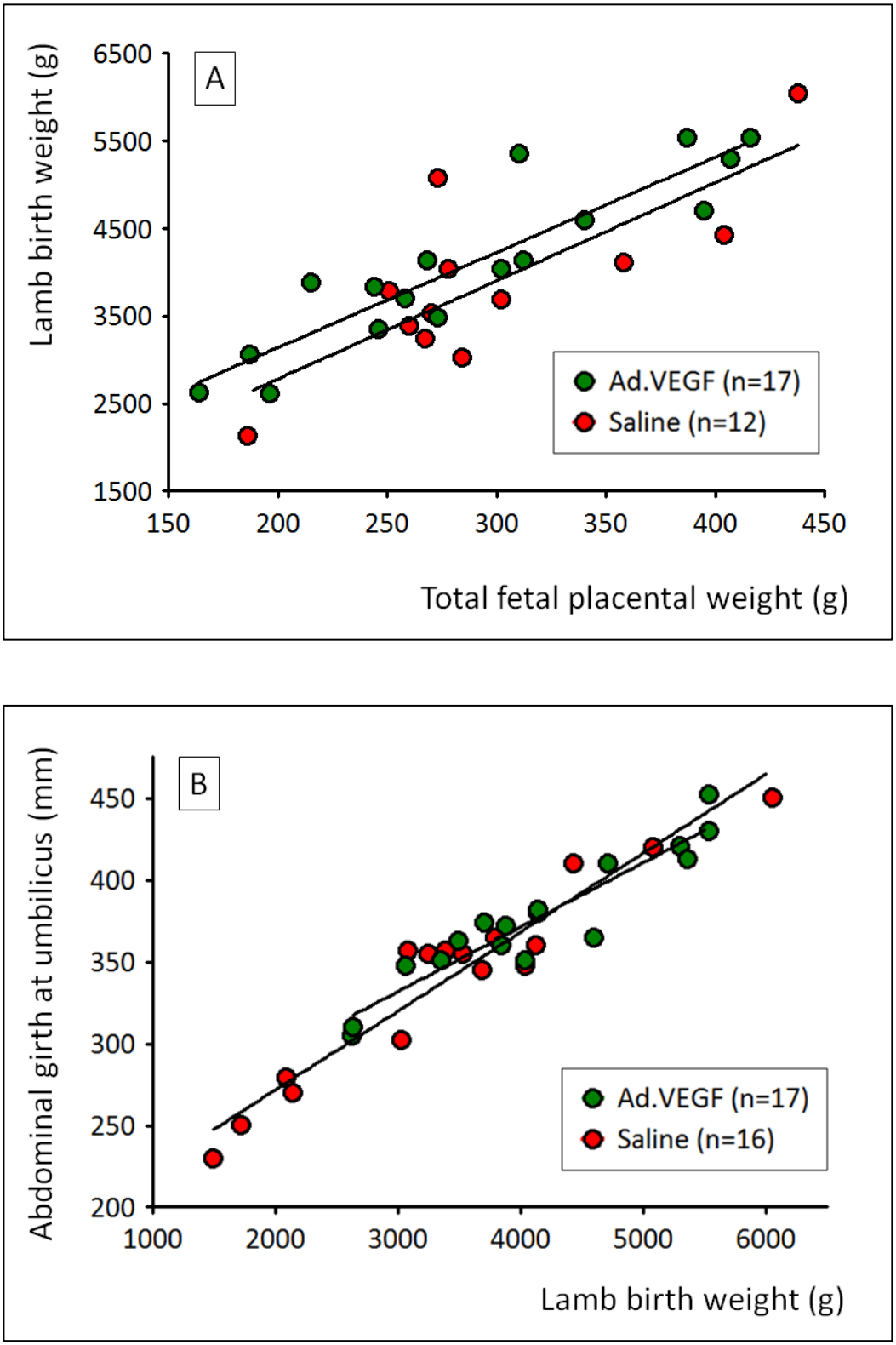

Scattergrams of total fetal placental weight and lamb birth weight [A] and birth weight versus girth at the level of the umbilicus [B], respectively. Placental data was unavailable for 4 lambs (birth weights 1496, 1720, 2090 and 3080g). Correlations coefficients are detailed in the text.

Table 5.4 – Metabolic, haematological and venous blood gas parameters in birth plasma samples and physical measurements of lambs taken immediately after birth

	Saline (n=15)	**Ad.VEGF (n=17)**	**P Value**
Biparietal head diameter (mm)	63.6 ± 1.72	67.4 ± 1.17	0.072
Abdominal girth (mm)	341 ± 15.3	376 ± 9.6	0.059
Glucose (mg/dl)	38.04 ± 4.125	51.44 ± 6.020	0.089
Lactate (mmol/l)	6.49 ± 0.528	7.82 ± 0.607	0.116
Insulin (ng/ml)	0.461 ± 0.0667	0.440 ± 0.0472	0.788
IGF-1 (ng/ml)	0.122 ± 0.0151	0.147 ± 0.0171	0.287
Haematocrit (%)	44.96 ± 1.249	44.09 ± 1.609	0.681
Haemoglobin (g/dl)	13.53 ± 0.383	13.32 ± 0.438	0.733
Methaemoglobin (g/dl)	1.83 ± 0.056	1.84 ± 0.043	0.857
Carboxyhaemoglobin (g/dl)	3.56 ± 0.106	3.49 ± 0.113	0.632
Venous oxygen saturation (%)	48.89 ± 3.400	47.37 ± 2.712	0.726
Venous oxygen content (mmol/l)	8.81 ± 2.700	8.39 ± 0.639	0.661

were not significantly different between groups. Four ewes in the Ad.VEGF group and five in the Saline group produced insufficient colostrum to meet initial requirements of 50ml/kg and hence their lambs were supplemented using the donor colostrum pool. Irrespective of treatment group, the colostrum yield was correlated with total fetal placental weight ($r=0.430$, $n=32$, $p=0.008$). Although colostrum IgG concentrations were unrelated to lamb birth weight ($r=-0.069$, $n=32$, $p=0.708$), the large differences seen in colostrum yield translated into large differences in total colostrum content, which also correlated positively with birth weight ($r=0.667$, $n=32$, $p<0.001$).

5.3.4.5 Additional neonatal care

Figure 5.14 summarises the additional neonatal care measures required to ensure lamb

Table 5.5 – Routine vital signs (cardiorespiratory and temperature) taken on all lambs in the first 24 hours of life and immunoglobulin G levels in lamb / maternal plasma at 24 hours of age

	Saline (n=15)	**Ad.VEGF (n=17)**	**P Value**
Heart rate (min^{-1}) at 1 hour	232 ± 13.3	246 ± 6.24	0.342
Respiratory rate (min^{-1}) at 1 hour	71 ± 3.10	72 ± 2.71	0.960
Rectal temperature (^{o}C) at 1 hour	39.8 ± 0.20	39.9 ± 0.14	0.757
Time to standing (min)	107.5 ± 28.19	96.8 ± 19.80	0.752
Shoulder height (cm) at 24 hours	33 ± 1.0	35 ± 0.7	0.237
Lamb IgG (mg/ml) at 24 hours	22.9 ± 1.85	23.1 ± 4.06	0.975
Maternal IgG (mg/ml) at 24 hours	12.3 ± 0.79	12.0 ± 1.81	0.882

Table 5.6 – Colostrum yield, nutrient composition and immunoglobulin G content at birth

	Saline (n=15)	**Ad.VEGF (n=17)**	**P Value**
Colostrum yield (ml)	266 ± 39.1	314 ± 48.5	0.452
IgG concentration (mg/ml)	50.8 ± 3.48	56.8 ± 5.74	0.396
Total IgG content (g)	12.7 ± 1.84	15.9 ± 2.20	0.278
Butterfat concentration (g/100g)	7.74 ± 1.274	7.43 ± 0.958	0.845
Total butterfat (g)	23.0 ± 4.42	23.0 ± 3.74	0.997
Lactose (g/100g)	1.54 ± 0.15	1.72 ± 0.12	0.398
Total lactose (g)	5.03 ± 0.92	4.46 ± 0.79	0.631
Crude protein (g/100g)	18.5 ± 1.11	19.3 ± 1.06	0.572
Total crude protein (g)	46.4 ± 6.75	56.6 ± 8.17	0.352
Total energy concentration (kJ/kg)	2459 ± 41.8	2449 ± 32.4	0.838
Total energy content (kJ)	662 ± 95.9	769 ± 117.5	0.495

Figure 5.14 – Additional neonatal care measures required to ensure lamb survival

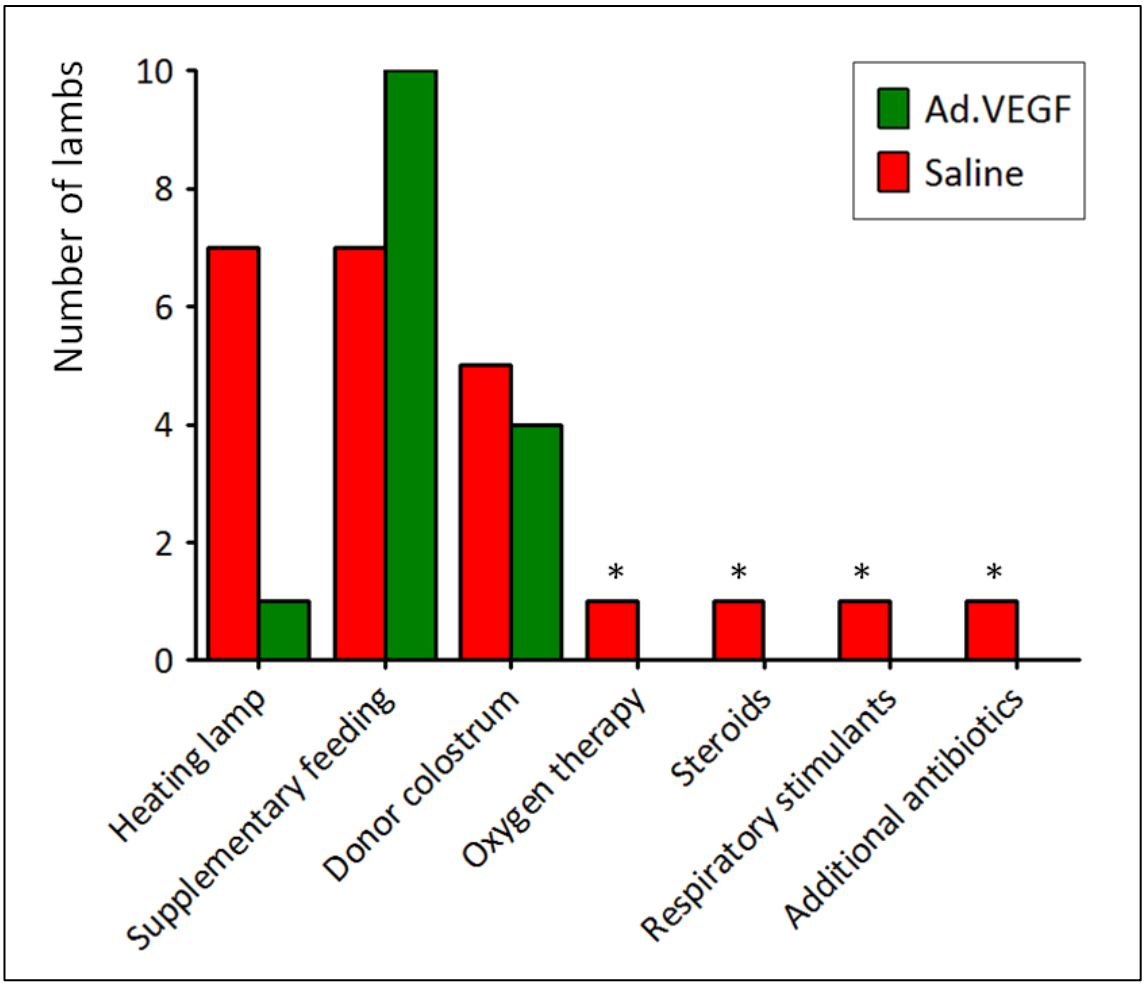

** All these interventions were required in one particular lamb, born by caesarean section weighing 2090g. Number of lambs studied throughout the neonatal period was 31 of 33, excluding one stillbirth and one accidental neonatal death (due to maternal crushing) in the Saline and Ad.VEGF groups, respectively.*

---

survival, by study group. For the 10 and 7 lambs in the Ad.VEGF and Saline groups, respectively, requiring supplementary feeding in the neonatal period, there were no significant group differences in the number of additional feeds (6±3.0 vs. 13±5.4) or in the duration of supplementary feeding (64±24.0 vs. 70±24.2 hours) required to ensure appropriate weight gain. Those lambs requiring supplementary feeding for longer than 48 hours (n=7) were of lower birth weight than spontaneously suckling lambs (n=25) (2931±467.3 vs. 4114±173.9, p=0.007). Only four lambs (two Ad.VEGF and two Saline) required supplementary feeding beyond 72 hours of age and these comprised the first, second, fourth and seventh smallest

Table 5.7 – Serum urea and electrolytes and liver enzymes at 8 days of postnatal age

	Saline (n=15)	**Ad.VEGF (n=16)**	**P Value**
Sodium (mmol/l)	149.2 ± 0.34	149.2 ± 0.46	0.983
Potassium (mmol/l)	6.15 ± 0.118	5.98 ± 0.130	0.339
Urea (mmol/l)	7.43 ± 0.663	7.86 ± 0.563	0.624
Creatinine (µmol/l)	50.9 ± 1.29	50.3 ± 1.08	0.714
Chloride (mmol/l)	106.1 ± 0.42	105.6 ± 0.50	0.506
Albumin (g/l)	27.6 ± 0.45	27.7 ± 0.25	0.847
Alanine transaminase (IU/l)	3.93 ± 0.248	4.19 ± 0.344	0.558
Aspartate aminotransferase (IU/l)	51.6 ± 1.10	53.3 ± 3.34	0.644
Gamma-glutamyl transferase (IU/l)	289 ± 34.9	306 ± 30.2	0.715
Alkaline phosphatase (IU/l)	1034 ± 81.4	1011 ± 86.1	0.849
Glutamate dehydrogenase (IU/l)	27.4 ± 12.40	15.0 ± 3.09	0.346

Serum urea, creatinine, electrolytes and liver enzymes at 8 days of postnatal age in 31 surviving prenatally growth-restricted lambs whose overnourished adolescent mothers received mid-gestation bilateral uterine artery injections of Ad.VEGF or saline. There were no significant differences between levels in male versus female lambs and no gender x treatment interaction.

---

lambs by initial birth weight, indicating that small size at birth was a strong predictor of the need for prolonged supplementary feeding.

5.3.4.6 Serum biochemistry and liver function

Table 5.7 shows values of serum biochemistry and liver function at 8 days of postnatal age, by study group and gender. There were no differences between Ad.VEGF and Saline groups in any parameters. Irrespective of treatment group, lamb birth weight was positively correlated with sodium (r=0.562, n=15, p=0.029) and negatively correlated with potassium (r=–0.542, n=15, p=0.037), ALP (r=–0.563, n=15, p=0.029) and GLDH (r=–0.609, n=15, p=0.016) in Saline but not

Ad.VEGF groups. By contrast, birth weight was positively correlated with chloride (r=0.554, n=16, p=0.026) and albumin (r=0.555, n=16, p=0.026) and negatively correlated with ALT (r= -0.536, n=16, p=0.032) and albumin (r=–0.516, n=16, p=0.041) only within the Ad.VEGF group.

5.3.5 Postnatal growth and anabolic hormones

5.3.5.1 Live weight

Figure 5.15A shows serial measurements of lamb body weight from birth until necropsy at 12 weeks of age. There was a tendency towards increased live weight in Ad.VEGF relative to Saline groups at 14 days (9.4±0.43 vs. 8.1±0.53 kg, p=0.066), 21 days (11.6±0.50 vs. 10.1±0.62 kg, p=0.071), 28 days (14.0±0.58 vs. 12.3±0.69 kg, p=0.07) and 35 days of age (16.9±0.72 vs. 14.8±0.81 kg, p=0.061). Subsequently live weight was significantly increased in Ad.VEGF versus Saline groups at 42 days (20.0±0.70 vs. 17.5±0.91 kg, p=0.041), 49 days (23.0±0.72 vs. 20.4±1.00 kg, p=0.037), 56 days (26.5±0.73 vs. 23.2±1.05 kg, p=0.015), 63 days (29.5±0.77 vs. 26.1±1.11 kg, p=0.016), 70 days (31.8±0.81 vs. 28.5±1.15 kg, p=0.024), 77 days (35.2±0.91 vs. 31.6±1.18 kg, p=0.021) and 82±0.3 days of age (37.1±0.89 vs. 33.5±1.17 kg, p=0.019).

Correspondingly overall absolute postnatal growth velocity from birth until necropsy was increased in Ad.VEGF relative to Saline groups (397±8.7 vs. 362±11.7 g/day, p=0.023). In contrast, fractional growth velocity was not significantly different (10.0±0.61 vs. 10.7±0.76 % per day, respectively, from birth until 82±0.3 days of age). Fractional growth velocity demonstrated a strong and inverse relationship with birth weight, irrespective of treatment group (r=–0.910, n=31, p=<0.001), as illustrated in Figure 5.15B.

5.3.5.2 Abdominal girth

Figure 5.16A depicts serial upward changes in abdominal girth at the umbilicus from birth until necropsy. Girth was increased in Ad.VEGF relative to Saline groups at 56 days (88±1.2 vs. 84±1.5 cm, p=0.019), 77 days (104±1.3 vs. 99±1.5 cm, p=0.026) and 82 days of age (108±1.4 vs. 104±1.1 cm, p=0.032). In addition, there was a tendency towards higher abdominal girth in Ad.VEGF compared to Saline groups at 7 days (48±1.0 vs. 45±1.4 cm, p=0.063), 14 days (54±0.9 vs. 51±1.4 cm, p=0.061), 42 days (75±1.2 vs. 71±1.8 cm, p=0.07), 63 days (92±1.3 vs. 89±1.4 cm, p=0.1) and 70 days of age (96±1.2 vs. 93±1.7 cm, p=0.092).

5.3.5.3 Shoulder height

Figure 5.16B shows serial increases in shoulder height from birth until necropsy. Lambs in the Ad.VEGF group were taller at 28 days (44±0.5 vs. 42±0.7 cm, p=0.036), 35 days (46±0.5 vs.

Figure 5.15 – Absolute and fractional postnatal growth

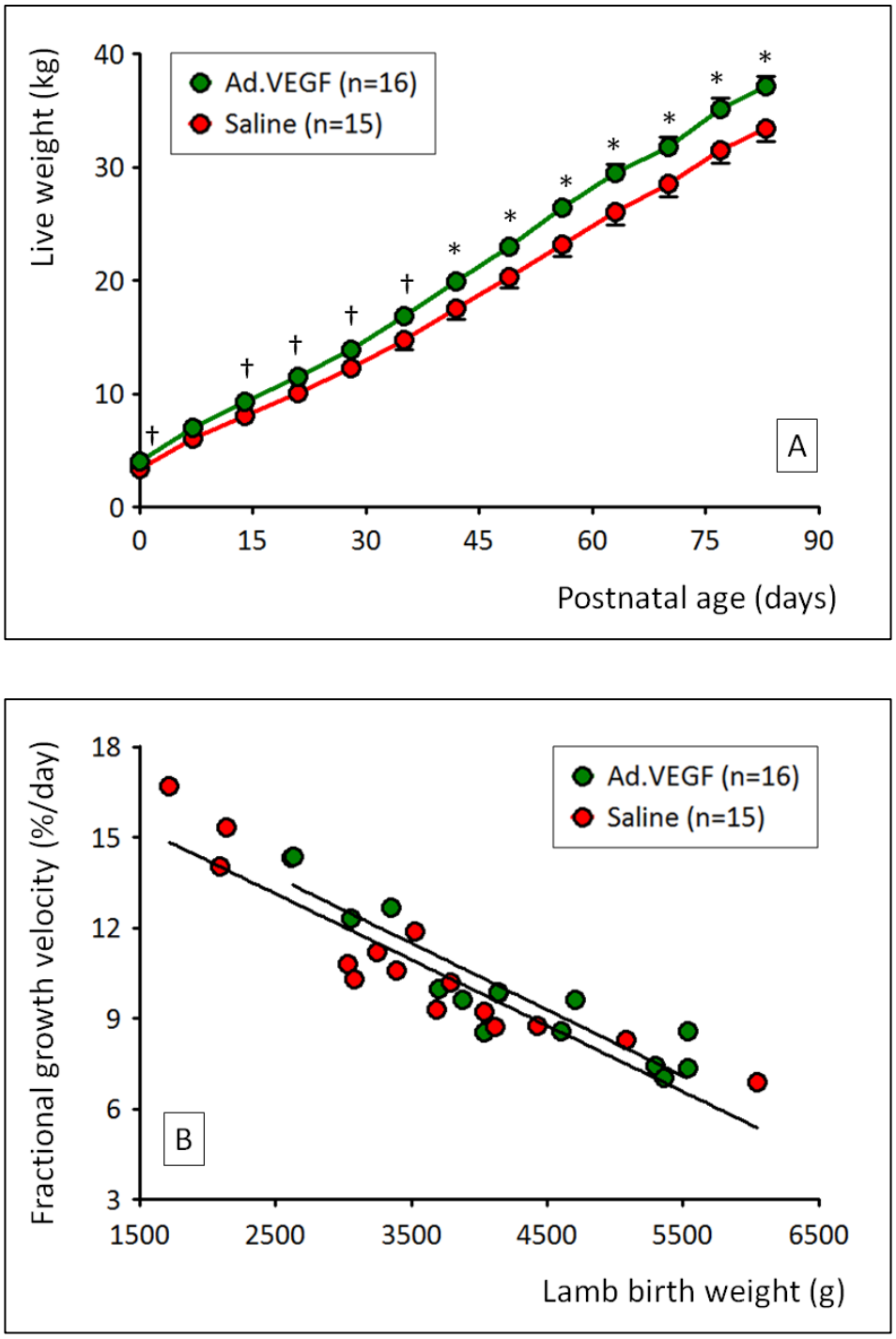

*[A] Serial measurements of live weight made at weekly intervals from birth until 83±0.2 days of postnatal age in 31 surviving prenatally growth-restricted lambs whose overnourished adolescent mothers received mid-gestation bilateral uterine artery injections of Ad.VEGF or saline. † p=0.05-0.1 * p<0.05. [B] Scattergram of lamb birth weight versus fractional growth velocity for weight to weaning (= final live weight - birth weight, expressed as a percentage of lamb birth weight and per day of postnatal age. Correlation coefficients are detailed in the text.*

Figure 5.16 – Lamb abdominal girth and shoulder height measurements

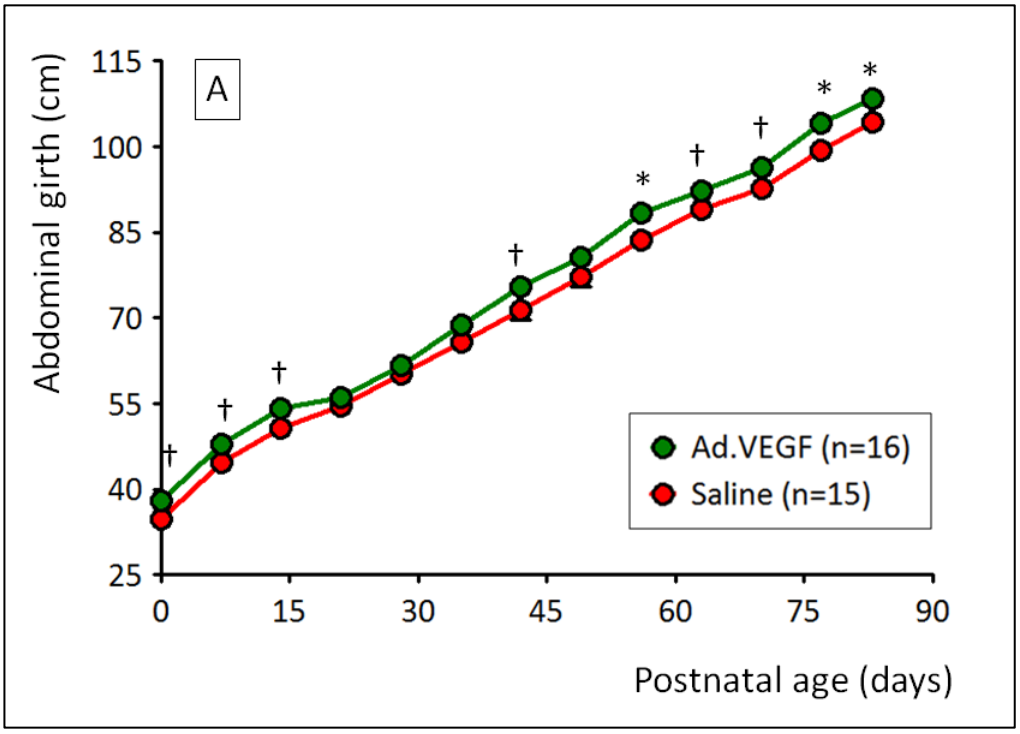

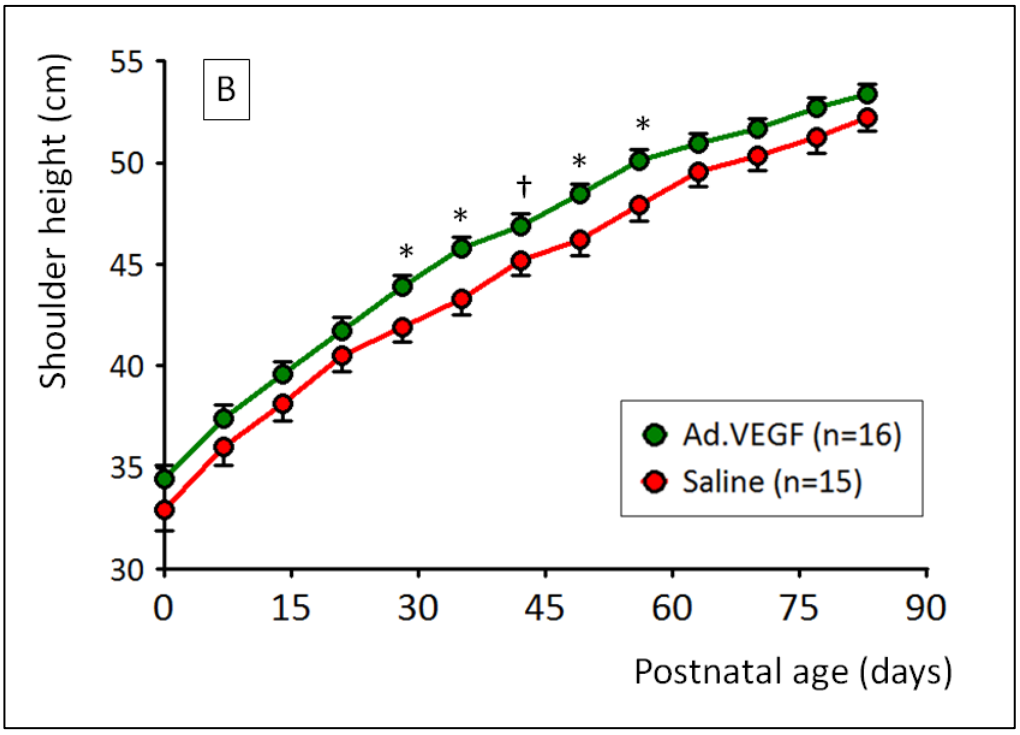

*Serial measurements of abdominal girth at the level of the umbilicus [A] and height at the anterior shoulder [B] at weekly intervals from birth until 83±0.2 days of postnatal age in 31 surviving prenatally growth-restricted lambs whose overnourished adolescent mothers received mid-gestation bilateral uterine artery injections of Ad.VEGF or saline. † p=0.05-0.1 * p<0.05.*

44±0.8 cm, p=0.013), 49 days (49±0.5 vs. 47±0.7 cm, p=0.018) and 56 days of age (51±0.5 vs. 49±0.8 cm, p=0.031). There was also a tendency towards increased shoulder height in Ad.VEGF versus Saline groups at 42 days of age (47±0.6 vs. 45±0.7 cm, p=0.087).

Lamb birth weight and all three measures of offspring size (live weight, shoulder height and umbilical girth) were independent of gender throughout the postnatal period up to weaning.

5.3.5.4 Insulin

Figure 5.17A shows serial measurements of plasma insulin from birth until necropsy. Insulin concentrations were relatively low at birth, increased 5 fold by the end of the first week of life and thereafter stabilised for the rest of the suckling period. There was a tendency towards higher insulin levels in Ad.VEGF compared with Saline groups at 7 days of age (71.6±7.21 vs. 55.1±6.23 µU/ml, p=0.097) but subseqeuntly no other significant differences between groups at any point up to 12 weeks postnatal age. Insulin concentrations were independent of gender.

5.3.5.5 IGF-1

Figure 5.17B illustrates serial measurements of plasma IGF-1 from birth until necropsy. IGF-1 concentrations were relatively low at birth, increased ~3 fold by the end of the first week of life and thereafter largely plateaued for the rest of the suckling period. There were no significant differences in IGF-1 between Ad.VEGF and Saline groups at any stage but males tended to have greater IGF-1 concentrations than females at 7 days (p=0.056) and levels were significantly higher in males versus females from 14 days of age onwards (p<0.001-0.043).

5.3.6 Immune challenge

Figure 5.18 illustrates the mean levels of SAA prior to and 24 and 48 hours following routine vaccination at 58±0.4 days of age, by study group. There were no significant differences between Ad.VEGF and Saline groups at baseline or after challenge. Levels at each stage were compared by one-way ANOVA and post-hoc LSD tests. SAA levels were increased >500-fold at 24 and 48 hours relative to baseline levels in all lambs, commensurate with an acute phase response and overall were not significantly different between 24 and 48 hours (29.5±5.10 versus 29.2±4.93, respectively, p=0.966). Similarly there was no detectable difference when the individual post-challenge data were combined. There were no significant correlations between SAA levels and lamb birth weight and placental weight, however peak/mean SAA levels correlated with neonatal plasma IgG concentrations for the Saline group (r=0.636/0.609, n=15, p=0.011/0.016) but not within the Ad.VEGF group (r=0.187/0.200, n=16, p=0.487/0.458).

Figure 5.17 – Lamb plasma insulin and insulin-like growth factor 1 levels from birth to weaning

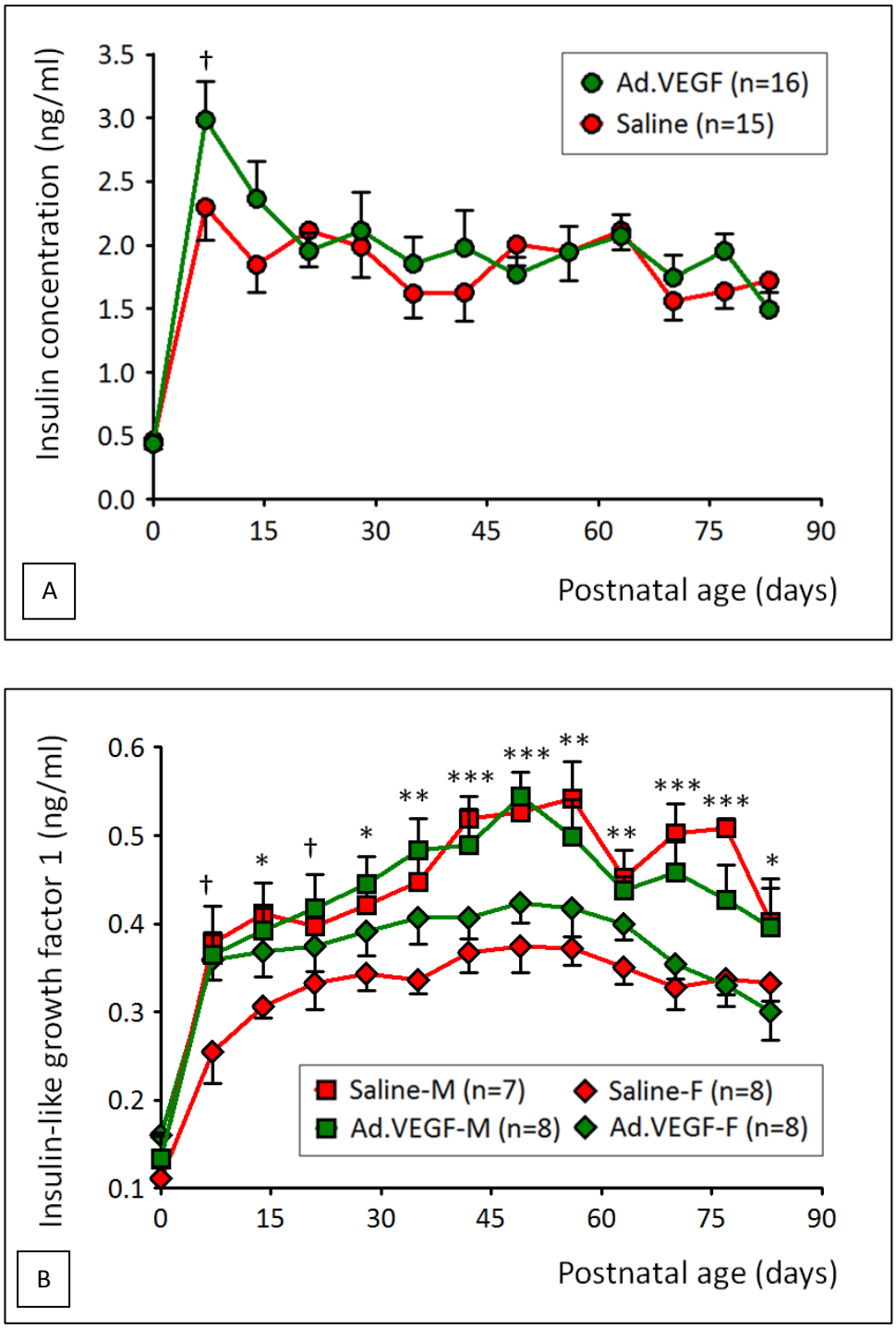

*Serial measurements of plasma insulin [A] and IGF-1 [B], measured by radioimmunoassay, at weekly intervals from birth until 83±0.2 days of postnatal age in 31 surviving prenatally growth-restricted lambs whose overnourished adolescent mothers received mid-gestation bilateral uterine artery injections of Ad.VEGF or saline. † p=0.05-0.1 * p<0.05, ** p<0.01, *** p<0.001, as indicated. IGF-1 levels did not differ between Ad.VEGF and saline groups but were signficantly higher in male (squares) vs. females (diamonds), thus IGF-1 is presented by gender.*

Figure 5.18 – Lamb serum amyloid A concentration before and after routine vaccination

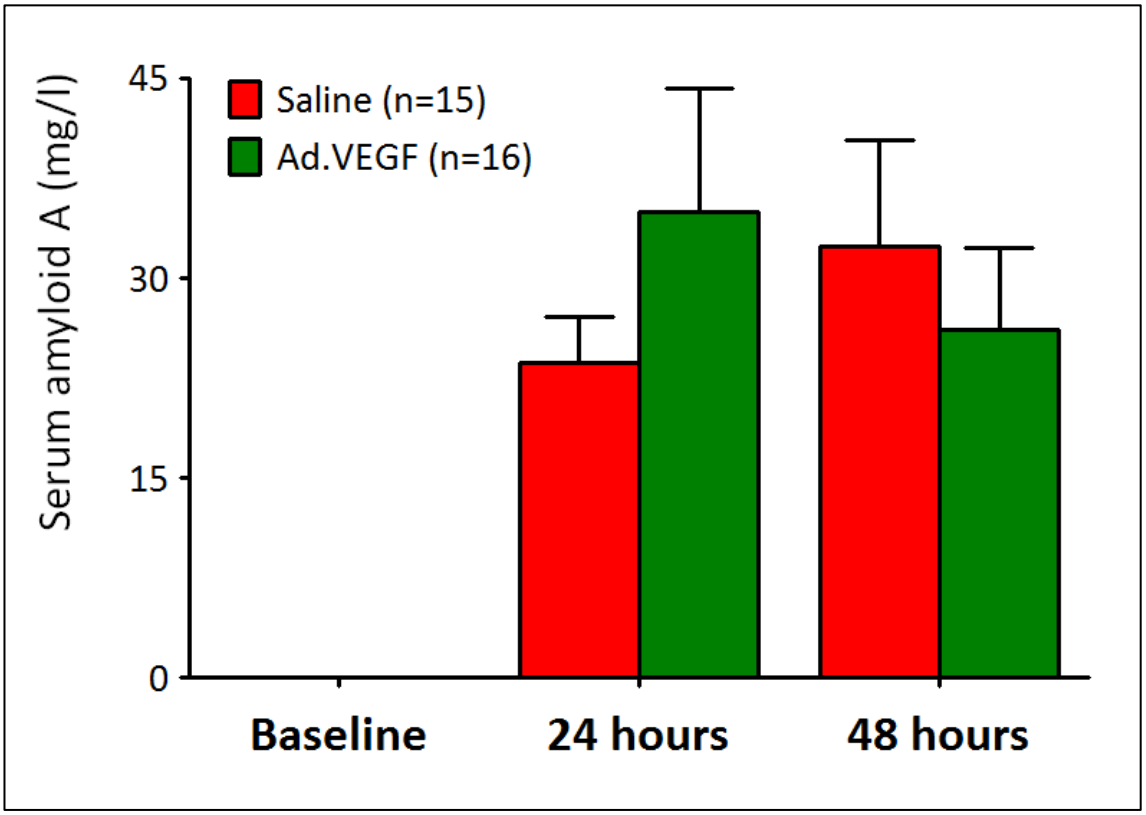

Serial levels of the acute phase reactant serum amyloid A (measured by ELISA) at baseline and 24/48 hours following routine vaccination with Heptatvac P Plus® at 58±0.4 days postnatal age in 31 surviving prenatally growth-restricted lambs whose overnourished adolescent mothers received mid-gestation bilateral uterine artery injections of Ad.VEGF or saline. There were no significant differences between Ad.VEGF or saline groups, or between males and females. Levels were increased (p<0.001) at 24 and 48 hours relative to baseline (0.049±0.0447 and 0.058±0.0255 mg/l in Ad.VEGF saline groups, respectively).

5.3.7 Metabolic challenge

Measurements of insulin and various metabolite responses to an intravenous 0.25mg/kg glucose bolus at 68±0.5 days of age are shown below. For each metabolite, the three baseline values (–20, –10 and 0 minutes relative to the glucose infusion) were averaged to find the baseline fasting mean. Fasting baseline values for each metabolite are shown in Table 5.8, by study group and gender. There were no significant differences in fasting metabolite levels between Ad.VEGF and Saline groups, however urea levels were higher (p=0.004) and non-

Table 5.8 – Fasting plasma metabolite levels and area under the curve for glucose, insulin and NEFA following an intravenous glucose bolus at 7 weeks of age

	Saline-F (n=8)	Saline-M (n=7)	Ad.VEGF-F (n=8)	Ad.VEGF-M (n=8)	P Values		
					Treatment	Gender	Interaction
Fasting glucose (mg/dl)	85.3 ± 1.15	82.9 ± 1.96	85.1 ± 3.90	82.9 ± 1.32	0.946	0.822	0.990
Fasting insulin (ng/ml)	1.24 ± 0.089	1.38 ± 0.179	1.60 ± 0.211	1.24 ± 0.135	0.499	0.350	0.131
Fasting NEFA (mmol/l min)	0.47 ± 0.045	0.41 ± 0.024	0.56 ± 0.055	0.46 ± 0.042	0.111	0.085	0.585
Fasting glycerol (mmol/l)	93.9 ± 1.67	86.0 ± 6.81	111.9 ± 14.58	92.1 ± 10.62	0.232	0.304	0.551
Fasting urea (mmol/l)	7.97 ± 0.416	7.19 ± 0.352	8.25 ± 0.337	6.71 ± 0.336	0.783	**0.004**	0.302
Fasting glucose : insulin ratio	1.38 ± 0.264	1.58 ± 0.564	1.07 ± 0.170	1.12 ± 0.139	0.222	0.692	0.821
Fasting insulin : glucose ratio	0.91 ± 0.160	1.19 ± 0.373	1.12 ± 0.200	1.05 ± 0.199	0.890	0.660	0.469
HOMA index	113 ± 13.3	123 ± 16.5	150 ± 29.0	110 ± 7.7	0.522	0.417	0.187
Glucose AUC (mg/min/dl)	2050 ± 360	2216 ± 324	2570 ± 425	2720 ± 281	0.430	0.659	0.983
Insulin AUC (ng/ml min)	71.0 ± 11.53	88.4 ± 18.86	104.7 ± 7.65	117.4 ± 19.88	**0.040**	0.876	0.329
NEFA AUC (mmol/min/l)	12.21 ± 5.535	6.58 ± 3.427	20.09 ± 3.20	16.12 ± 3.20	**0.038**	0.236	0.585

Fasting plasma metabolite levels and indices of insulin resistance before and area under the curve (AUC) following an intravenous glucose bolus (metabolic challenge) at 68±0.5 days postnatal age in 31 surviving prenatally growth-restricted lambs whose overnourished adolescent mothers received mid-gestation bilateral uterine artery injections of Ad.VEGF or saline. Abbreviations: HOMA index = homeostatic model assessment index; NEFA = non-esterified fatty acids.

esterified fatty acid levels tended also to be higher (p=0.085) in female lambs compared to males. The area under the curve (AUC) for each metabolite was calculated minus this baseline i.e. the increase or decrease in a given metabolite relative to baseline values across the 2 hour test period. AUC are summarised in Table 5.8 and discussed individually by metabolite below.

There were no significant gender differences in AUC for any parameter. Moreover there were no differences in any indices of insulin resistance (homeostatic model assessment (HOMA) index, or fasting glucose to insulin or insulin to glucose ratios) by treatment or gender. There were no differences between Ad.VEGF and Saline groups in appetite index, taken as the acute live weight gain in the first 15 minutes after feeding was resumed following a five hour fast for metabolic challenge (191±78g versus 233±78g, respectively, p=0.714).

5.3.7.1 Glucose response

Figure 5.19A shows serial measurements of plasma glucose by study group. Glucose concentrations were significantly higher in Ad.VEGF compared to Saline groups at 15 minutes post glucose infusion (156.81±4.379 vs. 146.51±4.604 mg/dl, p=0.023) and there was a tendency towards higher concentrations in Ad.VEGF versus Saline groups at 20, 25 and 45 minutes (146.23±4.769 vs. 134.51±4.036 mg/dl, p=0.073; 134.83±4.519 vs. 123.60±3.805 mg/dl, p=0.069; and 105.66±4.067 vs. 96.45±2.992 mg/dl, p=0.082, respectively).

Despite the significant differences at these individual time points, overall glucose AUC was not significantly different between groups (see Table 5.8). Interim AUC values were also calculated at each consecutive time point and similarly did not differ between groups (data not shown). Irrespective of treatment group, baseline fasting glucose demonstrated a weak negative correlation with birth weight (r=-0.407, n=31, p=0.023) but not with lamb body weight or dimensions at the time of glucose challenge.

5.3.7.2 Insulin response

Figure 5.19B illustrates serial measurements of plasma insulin by study group. There was a tendency towards higher insulin concentrations in Ad.VEGF compared to Saline groups at 25 and 30 minutes post glucose infusion (89.54±5.823 vs. 72.97±5.591 μU/ml, p=0.05; and 85.80±5.736 vs. 69.00±6.266 μU/ml, p=0.057, respectively) and insulin concentrations were significantly higher in Ad.VEGF versus Saline groups at 45 and 60 minutes (64.94±6.143 vs. 43.30±5.046 μU/ml, p=0.011; and 45.06±4.763 vs. 31.69±3.431 μU/ml, p=0.032, respectively). Overall, insulin AUC was significantly increased in Ad.VEGF relative to Saline groups (see Table 5.8). Fasting insulin : glucose and insulin AUC : glucose AUC ratios were not significantly

Figure 5.19 – Glucose and insulin responses to glucose challenge

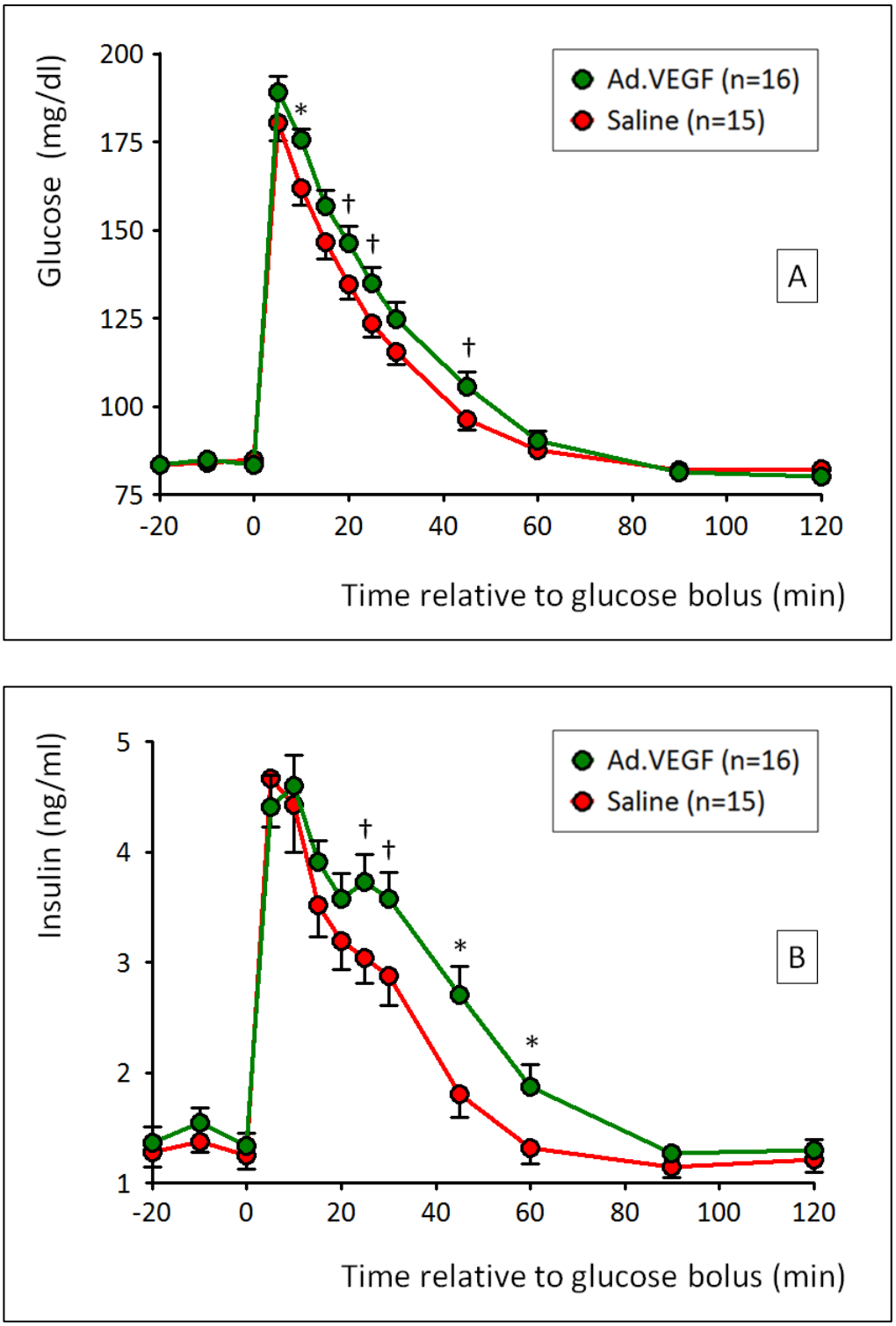

*Serial measurements of plasma glucose [A] and insulin [B] at regular intervals up to 120 minutes following a standardised intravenous glucose infusion administered at 68±0.5 days postnatal age in 31 surviving prenatally growth-restricted lambs whose overnourished adolescent mothers received mid-gestation bilateral uterine artery injections of Ad.VEGF or saline. † p=0.05-0.1, * p<0.05.*

Figure 5.20 – Non-esterified fatty acid response to glucose challenge

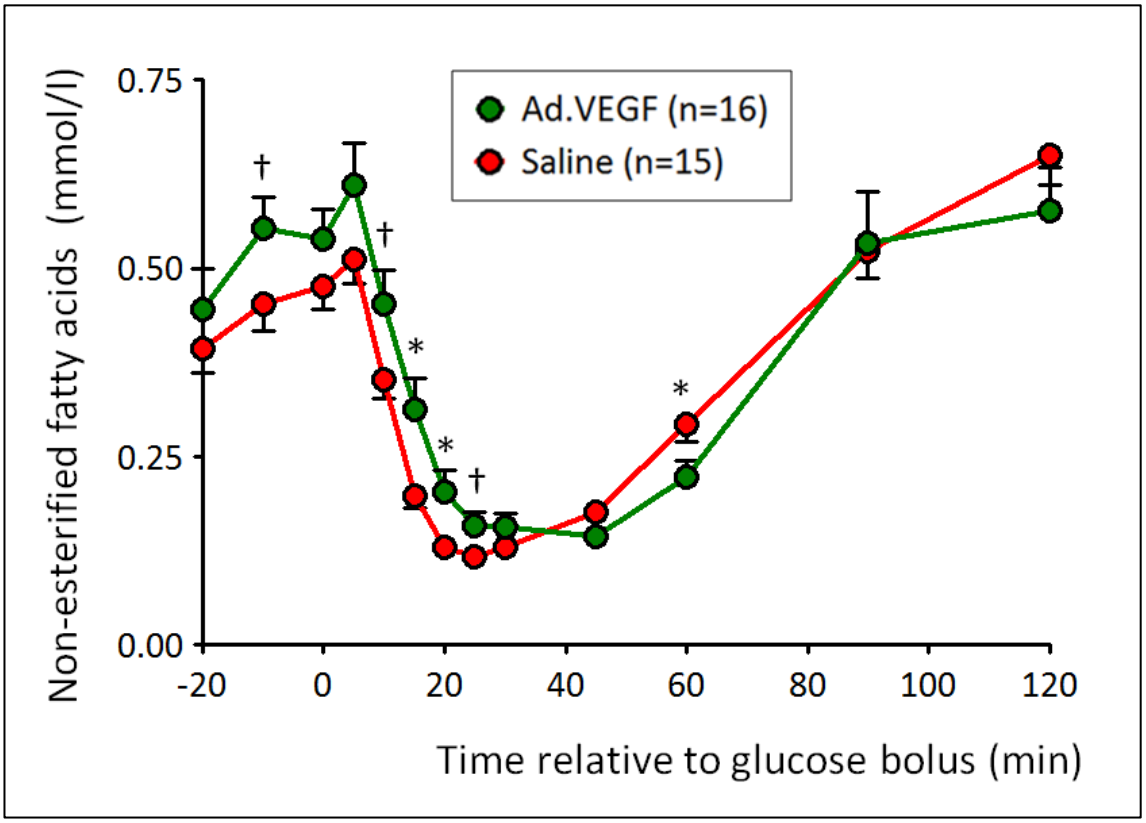

*Serial measurements of plasma non-esterified fatty acid (NEFA) at regular intervals up to 120 minutes following a standardised intravenous glucose infusion administered at 68±0.5 days postnatal age in 31 surviving prenatally growth-restricted lambs whose overnourished adolescent mothers received mid-gestation bilateral uterine artery injections of Ad.VEGF or saline. † p=0.05-0.1, * p<0.05.*

---

different between treatment groups. Insulin parameters were not significantly correlated with birth weight, fetal : placental weight ratios or weight / girth at the time of metabolic challenge.

5.3.7.3 NEFA response

Figure 5.20 details serial measurements of plasma NEFA by study group. Although baseline values tended to be higher in Ad.VEGF relative to Saline groups at 10 minutes prior to glucose infusion (p=0.073), mean baseline NEFA levels did not differ between groups (see Table 5.8). There was a tendency towards higher NEFA concentrations in Ad.VEGF versus Saline groups at 10 minutes post glucose infusion (0.45±0.045 vs. 0.35±0.026 mmol/l, p=0.069) and NEFA concentrations were significantly higher in Ad.VEGF compared with Saline groups at 15, 20 and

25 minutes (0.31±0.040 vs. 0.20±0.016 mmol/l, p=0.015; 0.20±0.028 vs. 0.13±0.013 mmol/l, p=0.026; and 0.16±0.018 vs. 0.12±0.009 mmol/l, p=0.048, respectively). By contrast, NEFA concentrations were lower in Ad.VEGF versus Saline groups at 60 minutes (0.22±0.021 vs. 0.29±0.022 mmol/l, p=0.031). Overall, NEFA AUC was significantly increased in Ad.VEGF relative to Saline groups (see Table 5.8). There appeared to be an upward shift of the curve in Ad.VEGF relative to Saline groups. Despite a tendency towards higher baseline levels in females versus males, NEFA AUC did not differ by gender.

5.3.8 Body composition analysis

Table 5.9 summarises body composition as measured by DEXA at 74±0.4 days gestation. At this point, lambs prenatally treated with Ad.VEGF were larger than those treated with saline (32.6±0.86 vs. 29.8±1.01kg, respectively, p=0.047) but there were no significant differences between males and females (p=0.280) and no treatment x gender interaction (p=0.244). There was a tendency towards higher bone mineral density, total bone mineral content and lean tissue mass in Ad.VEGF relative to Saline groups. There were no significant differences between groups in body fat, either in absolute or relative terms, neither were there any significant differences between males and females in the degree of adiposity as assessed by DEXA. Bone mineral content and lean tissue mass were positively correlated with birth weight (r=0.570, n=30, p=0.001 and r=0.813, n=30, p=<0.001) and current live weight (r=0.802, n=30, p=<0.001 and r=0.887, n=30, p=<0.001), abdominal girth (r=0.687, n=30, p=<0.001 and r=0.852, n=30, p=<0.001) and shoulder height (r=0.636, n=30, p=<0.001 and r=0.855, n=30, p=<0.001) at the time of examination. Lean tissue mass was also inversely correlated with fractional growth velocity to weaning (r=–0.610, n=30, p=0.001).

Table 5.9 – Body composition analysis by dual energy X-ray absorptiometry

	Saline (n=15)	**Ad.VEGF (n=16)**	**P Value**
Bone Mineral Density (g/cm)	0.482 ± 0.0099	0.510 ± 0.0096	0.057
Bone Mineral Content (g)	783.1 ± 27.80	856.7 ± 27.19	0.069
Lean Tissue Mass (kg)	26.32 ± 0.943	28.65 ± 0.772	0.066
Fat Mass (kg)	2.43 ± 0.350	3.02 ± 0.339	0.222
% Body Fat	8.03 ± 1.14	9.26 ± 1.01	0.383

There were no significant differences between males and females for any parameters.

5.3.9 Necropsy parameters

5.3.9.1 Blood results

Table 5.10 shows the concentrations of various metabolic hormones and haematological parameters in lamb blood sampled on the day prior to necropsy. There were no significant differences between Ad.VEGF and Saline groups. Peripheral plasma IGF-1 concentrations were higher in male compared with female lambs (51.48±4.295 vs. 40.86±2.457 pmol/ml, p=0.015) whilst leptin concentrations were lower in males versus females (2.53±0.467 vs. 4.49±0.591 ng/ml, p=0.043). Irrespective of treatment group and gender, leptin correlated strongly with perirenal fat weight (both absolute and relative) at subsequent necropsy (r=0.744 and r=0.756, respectively, p=<0.001). Haemoglobin levels tended to be higher in female versus male lambs (p=0.05), in keeping with a lower relative blood volume (p<0.001) in female compared to male lambs (see Section 5.3.9.3 below), suggesting relative haemoconcentration.

5.3.9.2 Absolute organ weights and measurements

Table 5.11 shows major lamb organ weights and additional post mortem measurements taken at necropsy at 82±0.2 days postnatal age, by study group and gender. Lambs in the Ad.VEGF group were heavier (live weight and carcass weight) with greater abdominal girth than those in the Saline group. Male lambs did not weigh more than female lambs at this stage. Liver and perirenal fat weights were also significantly greater and there was a tendency towards decreased adrenal weight in Ad.VEGF versus Saline groups. Blood, hock and tibial bone weights were greater in male versus female lambs (1369±58.9 vs. 1188±40.8 g, p=0.016; 1116±35.2 vs. 1013±25.9 g, p=0.022; and 59.2±1.73 vs. 52.5±1.70 g, p=0.012; respectively) whilst perirenal fat weight was lower in males versus females (229.4±20.50 vs. 416.8±42.48 g, p=<0.001). There was also a significant interaction between study group and gender with respect to perirenal fat weight, such that this was highest in the Ad.VEGF-treated female lambs (p=0.034). All remaining absolute organ weights were unaffected by treatment or gender.

5.3.9.3 Relative organ weights

Table 5.12 details the major lamb internal organ weights, expressed relative to residual lamb carcass weight, by treatment group and gender. The relative adrenal weight was significantly lower in Ad.VEGF versus Saline groups. Relative brain weight and brain to liver ratios (shown in Figure 5.21A), two different indices of fetal brain sparing, also tended to be lower in Ad.VEGF relative to Saline groups. There was also a lower relative heart weight and tendency towards lower relative lung weight in Ad.VEGF compared with Saline groups. Relative perirenal fat

Table 5.10 – Measurement of metabolic hormones and haematological parameters at 82 days of postnatal age

	Saline-F (n=8)	Saline-M (n=7)	Ad.VEGF-F (n=8)	Ad.VEGF-M (n=8)	P Values		
					Treatment	Gender	Interaction
Leptin (ng/ml)	4.07 ± 0.921	2.43 ± 0.589	4.91 ± 0.987	2.62 ± 0.744	0.519	**0.018**	0.683
IGF-1 (ng/ml)	0.32 ± 0.020	0.39 ± 0.037	0.29 ± 0.014	0.39 ± 0.054	0.626	**0.043**	0.738
Insulin (ng/ml)	1.66 ± 0.338	1.79 ± 0.202	1.31 ± 0.085	1.69 ± 0.174	0.342	0.292	0.593
Haematocrit (%)	39.1 ± 0.92	36.4 ± 2.08	40.9 ± 0.52	39.2 ± 0.97	0.092	0.124	0.715
Haemoglobin (g/dl)	12.9 ± 0.32	12.1 ± 0.44	12.8 ± 0.15	12.8 ± 0.37	0.097	0.050	0.740

Plasma measurements of leptin, IGF-1, insulin, haematocrit and haemoglobin at 82±0.2 days postnatal age in 31 surviving prenatally growth-restricted lambs whose overnourished adolescent mothers received mid-gestation bilateral uterine artery injections of Ad.VEGF or saline. Comparisons were made using the General Linear Model. Abbreviations: IGF-1 = insulin-like growth factor 1.

Table 5.11 – Weights of major lamb organs, hock, blood and residual carcass, and weight and length of the tibial bone

	Saline-F (n=8)	Saline-M (n=7)	Ad.VEGF-F (n=8)	Ad.VEGF-M (n=8)	P Values		
					Treatment	Gender	Interaction
Live weight (kg)	31.9 ± 1.43	35.3 ± 1.76	36.9 ± 1.10	37.4 ± 1.53	**0.019**	0.195	0.322
Abdominal girth (cm)	103.1 ± 1.56	105.9 ± 1.28	108.9 ± 1.47	107.9 ± 2.47	**0.032**	0.632	0.306
Brain weight (g)	69.6 ± 1.11	71.2 ± 2.95	72.5 ± 0.91	72.5 ± 2.17	0.294	0.690	0.709
Pituitary weight (g)	0.53 ± 0.046	0.50 ± 0.054	0.61 ± 0.046	0.54 ± 0.028	0.210	0.292	0.650
Weight of both adrenals (g)	1.78 ± 0.050	1.84 ± 0.051	1.61 ± 0.069	1.76 ± 0.085	0.081	0.144	0.571
Pancreas weight (g)	33.8 ± 2.34	38.9 ± 2.26	39.3 ± 1.13	39.5 ± 2.06	0.163	0.186	0.225
Liver weight (g)	560 ± 24.4	630 ± 24.7	651 ± 20.2	659 ± 22.9	**0.016**	0.104	0.188
Spleen weight (g)	135 ± 11.8	155 ± 20.2	149 ± 12.2	149 ± 6.7	0.811	0.420	0.456
Perirenal fat weight (g)	308 ± 36.4	226 ± 33.7	498 ± 53.7	233 ± 26.1	**0.024**	**<0.001**	**0.034**
Weight of both kidneys (g)	106 ± 5.2	124 ± 7.3	124 ± 5.4	122 ± 6.1	0.249	0.202	0.116

Heart weight (g)	186 ± 14.0	178 ± 18.3	183 ± 10.4	170 ± 8.8	0.691	0.439	0.892
Weight of both lungs (g)	470 ± 43.4	504 ± 16.3	485 ± 17.0	507 ± 31.1	0.798	0.324	0.826
Thymus weight (g)	46.5 ± 4.05	40.1 ± 3.05	48.9 ± 3.56	45.7 ± 3.15	0.202	0.178	0.657
Weight of both testes (g)		39.8 ± 6.38		50.8 ± 8.57	0.322		
Weight of both ovaries (g)	1.49 ± 0.128		1.24 ± 0.155		0.267		
Hock weight (g)	965 ± 40.4	1112 ± 51.2	1050 ± 29.3	1120 ± 51.6	0.400	**0.022**	0.399
Blood weight (g)	1122 ± 68.2	1385 ± 100	1237 ± 46.0	1355 ± 73.7	0.691	**0.016**	0.344
Tibia weight (g)	50.8 ± 3.43	58.0 ± 1.63	53.9 ± 1.57	60.2 ± 2.99	0.388	**0.012**	0.868
Tibia length (cm)	96.7 ± 2.23	98.9 ± 2.14	98.4 ± 1.32	100.1 ± 1.50	0.429	0.294	0.875
Residual carcass weight (kg)	19.3 ± 1.04	20.5 ± 1.05	25.7 ± 0.91	25.4 ± 1.00	**0.038**	0.868	0.334

Table 5.12 – Relative weights of major lamb organs (in g per kg empty carcass weight) plus relative carcass weight (per kg live weight at necropsy)

	Saline-F (n=7)	Saline-M (n=7)	Ad.VEGF-F (n=8)	Ad.VEGF-M (n=8)	P Values		
					Treatment	Gender	Interaction
Brain	3.66 ± 0.232	3.49 ± 0.078	3.43 ± 0.143	3.37 ± 0.146	0.112	0.812	0.387
Pituitary	0.028 ± 0.003	0.024 ± 0.002	0.027 ± 0.002	0.025 ± 0.001	0.891	0.225	0.756
Adrenals	0.094 ± 0.006	0.091 ± 0.005	0.072 ± 0.002	0.083 ± 0.005	**0.004**	0.369	0.133
Pancreas	1.75 ± 0.093	1.90 ± 0.058	1.78 ± 0.099	1.87 ± 0.050	0.971	0.144	0.719
Liver	29.2 ± 1.22	30.9 ± 0.77	29.2 ± 0.79	30.8 ± 1.61	0.974	0.150	0.967
Spleen	7.06 ± 0.739	7.48 ± 0.723	6.56 ± 0.348	6.68 ± 0.257	0.238	0.626	0.786
Perirenal fat	15.8 ± 1.30	10.9 ± 1.42	21.8 ± 1.71	10.7 ± 1.01	0.055	**<0.001**	**0.037**
Kidneys	5.53 ± 0.269	6.06 ± 0.173	5.54 ± 0.121	5.67 ± 0.332	0.433	0.165	0.391
Heart	9.68 ± 0.654	8.61 ± 0.571	8.18 ± 0.483	7.89 ± 0.241	**0.044**	0.200	0.460
Lungs	24.3 ± 1.67	24.7 ± 0.65	21.7 ± 0.62	23.5 ± 1.10	0.072	0.295	0.529

Thymus	0.0025 ± 0.0004	0.0020 ± 0.0002	0.0022 ± 0.0002	0.0022 ± 0.0002	0.928	0.310	0.373
Testes		1.88 ± 0.210		2.54 ± 0.319	0.106		
Ovaries	0.080 ± 0.012		0.057 ± 0.008		0.130		
Hock	50.1 ± 1.20	54.5 ± 1.68	47.0 ± 0.90	53.1 ± 1.11	0.084	**<0.001**	0.500
Tibia	2.64 ± 0.155	2.86 ± 0.113	2.42 ± 0.107	2.85 ± 0.140	0.384	**0.020**	0.430
Blood	57.9 ± 1.17	67.2 ± 2.06	55.4 ± 1.91	63.5 ± 2.04	0.113	**<0.001**	0.757
Carcass	1.75 ± 0.093	1.90 ± 0.058	1.78 ± 0.099	1.87 ± 0.050	0.624	**0.003**	0.434

Figure 5.21 – Indices of asymmetrical growth and relative perirenal fat depot by group/gender

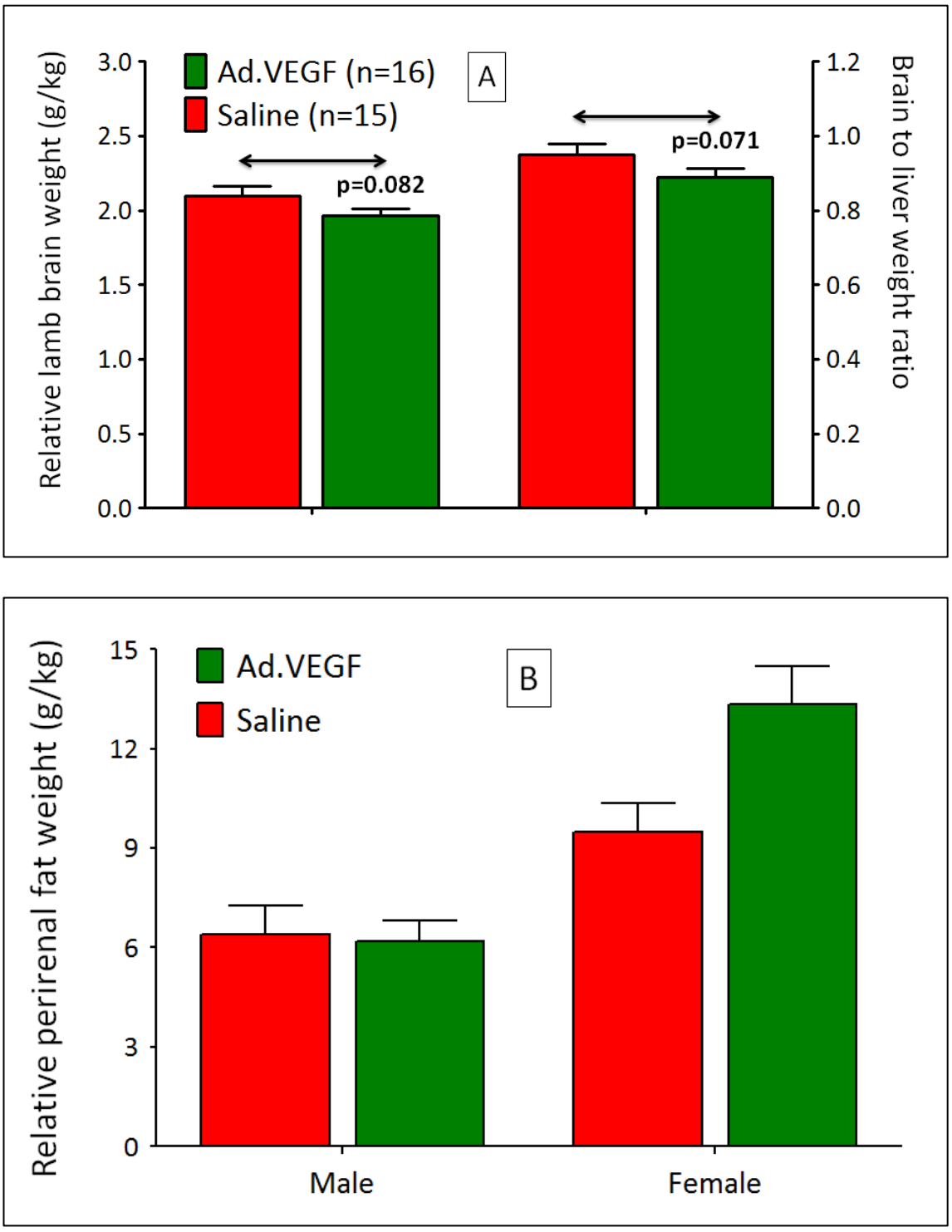

Relative lamb brain weight, brain to liver weight ratios [A] and relative perirenal fat weight [B] at necropsy at 83±0.2 days postnatal age in 31 surviving prenatally growth-restricted lambs whose overnourished adolescent mothers received mid-gestation bilateral uterine artery injections of Ad.VEGF or saline. Relative perirenal fat data is presented separately by gender as it was greater in females versus males (p<0.001) with a significant treatment/sex interaction.

weights were significantly higher in female versus male lambs (11.68±0.908 vs. 6.29±0.514 g/kg, p=<0.001) and tended also to be higher in Ad.VEGF versus Saline groups (p=0.055). In keeping with the pattern seen for absolute perirenal fat weight, there was a significant interaction between treatment group and gender, such that relative perirenal fat weight was highest in the Ad.VEGF-treated female lambs (p=0.042), illustrated in Figure 5.21B. By contrast, there were no significant treatment group or gender differences in relative liver weight when these were expressed per kg of lamb body weight, indicating proportionate shifts in hepatic growth. Weight of the blood following exsanguination (an index of circulating blood volume and/or density of its cellular components) was lower in females than males (p<0.001) and tended also to be lower in Ad.VEGF versus Saline groups, with no significant interaction between treatment and gender. Relative hock weight tended to be higher in Ad.VEGF versus saline-treated lambs (p=0.084), providing further evidence of increased musculoskeletal mass.

5.3.9.4 Gross abnormalities

Several anomalies were found during the course of the lamb dissections. The lamb in the Ad.VEGF group which contracted pneumonia in the eleventh week of life was noted to have macroscopically abnormal lungs weighing 810g (which was more than 2 standard deviations above the 610g mean). Histological examination revealed diffuse collapse with eosinophil infiltrate around the airways and blood vessels. A second lamb in the Ad.VEGF group, which had followed an uneventful postnatal course, was found to have an enlarged heart at necropsy, weighing 530g (greater than 7 standard deviations above the 282g mean). When examined histologically the myocardium appeared hyperplastic but otherwise normal and this was presumed to have been secondary to a congenital abnormality e.g. valvular stenosis or septal defect. A third lamb in the Ad.VEGF group was found to have a hydrocoele of the right testicle and one lamb in the Saline group had discordantly sized testes. Both these gonadal defects have been observed on multiple occasions in lambs during the course of previous research studies and consequently were not unexpected.

5.4 Discussion

5.4.1 Ad.VEGF increased fetal growth velocity

The most important finding of this study was that the positive effect of Ad.VEGF therapy on fetal growth velocity observed in the late gestation study (see Section 4.4.1) was reproduced. Measurements of the fetal AC were once again noted to be greater at 3 and 4 weeks following Ad.VEGF treatment compared with inactive treatment (saline), using an experimental design featuring randomisation and a blind assessor. The change in AC relative to baseline following

Ad.VEGF treatment at these two time points was remarkably similar in this study compared to the late gestation study (75.8±2.16 vs. 75.6±3.62mm, and 93.1±2.57 vs. 92.1±4.31mm, at 3 and 4 weeks, respectively), which adds precision to the estimate of the effect size of Ad.VEGF treatment. In addition to the impact on fetal AC measurements, a simultaneous shift in renal growth was also observed here, which was not seen in the previous study. Measurements of RV were also significantly greater at 3 and 4 weeks in Ad.VEGF compared with Saline groups. Furthermore RV measurements tended to be higher in Ad.VEGF versus Saline groups at >6 weeks post-treatment (p=0.061) at a time when AC measurements were no longer different. This thesis has introduced RV as a novel marker of ovine fetal growth (discussed extensively in Chapter 3). RV correlates well with fetal weight in late gestation irrespective of the degree of FGR and is technically easier to measure than the AC, which becomes increasingly variable towards term. This may explain the tendency towards higher RV in Ad.VEGF versus Saline groups at 133 days gestation. Comparison of the change in AC and RV measurements relative to baseline between Ad.VEGF and Saline groups indicated that Ad.VEGF treatment increased renal growth by 23.2% and 17.1% and abdominal growth by 16.4% and 14.8%, at 3 and 4 weeks post-treatment, respectively. The potential clinical significance of an ~18% increase in fetal growth (on average) over a 3 to 4 week period is discussed in Chapter 7. Notably, despite randomisation, fetuses allocated to the Ad.VEGF group had lower initial mean umbilical artery pulsatility indices than those allocated to the Saline group. As mid-gestation UA PI values are negatively correlated with term birth weight (see Section 3.3.6) this suggests that these pregnancies were more compromised at baseline and the fetuses were tracking to be smaller, which is consequently biased against the hypothesis that Ad.VEGF would improve fetal growth.

5.4.2 Ad.VEGF tended to increase birth weight and gestation length

As stated above, when fetal growth was reassessed using ultrasound at 133 days gestation there were no significant differences between study groups in fetal AC measurements but there remained a tendency towards higher RV measurements in fetuses of Ad.VEGF- relative to saline-treated ewes (p=0.061). After spontaneous delivery near to term, lamb birth weight and abdominal girth (which directly reflects the ultrasonograhic AC measurement) also tended to be higher in Ad.VEGF versus Saline groups (p=0.081), in keeping with the late gestation ultrasound findings. RV measurements at 133 days gestation correlated strongly with lamb birth weight at ~141 days gestation, irrespective of study group (r=0.825, n=29, p<0.001), reinforcing the strength of the RV ultrasound parameter as a predictor of lamb birth weight. The mean increase in lamb birth weight in the Ad.VEGF relative to the Saline group was 681g (approximately 20%) which was in agreement with the 18% shift in fetal growth by ultrasound.

It is interesting that the significance level of the group comparison was so strongly affected by the presence of a particularly large lamb in the Saline group (see Section 5.3.4.1). This highlights the challenges of working with a paradigm in which only 52% of pregnancies are expected to exhibit a major degree of FGR (Wallace et al. 2004b), wherein Ad.VEGF would only be expected to exert a therapeutic effect in one half of all cases treated. The combination of maternal overnutrition and the failure to induce placental insufficiency can on occasion produce a fetus or lamb of even greater size than in moderate (control) intake pregnancies, which introduces a large degree of variability in the overnourished group. This could potentially have masked the true effect of treatment in the smallest fetuses. In the late gestation study the inclusion of a contemporaneous group of control-intake ewes meant that the proportions of markedly growth-restricted fetuses could be determined with a reasonable degree of certainty and compared between Ad.VEGF and Saline/Ad.LacZ-treated groups. The lack of genetically matched control-intake ewes in the present study meant it was not possible to do this and an attempt to use historical control data for lambs born near term did not reveal any significant differences in the proportions of marked growth-restricted versus non-FGR lambs. Physical measurements at the time of birth (abdominal girth and biparietal head diameter) also tended to be greater in Ad.VEGF versus Saline groups, suggesting proportionate increases in brain and somatic growth. This would seem to imply that Ad.VEGF had no effect of fetal brain sparing herein, however at 3 months of age there was evidence at post-mortem examination to the contrary (see Section 5.4.6).

There was a tendency towards increased placental efficiency following Ad.VEGF treatment in agreement with the findings of the late gestation study, in which fetal to placental weight ratio was found to be significantly greater in Ad.VEGF-treated overnourished versus control-intake pregnancies (see Section 4.3.4.2) accompanied by an upregulation in the caruncular expression of VEGF receptors FLT1 and KDR relative to Saline/Ad.LacZ-treated overnourished pregnancies (see Section 4.3.5.7). However, in the present study, maternal plasma oestradiol-17β levels were equivalent in both groups throughout gestation, suggesting that Ad.VEGF did not impact placental secretory function. Other possible mechanisms behind increased placental efficiency include increased placental vascularity or transport capacity, as discussed in Chapters 4 and 7.

There was also a tendency towards increased gestation length in Ad.VEGF versus Saline groups ($p=0.074$). During lambing, considerable neonatal complications are associated with as little as two to three days' prematurity (Wallace JM, personal communication). However with regards to human pregnancy it could be argued that, even if this represents a true effect of prenatal Ad.VEGF gene therapy, a mean difference of two days (0.01 gestation, equivalent to four days

in the human) is unlikely to be of major clinical significance. Importantly, the tendency towards increased birth weight in the Ad.VEGF group was not explained only by this slight prolongation of pregnancy, as the significance levels for the birth weight differences did not change greatly after correcting mathematically for gestation length (p=0.084 versus p=0.081).

5.4.3 Ad.VEGF increased absolute postnatal growth rates to weaning

The original hypothesis was that the potential mitigation of FGR by Ad.VEGF treatment would result in an attenuation of the catch-up growth that is characteristic of this ovine paradigm. Consequently it was a relatively surprising observation that lambs born following Ad.VEGF continued to grow at a faster rate during the first 12 weeks and hence were significantly larger than their saline-treated counterparts from 6 weeks of age onwards. Interestingly this increase in postnatal growth was apparent when expressed in absolute terms, but not when expressed as a fraction of lamb birthweight. This suggests that there was no disassociation of the normal positive relationship seen between initial weight and fractional growth velocity. Previously, when the postnatal growth trajectories of small lambs born to overnourished mothers were compared with those of normally grown offspring from control-intake pregnancies, absolute growth rates to weaning were not significantly different (368±13.4 vs. 359±10.9 g/day, $p>0.05$), indicating that lambs born following FGR were indeed catching up in early postnatal life (Wallace et al. 2010a). As a result fractional growth rates were higher in prenatally growth-restricted lambs ($p<0.001$) and these differences were more pronounced in male lambs compared to females: 11.2 vs. 6.6 and 9.1 vs. 6.8%/day, n=9 and 16, respectively (Wallace et al. 2010b). In the present study mean fractional growth rates in the Ad.VEGF group (10.0%) were similar in magnitude to that previously observed in lambs born to (untreated) overnourished mothers (10.1%), suggesting that the increased absolute postnatal growth rates following Ad.VEGF treatment herein were not excessive relative to baseline and probably just reflected the relative size advantage of these lambs at birth (p=0.081), magnified as the weeks went on. Measurements of abdominal girth and shoulder height followed a similar pattern to lamb body weight, with significant differences between Ad.VEGF and Saline groups at various time points between birth and necropsy at 12 weeks. Measurements of shoulder height began to plateau after ~7 weeks, following which there were no further significant differences between groups. Relative to lambs of control-intake dams, prenatally growth-restricted lambs have been shown to have significantly reduced girth and shoulder height up to 68 days of age, with gender differences beginning to emerge from 58 days postnatal age (Wallace et al. 2013). In the present study no significant male/female differences were evident for these parameters.

5.4.4 Ad.VEGF increased glucose-stimulated insulin secretion / NEFA suppression

A further hypothesis was that mitigation of FGR by Ad.VEGF treatment would result in an attenuation of the increased glucose-stimulated insulin secretion that is characteristic of this ovine paradigm. However, surprisingly, in the present study there was a significant *increase* in insulin secretion, reflected by a greater insulin AUC following an intravenous glucose tolerance test in Ad.VEGF versus Saline groups. This appeared to relate to a greater second phase insulin response, as significant differences at individual time points did not become apparent until 25 minutes following glucose administration. Insulin secretion has been shown to be biphasic in rats and humans with a brief spike lasting approximately 10 minutes, followed by a more sustained response, although the usefulness of distinguishing between them is questionable, given that both phases appear to be impaired in diabetes (Gerich 2002). With respect to the glucose curves, although there were some differences in plasma levels at individual time points, overall glucose AUC did not differ between groups. NEFA AUC was also increased following glucose infusion, although this most likely represents a response to enhanced insulin secretion rather than altered fat metabolism *per se*. Perhaps most reassuringly, there were no significant differences between Ad.VEGF and Saline in any indices of insulin sensitivity, namely insulin AUC : glucose AUC ratio, fasting plasma insulin : glucose ratio or the HOMA index. This suggests that the enhanced insulin secretion seen following Ad.VEGF did not reflect relative insulin resistance, and therefore does not suggest any detriment to the metabolic phenotype, rather an increased capacity to secrete insulin without any alteration in insulin action *per se*. There were also no significant differences in the fasting levels of glucose, insulin, NEFA, glycerol or urea, suggesting that Ad.VEGF had no impact (positive or negative) on basal metabolic function. Interestingly plasma glucose tended to be higher at birth in Ad.VEGF versus Saline groups ($p=0.089$), which was in the expected direction in keeping with improved fetal growth and implies higher transplacental glucose transfer pre-delivery. This finding is also in keeping with the tendency towards increased caruncular GLUT1 expression following Ad.VEGF treatment in the late gestation study (see Section 4.4.7).

5.4.5 Ad.VEGF tended to increase lean tissue mass and bone mineral density

Given the increased absolute growth rates, as discussed above, it became especially important to assess whether this might be a reflection of an associated increase in adiposity, as this might have a bearing on the risk of metabolic syndrome. It has previously been shown that, relative to the normally grown lambs of control-intake ewes, prenatally growth-restricted lambs have reduced BMD ($p<0.02$) and higher percentage total body fat ($p<0.001$) on DEXA examination at 11 weeks of age (Wallace et al. 2010b). It was initially reassuring that despite the increased

growth rates following Ad.VEGF, there were no differences in fat mass or percentage body fat between Ad.VEGF and Saline groups when examined at 11 weeks of age. Rather there was a tendency towards increased BMD, bone mineral content and lean tissue mass in Ad.VEGF versus Saline groups, all of which are in the direction of normal. However, at the point of necropsy at 12 weeks of age there some notable differences in the weight of the perirenal fat depot between groups. As expected, perirenal fat stores were greater in females than males ($p<0.001$) however there were also a tendency towards increased relative perirenal fat weight (g/kg fetus) in Ad.VEGF versus Saline groups and a significant interaction between gender and treatment group. Consequently relative perirenal fat weight was highest in female lambs treated prenatally with Ad.VEGF ($p<0.001$). This appears to indicate that females may be more sensitive to putatively enhanced nutrient supply *in utero*, although there were no gender differences in fetal growth velocity or lamb birth weight in the present study. No significant gender differences in fat deposition have previously been observed in response to increasing fetal nutrient supply in late gestation sheep pregnancy, which is largely under the regulation of insulin and leptin (Muhlhausler et al. 2002; Muhlhausler et al. 2003), neither of which were influenced by Ad.VEGF treatment in the present study. However it seems more likely that this relative increase in perinatal fat mass was established during fetal rather than neonatal life as the perirenal fat depot is largely laid down in late pregnancy. Irrespective, there was no evidence that female and/or Ad.VEGF-treated lambs had a worse metabolic profile than male and/or saline-treated lambs. Furthermore the perirenal fat is but one of several major fat depots in the body and it is a potential limitation of this study that the effect of Ad.VEGF on overall adiposity was not assessed beyond this individual proxy measure. It is interesting that the DEXA assessment of body fat did not reveal any differences between Ad.VEGF and Saline groups, although notably it also failed to detect gender differences, which have previously been shown at this stage of life (Carr et al. 2012). Furthermore, DEXA is less sensitive than measurement of the dissected fat depot at necropsy.

Ultimately it would be necessary to follow-up the offspring for a longer period to see whether any changes in relative adiposity persisted into adulthood and/or were associated with an adverse phenotype. Perhaps reassuringly, it has recently been shown that feeding an optimum diet (as opposed to ad libitum feeding) in the postnatal period can reverse the adverse metabolic phenotype in female but not male lambs following FGR induced by overnourishment of adolescent dams (Wallace et al. 2012). Consequently if Ad.VEGF does increase relative adiposity in females, it may be easier to ameliorate through dietary modification than in males.

More positively, Ad.VEGF therapy tended to increase lean tissue mass and BMD. The latter has

been shown to be reduced both in human FGR (Verkauskiene et al. 2007) and in this particular animal model (Wallace et al. 2010b). In the late gestation study, Ad.VEGF had no demonstrable effect on skeletal growth as assessed by serial ultrasound measurement of the femur and tibia, and by direct measurement of the same bones at necropsy. In the present study, there was no effect of Ad.VEGF on length or weight of the tibial bone at 12 weeks of postnatal age. Together these findings imply that although skeletal size is not affected, there may be an improvement in the quality of the skeleton, perhaps through increased bone mineralisation. The timing of this potential improvement in BMD (e.g. prenatal versus postnatal) is however not known. There was also a tendency towards higher lean tissue mass by DEXA in Ad.VEGF versus Saline groups, irrespective of gender. This was in keeping with significantly increased residual carcass weights at postnatal necropsy, reflecting musculoskeletal mass. Despite the female-specific effects on relative perirenal fat weight discussed above, this suggested that increased absolute postnatal growth rates of the Ad.VEGF-treated lambs reflected enhanced lean tissue accretion.

5.4.6 Ad.VEGF tended to mitigate brain sparing / disproportionate adrenal growth

In this study no data was available on serial ultrasound fetal BPD:AC ratios as head measurements were not included in the set of measurements taken at ultrasound examination. Furthermore there were no significant differences between groups in the ratio of biparietal head diameter (measuring using calipers) to abdominal girth at the time of birth. However, despite this lack of early evidence of a mitigating effect of Ad.VEGF on fetal brain sparing, at the point of necropsy at 12 weeks gestation there were some clues that this had taken place, presumably during prenatal life. There was a tendency towards reduced relative fetal brain weights and brain to liver weight ratios in Ad.VEGF versus Saline groups, which mirrored what had been observed at necropsy in late gestation (see Section 4.3.4.5). Although there were no control-intake pregnancies here to directly compare with, this is in keeping with an attenuation of the fetal brain sparing effect, which likely reflects a reduced need for fetal adaptation and is therefore an encouraging finding (Section 4.4.2). Furthermore at postnatal necropsy there was also a reduction in the relative adrenal weight in Ad.VEGF relative to Saline groups. This was once again in keeping with what had been observed at fetal necropsy in the late gestation study and may represent an attenuation of the accelerated maturation of the adrenal gland that is characteristic of this and many other animal models of FGR. Interesting there was a negative correlation between relative adrenal weight and gestation length in the Saline group ($r=-0.658$, $n=15$, $p=0.020$), suggesting that the greater the relative size of the adrenal, the earlier spontaneous delivery occurred. In spite of the lack of any measurable differences in plasma cortisol between control- and high-intake ewes when previously

measured at ~128 days gestation (Wallace et al. 2000), this supports the concept of a functional relationship between premature activation of the hypothalamic-pituitary-adrenal axis and the initiation of labour in this paradigm. Interestingly there appeared to be a dissociation of this relationship following Ad.VEGF treatment (r=-0.246, n=16, p=0.376), which is in keeping with the slightly increased gestation length seen in this group. Incidentally it is currently not known whether an increase in plasma cortisol occurs between 128 and 145 days gestation, in overnourished pregnancies as the associated prematurity precludes a comprehensive assessment nearer to term.

5.4.7 Ad.VEGF was not associated with any complications in the perinatal period

As in the previous study there were no adverse responses of the mother or fetus to the injection or occlusion procedure and all Ad.VEGF-treated pregnancies continued until term, following an uncomplicated course. At delivery particular attention was paid to blood loss at delivery as a theoretical association between enhanced uterine blood flow and postpartum haemorrhage was anticipated. No such complications were encountered. Furthermore there were no unexpected problems in the neonatal period and no significant differences in the level of neonatal care required to ensure lamb survival. Fetal serum biochemistry and liver function were not altered. The latter observation was particularly reassuring as there is a particular concern that adenovirus vectors can induce liver inflammation (Worgall et al. 1997), although it does not appear that any fetal transfer of the vector occurs following administration during sheep pregnancy (David et al. 2008). Furthermore, as the hepatic transaminases are acute phase reactants and are often raised non-specifically in illness, low levels are suggestive of an absence of systemic inflammation. Collectively the above observations support the safety of Ad.VEGF as a prenatal therapy.

5.4.8 Ad.VEGF did not impact upon colostrum quantity, quality or antibody levels

In the sheep, the functional development of the mammary gland is virtually complete by the end of gestation, with negligible growth observed postnatally (Anderson 1975). Gestational mammary development is nutritionally sensitive, since maternal undernutrition results in a reduction in mammary weight at term (Swanson et al. 2008) and vascularity within the gland is also influenced by maternal diet, and in particular its selenium content (Vonnahme et al. 2011; Neville et al. 2013). It was considered that Ad.VEGF therapy might potentially have an effect on mammary gland development via two different mechanisms: (1) directly by systemic spread of the vector or raised plasma VEGF levels secondary to over-expression; or (2) indirectly through enhanced placental secretory function. However in this study it did not appear that Ad.VEGF

had any effect on the growth, development or function of the mammary gland as there were no significant differences in the colostrum yield, nutrition composition, IgG concentration or IgG content. This in agreement with the lack of any measurable change in circulating levels of oestradiol-17β levels throughout the second half of pregnancy following Ad.VEGF treatment, as mammary development is principally driven by oestrogen (Flint & Knight 1997). The positive correlation between placental size and colostrum yield seen herein illustrates the importance of placental secretory function for physiological mammary development. Although colostrum IgG and nutrient concentrations are unperturbed in this paradigm, the reduction in placental size and overall colostrum yield translates into large differences in IgG and nutrient content. This is important because it is the total volume of colostrum available to the lamb that matters with respect to the provision of passive immunity. In the present study 9 of 32 (28%) live born lambs required the use of donor colostrum to meet the minimum requirement of 50ml/kg body weight. The outlook for these lambs without supplementation would probably have been poor. However the provision of pooled donor colostrum appeared to be effective, given that plasma IgG levels were unrelated to birth weight by 24 hours of age ($r=0.094$, $n=32$, $p=0.615$). Moreover this suggests that early function of the neonatal gut is relatively unimpaired in these prenatally growth-restricted lambs and that the absorptive capacity was sufficient to normalise circulating IgG levels within 24 hours. This is in keeping with the lack of any differences in fetal small intestinal crypt cell proliferation and an increase in relative small intestinal weight in overnourished versus control-intake pregnancies within the late gestation study (see Sections 4.3.5.2 and 4.3.4.5, respectively), which suggests that there is a relative preservation of gut development (similar to that seen in the brain) in the face of a reduced fetal nutrient supply.

5.4.9 Ad.VEGF did not influence the inflammatory response to routine vaccination

In the present study there were no significant differences between groups in the levels of serum amyloid A, an acute phase reactant that is released in response to infection and inflammation, at baseline or at 24 or 48 hours following routine vaccination with a combined Clostridium and Pasteurella vaccine. Interest in serum amyloid A levels in relation to postnatal growth and metabolism has been stimulated by previous observations of an association with both obesity (Zhao et al. 2010) and insulin resistance (Leinonen et al. 2003). The lack of any effect of Ad.VEGF on serum amyloid A levels is therefore in keeping with the absence of any excessive adiposity or insulin resistance, both of which are reassuring, along with the adequate serum IgG levels at 24 hours and absence of any evidence of hepatic inflammation at 7 days of age (Sections 5.3.4.3 and 5.3.4.6). When previously measured in this FGR paradigm in lambs of the same age, peak serum amyloid A levels were increased in prenatally growth-restricted

relative to normally grown lambs (357±42.4 vs. 219±49.0mg/l, p=0.005) and were also greater in males than females (356±53.3 vs. 233±41.1mg/l, p=0.014) (Carr et al. 2012). By contrast, in the present study no gender differences were present. Interestingly, when immune response to vaccination was previously re-tested at 13 weeks postnatal age, differences by prenatal nutrition tended to be in the opposite direction (69±13.4 vs. 141±34.9mg/l, p=0.051) and serum amyloid A levels were independent of gender (Carr et al. 2012). This appears to suggest an alteration in the ontogeny of the immune system following prenatal growth restriction. It is unknown whether Ad.VEGF might have impacted immune responses at a later gestation as no comparable data at 13 weeks was available for the present study. However it would seem unlikely given the lack of any clear difference when examined at 6 weeks.

5.5 Conclusions

Mid-gestation delivery of Ad.VEGF gene therapy in FGR pregnancies induced by overnourishing adolescent sheep dams resulted in a significant increase in fetal growth velocity at 3 and 4 weeks post-treatment and tended to increase gestation length by approximately two days. Pregnancies following Ad.VEGF tended to have increased placental efficiency, and lambs tended to be heavier at birth with greater abdominal girth and higher plasma glucose. Ad.VEGF had no effect on colostrum quantity or quality and there were no differences in the level of neonatal care required to ensure lamb survival between groups. Absolute postnatal growth rates were increased following Ad.VEGF but fractional growth velocity was unaltered. There was no effect on the immune response to routine vaccination. Ad.VEGF-treated lambs demonstrated increased insulin secretion and NEFA suppression following an intravenous glucose challenge. However fasting levels of glucose, insulin, urea, NEFA and glycerol were unchanged, as were the insulin to glucose ratios and HOMA indices, suggesting that this observation was not due to insulin resistance. On DEXA analysis lean tissue mass and bone mineral density/content tended to be increased. At necropsy at ~12 weeks postnatal age, relative perirenal fat stores were increased in Ad.VEGF-treated female but not male lambs. Otherwise there appeared to be enhanced lean tissue accretion which, along with the increased glucose-stimulated insulin secretion, likely represents a greater anabolic drive in the Ad.VEGF-treated animals. Whether this simply reflects their relative size advantage at birth or some form of intratuerine programming effect remains unclear, and this is investigated and discussed further in Chapter 6.

Chapter 6

Epigenetic Status of Growth Related Genes in Hepatic Tissues of Fetuses and Lambs Following Fetal Growth Restriction & Prenatal Ad.VEGF Gene Therapy

6.1 Introduction

This chapter describes a programme of work to evaluate the impact of FGR and Ad.VEGF gene therapy upon the epigenetic status of key genes related to postnatal growth and metabolism.

6.1.1 Background

As discussed in Section 1.1.3.8, FGR and its proxy measures small-for-gestational age (SGA) and low birth weight (LBW) are associated with an increased risk of adult cardiovascular, renal and metabolic diseases. Several different mechanisms for this "intrauterine programming" effect have been proposed, which can broadly be considered as structural, functional or epigenetic in nature - currently much attention is focused on the latter because of the implications for the long term health of the affected individual (Santos & Joles 2012).

Epigenetic modifications result in changes in gene expression in the absence of any alteration in the actual DNA sequence. There are three main processes involved in epigenetics, namely DNA methylation, histone modification and microRNAs. These mechanisms appear to work in concert with one another and have been comprehensively reviewed by (Chen & Zhang 2011). It has been demonstrated that changes in the intrauterine environment can influence the fetal epigenome resulting in an altered phenotype for a given genotype. This is perhaps best illustrated by the seminal experiments using the agouti mouse, in which variable dietary methyl supplementation of the mother resulted in a range of different offspring phenotypes (coat colours) secondary to variable DNA methylation (Wolff et al. 1998; Cooney et al. 2002).

DNA methylation is by far the best characterised epigenetic mechanism. It occurs at specific palindromic sequences in which a cystosine (C) residue is directly followed by a guanine (G). These pairings are termed CpG dinucleotides - the intervening "p" is used to distinguish this pairing from the complementary CG pairing between the sense and anti-sense strands of DNA. CpG dinucleotides occur non-randomly throughout the genome, usually within short stretches of G:C-rich and CpG dense DNA, which are termed CpG islands. CpG islands often occur close to or within the promoter regions of genes. The cytosine residue within CpG dinucleotides will occasionally covalently acquire a methyl group at its 5-carbon position. The overall degree of methylation at the C residues within CpG islands is highly variable between different genomic regions and between different cell and tissue types. By contrast, cytosines outwith CpG islands

are usually unmethylated throughout most of the genome. This is partly due to the fact that there is a high rate of spontaneous decay of methylated cytosines to uracil, following which the DNA repair process consistently replaces them with a unmethylated cytosine such that the natural tendency overall is towards a state of demethylation. Consequently it is believed that maintenance of DNA methylation at certain sites is an active process mediated by the DNA methyltransferases (Delcuve et al. 2009). Methylated cytosines inhibit the attachment of various transcription factors, both directly and indirectly through forming bonds with methyl-CpG-binding domain (MBD) proteins (Kass et al. 1997) - illustrated in Figure 6.1. Consequently hypermethylation is associated with reduced gene expression or gene silencing, whilst relative hypomethylation is associated with enhanced gene expression. In addition to its putative role in intrauterine programming, DNA methylation is the mechanism behind genetic imprinting, whereby one parental allele is silenced by hypermethylation. Imprinting may be physiological, as occurs in the fetal H19 and IGF-2 genes, or pathological, for example as seen in Silver-Russell syndrome (Rossignol et al. 2008). There is also recent evidence that exposure to environmental toxins *in utero* such as nicotine (Wang et al. 2011b) and alcohol (Resendiz et al. 2013) can have directly harmful effects on CpG methylation. Aberrant DNA methylation is also seen in some other disease states and is especially important in cancer biology (Dawson & Kouzarides 2012).

Histone modification and miRNAs contribute an additional layer of epigenetic control. Histones are octameric globular protein structures around which DNA is coiled to form nucleosomes, which are packaged together as chromatin, a relatively dense aggregation of DNA and protein. The accessibility of transcription factors, DNA helicase, RNA polymerase and other proteins involved in the regulation of gene expression can be facilitated or impeded by the modification of the histones on their tail ends, which protrude out of the nucleosomes. Such modifications can occur biochemically by way of methylation, acetylation, phosphorylation, biotinylation, ubiquitination and ADP-ribosylation (Munshi et al. 2009). MicroRNAs (miRNAs) are relatively short non-coding sequences of single-stranded RNA that combine with mRNAs in a specific fashion, resulting in their degradation or inhibition of their translation into proteins (Chuang & Jones 2007). Unlike the other two mechanisms, the miRNAs act at a post-transcriptional level.

The work detailed in this chapter focused on assessment of DNA methylation in various genes of interest. There are currently numerous different approaches that can be used to assess DNA methylation. At the most basic level, global DNA methylation can be determined in any tissue by quantification of mRNA expression of DNA methyltransferases using qRT-PCR or detection of 5-methyl-cytosine residues by means of immunohistochemistry or DNA dot blot analysis (Grazul-Bilska et al. 2011). Unfortunately these methods do not give any information about

Figure 6.1 – Putative effect of DNA methylation on gene expression

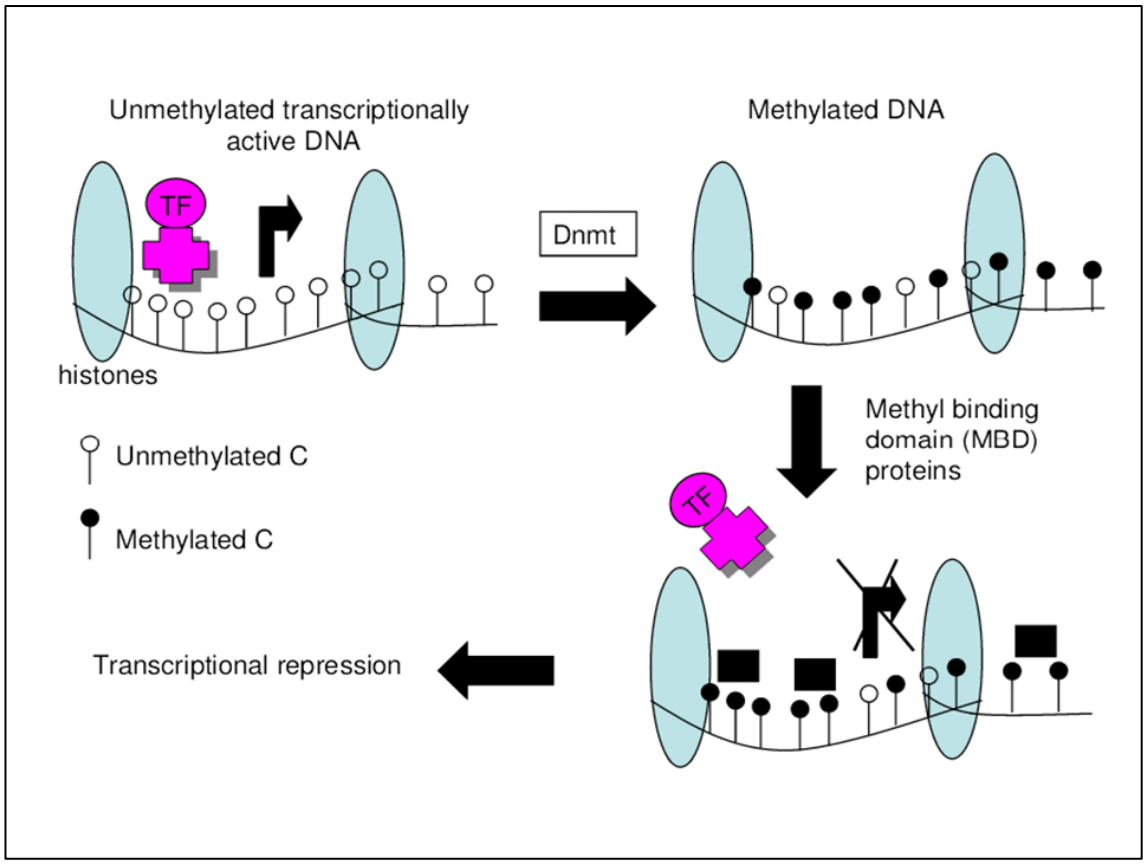

Diagram illustrating unmethylated DNA, which allows transcription factors (TF) to bind freely, compared with methylated DNA following the action of DNA methyltransferases (Dnmt). Methylated DNA allows methyl binding domain (MBD) proteins to bind, which obstruct the access of transcription factors resulting and thereby inhibit gene expression. Figure reproduced with permission from a presentation by Dr Mandy Drake, Scottish Senior Clinical Fellow and Honorary Consultant in Paediatric Endocrinology, University of Edinburgh.

---

which individual genes might be differentially methylated. More specific information can be gained by interrogating individual CpG sites. Broadly speaking this can either be achieved by methyl-specific PCR or by a bisulphite sequencing method. Methyl-specific PCR necessitates two reactions using different sets of primers, one which amplifies methylated DNA at the site of interest and one which amplifies unmethylated DNA. The ratio between the amount of PCR product from the two reactions can then be calculated, however as they are run separately there may be amplification bias or other inequalities. An extension of this technique called Methylight uses an additional oligonucleotide probe to increase the sensitivity and specificity

(Trinh et al. 2001). However both these approaches are limited by the fact they quantify the amount of fully methylated relative to fully unmethylated DNA, and are unable to distinguish variable degrees of methylation between these two states. The ability to detect more subtle shifts in methylation is particularly important within the field of intrauterine programming as the somatotrophic axis genes are unlikely to be turned completely on or off (like, for example, proto-oncogenes or tumour suppressor genes, respectively (Teodoridis et al. 2005)) but rather may be expected to exhibit relative degrees of hyper- or hypomethylation sufficient to differentially impact gene expression. Bisulphite sequencing methods have the advantage that individual CpG sites can be investigated at high resolution. Sodium bisulphite is a compound that actively degrades unmethylated cystosines to uracils (which are then converted to thymine during subsequent PCR) whilst leaving methylated cytosines intact (Hayatsu 2008). This effectively creates a C / T single nucleotide polymorphism at each CpG site, where methylated cytosines are represented by "C"s and unmethylated cytosines by "T"s. This is illustrated in Figure 6.2. The C / T ratios can then be examined by one of a number of different methodologies including pyrosequencing, Sequenom™ MassArray™, immunoprecipitation or cloning followed by direct sequencing.

Pyrosequencing is a technique in which a sequencing primer is hybridised to the PCR amplicon and combined with four enzymes (DNA polymerase, ATP sulphurylase, luciferase and apyrase) and two substrates (adenosine 5' phosphosulphate (APS) and luciferin) - see Marsh (2007) for an overview. The expected order of bases of the amplicon is inputed into the sequencer to calculate the dispensation order of deoxyribonucleotide triphosphates (dNTPs) that are added into the reaction sequentially. For example, if an adenosine residue were to be expected next then the complementary dNTP, in this case deoxyribothymidine triphosphate (dTTP), would be added and would be incorporated into the DNA strand, catalysed by DNA polymerase. This reaction is accompanied by the release of an equimolar amount of pyrophosphate (PPi), which is then converted to ATP by ATP sulphurylase in the presence of APS. The resultant ATP triggers the conversion of luciferin to oxyluciferin by luciferase, which emits a quantity of visible light that is proportional to the amount of ATP/dNTP/nucleotide present. The amount of light detected is illustrated as a "pyrogram", on which the height of each peak indicates the number of nucleotides incorporated. Meanwhile the apyrase mops up any unincorporated nucleotides and ATP ready for the addition of the next dNTP according to the predetermined dispensation order. The general pyrosequencing reaction is illustrated in Figure 6.3. With respect to CpG dinucleotides, these can be specifically highlighted where these occur within the dispensation order as a "Y", indicating that a mixture of C and T nucleotides (representing methylated and unmethylated cytosines, respectively) of unknown proportions is expected.

Figure 6.2 – Effects of sodium bisulphite conversion on CpG dinucleotides

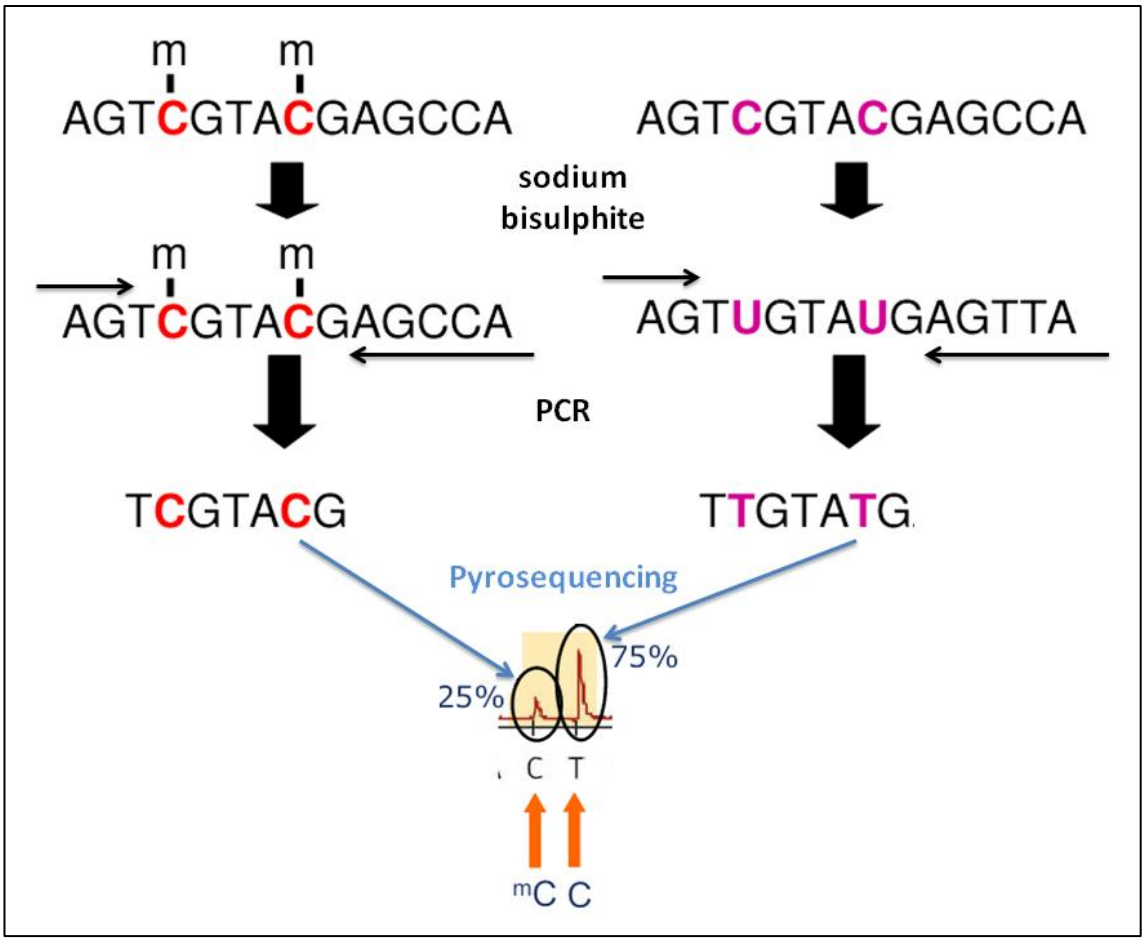

Illustration of the differential effects of sodium bisulphite on methylated (red) and unmethylated (pink) cytosine (C) residues within CpG dinucleotides. Unmethylated cytosines are degraded to uracil (U) whilst methylated cytosines are preserved. During subsequent polymerase chain reaction (PCR), uracil is converted to thiamine (T) whilst cystosine remains unchanged. Primers (black arrows) specifically designed to avoid CpG sites amplify all template DNA resulting in a mixture of Cs and Ts at the CpG sites of interest within the amplicon. The ratio of C : T is proportional to the amount of methylated and unmethylated sites, respectively, and can be quantified by pyrosequencing and measurement of the relative height of the two peaks. Figure adapted with permission from a presentation by Dr Mandy Drake, Scottish Senior Clinical Fellow and Honorary Consultant in Paediatric Endocrinology, University of Edinburgh.

The pyrosequencer will release the complementary dNTPs into the reaction in close succession. The proportion of C to T present can be determined by the measuring the ratio of the two peaks on the pyrogram and reflects percentage DNA methylation at that locus.

Figure 6.3 – Pyrosequencing

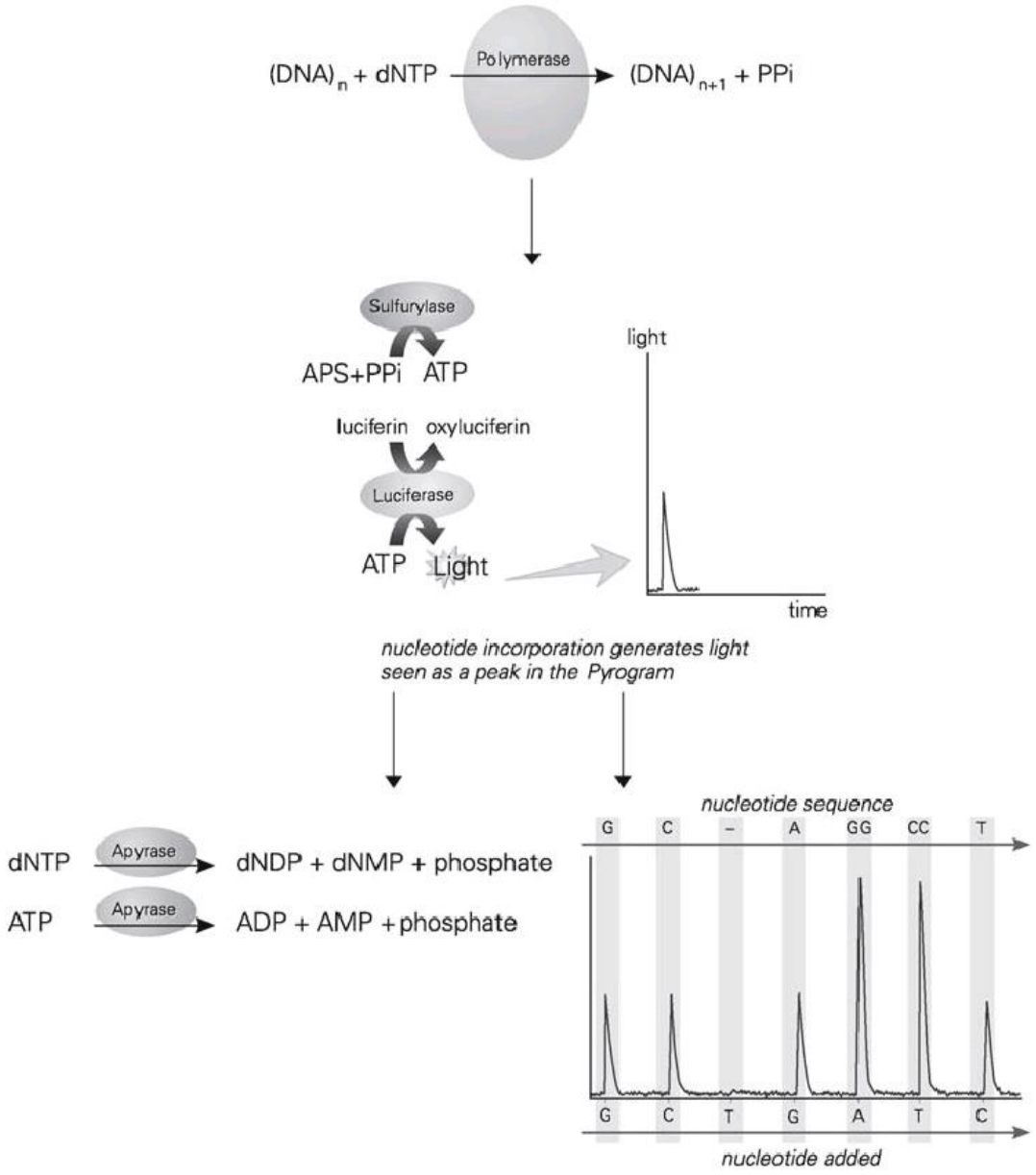

Diagram illustrating the various chemical reactions involved in the pyrosequencing process - please see text for full explanation. Abbreviations: DNA = deoxyribonucleic acid; dNTP = deoxyribonucleotide triphosphate; PPi = pyrophosphate; APS = adenosine 5' phosphosulphate; ATP = adenosine triphosphate; dNDP = deoxyribonucleotide diphosphate; dNMP = deoxyribonucleotide monophosphate; ADP = adenosine diphosphate; AMP = adenosine monophosphate; G = guanine; C = cytosine; A = adenosine; T = thymine. Figure reproduced with permission from Marsh (2007).

Assessment of gene-specific, as opposed to global, DNA methylation during sheep pregnancy is limited to only a few reports to date, with most epigenetic studies using other species such as rodents. Reports relating to sheep models of FGR are detailed in the Discussion (Section.6.4). However, it is clear that maternal nutrition in general can impact fetal DNA methylation. For example, DNA methylation of IGF2R and H19 is increased in sheep dams fed a diet comprised of alfalfa haylage compared with corn (Lan et al. 2013) and moderate maternal undernutrition reduces DNA methlyation of the proopimelacanocortin and glucocorticoid receptor genes in the fetal hypothalamus (Begum et al. 2012).

6.1.2 Aims

The aims of this work were to:

- To identify ovine genes related to postnatal growth and metabolism that contain one or more CpG islands according to conventional definitions
- To work up functioning assays to quantify the degree of methylation at specific CpG sites within these CpG islands using bisulphite conversion, PCR and pyrosequencing
- To determine if DNA methylation patterns in growth related genes differ between growth-restricted and normally grown fetuses of overnourished and control-fed adolescent ewes
- To examine for any changes in methylation status of growth related genes associated with maternal Ad.VEGF gene therapy in late gestation fetuses and in postnatal lamb tissues
- To evaluate whether there are any differences in DNA methylation patterns in growth related genes between male and female fetuses and lambs

6.2 Methods

DNA extraction and sodium bisulphite conversion was performed at University College London. PCR and pyrosequencing were performed in collaboration with The Genome Centre at Barts and the London School of Medicine and Dentistry, Queen Mary University London.

6.2.1 Identification of CpG islands

Genomic DNA sequences for various ovine genes relevant to postnatal growth and metabolism were searched for in the US National Center for Biotechnology Information (NCBI) Nucleotide database. All available sequences were imported into Methyl Primer Express® software version 1.0 (Applied Biosystems, Foster City, CA, USA) to determine the presence or absence of CpG islands according to the following criteria:

- Length >200bp
- GC content >55%
- Observed : expected CpG ratio (= no. of CpG / no. of C x no. of G) >0.65

The original criteria for GC content and observed : expected CpG ratios were >50% and >0.60 (Gardiner-Garden & Frommer 1987) however it has been proposed that increasing the cut-offs to those detailed above makes identification of CpG islands more specific as it is more likely to exclude other GC-rich genomic sequences such as Alu repeats, which are repetitive elements that occur in non-coding regions (Takai & Jones 2002). It has also been recommended that the minimum length be increased to >500bp, however this was not done here due to the relatively short length of the published sheep genomic DNA sequences, and particularly a lack of extensive non-coding sequences in which CpG islands are likely to lie. Nevertheless a total of 24 CpG islands were identified in ten different genes relating to the somatotrophic axis. These are detailed in Table 6.1 and gene structures are described below.

6.2.1.1 Insulin and insulin-like growth factor 2

The insulin and insulin-like growth factor (IGF)-2 genes are contiguous and are similar in their structural arrangement and expression profile in sheep and humans (Ohlsen et al. 1994). The human IGF-2 gene contains ten exons. The first seven are non-coding and are alternatively spliced to exons 8, 9 and 10, which together encode the IGF-2 precursor protein. The ovine IGF-2 gene has a similar exonic arrangement, although no equivalent of non-coding exon 2 has been identified. It also appears to lack the proposed CCAAT/enhancer binding protein (C/EBP) site that is located upstream of human exon 1 (van Dijk et al. 1992). The intergenic region between insulin and IGF-2 is approximately 750 nucleotides shorter than in the human and contains a stretch of 85 nucleotides with a particularly high C:G density (96%). There are four putative promotors (P1 to P4), which precede exons 1, 4, 6 and 7, respectively. Of these P3 and P4 are considered to be the major promoters utilised in fetal and non-hepatic adult tissue, whilst P1 is only active in adult liver. The linked insulin gene is comprised of three exons, which lie proximal to IGF-2 exon 1. CpG islands were identified proximal to insulin exon 1 and IGF-2 exons 1, 4, 5, 6, 7, 8, 9 and 10.

6.2.1.2 Insulin-like growth factor 1

The ovine IGF-1 is highly homologous with the human IGF-1 gene, with the exception of a single nucleotide substitution (alanine in place of proline at position 66) and the presence of an additional glutamine residue at the boundary between exons 1 and 2 (Wong et al. 1989).

Table 6.1 – Details of 24 CpG islands identified within the genes of the ovine somatotrophic axis

CpG Island No.	Gene	Accession No.	Length of Gene (bases)	Length of CpG Island (bases)	%CG
1	Insulin Exons 1 to 3	U00659	1520	980	71.4
2	IGF-2 Exon 1	U00659	873	180	71.4
3	IGF-2 Exon 4	U00664	1760	1323	68.8
4	IGF-2 Exon 5	U00664	800	800	68.8
5	IGF-2 Exon 6	U00664	1932	1520	68.8
6	IGF-2 Exon 7	U00665	547	262	68.3
7	IGF-2 Exon 8	U00666	889	440	61.6
8	IGF-2 Exon 9	U00667	611	496	69.0
9	IGF-2 Exon 10	U00668	720	622	59.8
10	IGF-1 Exon 2	X51357	1808	515	55.7
11	IGF-1 Exon 3	X51358	560	496	55.4
12	IGF-1 Exon 3	X69473	573	379	56.2
13	IGF-1 Exon 4	X69474	526	469	55.7
14	H19	AJ566210	8767	1160	64.0
15	H19	AJ566210	8767	818	64.9
16	H19	AJ566210	8767	1502	67.8
17	H19	AJ566210	8767	1939	67.2
18	H19	AJ566210	8767	628	69.4
19	GH	X12546.1	2162	320	55.9
20	GH Receptor Exon 1B	S78252	1379	215	55.8
21	Insulin Receptor	‡	264	226	56.2
22	NRC31	HM204706	4791	2984	65.6
23	IGF1R Exon 3	EF669473	346	343	69.4
24	IGF2R Intron 2 DMR	AY182033	3048	2619	72.3

‡ No accession number available - sequence published by McGrattan et al. (1998)

The IGF-1 gene has five exons. In the sheep there are two known variants of exon 1 (1W and 1A), whilst exon 4 has not been shown to be expressed at all (Dickson et al. 1991). Accordingly ovine IGF-1 mRNA is comprised of exons 1,2,3 and 5, with alternative splicing of the first exon (1/1A/1W). The putative promoter site for IGF-1 is located proximal to exon 1 but is reportedly not GC-rich (Ohlsen et al. 1993) therefore unsurprisingly no conventional CpG island was found at this location in the ovine sequence. However three separate downstream CpG islands were identified preceding exons 2, 3 and 4, respectively.

6.2.1.3 H19

H19 is composed of five exons, separated by four very short intronic sequences. Unlike insulin, IGF-1 and IGF-2, there is little homology with the human gene with respect to its nucleotide sequence, with the exception of specific regions (particularly exon 1), although the overall size and structure of the gene is relatively well conserved (Lee et al. 2002). The H19 gene has a very high GC content, which is characteristic of imprinted genes. There is a differentially methylated region (DMR) upstream of the H19 gene that tends to be predominantly methylated in one of the two parental alleles (Young et al. 2003). Studies in parthenogenetic pregnancies suggest that H19 is paternally imprinted in the sheep (Feil et al. 1998; Hagemann et al. 1998) whilst, conversely, IGF-2 is maternally imprinted (McLaren & Montgomery 1999). Five different CpG islands of reasonable size were identified across the H19 gene, ranging from 620 to 1939 bases in length (see Table 6.1).

6.2.1.4 Growth hormone

The ovine GH gene contains five exons interspersed by four introns and shows 97.5% sequence homology with the bovine form (Orian et al. 1988). It has also been shown that sheep may be homozygous or heterozygous for two different alleles (GH1 and GH2) although the latter is more commonly seen in domesticated breeds (Ofir & Gootwine 1997). Here a single CpG island was identified within the GH gene, preceding and extending into exon 5.

6.2.1.5 Growth hormone receptor

The ovine growth hormone receptor gene is known to contain seven different alternatively spliced untranslated regions. Exon 1A is only expressed in liver and contains a developmentally regulated liver-specific promoter (P1) which lies upstream of the transcription initiation site (Adams et al. 1990). Exon 1B maps upstream of exon 1A and coding exon 2, which contains the translation initiation site. It is differentially expressed across a range of different tissues, predominates in skeletal muscle, and contains a putative second promoter, P2 (Adams 1995).

A single CpG island was identified within the ovine GHR gene, preceding and extending into the non-coding sequence of exon 1B.

6.2.1.6 Insulin receptor

For the insulin receptor gene, a relatively short partial ovine sequence that demonstrates 84% nucleotide homology with human exons 11, 12 and 13 (McGrattan et al. 1998) was examined and a single CpG island identified within the intronic region. This gene also features alternative splicing resulting in two different isoforms with differing specificity for insulin.

6.2.1.7 Glucocorticoid receptor

The glucocorticoid receptor is also known as the nuclear receptor subfamily 3, group C, member 1 (NRC31). An as-of-yet unpublished sequence listed in NCBI Nucleotide database (accession number HM204706.1) which spans both the promoter region and partial coding sequence was examined and a single large CpG island (2984bp) identified within the promoter.

6.2.1.8 Insulin-like growth factor 1 receptor

The human IGF1R gene contains a CG-rich promoter region that lacks conventional TATA and CCAAT elements. The transcription start site is approximately 1000 base pairs proximal to the translation start site (Sepp-Lorenzino 1998). The ovine IGF1R gene is highly homologous with that of other mammalian species and three different allelic sequences have been characterised (Byun et al. 2008). Although the published ovine sequence is relatively short and lacks the long 5' untranslated region of the human gene, nevertheless a single CpG island was identified that precedes and extends into exon 3.

6.2.1.9 Insulin-like growth factor 2 receptor

IGF2R, like H19 and IGF-2, is an imprinted gene that is known to contain an important CpG island located within the second intron, which is known as region 2 in the mouse (Wutz & Barlow 1998) and differentially methylated region (DMR) 2 in the sheep (Young et al. 2001; Young et al. 2003). The CpG island at this location was more GC rich than any of the islands identified within the other nine genes (72.3% - see Table 6.1), which is in keeping with its putative role as a key regulator of IGF2R gene expression via uniparental imprinting.

6.2.2 Primer design

In order to design primers for bisulphite-converted DNA, the genomic DNA sequences first needed to be modified to take into account the genome-wide degradation of unmethylated

cytosine to thymine that is anticipated following bisulphite treatment and PCR. To achieve this DNA sequences were first imported into Microsoft Word (Microsoft Corporation, Redmond, WA, USA). Using the "find and replace" function, all instances of "CG" in the sequence were converted to "X" in order to preserve these particular cytosines, which may or may not be methylated and therefore vulnerable to sodium bisulphite. Next all the remaining "C"s were converted to "T"s in line with the expected effects of sodium bisulphite on unmethylated cystosines. Finally "X"s were converted back into "CG"s and highlighted as regions of interest.

Forward/reverse and sequencing primers, for the PCR and pyrosequencing steps, respectively, were designed within the modified DNA sequences using the PyroMark Assay Design software version 2.0.1.15 (Qiagen, Uppsala, Sweden) and are shown in Tables 6.2 and 6.3. Although PCR and pyrosequencing are completely separate reactions, the software designs all primers together as even a strong PCR product is redundant if no appropriate sequencing primer is able to bind to it during the subsequent step. Potential primer sets generated by the software were ranked according to a scoring system (maximum = 100) taking into account various factors including primer melting and annealing temperatures, risk of hairpin (or other secondary structure) formation and % GC. The ideal length of a PCR product for subsequent pyrosequencing is approximately 100 base pairs. Amplicon length is somewhat of a compromise. On the one hand, shorter amplicons are likely to contain fewer CpG sites for interrogation, limiting the amount of methylation information gained. On the other hand, longer amplicons are more likely to fail the pyrosequencing step. Wherever possible forward and reverse primers that did not include any CpG sites within their sequences were chosen to minimise the chance of any methylation-specific amplification bias.

Primer sets were successfully designed for 21 out of 24 CpG island sequences. Design is more challenging when dealing with bisulphite-converted DNA as the majority of the genetic code is effectively simplified from four to three bases. This means that the risks of primers binding non-specifically to other parts of the genome as well as to the region of interest is increased. Nevertheless primer specificity can be checked at the sequencing stage to ensure an amplicon of the expected size has been produced. As the sense and anti-sense DNA strands are no longer complementary post sodium bisulphite conversion, primer sets for the remaining 3 of 24 CpG islands were designed using the modified reverse DNA sequence as an alternative.

6.2.3 DNA extraction

DNA was extracted from snap-frozen liver samples obtained from necropsy of fetuses at ~131 days gestation and lambs at ~83 days postnatal age (see Sections 4.2.5.2 and 5.2.6).

Table 6.2 – PCR primers for 14 functioning assays interrogating CpG sites in 10 genes of interest

Assay	Target	Primer	Sequence
1	Insulin	Forward	5'-[Biotin]AGTTATGAAGATTTTTAAGGGGGTTTTAT-3'
		Reverse	5'-AAACCCTCCACCCCTAAATTAACCT-3'
2	IGF-2 Exon 1	Forward	5'-[Biotin]ACCTTAATACAACCAAATCACC-3'
		Reverse	5'-ATAGGTATTTGTTTAGGTTATTAT-3'
3	IGF-2 Exon 4	Forward	5'-TTTGGAATTTTTTAAGTTTTATATTGAGGA-3'
		Reverse	5'- [Biotin]ACCCAAACATATAAATCAACAAACTC-3'
4	IGF-2 Exon 6	Forward	5'-GGGTTTTTAAATATTTTAGAATAGTGATT-3'
		Reverse	5'-[Biotin]AACTCCAACCAAAAAAAAACCAAACTTA-3'
5	IGF-1 Exon 2	Forward	5'-GGGAGTGTGTGAAGAGTTGAAT-3'
		Reverse	5'-[Biotin]ACTAAAAAAAAAAATCCATCCAAAATCTAC-3'
6	IGF-1 Exon 3	Forward	5'-TGAATGATAGTTTGTGGTTGGTAGTTA-3'
		Reverse	5'-[Biotin]AAAAAAAACTCCATCCAAAATCTACA-3'
7	IGF-1 Exon 4	Forward	5'-GATATGTTTAAGGTTTAGAAGGTAAGTT-3'
		Reverse	5'-[Biotin]TACTACTAAATTACTACAACCACATAACTC-3'
8	H19	Forward	5'-ATTAGTTTTGGAAGGTGTTGG-3'
		Reverse	5'-[Biotin]ATAAATCTTCCCTTCCTTTAAATCAACCT-3'
9	GH	Forward	5'-GGGAGGTTAGTTGAGTTTTTTAGTTGTTAG-3'
		Reverse	5'-[Biotin]TACCTAACCCCACCCCCTAA-3'
10	IGF1R	Forward	5'-GTGTTGGGAGGGTAGTTGG-3'
		Reverse	5'-[Biotin]CACCCCCAATACCTAAACAACTACAAC-3'
11	IGF2R	Forward	5'-AGAGTAGAAATTTTTTTTGGAGTGTT-3'
		Reverse	5'-[Biotin] AACACCTTACTCAAAACCTACCA-3'
12	GHR	Forward	5'-GTTTTGTTTTTTTTTTGGGAATAGG-3'
		Reverse	5'-[Biotin]CCTCCTAAAAAAAAATATTAATAATTACAA-3'
13	NRC31	Forward	5'-GAGTTATATAAATGGTAGTATGTGT-3'
		Reverse	5'-[Biotin]CAACCCCCTTCCCAAACT-3'
14	Insulin Receptor	Forward	5'-GTTTTTTAGAAGGTTTGGGGATGAAAATT-3'
		Reverse	5'-[Biotin]-AACCCACTCTCAAATCCTCAAAAAACTAA-3'

Table 6.3 – Sequencing primers for 14 functioning assays covering CpG sites in genes of interest

Assay	Target	PCR Primer Score	PCR Product Size	Sequencing Primer
1	Insulin	66	132	5'-ACCCCTAAATTAACCTC-3'
2	IGF-2 Exon 1	95	110	5'-ATAGGTATTTGTTTAGGTTATTAT-3'
3	IGF-2 Exon 4	82	114	5'-AGTTTTATATTGAGGATTTTGT-3'
4	IGF-2 Exon 6	65	154	5'-TTTTAGAATAGTGATTTTAGATGTT-3'
5	IGF-1 Exon 2	80	145	5'-GTGTTGGTAGTTATTTTTAGTT-3'
6	IGF-1 Exon 3	83	119	5'-AGTTTTAGAGATTTTTTATTTTAAT-3'
7	IGF-1 Exon 4	93	100	5'-GGGGAGGAGGTGAGGG-3'
8	H19	88	117	5'-TTGGAAGGTGTTGGT-3'
9	GH	59	174	5'-TTGTTAGTTATTTGTTGTTATTTTT-3'
10	IGF1R	70	110	5'-GGGAGGGTAGTTGGG-3'
11	IGF2R	85	231	5'-AAAGGTGAGGTAGGA-3'
12	GHR	76	80	5'-TTTTTTTTTGGGAATAGGG-3'
13	NRC31	70	97	5'-AGTATGTGTAGTTTAAGGTAGG-3'
14	Insulin Receptor	89	104	5'-GATGAAAATTAAGTTGTGTAGGTA-3'

DNA was extracted using the using the DNEasy Blood & Tissue Kit (Qiagen). To start, approximately 25mg of liver tissue was thawed, cut into small pieces and placed into a 1.5ml centrifuge tube, to which was added 180µl tissue lysis buffer 1 and 20µl proteinase K. After mixing thoroughly tubes were incubated at 56°C in a heated block and intermittently vortexed until the tissue had been completely lysed. Next 200µl lysis buffer 2 and 200µl 100% ethanol were added and tubes were thoroughly mixed to produce a homogeneous solution. The mixture was transferred into a DNEasy Mini spin column (Qiagen), which was mounted in a 2ml collection tube and centrifuged at 8000rpm (6000g) for 1 minute. The flow-through was

discarded and the spin column was refilled with 500µl wash buffer 1, remounted in a new 2ml collection tube and centrifuged at 8000rpm (6000g) for 1 minute. The flow-through was again discarded and the spin column refilled with 500µl wash buffer 2, remounted in a new 2ml collection tube and centrifuged at 14000rpm (20000g) for 3 minutes. Membranes were checked to ensure that they were dry to avoid any transfer of ethanol into subsequent steps. The spin column was then placed into a new 2ml collection tube and 200µl elution buffer was pipetted directly onto the membrane, incubated at room temperature for 1 minute and was centrifuged at 8000rpm (6000g) for 1 minute. In order to maximise the final DNA yield, the flow-through was then pipetted back onto the membrane and the last centrifuge step was repeated. The exact concentration of DNA in each sample was determined using a NanoDrop® ND-1000 spectrophotometer (NanoDrop Technologies Inc., Wilmington, DE, USA). Samples were checked for any RNA contamination by capillary electrophoresis using an Agilent 2100 Bioanalyser (Agilent Technologies) before being stored at -20°C pending bisulphite conversion.

6.2.4 Control sample preparation

In order to ensure the capability of the pyrosequencing assay (see below) to detect absent and complete methylation in the genes of interest, it was necessary to generate an unmethylated and fully methylated control DNA sample, respectively. Additional hepatic DNA was extracted for this purpose from a single normally grown fetus of one of the control-intake ewes in the late gestation study (Chapter 4). Both control samples were subsequently bisulphite converted alongside all of the test samples and run concurrently on the same PCR/pyrosequencing plates.

To generate the unmethylated control, genome wide amplification (GWA) was performed on the template DNA using the GenomiPhi™ DNA Amplification Kit (GE Healthcare, Little Chalfont, Buckinghamshire). During PCR, new DNA synthesised by DNA polymerase does not contain any methylated cytosine residues as it is the antisense strand that is read when the new cystosine is produced. Therefore regardless of whether the original cytosine happened to be methylated or unmethylated it is actually the complementary guanine that is read by the DNA polymerase, in response to which a new (unmethylated) cytosine residue is laid down. When a nested GWA approach is used, eventually after numerous PCR cycles the proportion of original DNA (and any methylation therein) becomes negligible. To further refine the approach, an adaptation of the GWA methodology (utilising DNA polymerase derived from the bacteriophage ϕ29) was introduced, as previously described by Umetani et al. (2005). The reason for this modification is that conventional GWA using thermal cycling is associated with unequal amplification of certain parts of the genome such that CG rich areas such as CpG islands, which are obviously very important regions for DNA methylation studies, are not efficiently amplified (McDowell et

al. 1998). By contrast, continuous amplification method using ϕ29 DNA transferase at a constant temperature (30°C) results in more homogeneous amplification and greater accuracy.

To generate the fully methylated control, the template DNA was treated with the enzyme CpG methylase, M.*Sss*I (EC.2.1.1.37, Zymo Research Corporation), which acts to rapidly, completely and reproducibly methylate all the cytosine residues in double-stranded DNA, including those within the CpG dinucleotides (Nur et al. 1985; Renbaum et al. 1990). M.*Sss*I is a recombinant enzyme that is isolated from a strain of E.Coli that expresses the methyltransferase gene from Spiroplasma sp. strain MQ1. To prepare the control, 4µl of genomic DNA at a concentration of 200ng/µl was added to 2µl of CpG reaction buffer, 1µl of 20X SAM (s-adenosylmethionine, 12mM in a low pH buffer), 1µl of CpG methylase (at a concentration of 4 units/µl) and 12µl nuclease-free water (P1195, Promega UK Ltd, Southampton). The mixture was then incubated overnight at 30°C in a heated block to maximise completeness of the hypermethylation. An additional 1µl CpG methylase was added to the reaction two hours into the incubation period to further drive methylation to completion.

6.2.5 Bisulphite conversion

From each sample 400ng of genomic DNA was modified with sodium bisulphite (optimal range 200-500ng) using the EZ DNA Methylation-Gold™ Kit (D5005, Zymo Research Corporation, Irvine, CA, USA). Based on the initial DNA concentration, each sample was individually diluted with nuclease-free water (Promega) in order to achieve a volume of 20µl at a concentration of 20ng/µl in a PCR tube. To this was added 130µl of CT conversion reagent. Tubes were placed into a PTC-100 Thermocycler (MJ Research, Inc., Watertown, MA, USA) at 98°C for 10 minutes followed by 64°C for 2.5 hours. Thereafter tubes were incubated for 20 hours (overnight) at 4°C. The next morning, each sample was transferred into 600µl binding buffer in a Zymo-Spin™ IC column, which was then capped and inverted repeatedly to mix. Spin columns were centrifuged at maximum speed (10000g) for 30 seconds and the flow-through was discarded. Next 100µl of wash buffer was added to each spin column and the centrifugation step was repeated. After discarding the flow-through, 200µl desulphonation buffer was added to each column, which were then incubated at room temperature for 20 minutes before being spun again at 10000g for 30 seconds. This was followed by two wash steps, wherein 200µl wash buffer was added and the centrifugation step was repeated each time. Finally the column was placed into a fresh 1.5ml microcentrifuge tube to which was added 10µl elution buffer. After centrifugation again at 10000g for 30 minutes, the resultant eluted DNA (flow-through) was stored at -20°C pending the PCR step. All samples for each study were bisulphite-converted in a single batch to avoid the introduction of any conversion bias.

6.2.6 Polymerase chain reaction

PCR was performed on the bisulphite-converted DNA samples using the forward and reverse primers designed as detailed in Section 6.2.2 and synthesised by Metabion International AG (Martinsried, Germany). All other reagents were provided as part of the AmpliTaq Gold® DNA Polymerase, LD (low DNA) kit using a Hot Start, Strong Finish™ protocol (Applied Biosystems). The LD DNA polymerase is encoded by a modified form of the *Thermus aquaticus* polymerase gene and further purified in order to reduce bacterial DNA contamination from incorporation into an *Escherichia coli* host (Lawyer et al. 1989). The "hot start" technique features initiation of the amplification reaction at a temperature higher than that of optimal primer annealing in order to minimise unwanted priming and non-specific product formation (Chou et al. 1992).

PCR reactions were set up in 96-well plates. All samples for each study were processed across a single plate, negating any inter-assay variation. In each well, 4µl of bisulphite-converted DNA at 5ng/µl concentration was added to 50µl PCR MasterMix, which was made up as follows to give a final concentration of magnesium chloride ($MgCl_2$) of 2mM:

- Nuclease free water (Promega UK Ltd) 30.8µl
- GeneAmp 10X PCR Gold Buffer 5.0µl
- 25mM $MgCl_2$ solution 4.0µl
- Deoxyadenosine triphosphate (dATP) 1.0µl
- Deoxycytidine triphosphate (dCTP) 1.0µl
- Deoxyguanosine triphosphate (dGTP) 1.0µl
- Deoxythymidine triphosphate (dTTP) 1.0µl
- Forward primer 1.0µl
- Reverse primer 1.0µl
- AmpliTaq Gold® DNA polymerase LD (5 units/µl) 0.2µl

Plates were processed through a PTC-225 Peltier Thermal Cycler (MJ Research). Samples were initially incubated at 95°C for 5 minutes, following which the following cycle was initiated and repeated a total of 45 times:

- 95°C for 15 seconds
- 57°C for 30 seconds (annealing temperature)
- 72°C for 15 seconds

To finish, plates were incubated at 72°C for a further 5 minutes and then 4°C for 10 minutes. Subsequently the resultant PCR products were subjected to gel electrophoresis to check that an amplicon of the expected size had been generated by the assay. Of the 24 initially designed primer sets, 21 were tested at the PCR stage - the remaining three were not needed as others had worked well for the same gene. Of these 21 assays, 19 generated appropriate products, which were then taken forward to pyrosequencing. The reaction conditions were satisfactory for all these assays bar one, which was the insulin receptor. An incremental adjustment of $MgCl_2$ concentration from 2mM to 3mM (by increasing the volume of $MgCl_2$ in the MasterMix from 4.0µl to 6.0µl and reducing the volume of water from 30.8µl to 28.8µl) and a reduction in annealing temperature from 57°C to 54°C solved this problem and produced a working assay.

6.2.7 Pyrosequencing

Pyrosequencing was performed on PCR products from the above reaction, using sequencing primers designed as described in Section 6.2.2 and synthesised by Metabion International AG. To begin, 20µl of PCR product from each sample was added to 37µl Pyromark binding buffer (Ref. 979006, Qiagen) and 3µl streptavidin sepharose beads (Ref. 17-5113-01, GE Healthcare) in an Abgene-skirted 96-well plate (Ref. 732-4888, Merk Ltd, Feltham, Middlesex). A PCR plate seal was applied and the plate was continuously shaken on a high-speed microplate shaker (Illumina, San Diego, Ca, USA) at 1600rpm for 20 minutes to allow the biotinylated product to bind to the streptavidin, without allowing sedimentation to the bottom of the well resulting in inability to retrieve it. Subsequently a vacuum Prep workstation (Pyrosequencing®, Qiagen) was used to wash and denature the beads and transfer them to a new plate. The patency of all pins on the vacuum Prep tool was first checked by aspirating MilliQ water (Millipore, Billerica, MA, USA). Any pins with delayed aspiration rates were immediately replaced with new filter probes (Ref. 979010, Qiagen). Thereafter the plate was removed from the shaker and immediately transferred to the vacuum prep station. Water was aspirated for 10 seconds then the vacuum tool was held in the air and shaken lightly to ensure that all water had drained away. Thereafter samples were aspirated from the Abgene PCR plate. The tool was immersed in 70% ethanol (Ref. 104766P, Merk Ltd) for 5 seconds, and then transferred into 0.2M sodium hydroxide (Ref. 102524X, AnalaR NORMAPUR®, VWR) for 5 seconds to denature the DNA and to render it single-stranded in order to allow the sequencing primer to bind. Next it was immersed in PyroMark wash buffer (Ref. 979008, Qiagen), leaving only the beads on the tips of the pins. The beads were then transferred into a PSQ low plate (Ref. 979002, Qiagen) containing 43.5µl annealing buffer and 1.5µl sequencing primer at 10µM (diluted in annealing buffer) and briefly agitated. The last three steps were repeated in order to increase the yield.

Plates were then incubated at 80°C for 2 minutes (PTC-225) to destroy the streptavidin beads and release the PCR product, and allowed to cool to room temperature before being placed into a PSQ 96MA pyrosequencer (Qiagen). PSQ 96MA software version 2.1 (Qiagen) was used to calculate the required amounts of the PyroMark Gold Q96 reagents (Ref. 972804, Qiagen). The substrate mix and enzyme mix were each resuspended in 620µl MilliQ water prior to being loaded into a PyroMark Q96 cartridge (Ref. 979004, Qiagen) together with the required volumes of dATP, dGTP, dTTP and dCTP. The pyrosequencing process itself is illustrated by the example pyrogram in Figure 6.4. First the enzyme mixture was added to each well containing PCR product (indicated by the letter E), shortly followed by substrate mixture (S). Thereafter the complementary dNTP for each nucleotide in the dispensation order (expected sequence) was added in turn until the reaction was completed. Pyro-Q-CpG software version 1.0.9 (Biotage) was used to analyse the pyrograms in order to determine the percentage DNA methylation at each individual CpG site by measuring the ratio of the C/T peaks. Satisfactory pyrosequencing assays were established for 16 of the 19 acceptable PCR products. For the H19 gene there was a choice of three different assays that had been developed within the same sequence (albeit in three different CpG islands) therefore the assay with the strongest PCR product was chosen to take forward for sample analysis. Consequently a total of 14 assays were run on each fetal and lamb DNA sample, covering a total of 10 genes of interest and providing a quantification of the degree of methylation at 57 individual CpG sites. The forward and reverse PCR primers and pyrosequencing primers for these 14 assays are detailed in Tables 6.2 and 6.3, respectively.

6.2.8 Data analysis

Percentage DNA methylation was compared between groups at each individual CpG site and also as an average according to individual assays and genes of interest. Data was tested for normality and equality of variance using Q-Q plots and Levene's test, respectively. For the fetal study, the four groups were compared by one-way ANOVA. For the postnatal study, in view of anticipated gender differences, the General Linear Model was used in order to examine for the effect of prenatal Ad.VEGF treatment, gender and their potential interaction and therefore the results are presented as four groups (Ad.VEGF-M, Ad.VEGF-F, Saline-M and Saline-F). For both studies, DNA methylation was correlated with a number of relevant *in vivo* parameters using Pearson's product moment test. All data are presented as mean ± standard error of the mean (SEM) unless otherwise stated. Formal statistical significance was considered to have been reached where $p<0.05$ and a tendency towards significance was defined as $p<0.1$.

Figure 6.4 – Example pyrogram illustrating use of C/T ratios to quantify methylation status

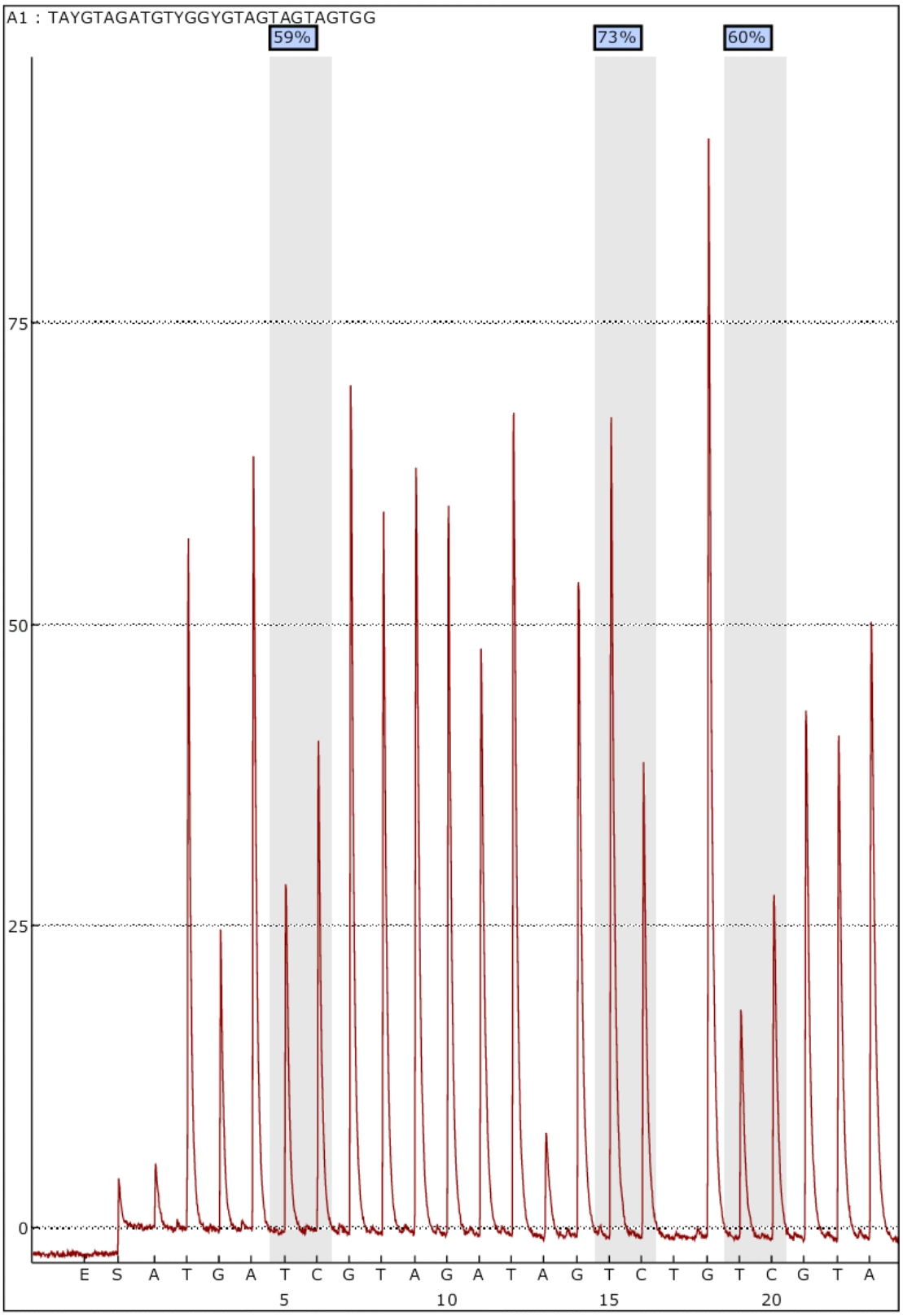

Abbreviations: E = enzyme mix; S = substrate mix; Y = CpG site; A = adenosine; T = thymine; C = cytosine; G = guanine. Example shown is IGF1R - the sequencing primer contains three CpG dinucleotides. In this animal these cytosines were 59%, 70% and 63% methylated, respectively.

6.3 Results

Although results were obtained from all 14 assays that were developed, the DNA methylation information generated for NRC31 was very limited as there was zero detectable methylation at the majority of the 7 individual CpG sites investigated for most of the samples. In the instances where DNA methylation was quantified, the amount present was minimal for both cohorts. In the postnatal samples, which were analysed first, there was zero detectable methylation in 26 (90%), 20 (69%), 22 (81%), 27 (93%), 29 (100%) and 29 (100%) of 29 animals at positions 1, 2, 3, 5, 6 and 7 respectively. Consequently no meaningful comparisons between the study groups were possible at these loci. DNA methylation information at position 4 was obtained in 19 of 29 animals (66%) and was minimal (mean ~2%). There were no significant differences between H+Ad.VEGF and H+Saline groups (2.14±0.34 versus 1.85±0.14, p=0.483) or male and female lambs (1.84±0.10 versus 2.22±0.43, p=0.295). In the fetal cohort there was no detectable DNA methylation in 52 (91%), 50 (88%), 54 (95%), 57 (100%), 46 (81%), 55 (96%) and 55 (96%) of 57 animals at positions 1 to 7, respectively. Unfortunately no results were available from the fully methylated and unmethylated control samples for NRC31 (see below), which meant that it was not possible to say whether this lack of detectable methylation was due to a genuine absence of methylcytosine at these CpG sites, or whether this assay was lacking the required sensitivity.

6.3.1 Overview

Mean DNA methylation for each gene of interest is shown in Figure 6.5, presented separately for the fetal and postnatal studies. Due to the (probably technical) problems with NRC31 as discussed above, meaningful comparisons were only possible for the remaining nine genes of interest. Overall DNA methylation status varied greatly between different genes. The degree of methylation ranged from as low as 1.49±0.05% for the GH receptor gene up to 87.9±0.26% for the insulin gene. In general, mean levels of methylation were similar in magnitude across the two studies and were marginally higher (4–14%, $p<0.001$) in the lamb study relative to the fetal study. Interestingly however, IGF-2 and IGF1R both showed the opposite trend, with DNA methylation that was 41–45% lower in lambs versus fetuses ($p<0.001$). It should be noted that the two cohorts are not directly comparable as the hepatic DNA for each batch was bisulphite converted separately and also the fetal cohort included both control-intake and overnourished ewes whilst the postnatal cohort comprised overnourished ewes only. However as there were no significant differences between control-intake and high-intake pregnancies with respect to fetal DNA methylation (see Section 6.3.2) it did not seem unreasonable to make a tentative general comparison, whilst keeping these issues in mind.

Figure 6.5 – Comparison of overall DNA methylation of nine genes between fetuses and lambs

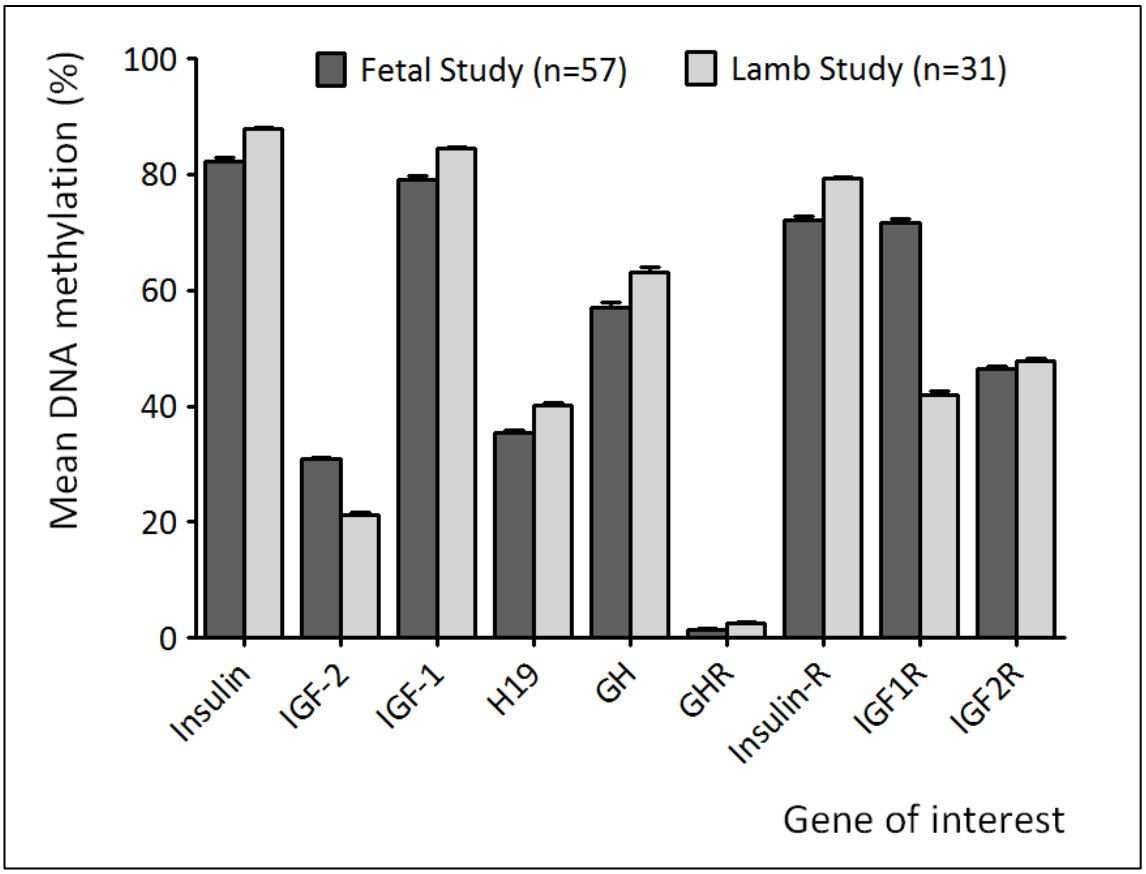

Mean DNA methylation was calculated by averaging the mean measurements at all individual CpG dinucleotides examined within each gene (ranging from 1 to 14). Abbreviations: IGF = insulin-like growth factor; GH = growth hormone; R = receptor.

Figure 6.6 shows the degree of methylation in the fully methylated and unmethylated control DNA samples. Unfortunately results were only obtained for eight out of ten genes of interest. This is because the IGF2R and NRC31 assays required a considerable amount of optimisation and needed to be repeated several times, during which both control samples were used up.

For the remaining eight genes a high degree of methylation was seen in the sample treated with M.*Sss*I (81.6–95.1%) and was highest in the insulin gene, in keeping with the results from the analysed samples. Most strikingly, despite very low levels of methylation in the GHR gene across the cohort, there is clearly the potential for this gene to become heavily methylated, as indicated by the 94% methylation status of the GHR in the control sample treated with M.*Sss*I. Conversely, treatment of hepatic DNA using a nested GWA resulted in low levels of detectable methylation for 7 of 8 genes (0.1–9.3%) with the notable exception of the insulin gene (39.7%).

Figure 6.6 – DNA methylation profiles of eight genes in fully methylated/unmethylated controls

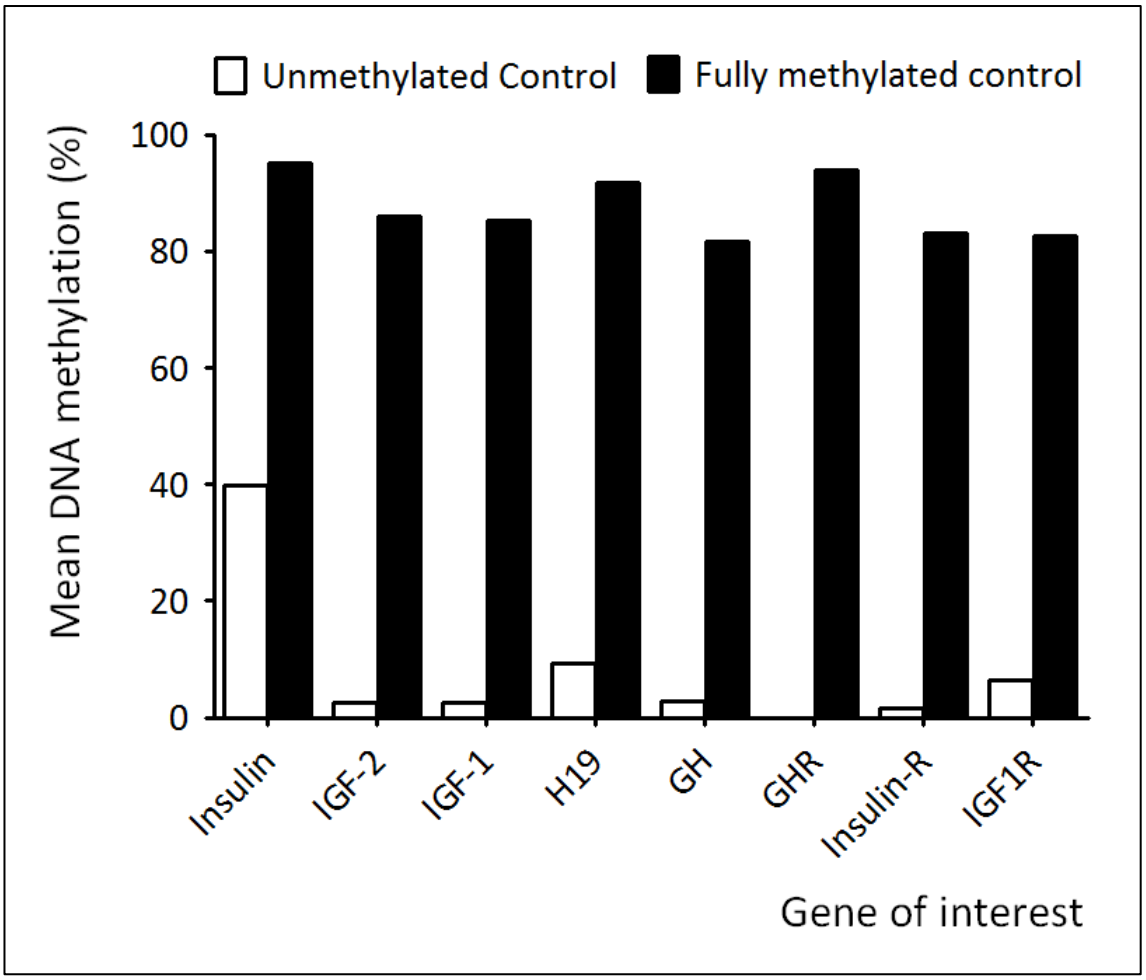

Mean DNA methylation was calculated by averaging the mean measurements at all individual CpG dinucleotides examined within each gene (ranging from 1 to 14). Abbreviations: IGF = insulin-like growth factor; GH = growth hormone; R = receptor. Control samples were derived from a single normally growth fetus whose mother was fed a control intake during pregnancy. The fully methylated control was prepared by treatment with the methylating enzyme M.SssI. The unmethylated control sample was prepared using a nested genome wide amplification kit.

6.3.2 Fetal study

Table 6.4 presents the DNA methylation at each individual CpG dinucleotide across nine genes of interest in the 57 fetal samples taken from the late gestation study (Chapter 4). There were no significant differences between the four study groups at any of the 50 loci. Similarly when these were averaged by sequence and by gene, there were no differences between C+Saline, H+Ad.VEGF, H+Ad.LacZ or H+Saline groups (Table 6.5). Furthermore there were no significant

Table 6.4 – DNA methylation at 50 individual CpG sites in nine genes in late gestation fetal liver

	Gene / CpG Position	C+Saline (n=12)	H+Ad.VEGF (n=18)	H+Saline (n=13)	H+Ad.LacZ (n=14)	P Value
1	Insulin Position 1	72.5 ± 1.63	73.9 ± 1.38	73.3 ± 1.46	71.1 ± 1.40	0.579
2	Insulin Position 2	84.4 ± 1.50	85.8 ± 1.32	85.1 ± 1.41	84.9 ± 1.22	0.892
3	Insulin Position 3	80.7 ± 1.22	79.2 ± 4.00	82.2 ± 1.17	83.2 ± 1.09	0.727
4	Insulin Position 4	86.4 ± 1.36	88.3 ± 1.13	87.4 ± 1.35	87.2 ± 1.07	0.755
5	Insulin Position 5	84.3 ± 1.47	85.6 ±1.21	85.3 ± 1.64	84.8 ± 1.00	0.910
6	IGF-2 Exon 1 Position 1	69.5 ± 2.21	71.0 ± 1.77	69.8 ± 2.13	68.7 ± 1.52	0.853
7	IGF-2 Exon 1 Position 2	71.5 ± 1.54	72.7 ± 1.36	72.6 ± 1.50	71.3 ± 1.34	0.857
8	IGF-2 Exon 1 Position 3	58.4 ± 2.09	60.0 ± 1.69	57.3 ± 1.39	60.7 ± 1.45	0.485
9	IGF-2 Exon 4 Position 1	17.2 ± 1.12	16.6 ± 1.16	17.8 ± 0.99	16.8 ± 1.62	0.911
10	IGF-2 Exon 4 Position 2	28.8 ± 0.94	27.7 ± 0.85	28.4 ± 0.74	27.2 ± 1.44	0.704
11	IGF-2 Exon 6 Position 1	2.83 ± 0.22	2.46 ± 0.13	2.43 ± 0.92	2.87 ± 0.24	0.802
12	IGF-2 Exon 6 Position 2	3.72 ± 0.24	3.28 ± 0.27	3.08 ± 0.12	3.73 ± 0.20	0.297
13	IGF-1 Exon 2 Position 1	83.8 ± 1.90	85.0 ± 1.50	86.6 ± 1.82	85.0 ± 1.46	0.728
14	IGF-1 Exon 2 Position 2	8.8 ± 0.55	8.0 ± 0.40	9.7 ± 0.75	8.6 ± 0.66	0.199
15	IGF-1 Exon 2 Position 3	83.3 ± 1.40	84.9 ± 1.35	84.5 ± 1.99	84.0 ± 1.60	0.912
16	IGF-1 Exon 2 Position 4	85.1 ± 1.62	85.9 ± 1.27	86.4 ± 1.76	85.5 ± 1.19	0.938
17	IGF-1 Exon 2 Position 5	85.3 ± 1.62	86.3 ± 1.30	84.4 ± 1.65	84.9 ± 1.55	0.792
18	IGF-1 Exon 2 Position 6	78.1 ± 1.47	78.9 ± 1.26	78.8 ± 2.17	79.7 ± 2.30	0.949
19	IGF-1 Exon 3 Position 1	78.1 ± 1.72	80.5 ± 1.42	78.7 ± 1.73	79.7 ± 1.90	0.847
20	IGF-1 Exon 3 Position 2	81.6 ± 1.73	82.7 ± 1.48	80.6 ± 1.62	82.2 ± 1.79	0.816
21	IGF-1 Exon 3 Position 3	80.1 ± 1.94	82.2 ± 1.45	79.8 ± 1.57	81.2 ± 1.90	0.707
22	IGF-1 Exon 3 Position 4	79.0 ± 1.95	80.4 ± 1.47	77.9 ± 1.67	78.9 ± 2.08	0.776
23	IGF-1 Exon 4 Position 1	89.1 ± 1.51	91.0 ± 1.21	91.1 ± 1.45	88.4 ± 1.79	0.476
24	IGF-1 Exon 4 Position 2	89.0 ± 1.39	91.0 ± 1.19	91.6 ± 1.36	88.7 ± 1.47	0.373

25	IGF-1 Exon 4 Position 3	75.4 ± 1.76	76.8 ± 1.37	77.2 ± 1.20	74.9 ± 1.34	0.623
26	H19 Position 1	36.6 ± 0.99	36.9 ± 1.04	35.4 ± 0.92	35.3 ± 1.14	0.567
27	H19 Position 2	39.4 ± 0.85	38.7 ± 0.89	37.8 ± 0.70	37.4 ± 0.78	0.385
28	H19 Position 3	35.9 ± 0.98	35.5 ± 1.17	35.1 ± 0.76	35.2 ± 0.87	0.951
29	H19 Position 4	28.1 ± 0.88	28.2 ± 1.05	26.8 ± 0.87	26.8 ± 1.00	0.615
30	H19 Position 5	34.8 ± 1.14	34.7 ± 1.18	34.5 ± 0.97	33.9 ± 1.28	0.960
31	H19 Position 6	42.0 ± 1.88	40.7 ± 1.11	38.4 ± 1.65	39.4 ± 1.24	0.360
32	GH Position 1	53.8 ± 2.21	57.2 ± 2.38	54.8 ± 2.40	53.1 ± 2.07	0.593
33	GH Position 2	59.2 ± 1.45	59.7 ± 1.27	59.1 ± 1.20	58.4 ± 1.28	0.899
34	GH Receptor Position 1	1.64 ± 0.08	1.47 ± 0.09	1.52 ±0.13	1.37 ± 0.11	0.435
35	Insulin Receptor Position 1	69.5 ± 1.12	69.5 ± 1.25	70.7 ± 1.13	68.0 ± 1.25	0.548
36	Insulin Receptor Position 2	75.3 ± 1.37	74.9 ± 1.16	74.9 ± 0.95	73.9 ± 1.50	0.896
37	IGF1R Position 1	67.5 ± 1.58	66.4 ± 1.31	68.7 ± 1.17	67.4 ± 1.60	0.697
38	IGF1R Position 2	78.6 ± 1.46	77.8 ± 1.26	79.3 ± 1.26	79.0 ± 1.28	0.854
39	IGF1R Position 3	67.6 ± 1.77	67.0 ± 1.68	67.5 ± 1.21	66.6 ± 1.52	0.968
40	IGF2R Position 1	49.2 ± 3.47	44.9 ± 1.33	45.3 ± 0.70	44.9 ± 0.75	0.294
41	IGF2R Position 2	48.3 ± 0.71	45.0 ± 2.31	45.8 ± 0.63	45.3 ± 0.77	0.485
42	IGF2R Position 3	41.6 ± 3.19	43.6 ± 1.21	43.4 ± 0.85	43.2 ± 0.89	0.844
43	IGF2R Position 4	49.7 ± 0.70	48.9 ± 1.03	49.5 ± 0.80	46.7 ± 1.16	0.146
44	IGF2R Position 5	39.4 ± 0.86	38.7 ± 0.64	40.2 ± 2.16	38.8 ± 2.16	0.900
45	IGF2R Position 6	54.0 ± 2.03	51.5 ± 1.66	49.7 ± 1.97	46.3 ± 1.19	0.101
46	IGF2R Position 7	41.4 ± 0.60	40.2 ± 1.66	43.2 ± 1.99	39.3 ± 1.36	0.348
47	IGF2R Position 8	55.4 ± 2.17	56.6 ± 1.97	56.9 ± 3.60	52.3 ± 1.59	0.518
48	IGF2R Position 9	21.0 ± 1.44	26.0 ± 2.79	22.6 ± 0.96	22.1 ± 1.62	0.319
49	IGF2R Position 10	78.0 ± 3.63	72.6 ± 5.04	79.2 ± 4.20	73.4 ± 3.87	0.662
50	IGF2R Position 11	48.6 ± 1.04	44.9 ± 2.72	45.1 ± 2.15	48.1 ± 4.21	0.751

P values shown are for overall ANOVA. There were no significant differences between groups.

Table 6.5 – Mean DNA methylation in nine genes of interest in late gestation fetal liver tissue

	C+Saline (n=12)	H+Ad.VEGF (n=18)	H+Saline (n=13)	H+Ad.LacZ (n=14)	P Value
Insulin	81.6 ± 1.39	82.6 ± 1.61	82.7 ± 1.36	82.2 ± 0.93	0.963
IGF-1 Exon 2	*70.7 ± 1.32*	*71.5 ± 1.11*	*71.7 ± 1.52*	*71.3 ± 1.19*	*0.959*
IGF-1 Exon 3	*79.9 ± 1.81*	*81.5 ± 1.44*	*79.2 ± 1.62*	*80.5 ± 1.90*	*0.795*
IGF-1 Exon 4	*84.5 ± 1.34*	*86.3 ± 1.14*	*86.7 ± 1.18*	*84.0 ± 1.46*	*0.398*
IGF-1	78.4 ± 1.46	79.7 ± 1.21	79.2 ± 1.36	79.6 ± 1.47	0.784
IGF-2 Exon 1	*66.5 ± 1.81*	*67.9 ± 1.51*	*66.6 ± 1.39*	*66.9 ± 1.31*	*0.894*
IGF-2 Exon 4	*23.0 ± 0.99*	*22.1 ± 0.95*	*23.1 ± 0.79*	*22.0 ± 1.61*	*0.849*
IGF-2 Exon 6	*3.21 ± 0.21*	*2.84 ± 0.22*	*3.69 ± 0.77*	*3.34 ± 0.20*	*0.200*
IGF-2	31.0 ± 0.57	31.0 ± 0.45	31.3 ± 0.34	31.3 ± 0.48	0.909
H19	36.1 ± 0.99	35.8 ± 0.99	34.7 ± 0.79	34.7 ± 1.03	0.630
GH	56.5 ± 1.39	58.4 ± 1.66	57.0 ± 1.57	55.7 ± 1.34	0.624
GHR	1.64 ± 0.08	1.47 ± 0.09	1.52 ±0.13	1.37 ± 0.11	0.435
Insulin Receptor	72.4 ± 1.20	72.2 ± 1.15	72.8 ± 0.96	71.0 ± 1.36	0.763
IGF1R	71.7 ± 1.46	71.0 ± 1.26	72.4 ± 1.18	71.3 ± 1.31	0.873
IGF2R	47.9 ± 0.57	46.4 ± 1.04	47.1 ± 0.84	45.3 ±0.74	0.248

differences when comparing control-intake versus high-intake, or marked FGR versus non-FGR pregnancies. Combining the H+Ad.LacZ and H+Saline groups, as had been done previously (see Chapter 4), also had no significant impact on the results. There were no gender differences in DNA methylation of eight of nine genes with the single exception of IGF2R, which was higher in female compared with male lambs (47.5±0.56 versus 45.4±0.69, respectively, p=0.018). When examining the individual CpG sites, % DNA methylation was found to be higher at position 8 (p=0.039) and tended to be greater at positions 1, 2 and 9 too (p=0.058, p=0.079 and p=0.086).

There were no significant correlations between the degree of DNA methylation of these nine genes of interest and *in vivo* parameters such as fetoplacental weights, ultrasonographic fetal growth velocity (delta AC and RV), post-mortem physical measurements and internal organ weights. Neither insulin nor IGF-1 gene DNA methylation levels correlated with their respective determinations in plasma. There were however a number of significant correlations between the methylation status of different genes. Irrespective of fetal gender, insulin was correlated with IGF-1, H19 and GH ($r=0.676–0.929$, $n=57$, $p<0.001–0.016$), IGF-1 was correlated with H19 and GH ($r=0.589–0.769$, $n=57$, $p<0.001–0.003$) and H19 with GH ($r=0.719$, $n=57$, $p<0.008$). The strength of these correlations were very similar when only control- or high-intake pregnancies were included, further implying a lack of any effect of prenatal nutrition. Interestingly neither IGF-1 or IGF-2 correlated with either one of their receptors (IGF1R and IGF2R) and GH did not correlate with GHR. Meanwhile insulin correlated with its receptor only in the overnourished pregnancies ($r=0.373$, $n=45$, $p=0.014$).

6.3.3 Lamb study

Mean DNA methylation at 50 individual CpG dinucleotides across nine genes of interest in 31 lambs surviving at the conclusion of the postnatal study (see Chapter 5) is shown in Table 6.6. In keeping with the findings in the fetal cohort (see above), no significant effect of Ad.VEGF on DNA methylation was observed at any of these sites. However some gender differences and gender X treatment interactions were apparent at this postnatal stage. DNA methylation was lower in females versus males at two different CpG sites within the insulin gene. By contrast, methylation was greater in females versus males at two CpG dinucleotides preceding IGF-1 exons 2 and 3, and tended also to be increased at a single position before exon 4. Accordingly overall insulin gene methylation was lower ($p=0.007$) and IGF-1 tended to be higher ($p=0.053$) in female relative to male lambs (see Table 6.7). DNA methylation also tended to be higher in female versus male lambs at isolated CpG sites in IGF-2 and GH, but no significant gender differences were seen in the average methylation of these genes. Whilst there were some minor interactions between gender and treatment group (one significant at $p=0.04$ and two with $p=0.05$-0.01), notably in all cases it was the saline- and not Ad.VEGF-treated females that were the outlying group and no such interactions were evident in the averages by gene.

6.3.4 Gender effects

In order to further examine the impact of gender on DNA methylation, additional data was incorporated from an additional six lambs from the term/postnatal cohort who had been surplus to requirements for the main study, but who had been managed identically both pre-

Table 6.6 – DNA methylation at 50 individual CpG sites in nine genes of interest in postnatal lamb liver tissue

	Gene / CpG Position	Saline-F (n=8)	Ad.VEGF-F (n=8)	Saline-M (n=7)	Ad.VEGF-M (n=8)	P Values		
						Treatment	Gender	Interaction
1	Insulin Position 1	80.1 ± 0.99	78.9 ± 1.80	82.5 ± 0.50	81.2 ± 0.68	0.453	0.145	0.844
2	Insulin Position 2	90.7 ± 0.44	91.5 ± 0.21	92.1 ± 0.29	92.1 ± 0.31	0.313	**0.015**	0.238
3	Insulin Position 3	83.5 ± 1.45	85.0 ± 0.46	86.5 ± 0.77	86.3 ± 0.55	0.128	**0.003**	0.090
4	Insulin Position 4	92.1 ± 2.22	91.7 ± 1.27	93.0 ± 1.29	92.2 ± 0.67	0.646	0.853	0.920
5	Insulin Position 5	90.2 ± 0.49	86.9 ± 2.56	90.6 ± 0.55	90.5 ± 0.70	0.327	0.518	0.353
6	IGF-2 Exon 1 Position 1	34.2 ± 1.00	32.6 ± 1.06	31.2 ± 0.83	31.6 ± 0.77	0.368	0.058	0.173
7	IGF-2 Exon 1 Position 2	39.1 ± 1.23	36.9 ± 1.18	36.4 ± 0.80	36.9 ± 0.78	0.155	0.053	0.066
8	IGF-2 Exon 1 Position 3	25.1 ± 1.73	25.6 ± 1.52	27.4 ± 0.94	25.5 ± 2.17	0.549	0.520	0.618
9	IGF-2 Exon 4 Position 1	21.3 ± 1.60	19.0 ± 1.13	19.7 ± 1.09	19.1 ± 0.61	0.124	0.433	0.319
10	IGF-2 Exon 4 Position 2	37.5 ± 2.25	35.0 ± 1.47	35.4 ± 2.19	34.7 ± 0.89	0.353	0.762	0.579
11	IGF-2 Exon 6 Position 1	4.73 ± 0.26	5.15 ± 0.47	4.96 ± 0.80	4.01 ± 0.29	0.704	0.719	0.182
12	IGF-2 Exon 6 Position 2	3.89 ± 0.44	5.47 ± 0.69	4.47 ± 0.10	4.11 ± 0.45	0.375	0.569	0.166
13	IGF-1 Exon 2 Position 1	89.2 ± 1.31	88.6 ± 0.99	86.3 ± 1.05	85.5 ± 1.01	0.603	**0.041**	0.800
14	IGF-1 Exon 2 Position 2	4.08 ± 0.82	4.86 ± 0.29	4.74 ± 0.13	4.57 ± 0.33	0.374	0.708	0.205
15	IGF-1 Exon 2 Position 3	87.5 ± 0.73	88.4 ± 0.30	87.7 ± 0.48	88.3 ± 0.31	0.145	0.913	0.870

16	IGF-1 Exon 2 Position 4	91.9 ± 0.82	91.9 ± 0.40	92.3 ± 0.38	92.4 ± 0.41	0.785	0.403	0.862
17	IGF-1 Exon 2 Position 5	89.7 ± 0.74	90.5 ± 0.59	90.7 ± 0.45	89.8 ± 0.67	0.922	0.901	0.151
18	IGF-1 Exon 2 Position 6	81.1 ± 0.48	81.9 ± 0.53	81.6 ± 0.78	80.5 ± 0.47	0.656	0.541	0.199
19	IGF-1 Exon 3 Position 1	87.1 ± 0.55	87.6 ± 0.36	86.2 ± 0.45	86.4 ± 0.23	0.369	**0.046**	0.698
20	IGF-1 Exon 3 Position 2	89.8 ± 0.68	89.7 ± 0.24	89.9 ± 0.42	89.6 ± 0.44	0.799	0.734	0.715
21	IGF-1 Exon 3 Position 3	89.1 ± 0.56	89.7 ± 0.25	88.8 ± 0.71	88.6 ± 0.56	0.830	0.420	0.540
22	IGF-1 Exon 3 Position 4	85.0 ± 0.34	85.5 ± 0.52	83.9 ± 0.71	84.6 ±0.35	0.242	0.169	0.979
23	IGF-1 Exon 4 Position 1	95.9 ± 1.42	96.8 ± 0.77	97.0 ± 1.16	96.6 ± 0.82	0.792	0.078	0.850
24	IGF-1 Exon 4 Position 2	99.9 ± 0.09	99.4 ± 0.34	100 ± 0.02	99.0 ± 0.72	0.155	0.942	0.540
25	IGF-1 Exon 4 Position 3	82.7 ± 3.54	79.8 ± 0.88	80.0 ± 0.79	79.0 ± 0.73	0.236	0.544	0.515
26	H19 Position 1	37.6 ± 1.38	38.1 ± 0.51	38.3 ± 0.94	37.5 ± 0.76	0.932	0.990	0.466
27	H19 Position 2	41.8 ± 1.16	41.1 ± 0.76	42.4 ± 0.61	41.6 ± 1.07	0.419	0.799	0.998
28	H19 Position 3	42.4 ± 1.00	42.2 ± 0.61	42.9 ± 0.71	42.0 ± 0.96	0.403	0.659	0.807
29	H19 Position 4	31.0 ± 2.22	30.1 ± 0.56	30.9 ± 0.89	28.6 ± 1.30	0.288	0.828	0.561
30	H19 Position 5	42.5 ± 2.14	42.9 ± 0.59	40.6 ± 0.90	41.1 ± 0.72	0.777	0.274	0.933
31	H19 Position 6	45.9 ± 1.51	46.4 ± 0.60	46.3 ± 0.81	45.4 ± 0.78	0.710	0.750	0.560
32	GH Position 1	71.9 ± 5.69	59.3 ± 3.77	67.2 ± 4.93	66.7 ± 3.55	0.149	0.768	0.186
33	GH Position 2	60.8 ± 1.10	62.1 ± 0.84	59.6 ± 0.72	59.6 ± 1.05	0.508	0.067	0.496
34	GH Receptor Position 1	2.53 ± 0.42	2.28 ± 0.21	2.45 ± 0.29	3.41 ± 0.81	0.450	0.271	0.211

35	Insulin Receptor Position 1	75.6 ± 1.93	76.0 ± 1.20	76.8 ± 1.12	75.8 ± 0.81	0.453	0.283	0.925
36	Insulin Receptor Position 2	83.6 ± 0.77	81.9 ± 0.76	81.5 ± 0.57	81.5 ± 0.41	0.164	0.147	0.153
37	IGF1R Position 1	36.7 ± 1.99	34.5 ± 0.99	36.4 ± 1.28	36.3 ± 0.65	0.258	0.723	0.288
38	IGF1R Position 2	49.6 ± 2.43	46.6 ± 1.06	48.4 ± 1.52	48.6 ± 1.05	0.245	0.806	0.219
39	IGF1R Position 3	51.4 ± 7.88	40.4 ± 0.92	41.3 ± 1.40	42.3 ± 1.21	0.152	0.156	**0.040**
40	IGF2R Position 1	50.9 ± 0.74	49.1 ± 1.19	49.2 ± 1.39	49.7 ± 1.15	0.793	0.613	0.485
41	IGF2R Position 2	49.3 ± 1.97	48.1 ± 1.47	46.1 ± 1.24	46.2 ± 0.96	0.793	0.203	0.738
42	IGF2R Position 3	45.4 ± 0.87	45.0 ± 1.21	45.0 ± 1.10	44.6 ± 0.92	0.814	0.861	0.898
43	IGF2R Position 4	47.8 ± 1.67	47.2 ± 1.63	47.1 ± 1.63	47.7 ± 1.13	0.954	0.947	0.775
44	IGF2R Position 5	42.1 ± 1.17	42.1 ± 0.79	43.5 ± 1.38	42.6 ± 0.87	0.756	0.665	0.602
45	IGF2R Position 6	51.8 ± 1.78	50.3 ± 1.59	49.4 ± 1.81	50.5 ± 0.60	0.939	0.587	0.522
46	IGF2R Position 7	45.4 ± 1.30	44.6 ± 1.11	43.5 ± 2.20	43.0 ± 1.02	0.924	0.308	0.823
47	IGF2R Position 8	52.8 ± 1.63	47.4 ± 3.78	52.3 ± 1.49	50.6 ± 0.71	0.258	0.627	0.601
48	IGF2R Position 9	38.2 ± 1.15	37.9 ± 1.10	36.7 ± 1.93	36.0 ± 2.29	0.957	0.562	0.751
49	IGF2R Position 10	64.8 ± 3.46	64.7 ± 1.87	65.3 ± 2.44	65.8 ± 2.19	0.973	0.940	0.880
50	IGF2R Position 11	49.0 ± 1.66	48.6 ± 1.32	46.5 ± 2.81	45.0 ± 1.07	0.810	0.228	0.614

Table 6.7 – Mean DNA methylation in nine genes of interest in postnatal lamb liver

Gene / CpG Position	Saline-F (n=8)	Ad.VEGF-F (n=8)	Saline-M (n=7)	Ad.VEGF-M (n=8)	P Values		
					Treatment	Gender	Interaction
Insulin	87.3 ± 0.84	86.8 ± 0.65	88.9 ± 0.26	88.5 ± 0.36	0.526	**0.007**	0.868
IGF-1 Exon 2	*73.9 ± 0.26*	*74.3 ± 0.24*	*73.9 ± 0.30*	*73.5 ± 0.21*	*0.780*	*0.261*	*0.870*
IGF-1 Exon 3	*87.8 ± 0.47*	*88.1 ± 0.21*	*87.2 ± 0.46*	*87.3 ± 0.30*	*0.501*	*0.181*	*0.659*
IGF-1 Exon 4	*92.8 ± 1.35*	*92.0 ± 0.13*	*92.3 ± 0.45*	*91.5 ± 0.29*	*0.118*	*0.270*	*0.731*
IGF-1	84.8 ± 0.51	84.8 ± 0.14	84.5 ± 0.30	84.1 ± 0.15	0.443	0.053	0.639
IGF-2 Exon 1	*32.8 ± 1.20*	*31.7 ± 1.01*	*31.7 ± 0.75*	*31.3 ± 1.12*	*0.293*	*0.254*	*0.472*
IGF-2 Exon 4	*29.4 ± 1.71*	*27.0 ± 1.28*	*27.6 ± 1.58*	*26.9 ± 0.59*	*0.211*	*0.633*	*0.436*
IGF-2 Exon 6	*4.44 ± 0.33*	*5.55 ± 0.56*	*5.06 ± 0.77*	*4.01 ± 0.27*	*0.819*	*0.722*	*0.460*
IGF-2	22.0 ± 1.05	21.5 ± 0.65	21.2 ± 0.67	20.7 ± 0.56	0.406	0.366	0.835
H19	40.2 ± 1.41	40.1 ± 0.48	40.2 ± 0.48	39.4 ± 0.67	0.532	0.860	0.661
GH	66.4 ± 3.29	60.7 ±1.91	63.4 ± 2.26	63.1 ± 1.72	0.257	0.817	0.310
GHR	2.53 ± 0.42	2.28 ± 0.21	2.45 ± 0.29	3.41 ± 0.81	0.450	0.271	0.211
Insulin Receptor	79.6 ± 1.28	79.0 ± 0.87	79.2 ± 0.61	78.6 ± 0.43	0.234	0.283	0.573
IGF1R	43.4 ± 2.30	40.5 ± 0.96	42.0 ± 1.38	42.4 ± 0.94	0.202	0.544	0.132
IGF2R	47.4 ± 0.47	48.8 ± 1.16	47.7 ± 0.78	48.8 ± 1.16	0.686	0.533	0.867

Figure 6.7 – Comparison of insulin and IGF-1 gene methylation between male and female lambs

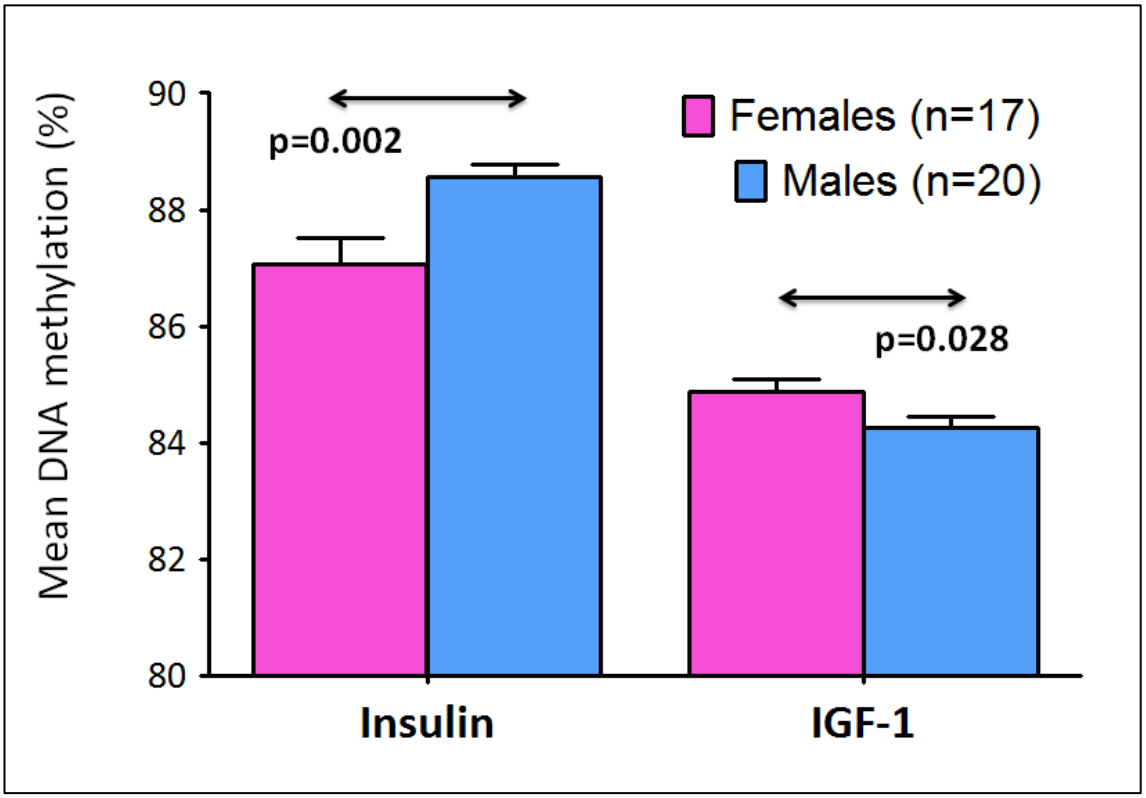

Mean DNA methylation was calculated by averaging the mean measurements at all individual CpG dinucleotides examined in the insulin and insulin-like growth factor (IGF)-1 genes (5 and 14, respectively) in DNA extracted from liver samples collected at ~12 weeks of age. All lambs were born to overnourished adolescent mothers who had received bilateral uterine artery injections of Ad.VEGF (n=16), Saline (n=15) or not undergone surgery (n=6). There were no significant differences between these three groups and no gender X treatment interaction. Comparisons were made using the General Linear Model.

---

and postnatally. Of the original 40 pregnant ewes in this cohort, only 33 had been randomised to Ad.VEGF or Saline groups. The remaining seven had been managed contemporaneously in exactly the same way as their operated counterparts up until delivery and the resultant lambs received all the same neonatal care measures and postnatal investigations. One of these seven was crushed by its mother, leaving six survivors (five male and one female) at 12 weeks of age. The lambs were necropsied and underwent liver sampling and DNA extraction with the others.

Addition of these six lambs further strengthened the gender differences in DNA methylation of the insulin and IGF-1 genes, which are depicted in Figure 6.7. Differences were independent of

the study group (Ad.VEGF, Saline or unoperated). Insulin gene methylation correlated negatively with fasting plasma insulin levels measured prior to glucose challenge at ~7 weeks of age (r=-0.422, n=37, p=0.013), illustrated in Figure 6.8, but not with randomly timed insulin concentrations measured at weekly intervals between birth and necropsy (p>0.05) during which time lambs had free access to their mother's food hopper and were freely suckling. Similarly IGF-1 gene methylation did not correlate significantly with *in vivo* measurements of plasma IGF-1 at any stage (p>0.05).

Figure 6.8 – Correlation between methylation of the insulin gene and fasting plasma insulin

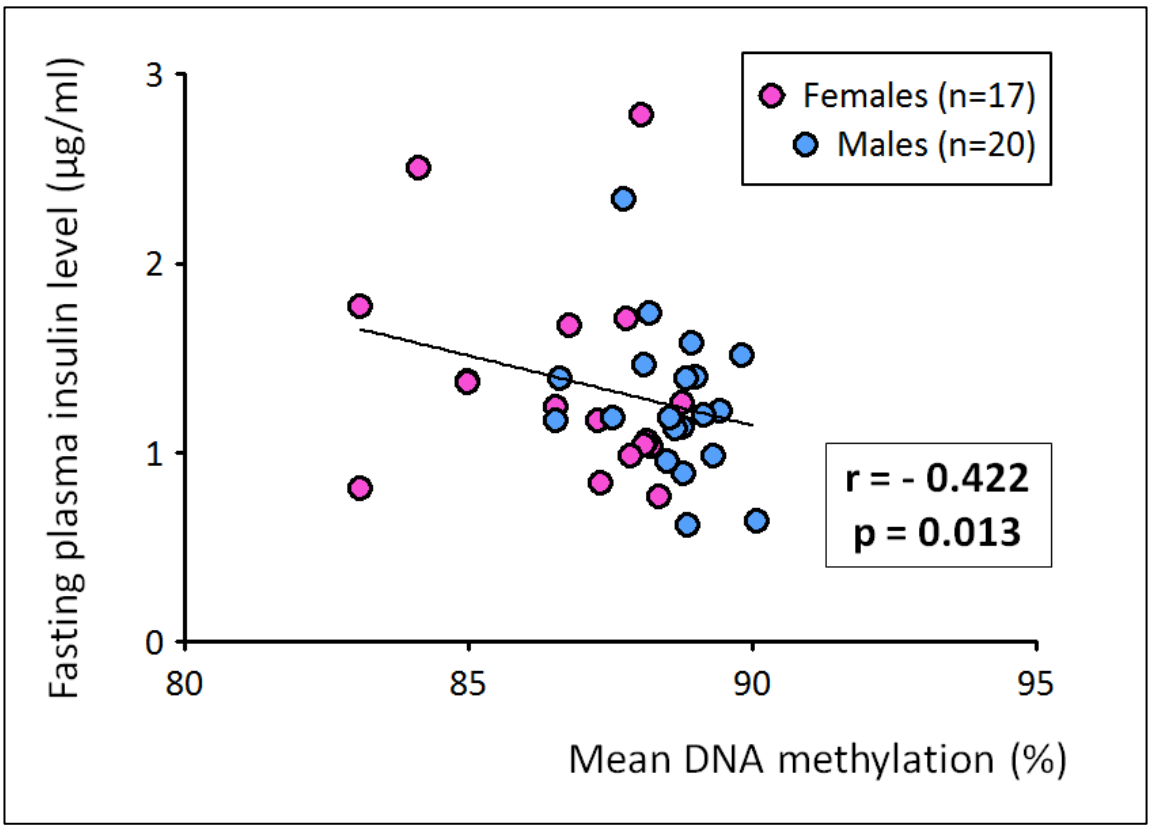

Scatterplot between mean insulin gene at 5 CpG dinucleotides examined in liver tissues at ~12 weeks of age and DNA methylation and fasting plasma insulin measured by radioimmunoassay at ~7 weeks of age. All lambs were born to overnourished adolescent mothers who had received bilateral uterine artery injections of Ad.VEGF (n=16), Saline (n=15) or had not undergone surgery (n=6). Correlation was assessed using Pearson's product moment test.

There were no consistent correlations between the methylation status of the genes examined and any other parameters in the postnatal study. However, interestingly GH gene methylation

was inversely related to lamb birth weight and necropsy weight in male lambs (r=-0.406, n=37, p=0.016; and r=-0.362, n=37, p=0.035, respectively) but not female lambs (p>0.05). Moreover the correlations observed between the methylation status of various genes (insulin, H19, GH and IGF-1) in the fetal cohort were not replicated in the postnatal study. The only consistent and significant correlation in this group was between IGF2 and IGF1R (r=0.476, n=37, p=0.004).

6.4 Discussion

6.4.1 Maternal Ad.VEGF therapy had no measurable effect on DNA methylation

From the results detailed above, there was no evidence that Ad.VEGF impacts the epigenetic status of the ten genes studied here in relation to postnatal growth and metabolism. The original rationale for performing these studies was the observation of enhanced absolute postnatal growth rates (see Section 5.3.5.1) and increased glucose-stimulated insulin secretion at 7 weeks postnatal age (see Section 5.3.7.2) following prenatal Ad.VEGF treatment. Although methylation status of the GH and insulin genes correlated inversely with lamb body weight (males only) and fasting insulin, respectively, no significant differences were seen according to treatment group. The lack of any measurable epigenetic effect of prenatal maternal Ad.VEGF therapy is reassuring and suggests that no permanent alterations in somatotrophic gene function have occurred as a consequence of attempting to therapeutically manipulate fetal nutrient supply. Consequently, it seems more likely that the increased postnatal growth and insulin secretion observed in Ad.VEGF-treated lambs reflect their relative size advantage at birth rather than altered epigenetic status of key genes related to postnatal growth and metabolism. However this is a relatively tentative conclusion as it remains possible that changes outwith the 57 CpG sites studied could have been missed. The bisulphite sequencing methods used herein provide a very high resolution assessment of methylation at specific loci, but are limited by the fact that only a small number can be examined in any one reaction. Furthermore the specific sites are limited to those around which functional primer sets can be designed, which largely depends on the neighbouring genes sequences. It is interesting that two of the three genes that showed significant gender differences in DNA methylation (IGF-1 and IGF2R) were the two genes with the greatest number of CpG dinucleotides assessed (13 and 11, respectively). It is possible that potential differences may have been missed in some other genes simply because too few CpG sites were assessed and/or the available sequences were too short. More recently array-based technologies have been developed for the human and mouse that can simultaneously examine a vast number of CpG sites (up to 450,000) in a single assay (Sandoval et al. 2011). However no such commercial kits were available for the sheep at the time of conducting (or writing up) the experiments detailed in this thesis. A

further limitation is that, although accepted criteria were used to identify CpG islands within published ovine gene sequences, the true biological significance of DNA methylation at these specific sites has largely not been assessed. Most of the ovine genes investigated herein were originally sequenced with the aim of examining their exonic arrangement rather than focusing on the 5' untranslated regions (i.e. the proximal introns) where the majority of CpG islands are known to lie (Kass et al. 1997). The methylation assays developed herein are novel and therefore direct comparisons with previous studies in the sheep is difficult. For example, Sinclair et al. (2007) reported alterations in DNA methylation following manipulation of dietary vitamin B and methionine content at 4% of 1400 loci in a gender-specific manner using restriction landmark genome scanning, however the identity of these loci was not explicitly dd. Wang et al. (2011a) recently examined methylation of the differentially methylated regions of IGF-2/H19 and IGF2R in cardiac tissue using combined bisulphite restriction analysis (COBRA) but found no significant changes secondary to ovine FGR induced by carunclectomy.

6.4.2 Fetal DNA methylation of growth related genes was not associated with FGR

In addition to evaluating the potential epigenetic effects of Ad.VEGF, it was also possible here to make comparisons between the normal and growth-restricted fetuses of control-intake and untreated high-intake ewes (receiving Ad.LacZ or saline), respectively, at late gestation but not postnatal time points. There were no significant differences in the DNA methylation status of eight different genes. Unfortunately no information was available for NRC31 and IGF2R genes. There were also no differences between marked FGR (fetal weight >2SD below control mean) when compared to non-FGR high-intake or control-intake pregnancies in any genes evaluated. Albeit subject to the same limitations as discussed above, these findings suggest that the FGR induced by overnourishment of the adolescent ewe is not epigenetically mediated at the level of the fetal/neonatal tissues, although it remains possible that the epigenetic status of various placental genes may be altered by changes in the intrauterine environment (Lee & Ding 2012).

In the human, genome-wide DNA methylation studies performed in monozygotic and dizygotic twins have highlighted the significant contribution that the intrauterine environment makes to the neonatal epigenome (Gordon et al. 2012). DNA methylation at LINE-1 repetitive elements, which is a surrogate for genome-wide methylation, correlates with birth weight centiles (Fryer et al. 2011) and hypo- and hyper-methylation of H19 and IGF2R, respectively, is seen in human FGR (Turner et al. 2010). Initial studies on individuals prenatally exposed to the Dutch famine (see Section 1.1.3.8) found reduced DNA methylation in the DMR of region of the IGF-2 gene (Heijmans et al. 2008) and the INSIGF gene, and increased methylation of the IL10, LEP, ABCA1 GNASAS and MEG3 genes (Tobi et al. 2009) only when the exposure occurred around the time

of conception and not in late gestation. The same group subsequently tested for differences at the same loci in adults born SGA following fetal growth restriction and found no differences in DNA methylation of IGF-2, GNASAS, INSIGF and LEP relative to appropriate-for-gestational-age controls (Tobi et al. 2011). The latter results suggest that not all long-term morbidity of FGR that is presumed to result from programming *in utero* is mediated by epigenetic mechanisms.

Nevertheless there is a growing body of evidence from different rat models that FGR can result in altered DNA methylation patterns in various genes. For example, FGR secondary to dietary restriction in the rat is characterised by neonatal catch up growth resulting in adult obesity and impaired glucose tolerance that is associated with hypermethylation of the promoter regions of the peroxisome proliferator-activated receptor (PPAR)-γ coactivator 1α and the insulin receptor genes as well as hypomethylation of the promoter regions of the PPAR-α and glucocorticoid receptor genes in the liver (Lillycrop et al. 2008; Burdge et al. 2009; Zeng et al. 2012). FGR secondary to bilateral uterine artery ligation in the rat results in hypermethylation of the IGF-1 gene (Fu et al. 2009) and gender-specific changes in hippocampal dual-specificity phosphatase 5 (DUSP5) methylation, which have been implicated in the impaired learning and memory seen following FGR (Ke et al. 2011). Genome-wide analysis in FGR rats suggests that methylation may be altered at up to 1400 different CpG sites in the pancreatic islet at 7 weeks of age (Thompson et al. 2010).

It is a potential limitation of this study that only effects on DNA methylation were examined, as it is feasible that epigenetic changes may alternatively be mediated via histone modification or miRNAs. FGR secondary to bilateral uterine artery ligation in the rat has been shown to modify histones in the IGF-1 (Fu et al. 2009), PPAR-γ (Joss-Moore et al. 2010) and the glucocorticoid receptor (Ke et al. 2010) genes in the liver, lung and hippocampus, respectively. FGR due to protein restriction in the rat increases methylation and reduces acetylation of histone H3 in the promoter region of the hepatic cholesterol 7α-hydroxyulase gene, which has been implicated in the pathogenesis of the hypercholesterolaemia that is observed in the adult offspring in this model (Sohi et al. 2011). FGR secondary to maternal undernutrition in the rat increases histone acetylation in the promotor region of the endothelin-1 gene in pulmonary vascular endothelial cells in an effect which is believed to contribute to the increased risk of hypoxia-induced pulmonary arterial hypertension in adult life (Xu et al. 2013). Although research into miRNAs in FGR to date is lacking, levels of miR132 are altered in growth-restricted rat pups after bilateral uterine artery ligation (Joss-Moore et al. 2011).

A further limitation of the current work is that patterns of methylation were only examined in hepatic tissue. Liver was chosen for this study as most of the previous work on the epigenetic

impact of FGR had been performed using this tissue type, and because the liver is an important metabolic organ. However it is now becoming clearer that the epigenetic changes observed in one tissue cannot necessarily be extrapolated to others. Even within a given tissue, there may be major differences between different cell types. Umbilical cord blood is often used to study neonatal epigenetic changes in the human as it is relatively easy to obtain (Fryer et al. 2009) however there are major differences between its constituents, for example the epigenomes of lymphocytes and monocytes have distinctly different profiles (Miao et al. 2008). This is particularly important when considering studies on the epigenetic status of the placenta, which are prevalent (Nelissen et al. 2011). Placental mRNA expression of IGF-2 is reduced in placentae from FGR pregnancies and associated with a loss of imprinting at two differentially methylated regions in the IGF-2 gene (Koukoura et al. 2011b). There is also hypomethylation of the H19 promoter region associated with increased mRNA expression of H19, which is consistent with reduced IGF-2 transcription (Koukoura et al. 2011a). Genome-wide placental DNA methylation has revealed differential methylation patterns throughout the genome with a slight overall tendency towards hypomethylation (Lambertini et al. 2011) and it has been suggested that placental methylation might be used as a marker of the intrauterine environment (Banister et al. 2011). Placental epigenetics may also give clues about causation of FGR, for example aberrant methylation of TBX15 gene is implicated in the pathophysiology of uteroplacental insufficiency (Chelbi et al. 2011). However given the high degree of tissue specificity, the coexistence of similar changes in fetal or neonatal tissues cannot be assumed.

6.4.3 Female fetuses had higher IGF2R gene methylation at 0.9 gestation

Irrespective of study group, the level of DNA methylation in the IGF2R gene was found to be significantly greater in female relative to male fetuses when examined in the liver tissue at 131 days gestation. IGF2R was the only gene to demonstrate any gender differences in the fetal cohort. There was no effect of FGR or prenatal Ad.VEGF gene therapy on IGF2R methylation. In the aforementioned study on individuals born following the Dutch famine, prenatal exposure had no effect on IGF2R methylation, however for the normal (unexposed) controls mean levels were 2.6% higher in males versus females in adult life (Tobi et al. 2009), which is the opposite pattern to that seen for these young lambs. Notably the epigenetic alterations in various other genes following periconceptual famine exposure were gender-specific, with effects on INSIGF and LEP restricted to men and GNASAS more pronounced in women. Other work in the human has shown that generally CpG sites show more methylation in males, with the exception of the DMRs of imprinted genes, in which DNA methylation appears to be more equal between sexes (El-Maarri et al. 2007). Unlike IGF1R, which mediates the mitogenic effects of IGF-1 and IGF-2,

IGF2R is a clearance receptor that antagonises IGF-2 action, and disruption of the IGF2R gene results in increased serum and tissue levels of IGF-2 and fetal overgrowth (Ludwig et al. 1996). Relative hypermethylation of the IGF2R gene in females might hypothetically be associated with reduced IGF2R gene expression and less IGF-2 clearance, however these potential effects have not been assessed here and no conclusions can be made regarding biological significance.

6.4.4 Female lambs had lower insulin gene methylation at 12 weeks of age

Irrespective of treatment group, female lambs were found to have less DNA methylation of the insulin gene compared with male lambs. Furthermore insulin gene methylation was negatively correlated with fasting plasma insulin levels, irrespective of gender. In spite of this however, there were no male versus female differences in fasting insulin levels, glucose-stimulated insulin secretion or any indices of insulin resistance (see Chapter 5) in this cohort, although glucose-stimulated insulin secretion has previously been shown to be lower in females compared with male lambs ($p<0.003$) at 7 weeks of age in the overnourished adolescent paradigm (Wallace et al. 2010b). In clinical studies, women have been shown to be less insulin resistant (Geer & Shen 2009) and to exhibit lower fasting insulin levels (Ferrara et al. 1995) compared with men. These latter changes would initially seem to be in the opposite direction to what would be expected from the insulin gene methylation differences seen here in the sheep. However the regulation of insulin gene transcription is highly complex (Melloul et al. 2002) and cleavage of insulin from its precursor protein *in vivo* is dependent on other factors including post-translational modification and diet. It was also interesting that the insulin gene demonstrated the highest levels of DNA methylation of all the genes examined in the present study (up to ~95%) and that these levels could only be reduced to ~40% by GWA, a technique which rendered the methylation status of all other genes <10%. The biological significance of these observations is unclear but they imply a high degree of resistant CpG methylation at this location in the insulin gene in the sheep fetus and young lamb. Irrespective of gender, insulin gene methylation correlated inversely with fasting insulin. This relationship is in the expected direction as higher degrees of DNA methylation would hypothetically be associated with less transcription and translation of the precursor protein preproinsulin. Insulin gene methylation was positively correlated with GH methylation, which did not did not differ by treatment group or gender but was inversely related to birth weight and live weight at necropsy in male lambs only. Again this relationship is biologically plausible, as increased GH gene methylation would hypothetically result in attenuated GH gene expression, GH protein levels and somatic growth.

6.4.5 Female lambs had greater IGF-1 gene methylation at 12 weeks of age

In contrast to the gender pattern for insulin gene methylation, DNA methylation of the IGF-1 gene was significantly greater in females versus males. Although DNA methylation status did not correlate with *in vivo* plasma measurements of IGF-1, the latter was significantly higher in males compared with female lambs throughout the first 12 weeks of life (see Section 5.3.5.5). Consequently the relative IGF-1 hypomethylation observed in males is in keeping with the greater IGF-1 protein levels, presumably as a result of increased transcription. With respect to both IGF-1 and insulin gene DNA methylation, it is interesting that there were no detectable differences when examined in late gestation in the fetal study. Obviously the two cohorts are not directly comparable, however this does suggest that these epigenetic gender differences emerge sometime between 0.9 gestation and 12 weeks of postnatal age, and probably during neonatal life. It may be that the changes only become apparent once the gastrointestinal tract and appetite axis become fully functional in the early neonatal period. Hence these changes may not actually be programmed *in utero* but represent dissimilarities that emerge alongside other sex differences such as fasting metabolite levels and relative adiposity during postnatal growth and development. In support of this concept, there is evidence that epigenetic changes can occur and can be prevented during postnatal life, for example amelioration of neonatal catch-up group by dietary manipulation in rat pups born following prenatal growth restriction appears to prevent the changes in IGF-1 methylation that otherwise occur in the first few weeks (Tosh et al. 2010) and is associated with an improved metabolic profile (Lim et al. 2011).

6.4.6 Methylation of IGF-2 and IGF1R was significantly lower in postnatal life

It was interesting that IGF-2 and IGF1R methylation was 41% lower in postnatal versus fetal tissues, whereas the other six comparable genes were very similar and consistently slightly higher in their degree of DNA methylation. Functionally IGF-2 is an important mediator of constitutive fetal growth but is largely replaced by IGF-1 around the time of birth and into the neonatal period (Fowden 2003). Accordingly disruption of the IGF-2 gene causes FGR without influencing postnatal growth rates (DeChiara et al. 1990) whilst overexpression causes fetal macrosomia (Efstratiadis 1998). IGF-2 also plays a role in the regulation of placental growth (Fowden & Forhead 2009), a role which becomes redundant after birth. Consequently it might be expected that IGF-2 methylation would be higher (rather than lower) during the postnatal period in view of the significant reduction that occurs in IGF-2 mRNA and protein expression. Alternatively it might be that non-epigenetic mechanisms (for example transcription factors, post-translational modification or antagonists) are responsible for the relative decline in IGF-2 levels that is observed approaching term (Mesiano et al. 1989).

6.5 Conclusions

There were no differences in DNA methylation of the insulin, IGF-2, IGF-1, H19, GH, GHR, insulin receptor or IGF1R genes in either fetal or lamb hepatic tissues following prenatal treatment with Ad.VEGF. In addition there were no differences in the IGF2R and glucocorticoid receptor genes in the lambs. This suggests that the increased postnatal growth rates and glucose-stimulated insulin secretion observed in Ad.VEGF-treated lambs most likely reflected their relative size advantage birth rather than an epigenetic effect. IGF-2 and IGF1R methylation was noted to be lower in postnatal relative to fetal life. IGF-1 gene methylation was higher in female versus male lambs at the postnatal stage, in keeping with the lower plasma IGF-1 levels observed in females compared with males. By contrast, insulin gene methylation was lower in female relative to male lambs and, irrespective of gender, was weakly correlated with fasting plasma insulin levels.

7.1 Discussion

The main aims of the research reported in this thesis were to evaluate the efficacy, safety and mechanisms of action of prenatal maternal Ad.VEGF gene therapy in fetal growth restriction induced by overnourishment of adolescent ewes. The aims were largely achieved and the positive results generated are encouraging, lending support to the notion that prenatal maternal Ad.VEGF gene therapy might, in the future, become the first effective treatment for severe early-onset FGR. This research has also given rise to several additional programmes of work, some ongoing and some scheduled, and together these are supporting the move towards clinical translation.

7.1.1 Effects of Ad.VEGF in ovine FGR

The following sections briefly summarise and draw together the most important findings from the two individual studies of Ad.VEGF in ovine FGR, which are detailed in Chapters 4 and 5.

7.1.1.1 Fetal growth and gestation length

In accordance with the original hypothesis, this work has provided first proof of principle that maternal uterine artery Ad.VEGF can increase fetal growth in pregnancies complicated by FGR. In two separate studies, mid-gestation delivery of Ad.VEGF to the uterine arteries in putatively growth-restricted sheep pregnancies produced a significant increase in fetal growth velocity, as indicated by increased ultrasonographic fetal abdominal circumference (AC) ± renal volume (RV) measurements, relative to fetuses receiving inactive control treatments (Ad.LacZ or saline). The precision around the estimate of treatment effect was high, given that the AC shift post-Ad.VEGF over this four week period was virtually equal in both studies (93 versus 92mm) despite different maternal donor genetics and a mean differential of one day in the timing of administration. The additional AC growth observed in Ad.VEGF-treated fetuses indicated a ~20% increase relative to the Ad.LacZ/saline comparator groups. In both studies these differences were significant at 3 and 4 weeks post-injection. The timing of these effects on fetal growth are entirely commensurate with the expected duration of adenoviral expression. It is important to note here that, with respect to clinical translation, it would not be necessary to completely normalise fetal growth. Rather the aim would be to moderately extend time spent safely *in utero* and to achieve a modest increase in weight prior to elective delivery because of fetal compromise. Consequently the fact that the effect appeared to tail off after 4

weeks is probably not important, given that the fetus would likely be delivered by this stage in the clinical situation. For example, hypothetically if we were to replicate these effects in treating a human fetus at the very threshold of viability, i.e. at 24 weeks gestation with an estimated weight of 500g, and to deliver at the peak of the effect (20% extra growth at 4 weeks), this might correspond to an additional 100g and delivery at 28 weeks gestation, which would be a respectable achievement. It is likely that the indication for delivery, deterioration in fetal wellbeing, would be the same in treated fetuses as in untreated fetuses. Clearly this extrapolation makes a number of different assumptions, and is rather speculative, particularly as this ovine model constitutes a relatively mild and late onset form of FGR (discussed further in Section 7.1.1.4 below). Nevertheless the fact remains that very modest increases in fetal growth, enough to delay delivery even by a few days or weeks, can translate into major improvements in survival and morbidity at this stage of pregnancy (Costeloe et al. 2000). For example, in one case series of extremely low birth weight infants born at 26 weeks of gestation, one-year survival was 78% with a birth weight of 601-700g versus 51% at 501-600g (Morse et al. 2006). In another series of extremely preterm babies, survival free of moderate or severe disability at 6 years of age was nearly three times greater (24% vs. 9%) at 25 compared to 24 weeks gestation (Marlow et al. 2005). As stated previously, gestational age at delivery is the single strongest predictor of neonatal outcome following FGR (Baschat et al. 2007) and thus a therapy capable of producing even a modest improvement in fetal growth or time spent *in utero* could make a significant difference to perinatal outcome in severe FGR. Interestingly, in the delivery cohort there was a trend towards a natural increase in gestation length in the Ad.VEGF-treated pregnancies of approximately two days, although these lambs still delivered slightly prematurely, three days prior to full term. This might possibly have been secondary to the attenuation of the increased relative adrenal growth that is seen in the model, which theoretically might initiate labour prematurely via increased fetal cortisol secretion. However, in clinical cases of severe early-onset FGR it is unlikely that pregnancies would be allowed to continue until spontaneous delivery at term, as was the case for these sheep experiments.

In both sheep studies, there was evidence of attenuated fetal brain sparing at post-mortem, in addition to the effects on ultrasonographic BPD:AC ratios, which were measured in the fetal study only. It is important to reiterate that growth of the fetal head in absolute terms was not altered, rather the abdominal (somatic) growth caught up with the preserved head growth. As discussed in detail in Section 4.4.2, this is likely to be a positive finding as it suggests that the need for the fetus to prioritise its brain growth has been reduced, implying a more favourable intrauterine environment and potentially enhanced fetal substrate supply. Although fetal brain

sparing is an adapative response (see Section 1.1.3.4), it is a marker of fetal hypoxia (Giussani et al. 2012) and appears to confer an increased risk of poorer neurodevelopemental outcomes in the longer term. Hence mitigation of the brain sparing effect is likely to be a positive feature.

7.1.1.2 Fetal weight and birth weight

Despite the positive effects of Ad.VEGF on ultrasonographic fetal growth velocity, when fetal weight at late gestation necropsy and birth weight at term were compared in absolute terms between treated and untreated groups, there was no significant difference and a tendency ($p=0.081$) towards a difference, respectively, in Ad.VEGF versus Ad.LacZ/saline-treated groups. However it must be borne in mind that in the sheep model of FGR that was used only ~52% of pregnancies are expected to demonstrate a marked degree of FGR (Wallace et al. 2004b). The proportion of markedly FGR pregnancies in the late gestation study was significantly reduced following Ad.VEGF treatment ($p=0.033$) to just 28%, which is well below the historical average. Although the term study lacked contemporaneous controls from which to estimate growth potential and determine the proportions of marked FGR, there was a conspicuous lack of very low birth weight lambs in the Ad.VEGF treated group: 0 of 17 versus 4 of 16 lambs <2500g in the Saline-treated group. Furthermore the mean difference between Ad.VEGF and saline-treated lambs overall was +681g (19.8%), which was very close to that used for the power calculation for this study (+719g; 20%). It was actually the variance introduced by the single very large lamb in the Saline group (discussed in Section 5.4.2) that reduced the statistical significance to $p>0.05$. Although no firm conclusions can be drawn from the these observations, together they imply that the effects of Ad.VEGF might be confined to, or at least greatest in magnitude in, the most compromised pregnancies. Consequently a more accurate estimation of effect size might be achieved if the study were to be repeated in only the most compromised overnourished adolescent pregnancies. Retrospective analysis of the ultrasound data (reported in Chapter 3) suggests that the umbilical artery Doppler indices and placentome index in mid-gestation are early predictors of eventual birth weight, and therefore selection of fetuses that are destined to become markedly FGR might be feasible using these parameters. In the postnatal study, Ad.VEGF-treated lambs demonstrated enhanced absolute postnatal growth velocity that was independent of any change in fractional growth rates and epigenetic status of key genes of the somatotrophic axis, and increased glucose-stimuated insulin secretion that was independent of any changes in markers of insulin resistance. These differences likely reflect their relative size advantage at birth rather than any intrauterine programming effect (discussed in Chapter 5).

7.1.1.3 Putative mechanisms of action

Prior to these studies in ovine FGR, most attention had been focused on the effects of Ad.VEGF at the level of the UtA, in particular the alterations in UBF, vascular reactivity, intima to media ratios and angiogenesis in the perivascular adventitia that had been shown following administration in normally developing sheep pregnancies (David et al. 2008; Mehta et al. 2011). These effects were not reproduced in the late gestation study detailed in this thesis, with the exception of bradykinin-induced relaxation of the UtA, which was strikingly enhanced following Ad.VEGF treatment. Possible reasons for the lack of differences in UBF and the other UtA parameters are discussed in detail in Chapter 4. However, an important and novel finding of this study was an upregulation of mRNA expression of both VEGF receptors (FLT1 and KDR) in the maternal placental compartment, downstream of the site of Ad.VEGF injection. Furthermore, placental efficiency (as indicated by the fetal to placental weight ratio) was significantly increased in Ad.VEGF-treated overnourished versus control-intake pregnancies in late gestation, and tended also to be increased in Ad.VEGF- versus saline-treated overnourished pregnancies at term. These observations suggest that effects at the placental level might be important in mediating the beneficial impact of Ad.VEGF on fetal growth. FLT1 and KDR are angiogenic factors and might therefore be expected to produce additional vascularisation in the placental bed during the remodelling phase of placental development in the final third of gestation (Borowicz et al. 2007). Although there was no evidence of enhanced placental secretory function, given that oestradiol levels did not change, there was a tendency towards higher GLUT1 mRNA expression in the maternal caruncle. Moreover, plasma glucose levels tended to be higher in Ad.VEGF treated lambs at birth, suggesting enhanced placental glucose transfer and fetal glucose supply.

Importantly there was no evidence in either of the studies of any transfer of the vector and/or transgene to the fetal placental compartment or fetus, which is in keeping with the findings in normal sheep pregnancy after uterine artery delivery of Ad.VEGF. More specifically, the effects of Ad.VEGF treatment on the mRNA expression of FLT1, KDR and GLUT1 were all confined to the maternal caruncle and there were no effects on the umbilical artery Dopplers, reflecting vascular resistance in the fetoplacental circulation. This is reassuring from a safety perspective and is a potential benefit of maternal Ad.VEGF therapy over pharmacological agents such as sildenafil citrate, which do cross the placenta in significant amounts. These findings may not be directly extrapolatable to human pregnancy, and this is discussed further in Section 7.1.3.1 below. However maternofetal transfer of VEGF-A_{165} and other isoforms is unlikely to occur as hydrophilic molecules usually cross the placenta via water-filled routes of a finite radius, which

restrict the passage of larger molecules like VEGF (Stulc 1989). This assumption has been supported by *ex vivo* experiments on human placenta, using VEGF-A_{165} (Brownbill et al. 2007).

7.1.1.4 Strengths and limitations of this work

The main strength of the studies detailed in this thesis lie in the use of a well-characterised large animal FGR model with key similarities to human uteroplacental insufficiency. In addition the study design incorporated elements that are considered important in human trials testing therapeutic interventions, namely randomisation and blinding. The randomisation procedure, which was based on the initial measures of the fetal abdominal circumference, renal volume and placentome index, did not result in a completely even allocation of all baseline parameters in the second study. The Ad.VEGF group demonstrated higher umbilical Doppler indices, which were not randomised for and which are associated with poorer placentation and fetal growth, however this is unlikely to have affected the interpretation of the results, as it actually biased the study against the hypothesis. Unbalanced characteristics at baseline are not uncommon in studies with relatively small numbers of animals or participants, and represents a chance imbalance rather than bias *per se*. Given the subjective nature of the ultrasound assessment of fetal growth, blinding is highly advantageous to avoid measurement bias. To my knowledge this represents the only study to date in which a prenatal intervention has been shown to increase fetal growth velocity when quantified by a masked assessor.

The main limitations of this work are the structural differences in placentation between sheep and humans and the relatively late onset of FGR in this particular model. Ultimately no animal model can completely represent the human condition and clinical trials in women with severe early-onset FGR will ultimately be needed (see Section 7.1.3 below). Placentation in ruminants such as the sheep is syndesmochorial. This is a subtype of the epitheliochorial placenta, which is the least invasive form (Kaufmann 1981). In ovine pregnancy here are six layers separating the maternal and fetal blood. Starting from the maternal side, these constitute: (1) maternal endothelium; (2) endometrial connective tissue; (3) endometrial epithelium; (4) trophoblast; (5) fetal connective tissue; and (6) fetal endothelium. By contrast, the process of trophoblast invasion of the maternal spiral arteries in the human destroys the maternal layers such that the maternal blood comes into direct contact with the trophoblast termed haemomonochorial placentation). The potential significance of these differences is two-fold. Firstly, it might be considered that viral vectors could more easily cross into the fetus in the human compared with the sheep, and this is discussed further below in Section 7.1.3.1. Secondly in the context of impaired trophoblast invasion, it remains unclear if a putative increase in UBF secondary to Ad.VEGF therapy would still be effective if the exchange barrier was greatly impaired, as might

be the case in the clinical situation. Furthermore inadequate villous development on the fetal side of the placenta (discussed in Section 1.1.2.3) might be a rate-limiting step for gaseous and nutrient impaired transfer, in which case theoretically increasing UBF might result in mismatch between the umbilical and uterine circulations. Reassuringly, however, the increase in fetal growth that was observed in the two sheep studies occurred in the absence of any significant change in the umbilical artery Doppler indices, which reflect fetoplacental resistance and blood flow, suggesting that a corresponding increase in umbilical blood flow is not actually necessary for therapeutic benefit.

The main rationale for choosing to use the overnourished adolescent sheep paradigm for these experiments was the relatively "natural" form of placentally-mediated FGR that is generated. However, as illustrated in Figure 3.1, despite the early insult on placental development, growth of the fetus is not impacted until the final third of gestation. In considering clinical translation it will be important to evaluate this therapy first of all in pregnancies with severe early-onset FGR, in which the growth of the fetus has slowed dramatically or completely arrested prior to a viable birth weight being achieved. In these pregnancies there is currently no other option for parents but to terminate the pregnancy or to await fetal demise *in utero,* should the fetus not reach a viable birthweight (~500g). The model used does not admittedly replicate this extreme form of FGR well. However, most of the other available models of FGR would have been completely unsuitable for these experiments as they involve surgical procedures that permanently compromise uteroplacental perfusion, which could not subsequently be restored by gene therapy treatment, e.g. carunclectomy, embolisation and arterial ligation. The single exception to this is FGR induced by maternal hyperthermia, which leads to an earlier perturbation of fetal growth that better mimics severe early-onset human FGR. However there is only a tendency towards a reduction in UBF ($p=0.07$) in absolute terms in this paradigm and UBF is actually increased relative to control (normothermic) pregnancies when expressed on a fetal weight specific basis (Regnault et al. 2003). This model features very high perinatal mortality rates: historically 29% of heat-stressed ewes will have a miscarriage or stillbirth, and 45% of live born lambs will die in the neonatal period (Shelton & Huston 1968). Furthermore it is relatively expensive to house sheep under constant hyperthermic conditions All these factors limited the suitability of the hyperthermia model for the studies detailed here.

A further potential criticism of the overnourished adolescent model might be the very aspects employed to maximise the genetic homogeneity, with the aim of controlling for various factors that confound the study of fetal growth. For example it is known that assisted reproduction is a risk factor for FGR (Jackson et al. 2004) and embryo transfer from an adult Greyface ewe into

a much smaller, peripuberal adolescent recipient is likely to result in an element of maternal constraint (see Section 1.1.2.2). For the purposes of the studies detailed in this thesis, all these factors were equally represented in groups receiving Ad.VEGF and inactive control treatments and the randomisation procedure effectively meant that the groups were similar in all respects other than the dietary manipulation and the treatment received. However there may have been pertubations of growth attributable to the assisted reproductive techniques, adolescent uterine environment and/or surgery to administer the vector/saline which were not directly measurable given the study design. Hence the additional effect of Ad.VEGF might differ in its magnitude if the study were to be repeated in naturally conceiving overnourished adolescent ewes or an adult sheep model of FGR. Similarly using a non-invasive means of accessing the uterine artery (Section 7.1.3.2.) might avoid the potentially negative effects of open abdominal surgery on fetal growth.

7.1.2 Ongoing work

7.1.2.1 Assessment of placental vascularity

Given the observed effects of Ad.VEGF on caruncular mRNA expression of VEGF receptors KDR and FLT1, an important question that remains unanswered is whether this had an impact on vascularity in the maternal and/or fetal placental compartments. Previously when proliferative growth in the maternal caruncle was compared between high- and control-intake adolescent sheep pregnancies at 50, 90 and 130 days gestation, various indices of vascularity were numerically lower at all stages of gestation in the placentae of overnourished dams, but these differences did not reach statistical significance (Redmer et al. 2009). This was in contrast to the fetal cotyledon, where vascular indices were actually increased secondary to high intakes at 90 days gestation, presumably as a form of compensation (discussed in Section 4.4.10). In the fetal study, placental tissues were immersion fixed in Carnoy's solution and embedded in paraffin for the subsequent quantification of placental vascularity. In collaboration with Professor Dale Redmer at North Dakota State University (NDSU), placental samples will be cut into 5µm sections, differentially stained to identify the maternal versus the fetal vessels within the placentome and subjected to image analysis to determine capillary area density, capillary number density, capillary surface density and area per capillary, as previously described by Borowicz et al. (2007). Gestational changes in these indices have been extensively examined in both normal and compromised sheep pregnancies and capillary area density is positively correlated with VEGF expression in both the carcuncle and cotyledon (Borowicz et al. 2007; Reynolds et al. 2010), thus there is a real possibility that adenovirus mediated over-expression of VEGF may impact placental vascular development and/or remodelling.

7.1.2.2 Expression of genes involved in placental transport

In both sheep studies there was a suggestion that Ad.VEGF might enhance placental transfer of glucose, as indicated by a tendency towards higher GLUT1 mRNA expression in the maternal caruncle in late gestation, and a tendency towards higher glucose levels in lamb plasma at birth. This effect may have contributed to enhanced fetal growth, either in addition to or independently of any (undetected) impact on UBF. Given the encouraging results for the glucose transporters, it is of obvious interest to examine for any evidence of altered amino acid and/or non-esterified fatty acid (NEFA) transport capacity, both of which are also important substrates for normal fetal growth (Hanson et al 1995; Glazier et al. 1997). In sheep, transfer of amino acids across the maternal-facing microvillous membrane is dependent on accumulative transporters, such as system A, and amino acid exchangers (Cleal & Lewis 2008). In addition there are facilitated transporters present in the fetal-facing basal membrane, which further promote transfer of amino acids into the fetal circulation, an example of which is T-type amino acid transporter, TAT-1 (Cleal et al. 2011). By contrast, NEFA are able to cross into the fetus by simple diffusion, however they first need to be released from the lipoprotein complexes that form in the maternal blood (Gude et al. 2004). Breakdown of these complexes is catalysed by lipoprotein lipase (LPL). It has been shown that levels of LPL protein are reduced in growth-restricted placentae (Magnusson et al. 2004), although this has not been measured to date in the overnourished adolescent paradigm. In collaboration with Drs Lucy Green and Jane Cleal, University of Southampton, mRNA expression of TAT-1 and LPL is being examined in the maternal and fetal placental tissues from the late gestation study. In addition, mRNA expression of the vitamin D and IGF1 receptor will be quantified, as these are considered important for the endocrine regulation of placental transport (Murphy et al. 2006). However, it must be borne in mind that there are potential limitations with this type of opportunistic *in vitro* analysis, considering that these studies were not specifically powered to detect differences in nutrient transporter gene expression. Given that the shift in fetal growth attributable to Ad.VEGF was relatively small compared with background differences between control- and high- intake pregnancies, greater numbers may be needed to detect a significant effect. Furthermore in the absence of reliable assays to quantify protein expression, differences in mRNA can be difficult to interpret. An alternative approach would be to study placental nutrient transport capacity dynamically by repeating the experiment in chronically catheterised animals, which would allow for rates of uptake and utilisation of various substrates by the gravid uterus as a whole, as well as the placenta and fetus, to be examined.

7.1.2.3 Assessment of small intestinal vascularity

Maternal nutrient restriction during sheep pregnancy has previously been shown to reduce jejunal capillary surface density in the offspring at three weeks of postnatal age (Meyer et al. 2013). In collaboration with Professor Joel Caton, NDSU, perfusion-fixed sections of fetal small intestine, prepared as described in Section 4.2.5.2 and depicted in Figure 4.4, and immersion-fixed in Carnoy's solution, will be examined to quantify jejunal vascularity. In the late gestation study, overnourishment of the adolescent ewe was associated with a significant increase in relative small intestinal weight relative to control-fed ewes, and Ad.VEGF therapy attenuated this effect. A comparison of fetal small intestinal vascularity between control- and (untreated) high-intake pregnancies will assess whether FGR *per se* has any impact on the number or density of mesenteric blood vessels in this paradigm. It will also be assessed whether Ad.VEGF attenuates any such effect. In addition, mRNA expression of key angiogenic factors and receptors will be examined using RT-PCR in snap-frozen fetal jejunal tissues and correlated with these vascular indices. Redistribution of the fetal cardiac output away from the developing gut (see Section 1.1.3.4) results in an insult to the mesenteric blood supply, which is implicated in the pathogenesis of necrotising enterocolitis (NEC) in the human newborn (Lin et al. 2008). Although NEC has not to date been observed as a consequence of FGR in the overnourished adolescent paradigm, secondary effects of Ad.VEGF therapy might include a reduced risk of this particular neonatal complication if successfully translated into the clinic.

7.1.2.4 Assessment of somatotrophic gene expression

In Chapter 6, the DNA methylation status of ten somatotrophic axis genes was quantified to examine whether the observed effects of prenatal Ad.VEGF treatment on postnatal growth and metabolism were epigenetically mediated. This work is being extended by determination of mRNA expression of these same ten genes in hepatic tissues by qRT-PCR. This will facilitate correlation between methylation status and gene expression, and also examine for a potential upregulation of the somatrophic axis through alternative, non-epigenetic mechanisms. As discussed in Section 6.4.2, DNA methylation status varies greatly between different cell and tissue types. It would therefore have been interesting to analyse additional tissue sets, such as the pancreas and perirenal fat, from these studies for the same 10 genes. However given the current lack of evidence of any baseline epigenetic differences in this particular sheep model of FGR and the relative expense of pyrosequencing, it was not considered worthwhile pursuing in these particular tissues. However, given the potential of Ad.VEGF to mitigate FGR, repeating the experiment in an established model of intrauterine programming (ovine or murine) might

be informative and would be a better means of investigating whether Ad.VEGF can benefit the longer term health of the offspring. This aspect is considered further in Section 7.1.2.6 below.

7.1.2.5 Evaluation of prenatal Ad.VEGF therapy in a guinea pig FGR model

At the time of writing, complementary experiments are underway to investigate the effects of Ad.VEGF treatment in a guinea pig model of FGR induced by periconceptual maternal undernutrition. Restriction of maternal caloric intake by 70% for 4 weeks pre-conception and for the first half of pregnancy, followed by 90% for the second half of pregnancy, results in a 40% reduction of fetal weight with asymmetrical growth restriction and fetal brain sparing. Although UBF has not specifically been measured in this model, there is evidence of uteroplacental insufficiency in the form of a reduced placental exchange surface area and increased thickness of the exchange barrier (Roberts et al. 2001). The guinea pig was chosen for additional experiments in view of it similarity to the human with respect to placentation and the relatively long length of gestation for a rodent. Guinea pigs have a haemochorial placenta and there is trophoblast invasion of the radial arteries (Mess 2007). Treatment of the uterine and radial arteries with Ad.VEGF, administered externally using a thermosensitive pluronic gel, reduced brain to liver weight ratios and tended to increase fetal weight compared to Ad.LacZ treatment (0.45±0.019 vs. 0.53±0.017, p=0.021, and 95±2.0 vs. 85±2.8g, p=0.061; respectively) (Mehta et al. 2012), replicating the findings of the sheep studies presented in this thesis. Although this data is provisional, it further supports the efficacy of prenatal Ad.VEGF gene therapy in FGR and the move towards clinical translation.

7.1.2.6 Assessment of longer term outcomes

An important consideration that has not been addressed by this particular programme of work is the effect of Ad.VEGF on long term morbidity. As discussed in Sections 4.4.2 and 7.1.1.1, it is becoming increasingly recognised that fetal adaptive mechanisms such as the brain sparing effect may actually indicate an increased risk of a poorer neurological outcome. In both the sheep studies detailed in this thesis, there was evidence that Ad.VEGF attenuated fetal brain sparing, which potentially represents an additional benefit of treatment. However it remains to be seen whether this translates into a measurable effect on motor or cognitive function. Additional funding is currently being sought to examine the impact of Ad.VEGF treatment on neurological outcomes using the guinea pig model of FGR described above. In addition, it will be important to examine the impact of prenatal Ad.VEGF therapy on health and wellbeing in adult life to investigate whether improving the fetal growth trajectory can mitigate the adverse metabolic phenotype that is often seen following FGR. However, this is likely to be a secondary

consideration for clinical translation as the primary aim will be to reduce: (a) perinatal mortality; and (b) neonatal morbidity in severe cases of FGR. However any additional benefit on the long term wellness of the individual would be very welcome and could have a significant positive impact at a public health level. Currently much attention is focused on the role of various preventive nutritional strategies in pregnancy and early childhood to reduce the burden of cardiovascular and metabolic disease in adulthood (Barouki et al. 2012; Balbus et al. 2013), however it remains to be seen whether prenatal treatment of established FGR might have a similar impact.

7.1.3 Moving towards clinical translation

On the back of the studies detailed in this thesis, funding has now been secured from the European Union via a Framework Programme 7 grant for a series of different work packages with the overall aim of translating Ad.VEGF therapy into the clinic for the treatment of severe early-onset FGR. The EVERREST project (Does vascular endothelial growth factor gene therapy safely improve outcome in severe early-onset fetal growth restriction?) includes a full reproductive toxicology programme, a bioethical study and a first in-woman phase I/IIa trial to be conducted across four European clinical centres of excellence. There are likely to be various challenges in the development of the clinical trial protocol for the latter. Patient numbers will be limited to 24, and a 3+3 dose escalation dosing regimen in serial patients will be used, with an emphasis on safety. Perinatal outcomes will be compared to data from historical controls that will be collected prospectively during the course of the study from the four participating centres. As the study will be underpowered to look at morbidity and mortality, long-term follow up will be essential.

Very few other therapies are at an equivalent stage of development for FGR or other obstetric complications. As discussed in Section 1.1.4.5, a randomised clinical trial of sildenafil for severe FGR is underway (STRIDER) despite the various concerns about efficacy and safety of this drug, in particular with respect to the risk of placental steal and preventing fetal compensation. Two potential advantages of prenatal Ad.VEGF gene therapy over sildenafil are: (a) that the former is capable of locally targeting the uteroplacental circulation by transducing only the uterine arterial circulation; and (b) that a sustained increase in UBF and/or fetal growth can be achieved using only a single dose. Other groups have begun to investigate the potential of gene therapy for obstetric conditions, but are not yet ready for clinical studies. Systemic delivery of adenoviruses encoding VEGF-A_{121} in a mouse model of pre-eclampsia reduces maternal hypertension and proteinuria (Woods et al. 2011), and placental-specific adenovirus-mediated over-expression of angiopoietin 2 has been shown to increase fetal weight in normal

mouse pregnancy (Katz et al. 2009), although efficacy in an animal model of FGR is yet to be reported. Currently the number of new therapies under development in Obstetrics is limited when compared to other medical fields, which is likely to be a reflection of the cost of reproductive toxicology experiments and long-term follow-up of the offspring, as well as specific concerns about teratogenicity and ethics.

7.1.3.1 Safety aspects of Ad.VEGF in pregnancy

It is reassuring that there were no obvious signs of toxicity from the adenoviral vector in the sheep studies. With respect to maternal wellbeing, ewes receiving Ad.VEGF or Ad.LacZ did not show any delay in their post-operative recovery that might have been suggestive of systemic infection, and their re-alimentation was equivalent to saline treated ewes. Analysis of neonatal blood samples obtained at 1 week of age did not show any detrimental effect on liver function or serum biochemistry. This is in agreement with previous investigations on maternal and fetal blood at 1 and 6 weeks following vector injection (David et al. 2008; Mehta et al. 2011), which also included routine haematological parameters. The lack of evidence of liver dysfunction is particularly encouraging. Given the equivalent size of the sheep and the human (both mother and her fetus), this suggests that the dose used is unlikely to be harmful and is likely to be clinically relevant. Given the differences between human and sheep placentation, there remains a possibility that Ad.VEGF may cross into the human fetus. Direct fetal administration of adenovirus has been shown to induce an immune response (McCray et al. 1995), which becomes more pronounced following repeated exposure (Iwamoto et al. 1999). For long-term gene therapy applications, an immune response may be detrimental. However given that transgene expression in the fetal tissues is not necessary for the beneficial effects described in this thesis, an immune reaction to mop up any spillover into the fetus would not be undesirable under the circumstances. This highlights the fact that this is ultimately a maternal therapy, albeit one that is indicated on fetal grounds. Moreover, there is some evidence from previous experiments that transfer of Ad.VEGF across the human placenta is unlikely to occur at all. This may relate to the availability of the Coxsackievirus and adenovirus receptor (CAR), a type 1 membrane receptor encoded by the CXADR gene that the adenovirus needs to bind to in order to gain access to the cell, via internalisation (Nemerow & Stewart 1999; Carson 2001). It has been demonstrated that CAR is continuously expressed on the fetal side of the placenta within the invasive cytotrophblast but not the syncytiotrophoblast, which renders the latter resistant to adenoviral infection and limits placental transfer (Koi et al. 2001). It appears that the ability of the adenovirus to infect the trophoblast is related to its state of differentiation, as transduction efficiency is reduced once the mononucleated cytotrophoblast cells terminally

differentiates into mulitnucleated syncytiotrophoblast cells (MacCalman et al. 1996; Parry et al. 1998). However, although susceptibilty to adenoviral infection is related to the presence or absence of CAR, adenoviral infection has been achieved in cell lines and animals that would otherwise be considered non-susceptible when modified viruses (e.g. gene therapy vectors) or high concentrations of wild-type viruses are delivered (Batra & Sharma 2002; Kim et al. 2002).

In collaboration with Professor Colin Sibley at the Maternal and Fetal Health Research Centre, University of Manchester, it has been shown that high-dose Ad.VEGF has no obvious adverse effects on the structure and function of human placental explants in culture. This has also been evaluated in the *ex vivo* dual perfused lobule. In both sets of experiments there was no detrimental effect of Ad.VEGF on placental cell survival, enzyme activity and hormone secretion. In the present studies, there were no gross abnormalities in fetal or maternal tissue at the time of necropsy. This is important as sustained over-expression of VEGF has been associated with tumorigenesis and reduced life span in mice (Lee et al. 2000; Kotimaa et al. 2012). This is one rationale for the use of a short acting vector such as the adenovirus, which prevents the long term expression that may otherwise occur with the use of lentiviral VEGF, for example (Azzouz et al. 2004; Jiang et al. 2008). Previous work in normal sheep pregnancy has included microscopic examination of a range of H&E-stained maternal and fetal tissues (including heart, lung, liver, kidney, adrenal, spleen, brain, thymus and gonad) and similarly failed to reveal any abnormalities following prenatal adenoviral delivery (David et al. 2008). Furthemore there were no adverse effects on maternal or fetal haemodynamic parameters when these were directly measured and no undesirable expression of Ad.VEGF was detectable in the peripheral maternal circulation or in any fetal tissues when examined by RT-PCR (David et al. 2008; Mehta et al. 2011).

Further toxicology studies are planned using the pregnant New Zealand white rabbit, which is considered to be the best model for this purpose as it most closely mimics human placentation during the second trimester, which is haemodichorial rather than haemomonochorial as is the case in the third trimester. This is important considering the timing of Ad.VEGF treatment for the eventual clinical trial, which would probably be around 22 to 24 weeks gestation. This work will involve exposing the pregnant rabbit to extremely high concentrations of vector in order to determine the safety window between therapeutic and toxic (titrated up to lethal) doses. Detailed histological examination of maternal and fetal tissues will be performed, as well as an investigation of vector biodistribution using quantitative PCR. For any subsequent clinical study it will be important to determine the most appropriate vector dose to maximise the treatment effect whilst minimising any potential adverse side-effects.

7.1.3.2 Delivery of the vector to the human uterine artery

During these studies there were no obvious adverse fetal responses to the injection procedure, although no vital signs were specifically monitored. In the previous studies in normal sheep pregnancy, fetal heart rate and blood pressure (measured invasively) were unaffected by UtA occlusion. Unlike the present study, in these experiments flow probes were implanted prior to vector injection in order to record baseline measurements of UBF. This revealed an acute drop in UBF of approximately 10% in the first three days following injection of Ad.VEGF or Ad.LacZ. It was supposed that this was due to the 5-minute vascular occlusion and associated trauma to the vessel wall. However in all cases UBF was restored by 5 to 7 days. In the longer term there was no evidence of damage to the UtA vessel wall, and no obvious oedema, inflammation or leucocyte infiltration at the time of necropsy (Mehta et al. 2011). It is not possible to say whether a similar drop in UBF occurred in the present studies as no baseline measurements were made. This was due to the fact that the adolescent ewes had already undergone a mini-laparotomy for embryo transfer, and two further laparotomies for flow probe placement and gene therapy administration, respectively, would have required additional regulatory approval from the Home Office, which we were advised by the local inspector would not be forthcoming on welfare grounds. Moreover monitoring did not begin until the third post-operative day to allow ewes to fully recover from the midline laparotomy. This potential acute drop in UBF remains a concern from the point of view of clinical translation as severely growth-restricted fetuses are already likely to be hypoxaemic (Akalin-Sel et al. 1994; Nicolini et al. 1990). However, on the other hand it could be argued that chronically hypoxaemic fetuses might be *more* tolerant of further temporary hypoxia. For example, it is recognised that uncompromised term fetuses are more vulnerable to hypoxic-ischaemic insults due to intrapartum asphyxia than compromised (preterm or growth-restricted) fetuses. Although the most compromised fetuses of overnourished adolescent ewes are modestly hypoxaemic in late gestation (Wallace et al. 2002), it is not known whether this is also the case mid-gestation.

In view of the risks of preterm labour and fetal loss following maternal laparotomy ± uterine manipulation during pregnancy in humans (McGory et al. 2007), access to the UtA for the trial will be via transfemoral catheterisation (Delotte et al. 2009). This is a clinical procedure that is already approved by the National Institute for Health and Clinical Excellence (NICE) and is used for the management of postpartum haemorrhage and menorrhagia due to uterine fibroids by embolisation. Occlusion would still be required but could be achieved via intraluminal balloon inflation. A critical safety consideration with respect to UtA occlusion is the availability of a collateral circulation to maintain oxygen supply to the fetus during the occlusion. Collateral

supply might come from the contralateral UtA or via the ovarian blood vessels. This was not a problem in the sheep experiments however there is evidence that the ovine uterus is relatively hyperperfused, which might protect the fetus against short term reductions in UBF of <50% (Skillman et al. 1985). It will be important to monitor the fetal heart rate using an external ultrasonic transducer during vascular occlusion and to have a low threshold to abandon the occlusion should a significant fetal bradycardia develop. Pre-oxygenation of the mother may be considered and is unlikely to be harmful in the short term, although there is evidence that prolonged exposure to maternal oxygen therapy is detrimental to the fetus (NICE 2007). In the context of a pre-viable fetus with absent growth velocity, the risk of the injection procedure and occlusion is likely to be outweighed by the high risk of intrauterine death in this particular scenario. However in less severe cases, this risk : benefit ratio may be altered. Extra-luminal delivery of Ad.VEGF (as used in the guinea pig experiments outlined above) is unlikely to be feasible in the human as this would probably necessitate a laparotomy.

7.1.3.3 Ethical barriers to implementation

Gene therapy treatment raises a great number of ethical issues, particularly where the fetus is involved. One specific concern about prenatal gene therapy in general is potential transmission to the fetal germline, which may potentially result in transgenerational adverse effects. There is also a potential risk of insertional mutagenesis, leading to tumour formation. One of the real benefits of using adenoviral vectors is that these risks are negated by the fact that they are non-integrating in nature. Any fetal intervention can precipitate preterm birth and this would further compound the problem for an affected fetus. However if Ad.VEGF were to be given at a non-viable stage then the risk imposed would be miscarriage rather than a potentially poor neonatal outcome, which is arguably less of a burden.

Informed consent will be essential for recruitment to the phase 1 clinical trial and for potential widespread dissemination of this therapy in the longer term. One particular issue is likely to be the potentially short interval between diagnosis and the proposed intervention. This may not allow women the time to fully process all the information in order to make an informed choice. A further issue is that, in the UK, the fetus officially has no rights *per se* until the time of birth. Nevertheless, understandably mothers do bestow moral status on their fetuses. This is based upon the fact that the fetus has an undeniable potential to become a person in its own right. The point of gestation at which the fetus is considered to satisfy such criteria is variable across cultures. Some would argue that this only occurs at the point of viability. Potential target pregnancies for this therapy would be those where the estimated fetal weight remains below 500g, which would technically not meet the criteria for viability.

After consenting to prenatal Ad.VEGF gene therapy, the mother essentially takes on the risks of the procedure. This is similar to the situation with respect to fetal surgical intervention. For example, prenatal repair of myelomeningocoele (spina bifida) when compared with standard postnatal surgery is associated with a reduced need for ventriculoperitoneal shunting and better neurological outcomes at 2 years of age, despite a significant increase in preterm birth rates and iatrogenic membrane rupture (Adzick et al. 2011). However this approach requires a hysterotomy in mid-pregnancy that is associated with considerable maternal morbidity due to uterine scar dehiscence and infection, and an increased risk of complications in future pregnancies (Clow & Crompton 1973). This highlights the potential fetomaternal conflict that may arise where an intervention for fetal benefit can cause maternal harm. It is essential that the mother maintains her autonomy in such situations, and that health professionals do not pressure her in any way towards interventions based on their own consideration of the fetus as a patient (Chervenak & McCullough 2002).

Another consideration that is unique to Fetal Medicine practice is the option of termination of pregnancy in some countries, which provides the parents with a 100% guarantee that the child will not suffer any residual morbidity. At University College Hospital between 2000 and 2012, approximately 10% of parents (n=7) chose to terminate pregnancies that were diagnosed as affected by severe early-onset FGR (DJ Carr, unpublished data) rather than take the risk of having a child with potentially severe handicap. However in some countries and cultures, termination of pregnancy may not be acceptable. Parents faced with severe early-onset FGR with a very poor outlook will still have the option of not continuing with the pregnancy, and it could be argued that choosing to receive experimental gene therapy represents a "gamble". Attitudes towards termination will be important to consider in developing the clinical trial protocol as this may introduce bias into recruitment, e.g. an ethnic mix that is not completely representative of the general population to which the results will be extrapolated. Furthermore, particularly as it seems unlikely that Ad.VEGF therapy will completely normalise fetal growth (see Section 7.1.1.1 above), it might be possible that treatment may shift a fetus otherwise destined to be stillborn just across the threshold of viability and constitute a poor perinatal outcome. This issue is not limited to consideration of Ad.VEGF gene therapy for FGR alone, but is relevant when considering other fetal interventions, such as maternal steroids to mature the fetal lungs, intrauterine fetal blood transfusion, fetoscopic tracheal occlusion for congenital diaphragmatic hernia or open fetal surgery for spina bifida surgery. Some parents might argue that a "partial cure" of this nature might be worse than no cure. This would be particularly true for patients who would not have otherwise chosen to continue the pregnancy, had the prenatal gene therapy option not been available. This possibility of a poor outcome

despite an attempt at *in utero* therapy will need to be explicitly discussed in order to ensure that the parents fully understand the implications, as such decisions cannot be reversed. In some cases, termination of pregnancy may remain an option following prenatal Ad.VEGF if beneficial effects on fetal growth and/or wellbeing are not seen. If preterm delivery ensues it may also be a reasonable option not to resuscitate the neonate, depending on birth weight and gestational age. This is currently the case for spontaneous preterm birth near the limit of viability. Such decisions require a detailed discussion with the neonatologists about prognosis.

Ultimately the risk-benefit ratio for prenatal gene therapy is still not clear, unlike some of the more common invasive fetal procedures such as laser ablation of placental vessels in twin-twin transfusion syndrome and fetal blood transfusion for haemolytic disease, where analysis of outcomes over the last 20 years has determined the risks and benefits. Consequently the issue of informed consent is challenging (Burger & Wilfond 2000). The relative lack of qualitative research in this area of practice leaves many questions unanswered about what parents would consider acceptable in the realm of fetal therapy. This highlights the need for a bioethical study, which will be performed prior to a phase I/IIa clinical trial. This study will aim to explore the attitudes of mothers and fathers, health professionals and other relevant stakeholders towards maternal Ad.VEGF gene therapy for fetal benefit across the European Union.

7.1.3.4 Wider applications: pre-eclampsia and late-onset FGR

As mentioned above, the proposed phase I/IIa clinical trial will aim to recruit only pregnancies affected by severe early-onset FGR (incidence 1:500) for which the only current alternatives are to perform a termination of pregnancy or to await fetal demise *in utero* should fetal weight never reach a viable threshold. However, should Ad.VEGF prove to be effective and safe, then the therapy may be of use for placental disorders in a much wider sense. Milder and later onset forms of FGR are much more common, affecting around 8% of pregnancies (Mandruzzato et al. 2008). Unlike early-onset FGR, the problem is usually more one of identification, as cases tend to present after the routine second trimester anomaly scan. Once FGR is diagnosed, the prospect of delivering the compromised fetus is far less of a problem at later gestations, however delivery does not appear to improve outcome, according to the results of the DIGITAT trial (see Section 1.1.4.6). Consequently treatment with Ad.VEGF in the late second or even third trimester may still be helpful depending on the safety profile of the therapy. The burden of mild FGR is considerable, as a large proportion of stillborn babies have evidence of unrecognised growth restriction (Cousens et al. 2011).

Pre-eclampsia is a pregnancy complication that is closely related to FGR and shares a similar

pathogenesis, i.e. impaired trophoblastic invasion of the spiral arteries (see Section 1.1.2.3). Pre-eclampsia complicates up to 10% of pregnancies (Sibai et al. 2005) and is a leading cause of maternal death (Cantwell et al. 2011), mainly due to complications of stroke and eclampsia. In addition to causing FGR, pre-eclampsia produces a maternal syndrome that is characterised by gestational hypertension, oedema and proteinuria. There is often widespread endothelial dysfunction that can lead to a number of superimposed crises including pulmonary oedema, renal failure, placental abruption, haemorrhagic stroke, HELLP (haemolysis, elevated liver enzymes and low platelets) syndrome. For the planned phase I/IIa trial of Ad.VEGF in FGR it will be important to exclude cases of established pre-eclampsia where possible, as maternal complications may indicate delivery before an assessment of the fetal response to therapy can be made. Ultimately maternal health takes priority over that of the fetus. However, should Ad.VEGF therapy prove effective for isolated FGR, an improvement in uteroplacental perfusion may also mitigate endothelial dysfunction and thereby reduce the severity of the maternal syndrome. The effects on maternal parameters such as blood pressure and urinary protein will need to be evaluated in due course.

7.2 Conclusions

In a well-established sheep model of placentally-mediated FGR induced by overnourishment of the pregnant adolescent ewe, bilateral uterine artery injections of Ad.VEGF in mid-gestation:

- Significantly increased fetal growth velocity (reflected by greater abdominal circumference ± renal volume measurements) at 3 and 4 weeks post-injection: ultrasonographic growth assessed by single operator blind to treatment; findings replicated in two separate studies
- Mitigated brain sparing, reflected by lower biparietal diameter : abdominal circumference ratios throughout the final third of gestation / lower brain : liver weight ratios at necropsy
- Reduced the incidence of marked FGR in late gestation (resulting in fewer fetuses with a birth weight >2 standard deviations below the normally-grown control-intake mean)
- Tended to increase lamb birth weight near term, gestation length and placental efficiency
- Attenuated disproportionate relative growth of the fetal adrenal gland and small intestine
- Increased the relaxation response of the uterine artery in response to bradykinin
- Increased caruncular expression of both VEGF receptors, FLT1 and KDR
- Tended to increase caruncular expression of GLUT1 and plasma glucose levels at birth

- Was not associated with any maternal, fetal or neonatal complications around the time of gene therapy treatment, at delivery near to term and during the first 12 weeks of life
- Increased absolute postnatal growth velocity without affecting fractional growth rates or the epigenetic status of key genes of the somatotrophic axis
- Increased glucose-stimulated insulin secretion and non-esterified fatty acid suppression without affecting indices of insulin resistance
- Tended to increase lean tissue mass and bone mineral density and significantly increased perirenal fat weight in female lambs only at 12 weeks of age

Despite these positive effects, no measurable effect of Ad.VEGF was seen on serial *in vivo* measurements of UBF. The lack of any sustained differences in UBF between control- and high-intake adolescent pregnancies however was highly suspicious, as was the lack of a normal 2-3 fold gestational increase in UBF during the second half of gestation. It appears likely therefore that the telemetric monitoring equipment used in this study was not functioning properly. The alternative explanation is that Ad.VEGF had no genuine impact on UBF and that its effect on fetal growth was mediated by other factors, such as placental nutrient transport capactity. No effect of Ad.VEGF was seen on IMR or neovascularisation in the perivascular adventitia. This may reflect differences in study design or adaptive responses to uteroplacental insufficiency, given that the latter was significantly increased in high- relative to control-intake pregnancies.

This work has demonstrated proof of principle that prenatal maternal Ad.VEGF gene therapy safely improves fetal growth in pregnancies complicated by FGR. There was no measurable effect on UBF, intima to media ratios or neovascularisation (all proposed mechanisms of action from previous work) however there was evidence of effects mediated downstream at the placental level, particularly an upregulation of FLT1, KDR and GLUT1 in the maternal caruncular tissues. These findings have led on to additional work to examine the effect of Ad.VEGF on placental vascularity and genes involved in placental nutrient transport in order to further investigate the mechanisms of action. In addition, funding has been secured to perform reproductive toxicology experiments, a bioethical study and first-in-woman phase I/IIa clinical trial in the move towards translation of this novel therapy into the clinic. There are likely to be considerable practical and ethical barriers to overcome in developing this treatment for human use. Safety will be key, given the limitations of the present study and the differences between species, particularly with respect to placentation. Nevertheless, prenatal maternal Ad.VEGF gene therapy has the potential to become the first effective treatment for severe early-onset fetal growth restriction.

- Abalos E, Duley L, Steyn DW, Henderson-Smart DJ. Antihypertensive drug therapy for mild to moderate hypertension during pregnancy. *Cochrane Database Syst Rev* 2007; (1): CD002252

- Abbas A, Snijders RJ, Nicolaides KH. Serum ferritin and cobalamin in growth retarded fetuses. *BJOG* 1994; 101: 215-219

- Abi-Nader KN, Mehta V, Wigley V, Filippi E, Tezcan B, Boyd M, Peebles DM, David AL. Doppler ultrasonography for the noninvasive measurement of uterine artery volume blood flow through gestation in the pregnant sheep. *Reprod Sci* 2010; 17: 13-19

- Acharya G, Erkinaro T, Makikallio K, Lappalainen T, Rasanen J. Relationships among Doppler-derived umbilical artery absolute velocities, cardiac function, and placental volume blood flow and resistance in fetal sheep. *Am J Physiol Heart Circ Physiol* 2004; 286: H1266-H1272

- Acharya G, Sitras V, Erkinaro T, Makikallio K, Kavasmaa T, Pakkila M, Huhta JC, Rasanen J. Experimental validation of uterine artery volume blood flow measurement by Doppler ultrasonography in pregnant sheep. *Ultrasound Obstet Gynecol* 2007; 29: 401-406

- Ackerman J, Gonzalez EF, Gilbert-Barness E. Immunological studies of the placenta in maternal connective tissue disease. *Pediatr Dev Pathol* 1999; 2: 19-24

- Adams TE, Baker L, Fiddes RJ, Brandon MR. The sheep growth hormone receptor: molecular cloning and ontogeny of mRNA expression in the liver. *Mol Cell Endocrinol* 1990; 73: 135-145

- Adams TE. Differential expression of growth hormone receptor messenger RNA from a second promoter. *Mol Cell Endocrinol* 1995; 108: 23-33

- Adams MB, Phillips ID, Simonetta G, McMillen IC. Differential effects of increasing gestational age and placental restriction on tyrosine hydroxylase, phenylethanolamine N-methyltransferase, and proenkephalin A mRNA levels in the fetal sheep adrenal. *J Neurochem*. 1998; 71: 394-401

- Adamson SL, Morrow RJ, Langille BL, Bull SB, Ritchie JW. Site-dependent effects of increases in placental vascular resistance on the umbilical arterial velocity waveform in fetal sheep. *Ultrasound Med Biol* 1990; 16: 19-27

- Adzick NS, Thom EA, Spong CY, Brock JW,3rd, Burrows PK, Johnson MP, Howell LJ, Farrell JA, Dabrowiak ME, Sutton LN, Gupta N, Tulipan NB, D'Alton ME, Farmer DL, MOMS Investigators. A randomized trial of prenatal versus postnatal repair of myelomeningocele. *N Engl J Med* 2011; 364: 993-1004

- Akalin-Sel T, Nicolaides KH, Peacock J, Campbell S. Doppler dynamics and their complex interrelation with fetal oxygen pressure, carbon dioxide pressure, and pH in growth-retarded fetuses. *Obstet Gynecol* 1994; 84: 439-444

- Alexander GR, Wingate MS, Mor J, Boulet S. Birth outcomes of Asian-Indian Americans. *Int J Gynaecol Obstet* 2007; 97: 215-220

- Alfirevic Z, Neilson JP. Doppler ultrasonography in high-risk pregnancies: Systematic review with meta-analysis. *Am J Obstet Gynecol* 1995; 172: 1379-1387

- al-Ghazali W, Chita SK, Chapman MG, Allan LD. Evidence of redistribution of cardiac output in asymmetrical growth retardation. *BJOG* 1989; 96: 697-704

- Allen VM, Joseph K, Murphy KE, Magee LA, Ohlsson A. The effect of hypertensive disorders in pregnancy on small for gestational age and stillbirth: a population based study. *BMC Pregnancy Childbirth* 2004; 4: 17

- Alvino G, Cozzi V, Radaelli T, Ortega H, Herrera E, Cetin I. Maternal and fetal fatty acid profile in normal and intrauterine growth restriction pregnancies with and without preeclampsia. *Pediatr Res* 2008; 64: 615-620

- Anandakumar C, Chew S, Wong YC, Malarvishy G, Po LU, Ratnam SS. Early asymmetric IUGR and aneuploidy. *J Obstet Gynaecol Res* 1996; 22: 365-370

- Ananth CV, Peltier MR, Chavez MR, Kirby RS, Getahun D, Vintzileos AM. Recurrence of ischemic placental disease. *Obstet Gynecol* 2007; 110: 128-133

- Anderson RR. Mammary gland growth in sheep. *J Anim Sci* 1975; 41: 118-123

- Arbeille P, Bosc M, Vaillant MC, Tranquart F. Nicotine-induced changes in the cerebral circulation in ovine fetuses. *Am J Perinatol* 1992; 9: 270-274

- Arroyo JA, Anthony RV, Parker TA, Galan HL. Differential expression of placental and vascular endothelial nitric oxide synthase in an ovine model of fetal growth restriction. *Am J Obstet Gynecol* 2006; 195: 771-777

- Arroyo JA, Winn VD. Vasculogenesis and angiogenesis in the IUGR placenta. *Semin Perinatol* 2008; 32: 172-177

- Askie LM, Duley L, Henderson-Smart DJ, Stewart LA, PARIS Collaborative Group. Antiplatelet agents for prevention of pre-eclampsia: a meta-analysis of individual patient data. *Lancet* 2007; 369: 1791-1798

- Atkinson T, Fowler VR, Garton GA, Lough AK. A rapid method for the accurate determination of lipid in animal tissues. *Analyst* 1972; 97: 562-568

- Aucott SW, Donohue PK, Northington FJ. Increased morbidity in severe early intrauterine growth restriction. *J Perinatol* 2004; 24: 435-440

- Avagliano L, Garo C, Marconi AM. Placental amino acids transport in intrauterine growth restriction. *J Pregnancy* 2012; 2012: 972562

- Azzouz M, Ralph GS, Storkebaum E, Walmsley LE, Mitrophanous KA, Kingsman SM, Carmeliet P, Mazarakis ND. VEGF delivery with retrogradely transported lentivector prolongs survival in a mouse ALS model. *Nature* 2004; 429: 413-417

- Babischkin JS, Suresch DL, Pepe GJ, Albrecht ED. Differential expression of placental villous angiopoietin-1 and -2 during early, mid and late baboon pregnancy. *Placenta* 2007; 28: 212-218

- Balbus JM, Barouki R, Birnbaum LS, Etzel RA, Gluckman PD S, Grandjean P, Hancock C, Hanson MA, Heindel JJ, Hoffman K, Jensen GK, Keeling A, Neira M, Rabadan-Diehl C, Ralston J, Tang KC. Early-life prevention of non-communicable diseases. *Lancet* 2013; 381: 3-4

- Banister CE, Koestler DC, Maccani MA, Padbury JF, Houseman EA, Marsit CJ. Infant growth restriction is associated with distinct patterns of DNA methylation in human placentas. *Epigenetics* 2011; 6: 920-927

- Barbera A, Jones OW, 3rd, Zerbe GO, Hobbins JC, Battaglia FC, Meschia G. Early ultrasonographic detection of fetal growth retardation in an ovine model of placental insufficiency. *Am J Obstet Gynecol* 1995a; 173: 1071-1074

- Barbera A, Jones OW,3rd, Zerbe GO, Hobbins JC, Battaglia FC, Meschia G. Ultrasonographic assessment of fetal growth: comparison between human and ovine fetus. *Am J Obstet Gynecol* 1995b; 173: 1765-1769

- Barker DJ, Gluckman PD, Godfrey KM, Harding JE, Owens JA, Robinson JS. Fetal nutrition and cardiovascular disease in adult life. *Lancet* 1993; 341: 938-941

- Barker DJ, Forsen T, Uutela A, Osmond C, Eriksson JG. Size at birth and resilience to effects of poor living conditions in adult life: longitudinal study. *BMJ* 2001; 323: 1273-1276

- Barker DJ, Osmond C, Forsen TJ, Kajantie E, Eriksson JG. Trajectories of growth among children who have coronary events as adults. *N Engl J Med* 2005; 353: 1802-1809

- Barker DJ. Adult consequences of fetal growth restriction. *Clin Obstet Gynecol* 2006; 49: 270-283

- Barouki R, Gluckman PD, Grandjean P, Hanson M, Heindel JJ. Developmental origins of non-communicable disease: implications for research and public health. *Environ Health* 2012; 11: 42

- Barry JS, Davidsen ML, Limesand SW, Galan HL, Friedman JE, Regnault TR, Hay WW, Jr. Developmental changes in ovine myocardial glucose transporters and insulin signaling following hyperthermia-induced intrauterine fetal growth restriction. *Exp Biol Med (Maywood)* 2006; 231: 566-575

- Barry JS, Anthony RV. The pregnant sheep as a model for human pregnancy. *Theriogenology* 2008; 69: 55-67

- Barut F, Barut A, Gun BD, Kandemir NO, Harma MI, Harma M, Aktunc E, Ozdamar SO. Intrauterine growth restriction and placental angiogenesis. *Diagn Pathol* 2010a; 5: 24

- Barut F, Barut A, Dogan Gun B, Kandemir NO, Aktunc E, Harma M, Harma MI, Ozdamar SO. Expression of heat shock protein 70 and endothelial nitric oxide synthase in placental tissue of preeclamptic and intrauterine growth-restricted pregnancies. *Pathol Res Pract* 2010b; 206: 651-656

- Baschat AA, Gembruch U, Reiss I, Gortner L, Diedrich K. Demonstration of fetal coronary blood flow by Doppler ultrasound in relation to arterial and venous flow

velocity waveforms and perinatal outcome - the 'heart-sparing effect'. *Ultrasound Obstet Gynecol*. 1997; 9: 162-172

- Baschat AA, Gembruch U, Reiss I, Gortner L, Harman CR, Weiner CP. Neonatal nucleated red blood cell counts in growth-restricted fetuses: relationship to arterial and venous doppler studies. *Am J Obstet Gynecol* 1999; 181: 190-195

- Baschat AA, Gembruch U, Harman CR. The sequence of changes in Doppler and biophysical parameters as severe fetal growth restriction worsens. *Ultrasound Obstet Gynecol* 2001; 18: 571-577

- Baschat AA. Doppler application in the delivery timing of the preterm growth-restricted fetus: another step in the right direction. *Ultrasound Obstet Gynecol* 2004; 23: 111-118

- Baschat AA, Cosmi E, Bilardo CM, Wolf H, Berg C, Rigano S, Germer U, Moyano D, Turan S, Hartung J, Bhide A, Muller T, Bower S, Nicolaides KH, Thilaganathan B, Gembruch U, Ferrazzi E, Hecher K, Galan HL, Harman CR. Predictors of neonatal outcome in early-onset placental dysfunction. *Obstet Gynecol* 2007; 109: 253-261

- Baschat AA, Viscardi RM, Hussey-Gardner B, Hashmi N, Harman C. Infant neurodevelopment following fetal growth restriction: Relationship with antepartum surveillance parameters. *Ultrasound Obstet Gynecol* 2009; 33: 44-50

- Baschat AA. Fetal growth restriction - from observation to intervention. *J Perinat Med* 2010; 38: 239-246

- Bastide A, Manning F, Harman C, Lange I, Morrison I. Ultrasound evaluation of amniotic fluid: outcome of pregnancies with severe oligohydramnios. *Am J Obstet Gynecol* 1986; 154: 895-900

- Batra RK, Sharma SWL. Utility of adenoviral vectors in animals models of human disease I: cancer. In: Curiel DT, Douglas JT *Adenoviral Vectors For Gene Therapy*. New York: Academia Press. 2002: 533-563

- Bavdekar A, Yajnik CS, Fall CH, Bapat S, Pandit AN, Deshpande V, Bhave S, Kellingray SD, Joglekar C. Insulin resistance syndrome in 8-year-old Indian children: small at birth, big at 8 years, or both? *Diabetes* 1999; 48: 2422-2429

- Begum G, Stevens A, Smith EB, Connor K, Challis JR, Bloomfield F, White A. Epigenetic changes in fetal hypothalamic energy regulating pathways are associated with maternal undernutrition and twinning. *FASEB J* 2012; 26: 1694-1703

- Bell AW, Hay WW,Jr, Ehrhardt RA. Placental transport of nutrients and its implications for fetal growth. *J Reprod Fertil Suppl* 1999; 54: 401-410

- Benavides-Serralde A, Scheier M, Cruz-Martinez R, Crispi F, Figueras F, Gratacos E, Hernandez-Andrade E. Changes in central and peripheral circulation in intrauterine growth-restricted fetuses at different stages of umbilical artery flow deterioration: new fetal cardiac and brain parameters. *Gynecol Obstet Invest* 2011; 71: 274-280

- Beppu M, Obayashi S, Aso T, Goto M, Azuma H. Endogenous nitric oxide synthase inhibitors in endothelial cells, endothelin-1 within the vessel wall, and intimal hyperplasia in perimenopausal human uterine arteries. *J Cardiovasc Pharmacol* 2002; 39: 192-200

- Berghella V. Prevention of recurrent fetal growth restriction. *Obstet Gynecol* 2007; 110: 904-912

- Bernstein PS, Minior VK, Divon MY. Neonatal nucleated red blood cell counts in small-for-gestational age fetuses with abnormal umbilical artery Doppler studies. *Am J Obstet Gynecol* 1997; 177: 1079-1084

- Bernstein IM, Horbar JD, Badger GJ, Ohlsson A, Golan A. Morbidity and mortality among very-low-birth-weight neonates with intrauterine growth restriction - the Vermont Oxford network. *Am J Obstet Gynecol* 2000; 182: 198-206

- Bersinger NA, Odegard RA. Serum levels of macrophage colony stimulating, vascular endothelial, and placenta growth factor in relation to later clinical onset of pre-eclampsia and a small-for-gestational age birth. *Am J Reprod Immunol* 2005; 54: 77-83

- Bharali DJ, Klejbor I, Stachowiak EK, Dutta P, Roy I, Kaur N, Bergey EJ, Prasad PN, Stachowiak MK. Organically modified silica nanoparticles: a nonviral vector for in vivo gene delivery and expression in the brain. *Proc Natl Acad Sci USA* 2005; 102: 11539-11544

- Blankenship TN, Enders AC. Modification of uterine vasculature during pregnancy in macaques. *Microsc Res Tech* 2003; 60: 390-401

- Blumenshine P, Egerter S, Barclay CJ, Cubbin C, Braveman PA. Socioeconomic disparities in adverse birth outcomes: a systematic review. *Am J Prev Med* 2010; 39: 263-272

- Bobryshev YV, Inder SJ, Cherian SM, Lord RS, Ao PY, Hawthorne WJ, Fletcher JP. Colonisation of prosthetic grafts by immunocompetent cells in a sheep model. *Cardiovasc Surg* 2001; 9: 166-176

- Boers KE, Vijgen SM, Bijlenga D, van der Post JA, Bekedam DJ, Kwee A, van der Salm PC, van Pampus MG, Spaanderman ME, de Boer K, Duvekot JJ, Bremer HA, Hasaart TH, Delemarre FM, Bloemenkamp KW, van Meir CA, Willekes C, Wijnen EJ, Rijken M, le Cessie S, Roumen FJ, Thornton JG, van Lith JM, Mol BW, Scherjon SA, DIGITAT Study Group. Induction versus expectant monitoring for intrauterine growth restriction at term: randomised equivalence trial (DIGITAT). *BMJ* 2010; 341: c7087

- Boers KE, van Wyk L, van der Post JA, Kwee A, van Pampus MG, Spaanderdam ME, Duvekot JJ, Bremer HA, Delemarre FM, Bloemenkamp KW, de Groot CJ, Willekes C, Rijken M, Roumen FJ, Thornton JG, van Lith JM, Mol BW, le Cessie S, Scherjon SA, DIGITAT Study Group. Neonatal morbidity after induction vs expectant monitoring in intrauterine growth restriction at term: a subanalysis of the DIGITAT RCT. *Am J Obstet Gynecol* 2012; 206: 344.e1-344.e7

- Borowicz PP, Arnold DR, Johnson ML, Grazul-Bilska AT, Redmer DA, Reynolds LP. Placental growth throughout the last two thirds of pregnancy in sheep: vascular development and angiogenic factor expression. *Biol Reprod* 2007; 76: 259-267

- Bourke DA, Aitken RP, Zuur G, Wallace JM. Use of fetal kidney ultrasound measurements for prediction of fetal size in late gestation sheep - a comparison of ultrasound indices and fetal organ data *Reprod Abstr Ser* 2002; 28: 1-35 [abstract]

- Bracero LA, Beneck D, Kirshenbaum N, Peiffer M, Stalter P, Schulman H. Doppler velocimetry and placental disease. *Am J Obstet Gynecol* 1989; 161: 388-393

- Braun T, Li S, Moss TJ, Connor KL, Doherty DA, Nitsos I, Newnham JP, Challis JR, Sloboda DM. Differential appearance of placentomes and expression of prostaglandin H synthase type 2 in placentome subtypes after betamethasone treatment of sheep late in gestation. *Placenta* 2011; 32: 295-303

- Brenner BM, Chertow GM. Congenital oligonephropathy: An inborn cause of adult hypertension and progressive renal injury? *Curr Opin Nephrol Hypertens* 1993; 2: 691-695

- Brett DJ, Corbett JL, Inskip MW. The energy content of ewes' milk. *Proceedings of the Australian Society of Animal Production* 1972; 9: 286

- Bricker L, Neilson JP, Dowswell T. Routine ultrasound in late pregnancy (after 24 weeks' gestation). *Cochrane Database Syst Rev* 2008; 4: CD001451

- Brocklehurst P, French R. The association between maternal HIV infection and perinatal outcome: a systematic review of the literature and meta-analysis. *BJOG* 1998; 105: 836-848

- Brodszki J, Lanne T, Marsal K, Ley D. Impaired vascular growth in late adolescence after intrauterine growth restriction. *Circulation* 2005; 111: 2623-2628

- Brown K, Heller DS, Zamudio S, Illsley NP. Glucose transporter 3 (GLUT3) protein expression in human placenta across gestation. *Placenta* 2011; 32: 1041-1049

- Brownbill P, McKeeman GC, Brockelsby JC, Crocker IP, Sibley CP. Vasoactive and permeability effects of vascular endothelial growth factor-165 in the term in vitro dually perfused human placental lobule. *Endocrinology* 2007; 148: 4734-4744

- Brownbill P, Mills TA, Soydemir DF, Sibley CP. Vasoactivity to and endogenous release of vascular endothelial growth factor in the in vitro perfused human placental lobule from pregnancies complicated by preeclampsia. *Placenta* 2008; 29: 950-955

- Bruce LA, Atkinson T, Hutchinson JSM, Shakespear RA, MacRae JC. The measurement of insulin-like growth factor 1 in sheep plasma. *J Endocrinol* 1991; 128: R1-R4

- Bujold E, Roberge S, Lacasse Y, Bureau M, Audibert F, Marcoux S, Forest JC, Giguere Y. Prevention of preeclampsia and intrauterine growth restriction with aspirin started in early pregnancy: a meta-analysis. *Obstet Gynecol* 2010; 116: 402-414

- Burdge GC, Lillycrop KA, Phillips ES, Slater-Jefferies JL, Jackson AA, Hanson MA. Folic acid supplementation during the juvenile-pubertal period in rats modifies the phenotype and epigenotype induced by prenatal nutrition. *J Nutr* 2009; 139: 1054-1060

- Burger IM, Wilfond BS. Limitations of informed consent for in utero gene transfer research: implications for investigators and institutional review boards. *Hum Gene Ther* 2000; 11: 1057-1063

- Byun SO, Zhou H, Hickford JG. Polymorphism of the ovine insulin-like growth factor I receptor (IGFIR) gene. *Mol Cell Probes* 2008; 22: 131-132

- Campbell S, Wilkin D. Ultrasonic measurement of fetal abdomen circumference in the estimation of fetal weight. *BJOG* 1975; 82: 689-697

- Cantwell R, Clutton-Brock T, Cooper G, Dawson A, Drife J, Garrod D, Harper A, Hulbert D, Lucas S, McClure J, Millward-Sadler H, Neilson J, Nelson-Piercy C, Norman J, O'Herlihy C, Oates M, Shakespeare J, de Swiet M, Williamson C, Beale V, Knight M, Lennox C, Miller A, Parmar D, Rogers J, Springett A. Saving mothers' lives: Reviewing maternal deaths to make motherhood safer: 2006-2008 - the eighth report of the confidential enquiries into maternal deaths in the united kingdom. *BJOG* 2011; 118(Suppl _1): 1-203

- CARE Study Group. Maternal caffeine intake during pregnancy and risk of fetal growth restriction: a large prospective observational study. *BMJ* 2008; 337: a2332

- Carr DJ, Aitken RP, Milne JS, Adam C, Wallace JM. Inflammatory response to routine vaccination at 6 and 13 weeks of age in relation to growth and body composition in low birthweight lambs. *Neonatal Society Summer Meeting, Canterbury UK*. 2012 Jun [poster presentation]

- Carson SD. Receptor for the group B coxsackieviruses and adenoviruses: CAR. *Rev Med Virol* 2001; 11: 219-226

- Carter AM. Animal models of human placentation - a review. *Placenta* 2007; 28(Suppl_ A): S41-S47

- Cellini C, Xu J, Arriaga A, Buchmiller-Crair TL. Effect of epidermal growth factor infusion on fetal rabbit intrauterine growth retardation and small intestinal development. *J Pediatr Surg* 2004; 39: 891-897

- Cetin I, Corbetta C, Sereni LP, Marconi AM, Bozzetti P, Pardi G, Battaglia FC. Umbilical amino acid concentrations in normal and growth-retarded fetuses sampled in utero by cordocentesis. *Am J Obstet Gynecol* 1990; 162: 253-261

- Cetin I, Marconi AM, Corbetta C, Lanfranchi A, Baggiani AM, Battaglia FC, Pardi G. Fetal amino acids in normal pregnancies and in pregnancies complicated by intrauterine growth retardation. *Early Hum Dev* 1992; 29: 183-186

- Chakraborty S, Joseph DV, Bankart MJ, Petersen SA, Wailoo MP. Fetal growth restriction: relation to growth and obesity at the age of 9 years. *Arch Dis Child Fetal Neonatal Ed* 2007; 92: F479-F483

- Chan FY, Pun TC, Lam C, Khoo J, Lee CP, Lam YH. Pregnancy screening by uterine artery Doppler velocimetry - which criterion performs best? *Obstet Gynecol* 1995; 85: 596-602

- Chan FY, Pun TC, Lam P, Lam C, Lee CP, Lam YH. Fetal cerebral Doppler studies as a predictor of perinatal outcome and subsequent neurologic handicap. *Obstet Gynecol* 1996; 87: 981-988

- Chandra KR, Matsumura T. Ontogenetic development of the immune system and effects of fetal growth retardation. *J Perinat Med* 1979; 7: 279-290

- Chard T, Costeloe K, Leaf A. Evidence of growth retardation in neonates of apparently normal weight. *Eur J Obstet Gynecol Reprod Biol* 1992; 45: 59-62

- Charlton V, Johengen M. Effects of intrauterine nutritional supplementation on fetal growth retardation. *Biol Neonate* 1985; 48: 125-142

- Chauhan SP, Sanderson M, Hendrix NW, Magann EF, Devoe LD. Perinatal outcome and amniotic fluid index in the antepartum and intrapartum periods: a meta-analysis. *Am J Obstet Gynecol* 1999; 181: 1473-1478

- Cheema R, Dubiel M, Gudmundsson S. Fetal brain sparing is strongly related to the degree of increased placental vascular impedance. *J Perinat Med* 2006; 34: 318-322

- Chelbi ST, Doridot L, Mondon F, Dussour C, Rebourcet R, Busato F, Gascoin-Lachambre G, Barbaux S, Rigourd V, Mignot TM, Tost J, Vaiman D. Combination of promoter hypomethylation and PDX1 overexpression leads to TBX15 decrease in vascular IUGR placentas. *Epigenetics* 2011; 6: 247-255

- Chen M, Zhang L. Epigenetic mechanisms in developmental programming of adult disease. *Drug Discov Today* 2011; 16: 1007-1018

- Chervenak FA, McCullough LB. A comprehensive ethical framework for fetal research and its application to fetal surgery for spina bifida. *Am J Obstet Gynecol* 2002; 187: 10-14

- Chitty LS, Altman DG, Henderson A, Campbell S. Charts of fetal size: 2. head measurements. *BJOG* 1994a; 101: 35-43

- Chitty LS, Altman DG, Henderson A, Campbell S. Charts of fetal size: 3. abdominal measurements. *BJOG* 1994b; 101: 125-131

- Chitty LS, Altman DG, Henderson A, Campbell S. Charts of fetal size: 4. femur length. *BJOG* 1994c; 101: 132-135

- Chitty LS, Altman DG. Charts of fetal size: kidney and renal pelvis measurements. *Prenat Diagn* 2003; 23: 891-897

- Chou Q, Russell M, Birch DE, Raymond J, Bloch W. Prevention of pre-PCR mis-priming and primer dimerization improves low-copy-number amplifications. *Nucleic Acids Res* 1992; 20: 1717-1723

- Christenson RK, Prior RL. Uterine blood flow and nutrient uptake during late gestation in ewes with different number of fetuses. *J Anim Sci* 1978; 46: 189-200

- Chuang JC, Jones PA. Epigenetics and microRNAs. *Pediatr Res* 2007; 61: 24R-29R

- Cianfarani S, Germani D, Rossi L, Argiro G, Boemi S, Lemon M, Holly JM, Branca F. IGF-I and IGF-binding protein-1 are related to cortisol in human cord blood. *Eur J Endocrinol* 1998; 138: 524-529

- Cleal JK, Lewis RM. The mechanisms and regulation of placental amino acid transport to the human foetus. *J Neuroendocrinol* 2008; 20: 419-426

- Cleal JK, Glazier JD, Ntani G, Crozier SR, Day PE, Harvey NC, Robinson SM, Cooper C, Godfrey KM, Hanson MA, Lewis RM. Facilitated transporters mediate net efflux of amino acids to the fetus across the basal membrane of the placental syncytiotrophoblast. *J Physiol* 2011; 589: 987-997

- Clow WM, Crompton AC. The wounded uterus: Pregnancy after hysterotomy. *BMJ* 1973; 1: 321-323

- Cnossen JS, Morris RK, ter Riet G, Mol BW, van der Post JA, Coomarasamy A, Zwinderman AH, Robson SC, Bindels PJ, Kleijnen J, Khan KS. Use of uterine artery Doppler ultrasonography to predict pre-eclampsia and intrauterine growth restriction: a systematic review and bivariable meta-analysis. *CMAJ* 2008; 178: 701-711

- Conde-Agudelo A, Rosas-Bermudez A, Kafury-Goeta AC. Birth spacing and risk of adverse perinatal outcomes: a meta-analysis. *JAMA* 2006; 295: 1809-1823

- Conde-Agudelo A, Papageorghiou AT, Kennedy SH, Villar J. Novel biomarkers for predicting intrauterine growth restriction: a systematic review and meta-analysis. *BJOG* 2013; 120 :681-694

- Constancia M, Hemberger M, Hughes J, Dean W, Ferguson-Smith A, Fundele R, Stewart F, Kelsey G, Fowden A, Sibley C, Reik W. Placental-specific IGF-II is a major modulator of placental and fetal growth. *Nature* 2002; 417: 945-948

- Cooney CA, Dave AA, Wolff GL. Maternal methyl supplements in mice affect epigenetic variation and DNA methylation of offspring. *J Nutr* 2002; 132: 2393S-2400S

- Costeloe K, Hennessy E, Gibson AT, Marlow N, Wilkinson AR. The EPICure study: outcomes to discharge from hospital for infants born at the threshold of viability. *Pediatrics* 2000; 106: 659-671

- Coulter CL, McMillen IC, Bird IM, Salkeld MD. Steroidogenic acute regulatory protein expression is decreased in the adrenal gland of the growth-restricted sheep fetus during late gestation. *Biol Reprod* 2002; 67: 584-590

- Cousens S, Blencowe H, Stanton C, Chou D, Ahmed S, Steinhardt L, Creanga AA, Tuncalp O, Balsara ZP, Gupta S, Say L, Lawn JE. National, regional, and worldwide estimates of stillbirth rates in 2009 with trends since 1995: a systematic analysis. *Lancet* 2011; 377: 1319-1330

- Cox P, Marton T. Pathological assessment of intrauterine growth restriction. *Best Pract Res Clin Obstet Gynaecol* 2009; 23: 751-764

- Crawford BS, Davis J, Harrigill K. Uterine artery atherosclerotic disease: histologic features and clinical correlation. *Obstet Gynecol* 1997; 90: 210-215

- Crowther CA, Verkuyl DA, Neilson JP, Bannerman C, Ashurst HM. The effects of hospitalization for rest on fetal growth, neonatal morbidity and length of gestation in twin pregnancy. *BJOG* 1990; 97: 872-877

- Cruz-Martinez R, Figueras F, Oros D, Padilla N, Meler E, Hernandez-Andrade E, Gratacos E. Cerebral blood perfusion and neurobehavioral performance in full-term small-for-gestational-age fetuses. *Am J Obstet Gynecol* 2009; 201: 474.e1-474.e7

- Currie MJ, Bassett NS, Gluckman PD. Ovine glucose transporter-1 and -3: CDNA partial sequences and developmental gene expression in the placenta. *Placenta* 1997; 18: 393-401

- Da Silva P, Aitken RP, Rhind SM, Racey PA, Wallace JM. Effect of maternal overnutrition during pregnancy on pituitary gonadotrophin gene expression and gonadal morphology in female and male foetal sheep at day 103 of gestation. *Placenta* 2003; 24: 248-257

- David AL, Torondel B, Zachary I, Wigley V, Abi-Nader K, Mehta V, Buckley SM, Cook T, Boyd M, Rodeck CH, Martin J, Peebles DM. Local delivery of VEGF adenovirus to the uterine artery increases vasorelaxation and uterine blood flow in the pregnant sheep. *Gene Ther* 2008; 15: 1344-1350

- David AL, Waddington SN. Candidate diseases for prenatal gene therapy. *Methods Mol Biol* 2012; 891: 9-39

- Davidson J, Mathieson J, Boyne AW. The use of automation in determining nitrogen by the Kjeldahl method, with final calculations by computer. *Analyst* 1970; 95: 181-193

- Dawson MA, Kouzarides T. Cancer epigenetics: From mechanism to therapy. *Cell* 2012; 150: 12-27

- de Boo HA, Eremia SC, Bloomfield FH, Oliver MH, Harding JE. Treatment of intrauterine growth restriction with maternal growth hormone supplementation in sheep. *Am J Obstet Gynecol* 2008; 199: 559.e1-559.e9

- de Jong CL, Gardosi J, Dekker GA, Colenbrander GJ, van Geijn HP. Application of a customised birthweight standard in the assessment of perinatal outcome in a high risk population. *BJOG* 1998; 105: 531-535

- de Rooij SR, Wouters H, Yonker JE, Painter RC, Roseboom TJ. Prenatal undernutrition and cognitive function in late adulthood. *Proc Natl Acad Sci USA*. 2010; 107: 16881-16886

- DeChiara TM, Efstratiadis A, Robertson EJ. A growth-deficiency phenotype in heterozygous mice carrying an insulin-like growth factor II gene disrupted by targeting. *Nature* 1990; 345: 78-80

- Degani S. Fetal biometry: clinical, pathological, and technical considerations. *Obstet Gynecol Surv* 2001; 56: 159-167

- Delcuve GP, Rastegar M, Davie JR. Epigenetic control. *J Cell Physiol* 2009; 219: 243-250

- Delotte J, Novellas S, Koh C, Bongain A, Chevallier P. Obstetrical prognosis and pregnancy outcome following pelvic arterial embolisation for post-partum hemorrhage. *Eur J Obstet Gynecol Reprod Biol* 2009; 145: 129-132

- Dicke JM, Crane JP. Sonographic recognition of major malformations and aberrant fetal growth in trisomic fetuses. *J Ultrasound Med* 1991; 10: 433-438

- Dickson MC, Saunders JC, Gilmour RS. The ovine insulin-like growth factor-I gene: characterization, expression and identification of a putative promoter. *J Mol Endocrinol* 1991; 6: 17-31

- Divon MY. Randomized controlled trials of umbilical artery Doppler velocimetry: How many are too many? *Ultrasound Obstet Gynecol* 1995; 6: 377-379

- Doctor BA, O'Riordan MA, Kirchner HL, Shah D, Hack M. Perinatal correlates and neonatal outcomes of small for gestational age infants born at term gestation. *Am J Obstet Gynecol* 2001; 185: 652-659

- Doize F, Vaillancourt D, Carabin H, Belanger D. Determination of gestational age in sheep and goats using transrectal ultrasonographic measurement of placentomes. *Theriogenology* 1997; 48: 449-460

- Downing GJ, Yarlagadda P, Maulik D. Effects of acute hypoxemia on umbilical arterial Doppler indices in a fetal ovine model. *Early Hum Dev* 1991; 25: 1-10

- Drenthen W, Pieper PG, Roos-Hesselink JW, van Lottum WA, Voors AA, Mulder BJ, van Dijk AP, Vliegen HW, Yap SC, Moons P, Ebels T, van Veldhuisen DJ, ZAHARA

Investigators. Outcome of pregnancy in women with congenital heart disease: a literature review. *J Am Coll Cardiol* 2007; 49: 2303-2311

- Dugoff L, Lynch AM, Cioffi-Ragan D, Hobbins JC, Schultz LK, Malone FD, D'Alton ME, FASTER Trial Research Consortium. First trimester uterine artery Doppler abnormalities predict subsequent intrauterine growth restriction. *Am J Obstet Gynecol* 2005; 193: 1208-1212

- Duley L, Henderson-Smart DJ, Meher S, King JF. Antiplatelet agents for preventing pre-eclampsia and its complications. *Cochrane Database Syst Rev* 2007; 2: CD004659

- Economides DL, Nicolaides KH, Campbell S. Metabolic and endocrine findings in appropriate and small for gestational age fetuses. *J Perinat Med* 1991; 19: 97-105

- Efstratiadis A. Genetics of mouse growth. *Int J Dev Biol* 1998; 42: 955-976

- Ehrhardt RA, Bell AW. Growth and metabolism of the ovine placenta during mid-gestation. *Placenta* 1995; 16: 727-741

- El-Maarri O, Becker T, Junen J, Manzoor SS, Diaz-Lacava A, Schwaab R, Wienker T, Oldenburg J. Gender specific differences in levels of DNA methylation at selected loci from human total blood: a tendency toward higher methylation levels in males. *Hum Genet* 2007; 122: 505-514

- Eremia SC, de Boo HA, Bloomfield FH, Oliver MH, Harding JE. Fetal and amniotic insulin-like growth factor-I supplements improve growth rate in intrauterine growth restriction fetal sheep. *Endocrinology* 2007; 148: 2963-2972

- Erkinaro T, Kavasmaa T, Pakkila M, Acharya G, Makikallio K, Alahuhta S, Rasanen J. Ephedrine and phenylephrine for the treatment of maternal hypotension in a chronic sheep model of increased placental vascular resistance. *Br J Anaesth* 2006; 96: 231-237

- Everett TR, Lees CC. Beyond the placental bed: placental and systemic determinants of the uterine artery doppler waveform. *Placenta* 2012; 33: 893-901

- Feil R, Khosla S, Cappai P, Loi P. Genomic imprinting in ruminants: allele-specific gene expression in parthenogenetic sheep. *Mamm Genome* 1998; 9: 831-834

- Ferrara A, Barrett-Connor E, Wingard DL, Edelstein SL. Sex differences in insulin levels in older adults and the effect of body size, estrogen replacement therapy, and glucose tolerance status. The Rancho Bernardo study, 1984-1987. *Diabetes Care* 1995; 18: 220-225

- Ferrazzi E, Bozzo M, Rigano S, Bellotti M, Morabito A, Pardi G, Battaglia FC, Galan HL. Temporal sequence of abnormal Doppler changes in the peripheral and central circulatory systems of the severely growth-restricted fetus. *Ultrasound Obstet Gynecol* 2002; 19: 140-146

- Figueras F, Cruz-Martinez R, Sanz-Cortes M, Arranz A, Illa M, Botet F, Costas-Moragas C, Gratacos E. Neurobehavioral outcomes in preterm, growth-restricted infants with and without prenatal advanced signs of brain-sparing. *Ultrasound Obstet Gynecol* 2011; 38: 288-294

- Fink JC, Schwartz SM, Benedetti TJ, Stehman-Breen CO. Increased risk of adverse maternal and infant outcomes among women with renal disease. *Paediatr Perinat Epidemiol* 1998; 12: 277-287

- FitzSimmons J, Fantel A, Shepard TH. Growth parameters in mid-trimester fetal Turner syndrome. *Early Hum Dev* 1994; 38: 121-129

- Flake AW, Villa-Troyer RL, Adzick NS, Harrison MR. Transamniotic fetal feeding. III. the effect of nutrient infusion on fetal growth retardation. *J Pediatr Surg* 1986; 21: 481-484

- Flint DJ, Knight CH. Interactions of prolactin and growth hormone (GH) in the regulation of mammary gland function and epithelial cell survival. *J Mammary Gland Biol Neoplasia* 1997; 2: 41-48

- Fok RY, Pavlova Z, Benirschke K, Paul RH, Platt LD. The correlation of arterial lesions with umbilical artery Doppler velocimetry in the placentas of small-for-dates pregnancies. *Obstet Gynecol* 1990; 75: 578-583

- Fouron JC, Teyssier G, Maroto E, Lessard M, Marquette G. Diastolic circulatory dynamics in the presence of elevated placental resistance and retrograde diastolic flow in the umbilical artery: a Doppler echographic study in lambs. *Am J Obstet Gynecol* 1991; 164: 195-203

- Fowden AL. The insulin-like growth factors and feto-placental growth. *Placenta* 2003; 24: 803-812
- Fowden AL, Forhead AJ. Endocrine regulation of feto-placental growth. *Horm Res* 2009; 72: 257-265
- Fryer AA, Nafee TM, Ismail KM, Carroll WD, Emes RD, Farrell WE. LINE-1 DNA methylation is inversely correlated with cord plasma homocysteine in man: a preliminary study. *Epigenetics* 2009; 4: 394-398
- Fryer AA, Emes RD, Ismail KM, Haworth KE, Mein C, Carroll WD, Farrell WE. Quantitative, high-resolution epigenetic profiling of CpG loci identifies associations with cord blood plasma homocysteine and birth weight in humans. *Epigenetics* 2011; 6: 86-94
- Fu Q, Yu X, Callaway CW, Lane RH, McKnight RA. Epigenetics: Intrauterine growth retardation (IUGR) modifies the histone code along the rat hepatic IGF-1 gene. *FASEB J* 2009; 23: 2438-2449
- Fujimoto A, Wilson MG. Growth retardation in wolf-hirschhorn syndrome. *Hum Genet* 1990; 84: 296-297
- Fulton D, Gratton JP, McCabe TJ, Fontana J, Fujio Y, Walsh K, Franke TF, Papapetropoulos A, Sessa WC. Regulation of endothelium-derived nitric oxide production by the protein kinase akt. *Nature* 1999; 399: 597-601
- Gagnon R, Challis J, Johnston L, Fraher L. Fetal endocrine responses to chronic placental embolization in the late-gestation ovine fetus. *Am J Obstet Gynecol* 1994; 170: 929-938
- Gagnon A, Wilson RD, Audibert F, Allen VM, Blight C, Brock JA, Desilets VA, Johnson JA, Langlois S, Summers A, Wyatt P, Society of Obstetricians and Gynaecologists of Canada Genetics Committee. Obstetrical complications associated with abnormal maternal serum markers analytes. *J Obstet Gynaecol Can* 2008; 30: 918-949
- Galan HL, Hussey MJ, Chung M, Chyu JK, Hobbins JC, Battaglia FC. Doppler velocimetry of growth-restricted fetuses in an ovine model of placental insufficiency. *Am J Obstet Gynecol* 1998; 178: 451-456

- Galan HL, Hussey MJ, Barbera A, Ferrazzi E, Chung M, Hobbins JC, Battaglia FC. Relationship of fetal growth to duration of heat stress in an ovine model of placental insufficiency. *Am J Obstet Gynecol* 1999; 180: 1278-1282

- Galan HL, Anthony RV, Rigano S, Parker TA, de Vrijer B, Ferrazzi E, Wilkening RB, Regnault TR. Fetal hypertension and abnormal doppler velocimetry in an ovine model of intrauterine growth restriction. *Am J Obstet Gynecol* 2005; 192: 272-279

- Ganguly A, McKnight RA, Raychaudhuri S, Shin BC, Ma Z, Moley K, Devaskar SU. Glucose transporter isoform-3 mutations cause early pregnancy loss and fetal growth restriction. *Am J Physiol Endocrinol Metab* 2007; 292: E1241-1255

- Gardiner-Garden M, Frommer M. CpG islands in vertebrate genomes. *J Mol Biol* 1987; 196: 261-282

- Gardosi J, Chang A, Kalyan B, Sahota D, Symonds EM. Customised antenatal growth charts. *Lancet* 1992; 339: 283-287

- Gardosi J, Mongelli M, Wilcox M, Chang A. An adjustable fetal weight standard. *Ultrasound Obstet Gynecol* 1995; 6: 168-174

- Gardosi J, Francis A. Adverse pregnancy outcome and association with small for gestational age birthweight by customized and population-based percentiles. *Am J Obstet Gynecol* 2009; 201: 28.e1-28.e8

- Geer EB, Shen W. Gender differences in insulin resistance, body composition, and energy balance. *Gend Med* 2009; 6(Suppl_1): 60-75

- Genger H, Enzelsberger H, Salzer H. Carnitine in therapy of placental insufficiency - initial experiences. *Z Geburtshilfe Perinatol* 1988; 192: 155-157

- Gerich JE. Is reduced first-phase insulin release the earliest detectable abnormality in individuals destined to develop type 2 diabetes? *Diabetes* 2002; 51(Suppl_1): S117-S121

- Gertler A, Simmons J, Keisler DH. Large-scale preparation of biologically active recombinant ovine obese protein (leptin). *FEBS Lett* 1998; 422: 137-140

- Ghi T, Contro E, Youssef A, Giorgetta F, Farina A, Pilu G, Pelusi G. Persistence of increased uterine artery resistance in the third trimester and pregnancy outcome. *Ultrasound Obstet Gynecol* 2010; 36: 577-581
- Ghidini A. Idiopathic fetal growth restriction: A pathophysiologic approach. *Obstet Gynecol Surv* 1996; 51: 376-382
- Giacca M, Zacchigna S. VEGF gene therapy: Therapeutic angiogenesis in the clinic and beyond. *Gene Ther* 2012; 19: 622-629
- Giles WB, Trudinger BJ, Cook CM. Fetal umbilical artery flow velocity-time waveforms in twin pregnancies. *BJOG* 1985; 92: 490-497
- Giles WB, Trudinger BJ, Stevens D, Alexander G, Bradley L. Umbilical artery flow velocity waveform analysis in normal ovine pregnancy and after carunculectomy. *J Dev Physiol* 1989; 11: 135-138
- Giles W, Bisits A. Clinical use of Doppler ultrasound in pregnancy: information from six randomised trials. *Fetal Diagn Ther* 1993; 8: 247-255
- Giles W, Falconer J, Read M, Leitch I. Ovine fetal umbilical artery Doppler systolic diastolic ratios and nitric oxide synthase. *Obstet Gynecol* 1997; 89: 53-56
- Giussani DA, Camm EJ, Niu Y, Richter HG, Blanco CE, Gottschalk R, Blake EZ, Horder KA, Thakor AS, Hansell JA, Kane AD, Wooding FB, Cross CM, Herrera EA. Developmental programming of cardiovascular dysfunction by prenatal hypoxia and oxidative stress. *PLoS One* 2012; 7: e31017
- Glazier JD, Cetin I, Perugino G, Ronzoni S, Grey AM, Mahendran D, Marconi AM, Pardi G, Sibley CP. Association between the activity of the system A amino acid transporter in the microvillous plasma membrane of the human placenta and severity of fetal compromise in intrauterine growth restriction. *Pediatr Res* 1997; 42: 514-519
- Gloor JM, Breckle RJ, Gehrking WC, Rosenquist RG, Mulholland TA, Bergstralh EJ, Ramin KD, Ogburn PL, Jr. Fetal renal growth evaluated by prenatal ultrasound examination. *Mayo Clin Proc* 1997; 72: 124-129
- Gluckman PD, Hanson MA. Maternal constraint of fetal growth and its consequences. *Semin Fetal Neonatal Med* 2004; 9: 419-425

- Godfrey KM, Lillycrop KA, Burdge GC, Gluckman PD, Hanson MA. Epigenetic mechanisms and the mismatch concept of the developmental origins of health and disease. *Pediatr Res* 2007; 61: 5R-10R

- Goetzinger KR, Cahill AG, Macones GA, Odibo AO. Echogenic bowel on second-trimester ultrasonography: evaluating the risk of adverse pregnancy outcome. *Obstet Gynecol* 2011; 117: 1341-1348

- Goland RS, Jozak S, Warren WB, Conwell IM, Stark RI, Tropper PJ. Elevated levels of umbilical cord plasma corticotropin-releasing hormone in growth-retarded fetuses. *J Clin Endocrinol Metab* 1993; 77: 1174-1179

- Goldberger ZD, Valle JA, Dandekar VK, Chan PS, Ko DT, Nallamothu BK. Are changes in carotid intima-media thickness related to risk of nonfatal myocardial infarction? A critical review and meta-regression analysis. *Am Heart J* 2010; 160: 701-714

- Gordon L, Joo JE, Powell JE, Ollikainen M, Novakovic B, Li X, Andronikos R, Cruickshank MN, Conneely KN, Smith AK, Alisch RS, Morley R, Visscher PM, Craig JM, Saffery R. Neonatal DNA methylation profile in human twins is specified by a complex interplay between intrauterine environmental and genetic factors, subject to tissue-specific influence. *Genome Res* 2012; 22: 1395-1406

- Gouin K, Murphy K, Shah PS, Knowledge Synthesis group on Determinants of Low Birth Weight and Preterm Births. Effects of cocaine use during pregnancy on low birthweight and preterm birth: systematic review and metaanalyses. *Am J Obstet Gynecol* 2011; 204: 340.e1-340.12

- Gramellini D, Folli MC, Raboni S, Vadora E, Merialdi A. Cerebral-umbilical Doppler ratio as a predictor of adverse perinatal outcome. *Obstet Gynecol* 1992; 79: 416-420

- Grazul-Bilska AT, Borowicz PP, Johnson ML, Minten MA, Bilski JJ, Wroblewski R, Redmer DA, Reynolds LP. Placental development during early pregnancy in sheep: vascular growth and expression of angiogenic factors in maternal placenta. *Reproduction* 2010; 140: 165-174

- Grazul-Bilska AT, Johnson ML, Borowicz PP, Minten M, Bilski JJ, Wroblewski R, Velimirovich M, Coupe LR, Redmer DA, Reynolds LP. Placental development during early pregnancy in sheep: cell proliferation, global methylation, and angiogenesis in the fetal placenta. *Reproduction* 2011; 141: 529-540

- Greenough A, Nicolaides KH, Lagercrantz H. Human fetal sympathoadrenal responsiveness. *Early Hum Dev* 1990; 23: 9-13

- Greenwood JD, Minhas K, di Santo JP, Makita M, Kiso Y, Croy BA. Ultrastructural studies of implantation sites from mice deficient in uterine natural killer cells. *Placenta* 2000; 21: 693-702

- GRIT Study Group. A randomised trial of timed delivery for the compromised preterm fetus: short term outcomes and Bayesian interpretation. *BJOG* 2003; 110: 27-32

- Grivell RM, Alfirevic Z, Gyte GM, Devane D. Antenatal cardiotocography for fetal assessment. *Cochrane Database Syst Rev* 2012; 12: CD007863

- Gross SJ. Intrauterine growth restriction: a genetic perspective. *Clin Obstet Gynecol* 1997; 40: 730-739

- Gude NM, Roberts CT, Kalionis B, King RG. Growth and function of the normal human placenta. *Thromb Res* 2004; 114: 397-407

- Gudmundsson S, Huhta JC, Wood DC, Tulzer G, Cohen AW, Weiner S. Venous Doppler ultrasonography in the fetus with nonimmune hydrops. *Am J Obstet Gynecol* 1991; 164: 33-37

- Gudmundsson S, Tulzer G, Huhta JC, Marsal K. Venous doppler in the fetus with absent end-diastolic flow in the umbilical artery. *Ultrasound Obstet Gynecol* 1996; 7: 262-267

- Guest SS, Evans CD, Winter RM. The online London Dysmorphology Database. *Genet Med* 1999; 1: 207-212

- Gulmezoglu AM, Hofmeyr GJ. Calcium channel blockers for potential impaired fetal growth. *Cochrane Database Syst Rev* 2000a; 2: CD000049

- Gulmezoglu AM, Hofmeyr GJ. Transcutaneous electrostimulation for suspected placental insufficiency (diagnosed by Doppler studies). *Cochrane Database Syst Rev* 2000b; 2: CD000079

- Gulmezoglu AM, Hofmeyr GJ. Betamimetics for suspected impaired fetal growth. *Cochrane Database Syst Rev* 2001; 4: CD000036

- Hagemann LJ, Peterson AJ, Weilert LL, Lee RS, Tervit HR. In vitro and early in vivo development of sheep gynogenones and putative androgenones. *Mol Reprod Dev* 1998; 50: 154-162

- Hagen AS, Orbus RJ, Wilkening RB, Regnault TR, Anthony RV. Placental expression of angiopoietin-1, angiopoietin-2 and tie-2 during placental development in an ovine model of placental insufficiency-fetal growth restriction. *Pediatr Res* 2005; 58: 1228-1232

- Hahn T, Barth S, Graf R, Engelmann M, Beslagic D, Reul JM, Holsboer F, Dohr G, Desoye G. Placental glucose transporter expression is regulated by glucocorticoids. *J Clin Endocrinol Metab* 1999; 84: 1445-1452

- Hale SA, Jones CW, Osol G, Schonberg A, Badger GJ, Bernstein IM. Sildenafil increases uterine blood flow in nonpregnant nulliparous women. *Reprod Sci* 2010; 17: 358-365

- Hales CN, Barker DJ, Clark PM, Cox LJ, Fall C, Osmond C, Winter PD. Fetal and infant growth and impaired glucose tolerance at age 64. *BMJ* 1991; 303: 1019-1022

- Halliday HL. Neonatal management and long-term sequelae. *Best Pract Res Clin Obstet Gynaecol* 2009; 23: 871-880

- Hanson MA, Spencer JAD, Rodeck CH. *Growth*. Cambridge: Cambridge University Press; 1995

- Hanson MA, Gluckman PD. Developmental origins of health and disease: Moving from biological concepts to interventions and policy. *Int J Gynaecol Obstet* 2011; 115(Suppl_1): S3-5

- Harrell FE,Jr, Lee KL, Califf RM, Pryor DB, Rosati RA. Regression modelling strategies for improved prognostic prediction. *Stat Med* 1984; 3: 143-152

- Harrington K, Carpenter RG, Goldfrad C, Campbell S. Transvaginal Doppler ultrasound of the uteroplacental circulation in the early prediction of pre-eclampsia and intrauterine growth retardation. *BJOG* 1997; 104: 674-681

- Hay WW, Jr. Placental-fetal glucose exchange and fetal glucose metabolism. *Trans Am Clin Climatol Assoc* 2006; 117: 321-339

- Hayatsu H. The bisulfite genomic sequencing used in the analysis of epigenetic states, a technique in the emerging environmental genotoxicology research. *Mutat Res* 2008; 659: 77-82

- He H, Venema VJ, Gu X, Venema RC, Marrero MB, Caldwell RB. Vascular endothelial growth factor signals endothelial cell production of nitric oxide and prostacyclin through flk-1/KDR activation of c-src. *J Biol Chem* 1999; 274: 25130-25135

- He ZX, Wu DQ, Sun ZH, Tan ZL, Qiao JY, Ran T, Tang SX, Zhou CS, Han XF, Wang M, Kang JH, Beauchemin KA. Protein or energy restriction during late gestation alters fetal growth and visceral organ mass: an evidence of intrauterine programming in goats. *Anim Reprod Sci* 2013; 137: 177-182

- Hecher K, Snijders R, Campbell S, Nicolaides K. Fetal venous, intracardiac, and arterial blood flow measurements in intrauterine growth retardation: Relationship with fetal blood gases. *Am J Obstet Gynecol* 1995; 173: 10-15

- Hecher K, Bilardo CM, Stigter RH, Ville Y, Hackeloer BJ, Kok HJ, Senat MV, Visser GH. Monitoring of fetuses with intrauterine growth restriction: a longitudinal study. *Ultrasound Obstet Gynecol* 2001; 18: 564-570

- Hedman M, Hartikainen J, Syvanne M, Stjernvall J, Hedman A, Kivela A, Vanninen E, Mussalo H, Kauppila E, Simula S, Narvanen O, Rantala A, Peuhkurinen K, Nieminen MS, Laakso M, Yla-Herttuala S. Safety and feasibility of catheter-based local intracoronary vascular endothelial growth factor gene transfer in the prevention of postangioplasty and in-stent restenosis and in the treatment of chronic myocardial ischemia: phase II results of the Kuopio angiogenesis trial (KAT). *Circulation* 2003; 107: 2677-2683

- Hefler LA, Reyes CA, O'Brien WE, Gregg AR. Perinatal development of endothelial nitric oxide synthase-deficient mice. *Biol Reprod* 2001; 64: 666-673

- Heijmans BT, Tobi EW, Stein AD, Putter H, Blauw GJ, Susser ES, Slagboom PE, Lumey LH. Persistent epigenetic differences associated with prenatal exposure to famine in humans. *Proc Natl Acad Sci USA* 2008; 105: 17046-17049

- Heistad DD, Marcus ML, Larsen GE, Armstrong ML. Role of vasa vasorum in nourishment of the aortic wall. *Am J Physiol* 1981; 240: H781-787

- Henderson AJ, Warner JO. Fetal origins of asthma. *Semin Fetal Neonatal Med* 2012; 17: 82-91

- Hendrix N, Berghella V. Non-placental causes of intrauterine growth restriction. *Semin Perinatol* 2008; 32: 161-165
- Herre HD, Kyank H, Adomssent S, Wilken HP. Effect of the protein-free calf-blood-extract (solcoseryl) on the excretion of estrogens in chronic placental insufficiency. *Zentralbl Gynakol* 1976; 98: 212-216
- Heydanus R, Van Splunder IP, Wladimiroff JW. Tertiary centre referral of small-for-gestational age pregnancies: A 10-year retrospective analysis. *Prenat Diagn* 1994; 14: 105-108
- Hofman PL, Cutfield WS, Robinson EM, Bergman RN, Menon RK, Sperling MA, Gluckman PD. Insulin resistance in short children with intrauterine growth retardation. *J Clin Endocrinol Metab* 1997; 82: 402-406
- Hofmeyr GJ, Lawrie TA, Atallah AN, Duley L. Calcium supplementation during pregnancy for preventing hypertensive disorders and related problems. *Cochrane Database Syst Rev* 2010; 8: CD001059
- Hofmeyr GJ. Abdominal decompression for suspected fetal compromise/pre-eclampsia. *Cochrane Database Syst Rev* 2012; 6: CD000004
- Holmes K, Roberts OL, Thomas AM, Cross MJ. Vascular endothelial growth factor receptor-2: structure, function, intracellular signalling and therapeutic inhibition. *Cell Signal* 2007; 19: 2003-2012
- Hoopmann M, Abele H, Wagner N, Wallwiener D, Kagan KO. Performance of 36 different weight estimation formulae in fetuses with macrosomia. *Fetal Diagn Ther* 2010; 27: 204-213
- Howarth C, Gazis A, James D. Associations of type 1 diabetes mellitus, maternal vascular disease and complications of pregnancy. *Diabet Med* 2007; 24: 1229-1234
- Hua M, Odibo AO, Macones GA, Roehl KA, Crane JP, Cahill AG. Single umbilical artery and its associated findings. *Obstet Gynecol* 2010; 115: 930-934
- Hubinont C, Nicolini U, Fisk NM, Tannirandorn Y, Rodeck CH. Endocrine pancreatic function in growth-retarded fetuses. *Obstet Gynecol* 1991; 77: 541-544

- Hunter GL, Adams CE, Rowson LE. Inter-breed ovum transfer in sheep. *J Agric Sci* 1955; 46: 143-149
- Hunter AG, Reneau JK, Williams JB. Factors affecting IgG concentration in day-old lambs. *J Anim Sci* 1977; 45: 1146-1151
- Hurliman AK, Speroff L, Stouffer RL, Patton PE, Lee A, Molskness TA. Changes in circulating levels and ratios of angiopoietins during pregnancy but not during the menstrual cycle and controlled ovarian stimulation. *Fertil Steril* 2010; 93: 1493-1499
- Ibanez L, Suarez L, Lopez-Bermejo A, Diaz M, Valls C, de Zegher F. Early development of visceral fat excess after spontaneous catch-up growth in children with low birth weight. *J Clin Endocrinol Metab* 2008; 93: 925-928
- Ignarro LJ. Biological actions and properties of endothelium-derived nitric oxide formed and released from artery and vein. *Circ Res* 1989; 65: 1-21
- Inaba Y, Chen JA, Bergmann SR. Carotid plaque, compared with carotid intima-media thickness, more accurately predicts coronary artery disease events: a meta-analysis. *Atherosclerosis*. 2012; 220: 128-133
- Irion GL, Clark KE. Direct determination of the ovine fetal umbilical artery blood flow waveform. *Am J Obstet Gynecol* 1990a; 162: 541-549
- Irion GL, Clark KE. Relationship between the ovine fetal umbilical artery blood flow waveform and umbilical vascular resistance. *Am J Obstet Gynecol* 1990b; 163: 222-229
- Iwamoto HS, Trapnell BC, McConnell CJ, Daugherty C, Whitsett JA. Pulmonary inflammation associated with repeated, prenatal exposure to an E1, E3-deleted adenoviral vector in sheep. *Gene Ther* 1999; 6: 98-106
- Jackson MR, Walsh AJ, Morrow RJ, Mullen JB, Lye SJ, Ritchie JW. Reduced placental villous tree elaboration in small-for-gestational-age pregnancies: relationship with umbilical artery Doppler waveforms. *Am J Obstet Gynecol* 1995; 172: 518-525
- Jackson RA, Gibson KA, Wu YW, Croughan MS. Perinatal outcomes in singletons following in vitro fertilization: a meta-analysis. *Obstet Gynecol* 2004; 103: 551-563

- Jaddoe VW, Bakker R, Hofman A, Mackenbach JP, Moll HA, Steegers EA, Witteman JC. Moderate alcohol consumption during pregnancy and the risk of low birth weight and preterm birth. The generation R study. *Ann Epidemiol* 2007; 17: 834-840

- Jaquet D, Gaboriau A, Czernichow P, Levy-Marchal C. Insulin resistance early in adulthood in subjects born with intrauterine growth retardation. *J Clin Endocrinol Metab* 2000; 85: 1401-1406

- Jarvis S, Glinianaia SV, Torrioli MG, Platt MJ, Miceli M, Jouk PS, Johnson A, Hutton J, Hemming K, Hagberg G, Dolk H, Chalmers J, Surveillance of Cerebral Palsy in Europe (SCPE) collaboration of European Cerebral Palsy Registers. Cerebral palsy and intrauterine growth in single births: European collaborative study. *Lancet* 2003; 362: 1106-1111

- Jauniaux E, Brown R, Rodeck C, Nicolaides KH. Prenatal diagnosis of triploidy during the second trimester of pregnancy. *Obstet Gynecol* 1996; 88: 983-989

- Jeanty P, Dramaix-Wilmet M, Elkhazen N, Hubinont C, van Regemorter N. Measurements of fetal kidney growth on ultrasound. *Radiology* 1982; 144: 159-162

- Jiang J, Fan CY, Zeng BF. Osteogenic differentiation effects on rat bone marrow-derived mesenchymal stromal cells by lentivirus-mediated co-transfection of human BMP2 gene and VEGF165 gene. *Biotechnol Lett* 2008; 30: 197-203

- Johnson ML, Redmer DA, Reynolds LP. Uterine growth, cell proliferation, and c-fos proto-oncogene expression throughout the estrous cycle in ewes. *Biol Reprod* 1997; 56: 393-401

- Jones CT, Ritchie JW, Walker D. The effects of hypoxia on glucose turnover in the fetal sheep. *J Dev Physiol* 1983; 5: 223-235

- Joss-Moore LA, Wang Y, Baack ML, Yao J, Norris AW, Yu X, Callaway CW, McKnight RA, Albertine KH, Lane RH. IUGR decreases PPARgamma and SETD8 expression in neonatal rat lung and these effects are ameliorated by maternal DHA supplementation. *Early Hum Dev* 2010; 86: 785-791

- Joss-Moore LA, Wang Y, Ogata EM, Sainz AJ, Yu X, Callaway CW, McKnight RA, Albertine KH, Lane RH. IUGR differentially alters MeCP2 expression and H3K9Me3 of the PPARgamma gene in male and female rat lungs during alveolarization. *Birth Defects Res A Clin Mol Teratol* 2011; 91: 672-681

- Kafatos AG, Vlachonikolis IG, Codrington CA. Nutrition during pregnancy: the effects of an educational intervention program in Greece. *Am J Clin Nutr* 1989; 50: 970-979
- Karsdorp VH, van Vugt JM, Dekker GA, van Geijn HP. Reappearance of end-diastolic velocities in the umbilical artery following maternal volume expansion: a preliminary study. *Obstet Gynecol* 1992; 80: 679-683
- Kass SU, Pruss D, Wolffe AP. How does DNA methylation repress transcription? *Trends Genet* 1997; 13: 444-449
- Kastrup J, Jorgensen E, Fuchs S, Nikol S, Botker HE, Gyongyosi M, Glogar D, Kornowski R. A randomised, double-blind, placebo-controlled, multicentre study of the safety and efficacy of BIOBYPASS (AdGVVEGF121.10NH) gene therapy in patients with refractory advanced coronary artery disease: the NOVA trial. *EuroIntervention* 2011; 6: 813-818
- Katz AB, Keswani SG, Habli M, Lim FY, Zoltick PW, Midrio P, Kozin ED, Herlyn M, Crombleholme TM. Placental gene transfer: Transgene screening in mice for trophic effects on the placenta. *Am J Obstet Gynecol* 2009; 201: 499.e1-499.e8
- Kaufmann P. Functional anatomy of the non-primate placenta. *Placenta* 1981; Suppl_1: 13-28
- Kaulfuss KH, Uhlich K, Gille U. Ultrasonographic examination of the placentoma development in pregnant sheep. *Dtsch Tierarztl Wochenschr* 1998; 105: 162-167
- Kaur S, Picconi JL, Chadha R, Kruger M, Mari G. Biophysical profile in the treatment of intrauterine growth-restricted fetuses who weigh <1000 g. *Am J Obstet Gynecol*. 2008; 199: 264.e1-264.e4
- Ke X, Schober ME, McKnight RA, O'Grady S, Caprau D, Yu X, Callaway CW, Lane RH. Intrauterine growth retardation affects expression and epigenetic characteristics of the rat hippocampal glucocorticoid receptor gene. *Physiol Genomics* 2010; 42: 177-189
- Ke X, McKnight RA, Caprau D, O'Grady S, Fu Q, Yu X, Callaway CW, Albertine KH, Lane RH. Intrauterine growth restriction affects hippocampal dual specificity phosphatase 5 gene expression and epigenetic characteristics. *Physiol Genomics* 2011; 43: 1160-1169
- Keith JC,Jr, Moskal T, Eggleston MK, Konczal C, Howerton TL. Thromboxane synthetase inhibition produces maternal and fetal vasodilation during ovine pregnancy-induced hypertension: a Doppler flow velocimetric study. *J Perinatol* 1992; 12: 210-214

- Khoury J, Henriksen T, Christophersen B, Tonstad S. Effect of a cholesterol-lowering diet on maternal, cord, and neonatal lipids, and pregnancy outcome: a randomized clinical trial. *Am J Obstet Gynecol* 2005; 193: 1292-1301

- Kim M, Zinn KR, Barnett BG, Sumerel LA, Krasnykh V, Curiel DT, Douglas JT. The therapeutic efficacy of adenoviral vectors for cancer gene therapy is limited by a low level of primary adenovirus receptors on tumour cells. *Eur J Cancer* 2002; 38: 1917-1926

- Kingdom JC, Burrell SJ, Kaufmann P. Pathology and clinical implications of abnormal umbilical artery Doppler waveforms. *Ultrasound Obstet Gynecol* 1997; 9: 271-286

- Kinney JS, Kumar ML. Should we expand the TORCH complex? A description of clinical and diagnostic aspects of selected old and new agents. *Clin Perinatol* 1988; 15: 727-744

- Kirkegaard I, Henriksen TB, Uldbjerg N. Early fetal growth, PAPP-A and free beta-hCG in relation to risk of delivering a small-for-gestational age infant. *Ultrasound Obstet Gynecol* 2011; 37: 341-347

- Kiserud T, Johnsen SL. Biometric assessment. *Best Pract Res Clin Obstet Gynaecol* 2009; 23: 819-831

- Kleijer ME, Dekker GA, Heard AR. Risk factors for intrauterine growth restriction in a socio-economically disadvantaged region. *J Matern Fetal Neonatal Med* 2005; 18: 23-30

- Knox GE. Influence of infection on fetal growth and development. *J Reprod Med* 1978; 21: 352-358

- Koi H, Zhang J, Makrigiannakis A, Getsios S, MacCalman CD, Kopf GS, Strauss JF, 3rd, Parry S. Differential expression of the coxsackievirus and adenovirus receptor regulates adenovirus infection of the placenta. *Biol Reprod* 2001; 64: 1001-1009

- Konje JC, Howarth ES, Kaufmann P, Taylor DJ. Longitudinal quantification of uterine artery blood volume flow changes during gestation in pregnancies complicated by intrauterine growth restriction. *BJOG* 2003; 110: 301-305

- Kotimaa AA, Zainana AM, Pulkkinen E, Huusko J, Heinonen SE, Kholova I, Stedt H, Lesch HP, Yla-Herttuala S. Endothelium-specific overexpression of human vascular

endothelial growth factor-D in mice leads to increased tumor frequency and a reduced lifespan. *J Gene Med* 2012; 14: 182-190

- Koukoura O, Sifakis S, Zaravinos A, Apostolidou S, Jones A, Hajiioannou J, Widschwendter M, Spandidos DA. Hypomethylation along with increased H19 expression in placentas from pregnancies complicated with fetal growth restriction. *Placenta* 2011a; 32: 51-57

- Koukoura O, Sifakis S, Soufla G, Zaravinos A, Apostolidou S, Jones A, Widschwendter M, Spandidos DA. Loss of imprinting and aberrant methylation of IGF2 in placentas from pregnancies complicated with fetal growth restriction. *Int J Mol Med* 2011b; 28: 481-487

- Kramer MS. Intrauterine growth and gestational duration determinants. *Pediatrics* 1987; 80: 502-511

- Kramer MS, Platt R, Yang H, McNamara H, Usher RH. Are all growth-restricted newborns created equal(ly)? *Pediatrics* 1999; 103: 599-602

- Krulewitch CJ, Herman AA, Yu KF, Johnson YR. Does changing paternity contribute to the risk of intrauterine growth retardation? *Paediatr Perinat Epidemiol* 1997; 11(Suppl_1): 41-47

- Lackman F, Capewell V, Richardson B, daSilva O, Gagnon R. The risks of spontaneous preterm delivery and perinatal mortality in relation to size at birth according to fetal versus neonatal growth standards. *Am J Obstet Gynecol* 2001; 184: 946-953

- Lambertini L, Lee TL, Chan WY, Lee MJ, Diplas A, Wetmur J, Chen J. Differential methylation of imprinted genes in growth-restricted placentas. *Reprod Sci* 2011; 18: 1111-1117

- Lan X, Cretney EC, Kropp J, Khateeb K, Berg MA, Penagaricano F, Magness R, Radunz AE, Khatib H. Maternal diet during pregnancy induces gene expression and DNA methylation changes in fetal tissues in sheep. *Front Genet* 2013; 4: 49

- Lang JM, Lieberman E, Cohen A. A comparison of risk factors for preterm labor and term small-for-gestational-age birth. *Epidemiology* 1996; 7: 369-376

- Lang U, Baker RS, Khoury J, Clark KE. Effects of chronic reduction in uterine blood flow on fetal and placental growth in the sheep. *Am J Physiol Regul Integr Comp Physiol* 2000; 279: R53-59

- Lang U, Baker RS, Braems G, Zygmunt M, Kunzel W, Clark KE. Uterine blood flow - a determinant of fetal growth. *Eur J Obstet Gynecol Reprod Biol* 2003; 110(Suppl_1): S55-S61

- Larson BL, Heary HL,Jr, Devery JE. Immunoglobulin production and transport by the mammary gland. *J Dairy Sci* 1980; 63: 665-671

- Lawyer FC, Stoffel S, Saiki RK, Myambo K, Drummond R, Gelfand DH. Isolation, characterization, and expression in escherichia coli of the DNA polymerase gene from thermus aquaticus. *J Biol Chem* 1989; 264: 6427-6437

- Lea RG, Hannah LT, Redmer DA, Aitken RP, Milne JS, Fowler PA, Murray JF, Wallace JM. Developmental indices of nutritionally induced placental growth restriction in the adolescent sheep. *Pediatr Res* 2005; 57: 599-604

- Lea RG, Wooding P, Stewart I, Hannah LT, Morton S, Wallace K, Aitken RP, Milne JS, Regnault TR, Anthony RV, Wallace JM. The expression of ovine placental lactogen, StAR and progesterone-associated steroidogenic enzymes in placentae of overnourished growing adolescent ewes. *Reproduction* 2007; 133: 785-796

- Lederman SA, Rauh V, Weiss L, Stein JL, Hoepner LA, Becker M, Perera FP. The effects of the world trade center event on birth outcomes among term deliveries at three lower manhattan hospitals. *Environ Health Perspect* 2004; 112: 1772-1778

- Lee RJ, Springer ML, Blanco-Bose WE, Shaw R, Ursell PC, Blau HM. VEGF gene delivery to myocardium: Deleterious effects of unregulated expression. *Circulation* 2000; 102: 898-901

- Lee RS, Depree KM, Davey HW. The sheep (ovis aries) H19 gene: Genomic structure and expression patterns, from the preimplantation embryo to adulthood. *Gene* 2002; 301: 67-77

- Lee SA, Ding C. The dysfunctional placenta epigenome: causes and consequences. *Epigenomics* 2012; 4: 561-569

- Leinonen E, Hurt-Camejo E, Wiklund O, Hulten LM, Hiukka A, Taskinen MR. Insulin resistance and adiposity correlate with acute-phase reaction and soluble cell adhesion molecules in type 2 diabetes. *Atherosclerosis* 2003; 166: 387-394

- Leinonen E, Wathen KA, Alfthan H, Ylikorkala O, Andersson S, Stenman UH, Vuorela P. Maternal serum angiopoietin-1 and -2 and tie-2 in early pregnancy ending in preeclampsia or intrauterine growth retardation. *J Clin Endocrinol Metab* 2010; 95: 126-133

- Leitich H, Egarter C, Husslein P, Kaider A, Schemper M. A meta-analysis of low dose aspirin for the prevention of intrauterine growth retardation. *BJOG* 1997; 104: 450-459

- Leury BJ, Bird AR, Chandler KD, Bell AW. Glucose partitioning in the pregnant ewe: effects of undernutrition and exercise. *Br J Nutr* 1990; 64: 449-462

- Li C, McDonald TJ, Wu G, Nijland MJ, Nathanielsz PW. Intrauterine growth restriction alters term fetal baboon hypothalamic appetitive peptide balance. *J Endocrinol* 2013; 217: 275-282

- Lillycrop KA, Phillips ES, Torrens C, Hanson MA, Jackson AA, Burdge GC. Feeding pregnant rats a protein-restricted diet persistently alters the methylation of specific cytosines in the hepatic PPAR alpha promoter of the offspring. *Br J Nutr* 2008; 100: 278-282

- Lim K, Armitage JA, Stefanidis A, Oldfield BJ, Black MJ. IUGR in the absence of postnatal "catch-up" growth leads to improved whole body insulin sensitivity in rat offspring. *Pediatr Res* 2011; 70: 339-344

- Limesand SW, Rozance PJ, Zerbe GO, Hutton JC, Hay WW,Jr. Attenuated insulin release and storage in fetal sheep pancreatic islets with intrauterine growth restriction. *Endocrinology* 2006; 147: 1488-1497

- Lin S, Shimizu I, Suehara N, Nakayama M, Aono T. Uterine artery Doppler velocimetry in relation to trophoblast migration into the myometrium of the placental bed. *Obstet Gynecol* 1995; 85: 760-765

- Lin PW, Nasr TR, Stoll BJ. Necrotizing enterocolitis: recent scientific advances in pathophysiology and prevention. *Semin Perinatol* 2008; 32: 70-82

- Liu S, Krewski D, Shi Y, Chen Y, Burnett RT. Association between gaseous ambient air pollutants and adverse pregnancy outcomes in Vancouver, Canada. *Environ Health Perspect* 2003; 111: 1773-1778

- Lodygensky GA, Seghier ML, Warfield SK, Tolsa CB, Sizonenko S, Lazeyras F, Huppi PS. Intrauterine growth restriction affects the preterm infant's hippocampus. *Pediatr Res* 2008; 63: 438-443

- Logan EF, Foster WH, Irwin D. A note on bovine colostrum as an alternative source of immunoglobulins for lambs. *Animal Production* 1978; 26: 93-96

- Loughna P, Chitty LS, Evans T, Chudleigh T. Fetal size and dating: charts recommended for clinical obstetric practice. *Ultrasound* 2009; 17: 161-167

- Loyaga-Rendon RY, Sakamoto S, Beppu M, Aso T, Ishizaka M, Takahashi R, Azuma H. Accumulated endogenous nitric oxide synthase inhibitors, enhanced arginase activity, attenuated dimethylarginine dimethylaminohydrolase activity and intimal hyperplasia in premenopausal human uterine arteries. *Atherosclerosis* 2005; 178: 231-239

- Ludwig T, Eggenschwiler J, Fisher P, D'Ercole AJ, Davenport ML, Efstratiadis A. Mouse mutants lacking the type 2 IGF receptor (IGF2R) are rescued from perinatal lethality in Igf2 and Igf1r null backgrounds. *Dev Biol* 1996; 177: 517-535

- Lumley J, Chamberlain C, Dowswell T, Oliver S, Oakley L, Watson L. Interventions for promoting smoking cessation during pregnancy. *Cochrane Database Syst Rev* 2009; 3: CD001055

- Luther JS, Redmer DA, Reynolds LP, Wallace JM. Nutritional paradigms of ovine fetal growth restriction: Implications for human pregnancy. *Hum Fertil (Camb)* 2005; 8: 179-187

- Luther J, Aitken R, Milne J, Matsuzaki M, Reynolds L, Redmer D, Wallace J. Maternal and fetal growth, body composition, endocrinology, and metabolic status in undernourished adolescent sheep. *Biol Reprod* 2007; 77: 343-350

- Ma Y, Zhu MJ, Uthlaut AB, Nijland MJ, Nathanielsz PW, Hess BW, Ford SP. Upregulation of growth signaling and nutrient transporters in cotyledons of early to mid-gestational nutrient restricted ewes. *Placenta* 2011; 32: 255-263

- Macara L, Kingdom JC, Kaufmann P, Kohnen G, Hair J, More IA, Lyall F, Greer IA. Structural analysis of placental terminal villi from growth-restricted pregnancies with abnormal umbilical artery Doppler waveforms. *Placenta* 1996; 17: 37-48

- MacCalman CD, Furth EE, Omigbodun A, Kozarsky KF, Coutifaris C, Strauss JF, 3rd. Transduction of human trophoblast cells by recombinant adenoviruses is differentiation dependent. *Biol Reprod* 1996; 54: 682-691

- MacRae JC, Bruce LA, Hovell FDD, Hart IC, Inkster J, Walker A, Atkinson T. Influence of protein nutrition on the response of growing lambs to exogenous bovine growth hormone. *J Endocrinol* 1991; 130: 53-61

- Magnusson AL, Waterman IJ, Wennergren M, Jansson T, Powell TL. Triglyceride hydrolase activities and expression of fatty acid binding proteins in the human placenta in pregnancies complicated by intrauterine growth restriction and diabetes. *J Clin Endocrinol Metab* 2004; 89: 4607-4614

- Mahomed K. Iron and folate supplementation in pregnancy. *Cochrane Database Syst Rev* 2000; 2: CD001135

- Mahomed K, Gulmezoglu AM. Vitamin D supplementation in pregnancy. *Cochrane Database Syst Rev* 2000; 2: CD000228

- Maier RF, Gunther A, Vogel M, Dudenhausen JW, Obladen M. Umbilical venous erythropoietin and umbilical arterial pH in relation to morphologic placental abnormalities. *Obstet Gynecol* 1994; 84: 81-87

- Makinen K, Manninen H, Hedman M, Matsi P, Mussalo H, Alhava E, Yla-Herttuala S. Increased vascularity detected by digital subtraction angiography after VEGF gene transfer to human lower limb artery: a randomized, placebo-controlled, double-blinded phase II study. *Mol Ther* 2002; 6: 127-133

- Makrides M, Duley L, Olsen SF. Marine oil, and other prostaglandin precursor, supplementation for pregnancy uncomplicated by pre-eclampsia or intrauterine growth restriction. *Cochrane Database Syst Rev* 2006; 3: CD003402

- Mandruzzato G, Antsaklis A, Botet F, Chervenak FA, Figueras F, Grunebaum A, Puerto B, Skupski D, Stanojevic M, WAPM. Intrauterine restriction (IUGR). *J Perinat Med* 2008; 36: 277-281

- Mangham LJ, Petrou S, Doyle LW, Draper ES, Marlow N. The cost of preterm birth throughout childhood in England and Wales. *Pediatrics* 2009; 123: e312-e327
- Manten GT, Sikkema MJ, Voorbij HA, Visser GH, Bruinse HW, Franx A. Risk factors for cardiovascular disease in women with a history of pregnancy complicated by preeclampsia or intrauterine growth restriction. *Hypertens Pregnancy* 2007; 26: 39-50
- Mari G, Deter RL. Middle cerebral artery flow velocity waveforms in normal and small-for-gestational-age fetuses. *Am J Obstet Gynecol* 1992; 166: 1262-1270
- Mari G, Abuhamad AZ, Uerpairojkit B, Martinez E, Copel JA. Blood flow velocity waveforms of the abdominal arteries in appropriate- and small-for-gestational-age fetuses. *Ultrasound Obstet Gynecol* 1995; 6: 15-18
- Mari G, Hanif F, Treadwell MC, Kruger M. Gestational age at delivery and Doppler waveforms in very preterm intrauterine growth-restricted fetuses as predictors of perinatal mortality. *J Ultrasound Med* 2007; 26: 555-559
- Mari G. Doppler ultrasonography in obstetrics: From the diagnosis of fetal anemia to the treatment of intrauterine growth-restricted fetuses. *Am J Obstet Gynecol* 2009; 200: 613.e1-613.e9
- Marie M, Findlay PA, Thomas L, Adam CL. Daily patterns of plasma leptin in sheep: effects of photoperiod and food intake. *J Endocrinol* 2001; 170: 277-286
- Marinova GV, Loyaga-Rendon RY, Obayashi S, Ishibashi T, Kubota T, Imamura M, Azuma H. Possible involvement of altered arginase activity, arginase type I and type II expressions, and nitric oxide production in occurrence of intimal hyperplasia in premenopausal human uterine arteries. *J Pharmacol Sci* 2008; 106: 385-393
- Marlow N, Wolke D, Bracewell MA, Samara M, EPICure Study Group. Neurologic and developmental disability at six years of age after extremely preterm birth. *N Engl J Med* 2005; 352: 9-19
- Marsh S. Pyrosequencing applications. *Methods Mol Biol* 2007; 373: 15-24
- Martos-Moreno GA, Barrios V, Saenz de Pipaon M, Pozo J, Dorronsoro I, Martinez-Biarge M, Quero J, Argente J. Influence of prematurity and growth restriction on the adipokine profile, IGF1, and ghrelin levels in cord blood: relationship with glucose metabolism. *Eur J Endocrinol* 2009; 161: 381-389

- Matilainen R, Heinonen K, Siren-Tiusanen H, Jokela V, Launiala K. Neurodevelopmental screening of in utero growth-retarded prematurely born children before school age. *Eur J Pediatr* 1987; 146: 453-457

- Maulik D, Yarlagadda P, Nathanielsz PW, Figueroa JP. Hemodynamic validation of Doppler assessment of fetoplacental circulation in a sheep model system. *J Ultrasound Med* 1989; 8: 177-181

- Maulik D. Fetal growth restriction: the etiology. *Clin Obstet Gynecol* 2006; 49: 228-235

- Maynard SE, Min JY, Merchan J, Lim KH, Li J, Mondal S, Libermann TA, Morgan JP, Sellke FW, Stillman IE, Epstein FH, Sukhatme VP, Karumanchi SA. Excess placental soluble fms-like tyrosine kinase 1 (sFlt1) may contribute to endothelial dysfunction hypertension, and proteinuria in preeclampsia. *J Clin Invest* 2003; 111: 649-658

- McCance DR, Pettitt DJ, Hanson RL, Jacobsson LT, Knowler WC, Bennett PH. Birth weight and non-insulin dependent diabetes: thrifty genotype, thrifty phenotype, or surviving small baby genotype? *BMJ* 1994; 308: 942-945

- McCowan LM, Mullen BM, Ritchie K. Umbilical artery flow velocity waveforms and the placental vascular bed. *Am J Obstet Gynecol* 1987; 157: 900-902

- McCowan L, Horgan RP. Risk factors for small for gestational age infants. *Best Pract Res Clin Obstet Gynaecol* 2009; 23: 779-793

- McCowan LM, Roberts CT, Dekker GA, Taylor RS, Chan EH, Kenny LC, Baker PN, Moss-Morris R, Chappell LC, North RA, SCOPE consortium. Risk factors for small-for-gestational-age infants by customised birthweight centiles: data from an international prospective cohort study. *BJOG* 2010; 117: 1599-1607

- McCray PB,Jr, Armstrong K, Zabner J, Miller DW, Koretzky GA, Couture L, Robillard JE, Smith AE, Welsh MJ. Adenoviral-mediated gene transfer to fetal pulmonary epithelia in vitro and in vivo. *J Clin Invest* 1995; 95: 2620-2632

- McDowell DG, Burns NA, Parkes HC. Localised sequence regions possessing high melting temperatures prevent the amplification of a DNA mimic in competitive PCR. *Nucleic Acids Res* 1998; 26: 3340-3347

- McFadden DE, Kalousek DK. Two different phenotypes of fetuses with chromosomal triploidy: correlation with parental origin of the extra haploid set. *Am J Med Genet* 1991; 38: 535-538

- McGory ML, Zingmond DS, Tillou A, Hiatt JR, Ko CY, Cryer HM. Negative appendectomy in pregnant women is associated with a substantial risk of fetal loss. *J Am Coll Surg* 2007; 205: 534-540

- McGrattan PD, Wylie AR, Bjourson AJ. A partial cDNA sequence of the ovine insulin receptor gene: evidence for alternative splicing of an exon 11 region and for tissue-specific regulation of receptor isoform expression in sheep muscle, adipose tissue and liver. *J Endocrinol* 1998; 159: 381-387

- McIntire DD, Bloom SL, Casey BM, Leveno KJ. Birth weight in relation to morbidity and mortality among newborn infants. *N Engl J Med* 1999; 340: 1234-1238

- McKelvey WAC, Robinson JJ, Aitken RP, Henderson G. The evaluation of a laparoscopic insemination technique in ewes. *Theriogenology* 1985; 24: 519-535

- McLaren RJ, Montgomery GW. Genomic imprinting of the insulin-like growth factor 2 gene in sheep. *Mamm Genome* 1999; 10: 588-591

- McMillan WH, McDonald MF. Survival of fertilised ova from ewe lambs and adult uteri in the uteri of ewe lambs. *Animal Reproduction Science* 1985; 24: 519-535

- Mehta V, Abi-Nader KN, Peebles DM, Benjamin E, Wigley V, Torondel B, Filippi E, Shaw SW, Boyd M, Martin J, Zachary I, David AL. Long-term increase in uterine blood flow is achieved by local overexpression of VEGF-A(165) in the uterine arteries of pregnant sheep. *Gene Ther* 2011; 19: 925-935

- Mehta V, Boyd M, Barker H, Advic-Belltheus A, Carr D, Martin J, Zachary I, Peebles D, David AL. Local administration of ad.VEGF-A_{165} to the utero-placental circulation reduces brain sparing and may enhance fetal growth in an FGR model of guinea pig pregnancy. *Reprod Sci*. 2012; 19: 78A

- Mehta V, Abi-Nader KN, Shangaris P, Shaw SWS, Filippi E, Benjamin E, Boyd M, Peebles DM, Martin JF, Zachary IC, David AL. Local over-expression of VEGF-$D^{\Delta N \Delta C}$ in the uterine arteries of pregnant sheep results in long-term changes in uterine artery contractility and aniogenesis. 2013 [submitted]

- Mellor DJ, Mitchell B, Matheson IC. Reductions in lamb weight caused by pre-mating carunclectomy and mid-pregnancy placental ablation. *J Comp Pathol* 1977; 87: 629-633

- Melloul D, Marshak S, Cerasi E. Regulation of insulin gene transcription. *Diabetologia* 2002; 45: 309-326

- Meschia G. Circulation to female reproductive organs. In: Shepherd JT, Abboud FM *Handbook of Physiology.* Bethesda: American Physiological Society. 1983: 241-269

- Mesiano S, Young IR, Hey AW, Browne CA, Thorburn GD. Hypophysectomy of the fetal lamb leads to a fall in the plasma concentration of insulin-like growth factor I (IGF-I), but not IGF-II. *Endocrinology* 1989; 124: 1485-1491

- Mess A. The guinea pig placenta: Model of placental growth dynamics. *Placenta* 2007; 28: 812-815

- Meyer AM, Neville TL, Reed JJ, Taylor JB, Reynolds LP, Redmer DA, Hammer CJ, Vonnahme KA, Caton JS. Maternal nutritional plane and selenium supply during gestation impact visceral organ mass and intestinal growth and vascularity of neonatal lamb offspring. *J Anim Sci* 2013; 91: 2628-2639

- Miao F, Wu X, Zhang L, Riggs AD, Natarajan R. Histone methylation patterns are cell-type specific in human monocytes and lymphocytes and well maintained at core genes. *J Immunol* 2008; 180: 2264-2269

- Miller SL, Jenkin G, Walker DW. Effect of nitric oxide synthase inhibition on the uterine vasculature of the late-pregnant ewe. *Am J Obstet Gynecol* 1999; 180: 1138-1145

- Miller SL, Loose JM, Jenkin G, Wallace EM. The effects of sildenafil citrate (viagra) on uterine blood flow and well being in the intrauterine growth-restricted fetus. *Am J Obstet Gynecol* 2009; 200: 102.e1-102.e7

- Mitchell EK, Louey S, Cock ML, Harding R, Black MJ. Nephron endowment and filtration surface area in the kidney after growth restriction of fetal sheep. *Pediatr Res* 2004; 55: 769-773

- Moffett-King A. Natural killer cells and pregnancy. *Nat Rev Immunol* 2002; 2: 656-663

- Molina RD, Meschia G, Battaglia FC, Hay WW,Jr. Gestational maturation of placental glucose transfer capacity in sheep. *Am J Physiol* 1991; 261: R697-R704
- Moncada S, Vane JR. Pharmacology and endogenous roles of prostaglandin endoperoxides, thromboxane A2, and prostacyclin. *Pharmacol Rev* 1978; 30: 293-331
- Moore LG. Fetal growth restriction and maternal oxygen transport during high altitude pregnancy. *High Alt Med Biol* 2003; 4: 141-156
- Mori R, Ota E, Middleton P, Tobe-Gai R, Mahomed K, Bhutta ZA. Zinc supplementation for improving pregnancy and infant outcome. *Cochrane Database Syst Rev* 2012; 7: CD000230
- Morris RK, Malin GL, Tsourapas A, Roberts TE, Khan KS. An economic evaluation of alternative test-intervention strategies to prevent fetal growth restriction in singleton pregnancies. *Arch Dis Child Fetal Neonatal Ed* 2010; 95: Fa12
- Morrow RJ, Adamson SL, Bull SB, Ritchie JW. Effect of placental embolization on the umbilical arterial velocity waveform in fetal sheep. *Am J Obstet Gynecol* 1989; 161: 1055-1060
- Morrow RJ, Adamson SL, Bull SB, Ritchie JW. Acute hypoxemia does not affect the umbilical artery flow velocity waveform in fetal sheep. *Obstet Gynecol* 1990; 75: 590-593
- Morse SB, Wu SS, Ma C, Ariet M, Resnick M, Roth J. Racial and gender differences in the viability of extremely low birth weight infants: a population-based study. *Pediatrics* 2006; 117: e106-12
- Morsing E, Asard M, Ley D, Stjernqvist K, Marsal K. Cognitive function after intrauterine growth restriction and very preterm birth. *Pediatrics* 2011; 127: e874-82
- Morsing E, Gustafsson P, Brodszki J. Lung function in children born after foetal growth restriction and very preterm birth. *Acta Paediatr* 2012; 101: 48-54
- Mostello D, Chalk C, Khoury J, Mack CE, Siddiqi TA, Clark KE. Chronic anemia in pregnant ewes: maternal and fetal effects. *Am J Physiol* 1991; 261: R1075-R1083

- Muhlhausler BS, Roberts CT, McFarlane JR, Kauter KG, McMillen IC. Fetal leptin is a signal of fat mass independent of maternal nutrition in ewes fed at or above maintenance energy requirements. *Biol Reprod* 2002; 67: 493-499

- Muhlhausler BS, Roberts CT, Yuen BS, Marrocco E, Budge H, Symonds ME, McFarlane JR, Kauter KG, Stagg P, Pearse JK, McMillen IC. Determinants of fetal leptin synthesis, fat mass, and circulating leptin concentrations in well-nourished ewes in late pregnancy. *Endocrinology* 2003; 144: 4947-4954

- Muijsers GJ, Hasaart TH, Ruissen CJ, van Huisseling H, Peeters LL, de Haan J. The response of the umbilical and femoral artery pulsatility indices in fetal sheep to progressively reduced uteroplacental blood flow. *J Dev Physiol* 1990; 13: 215-221

- Munshi A, Shafi G, Aliya N, Jyothy A. Histone modifications dictate specific biological readouts. *J Genet Genomics* 2009; 36: 75-88

- Murotsuki J, Bocking AD, Gagnon R. Fetal heart rate patterns in growth-restricted fetal sheep induced by chronic fetal placental embolization. *Am J Obstet Gynecol* 1997; 176: 282-290

- Murphy VE, Smith R, Giles WB, Clifton VL. Endocrine regulation of human fetal growth: the role of the mother, placenta, and fetus. *Endocr Rev* 2006; 27: 141-169

- Nahum GG, Stanislaw H. Ultrasonographic prediction of term birth weight: how accurate is it? *Am J Obstet Gynecol* 2003; 188: 566-574

- Namgung R, Tsang RC, Specker BL, Sierra RI, Ho ML. Reduced serum osteocalcin and 1,25-dihydroxyvitamin D concentrations and low bone mineral content in small for gestational age infants: evidence of decreased bone formation rates. *J Pediatr* 1993; 122: 269-275

- Nardozza LM, Araujo Junior E, Barbosa MM, Caetano AC, Lee DJ, Moron AF. Fetal growth restriction: current knowledge to the general Obs/Gyn. *Arch Gynecol Obstet* 2012; 286: 1-13

- Nassar AH, Masrouha KZ, Itani H, Nader KA, Usta IM. Effects of sildenafil in nomega-nitro-L-arginine methyl ester-induced intrauterine growth restriction in a rat model. *Am J Perinatol* 2012; 29: 429-434

- Nelissen EC, van Montfoort AP, Dumoulin JC, Evers JL. Epigenetics and the placenta. *Hum Reprod Update* 2011; 17: 397-417
- Nelson-Piercy C. *Handbook of Obstetric Medicine (Fourth Edition)*. London: Informa Healthcare. 2010
- Nemerow GR, Stewart PL. Role of alpha(v) integrins in adenovirus cell entry and gene delivery. *Microbiol Mol Biol Rev* 1999; 63: 725-734
- Neville TL, Meyer AM, Reyaz A, Borowicz PB, Redmer DA, Reynolds LP, Caton JS, Vonnahme KA. Mammary gland growth and vascularity at parturition and during lactation in primiparous ewes fed differing levels of selenium and nutritional plane during gestation. *J Anim Sci Biotechnol* 2013; DOI 10.1186/2049-1891-4-6 [epub ahead of print]
- Newnham JP, Kelly RW, Roberts RV, MacIntyre M, Speijers J, Johnson T, Reid SE. Fetal and maternal Doppler flow velocity waveforms in normal sheep pregnancy. *Placenta* 1987; 8: 467-476
- NICE (National Institute for Health and Clinical Excellence). Intrapartum care: care of healthy women and their babies during childbirth. 2007 (updated 2008). Available at http://guidance.nice.org.uk/CG55. Last accessed on 10 June 2013.
- NICE (National Institute for Heath and Clinical Excellence). Antenatal care: routine care for the healthy pregnant woman. 2008. Available at http://guidance.nice.org.uk/CG62. Last accessed on 10 June 2013.
- Nicolaides KH, Campbell S, Bradley RJ, Bilardo CM, Soothill PW, Gibb D. Maternal oxygen therapy for intrauterine growth retardation. *Lancet* 1987; 1: 942-945
- Nicolini U, Hubinont C, Santolaya J, Fisk NM, Coe AM, Rodeck CH. Maternal-fetal glucose gradient in normal pregnancies and in pregnancies complicated by alloimmunization and fetal growth retardation. *Am J Obstet Gynecol* 1989; 161: 924-927
- Nicolini U, Hubinont C, Santolaya J, Fisk NM, Rodeck CH. Effects of fetal intravenous glucose challenge in normal and growth retarded fetuses. *Horm Metab Res* 1990; 22: 426-430

- Nieto-Diaz A, Villar J, Matorras-Weinig R, Valenzuela-Ruiz P. Intrauterine growth retardation at term: association between anthropometric and endocrine parameters. *Acta Obstet Gynecol Scand* 1996; 75: 127-131

- Niknafs P, Sibbald J. Accuracy of single ultrasound parameters in detection of fetal growth restriction. *Am J Perinatol* 2001; 18: 325-334

- Nimrod C, Clapp J,3rd, Larrow R, D'Alton M, Persaud D. Simultaneous use of Doppler ultrasound and electromagnetic flow probes in fetal flow assessment. *J Ultrasound Med* 1989; 8: 201-205

- Nur I, Szyf M, Razin A, Glaser G, Rottem S, Razin S. Procaryotic and eucaryotic traits of DNA methylation in spiroplasmas (mycoplasmas). *J Bacteriol* 1985; 164: 19-24

- Obayashi S, Aso T, Sato J, Hamasaki H, Azuma H. Intimal hyperplasia in human uterine arteries accompanied by impaired synergism between prostaglandin I2 and nitric oxide. *Br J Pharmacol* 1996; 119: 1072-1078

- Obayashi S, Beppu M, Aso T, Goto M, Azuma H. 17 beta-estradiol increases nitric oxide and prostaglandin I2 production by cultured human uterine arteries only in histologically normal specimens. *J Cardiovasc Pharmacol* 2001; 38: 240-249

- Ochi H, Suginami H, Matsubara K, Taniguchi H, Yano J, Matsuura S. Micro-bead embolization of uterine spiral arteries and changes in uterine arterial flow velocity waveforms in the pregnant ewe. *Ultrasound Obstet Gynecol* 1995; 6: 272-276

- Ochi H, Matsubara K, Kusanagi Y, Taniguchi H, Ito M. Significance of a diastolic notch in the uterine artery flow velocity waveform induced by uterine embolisation in the pregnant ewe. *Br J Obstet Gynaecol* 1998; 105: 1118-1121

- Odibo AO, Nelson D, Stamilio DM, Sehdev HM, Macones GA. Advanced maternal age is an independent risk factor for intrauterine growth restriction. *Am J Perinatol* 2006; 23: 325-328

- Ofir R, Gootwine E. Ovine growth hormone gene duplication - structural and evolutionary implications. *Mamm Genome* 1997; 8: 770-772

- Ohlsen SM, Dean DM, Wong EA. Characterization of multiple transcription initiation sites of the ovine insulin-like growth factor-I gene and expression profiles of three alternatively spliced transcripts. *DNA Cell Biol* 1993; 12: 243-251

- Ohlsen SM, Lugenbeel KA, Wong EA. Characterization of the linked ovine insulin and insulin-like growth factor-II genes. *DNA Cell Biol* 1994; 13: 377-388
- Ohshige A, Yoshimura T, Maeda T, Ito M, Okamura H. Increased platelet-activating factor-acetylhydrolase activity in the umbilical venous plasma of growth-restricted fetuses. *Obstet Gynecol* 1999; 93: 180-183
- Orian JM, O'Mahoney JV, Brandon MR. Cloning and sequencing of the ovine growth hormone gene. *Nucleic Acids Res* 1988; 16: 9046
- Osol G, Mandala M. Maternal uterine vascular remodeling during pregnancy. *Physiology (Bethesda)* 2009; 24: 58-71
- Ostlund E, Tally M, Fried G. Transforming growth factor-beta1 in fetal serum correlates with insulin-like growth factor-I and fetal growth. *Obstet Gynecol* 2002; 100: 567-573
- Ota E, Tobe-Gai R, Mori R, Farrar D. Antenatal dietary advice and supplementation to increase energy and protein intake. *Cochrane Database Syst Rev* 2012; 9: CD000032
- Ott WJ. The diagnosis of altered fetal growth. *Obstet Gynecol Clin North Am* 1988; 15: 237-263
- Owens JA, Falconer J, Robinson JS. Effect of restriction of placental growth on umbilical and uterine blood flows. *Am J Physiol* 1986; 250: R427-R434
- Owman C. Pregnancy induces degenerative and regenerative changes in the autonomic innervation of the female reproductive tract. In*: Development of the Autonomic Nervous System (Ciba Foundation Symposium 83).* London: Pitman Medical Press. 1981: 252-279
- Oyama K, Padbury J, Chappell B, Martinez A, Stein H, Humme J. Single umbilical artery ligation-induced fetal growth retardation: effect on postnatal adaptation. *Am J Physiol* 1992; 263: E575-E583
- Painter RC, Roseboom TJ, Bleker OP. Prenatal exposure to the dutch famine and disease in later life: An overview. *Reprod Toxicol* 2005; 20: 345-352
- Palmer SK, Zamudio S, Coffin C, Parker S, Stamm E, Moore LG. Quantitative estimation of human uterine artery blood flow and pelvic blood flow redistribution in pregnancy. *Obstet Gynecol* 1992; 80: 1000-1006

- Paolini CL, Marconi AM, Ronzoni S, Di Noio M, Fennessey PV, Pardi G, Battaglia FC. Placental transport of leucine, phenylalanine, glycine, and proline in intrauterine growth-restricted pregnancies. *J Clin Endocrinol Metab* 2001; 86: 5427-5432

- Papageorghiou AT, Fratelli N, Leslie K, Bhide A, Thilaganathan B. Outcome of fetuses with antenatally diagnosed short femur. *Ultrasound Obstet Gynecol* 2008; 31: 507-511

- Pardi G, Cetin I, Marconi AM, Lanfranchi A, Bozzetti P, Ferrazzi E, Buscaglia M, Battaglia FC. Diagnostic value of blood sampling in fetuses with growth retardation. *N Engl J Med* 1993; 328: 692-696

- Parraguez VC, Atlagich M, Diaz R, Bruzzone ME, Behn C, Raggi LA. Effect of hypobaric hypoxia on lamb intrauterine growth: comparison between high- and low-altitude native ewes. *Reprod Fertil Dev* 2005; 17: 497-505

- Parry S, Holder J, Halterman MW, Weitzman MD, Davis AR, Federoff H, Strauss JF, 3rd. Transduction of human trophoblastic cells by replication-deficient recombinant viral vectors. Promoting cellular differentiation affects virus entry. *Am J Pathol* 1998; 152: 1521-1529

- Patterson RM, Gibbs CE, Wood RC. Birth weight percentile and perinatal outcome: recurrence of intrauterine growth retardation. *Obstet Gynecol* 1986; 68: 464-468

- Peebles DM. Fetal consequences of chronic substrate deprivation. *Semin Fetal Neonatal Med* 2004; 9: 379-386

- Pena-Rosas JP, De-Regil LM, Dowswell T, Viteri FE. Daily oral iron supplementation during pregnancy. *Cochrane Database Syst Rev* 2012; 12: CD004736

- Persson B, Stangenberg M, Lunell NO, Brodin U, Holmberg NG, Vaclavinkova V. Prediction of size of infants at birth by measurement of symphysis fundus height. *BJOG* 1986; 93: 206-211

- Petrou S, Henderson J, Bracewell M, Hockley C, Wolke D, Marlow N, EPICure Study Group. Pushing the boundaries of viability: the economic impact of extreme preterm birth. *Early Hum Dev* 2006; 82: 77-84

- Phillips DI. Insulin resistance as a programmed response to fetal undernutrition. *Diabetologia* 1996; 39: 1119-1122

- Phillips DI, Walker BR, Reynolds RM, Flanagan DE, Wood PJ, Osmond C, Barker DJ, Whorwood CB. Low birth weight predicts elevated plasma cortisol concentrations in adults from 3 populations. *Hypertension* 2000; 35: 1301-1306

- Phillips ID, Anthony RV, Simonetta G, Owens JA, Robinson JS, McMillen IC. Restriction of fetal growth has a differential impact on fetal prolactin and prolactin receptor mRNA expression. *J Neuroendocrinol* 2001; 13: 175-181

- Pijnenborg R, Bland JM, Robertson WB, Brosens I. Uteroplacental arterial changes related to interstitial trophoblast migration in early human pregnancy. *Placenta*. 1983; 4: 397-413

- Platz E, Newman R. Diagnosis of IUGR: Traditional biometry. *Semin Perinatol* 2008; 32: 140-147

- Prefumo F, Sebire NJ, Thilaganathan B. Decreased endovascular trophoblast invasion in first trimester pregnancies with high-resistance uterine artery Doppler indices. *Hum Reprod* 2004; 19: 206-209

- Quirke JF, Hanrahan JP. Comparison of the survival in the uteri of adult ewes of cleaved ova from adult ewes and ewe lambs. *J Reprod Fertil* 1977; 51: 487-489

- Rajagopalan S, Mohler E, 3rd, Lederman RJ, Saucedo J, Mendelsohn FO, Olin J, Blebea J, Goldman C, Trachtenberg JD, Pressler M, Rasmussen H, Annex BH, Hirsch AT, Regional Angiogenesis With Vascular Endothelial Growth Factor trial. Regional angiogenesis with vascular endothelial growth factor (VEGF) in peripheral arterial disease: design of the RAVE trial. *Am Heart J* 2003; 145: 1114-1118

- RCOG (Royal College of Obstetricians and Gynaecologists). Green–top guideline no. 31: The investigation and management of the small–for–gestational–age fetus, second edition. 2013. Available at http://www.rcog.org.uk/womens-health/investigation-and-management-small-gestational-age-fetus-green-top-31 . Last accessed on 10 Jun 2013

- Redmer DA, Aitken RP, Milne JS, Reynolds LP, Wallace JM. Influence of maternal nutrition on messenger RNA expression of placental angiogenic factors and their receptors at midgestation in adolescent sheep. *Biol Reprod* 2005; 72: 1004-1009

- Redmer DA, Luther JS, Milne JS, Aitken RP, Johnson ML, Borowicz PP, Borowicz MA, Reynolds LP, Wallace JM. Fetoplacental growth and vascular development in

overnourished adolescent sheep at day 50, 90 and 130 of gestation. *Reproduction* 2009; 137: 749-757

- Redmer DA, Milne JS, Aitken RP, Johnson ML, Borowicz PP, Reynolds LP, Caton JS, Wallace JM. Decreasing maternal nutrient intake during the final third of pregnancy in previously overnourished adolescent sheep: Effects on maternal nutrient partitioning and feto-placental development. *Placenta* 2012; 33: 114-121

- Refuerzo JS, Sokol RJ, Aranda JV, Hallak M, Hotra JW, Kruger M, Sorokin Y. Sildenafil citrate and fetal outcome in pregnant rats. *Fetal Diagn Ther* 2006; 21: 259-263

- Regev RH, Lusky A, Dolfin T, Litmanovitz I, Arnon S, Reichman B, Israel Neonatal Network. Excess mortality and morbidity among small-for-gestational-age premature infants: a population-based study. *J Pediatr* 2003; 143: 186-191

- Regnault TR, Galan HL, Parker TA, Anthony RV. Placental development in normal and compromised pregnancies - a review. *Placenta* 2002; 23(Suppl_A): S119-S129

- Regnault TR, de Vrijer B, Galan HL, Davidsen ML, Trembler KA, Battaglia FC, Wilkening RB, Anthony RV. The relationship between transplacental O2 diffusion and placental expression of PlGF, VEGF and their receptors in a placental insufficiency model of fetal growth restriction. *J Physiol* 2003; 550: 641-656

- Renbaum P, Abrahamove D, Fainsod A, Wilson GG, Rottem S, Razin A. Cloning, characterization, and expression in escherichia coli of the gene coding for the CpG DNA methylase from spiroplasma sp. strain MQ1 (M.SssI). *Nucleic Acids Res* 1990; 18: 1145-1152.

- Resendiz M, Chen Y, Ozturk NC, Zhou FC. Epigenetic medicine and fetal alcohol spectrum disorders. *Epigenomics* 2013; 5: 73-86

- Reynolds LP, Redmer DA. Uteroplacental vascular development and placental function. *J Anim Sci* 1995; 73: 1839-1851

- Reynolds LP, Ferrell CL, Robertson DA, Ford SP. Metabolism of the gravid uterus, fetus and utero-placenta at several stages of gestation in cows. *J Agric Sci* 1986; 106: 437-444

- Reynolds LP, Borowicz PP, Caton JS, Vonnahme KA, Luther JS, Buchanan DS, Hafez SA, Grazul-Bilska AT, Redmer DA. Uteroplacental vascular development and placental function: an update. *Int J Dev Biol* 2010; 54: 355-366

- Rich-Edwards JW, Stampfer MJ, Manson JE, Rosner B, Hankinson SE, Colditz GA, Willett WC, Hennekens CH. Birth weight and risk of cardiovascular disease in a cohort of women followed up since 1976. *BMJ* 1997; 315: 396-400

- Rigano S, Bozzo M, Ferrazzi E, Bellotti M, Battaglia FC, Galan HL. Early and persistent reduction in umbilical vein blood flow in the growth-restricted fetus: a longitudinal study. *Am J Obstet Gynecol* 2001; 185: 834-838

- Rizzo G, Capponi A, Arduini D, Romanini C. The value of fetal arterial, cardiac and venous flows in predicting pH and blood gases measured in umbilical blood at cordocentesis in growth retarded fetuses. *BJOG* 1995; 102: 963-969

- Rizzo G, Capponi A, Chaoui R, Taddei F, Arduini D, Romanini C. Blood flow velocity waveforms from peripheral pulmonary arteries in normally grown and growth-retarded fetuses. *Ultrasound Obstet Gynecol* 1996; 8: 87-92

- Roberfroid D, Huybregts L, Lanou H, Henry MC, Meda N, Menten J, Kolsteren P, MISAME Study Group. Effects of maternal multiple micronutrient supplementation on fetal growth: a double-blind randomized controlled trial in rural Burkina Faso. *Am J Clin Nutr* 2008; 88: 1330-1340

- Roberts CT, Sohlstrom A, Kind KL, Earl RA, Khong TY, Robinson JS, Owens PC, Owens JA. Maternal food restriction reduces the exchange surface area and increases the barrier thickness of the placenta in the guinea-pig. *Placenta* 2001; 22: 177-185

- Robinson JJ, McDonald I, Fraser C, Crofts RMJ. Studies on reproduction in prolific ewes I: growth of the products of conception. *J Agric Sci* 1977; 88: 539-552

- Robinson JS, Kingston EJ, Jones CT, Thorburn GD. Studies on experimental growth retardation in sheep. The effect of removal of a endometrial caruncles on fetal size and metabolism. *J Dev Physiol* 1979; 1: 379-398

- Robinson JJ, Wallace JM, Aitken RP. Fertilization and ovum recovery rates in superovulated ewes following cervical insemination or laparoscopic intrauterine insemination at different times after progestagen withdrawal and in one or both uterine horns. *Journal of Reproduction and Fertility* 1989; 87: 771-782

- Robinson V. Finding alternatives: An overview of the 3Rs and the use of animals in research. *Sch Sci Rev* 2005; 87: 1-4

- Ronzoni S, Marconi AM, Paolini CL, Teng C, Pardi G, Battaglia FC. The effect of a maternal infusion of amino acids on umbilical uptake in pregnancies complicated by intrauterine growth restriction. *Am J Obstet Gynecol* 2002; 187: 741-746

- Rosengart TK, Lee LY, Patel SR, Sanborn TA, Parikh M, Bergman GW, Hachamovitch R, Szulc M, Kligfield PD, Okin PM, Hahn RT, Devereux RB, Post MR, Hackett NR, Foster T, Grasso TM, Lesser ML, Isom OW, Crystal RG. Angiogenesis gene therapy: phase I assessment of direct intramyocardial administration of an adenovirus vector expressing VEGF121 cDNA to individuals with clinically significant severe coronary artery disease. *Circulation* 1999; 100: 468-474

- Ross MG, Beall MH. Adult sequelae of intrauterine growth restriction. *Semin Perinatol* 2008; 32: 213-218

- Rossignol S, Netchine I, Le Bouc Y, Gicquel C. Epigenetics in Silver-Russell syndrome. *Best Pract Res Clin Endocrinol Metab* 2008; 22: 403-414

- Roza SJ, Steegers EA, Verburg BO, Jaddoe VW, Moll HA, Hofman A, Verhulst FC, Tiemeier H. What is spared by fetal brain-sparing? Fetal circulatory redistribution and behavioral problems in the general population. *Am J Epidemiol* 2008; 168: 1145-1152

- Rush D, Stein Z, Susser M. A randomized controlled trial of prenatal nutritional supplementation in New York City. *Pediatrics* 1980; 65: 683-697

- Russel AJF, Doney JM, Gunn RG. Subjective assessment of body fat in live sheep. *J Agric Sci* 1969; 72: 451-454

- Sakata M, Kurachi H, Imai T, Tadokoro C, Yamaguchi M, Yoshimoto Y, Oka Y, Miyake A. Increase in human placental glucose transporter-1 during pregnancy. *Eur J Endocrinol* 1995; 132: 206-212

- Salafia CM. Placental pathology of fetal growth restriction. *Clin Obstet Gynecol* 1997; 40: 740-749

- Samangaya RA, Mires G, Shennan A, Skillern L, Howe D, McLeod A, Baker PN. A randomised, double-blinded, placebo-controlled study of the phosphodiesterase type

5 inhibitor sildenafil for the treatment of preeclampsia. *Hypertens Pregnancy* 2009; 28: 369-382

- Sandoval J, Heyn H, Moran S, Serra-Musach J, Pujana MA, Bibikova M, Esteller M. Validation of a DNA methylation microarray for 450,000 CpG sites in the human genome. *Epigenetics* 2011; 6: 692-702

- Sanlaville D, Aubry MC, Dumez Y, Nolen MC, Amiel J, Pinson MP, Lyonnet S, Munnich A, Vekemans M, Morichon-Delvallez N. Maternal uniparental heterodisomy of chromosome 14: chromosomal mechanism and clinical follow up. *J Med Genet* 2000; 37: 525-528

- Santos MS, Joles JA. Early determinants of cardiovascular disease. *Best Pract Res Clin Endocrinol Metab* 2012; 26: 581-597

- Satterfield MC, Bazer FW, Spencer TE, Wu G. Sildenafil citrate treatment enhances amino acid availability in the conceptus and fetal growth in an ovine model of intrauterine growth restriction. *J Nutr* 2010; 140: 251-258

- Savvidou MD, Yu CK, Harland LC, Hingorani AD, Nicolaides KH. Maternal serum concentration of soluble fms-like tyrosine kinase 1 and vascular endothelial growth factor in women with abnormal uterine artery doppler and in those with fetal growth restriction. *Am J Obstet Gynecol* 2006; 195: 1668-1673

- Say L, Gulmezoglu AM, Hofmeyr GJ. Hormones for suspected impaired fetal growth. *Cochrane Database Syst Rev* 2003a; 1: CD000109

- Say L, Gulmezoglu AM, Hofmeyr GJ. Maternal nutrient supplementation for suspected impaired fetal growth. *Cochrane Database Syst Rev* 2003b; 1: CD000148

- Scherjon SA, Smolders-DeHaas H, Kok JH, Zondervan HA. The "brain-sparing" effect: antenatal cerebral doppler findings in relation to neurologic outcome in very preterm infants. *Am J Obstet Gynecol* 1993; 169: 169-175

- Scherjon SA, Oosting H, Smolders-DeHaas H, Zondervan HA, Kok JH. Neurodevelopmental outcome at three years of age after fetal 'brain-sparing'. *Early Hum Dev* 1998; 52: 67-79

- Scherjon S, Briet J, Oosting H, Kok J. The discrepancy between maturation of visual-evoked potentials and cognitive outcome at five years in very preterm infants with and without hemodynamic signs of fetal brain-sparing. *Pediatrics* 2000; 105: 385-391
- Schroeder HJ. Models of fetal growth restriction. *Eur J Obstet Gynecol Reprod Biol* 2003; 110(Suppl_1): S29-39
- Schulz LC. The dutch hunger winter and the developmental origins of health and disease. *Proc Natl Acad Sci USA* 2010; 107: 16757-16758
- Sepp-Lorenzino L. Structure and function of the insulin-like growth factor I receptor. *Breast Cancer Res Treat* 1998; 47: 235-253
- Shah PS, Shah V, Knowledge Synthesis Group On Determinants Of Preterm/lBW Births. Influence of the maternal birth status on offspring: a systematic review and meta-analysis. *Acta Obstet Gynecol Scand* 2009; 88: 1307-1318
- Shah PS, Knowledge Synthesis Group on determinants of preterm/low birthweight births. Paternal factors and low birthweight, preterm, and small for gestational age births:a systematic review. *Am J Obstet Gynecol* 2010a; 202: 103-123
- Shah PS, Knowledge Synthesis Group on Determinants of LBW/PT births. Parity and low birth weight and preterm birth: a systematic review and meta-analyses. *Acta Obstet Gynecol Scand* 2010b; 89: 862-875
- Shah PS, Shah J, Knowledge Synthesis Group on Determinants of Preterm/LBW Births. Maternal exposure to domestic violence and pregnancy and birth outcomes: a systematic review and meta-analyses. *J Womens Health* 2010; 19: 2017-2031
- Shah PS, Zao J, Ali S, Knowledge Synthesis Group of Determinants of preterm/LBW births. Maternal marital status and birth outcomes: a systematic review and meta-analyses. *Matern Child Health J* 2011; 15: 1097-1109
- Shelton M, Huston JE. Effects of high temperature stress during gestation on certain aspects of reproduction in the ewe. *J Anim Sci* 1968; 27: 153-158
- Sibai B, Dekker G, Kupferminc M. Pre-eclampsia. *Lancet* 2005; 365: 785-799

- Sieroszewski P, Suzin J, Karowicz-Bilinska A. Ultrasound evaluation of intrauterine growth restriction therapy by a nitric oxide donor (L-arginine). *J Matern Fetal Neonatal Med* 2004; 15: 363-366

- Silver LE, Decamps PJ, Korst LM, Platt LD, Castro L. Intrauterine growth restriction is accompanied by decreased renal volume in the human fetus. *Am J Obstet Gynecol* 2003; 188: 1320-1325

- Simchen MJ, Beiner ME, Strauss-Liviathan N, Dulitzky M, Kuint J, Mashiach S, Schiff E. Neonatal outcome in growth-restricted versus appropriately grown preterm infants. *Am J Perinatol* 2000; 17: 187-192

- Simon A, Gariepy J, Chironi G, Megnien JL, Levenson J. Intima-media thickness: A new tool for diagnosis and treatment of cardiovascular risk. *J Hypertens* 2002; 20: 159-169

- Simon A, Megnien JL, Chironi G. The value of carotid intima-media thickness for predicting cardiovascular risk. *Arterioscler Thromb Vasc Biol* 2010; 30: 182-185

- Sinclair KD, Allegrucci C, Singh R, Gardner DS, Sebastian S, Bispham J, Thurston A, Huntley JF, Rees WD, Maloney CA, Lea RG, Craigon J, McEvoy TG, Young LE. DNA methylation, insulin resistance, and blood pressure in offspring determined by maternal periconceptional B vitamin and methionine status. *Proc Natl Acad Sci USA* 2007; 104: 19351-19356

- Skarsgard ED, Amii LA, Dimmitt RA, Sakamoto G, Brindle ME, Moss RL. Fetal therapy with rhIGF-1 in a rabbit model of intrauterine growth retardation. *J Surg Res* 2001; 99: 142-146

- Skillman CA, Plessinger MA, Woods JR, Clark KE. Effect of graded reductions in uteroplacental blood flow on the fetal lamb. *Am J Physiol* 1985; 249: H1098-H1105

- Smerieri A, Petraroli M, Ziveri MA, Volta C, Bernasconi S, Street ME. Effects of cord serum insulin, IGF-II, IGFBP-2, IL-6 and cortisol concentrations on human birth weight and length: pilot study. *PLoS One* 2011; 6: e29562

- Smith GC, Smith MF, McNay MB, Fleming JE. The relation between fetal abdominal circumference and birthweight: findings in 3512 pregnancies. *BJOG* 1997; 104: 186-190

- Smith GC, Pell JP, Walsh D. Pregnancy complications and maternal risk of ischaemic heart disease: a retrospective cohort study of 129,290 births. *Lancet* 2001; 357: 2002-2006

- Snijders RJ, Sherrod C, Gosden CM, Nicolaides KH. Fetal growth retardation: Associated malformations and chromosomal abnormalities. *Am J Obstet Gynecol* 1993a; 168: 547-555

- Snijders RJ, Abbas A, Melby O, Ireland RM, Nicolaides KH. Fetal plasma erythropoietin concentration in severe growth retardation. *Am J Obstet Gynecol* 1993b; 168: 615-619

- Sohi G, Marchand K, Revesz A, Arany E, Hardy DB. Maternal protein restriction elevates cholesterol in adult rat offspring due to repressive changes in histone modifications at the cholesterol 7alpha-hydroxylase promoter. *Mol Endocrinol* 2011; 25: 785-798

- Sokol GM, Liechty EA, Boyle DW. Comparison of steady-state diffusion and transit time ultrasonic measurements of umbilical blood flow in the chronic fetal sheep preparation. *Am J Obstet Gynecol* 1996; 174: 1456-1460

- Sonesson SE, Fouron JC, Teyssier G, Bonnin P. Effects of increased resistance to umbilical blood flow on fetal hemodynamic changes induced by maternal oxygen administration: a Doppler velocimetric study on the sheep. *Pediatr Res* 1993; 34: 796-800

- Spinillo A, Gardella B, Preti E, Zanchi S, Stronati M, Fazzi E. Rates of neonatal death and cerebral palsy associated with fetal growth restriction among very low birthweight infants. A temporal analysis. *BJOG* 2006; 113: 775-780

- Stallmach T, Karolyi L, Lichtlen P, Maurer M, Hebisch G, Joller H, Marti HH, Gassmann M. Fetuses from preeclamptic mothers show reduced hepatic erythropoiesis. *Pediatr Res* 1998; 43: 349-354

- Steegers EA, Van Lakwijk HP, Jongsma HW, Fast JH, De Boo T, Eskes TK, Hein PR. (Patho)physiological implications of chronic dietary sodium restriction during pregnancy; a longitudinal prospective randomized study. *BJOG* 1991; 98: 980-987

- Stewart DJ, Hilton JD, Arnold JM, Gregoire J, Rivard A, Archer SL, Charbonneau F, Cohen E, Curtis M, Buller CE, Mendelsohn FO, Dib N, Page P, Ducas J, Plante S, Sullivan J, Macko J, Rasmussen C, Kessler PD, Rasmussen HS. Angiogenic gene therapy in patients with nonrevascularizable ischemic heart disease: a phase 2 randomized,

controlled trial of AdVEGF(121) (AdVEGF121) versus maximum medical treatment. *Gene Ther* 2006; 13: 1503-1511

- Street ME, Seghini P, Fieni S, Ziveri MA, Volta C, Martorana D, Viani I, Gramellini D, Bernasconi S. Changes in interleukin-6 and IGF system and their relationships in placenta and cord blood in newborns with fetal growth restriction compared with controls. *Eur J Endocrinol* 2006; 155: 567-574

- Stulc J. Extracellular transport pathways in the haemochorial placenta. *Placenta* 1989; 10: 113-119

- Sung JF, Fan X, Dhal S, Dwyer BK, Jafari A, El-Sayed YY, Druzin ML, Nayak NR. Decreased circulating soluble Tie2 levels in preeclampsia may result from inhibition of vascular endothelial growth factor (VEGF) signaling. *J Clin Endocrinol Metab* 2011; 96: E1148-E1152

- Supramaniam VG, Jenkin G, Loose J, Wallace EM, Miller SL. Chronic fetal hypoxia increases activin A concentrations in the late-pregnant sheep. *BJOG* 2006; 113: 102-109

- Swanson TJ, Hammer CJ, Luther JS, Carlson DB, Taylor JB, Redmer DA, Neville TL, Reed JJ, Reynolds LP, Caton JS, Vonnahme KA. Effects of gestational plane of nutrition and selenium supplementation on mammary development and colostrum quality in pregnant ewe lambs. *J Anim Sci* 2008; 86: 2415-2423

- Takai D, Jones PA. Comprehensive analysis of CpG islands in human chromosomes 21 and 22. *Proc Natl Acad Sci USA* 2002; 99: 3740-3745

- Tekay A, Jouppila P. Fetal adrenal artery velocimetry measurements in appropriate-for-gestational age and intrauterine growth-restricted fetuses. *Ultrasound Obstet Gynecol* 2000; 16: 419-424

- Teodoridis JM, Hall J, Marsh S, Kannall HD, Smyth C, Curto J, Siddiqui N, Gabra H, McLeod HL, Strathdee G, Brown R. CpG island methylation of DNA damage response genes in advanced ovarian cancer. *Cancer Res* 2005; 65: 8961-8967

- Tervit HR. Embryo transfer and sperm sexing. *2nd International Congress for Sheep Veterinarians, Proceedings of the Society's 19th Seminar*. 1989: 144-157

- Teyssier G, Fouron JC, Sonesson SE, Bonnin P, Skoll A. Circulatory changes induced by isovolumic increase in red cell mass in fetal lambs. *Arch Dis Child Fetal Neonatal Ed* 1998; 79: F180-F184

- Thakor AS, Herrera EA, Seron-Ferre M, Giussani DA. Melatonin and vitamin C increase umbilical blood flow via nitric oxide-dependent mechanisms. *J Pineal Res* 2010; 49: 399-406

- Thilaganathan B, Nicolaides KH. Erythroblastosis in birth asphyxia. *Ultrasound Obstet Gynecol* 1992; 2: 15-17

- Thilaganathan B, Athanasiou S, Ozmen S, Creighton S, Watson NR, Nicolaides KH. Umbilical cord blood erythroblast count as an index of intrauterine hypoxia. *Arch Dis Child Fetal Neonatal Ed* 1994; 70: F192-F194

- Thompson RF, Fazzari MJ, Niu H, Barzilai N, Simmons RA, Greally JM. Experimental intrauterine growth restriction induces alterations in DNA methylation and gene expression in pancreatic islets of rats. *J Biol Chem* 2010; 285: 15111-15118

- Thornton JG, Lilford RJ. Do we need randomised trials of antenatal tests of fetal wellbeing? *BJOG* 1993; 100: 197-200

- Thornton JG, Hornbuckle J, Vail A, Spiegelhalter DJ, Levene M, GRIT Study Group. Infant wellbeing at 2 years of age in the growth restriction intervention trial (GRIT): multicentred randomised controlled trial. *Lancet* 2004; 364: 513-520

- Thorpe-Beeston JG, Nicolaides KH, Snijders RJ, Felton CV, Vyas S, Campbell S. Relations between the fetal circulation and pituitary-thyroid function. *BJOG* 1991; 98: 1163-1167

- Thorpe-Beeston JG, Nicolaides KH. Fetal thyroid function. *Fetal Diagn Ther* 1993; 8: 60-72

- Thureen PJ, Trembler KA, Meschia G, Makowski EL, Wilkening RB. Placental glucose transport in heat-induced fetal growth retardation. *Am J Physiol* 1992; 263: R578-R585

- Tikkanen M. Placental abruption: Epidemiology, risk factors and consequences. *Acta Obstet Gynecol Scand* 2011; 90: 140-149

- Tobi EW, Lumey LH, Talens RP, Kremer D, Putter H, Stein AD, Slagboom PE, Heijmans BT. DNA methylation differences after exposure to prenatal famine are common and timing- and sex-specific. *Hum Mol Genet* 2009; 18: 4046-4053

- Tobi EW, Heijmans BT, Kremer D, Putter H, Delemarre-van de Waal HA, Finken MJ, Wit JM, Slagboom PE. DNA methylation of IGF2, GNASAS, INSIGF and LEP and being born small for gestational age. *Epigenetics* 2011; 6: 171-176

- Tolsa CB, Zimine S, Warfield SK, Freschi M, Sancho Rossignol A, Lazeyras F, Hanquinet S, Pfizenmaier M, Huppi PS. Early alteration of structural and functional brain development in premature infants born with intrauterine growth restriction. *Pediatr Res* 2004; 56: 132-138

- Tosh DN, Fu Q, Callaway CW, McKnight RA, McMillen IC, Ross MG, Lane RH, Desai M. Epigenetics of programmed obesity: Alteration in IUGR rat hepatic IGF1 mRNA expression and histone structure in rapid vs. delayed postnatal catch-up growth. *Am J Physiol Gastrointest Liver Physiol* 2010; 299: G1023-G1029

- Trinh BN, Long TI, Laird PW. DNA methylation analysis by MethyLight technology. *Methods* 2001; 25: 456-462

- Trudinger BJ, Giles WB, Cook CM, Bombardieri J, Collins L. Fetal umbilical artery flow velocity waveforms and placental resistance: Clinical significance. *BJOG* 1985; 92: 23-30

- Trudinger BJ, Connelly AJ, Giles WB, Hales JR, Wilcox GR. The effects of prostacyclin and thromboxane analogue (U46619) on the fetal circulation and umbilical flow velocity waveforms. *J Dev Physiol* 1989; 11: 179-184

- Trudinger B, Song JZ, Wu ZH, Wang J. Placental insufficiency is characterized by platelet activation in the fetus. *Obstet Gynecol* 2003; 101: 975-981

- Tulzer G, Gudmundsson S, Wood DC, Cohen AW, Weiner S, Huhta JC. Doppler in non-immune hydrops fetalis. *Ultrasound Obstet Gynecol* 1994; 4: 279-283

- Turner CL, Mackay DM, Callaway JL, Docherty LE, Poole RL, Bullman H, Lever M, Castle BM, Kivuva EC, Turnpenny PD, Mehta SG, Mansour S, Wakeling EL, Mathew V, Madden J, Davies JH, Temple IK. Methylation analysis of 79 patients with growth restriction reveals novel patterns of methylation change at imprinted loci. *Eur J Hum Genet*. 2010; 18: 648-655

- Tyson JE, Kennedy K, Broyles S, Rosenfeld CR. The small for gestational age infant: Accelerated or delayed pulmonary maturation? increased or decreased survival? *Pediatrics* 1995; 95: 534-538

- Ueland K, Novy MJ, Peterson EN, Metcalfe J. Maternal cardiovascular dynamics. IV. the influence of gestational age on the maternal cardiovascular response to posture and exercise. *Am J Obstet Gynecol* 1969; 104: 856-864

- Umetani N, de Maat MF, Mori T, Takeuchi H, Hoon DS. Synthesis of universal unmethylated control DNA by nested whole genome amplification with phi29 DNA polymerase. *Biochem Biophys Res Commun* 2005; 329: 219-223

- Urban J, Iwaszkiewicz-Pawlowska A. Concentration of free fatty acids (FFA) in amniotic fluid and maternal and cord serum in cases of intrauterine growth retardation. *J Perinat Med* 1986; 14: 259-262

- van Assche FA, Aerts L. The fetal endocrine pancreas. *Contrib Gynecol Obstet* 1979; 5: 44-57

- van den Hof MC, Nicolaides KH. Platelet count in normal, small, and anemic fetuses. *Am J Obstet Gynecol* 1990; 162: 735-739

- van der Veen F, Fox H. The human placenta in idiopathic intrauterine growth retardation: a light and electron microscopic study. *Placenta* 1983; 4: 65-77

- van Dijk MA, Rodenburg RJ, Holthuizen P, Sussenbach JS. The liver-specific promoter of the human insulin-like growth factor II gene is activated by CCAAT/enhancer binding protein (C/EBP). *Nucleic Acids Res* 1992; 20: 3099-3104

- van Huisseling H, Hasaart TH, Muijsers GJ, de Haan J. Umbilical artery pulsatility index and placental vascular resistance during acute hypoxemia in fetal lambs. *Gynecol Obstet Invest* 1991a; 31: 61-66

- van Huisseling H, Muijsers GJ, de Haan J, Hasaart TH. Fetal hypertension induced by norepinephrine infusion and umbilical artery flow velocity waveforms in fetal sheep. *Am J Obstet Gynecol* 1991b; 165: 450-455

- van Huisseling H, Muijsers GJ, de Haan J, Hasaart TH. The acute response of the umbilical artery pulsatility index to changes in blood volume in fetal sheep. *Eur J Obstet Gynecol Reprod Biol* 1992; 43: 149-155

- van Wyk L, Boers KE, van der Post JA, van Pampus MG, van Wassenaer AG, van Baar AL, Spaanderdam ME, Becker JH, Kwee A, Duvekot JJ, Bremer HA, Delemarre FM, Bloemenkamp KW, de Groot CJ, Willekes C, Roumen FJ, van Lith JM, Mol BW, le Cessie S, Scherjon SA, DIGITAT Study Group. Effects on (neuro)developmental and behavioral outcome at 2 years of age of induced labor compared with expectant management in intrauterine growth-restricted infants: long-term outcomes of the DIGITAT trial. *Am J Obstet Gynecol* 2012; 206: 406.e1-406.e7

- Vannucci RC, Vannucci SJ. Glucose metabolism in the developing brain. *Semin Perinatol* 2000; 24: 107-115

- Vatnick I, Ignotz G, McBride BW, Bell AW. Effect of heat stress on ovine placental growth in early pregnancy. *J Dev Physiol* 1991; 16: 163-166

- Veille JC, Kanaan C. Duplex doppler ultrasonographic evaluation of the fetal renal artery in normal and abnormal fetuses. *Am J Obstet Gynecol* 1989; 161: 1502-1507

- Verhaeghe J, Van Herck E, Bouillon R. Umbilical cord osteocalcin in normal pregnancies and pregnancies complicated by fetal growth retardation or diabetes mellitus. *Biol Neonate* 1995; 68: 377-383

- Verkauskiene R, Beltrand J, Claris O, Chevenne D, Deghmoun S, Dorgeret S, Alison M, Gaucherand P, Sibony O, Levy-Marchal C. Impact of fetal growth restriction on body composition and hormonal status at birth in infants of small and appropriate weight for gestational age. *Eur J Endocrinol* 2007; 157: 605-612

- Vickers MH, Breier BH, Cutfield WS, Hofman PL, Gluckman PD. Fetal origins of hyperphagia, obesity, and hypertension and postnatal amplification by hypercaloric nutrition. *Am J Physiol Endocrinol Metab* 2000; 279: E83-E87

- Viegas OA, Scott PH, Cole TJ, Eaton P, Needham PG, Wharton BA. Dietary protein energy supplementation of pregnant asian mothers at Sorrento, Birmingham. II: selective during third trimester only. *BMJ* 1982; 285: 592-595

- Viehweg B, Ruckhaberle KE, Zimmermann G, Beyreiss K, Petzold J, Forberg J. Therapy of suspected intrauterine fetal retardation. *Zentralbl Gynakol* 1987; 109: 818-829

- Ville Y, Proudler A, Kuhn P, Nicolaides KH. Aldosterone concentration in normal, growth-retarded, anemic, and hydropic fetuses. *Obstet Gynecol* 1994; 84: 511-514

- von Dadelszen P, Dwinnell S, Magee LA, Carleton BC, Gruslin A, Lee B, Lim KI, Liston RM, Miller SP, Rurak D, Sherlock RL, Skoll MA, Wareing MM, Baker PN, Research into Advanced Fetal Diagnosis and Therapy (RAFT) Group. Sildenafil citrate therapy for severe early-onset intrauterine growth restriction. *BJOG* 2011; 118: 624-628

- Vonnahme KA, Wilson ME, Li Y, Rupnow HL, Phernetton TM, Ford SP, Magness RR. Circulating levels of nitric oxide and vascular endothelial growth factor throughout ovine pregnancy. *J Physiol* 2005; 565: 101-109

- Vonnahme KA, Wienhold CM, Borowicz PP, Neville TL, Redmer DA, Reynolds LP, Caton JS. Supranutritional selenium increases mammary gland vascularity in postpartum ewe lambs. *J Dairy Sci* 2011; 94: 2850-2858

- Wali JA, de Boo HA, Derraik JG, Phua HH, Oliver MH, Bloomfield FH, Harding JE. Weekly intra-amniotic IGF-1 treatment increases growth of growth-restricted ovine fetuses and up-regulates placental amino acid transporters. *PLoS One* 2012; 7: e37899

- Wallace JM, Aitken RP, Cheyne MA. Nutrient partitioning and fetal growth in rapidly growing adolescent ewes. *J Reprod Fertil* 1996; 107: 183-190

- Wallace JM, Aitken RP, Cheyne MA, Humblot P. Pregnancy-specific protein B and progesterone concentrations in relation to nutritional regimen, placental mass and pregnancy outcome in growing adolescent ewes carrying singleton fetuses. *J Reprod Fertil* 1997a; 109: 53-58

- Wallace JM, Da Silva P, Aitken RP, Cruickshank MA. Maternal endocrine status in relation to pregnancy outcome in rapidly growing adolescent sheep. *J Endocrinol* 1997b; 155: 359-368.

- Wallace JM, Bourke DA, Aitken RP, Cruickshank MA. Switching maternal dietary intake at the end of the first trimester has profound effects on placental development and fetal growth in adolescent ewes carrying singleton fetuses. *Biol Reprod* 1999; 61: 101-110

- Wallace JM, Bourke DA, Aitken RP, Palmer RM, Da Silva P, Cruickshank MA. Relationship between nutritionally-mediated placental growth restriction and fetal growth, body composition and endocrine status during late gestation in adolescent sheep. *Placenta* 2000; 21: 100-108

- Wallace J, Bourke D, Da Silva P, Aitken R. Nutrient partitioning during adolescent pregnancy. *Reproduction* 2001; 122: 347-357
- Wallace JM, Bourke DA, Aitken RP, Leitch N, Hay WW,Jr. Blood flows and nutrient uptakes in growth-restricted pregnancies induced by overnourishing adolescent sheep. *Am J Physiol Regul Integr Comp Physiol* 2002; 282: R1027-36
- Wallace JM, Milne JS, Aitken RP. Maternal growth hormone treatment from day 35 to 80 of gestation alters nutrient partitioning in favor of uteroplacental growth in the overnourished adolescent sheep. *Biol Reprod*. 2004a; 70: 1277-1285
- Wallace JM, Aitken RP, Milne JS, Hay WW, Jr. Nutritionally mediated placental growth restriction in the growing adolescent: Consequences for the fetus. *Biol Reprod* 2004b; 71: 1055-1062
- Wallace JM, Milne JS, Aitken RP. The effect of overnourishing singleton-bearing adult ewes on nutrient partitioning to the gravid uterus. *Br J Nutr* 2005b; 94: 533-539
- Wallace JM, Regnault TR, Limesand SW, Hay WW Jr, Anthony RV. Investigating the causes of low birth weight in contrasting ovine paradigms. *J Physiol* 2005a; 565: 19-26
- Wallace JM, Luther JS, Milne JS, Aitken RP, Redmer DA, Reynolds LP, Hay WW, Jr. Nutritional modulation of adolescent pregnancy outcome - a review. *Placenta* 2006a; 27(Suppl_A): S61-8
- Wallace JM, Milne JS, Redmer DA, Aitken RP. Effect of diet composition on pregnancy outcome in overnourished rapidly growing adolescent sheep. *Br J Nutr* 2006b; 96: 1060-1068
- Wallace JM, Matsuzaki M, Milne J, Aitken R. Late but not early gestational maternal growth hormone treatment increases fetal adiposity in overnourished adolescent sheep. *Biol Reprod* 2006c; 75: 231-239
- Wallace JM, Milne JS, Aitken RP, Hay WW,Jr. Sensitivity to metabolic signals in late-gestation growth-restricted fetuses from rapidly growing adolescent sheep. *Am J Physiol Endocrinol Metab* 2007; 293: E1233-41
- Wallace JM, Milne JS, Matsuzaki M, Aitken RP. Serial measurement of uterine blood flow from mid to late gestation in growth restricted pregnancies induced by overnourishing adolescent sheep dams. *Placenta* 2008a; 29: 718-724

- Wallace JM, Milne JS, Aitken RP, Reynolds LP, Redmer DA. Putative role for oestrogen as the missing link between nutrition and feto-placental growth restriction in overnourished adolescent sheep. *Proc Physiol Soc* 2008b; 11: PC37 [abstract]

- Wallace JM, Milne JS, Aitken RP. Effect of weight and adiposity at conception and wide variations in gestational dietary intake on pregnancy outcome and early postnatal performance in young adolescent sheep. *Biol Reprod* 2010a; 82: 320-330

- Wallace JM, Aitken RP, Milne JS, Bake T, Adam C. Nutritionally-mediated placental growth restriction reduces size at birth and influences growth, body composition and metabolism in early postnatal life. *Fetal and Neonatal Physiological Society (FNPS) 37th Annual Meeting, Winchester, UK.* 2010b [poster presentation]

- Wallace JM, Milne JS, Green LR, Aitken RP. Postnatal hypothalamic-pituitary-adrenal function in sheep is influenced by age and sex, but not by prenatal growth restriction. *Reprod Fertil Dev* 2011; 23: 275-284

- Wallace JM, Milne JS, Adam CL, Aitken RP. Adverse metabolic phenotype in low-birth-weight lambs and its modification by postnatal nutrition. *Br J Nutr* 2012; 107: 510-522

- Wallace JM, Milne JS, Aitken RP, Adam CL. Impact of embryo donor adiposity, birth weight and gender on early postnatal growth, glucose metabolism and body composition in the young lamb. *Reprod Fertil Dev* 2013 [in press]

- Walton A, Hammond J. The maternal effects on growth and conformation in Shire horse - Shetland pony crosses. *Proc R Soc Lond B* 1938; 125: 311-335

- Wang KC, Zhang L, McMillen IC, Botting KJ, Duffield JA, Zhang S, Suter CM, Brooks DA, Morrison JL. Fetal growth restriction and the programming of heart growth and cardiac insulin-like growth factor 2 expression in the lamb. *J Physiol* 2011a; 589: 4709-4722

- Wang T, Chen M, Liu L, Cheng H, Yan YE, Feng YH, Wang H. Nicotine induced CpG methylation of Pax6 binding motif in StAR promoter reduces the gene expression and cortisol production. *Toxicol Appl Pharmacol* 2011b; 257: 328-337

- Wang Y, Tasevski V, Wallace EM, Gallery ED, Morris JM. Reduced maternal serum concentrations of angiopoietin-2 in the first trimester precede intrauterine growth restriction associated with placental insufficiency. *BJOG* 2007; 114: 1427-1431

- Ward VL, Estroff JA, Nguyen HT, Lakshmanan Y, Hayward A, Jaramillo D, Zurakowski D, Dunning PS, Peters CA, Barnewolt CE. Fetal sheep development on ultrasound and magnetic resonance imaging: a standard for the in utero assessment of models of congenital abnormalities. *Fetal Diagn Ther* 2006; 21: 444-457

- Wareing M, Myers JE, O'Hara M, Baker PN. Sildenafil citrate (Viagra) enhances vasodilatation in fetal growth restriction. *J Clin Endocrinol Metab* 2005; 90: 2550-2555

- Weiner CP, Robillard JE. Atrial natriuretic factor, digoxin-like immunoreactive substance, norepinephrine, epinephrine, and plasma renin activity in human fetuses and their alteration by fetal disease. *Am J Obstet Gynecol* 1988; 159: 1353-1360

- Weiner CP, Williamson RA. Evaluation of severe growth retardation using cordocentesis--hematologic and metabolic alterations by etiology. *Obstet Gynecol* 1989; 73: 225-229

- Weiss JL, Malone FD, Vidaver J, Ball RH, Nyberg DA, Comstock CH, Hankins GD, Berkowitz RL, Gross SJ, Dugoff L, Timor-Tritsch IE, D'Alton ME, FASTER Consortium. Threatened abortion: a risk factor for poor pregnancy outcome, a population-based screening study. *Am J Obstet Gynecol* 2004; 190: 745-750

- Wenstrom KD, Andrews WW, Bowles NE, Towbin JA, Hauth JC, Goldenberg RL. Intrauterine viral infection at the time of second trimester genetic amniocentesis. *Obstet Gynecol*. 1998; 92: 420-424

- Wilcox GR, Trudinger BJ, Cook CM, Wilcox WR, Connelly AJ. Reduced fetal platelet counts in pregnancies with abnormal Doppler umbilical flow waveforms. *Obstet Gynecol* 1989; 73: 639-643

- Wilcox MA, Newton CS, Johnson IR. Paternal influences on birthweight. *Acta Obstet Gynecol Scand* 1995; 74: 15-18

- Wilkins-Haug L, Quade B, Morton CC. Confined placental mosaicism as a risk factor among newborns with fetal growth restriction. *Prenat Diagn* 2006; 26: 428-432

- Williams SJ, McMillen IC, Zaragoza DB, Olson DM. Placental restriction increases the expression of prostaglandin endoperoxide G/H synthase-2 and EP2 mRNA in the fetal sheep kidney during late gestation. *Pediatr Res* 2002; 52: 879-885

- Winer N, Branger B, Azria E, Tsatsaris V, Philippe HJ, Roze JC, Descamps P, Boog G, Cynober L, Darmaun D. L-arginine treatment for severe vascular fetal intrauterine growth restriction: a randomized double-bind controlled trial. *Clin Nutr* 2009; 28: 243-248

- Wladimiroff JW, Tonge HM, Stewart PA. Doppler ultrasound assessment of cerebral blood flow in the human fetus. *BJOG* 1986; 93: 471-475

- Wolfe HM, Gross TL, Sokol RJ. Recurrent small for gestational age birth: perinatal risks and outcomes. *Am J Obstet Gynecol* 1987; 157: 288-293

- Wolff GL, Kodell RL, Moore SR, Cooney CA. Maternal epigenetics and methyl supplements affect agouti gene expression in Avy/a mice. *FASEB J* 1998; 12: 949-957

- Wong EA, Ohlsen SM, Godfredson JA, Dean DM, Wheaton JE. Cloning of ovine insulin-like growth factor-I cDNAs: heterogeneity in the mRNA population. *DNA* 1989; 8: 649-657

- Woods AK, Hoffmann DS, Weydert CJ, Butler SD, Zhou Y, Sharma RV, Davisson RL. Adenoviral delivery of VEGF121 early in pregnancy prevents spontaneous development of preeclampsia in BPH/5 mice. *Hypertension* 2011; 57: 94-102

- Wutz A, Barlow DP. Imprinting of the mouse Igf2r gene depends on an intronic CpG island. *Mol Cell Endocrinol* 1998; 140: 9-14

- Xu XF, Lv Y, Gu WZ, Tang LL, Wei JK, Zhang LY, Du LZ. Epigenetics of hypoxic pulmonary arterial hypertension following intrauterine growth retardation rat: epigenetics in PAH following IUGR. *Respir Res*. 2013: DOI 10.1186/1465-9921-14-20 [epub ahead of print]

- Yajnik CS. Early life origins of insulin resistance and type 2 diabetes in India and other Asian countries. *J Nutr* 2004; 134: 205-210

- Yasmeen S, Wilkins EE, Field NT, Sheikh RA, Gilbert WM. Pregnancy outcomes in women with systemic lupus erythematosus. *J Matern Fetal Med* 2001; 10: 91-96

- Yasuda M, Takakuwa K, Tokunaga A, Tanaka K. Prospective studies of the association between anticardiolipin antibody and outcome of pregnancy. *Obstet Gynecol* 1995; 86: 555-559

- Young LE, Fernandes K, McEvoy TG, Butterwith SC, Gutierrez CG, Carolan C, Broadbent PJ, Robinson JJ, Wilmut I, Sinclair KD. Epigenetic change in IGF2R is associated with fetal overgrowth after sheep embryo culture. *Nat Genet* 2001; 27: 153-154

- Young LE, Schnieke AE, McCreath KJ, Wieckowski S, Konfortova G, Fernandes K, Ptak G, Kind AJ, Wilmut I, Loi P, Feil R. Conservation of IGF2-H19 and IGF2R imprinting in sheep: effects of somatic cell nuclear transfer. *Mech Dev* 2003; 120: 1433-1442

- Zachary I. VEGF signalling: integration and multi-tasking in endothelial cell biology. *Biochem Soc Trans* 2003; 31: 1171-1177

- Zachary I, Morgan RD. Therapeutic angiogenesis for cardiovascular disease: biological context, challenges, prospects. *Heart* 2011; 97: 181-189

- Zachary I, Mathur A, Yla-Herttuala S, Martin J. Vascular protection: a novel nonangiogenic cardiovascular role for vascular endothelial growth factor. *Arterioscler Thromb Vasc Biol* 2000; 20: 1512-1520

- Zamudio S, Baumann MU, Illsley NP. Effects of chronic hypoxia in vivo on the expression of human placental glucose transporters. *Placenta* 2006; 27: 49-55

- Zeng Y, Gu P, Liu K, Huang P. Maternal protein restriction in rats leads to reduced PGC-1alpha expression via altered DNA methylation in skeletal muscle. *Mol Med Rep* 2012. DOI 10.3892/mmr.2012.1134 [epub ahead of print]

- Zezula-Szpyra A, Gawronska B, Skipor J. Vasa vasorum of blood and lymph vessels in the broad ligament of the sheep uterus analyzed by scanning electron microscopy. *Rocz Akad Med Bialymst* 1997; 42(Suppl_2): 134-146

- Zhang EG, Smith SK, Baker PN, Charnock-Jones DS. The regulation and localization of angiopoietin-1, -2, and their receptor Tie2 in normal and pathologic human placentae. *Mol Med* 2001; 7: 624-635

- Zhao Y, He X, Shi X, Huang C, Liu J, Zhou S, Heng CK. Association between serum amyloid A and obesity: a meta-analysis and systematic review. *Inflamm Res* 2010; 59: 323-334

- Zhu BP, Rolfs RT, Nangle BE, Horan JM. Effect of the interval between pregnancies on perinatal outcomes. *N Engl J Med* 1999; 340: 589-594

- Zoma WD, Baker RS, Clark KE. Effects of combined use of sildenafil citrate (Viagra) and 17beta-estradiol on ovine coronary and uterine hemodynamics. *Am J Obstet Gynecol* 2004; 190: 1291-1297

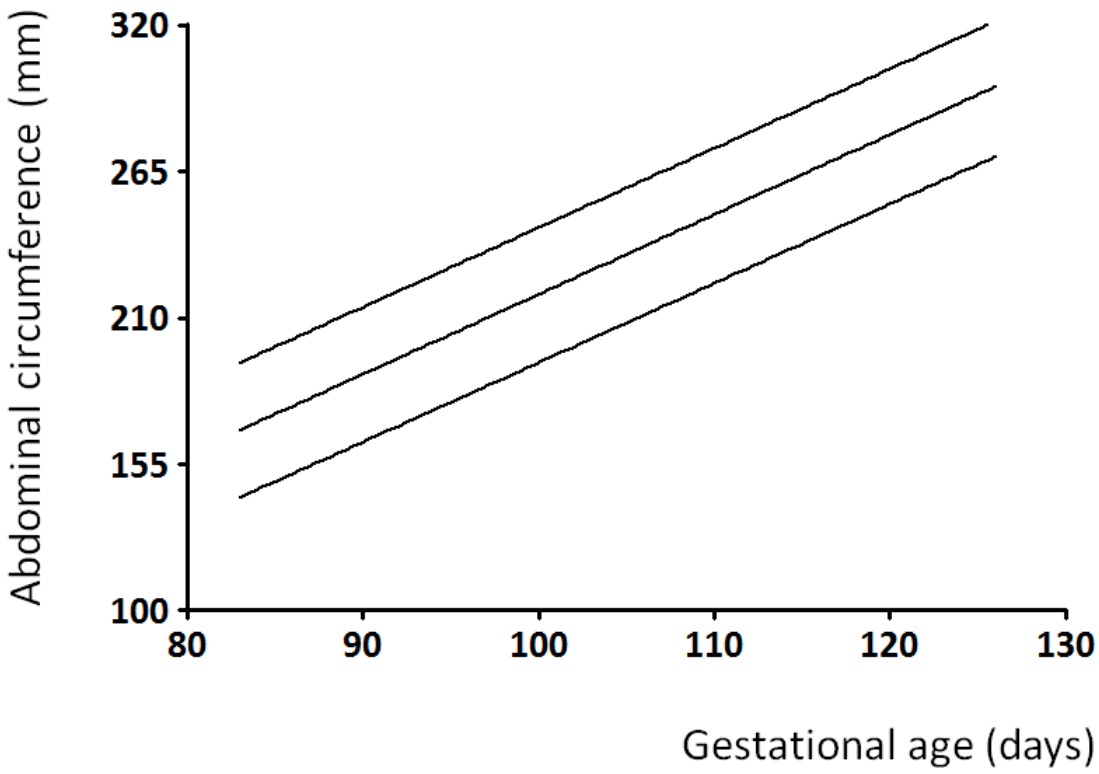
Abdominal circumference (mm)
320
265
210
155
100
80
90
100
110
120
130
Gestational age (days)

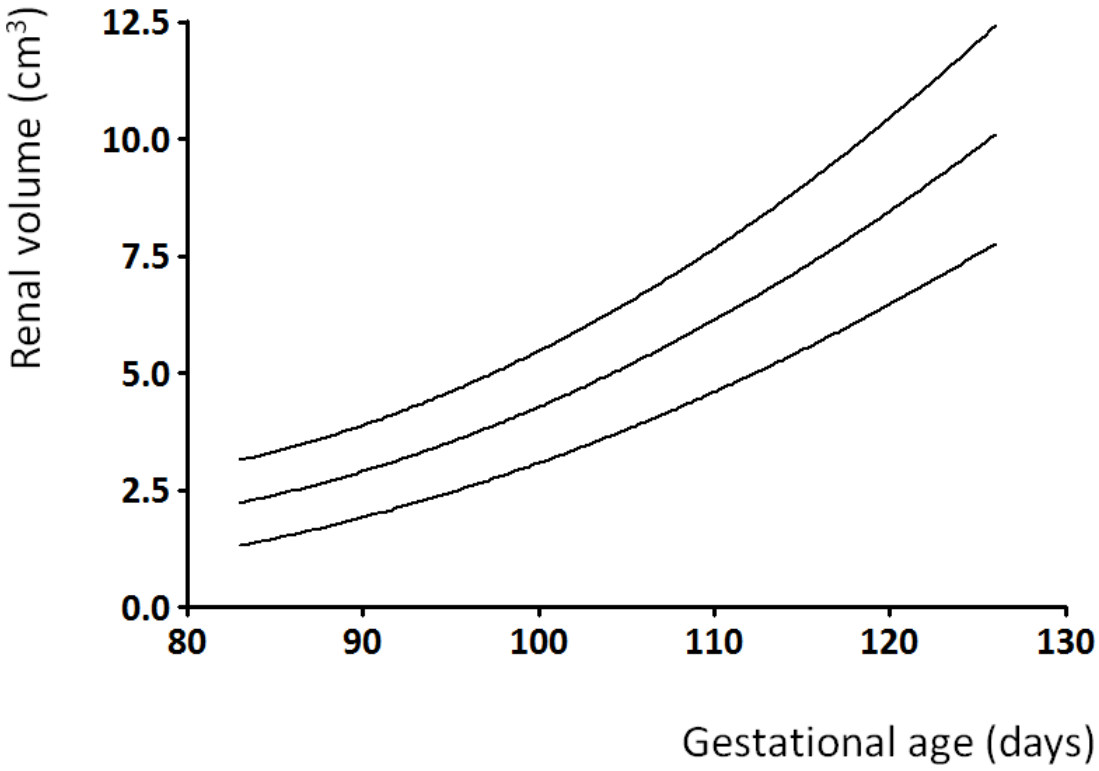
Renal volume (cm³)
12.5
10.0
7.5
5.0
2.5
0.0
80
90
100
110
120
130
Gestational age (days)

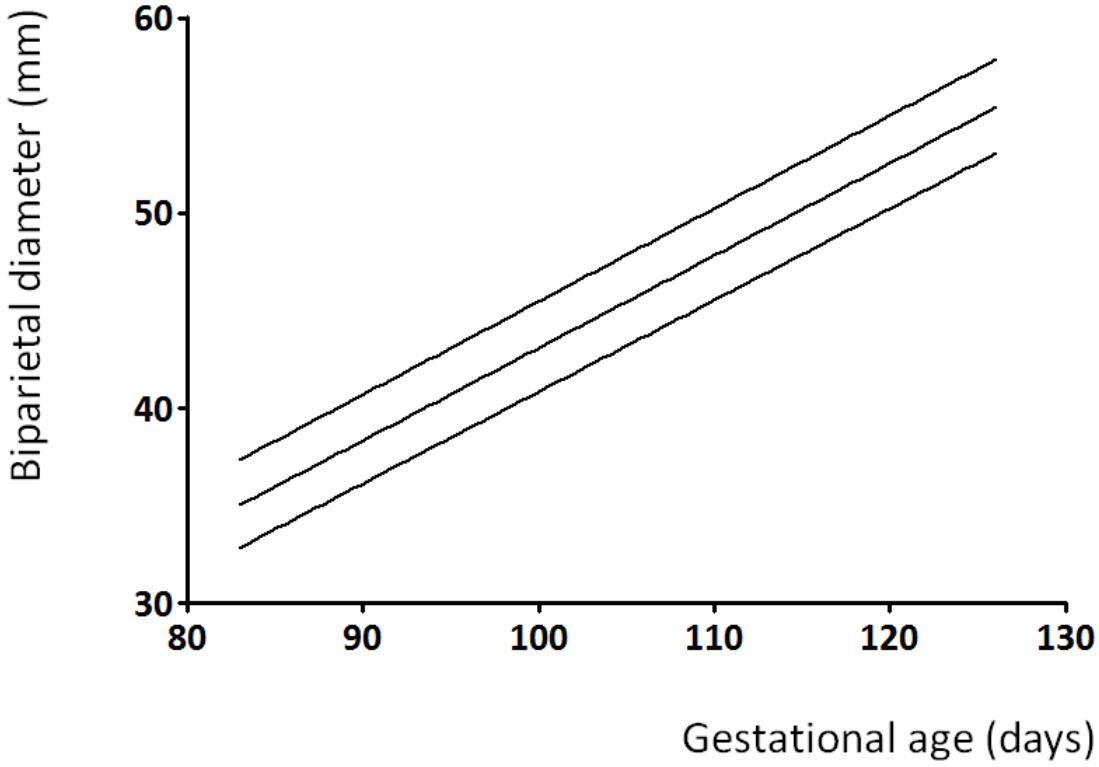
Biparietal diameter (mm)
60
50
40
30
80
90
100
110
120
130
Gestational age (days)

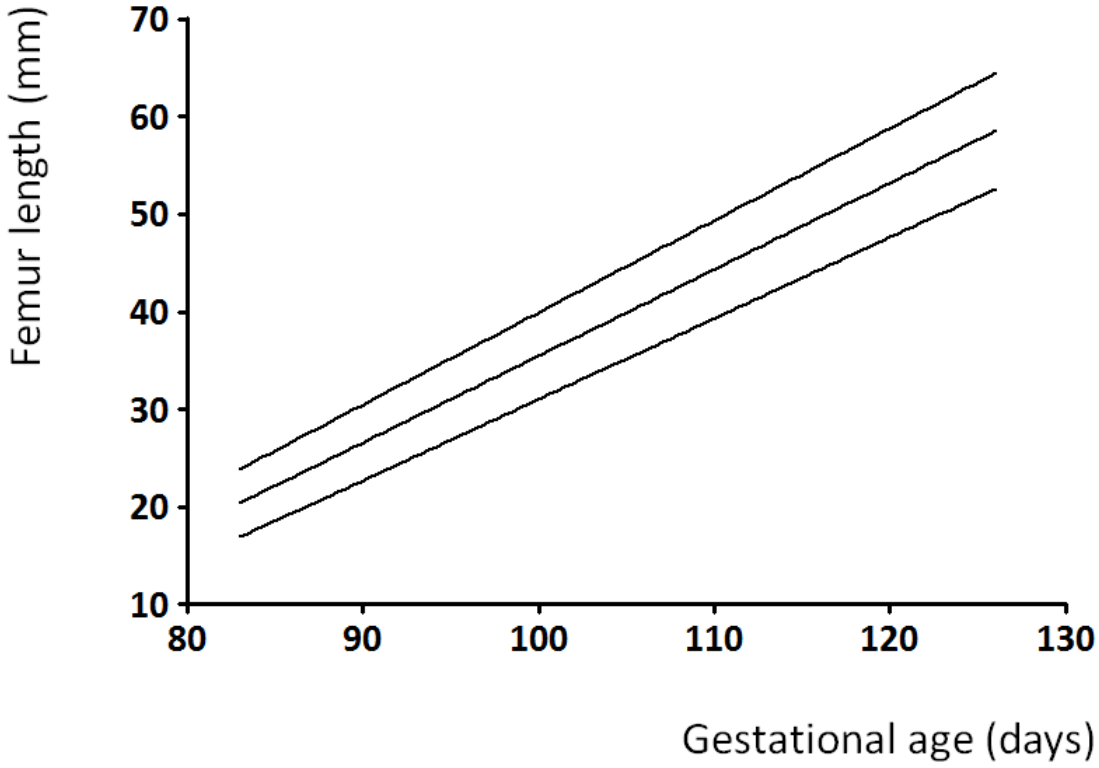
Femur length (mm)
70
60
50
40
30
20
10
80
90
100
110
120
130
Gestational age (days)

Weight		BPD	
Sex		Girth at umbilicus	
		AC (ultrasound plane)	

	Weight	Freeze	Fix	Comments
Fetal brain		✓ Whole		
Fetal pituitary		✓ Tissue-tek		
Fetal umbilical cord		✓		
Fetal adrenals		✓	✓	
Fetal pancreas		✓ **Hepatic portion**	✓ **Splenic portion**	
Fetal gut (100cm sample)*		✓	✓ x 3 (Carnoy's x 2)	
Fetal stomach complex*		✓		
Fetal small intestine*		✓		
Fetal large intestine*		✓		
Fetal liver		✓ x 2	✓ **Right lobe**	
Fetal spleen		✓	✓	
Fetal perirenal fat		✓	✓	
Fetal kidneys		✓ x 2 mid	✓ x 2 mid	
Fetal skin (thigh)		✓		
Fetal muscle (quadriceps)		✓	✓	
Fetal heart			✓	
- Fetal left ventricle (myocardium only)		✓		
- Fetal right ventricle (myocardium only)		✓		
Fetal lung (right lower lobe)		✓	✓	
Fetal thymus		✓	✓	
Fetal thyroid		✓	✓	
Fetal gonad		✓ Tissue-tek	✓	
Fetal eye / retina		✓	✓	

Femur length		*Tibia length*			
Fetal bone marrow (femur)		✓			
Fetal carcass		✓ at –20ºC			

* JC responsible for processing these samples

Fix in NBF unless stated otherwise

	Number	Weight (g)	Size	Morphology
Placentomes for freezing (x4)				
Placentomes for immersion fix (x4)				
Fetal perfused placentomes (*if done*)				
Remaining placentomes			>5cm	
			2-5cm	
			1-2cm	
			<1cm	
Residual uterus (g)				
Residual membranes (g)				
Uterine wall sample for vector spread				

Date	
Time killed	
Weight of gravid uterus	

	Weight	Freeze	Fix	Organ Bath Samples	Comments
UA1 (Gravid)		✓ x 2	✓		
UA2 (Gravid)		✓ x 2	✓		
UA3 (Gravid)		✓ x 2	✓	✓ x 2 (4-5cm length)	
UA4 (Gravid)		✓ x 2	✓	✓ x 2 (4-5cm length)	
UA1 (Non-gravid)		✓ x 2	✓		
UA2 (Non-gravid)		✓ x 2	✓		
UA3 (Non-gravid)		✓ x 2	✓	✓ x 2 (4-5cm length)	
UA4 (Non-gravid)		✓ x 2	✓	✓ x 2 (4-5cm length)	
Liver					
Blood					
Perirenal fat					
Carcass					

Ewe No ……..… **Pen No** ……..…….. **Lamb No** ……..

Date of birth ……..…… **Time of birth** ……..…….. **Present?** **Y / N**

Mode of delivery (please circle) **Spontaneous vaginal / Assisted vaginal / Caesarean**

If not spontaneous rate difficulty of delivery: *Easy / Average / Hard*

Details ……

……

……

Estimated blood loss **Average / Excessive**

Reason for excessive loss e.g. tear? ……

Colostrum yield ……..ml

Total placental weight ……..…… g **Membrane weight** …… g

Cotyledon number …….. **Cotyledon weight** ……..…… g

Initial Asssessment of Lamb (at delivery or at first encounter) – *please circle one option per row*

AIRWAY	Patent (no action)	Routine suction needed		Extensive suction needed
BREATHING	Normal	Fast	Slow	Absent
HEART RATE	Normal	Slow (e.g. less than 100 bpm)		Absent
MUSCLE TONE	Normal	Floppy	Stiff (neck back etc.)	Absent

Birthweight ……..g **Sex** **Male / Female**

Time to standing ……..……min **Heart Rate (at 1h)** ……bpm

Girth at umbilicus ……..……..cm **Resp. Rate (at 1h)** …….. /min

Biparietal diameter ……..……..mm **O2 Sats (at 1h)** ……..%

Height to shoulder (at 24h) ……..cm **Temperature (at 1h)** ……..°C

Dystosel (Se + Vit E) – *tick*					
Dam analgesia (if required)	*Day 0*	*Day 1*	*Day 2*		
Finedyne *Date / time*					
Dam antibiotics (if required)	*Day 0*	*Day 1*	*Day 2*		
Duphapen-Strep *Date / time*					
Lamb antibiotics (routine use)	*Day 0*	*Day 1*	*Day 2*	*Day 3*	*Day 4*
Baytril *Date / time*					

Lamb No …… **Date ……..……**

	Weight	Freeze	Fix	Comments
Brain		✓ Whole		
Pituitary		✓ Tissue-tek		
Adrenals		✓	✓	
Pancreas		✓ Hepatic portion	✓ Splenic portion	
Jejunum			✓ x 2 Carnoy's + NBF	
Liver		✓ x 2	✓ Right lobe	
Spleen		✓	✓	
Perirenal fat		✓	✓	
Kidneys		✓ x 2 mid	✓ x 2 mid	
Muscle (longissimus dorsi)		✓	✓	
Heart				
Lungs		✓	✓ right lower lobe (peripheral)	
Thymus				
Thyroid				
Gonads				
Hock weight (x4)				
Bone weight		✓ –20°C		
Bone length				
Blood				
Head				
Carcass				